Technische Universität München
TUM School of Natural Sciences

Understanding infrared divergences in de Sitter space with effective field theory

Andrea Federico Sanfilippo

Vollständiger Abdruck der von der TUM School of Natural Sciences der Technischen Universität München zur Erlangung eines

Doktors der Naturwissenschaften (Dr. rer. nat.)

genehmigten Dissertation.

Vorsitz:
Prof. Dr. Bastian Märkisch

Prüfende der Dissertation:
1. Prof. Dr. Martin Beneke
2. Prof. Dr. Björn Garbrecht
3. Prof. Dr. Ivo Sachs

Die Dissertation wurde am 17.07.2025 bei der Technischen Universität München eingereicht und durch die TUM School of Natural Sciences am 29.10.2025 angenommen.

Abstract

In this thesis, the infrared dynamics of the real, massless, minimally coupled, self-interacting scalar field in de Sitter space is studied, with a focus on effective-field-theory approaches. The two-point function of the field is studied using Stochastic Inflation, as well as the Euclidean formulation of the quantum theory, and the correspondence of the two results in a certain approximation is shown. The method of regions is then introduced to simplify the computation of late-time in-in correlation functions in Lorentzian de Sitter space, and the developed method is applied to the massless theory. Finally, the quantum-field-theoretic formulation of the Soft de Sitter Effective Theory is developed, and it is shown how the renormalization and matching procedure for this effective field theory can be carried out systematically using several examples. This framework is then applied to address the issue of infrared divergences in the case of one-point functions.

Zusammenfassung

In dieser Doktorarbeit wird die Infrarotdynamik des reellen, masselosen, minimal gekoppelten, selbstwechselwirkenden Skalarfeldes im de Sitter-Raum untersucht, mit Fokus auf effektiven Feldtheorien. Die Zweipunktfunktion des Feldes wird mittels Stochastischer Inflation, sowie der euklidischen Formulierung der Quantentheorie, untersucht, und die Korrespondenz der beiden Ergebnisse in einer bestimmten Näherung wird gezeigt. Die Methode der Regionen wird eingeführt, um die Berechnung von in-in-Korrelationsfunktionen bei späten Zeiten zu vereinfachen, und die entwickelte Methodik wird an der masselosen Theorie angewandt. Zuletzt wird die quantenfeldtheoretische Formulierung der Soft de Sitter Effective Theory entwickelt und es wird anhand von mehreren Beispielen gezeigt, wie die Renormierungs- und Matchingprozeduren für diese effektive Feldtheorie systematisch durchgeführt werden können. Die Infrarotdivergenzen im Fall von Einpunktfunktionen werden dann in diesem Rahmen behandelt.

Contents

Chapter 1

Introduction

The most fundamental features of our universe that are observable today are spatial homogeneity on large scales, as well as spatial flatness. Similarly, the Cosmic Microwave Background (CMB) radiation, which, to date, was mapped out most accurately by the Planck satellite [1], has a temperature distribution which is very close to being isotropic, with a mean value of 2.73 K and deviations of the order of 10^{-5} K. These observations naturally lead one to ask why our universe looks so very nearly homogeneous and isotropic, and what mechanism could have seeded the inhomogeneities that are observed.

The assumption that the the by-now standard ΛCDM model of cosmological evolution [2–4] accurately describes the history of the cosmos right after the initial moment, the Big Bang, leads to the conclusion that spatial homogeneity and flatness would already have to be featured by the initial state of the universe, which would translate into finely tuned initial conditions for the cosmological evolution. In particular, since the cosmic evolution according to this model increases spatial curvature with time, obtaining the near-flatness of the universe we observe today would have required a deviation from flatness of the order of 10^{-16} at the time of Big-Bang Nucleosynthesis [5]. The challenge of explaining why such initial conditions should have been present is known as the flatness problem. Furthermore, different patches of the CMB sky that we observe today would not have been in causal contact at any point in the past, such that these patches would never have had the chance to thermalize. The initial temperature of the primordial cosmos should therefore have been very finely tuned on a global scale as well, in order to evolve into the Universe that we observe today. This is called the horizon problem. While there is no logical inconsistency in assuming such highly fine-tuned initial conditions for the cosmic evolution, it would still be desirable to have a dynamical mechanism to realize such an initial state for the evolution according to the ΛCDM model. This necessitates an intervening phase of cosmic evolution between the Big Bang and the onset of the era that is modeled accurately by ΛCDM.

The inflationary paradigm [6–8] offers an elegant mechanism to resolve these puzzles. A phase of quasi-exponential expansion of the universe before the beginning of the radiation-domination era quickly flattens any curvature perturbations that were present at its beginning, driving the spatial curvature of the universe to zero, irrespective of its initial state. In addition, such an inflationary phase effectively enlarges the past causal horizon of any spacetime event after the end of inflation, which makes it possible for regions of the sky that are causally disconnected today to have been in causal contact with each other in the past. This resolves the horizon and flatness problems, provided that the universe expanded by a factor exceeding about e^{60} [5], also known as "60 e-folds". Furthermore, when populated by quantum fields, the inflationary spacetime leads to a physical picture in which the inhomogeneities of the Universe that we observe today in the CMB and in the large-scale structure (LSS) of matter are seeded by the fluctuations of these fields, as was first realized in [9]. As the spacetime expands, the physical wavenumber k_{ph} of the fluctuations is redshifted, and once the wavenumber of a particular field mode drops below the rate of expansion of the spacetime $k_{\mathrm{ph}} < H$ (it "exits the horizon") it stops evolving in time. Therefore, any energy over-density or under-density that is carried by the mode in questions remains frozen until the end of inflation, after which it can re-enter the horizon and become dynamical again. At this point it can pass its energy density on to any matter and radiation that it interacts with, and thus act as a seed for local inhomogeneity. These inhomogeneities eventually evolve into the ones we observe today. For this reason, the modes of the quantum fields that satisfy $k_{\rm ph} < H$ at the end of inflation, which we will call "superhorizon" modes and which define what we will call the "late-time limit", are the ones that are most phenomenologically relevant.

This deep and elegant paradigm has become the leading working theory of early-universe cosmology. The effort of turning this qualitative picture into a quantitative physical theory which yields testable predictions has led to the discovery of many fascinating and challenging problems that arise when trying to formulate quantum field theory in classical, cosmological spacetimes. Trying to better understand one of these puzzles, the issue of infrared divergences arising in massless scalar field theories in de Sitter spacetime, will be the main topic of this thesis. It is our opinion that this problem is of both theoretical and phenomenological interest, as we will motivate below, and that it is thus worthwhile to seek its resolution.

1.1 Single-field, slow-roll inflation

Inflation is a useful, broad framework to think about early-universe cosmology, but the mechanism by which it can be realized is not unique. There are several classes of inflationary models, see [5] for an overview and [10–12] for more detailed and extensive reviews. The simplest inflationary models are known as "single-field, slow roll inflation", in which inflation is driven by a single, real scalar field ϕ, called the inflaton field. This concept was introduced in the early works [8,13,14] and it was developed in several subsequent works by different authors, leading to a variety of realizations of the idea, see [12] for a specialized review of the topic. These manifold realizations have also motivated the construction of a framework to parametrize the details of the various single-field inflationary models by means of a single effective-field-theory (EFT) description of them, which is known as the EFT of inflation [15][1]. These models constitute the main physical picture and motivation that we will have in the back of our mind in the following.

Single-field, slow-roll inflationary models are defined by the action

$$S = S_{\rm EH} + S_\phi \tag{1.1.1}$$

$$= \int \mathrm{d}^4x\, \sqrt{-g}\left[\frac{R}{16\pi G_N} + \frac{1}{2}g^{\mu\nu}\partial_\mu\phi\partial_\nu\phi - V(\phi)\right]. \tag{1.1.2}$$

The key idea is to assume that the inflaton field ϕ has a non-vanishing vacuum expectation value (vev) $\phi_0(t)$, which we can assume to be spatially homogeneous but time-dependent, at the beginning of the inflationary era, and this vev is what drives the quasi-exponential expansion of the universe. This can be seen explicitly by inspecting the energy-momentum tensor $T_{\mu\nu}$ associated to the inflaton, which reads

$$T_{\mu\nu} \equiv \frac{2}{\sqrt{-g}}\frac{\delta S_\phi}{\delta g^{\mu\nu}} = \partial_\mu\phi\partial_\nu\phi - g_{\mu\nu}\left[\frac{1}{2}g^{\alpha\beta}\partial_\alpha\phi\partial_\beta\phi - V(\phi)\right]. \tag{1.1.3}$$

Comparing this result to the energy-momentum tensor of a perfect fluid with density ρ, pressure p and four-velocity u^μ in a homogeneous universe [17],

$$T_{\mu\nu} = (p+\rho)u_\mu u_\nu - p g_{\mu\nu}\,, \tag{1.1.4}$$

we see that, plugging $\phi = \phi_0(t)$ into (1.1.3), and assuming that we are in the comoving frame of the fluid, such that $u^\mu = (1,0,0,0)$, we can identify

$$\rho(t) = \frac{1}{2}\dot\phi_0^2(t) + V(\phi_0(t))\,, \tag{1.1.5}$$

$$p(t) = \frac{1}{2}\dot\phi_0^2(t) - V(\phi_0(t))\,. \tag{1.1.6}$$

[1]It should not to be confused with the EFT for inflation [16].

Provided that the potential energy of the field dominates over the kinetic energy,

$$V(\phi(t)) \gg \dot{\phi}^2(t) \tag{1.1.7}$$

which is the so-called slow-roll condition, we have the relation

$$p(t) \approx -\rho(t)\,, \tag{1.1.8}$$

and, neglecting corrections proportional to $\dot{\phi}_0$, the energy-momentum tensor takes the form

$$T_{\mu\nu} = V(\phi_0(t))g_{\mu\nu}\,. \tag{1.1.9}$$

Thus, under the conditions described above, the scalar field acts like a perfect fluid with negative pressure. This has the same effect as a positive cosmological constant, which causes the spacetime to expand exponentially, up to small corrections proportional to $\dot{\phi}_0$. These corrections can be organized systematically by defining the so-called slow-roll parameters

$$\varepsilon_{\rm sr} \equiv \frac{1}{16\pi G_N}\left(\frac{V'(\phi_0)}{V(\phi_0)}\right)^2\,, \quad \eta_{\rm sr} \equiv \frac{1}{8\pi G_N}\frac{V''(\phi_0)}{V(\phi_0)}\,, \tag{1.1.10}$$

where the prime denotes the derivative of the potential with respect to its field argument, which are both small. Since the kinetic energy of the field is very small with respect to its potential energy, the setup described above can be visualized as the inflaton field ϕ slowly "rolling down" the potential $V(\phi)$.

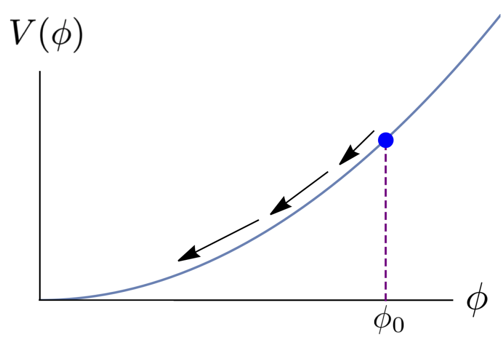

Figure 1.1: The classical inflaton field rolling down an exemplary potential $V(\phi)$, and thereby driving inflation.

So far, all these considerations have been classical. When quantizing the theory, on top of the classical field profile $\phi_0(t)$ of the inflaton field there will be small quantum fluctuations $\delta\phi$. We can therefore decompose the quantized field as

$$\phi(t,\vec{x}) = \phi_0(t) + \delta\phi(t,\vec{x})\,. \tag{1.1.11}$$

By plugging this field decomposition into the action S_ϕ one finds the following quadratic terms for $\delta\phi$:

$$S_\phi^{(\delta\phi)^2} = \frac{1}{2}\int \mathrm{d}^4x\,\sqrt{-g}\Big[g^{\mu\nu}\partial_\mu(\delta\phi)\partial_\nu(\delta\phi) - V''(\phi_0)(\delta\phi)^2\Big]\,. \tag{1.1.12}$$

This coincides with the action for a real scalar field with a very small mass proportional to $V''(\phi_0) \sim \eta_{\rm sr}$, which couples minimally to the background inflationary metric. To first approximation in the slow-roll parameters, which means that we neglect any terms proportional to $\varepsilon_{\rm sr}$ and $\eta_{\rm sr}$, the quantum fluctuation of the inflaton field thus behaves like a massless, minimally coupled, real scalar field propagating in a background de Sitter space. In the present discussion we treated the metric as a classical variable, to keep it simple. However, in more realistic inflationary models quantized metric fluctuations must be included in the description as well, and they are then described by a massless spin-2 field propagating in the inflationary spacetime.

As we discussed above, in the inflationary picture these quantum fluctuations are the ones that seeded the initial conditions for the evolution of the universe into what we observe today, and the details of their dynamics during inflation can therefore be related to the properties of today's universe. This then offers a way to constrain the details of how the inflationary phase was realized, as is nicely reviewed in Lecture 3 of [5]. To be able to do so, it is therefore of great interest to understand the dynamics of very light, and in particular massless, fields evolving in a de Sitter background geometry, since this constitutes the zeroth-order approximation to a more realistic inflationary scenario. Therefore, in this thesis, we will work in a simplified setting and consider a massless, self-interacting scalar field ϕ, which can be thought of as modeling the inflaton fluctuation $\delta\phi$, in rigid de Sitter space, without including metric fluctuations. Once this simplified and idealized setting is under control, deviations from it can then be included systematically.

1.2 Classical geometry of de Sitter space

In this section, we define the de Sitter spacetime, which will be the backdrop for the work that we will carry out in the rest of this thesis, as a Lorentzian manifold, following the presentation in [18] (see also [19]). We introduce the different coordinate charts that we will use in the following chapters, an invariant measure of distance in de Sitter space, and the isometries of the spacetime expressed in a particular coordinate system.

1.2.1 Definition of the manifold and coordinate charts

The de Sitter spacetime is defined as the solution of the Einstein field equations in a vacuum, with a positive cosmological constant Λ:

$$R_{\mu\nu} - \frac{1}{2}Rg_{\mu\nu} + \Lambda g_{\mu\nu} = 0\,. \tag{1.2.1}$$

Geometrically, this spacetime can be characterized in an arbitrary number of dimensions d as a maximally symmetric Lorentzian manifold with positive constant sectional curvature H^2, which is related to Λ by

$$\Lambda = \frac{(d-1)(d-2)}{2H^2}\,. \tag{1.2.2}$$

This means that the components of the Riemann curvature tensor with respect to a given chart are given by

$$R_{\lambda\mu\nu\rho} = H^2(g_{\lambda\nu}g_{\mu\rho} - g_{\lambda\rho}g_{\mu\nu})\,, \tag{1.2.3}$$

by which we immediately find the following results for the Ricci tensor and Riemann scalar:

$$R_{\mu\nu} \equiv R^{\lambda}{}_{\mu\lambda\nu} = (d-1)H^2 g_{\mu\nu}\,, \tag{1.2.4}$$

$$R \equiv g^{\mu\nu}R_{\mu\nu} = d(d-1)H^2\,. \tag{1.2.5}$$

H is called the Hubble parameter, and it can be thought of as the rate of expansion of the spacetime, which will become evident in a moment.

A useful way to visualize the geometry of de Sitter space is offered by the so-called embedding-space formalism: d-dimensional de Sitter space, which we will denote as dS_d, can be represented as a hyperboloid of curvature radius $1/H$ in $(d+1)$-dimensional Minkowski space, by means of the following constraint equation on the embedding-space coordinates X^A, $A=(0,...,d)$:

$$\eta_{AB}X^AX^B = (X^0)^2 - \sum_{i=1}^{d}(X^i)^2 = -\frac{1}{H^2}\,, \tag{1.2.6}$$

where we are denoting the Minkowski metric of the embedding space by $\eta_{AB} = \mathrm{diag}(1,-1,...,-1)$. This representation makes the isometry group of dS_d manifest, since it is given by the transformations that leave the equation (1.2.6) invariant. They are simply given by the isometries of $(d+1)$-dimensional Minkowski space which leave the origin of the coordinate system invariant, which is the Lorentz group $\mathrm{SO}(1,d)$. This group has dimension $(d+1)d/2$, which is the same as the dimension of the Poincaré group in d dimensions, which reflects the fact that dS_d is maximally symmetric. We will discuss this isometry group further below in section 1.2.3.

The induced metric on the manifold defined by the constraint equation (1.2.6) defines the de Sitter metric. Given a particular coordinate chart that parametrizes the surface of the hyperboloid, or a part of it, by expressing the embedding-space coordinates X^A in terms of the coordinates of the chart x^μ as $X^A(x)$, the induced line element $\mathrm{d}s^2$ can be computed using the equation [18]

$$\mathrm{d}s^2 = \eta_{AB}\mathrm{d}X^A(x)\mathrm{d}X^B(x)\,. \tag{1.2.7}$$

There are several different coordinate charts which cover different portions of the de Sitter manifold, corresponding to different foliations of it, and we briefly summarize the properties of the ones that will be relevant for us in the following chapters.

1) **Global coordinates.** This chart covers the entirety of the de Sitter manifold, which gives rise to its name. It is defined by the coordinates $(t,\vec{\omega})$, which are related to the embedding-space coordinates by

$$X^0 = \frac{1}{H}\sinh(Ht)\,, \tag{1.2.8}$$

$$X^i = \frac{\omega^i}{H}\cosh(Ht)\,, \quad 1 \le i \le d \tag{1.2.9}$$

where $t \in (-\infty,\infty)$ and the ω^i's parametrize the unit $(d-1)$-sphere S^{d-1}:

$$\sum_{i=1}^{d}(\omega^i)^2 = 1\,. \tag{1.2.10}$$

Therefore, in this coordinate system, the spatial slices at a given time t are given in terms of $(d-1)$-spheres, so this parametrization of de Sitter space is also known as "closed slicing". Using (1.2.7) we find that the line element in these coordinates reads

$$\mathrm{d}s^2 = \mathrm{d}t^2 - \frac{1}{H^2}\cosh^2(Ht)\mathrm{d}\Omega^2_{d-1}\,, \tag{1.2.11}$$

with $\mathrm{d}\Omega^2_{d-1}$ the line element on S^{d-1}. From this form of the line element it becomes apparent that the spatial slices start with infinite radius at $t=-\infty$, then shrink to their smallest radius at $t=0$, which is $1/H$, and then expand to infinite radius again as $t\to\infty$. While this does not resemble the inflationary spacetime that we have in mind, and that we would like to approximate by working in de Sitter space, these coordinates are still useful to define the Euclidean version of de Sitter space, and we will need them in chapter 2.

2) **Planar coordinates.** This chart covers only half of the de Sitter manifold, the so-called Poincaré, or expanding, patch, which is the one that is appropriate to approximate the inflationary spacetime. They are defined by the coordinates $(t,\vec{x})$, which are related to the embedding-space coordinates by

$$X^0 = \frac{1}{H}\sinh(Ht) + \frac{He^{Ht}}{2}|\vec{x}|^2\,, \tag{1.2.12}$$

$$X^1 = \frac{1}{H}\cosh(Ht) - \frac{He^{Ht}}{2}|\vec{x}|^2\,, \tag{1.2.13}$$

$$X^i = e^{Ht}x^i\,, \quad 2 \le i \le d\,, \tag{1.2.14}$$

with $t \in (-\infty, \infty)$ and $\vec{x} \in \mathbb{R}^{d-1}$. In this coordinate system, the spatial slices at a given time t are given by flat, $(d-1)$-dimensional Euclidean slices, so this parametrization of de Sitter space is also known as "flat slicing". Using (1.2.7) we find that these coordinates induce the metric

$$\mathrm{d}s^2 = \mathrm{d}t^2 - e^{2Ht}\mathrm{d}\vec{x}^2\,, \tag{1.2.15}$$

from which we see that the spatial slices start out with zero volume at $t = -\infty$, and then start expanding exponentially as time elapses, with expansion rate H, and their volume tends to infinity as $t \to \infty$. The expansion is characterized by the scale factor $a(t)$, which is defined as

$$a(t) \equiv e^{Ht}\,. \tag{1.2.16}$$

This reflects the inflationary picture we have in mind, and, therefore, these are the coordinates in which we will work for the bulk of the thesis, in chapters 3 and 4. In this parametrization it also becomes evident that de Sitter space is a special case of the homogeneous and isotropic Friedmann-Lemaître-Robertson-Walker (FLRW) universe [17], which is defined by the metric

$$\mathrm{d}s^2 = \mathrm{d}t^2 - a(t)^2\left[\frac{\mathrm{d}r^2}{1-Kr^2} + r^2\mathrm{d}\Omega^2_{d-2}\right]. \tag{1.2.17}$$

Comparing this form to (1.2.15) in spatial spherical coordinates we see that de Sitter space is a spatially flat ($K = 0$) and exponentially expanding FLRW universe.

3) **Conformal coordinates.** They are closely related to the planar coordinates, and they can be obtained from them by defining the conformal time variable η via

$$\mathrm{d}t = a(\eta)\mathrm{d}\eta\,. \tag{1.2.18}$$

This differential equation is solved by

$$\eta = -\frac{1}{a(\eta)H}\,, \quad \eta \in (-\infty, 0)\,. \tag{1.2.19}$$

Using the conformal time variable in (1.2.15), the line element takes the form

$$\mathrm{d}s^2 = a(\eta)^2\left[\mathrm{d}\eta^2 - \mathrm{d}\vec{x}^2\right], \tag{1.2.20}$$

which is equivalent to the flat-space line element, up to a conformal factor $a(\eta)^2$. This shows that de Sitter space is a so-called conformally flat spacetime.

4) **Static coordinates.** While we will not use this coordinate system for explicit computations in the following, it is useful to briefly discuss it to develop our physical intuition about de Sitter space, since these are the coordinates that a static observer in this spacetime would use. They are defined by the coordinates $(t, r, \vec{\omega})$, which are related to the embedding coordinates by

$$X^0 = \sqrt{\frac{1}{H^2} - r^2}\,\sinh(Ht)\,, \tag{1.2.21}$$

$$X^1 = \sqrt{\frac{1}{H^2} - r^2}\,\cosh(Ht)\,, \tag{1.2.22}$$

$$X^i = r\omega^i\,, \quad 2 \le i \le d\,, \tag{1.2.23}$$

with $t \in (-\infty, \infty)$, $r \in [0, 1/H)$ and the ω^i now parametrize the unit sphere S^{d-2}. The line element reads

$$\mathrm{d}s^2 = (1 - H^2r^2)\mathrm{d}t^2 - \frac{\mathrm{d}r^2}{1 - H^2r^2} - r^2\mathrm{d}\Omega^2_{d-2} \tag{1.2.24}$$

and we see that the induced metric is time-independent, which gives rise to the name of this set of coordinates, and it is singular at $r = 1/H$. This singularity signals the presence of the cosmological horizon of de Sitter space, which is generated by the exponential expansion of the spacetime, and its presence is manifest in this particular choice of coordinates, but not in the other three coordinate charts we discussed previously. Light rays emitted from beyond this radial distance will not reach an observer at the origin of the coordinate system. In these coordinates, the vector ∂_t is a time-like Killing vector field,

$$||\partial_t||^2 \equiv g_{tt} = 1 - H^2 r^2 > 0\,, \quad \text{for } 0 \leq r < \frac{1}{H}\,, \tag{1.2.25}$$

and it becomes a null vector at the cosmological horizon, so the time coordinate has a fixed point there.

This set of coordinates is closely analogous to the coordinates which yield the Schwarzschild metric for a spinless, uncharged black hole [17]. As in that case, one can define Kruskal coordinates to remove the coordinate singularity present in (1.2.24), thereby extending the static coordinates to cover all of de Sitter space. We will not further discuss them here and refer to [18] for their exposition.

1.2.2 The de Sitter-invariant distance function Z

We have now introduced several coordinate systems to parametrize different portions of the de Sitter manifold, but we will also need to characterize the distance of any two points, x and y, in any of the above parametrizations, in a coordinate-invariant way. The appropriate tool to do so is the de Sitter-invariant distance function Z, which is defined in the embedding space as [18]

$$-\frac{1}{H^2} Z(X, Y) = \eta_{AB} X^A Y^B\,, \tag{1.2.26}$$

and it measures the chord distance between two points on the de Sitter hyperboloid. This definition is manifestly invariant under the action of the isometry group $\mathrm{SO}(1, d)$. Via the above equation, we can determine the form of Z in any particular chart of dS_d by simply plugging in the embedding-space coordinates X^A expressed in terms of the chart x^μ. For instance, for the different coordinates we defined above we find

$$Z(x, y) = -\sinh(Ht_x)\sinh(Ht_y) + \cosh(Ht_x)\cosh(Ht_y)(\vec{\omega}_x \cdot \vec{\omega}_y) \quad \text{(global)}\,, \tag{1.2.27}$$

$$Z(x, y) = \cosh(H(t_x - t_y)) - \frac{H^2 e^{H(t_x + t_y)}}{2} |\vec{x} - \vec{y}|^2 \quad \text{(planar)}\,, \tag{1.2.28}$$

$$Z(x, y) = 1 + \frac{(\eta_x - \eta_y)^2 - |\vec{x} - \vec{y}|^2}{2\eta_x \eta_y} \quad \text{(conformal)}\,, \tag{1.2.29}$$

$$Z(x, y) = \cosh(H(t_x - t_y))\sqrt{1 - H^2(r_x^2 + r_y^2) + H^4 r_x^2 r_y^2} + H^2 r_x r_y (\vec{\omega}_x \cdot \vec{\omega}_y) \quad \text{(static)}\,. \tag{1.2.30}$$

We will use some of these results below in chapter 2.

1.2.3 Isometries of de Sitter space

Let us now discuss more in depth the isometry group of de Sitter space $\mathrm{SO}(1, d)$, which we introduced above, and derive the explicit form of their generators in conformal coordinates. While the elements of this symmetry group act linearly on the embedding-space coordinates X^A, which is one of the advantages of that formalism, it will act non-linearly on quantities expressed in terms of a particular coordinate chart of de Sitter manifold.

The line element we found above in these coordinates, using the scale factor $a(\eta) = (-H\eta)^{-1}$, reads

$$\mathrm{d}s^2 = \frac{1}{(-H\eta)^2}\left[\mathrm{d}\eta^2 - \mathrm{d}\vec{x}^2\right]\,, \tag{1.2.31}$$

and we can directly read off the form of the metric in conformal coordinates from it:

$$g_{\mu\nu} = \frac{1}{(-H\eta)^2}\eta_{\mu\nu}\,. \tag{1.2.32}$$

The line element (1.2.31) is manifestly invariant under spatial translations and rotations, which account for

$$d-1+\frac{(d-1)(d-2)}{2} = \frac{d(d-1)}{2} \tag{1.2.33}$$

of the $(d+1)d/2$ isometries. The remaining isometries are less obvious, and they can be found by means of Killing's equation: we parametrize the Killing vectors V as

$$V = V^\mu \partial_\mu\,, \tag{1.2.34}$$

where

$$\partial_0 = \frac{\partial}{\partial\eta}\,, \quad \partial_i = \frac{\partial}{\partial x^i}\,, \tag{1.2.35}$$

and the components $V_\mu = g_{\mu\nu}V^\nu$ then satisfy Killing's equation [17]

$$\nabla_\mu V_\nu + \nabla_\nu V_\mu = 0\,. \tag{1.2.36}$$

We now write out

$$\nabla_\mu V_\nu = \partial_\mu V_\nu - \Gamma^\lambda_{\mu\nu}V_\lambda\,, \tag{1.2.37}$$

with the Christoffel symbols

$$\Gamma^\lambda_{\mu\nu} = \frac{1}{2}g^{\lambda\alpha}\Big[\partial_\mu g_{\alpha\nu} + \partial_\nu g_{\alpha\mu} - \partial_\alpha g_{\mu\nu}\Big]\,, \tag{1.2.38}$$

and in the present coordinates they read

$$\Gamma^\lambda_{\mu\nu} = -\frac{1}{\eta}\Big[\delta^\lambda_0\delta^\mu_\nu + \delta^\lambda_i(\delta^0_\mu\delta^i_\nu + \delta^0_\nu\delta^i_\mu)\Big]\,, \tag{1.2.39}$$

so Killing's equation becomes

$$\partial_\mu V_\nu + \partial_\nu V_\mu + \frac{2}{\eta}\Big[\delta^\mu_\nu V_0 + (\delta^0_\mu\delta^i_\nu + \delta^0_\nu\delta^i_\mu)V_i\Big] = 0\,. \tag{1.2.40}$$

It can be immediately checked that the vectors

$$P_i = \partial_i\,, \tag{1.2.41}$$
$$R^i{}_j = x^i\partial_j - x_j\partial^i \tag{1.2.42}$$

satisfy (1.2.40), which are the generators of spatial translations and rotations, and further that

$$D = -\eta\partial_\eta - x^i\partial_i\,, \tag{1.2.43}$$
$$K^i = 2x^i\eta\partial_\eta + 2x^ix^j\partial_j + (\eta^2 - \vec{x}^2)\partial^i\,, \tag{1.2.44}$$

where summation over repeated indices is implied, also satisfy (1.2.40). The vector D generates dilations, while the vectors K^i generate special conformal transformations, and they can be written more compactly as

$$D = -x^\mu\partial_\mu\,, \tag{1.2.45}$$
$$K^i = 2x^ix^\mu\partial_\mu - x^2\partial^i\,. \tag{1.2.46}$$

Together, the $(d+1)d/2$ generators P_i, $R^i{}_j$, D and K^i generate the group $\mathrm{SO}(1,d)$.

Any quantity that is de Sitter-invariant must be left invariant by the action of any of the Killing vectors of $\mathrm{SO}(1,d)$, which we derived in the case of conformal coordinates in this section. This is equivalent to requiring that the quantity in question should be invariant under the action of an infinitesimal group element. In the special case of correlation functions of quantum fields computed in de Sitter space, this requirement can be used to constrain their form. This constraint becomes especially powerful when considering correlators evaluated at the future boundary of de Sitter space, which corresponds to $\eta \to 0$ in the present set of coordinates, which is due to the fact that the de Sitter-group is isomorphic to the conformal group in $d-1$ dimensions [20, 21]. At the $\eta = 0$-boundary the action of the generators on de Sitter-invariant correlation functions becomes equivalent to the action of the generators of the conformal group in $d-1$ Euclidean dimensions on the correlation functions of a Euclidean $(d-1)$-dimensional conformal field theory (CFT), as was first noticed for the case of graviton correlation functions in [22] and for the scalar case in [23]. When combined with the requirements imposed by analyticity and unitarity, the constraints on correlation functions can be strong enough to fix their form completely. This was exploited in the pioneering work [24] and then fully developed into the program known as the Cosmological Bootstrap in the series of papers [25–28], see [29] for a review of the topic. Since the late-time limit $\eta \to 0$ of correlation functions is also the one that is most relevant for making contact with cosmological observables that are measured today, this research program constitutes a very promising and rapidly developing field.

1.3 Real scalar field in de Sitter space, quantization, choice of the vacuum

After introducing and discussing the background geometry in which we will work, we now discuss the free, real scalar field in de Sitter space. This topic is by now standard, and its discussion can be found in textbooks on quantum field theory in curved spacetime, see [30–32], and we will briefly review the points that are most important for us. The action of a free, real scalar field with mass m in a generic d-dimensional curved spacetime is defined as

$$S = \frac{1}{2}\int \mathrm{d}^d x \, \sqrt{-g}\Big[g^{\mu\nu}\partial_\mu\phi(x)\partial_\nu\phi(x) - \Big(m^2 + \xi R\Big)\phi^2(x)\Big] \,. \tag{1.3.1}$$

Here, ξ is the parameter that controls the non-minimal coupling of the field ϕ to the background metric via the Riemann scalar R. Specializing to de Sitter space, which has a constant value of R, see (1.2.5), the effect of a non-minimal coupling to the metric can be fully absorbed into the mass parameter[2] m. Therefore, we set $\xi = 0$ and consider a minimally coupled scalar field from now on.

The equation of motion is obtained from S by requiring it to be extremal under variations of ϕ:

$$\frac{\delta S}{\delta\phi(x)} = 0 \,, \tag{1.3.2}$$

and it reads

$$\left[\frac{1}{\sqrt{-g}}\partial_\mu g^{\mu\nu}\sqrt{-g}\partial_\nu + m^2\right]\phi(x) = 0 \,, \tag{1.3.3}$$

where one can define

$$\Box_x \equiv \frac{1}{\sqrt{-g(x)}}\partial^x_\mu g^{\mu\nu}(x)\sqrt{-g(x)}\partial^x_\nu \tag{1.3.4}$$

as the curved-spacetime generalization of the d'Alembert operator. The equation of motion (1.3.3) holds for any form of the metric $g_{\mu\nu}$, but to solve it an explicit parametrization has to be plugged in. In the planar coordinates introduced in section 1.2.1, the above equation reads

$$\left[\frac{\partial^2}{\partial t^2} + H(d-1)\frac{\partial}{\partial t} - \frac{\vec{\partial}^2}{a(t)^2} + m^2\right]\phi(t,\vec{x}) = 0 \,. \tag{1.3.5}$$

[2] This is no longer true when including metric perturbations, which, however, we will not consider in this thesis.

To solve it, it is useful to switch to conformal coordinates, using the conformal time variable η instead of t, and to perform a spatial Fourier-transform of the field,

$$\phi(\eta, \vec{x}) = \int \frac{\mathrm{d}^{d-1}k}{(2\pi)^{d-1}} e^{i\vec{k}\cdot\vec{x}} \phi_{\vec{k}}(\eta)\,, \tag{1.3.6}$$

which yields

$$\left[(-H\eta)^2 \frac{\partial^2}{\partial\eta^2} + H(d-2)(-H\eta)\frac{\partial}{\partial\eta} + (-H\eta)^2\vec{k}^2 + m^2\right]\phi_{\vec{k}}(\eta) = 0\,. \tag{1.3.7}$$

This equation can be solved in terms of a superposition of Bessel functions of the first and second kind,

$$\phi_{\vec{k}}(\eta) = (-H\eta)^{\frac{d-1}{2}}\left[A_{\vec{k}} J_\nu(-k\eta) + B_{\vec{k}} Y_\nu(-k\eta)\right] \tag{1.3.8}$$

where we have introduced the mass parameter

$$\nu \equiv \sqrt{\left(\frac{d-1}{2}\right)^2 - \frac{m^2}{H^2}}\,, \tag{1.3.9}$$

and the coefficients $A_{\vec{k}}$ and $B_{\vec{k}}$ are not yet uniquely defined. The combination

$$-k\eta = \frac{k}{a(\eta)H} \tag{1.3.10}$$

which appears as the argument of the Bessel functions in (1.3.8) defines the modulus of the physical three-momentum variable $\vec{k}_{\mathrm{ph}} \equiv \vec{k}/a(\eta)$, which we mentioned above, in Hubble units.

So far the discussion has been classical. To quantize the scalar field, we proceed in the standard way, following the conventions of [30], and write the following Fourier-decomposition of the field operator:

$$\phi(\eta, \vec{x}) = \int \frac{\mathrm{d}^{d-1}k}{(2\pi)^{d-1}}\left[e^{i\vec{k}\cdot\vec{x}}\phi_{\vec{k}}(\eta) a_{\vec{k}} + e^{-i\vec{k}\cdot\vec{x}}\phi^*_{\vec{k}}(\eta) a^\dagger_{\vec{k}}\right]. \tag{1.3.11}$$

The operators $a_{\vec{k}}$ and $a^\dagger_{\vec{k}}$ are the standard annihilation and creation operators, respectively, and the mode function $\phi_{\vec{k}}(\eta)$, and its complex conjugate, appearing in (1.3.11) are assumed to solve the equation of motion (1.3.7). Assuming the canonical commutation relations

$$[a_{\vec{p}}, a_{\vec{k}}] = [a^\dagger_{\vec{p}}, a^\dagger_{\vec{k}}] = 0\,, \tag{1.3.12}$$

$$[a_{\vec{p}}, a^\dagger_{\vec{k}}] = (2\pi)^{d-1}\delta^{(d-1)}(\vec{p} - \vec{k})\,, \tag{1.3.13}$$

for the creation and annihilation operators implies that the mode functions $\phi_{\vec{k}}(\eta)$ should be normalized according to the Klein-Gordon inner product

$$i\left[\phi^*_{\vec{k}}(\eta)\partial_\eta\phi_{\vec{k}}(\eta) - \phi_{\vec{k}}(\eta)\partial_\eta\phi^*_{\vec{k}}(\eta)\right] = 1\,. \tag{1.3.14}$$

This condition fixes one of the undetermined constants appearing in (1.3.8), but the other one is left undetermined. In flat spacetime the second constraint equation to determine the analogous second unknown coefficient in the general solution for the mode functions comes from the requirement that the vacuum state, which is defined as the lowest-energy Eigenstate of the Hamiltonian of the quantized theory, is annihilated by $a_{\vec{k}}$ for any value of $\vec{k}$, see the discussion in [31]. However, in general curved spacetimes, there is no globally defined lowest-energy Eigenstate of the Hamiltonian, because there is no globally well-defined notion of energy as a conserved quantity. This leads to the well-known ambiguity of the notion of a vacuum state in quantum field theory in curved spacetime, and it must simply be chosen.

However, when working in de Sitter space in planar coordinates, there is a natural choice for it, which is known as the Bunch-Davies vacuum [33]. It corresponds to choosing $A_{\vec{k}}$ and $B_{\vec{k}}$ in (1.3.8) such that[3]

$$\phi_{\vec{k}}(\eta) = \sqrt{\frac{\pi}{4H}}(-H\eta)^{\frac{d-1}{2}} H^{(1)}_{\nu}(-k\eta)\,, \tag{1.3.15}$$

where

$$H^{(1)}_{\nu}(z) = J_{\nu}(z) + iY_{\nu}(z) \tag{1.3.16}$$

denotes the Hankel function of the first kind. This is the choice of vacuum state which we will assume for the remainder of the thesis. With this choice, the mode functions expressed in terms of the conformal time variable η have the property that they reduce to massless flat-space mode functions, up to an overall power of the scale factor, in the infinite past:

$$\lim_{\eta\to-\infty}\phi_{\vec{k}}(\eta) = (-H\eta)^{\frac{d-2}{2}}\frac{e^{-ik\eta}}{\sqrt{2k}}\,. \tag{1.3.17}$$

The reason why this choice is natural is the following: in planar coordinates any effects of the expansion of the spacetime in the infinite past are exponentially suppressed. In this case it is reasonable to assume the choice of the so-called adiabatic vacuum, which coincides with the Bunch-Davies vacuum in this case [30]. Physically, (1.3.17) reflects the intuition that the mode functions selected by this choice of the vacuum should reduce to flat-space ones at very early times, again up an overall power of the scale factor, because the fact that the spacetime is dynamical is negligible at that point in time. Since in this limit the magnitude of the physical momentum $k/a(\eta)$ of the mode function in question tends to infinity as well, so the mass of the field can be neglected compared to it, which is why we recover the functional form of a massless flat-space mode function.

Taking the opposite limit instead, $\eta \to 0$, the mode function we found behaves as

$$\lim_{\eta\to 0}\phi_{\vec{k}}(\eta) = (-\eta)^{\Delta_+}\varphi_+(\vec{k}) + (-\eta)^{\Delta_-}\varphi_-(\vec{k})\,, \tag{1.3.18}$$

where we are using a similar notation to [25], and we have defined

$$\Delta_{\pm} = \frac{d-1}{2} \mp \sqrt{\left(\frac{d-1}{2}\right)^2 - \frac{m^2}{H^2}}\,. \tag{1.3.19}$$

This behaviour is, in fact, not peculiar to scalar fields, but is exhibited by fields of generic spin s, which show the same late-time behaviour with a different form of $\Delta_{\pm}$, which then also depends on s [25]. This observation forms the basis for the formalism of the Cosmological Bootstrap, and the $\Delta_{\pm}$ can be interpreted as the conformal dimensions of two primary operators belonging to the boundary CFT, which emerge in the late-time limit from the full field ϕ. However, for us, the most relevant point about this observation is that from (1.3.19) it is evident that Δ_+ is positive and close to zero for small values of m^2/H^2, and it becomes exactly zero for massless scalar fields. This is another important reason why very light, and in particular massless, fields are relevant for the phenomenology of inflation: they are the ones that experience the smallest amount of suppression by the (quasi-)exponential expansion of the spacetime, and, therefore, they give the largest contributions to observables evaluated at late times.

1.4 In-in correlation functions and the Schwinger-Keldysh formalism

Having now defined the quantum-field theoretic framework that we are going to work in we are in the position to define the observables that we will be interested in computing, as well as the necessary formalism to compute them.

[3] We are using a non-standard convention for the constant phase of the mode function, but this will not affect any of the computations we will carry out.

In cosmology, and in particular inflationary cosmology, we are in a different situation with respect to particle physics scattering experiments. In the latter case, the physical picture is that an experimentalist is preparing a non-interacting multi-particle state in the infinite past, called the in-state, and then, as the in-state is let evolve in time, interactions are adiabatically turned on and then off again, and the outcome of the time evolution of the state is measured by projecting the time-evolved in-state onto a different, non-interacting multi-particle state in the infinite future, called the out-state. The set of all such inner products is given by the S-matrix of the theory in question. The crucial point in order to be able to define the S-matrix is the knowledge of the vacuum states in the infinite past and infinite future of the interacting theory, which in flat-space QFT are simply related by a complex phase [34, 35]. This is not the case if one wishes to describe the dynamics of quantum fields in a background spacetime which is evolving in time, and is not merely transitioning from a static configuration in the infinite past to a different static configuration in the infinite future, such as de Sitter space. Due to the evolution of the spacetime, this setting is akin to a physical state that is out of equilibrium, which makes the deterministic prediction of the time evolution of said state impossible. However, as we discussed above, since de Sitter space is exponentially expanding, at very early times its expansion was very slow, such that one can expect the dynamics of quantum fields in the de Sitter background at early times to be close to the flat-space scenario, which selects a particular vacuum state as the preferred one. This was precisely the motivation for choosing the Bunch-Davies vacuum. Once the in-vacuum state $|\Omega\rangle$ of the theory is defined, instead of computing time-ordered in-out correlation functions, one can instead consider the expectation value of a product of fields evaluated at a fixed correlation time t:

$$\langle \Omega | \phi(t, \vec{x}_1) ... \phi(t, \vec{x}_n) | \Omega \rangle \,. \tag{1.4.1}$$

From now on, we will abbreviate $\langle \Omega | ... | \Omega \rangle = \langle ... \rangle$. As argued by [36, 37], these "equal-time, in-in correlation functions" are the appropriate observables to consider in cosmology.

The formalism to compute these objects was first introduced in [38,39], and is therefore called "Schwinger-Keldysh", or sometimes "in-in", formalism. It was outlined again in [37], and we will follow the presentation in this reference for the precise definition of the quantities we wish to compute. In the interaction picture, the expectation value of an operator $Q(t)$ in the interacting theory with Hamiltonian

$$H(t) = H_0(t) + H_I(t) \tag{1.4.2}$$

is defined as follows:

$$\langle Q(t) \rangle = \left\langle \overline{T} \left\{ \exp\left[i \int_{-\infty}^{t} \mathrm{d}t' \; H_I(t') \right] \right\} Q_I(t) T \left\{ \exp\left[-i \int_{-\infty}^{t} \mathrm{d}t' \; H_I(t') \right] \right\} \right\rangle . \tag{1.4.3}$$

For us, the operator $Q(t)$ will be

$$Q(t) = \phi(t, \vec{x}_1) ... \phi(t, \vec{x}_n) \,, \tag{1.4.4}$$

and we have suppressed the position arguments, which will play no role in the following definitions. In the above equation, $\overline{T}$ and T denote the (anti-)time-ordering operator, respectively, and the subscript I is used to denote the interaction-picture version of an operator. The physical picture associated to this equation is the following: the ket-vacuum state $|\Omega\rangle$, which is defined at $t = -\infty$, is evolved forward in time by means of the standard interaction-picture time-evolution operator

$$U(t, -\infty) \equiv T \left\{ \exp\left[-i \int_{-\infty}^{t} \mathrm{d}t' \; H_I(t') \right] \right\} \tag{1.4.5}$$

until the correlation time t, and the same is done for the bra-state $\langle \Omega |$, on which the complex-conjugate time-evolution operator $U^\dagger(t, -\infty)$ acts, which replaces $T \to \overline{T}$ and $i \to -i$ in the exponential. The resulting time-evolved vacuum states are then used to compute the expectation value of the operator at correlation time t. From (1.4.3), [37] derives the following nested-commutator formula to compute this quantity:

$$\langle Q(t) \rangle = \sum_{n=0}^{\infty} i^n \int_{-\infty}^{t} \mathrm{d}t_n \int_{-\infty}^{t_n} \mathrm{d}t_{n-1} ... \int_{-\infty}^{t_2} \mathrm{d}t_1 \left\langle \Big[H_I(t_1), \Big[H_I(t_2), ..., \Big[H_I(t_n), Q_I(t) \Big] \Big] \Big] \right\rangle , \tag{1.4.6}$$

and, in fact, this formula holds already as an operator statement, without the need to sandwich both sides of the equation between vacuum states. Working with quantized field operators, one can use the above formula to compute in-in correlation functions, analogously to the framework of second quantization in flat-space QFT.

The above formula is very useful to prove operator identities, but to carry out practical computations it becomes quite cumbersome quite fast. For this purpose a path-integral formalism for computing in-in correlators is preferable, since it allows one to define diagrammatic rules and to formulate the perturbation-theory expansion of the correlators as an expansion in Feynman(-like) diagrams. Such a formalism exists, and the path integral to compute these quantities is referred to in the literature as "closed-time-path" (CTP) or Schwinger-Keldysh path integral. As reviewed in [40], this formalism is widely used in the contexts of non-equilibrium field theory and thermal field theory, since it is able to incorporate dissipative effects, as well as non-Gaussian initial states for the fields. It was discussed in the context of QFT in generic curved spacetimes in [41], and more recently in the Appendix of [37] as well. A more modern review, which specializes to the application to cosmology, is given in [42]. We will draw from all of these reference to establish the formalism and conventions we will use in the following. The Lagrangian in-in path integrals reads

$$\langle\phi(t,\vec{x}_1)...\phi(t,\vec{x}_n)\rangle = \int\mathcal{D}[\phi_+,\phi_-]\exp\left[i\int_{-\infty}^{t}\mathrm{d}t'\mathrm{d}^{d-1}x\,\sqrt{-g}\mathcal{L}[\phi_+(t',\vec{x})] - i\int_{-\infty}^{t}\mathrm{d}t'\mathrm{d}^{d-1}x\,\sqrt{-g}\mathcal{L}[\phi_-(t',\vec{x})]\right]$$
$$\times\,\phi_+(t,\vec{x}_1)...\phi_+(t,\vec{x}_n)\langle\phi_+(-\infty)|\Omega\rangle\langle\Omega|\phi_-(-\infty)\rangle\prod_{\vec{x}}\delta\Big(\phi_+(t,\vec{x})-\phi_-(t,\vec{x})\Big)\,. \tag{1.4.7}$$

Let us go through the elements appearing in this equation one by one.

The appearance of both the time-ordering and anti-time-ordering operators in the definition of the in-in correlation function (1.4.3) have as a consequence the necessity to introduce two different branches in the path integral, one which represents the standard time evolution forward in time from $-\infty$ to t, corresponding to the action of $U(t,-\infty)$, and the second branch corresponding to the action of $U^\dagger(t,-\infty)$, which can be interpreted as backwards time evolution from t back to $-\infty$. The definition of these two branches necessitates the doubling of the field variables $\phi\to\phi_\pm$, where the ϕ_+-field is associated to the regular forward time evolution, while the ϕ_--field is associated to the backward time evolution. The two sets of variables should agree at the correlation time t, which is enforced by the functional delta distribution, and the path integral is then summing over all possible field configurations of $\phi_\pm$. Since the $\phi_\pm$ are equivalent at time t, we can pick either of these variables to express the configuration of field Eigenvalues appearing in the integrand of the path integral, and above we used only plus fields. From this picture it is clear why the time integrals appearing in the exponentials of (1.4.7) have as an upper boundary the time at which the operators that appear in the expectation value are evaluated. One might wonder what would happen if one were to insist on extending the time integration to run up to $+\infty$, which would be more in line with the usual in-out path integral. The answer is that the contributions from the forward and backward branch after the time t would cancel out exactly, and would therefore introduce an unnecessary redundancy in the formula [40]. To avoid this, we only integrate up to the correlation time t. The final component which appears in (1.4.7) is $\langle\phi_+(-\infty)|\Omega\rangle\langle\Omega|\phi_-(-\infty)\rangle$, which is the modulus squared of the wavefunction of the vacuum [37]. It has the role of specifying the initial conditions at $t=-\infty$ of the field configurations over which the path integral is summing, and, as shown in [37], in the case where the theory should reduce to a free theory in the infinite past, this initial condition is implemented by this factor by means of a very similar $i\varepsilon$-prescription to the standard QFT-case: the lower boundaries of the time integrals appearing in the exponential in (1.4.7) associated to $\phi_\pm$ are deformed to $-\infty(1\mp i\varepsilon)$, respectively. This is the way that the $i\varepsilon$-prescription appears in the Schwinger-Keldysh path integral, and it has the practical effect of damping the contributions from the integrals over the mode functions at very early times, thus rendering the time integrals involved in the computations of diagrams convergent. It is crucial to take this into account while doing practical computations in this formalism. While the $i\varepsilon$-prescription appears naturally in the path-integral formulation of the in-in formalism, it was absent in the original derivation of the operator formula (1.4.6), even though the two formalism should be equivalent. This discrepancy has been resolved in the more recent works [43, 44], which showed how to incorporate its effect.

From the path-integral representation of the in-in correlator (1.4.7) one can then derive a set of Feynman rules to compute the correlation function in question perturbatively. Due to the doubling of the field variables over which we are integrating, and the two different time-evolution branches appearing in the formula, the diagrammatic rules to compute these quantities are more complicated than their in-out counterparts. Since we will need to connect fields which are associated to both time branches in (1.4.7) to each other, in all possible combinations, we will need four types of propagators, which are the following:

$$
\begin{aligned}
G_{++}(t_x,\vec{x};t_y,\vec{y}) &\equiv \langle T\{\phi(t_x,\vec{x})\phi(t_y,\vec{y})\}\rangle\,, &(1.4.8)\\
G_{+-}(t_x,\vec{x};t_y,\vec{y}) &\equiv \langle \phi(t_y,\vec{y})\phi(t_x,\vec{x})\rangle\,, &(1.4.9)\\
G_{-+}(t_x,\vec{x};t_y,\vec{y}) &\equiv \langle \phi(t_x,\vec{x})\phi(t_y,\vec{y})\rangle\,, &(1.4.10)\\
G_{--}(t_x,\vec{x};t_y,\vec{y}) &\equiv \langle \overline{T}\{\phi(t_x,\vec{x})\phi(t_y,\vec{y})\}\rangle\,, &(1.4.11)
\end{aligned}
$$

and the (anti-)time-ordered two-point functions are defined as:

$$
\begin{aligned}
G_{++}(t_x,\vec{x};t_y,\vec{y}) &= \theta(t_x-t_y)\langle \phi(t_x,\vec{x})\phi(t_y,\vec{y})\rangle + \theta(t_y-t_x)\langle \phi(t_y,\vec{y})\phi(t_x,\vec{x})\rangle\,, &(1.4.12)\\
G_{--}(t_x,\vec{x};t_y,\vec{y}) &= \theta(t_x-t_y)\langle \phi(t_y,\vec{y})\phi(t_x,\vec{x})\rangle + \theta(t_y-t_x)\langle \phi(t_x,\vec{x})\phi(t_y,\vec{y})\rangle\,. &(1.4.13)
\end{aligned}
$$

The Feynman rules derived from the Schwinger-Keldysh path integral can be found in the Appendix of [37], as well as in [42], and the procedure works as follows:

- Double each interaction term present in the classical action appearing in the exponent of the path integral, where the interactions which are associated to the forward contour come with a factor $-i$ (which is the standard situation), while the interactions associated to the backward contour come with a factor $+i$. Somewhat confusingly, the first type of vertex is referred to as a $(+)$-vertex in the literature, while the second type is referred to as a $(-)$-vertex. The Feynman rule associated to each type of interaction can be determined as usual. When considering a diagram with n vertices, one must sum over all 2^n diagrams resulting from choosing each vertex to be a $(+)$-vertex or a $(-)$-vertex.

- A line in a diagram which connects two $(+)$-vertices, or a $(+)$-vertex to an external point, at the spacetime points $(t_x,\vec{x})$ and $(t_y,\vec{y})$ is associated to $G_{++}(t_x,\vec{x};t_y,\vec{y})$, which is just the usual Feynman propagator.

- Similarly, a line in a diagram which connects two $(-)$-vertices, or a $(-)$-vertex to an external point, at the spacetime points $(t_x,\vec{x})$ and $(t_y,\vec{y})$ is associated to $G_{--}(t_x,\vec{x};t_y,\vec{y})$.

- A line in a diagram which connects a $(+)$-vertex at the spacetime point $(t_x,\vec{x})$ to a $(-)$-vertex at the spacetime point $(t_y,\vec{y})$ is associated to the unordered propagator $G_{+-}(t_x,\vec{x};t_y,\vec{y})$, while a line in a diagram which connects a $(-)$-vertex at the spacetime point $(t_x,\vec{x})$ to a $(+)$-vertex at the spacetime point $(t_y,\vec{y})$ is associated to $G_{-+}(t_x,\vec{x};t_y,\vec{y})$. Notice the correlation of the ordering of the subscripts $\pm$ to the ordering of field in the two-point functions in (1.4.9) and (1.4.10).

- As in the standard in-out path integral, one then must integrate over all spacetime points associated to the vertices appearing in the diagram in question. While the spatial integrals run over the entire spatial volume of the spacetime, the time integrals are bounded from above by the correlation time t. In particular, all time arguments t_n of the vertices satisfy $t_n \leq t$.

These rules have the following important consequence, if one is computing equal-time correlation functions of a real field: the 2^n diagrams which one is summing over at each order in the perturbative expansion will come in complex-conjugated pairs, since replacing all $(+)$-vertices with $(-)$-vertices, and vice-versa, in a diagram is equivalent to taking its complex conjugate [42]. Therefore, the resulting correlation function will be real-valued at each order in the expansion. This will constitute a useful consistency check on our computations.

To use the Schwinger-Keldysh formalism one thus has to deal with these more complicated rules, which make computations more cumbersome than in the more familiar in-out setting. Let us mention at this point that, if one is only interested in carrying out computations which assume Gaussian initial conditions for the fields, the above formalism can be traded for alternative formalisms, such as [45] which expresses the in-in path integral in terms of the in-out one, and, more prominently, the wavefunction-of-the-universe formalism, see [46–48] for introductory discussions of different aspects of this formalism in the context of cosmology. We will not use these formalism in this thesis.

However, the higher degree of complexity of the Schwinger-Keldysh path integral pays off by allowing one to include the effects of more complicated initial conditions in the computation of correlation functions, where the initial state may be non-Gaussian, and even mixed. This is implemented in practice by writing [40]

$$\langle\phi(t,\vec{x}_1)...\phi(t,\vec{x}_n)\rangle = \mathrm{tr}(\rho_D(-\infty)\phi(t,\vec{x}_1)...\phi(t,\vec{x}_n))\,, \tag{1.4.14}$$

where now $\rho_D(-\infty)$ is the generic density matrix describing the initial state at $t=-\infty$ and tr(...) denotes the trace operation. The path integral formula resulting from this more general expression is (1.4.7) with the replacement

$$\langle\phi_+(-\infty)|\Omega\rangle\langle\Omega|\phi_-(-\infty)\rangle \to \langle\phi_+(-\infty)|\rho_D(-\infty)|\phi_-(-\infty)\rangle\,, \tag{1.4.15}$$

and we recognize that the formula (1.4.7) simply used the density matrix associated to the pure state $|\Omega\rangle$, which is just $\rho_\Omega(-\infty)=|\Omega\rangle\langle\Omega|$. Using the notation and conventions of [49], the generic matrix element of the density matrix $\langle\phi_+(-\infty)|\rho_D(-\infty)|\phi_-(-\infty)\rangle$ can be usefully parametrized as follows:

$$\langle\phi_+(-\infty)|\rho_D(-\infty)|\phi_-(-\infty)\rangle = \exp\Big(iF[\phi_\pm]\Big)\,, \tag{1.4.16}$$

with the functional

$$F[\phi_\pm] \equiv \sum_{n=0}^{\infty}\frac{1}{n!}\int\left[\prod_{i=1}^{n}\mathrm{d}^{d-1}x_i\right]\Xi_n^{\sigma_1,...,\sigma_n}(\vec{x}_1,...,\vec{x}_n)\phi_{\sigma_1}(-\infty,\vec{x}_1)...\phi_{\sigma_1}(-\infty,\vec{x}_n)\,. \tag{1.4.17}$$

In the above expression we are implicitly summing over all CTP-indices $\sigma_i=\pm$. This functional is localized at the initial time at which the vacuum state is defined, which for us is $-\infty$, and the non-local functions $\Xi_n^{\sigma_1,...,\sigma_n}$ parametrize the density matrix $\rho_D(-\infty)$. Assuming that the density matrix $\rho_D(-\infty)$ is Hermitean imposes the following constraint on the initial-condition functions:

$$i\Xi_n^{\sigma_1,...,\sigma_n}(\vec{x}_1,...,\vec{x}_n) = \Big[i\Xi_n^{-\sigma_1,...,-\sigma_n}(\vec{x}_1,...,\vec{x}_n)\Big]^*\,. \tag{1.4.18}$$

A general Gaussian initial state can be completely parametrized by means of the initial-condition functions $\Xi_n^{\sigma_1,...,\sigma_n}$ with $n=0,1,2$, while a generic non-Gaussian initial state can be fully described by allowing for non-vanishing $\Xi_n^{\sigma_1,...,\sigma_n}$ for $n\geq 3$ [40]. In the latter case, the functions $\Xi_n^{\sigma_1,...,\sigma_n}$ are treated as non-local "vertices" to be inserted in diagrams just like normal vertices, see [49]. While we will restrict ourselves to using Gaussian initial conditions for the computations that we will carry out in chapter 3, the above formalism to include non-Gaussian initial conditions will be very useful in chapter 4.

1.5 Two-point function of the free scalar field, infrared divergence in the massless theory

The basic building block for the perturbative computation of correlation functions in the in-in formalism is the unordered two-point function $\langle\phi(t_x,\vec{x})\phi(t_y,\vec{y})\rangle$, which is also known as the Wightman function, as can be seen from the four propagators (1.4.8)-(1.4.11). For the real scalar field in de Sitter space, this quantity can be computed in any number of dimensions using the Fourier decomposition (1.3.11) of the field operator, together with the commutation relations (1.3.13) and the Bunch-Davies mode functions (1.3.15):

$$\langle\phi(\eta_x,\vec{x})\phi(\eta_y,\vec{y})\rangle = \frac{\pi}{4H}(-H\eta_x)^{\frac{d-1}{2}}(-H\eta_y)^{\frac{d-1}{2}}\int\frac{\mathrm{d}^{d-1}k}{(2\pi)^{d-1}}e^{i\vec{k}\cdot(\vec{x}-\vec{y})}H_\nu^{(1)}(-k\eta_x)H_\nu^{(1)*}(-k\eta_y)\,. \tag{1.5.1}$$

This integral can be evaluated by decomposing the vector $\vec{k}$ using spherical coordinates, which trivializes the integration over the $d-3$ azimuthal angles and leaves the non-trivial integrations over the modulus of k and the angle between the vectors $\vec{k}$ and $(\vec{x}-\vec{y})$, which can be defined as the polar angle. These integrals can then be solved exactly by making use of known results for integrals over special functions, see e.g. [50, 51], and the result reads, see [52, 53] for the original derivation and [54] for this form,

$$\langle\phi(x)\phi(y)\rangle = \frac{H^{d-2}}{(4\pi)^{\frac{d}{2}}}\frac{\Gamma(\frac{d-1}{2}+\nu)\Gamma(\frac{d-1}{2}-\nu)}{\Gamma(\frac{d}{2})}\,{}_2F_1\left(\frac{d-1}{2}+\nu, \frac{d-1}{2}-\nu; \frac{d}{2}; \frac{1+Z(x,y)}{2}\right). \tag{1.5.2}$$

In the above equation ${}_2F_1(a,b;c;z)$ denotes the Gauss hypergeometric function and $Z(x,y)$ denotes the de Sitter-invariant distance function, which we introduced in section 1.2.2, between the two points at which the fields are evaluated. In conformal coordinates it reads

$$Z(x,y) = Z(\eta_x,\vec{x};\eta_y,\vec{y}) = 1 + \frac{(\eta_x-\eta_y)^2 - |\vec{x}-\vec{y}|^2}{2\eta_x\eta_y}\,. \tag{1.5.3}$$

While we have sketched the derivation of the result (1.5.2) using the mode functions in conformal coordinates, the result for the two-point function $\langle\phi(x)\phi(y)\rangle$ in the Bunch-Davies vacuum looks the same in any set of coordinates, and the only thing that changes is the functional form of Z.

Inspecting the result (1.5.2) we find that it is singular in the limit $\nu \to (d-1)/2$, which corresponds to taking the massless limit $m^2 \to 0$, since the hypergeometric function tends to one while the gamma function $\Gamma(\frac{d-1}{2}-\nu)$ blows up. Strikingly, this divergence is present irrespective of the number of dimensions d in which one is working. To understand where it is coming from, it is useful to go back to the integral representation (1.5.1) of the two-point function, and inspect the small-k behaviour of the integrand for $\nu = (d-1)/2$:

$$\lim_{k\to 0} e^{i\vec{k}\cdot(\vec{x}-\vec{y})} H^{(1)}_{\frac{d-1}{2}}(-k\eta_x) H^{(1)*}_{\frac{d-1}{2}}(-k\eta_y) \to \frac{1}{k^{d-1}}\,, \tag{1.5.4}$$

where we are only showing the leading k-dependence of the integrand in this limit, and ignoring any k-independent coefficients. Thus, it follows that in the integration region where the modulus of $\vec{k}$ is small, the integral in (1.5.1) takes the form

$$\int \frac{\mathrm{d}^{d-1}k}{k^{d-1}}\,, \tag{1.5.5}$$

which is logarithmically divergent in any number of dimensions. This is the origin of the singular behaviour of the two-point function in the limit of vanishing mass, and it can be identified as an infrared (IR) divergence, since it is caused by the behaviour of the integrand in the limit of small physical momentum $-k\eta$, measured in Hubble units. The modes of the field with small values of $-k\eta$ are called "superhorizon" modes, since they satisfy

$$\frac{k}{a(\eta)} < H \tag{1.5.6}$$

so their associated physical wavelength $\lambda_{\rm ph}$ satisfies the inverse relation:

$$\lambda_{\rm ph} = \left(\frac{k}{a(\eta)}\right)^{-1} > \frac{1}{H}\,. \tag{1.5.7}$$

As we discussed in section 1.2.1, $1/H$ is the radius of the cosmological horizon of de Sitter space, which explains the nomenclature. These are the modes that are responsible for the IR divergence of the free, massless scalar field theory. By the same token, field modes that satisfy

$$\frac{k}{a(\eta)} > H \tag{1.5.8}$$

are called "subhorizon".

This pathology of the free theory was noticed already in [55], and it was understood in [56] to be a reflection of the fact that the theory of a free, minimally coupled, massless scalar field in de Sitter space does not allow for the existence of a vacuum state which respects the full set of de Sitter isometries. Physically, this effect can be thought of as a consequence of gravitational particle production due to the expanding background: since the minimally coupled scalar theory does not enjoy conformal invariance, as the spacetime expands field modes with small physical momentum (in Hubble units) get copiously produced. In the absence of a potential term which can counteract this effect the field amplitude can therefore grow without bound, and the two-point correlation between any pair of fields diverges. The free, massless scalar field is not the only problematic type of field theory from this point of view, and similar IR pathologies have been found in other theories of massless field in de Sitter space, see [57] for a review of the subject. At first, this seems to pose a dilemma: above, we discussed that light, and in particular massless, fields are the most phenomenologically relevant degrees of freedom in inflationary models, but, at the same time, the quantum theory of these types of fields in de Sitter space seems to be ill-defined.

The resolution to this conundrum is that the free theory of a massless scalar field is also a theory in which the correlation properties of the scalar field cannot be measured, since an interaction term of some sort between the scalar field and itself, or some other field species, is needed for a measurement to take place. Therefore, the setting of physical interest is the interacting theory. Once a self-interaction is switched on, it is possible that it will eventually counteract the effect of gravitational particle production and stabilize the theory, removing the pathological behaviour in the IR. This would then define a new vacuum state, which, however, cannot be perturbatively related to any vacuum state of the free theory: it would be generated by nonperturbative effects. This line of thinking strongly suggests that the correct description of the dynamics of the massless, minimally coupled, interacting scalar field on superhorizon scales must be a non-perturbative one.

The study of this phenomenon will be the main focus of this thesis. To this end, we will switch on the simplest possible stable self-interaction of the massless field, a quartic self-interaction, which we implement by means of the action

$$S_{\text{int}} = -\frac{(\lambda, \kappa)}{4!} \int \mathrm{d}^d x \, \sqrt{-g}\phi^4(x) \,, \tag{1.5.9}$$

and examine the IR dynamics of the resulting theory using three different approaches. The self-coupling of the field will be called λ in chapter 2 and κ in chapters 3 and 4, for reasons that will become clear[4].

1.6 Outline of the thesis

The thesis is structured as follows:

- In chapter 2 we will introduce the formalism of Stochastic Inflation and the Euclidean formulation of the theory of the massless, minimally coupled, self-interacting scalar field in de Sitter space. We will use these two formalisms to study the interacting two-point function of the field ϕ. This chapter is based on unpublished original material.

- In chapter 3 we will turn to the Lorentzian field-theoretic formulation of the theory of the massless, minimally coupled, self-interacting scalar field in de Sitter space, and show how the computation of correlation functions in the late-time limit can be simplified using the Method of Regions. This chapter is partly based on original material published in

  M. Beneke, P. Hager and A. F. Sanfilippo, *Cosmological correlators in massless ϕ^4-theory and the method of regions*, *JHEP* **04** (2024) 006 [2312.06766]

  and on unpublished original material.

- In chapter 4 we will introduce the appropriate EFT framework to characterize infrared field modes of quantum fields in de Sitter space, which is known as Soft de Sitter Effective Theory (SdSET), we will

[4] The coupling κ should not be confused with the self-coupling of metric fluctuations, which we do not consider in this thesis.

construct this EFT from the ground up, discuss the renormalization and matching procedure in the SdSET, and discuss how it can be used to address and resolve the IR divergences that are observed in perturbation theory. This chapter is based on unpublished original material.

- We conclude in chapter 5.

Chapter 2

Massless scalar two-point function: the Stochastic and Euclidean approaches

This chapter is dedicated to the study of the two-point function of the massless, minimally coupled, self-interacting scalar field in de Sitter space. Above, we discussed that the naive perturbative approach to the computation of correlation functions in this setting fails due to the IR-divergent behaviour of the free two-point function, which makes the perturbative expansion of the theory, as it is usually constructed, ill-defined. Historically, the first formalism that was able to succeed in yielding a well-defined description of it is the formalism of Stochastic Inflation. It was introduced and developed in [58, 59] and finally presented in [60]. The key physical insight which underlies this formalism is that, in the limit of late times, in Hubble units, one can abandon the full quantum-field-theoretical description of a scalar field in de Sitter space in favour of an effective description which is classical and stochastic in nature. In the leading infrared approximation, which will be defined in the following, the dynamics of the fields are fully described by a Fokker-Planck equation [61], which is simple enough to be solved exactly, either analytically or numerically. By solving it numerically in the case of the quartically self-interacting, massless scalar field the non-perturbative result for the two-point function at late times was derived for the first time in [60]. This result is free of IR divergences, it decays exponentially at late times, and it is de Sitter-invariant up to the considered order of approximation. Most notably, the stochastic result depends on the square root of the self-coupling, $\sqrt{\lambda}$, which makes its non-perturbative nature manifest.

While the stochastic framework was very successful in its purpose, its relation to a full quantum-field-theoretic treatment of the scalar field in de Sitter space remained unclear at first. Furthermore, its extension beyond the leading infrared approximation remained elusive for quite some time. Building on the previous works [62, 63], the first difficulty was successfully removed in [64], which showed explicitly that the stochastic formalism is fully equivalent to the field-theoretic description, up to the considered order of approximation. This proof was repeated by several authors using several different approaches, including the wavefunction-of-the-universe formalism [47, 65], a density-matrix approach in the static patch of de Sitter space [66], the Yang-Feldman equation [67], a diagrammatic proof [68], and the Schwinger-Keldysh path integral [69]. The first work to push the stochastic formalism beyond the leading-order approximation was [70], which computed next-to-leading order corrections to the Fokker-Planck equation in terms of an equation involving second-order time derivatives. More recently, [71] showed how to further extend the approximation, in principle to any desired order, and also computed the next-to-leading order corrections to the Fokker-Planck equation, but in a form which keeps the partial differential equation first-order in time. This result was shortly followed by [72], which obtained the same result using the above-mentioned static-patch approach. The statements made in [71] suggest that this form of the equation, which is known as Kramers-Moyal equation [61], should persist to all orders of approximation. The successful extension of the stochastic formalism to higher orders established it as the correct all-order formalism to address the issue of IR-divergences in de Sitter space.

A complementary approach that is also successful in yielding an IR-finite description of the massless scalar field is based on the formulation of the theory in Euclidean de Sitter space, which for dS_d is the d-dimensional sphere S^d. The advantage of working in a compact, spherical spacetime to make the infrared structure of a theory more manifest was already noticed in [73] in the context of massless, Euclidean quantum electrodynamics, and then applied to scalar field theories in [74], where it was also shown how to implement dimensional regularization in this setting to handle UV divergences. In [75] it was then established for the first time that, due to the discrete mode expansion of fields on the sphere, the singular behaviour of the massless, minimally coupled, free scalar field can be fully traced back to the mode with vanishing angular momentum, the so-called "zero-mode". In the same paper, it was also shown that the inclusion of an interaction term and the exact treatment of the zero-mode in the interacting theory yields a well-defined, IR-finite theory on the sphere. Based on this observation, [76] developed a systematic, semi-perturbative prescription, which treats the zero-mode exactly and all other modes perturbatively, obtaining a well-defined scheme to compute correlation functions of massless scalars on the sphere. As was the case in the stochastic approach, the effective expansion parameter in the Euclidean formalism also turns out to be $\sqrt{\lambda}$. However, in the Euclidean treatment this non-perturbative effect is ascribed fully to a single mode of the field. In both approaches the self-regularization of the IR-pathology in the free theory is interpreted as the generation of a new, dynamical mass scale $m^2_{\rm dyn} \sim H^2\sqrt{\lambda}$ due to the self-interaction of the field.

The Euclidean formalism solves the problem of IR-divergences in a fully quantum-field-theoretical framework, but its application is restricted to the sphere, since it relies crucially on the mode expansion of the field being discrete. In the Lorentzian setting, which is the physically relevant one, the mode expansion is continuous, and the large IR effects in perturbatively computed correlators are ascribed to the continuum of superhorizon field modes, so the method discussed above is not applicable. What one can still do, however, is use the Euclidean formalism to compute correlators on the sphere and then analytically continue the results to Lorentizan signature, by appropriately extending the range of values of the kinematic invariants. This procedure was used in the case of massive scalar fields in [54] to study the properties of massive two-point functions at large invariant distances between the arguments of the fields. In the subsequent paper [77] it was then shown that for $m^2 > 0$ the analytically continued Euclidean correlation functions coincide with the in-in correlators computed in the Bunch-Davies (or Euclidean) vacuum in Lorentzian signature, which are the relevant physical observables, over the entire range of physical values for the kinematic invariants. This proof validated the discussed procedure in the case of massive scalar fields. Following this line of argument, [75] advocated for extending the application of this procedure to the massless case. While there is no technical obstacle in doing so, the physical meaning of the analytic continuation of these results is not immediately clear. Since the true vacuum of the interacting theory is non-perturbative, it is not at all obvious which correlation functions one should compute in the massless theory in Lorentzian signature in the first place, and how.

The goal of this chapter is to show that the perturbatively computed stochastic result and the analytically continued Euclidean result for the two-point function of the massless, minimally coupled, self-interacting scalar field agree order by order in $\sqrt{\lambda}$ up to $\mathcal{O}(\lambda^2)$ in the limit of large invariant separation between the spacetime points at which the fields are evaluated. An analogous study was carried out in the $O(N)$ vector model in the large-N limit in the series of papers [78–80], finding that both at leading- [78] and next-to-leading order [80] in the $1/N$ expansion the analytically continued result decays exponentially in the large-invariant-distance limit. Further, at leading order in the $1/N$ expansion the propagator of the interacting theory reduces to a free, massive propagator with mass [78]

$$m^2_{\rm dyn} = \sqrt{\frac{\lambda}{2V_d}}\,, \tag{2.0.1}$$

so at this order the interpretation of "dynamical mass generation" is exact. At next-to-leading order in the $1/N$ expansion the authors of [80] instead find that the interacting two-point function can be represented as a superposition of two free, massive two-point functions with two distinct masses, $m^2_{\rm dyn}$ and $3m^2_{\rm dyn}$, so starting from this order two numerically distinct mass scales, which however are both still parametrically

$\mathcal{O}(\sqrt{\lambda})$, are present in the problem. This treatment reproduces the results found in [81, 82], which employed the large-N expansion up to next-to-leading order in $1/N$ directly in Lorentzian de Sitter space, up to the same order of approximation. The finding of [78] was also reproduced in [71], which means that in this model the stochastic and Euclidean results agree, at least at leading order in $1/N$. This was confirmed again by [83].

We are interested in establishing the connection between the result for the two-point function computed in the two formalisms in the single-field case, which is done here for the first time. While we will not be able to carry out an all-order proof, we will confirm the correspondence of the two results to fifth order in the expansion in $\sqrt{\lambda}$, which includes the evaluation of a two-loop diagram in Euclidean de Sitter space, to leading-logarithmic order, in a sense that will be made precise below. Along the way, we will also discuss the high-order behaviour of the perturbative stochastic series for the two-point function in the massless theory, which turns out to have interesting mathematical properties, and discuss the implications of this structure for the analytic continuation of the Euclidean result. We conclude the chapter by formulating two conjectures about the all-order properties of the analytic continuation of the Euclidean series for the two-point function in the limit of large invariant distance.

2.1 The formalism of Stochastic Inflation

In this section we review and discuss the stochastic formalism as presented in [60]. As an application, we will use it to compute the stochastic two-point function of the masless, minimally coupled, self-interacting scalar field both non-perturbatively, making use of numerical results, and analytically, using perturbation theory to a fixed order, and examine the large-order behaviour of the perturbative result.

2.1.1 Derivation of the Fokker-Planck equation

The starting point for the derivation of the central equation of Stochastic Inflation, which is the Fokker-Planck equation, is the equation of motion of a self-interacting scalar field in de Sitter space in planar coordinates. We already wrote down the d-dimensional equation for the free, massive field in (1.3.5), and in the case of the four-dimensional self-interacting field it becomes

$$\frac{\partial^2}{\partial t^2}\phi(x) + 3H\frac{\partial}{\partial t}\phi(x) - \frac{\vec{\partial}^2}{a(t)^2}\phi(x) + V'(\phi) = 0\,. \tag{2.1.1}$$

Notice that both a non-minimal coupling to the metric and a mass term can be accounted for by appropriately choosing $V(\phi)$. From this equation, we wish to derive an effective equation of motion for the component of the full field ϕ which describes field modes with physical momenta much smaller than the Hubble scale, $|\vec{k}|/a(t) \ll H$. Following [60], we split the field in a superhorizon field $\bar{\phi}$ and a subhorizon field $\delta\phi$, as

$$\phi(x) = \bar{\phi}(x) + \delta\phi(x)\,. \tag{2.1.2}$$

The superhorizon field $\bar{\phi}$ is the variable of interest. We define it using the mode decomposition of the full quantum field ϕ (1.3.11), which we rewrite here for convenience using coordinate time t and $d = 4$,

$$\phi(t,\vec{x}) = \int \frac{\mathrm{d}^3k}{(2\pi)^3}\Big[\phi_{\vec{k}}(t)e^{i\vec{k}\cdot\vec{x}}a_{\vec{k}} + \phi^*_{\vec{k}}(t)e^{-i\vec{k}\cdot\vec{x}}a^\dagger_{\vec{k}}\Big]\,, \tag{2.1.3}$$

and cutting off the modes with $|\vec{k}| \equiv k > \epsilon a(t)H$, with $\epsilon \ll 1$, in the above expression by introducing an appropriate Heaviside distribution in the integrand:

$$\bar{\phi}(t,\vec{x}) \equiv \int \frac{\mathrm{d}^3k}{(2\pi)^3}\theta(\epsilon a(t)H - k)\Big[\phi_{\vec{k}}(t)e^{i\vec{k}\cdot\vec{x}}a_{\vec{k}} + \phi^*_{\vec{k}}(t)e^{-i\vec{k}\cdot\vec{x}}a^\dagger_{\vec{k}}\Big]\,. \tag{2.1.4}$$

In the above, ϵ is a small, but otherwise arbitrary, parameter, which can be interpreted as the cutoff up to which of the effective description we are constructing holds. The subhorizon field $\delta\phi$ can then be defined using (2.1.2) as the complement of $\bar{\phi}$:

$$\delta\bar{\phi}(t,\vec{x}) \equiv \int \frac{\mathrm{d}^3k}{(2\pi)^3}\theta(k-\epsilon a(t)H)\Big[\phi_{\vec{k}}(t)e^{i\vec{k}\cdot\vec{x}}a_{\vec{k}} + \phi^*_{\vec{k}}(t)e^{-i\vec{k}\cdot\vec{x}}a^\dagger_{\vec{k}}\Big]\,. \tag{2.1.5}$$

We now plug the field decomposition (2.1.2) into the equation of motion (2.1.1), under the assumption that the field amplitude of ϕ is dominated by the contribution from superhorizon field modes, which means that we can assume $\bar{\phi} \gg \delta\phi$. Since $\delta\phi$ is small, it follows that we can neglect its self-interactions altogether, and treat the mode functions appearing in (2.1.5) as if they were free. This is not the case for $\bar{\phi}$, but what we can do is drop all terms containing $\delta\phi$ from the nonlinear terms, and we can replace directly $V(\phi) \to V(\bar{\phi})$. Regarding the derivative terms we need to be more careful. Since by definition $\bar{\phi}$ contains modes with small physical momenta, which also imply that the field varies slowly with time, we can drop all second-time-derivative terms acting on $\bar{\phi}$, both in time and space, from the effective equation of motion. When taking first-time derivatives of $\delta\phi$, we see from (2.1.5) that they act both on the mode functions and on the θ-distribution, turning it into a δ-distribution:

$$\frac{\partial}{\partial t}\theta(k-\epsilon a(t)H) = -\epsilon a(t)H^2\delta(k-\epsilon a(t)H)\,. \tag{2.1.6}$$

From these terms, we thus get contributions to the effective equation of motion for $\bar{\phi}$ which are localized at $k=\epsilon a(t)H$, the boundary of validity of our desired effective description, and which cannot be neglected. The result for the effective equation of motion for $\bar{\phi}$ reads [60]

$$\frac{\partial}{\partial t}\bar{\phi}(t,\vec{x}) = -\frac{1}{3H}V'(\bar{\phi}) + f(t,\vec{x})\,, \tag{2.1.7}$$

where the term $f(t,\vec{x})$ stems precisely from the mentioned time derivatives acting on the θ-distribution, and it reads

$$f(t,\vec{x}) \equiv \epsilon a(t)H^2\int \frac{\mathrm{d}^3k}{(2\pi)^3}\delta(k-\epsilon a(t)H)\Big[\phi_{\vec{k}}(t)e^{i\vec{k}\cdot\vec{x}}a_{\vec{k}} + \phi^*_{\vec{k}}(t)e^{-i\vec{k}\cdot\vec{x}}a^\dagger_{\vec{k}}\Big]\,. \tag{2.1.8}$$

In the above equation, the appearing mode functions are the free-theory ones, and they can be approximated by their late-time limit as [59]

$$\phi_{\vec{k}}(t) = \frac{-iHe^{-ik\eta(t)}}{\sqrt{2}k^{\frac{3}{2}}}\,,\quad \eta(t) = -\frac{1}{a(t)H}\,, \tag{2.1.9}$$

since their physical momenta are constrained by the δ-distribution in the integrand to lie on the physical-momentum shell $k/(a(t)H) = \epsilon \ll 1$.

The superhorizon field appearing in (2.1.7), as well as the source term f, are both still operators at this point. However, as pointed out in [59], all the quantities that appear in (2.1.7) actually commute with each other, so we can effectively treat them as classical variables. Since, however, we cannot assign a definite numerical value to the source f at any point in spacetime, and we can at most determine its correlation properties, it follows that the equation (2.1.7) is a classical, stochastic differential equation for $\bar{\phi}$, and we can regard f as a stochastic noise term acting on $\bar{\phi}$. This type of stochastic differential equation is known as Langevin equation [61].

We can now study the correlation properties of f. Since it contains free-theory creation and annihilation operators $a_{\vec{k}}$, $a^\dagger_{\vec{k}}$, any of its correlation functions will decompose into products of two-point functions. We can therefore identify it as Gaussian noise. Using (2.1.9), together with the canonical commutation relations (1.3.13) one can show that its two-point correlation function reads

$$\langle f(t,\vec{x})f(t',\vec{x}')\rangle = \frac{H^3}{4\pi^2}\delta(t-t')\frac{\sin(\epsilon a(t)H|\vec{x}-\vec{x}'|)}{\epsilon a(t)H|\vec{x}-\vec{x}'|}\,. \tag{2.1.10}$$

We can now expand this expression for $\epsilon \ll 1$ and the above reduces to

$$\langle f(t,\vec{x})f(t',\vec{x}')\rangle = \frac{H^3}{4\pi^2}\delta(t-t') + \mathcal{O}(\epsilon)\,. \tag{2.1.11}$$

The noise at the point $(t,\vec{x})$ is therefore uncorrelated with the noise at the point $(t',\vec{x}')$, except for the case when $t = t'$, which is the defining property of white noise. The set of approximations we used to obtain (2.1.7), together with the treatment of f as Gaussian white noise, define the "leading infrared approximation" in which the stochastic formalism is valid.

The fact that $\bar{\phi}$ satisfies a Langevin equation means that we can associate a set of probability distribution functions (PDFs) ρ_n to it, which will generate the full set of its n-point correlation functions. The simplest one is the one-point PDF $\rho_1(t,\varphi)$, which we can define via the equation

$$\langle F[\bar{\phi}(t,\vec{x})]\rangle = \int_{-\infty}^{\infty} \mathrm{d}\varphi\ F[\varphi]\rho_1(t,\varphi)\,. \tag{2.1.12}$$

Here, F is any function of $\bar{\phi}$. From (2.1.7) it follows that $\rho_1(t,\varphi)$ must satisfy the following Fokker-Planck equation [60, 61]:

$$\frac{\partial\rho_1(\varphi,t)}{\partial t} = \frac{1}{3H}\frac{\partial}{\partial\varphi}\Big[V'(\varphi)\rho_1(\varphi,t)\Big] + \frac{H^3}{8\pi^2}\frac{\partial^2}{\partial\varphi^2}\rho_1(\varphi,t)\,. \tag{2.1.13}$$

$$= \Gamma_\varphi \rho_1(t,\varphi)\,, \tag{2.1.14}$$

where in the last step we introduced the Fokker-Planck operator

$$\Gamma_\varphi \equiv \frac{1}{3H}\frac{\partial}{\partial\varphi}V'(\varphi) + \frac{H^3}{8\pi^2}\frac{\partial^2}{\partial\varphi^2}\,. \tag{2.1.15}$$

In the above equation, the derivatives are understood as acting on everything to their right.

The Fokker-Planck equation (2.1.13) is the central equation of Stochastic Inflation. We derived it in $d = 4$ spacetime dimensions, but it can be generalized to d dimensions by using the following d-dimensional Fokker-Planck operator, which will be useful for the later discussion:

$$\Gamma_{\varphi,d} \equiv \frac{1}{H(d-1)}\left[\frac{\partial}{\partial\varphi}V'(\varphi) + \frac{1}{V_d}\frac{\partial^2}{\partial\varphi^2}\right], \tag{2.1.16}$$

with

$$V_d \equiv \frac{2\pi^{\frac{d+1}{2}}}{H^d\Gamma(\frac{d+1}{2})}\,. \tag{2.1.17}$$

Remarkably, V_d is nothing but the volume of d-dimensional Euclidean de Sitter space. The appearance of this quantity in this context seems surprising at first, however, the formal connection between the stochastic formalism and the Euclidean sphere was identified and discussed in [84–86] as an effective dimensional reduction of the problem to a zero-dimensional "field theory", due to the dominance of the constant zero-momentum mode of the field in the far infrared limit. As we will see below, the same observation will hold true in the Euclidean treatment of the problem.

2.1.2 One-point probability distribution function

We will now study the properties of the solutions of (2.1.13). We will first review the general properties of the one-point PDFs obtained from the Fokker-Planck equation, which hold for any choice of the potential $V(\varphi)$, and then specify to the case of the massless, minimally coupled, quartically self-interacting scalar field, for which we will explicitly compute the relaxation Eigenvalues. They will be important for the discussion of the stochastic two-point function.

General properties

The Fokker-Planck equation (2.1.13) is a first-order differential equation in time, so to solve it one must also supply a boundary condition for ρ_1 at an initial time, which we will call t_0. Any solution for $\rho_1(\varphi, t)$ in four dimensions can then be written in the form [60]

$$\rho_1(\varphi,t) = \exp\left[-\frac{4\pi^2}{3H^4}V(\varphi)\right]\sum_{n=0}^{\infty} a_n \Phi_n(\varphi) e^{-\Lambda_n(t-t_0)}\,, \tag{2.1.18}$$

where the $\Phi_n(\varphi)$ and Λ_n are the Eigenfunctions and Eigenvalues, respectively, of the Schrödinger-like equation

$$\left[-\frac{1}{2}\frac{\partial^2}{\partial\varphi^2} + W(\varphi)\right]\Phi_n(\varphi) = \frac{4\pi^2\Lambda_n}{H^3}\Phi_n(\varphi)\,, \tag{2.1.19}$$

where

$$W(\varphi) \equiv \frac{1}{2}\Big[v'(\varphi)^2 - v''(\varphi)\Big]\,, \quad v(\varphi) \equiv \frac{4\pi^2}{3H^4}V(\varphi)\,. \tag{2.1.20}$$

The Λ_n are also called "relaxation Eigenvalues" in the literature. Equation (2.1.19) follows directly when plugging the ansatz (2.1.18) into (2.1.13). The operator acting on the Φ_n is Hermitian, so they are orthonormal functions,

$$\int_{-\infty}^{\infty} \mathrm{d}\varphi\ \Phi_n(\varphi)\Phi_m(\varphi) = \delta_{nm}\,, \tag{2.1.21}$$

which form a complete set on the interval $(-\infty, \infty)$,

$$\sum_{n=0}^{\infty}\Phi_n(\varphi)\Phi_n(\varphi') = \delta(\varphi - \varphi')\,. \tag{2.1.22}$$

From the orthonormality of the Φ_n we can compute the coefficients a_n in (2.1.18) by projecting the one-point PDF evaluated at $t = t_0$ onto $\Phi_n(\varphi)$:

$$a_n \equiv \int \mathrm{d}\varphi\ \rho_1(\varphi, t_0) e^{v(\varphi)}\Phi_n(\varphi)\,. \tag{2.1.23}$$

These coefficients therefore encode the initial condition used to solve the Fokker-Planck equation for ρ_1.

The first summand in (2.1.18) plays a special role, since it defines the time-independent equilibrium distribution, which is the solution of the equation

$$0 = \frac{1}{3H}\frac{\partial}{\partial\varphi}\Big[V'(\varphi)\rho_{1\mathrm{eq}}(\varphi)\Big] + \frac{H^3}{8\pi^2}\frac{\partial^2}{\partial\varphi^2}\rho_{1\mathrm{eq}}(\varphi)\,. \tag{2.1.24}$$

The associated Eigenvalue is therefore vanishing,

$$\Lambda_0 = 0\,, \tag{2.1.25}$$

and the solution of (2.1.24) reads

$$\rho_{1\mathrm{eq}}(\varphi) = N \exp\left[-\frac{8\pi^2}{3H^4}V(\varphi)\right]\,, \tag{2.1.26}$$

where the normalization factor N ensures

$$\int_{-\infty}^{\infty}\mathrm{d}\varphi\ \rho_{1\mathrm{eq}}(\varphi) = 1\,, \tag{2.1.27}$$

and $\rho_{1\mathrm{eq}}$ is related to the lowest Eigenfunction via

$$\rho_{1\mathrm{eq}}(\varphi) = \Phi_0^2(\varphi)\,. \tag{2.1.28}$$

Since this piece of the general solution (2.1.18) is the only time-independent one, any solution of the Fokker-Planck equation will asymptote to the equilibrium one as $t \to \infty$, which motivates the nomenclature for both $\rho_{1\mathrm{eq}}$ and the Λ_n.

Once we have obtained a particular solution for ρ_1 we can use it to compute one-point functions $\langle \bar{\phi}^n(t) \rangle$ via (2.1.12). Any one-point function which respects the full set of isometries of de Sitter space must be both space- and time-independent, so we should use $\rho_{1\mathrm{eq}}$ to compute such one-point functions in the stochastic formalism. This can be done by picking an initial value for the one-point PDF which satisfies

$$\rho_1(\varphi, t_0) \sim \rho_{1\mathrm{eq}}(\varphi) , \tag{2.1.29}$$

which then sets $a_n = 0$ for all $n > 0$ in (2.1.18) at any time t. The fact that the equilibrium distribution $\rho_{1\mathrm{eq}}(\varphi)$, which can be generalized to d-dimensions, satisfies

$$0 = \frac{1}{H(d-1)} \left[\frac{\partial}{\partial \varphi} \Big[V'(\varphi) \rho(\varphi, t) \Big] + \frac{1}{V_d} \frac{\partial^2}{\partial \varphi^2} \rho(\varphi, t) \right] , \tag{2.1.30}$$

immediately implies a recursion relation among the one-point functions with different n:

$$0 = \int_{-\infty}^{\infty} \mathrm{d}\varphi \, \varphi^n \left[\frac{\partial}{\partial \varphi} \Big[V'(\varphi) \rho_{1\mathrm{eq}}(\varphi) \Big] + \frac{1}{V_d} \frac{\partial^2}{\partial \varphi^2} \rho_{1\mathrm{eq}}(\varphi) \right] = -n \langle V'(\bar{\phi}) \bar{\phi}^{n-1} \rangle + \frac{n(n-1)}{V_d} \langle \bar{\phi}^{n-2} \rangle , \tag{2.1.31}$$

which gives us

$$\langle V'(\bar{\phi}) \bar{\phi}^{n-1} \rangle = \frac{n-1}{V_d} \langle \bar{\phi}^{n-2} \rangle . \tag{2.1.32}$$

This observation immediately generalizes to any function $f(\bar{\phi})$,

$$\langle V'(\bar{\phi}) f(\bar{\phi}) \rangle = \frac{1}{V_d} \langle f'(\bar{\phi}) \rangle . \tag{2.1.33}$$

We will make use of this identity later.

Massless, minimally coupled, self interacting scalar field

So far we have kept the discussion quite general, since we have not yet specified the form of the potential $V(\varphi)$ entering the Fokker-Planck equation. We will now specify to the case of a massless, minimally coupled, self-interacting scalar field with the quartic potential

$$V(\varphi) = \frac{\lambda}{4!} \varphi^4 , \tag{2.1.34}$$

and study the Eigenvalues and Eigenfunctions that characterize the one-point PDF.

In the case of interest the equation (2.1.19) becomes

$$\left[-\frac{1}{2} \frac{\partial^2}{\partial \varphi^2} + \frac{\lambda \pi^2}{3H^4} \left(\frac{2\lambda \pi^2}{27 H^4} \varphi^6 - \varphi^2 \right) \right] \Phi_n(\varphi) = \frac{4\pi^2 \Lambda_n}{H^3} \Phi_n(\varphi) , \tag{2.1.35}$$

which we can rewrite using only dimensionless quantities by defining

$$z \equiv \frac{\lambda^{\frac{1}{4}}}{H} \varphi , \quad E_n \equiv \frac{\Lambda_n}{H\sqrt{\lambda}} , \tag{2.1.36}$$

from which we then get

$$\left[-\frac{1}{2} \frac{\partial^2}{\partial z^2} + \frac{\pi^2}{3} \left(\frac{2\pi^2}{27} z^6 - z^2 \right) \right] \Phi_n(z) = 4\pi^2 E_n \Phi_n(z) . \tag{2.1.37}$$

This diferential equation can be solved exactly in terms of bi-confluent Heun functions,

$$\Phi_n(z) = \exp\left(\frac{\pi^2 z^4}{18}\right)\left[C_{1,n}\mathrm{Hb}\Big(-2E_n\pi^2, \frac{\pi^2}{3}, \frac{1}{2}, 0, \frac{2\pi^2}{9}, z^2\Big) + C_{2,n} z\mathrm{Hb}\Big(-2E_n\pi^2, \frac{4\pi^2}{3}, \frac{3}{2}, 0, \frac{2\pi^2}{9}, z^2\Big)\right], \tag{2.1.38}$$

and we see that the solution has a symmetric and an antisymmetric part. From the node theorem for the Schrödinger equation we know that the Eigenfunction to the n-th Eigenvalue must have n zero-crossings, so we expect the lowest Eigenfunction to be even, with no zeroes, and then to find alternating odd and even Eigenfunctions as we solve for higher Eigenvalues. As already mentioned, the lowest Eigenvalue of (2.1.19) is simply

$$E_0 = 0 \tag{2.1.39}$$

with Eigenfunction

$$\Phi_0(\varphi) = \frac{\sqrt{2\lambda^{\frac{1}{4}}}}{\sqrt{H\sqrt{\frac{3}{\pi}}\Gamma(\frac{1}{4})}} \exp\left[-\frac{\lambda\pi^2}{18H^4}\varphi^4\right]. \tag{2.1.40}$$

As expected, it is even and has no zeroes. It determines the equilibrium PDF through (2.1.28):

$$\rho_{1\mathrm{eq}}(\varphi) = \frac{2\lambda^{\frac{1}{4}}}{H\sqrt{\frac{3}{\pi}}\Gamma(\frac{1}{4})} \exp\left(-\frac{\lambda\pi^2}{9H^4}\varphi^4\right), \tag{2.1.41}$$

and the d-dimensional generalization of it, which is obtained from (2.1.30) and will be relevant later, reads

$$\rho_{1\mathrm{eq}}(\varphi) = \frac{2}{\Gamma(\frac{1}{4})}\left(\frac{V_d\lambda}{4!}\right)^{\frac{1}{4}} \exp\left(-\frac{\lambda V_d}{4!}\varphi^4\right). \tag{2.1.42}$$

Even though we have the exact solution (2.1.38) available, the Heun functions are too cumbersome to work with in practice, so to determine the Eigenvalues and Eigenfunctions for $n \geq 1$ we resort to finding a numerical solution for both by means of the "shooting method" [87]. The strategy is to guess an initial value for E_n, plug it into (2.1.37) and solve the equation numerically. The resulting solution, when plotted as a function of z, will only approach zero for large values of z if the guessed value of E_n is close to a true Eigenvalue. By increasing, or decreasing, the guessed value of E_n systematically one can improve the convergence to zero of the numerical solution for large values of z, thus improving the approximation of the Eigenvalue in question. Finally, by counting the number of zero-crossings that the found numerical solution for Φ_n has, before falling off to zero, one can determine which value of n the found E_n and Φ_n correspond to, and proceed from there.

By using this method to solve (2.1.37) for $n \geq 1$ we find the following table of Eigenvalues, which we determined up to $n = 6$ to a precision of 10 decimal places,

n	Λ_n
0	0
1	$0.0363030441H\sqrt{\lambda}$
2	$0.1181383047H\sqrt{\lambda}$
3	$0.2190951808H\sqrt{\lambda}$
4	$0.3384183051H\sqrt{\lambda}$
5	$0.4736902674H\sqrt{\lambda}$
6	$0.6232085392H\sqrt{\lambda}$

Table 2.1: Relaxation Eigenvalues Λ_n for $n = 0, ..., 6$, determined numerically up to 10 decimal places.

Up to $n = 4$ we find agreement with [60, 87] ($n = 4$ is the highest eigenvalue computed in either of these references) after replacing $\lambda \to \lambda/6$ in their results to account for additional factor 6 in our potential. The plots we find for the normalized Eigenfunctions $\Phi_n(z)$ are shown in figure 2.1.

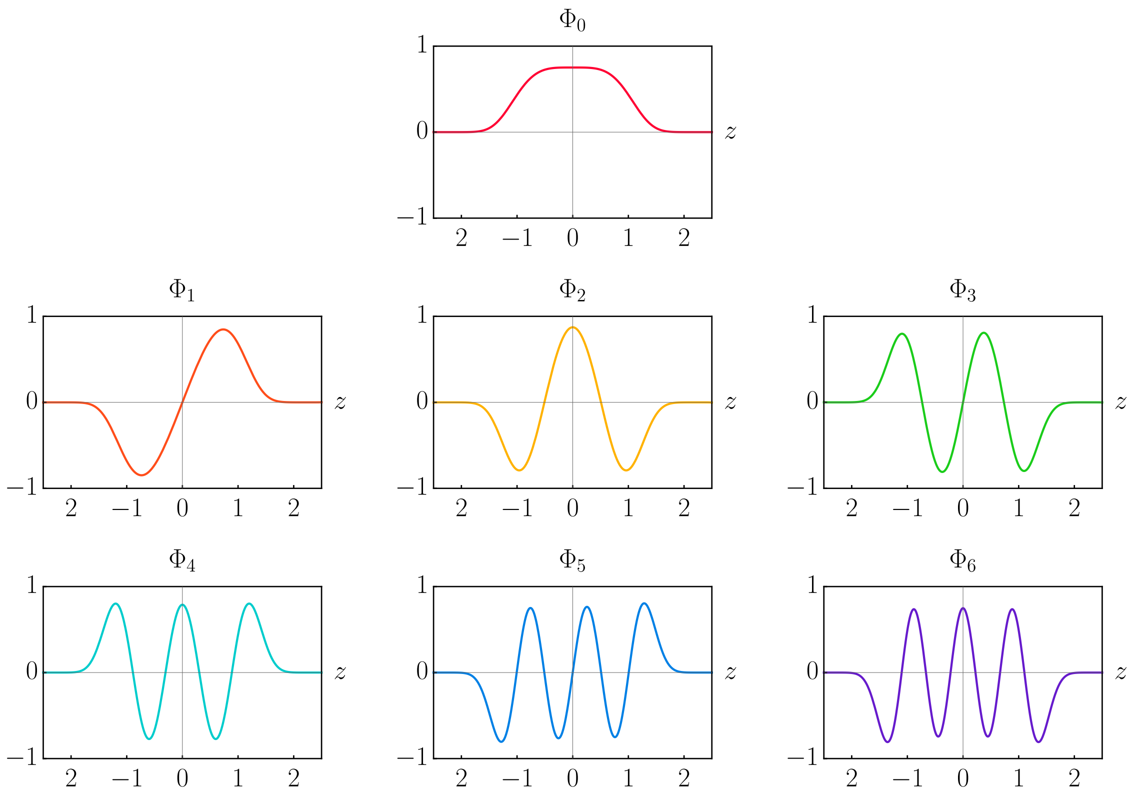

Figure 2.1: Plots of the first seven numerically computed Eigenfunctions. As expected, the Eigenfunctions with even n are even, while those with odd n are odd.

As expected, we see that the Eigenfunction Φ_n has n zero-crossings before falling off to zero at large values of z. The above results will be important for the determination of the stochastic two-point function, to which we now turn.

2.1.3 Stochastic two-point function: exact form, asymptotic expansion and Borel resummation

As mentioned above, the stochastic formalism is, of course, not limited to the computation of one-point correlation functions. Any n-point correlation function can be computed using the corresponding n-point PDF ρ_n, and in this section we will study the two-point function $G(t_1, \vec{x}_1; t_2, \vec{x}_2)$, following again the discussion in [60]. For our purposes it will be enough to study the two-point function evaluated at the same spatial point, $\vec{x}_1 = \vec{x}_2 = \vec{x}$. Even though it is not manifest, the stochastic result for this quantity is fully de Sitter-invariant, as shown in [60], so in principle one may obtain the two-point function at different spatial points by means of a de Sitter-boost.

The quantity of interest can be computed via the formula

$$G(t_1, \vec{x}; t_2, \vec{x}) \equiv G(t_1, t_2) = \int \mathrm{d}\varphi_1 \mathrm{d}\varphi_2\ \rho_2[\varphi_1(t_1, \vec{x}), \varphi_2(t_2, \vec{x})]\varphi_1\varphi_2 \tag{2.1.43}$$

which involves the two-point PDF $\rho_2[\varphi_1(t_1,\vec{x}),\varphi_2(t_2,\vec{x})]$, which we need to determine. It can be decomposed as

$$\begin{aligned}\rho_2[\varphi_1(t_1,\vec{x}),\varphi_2(t_2,\vec{x})] =& \Pi[\varphi_1(t_1,\vec{x})|\varphi_2(t_2,\vec{x})]\rho_1[\varphi_2(t_2,\varphi)]\theta(t_1-t_2)\\ &+\Pi[\varphi_2(t_2,\vec{x})|\varphi_1(t_1,\vec{x})]\rho_1[\varphi_1(t_1,\varphi)]\theta(t_2-t_1)\,,\end{aligned} \tag{2.1.44}$$

where $\Pi[\varphi_1(t_1,\vec{x}_1)|\varphi_2(t_2,\vec{x}_2)]$ is the conditional probability to find the field configuration $\bar{\phi}(t_1,\vec{x}_1)=\varphi_1$ provided that at an earlier time $\bar{\phi}(t_2,\vec{x}_2)=\varphi_2$ held, and $\rho_{1\mathrm{eq}}$ is the equilibrium one-point PDF (2.1.26). The initial condition for Π is

$$\Pi[\varphi_1(t,\vec{x})|\varphi_2(t,\vec{x})]\equiv\delta(\varphi_1-\varphi_2)\,, \tag{2.1.45}$$

and it satisfies the same Fokker-Planck equation as the one-point PDF $\rho_1(\varphi,t)$ separately in both arguments:

$$\frac{\partial}{\partial t_1}\Pi[\varphi_1(t_1,\vec{x}_1)|\varphi_2(t_2,\vec{x}_2)] =\Gamma_{\varphi_1}\Pi[\varphi_1(t_1,\vec{x}_1)|\varphi_2(t_2,\vec{x}_2)]\,, \tag{2.1.46}$$

$$\frac{\partial}{\partial t_2}\Pi[\varphi_1(t_1,\vec{x}_1)|\varphi_2(t_2,\vec{x}_2)] =\Gamma_{\varphi_2}\Pi[\varphi_1(t_1,\vec{x}_1)|\varphi_2(t_2,\vec{x}_2)]\,. \tag{2.1.47}$$

A de Sitter-invariant, late-time two-point function at coincident spatial points can depend on t_1 and t_2 only via the combination $|t_1-t_2|$, and when these two times are taken equal it must reduce to the de Sitter-invariant one-point function $\langle\bar{\phi}^2\rangle$. This implies that the expression we seek must have the form

$$G(t_1,t_2)=\langle\bar{\phi}^2\rangle\xi(|t_1-t_2|)\,,\quad \xi(0)=1\,, \tag{2.1.48}$$

where $\langle\bar{\phi}^2\rangle$ must be computed using the equilibrium one-point PDF $\rho_{1\mathrm{eq}}$. Since the only place in the defining equation of the two-point PDF (2.1.44) where the time variables do not enter in the combination t_1-t_2 is via the one-point PDFs, it then follows that the requirement (2.1.48) can be met if and only if the equilibrium solution for ρ_1 is used in this equation. Since no normalizable equilibrium solution in the case of the free massless, minimally coupled scalar field exists, this requirement cannot be met in that case, and it follows that no de Sitter-invariant two-point function exists. This is the stochastic avatar of the field-theoretic statement found in [56]. Once a self-interaction is switched on, however, an equilibrium solution does exist, and we can find an invariant solution for G.

Assuming that (2.1.48) can be fulfilled, the order of t_1 and t_2 does not matter, so we may fix a specific order without loss of generality. We will choose $t_1>t_2$. Then, the two-point PDF itself satisfies the Fokker-Planck equation

$$\frac{\partial}{\partial t_1}\rho_2[\varphi_1(t_1,\vec{x})\varphi_2(t_2,\vec{x})]=\Gamma_{\varphi_1}\rho_2[\varphi_1(t_1,\vec{x})\varphi_2(t_2,\vec{x})]\,, \tag{2.1.49}$$

which in turn implies that $G(t_1,t_2)$ will depend on the same Eigenvalues Λ_n and Eigenfunctions $\Phi_n(\varphi)$ we studied above. In particular, it may be expanded as

$$G(t_1,t_2)=\sum_{n=1}^{\infty}b_n e^{-\Lambda_n|t_1-t_2|}\,, \tag{2.1.50}$$

and the constraint (2.1.48) imposed by the requirement of de Sitter-invariance of the two-point function translates into the following constraint equation on the b_n:

$$\sum_{n=1}^{\infty}b_n=\langle\bar{\phi}^2\rangle\,. \tag{2.1.51}$$

This constraint may be regarded as an initial condition for G at $t_1=t_2$, in which case the coefficients b_n are defined as [60, 87]

$$b_n\equiv\left[\int_{-\infty}^{\infty}\mathrm{d}\varphi\;\varphi\Phi_0(\varphi)\Phi_n(\varphi)\right]^2\,. \tag{2.1.52}$$

In particular, $b_0 = 0$ if the potential under consideration is symmetric under the reflection $\phi \to -\phi$, since this implies that the product $\Phi_0^2 \sim \rho_{1\mathrm{eq}}$ appearing in the integrand of (2.1.52) will be an even function of φ. We can see that the definition (2.1.52) respects (2.1.51) using the completeness of the Eigenfunctions (2.1.22):

$$\begin{aligned}\sum_{n=1}^{\infty} b_n = \sum_{n=0}^{\infty} b_n &= \int \mathrm{d}\varphi \mathrm{d}\varphi' \ \varphi\varphi' \Phi_0(\varphi)\Phi_0(\varphi') \sum_{n=0}^{\infty} \Phi_n(\varphi)\Phi_n(\varphi') \\ &= \int \mathrm{d}\varphi \mathrm{d}\varphi' \ \varphi\varphi' \Phi_0(\varphi)\Phi_0(\varphi')\delta(\varphi - \varphi') = \langle \bar{\phi}^2 \rangle \, . \end{aligned} \tag{2.1.53}$$

As an application of the above formalism we can compute the first few coefficients b_n for the case of the quartically self-interacting massless scalar we already considered above. In this case, since $\Phi_0(\varphi)$ is an even function, and so are all Φ_n with n even, see (2.1.38), only the b_n with n odd will be non-vanishing. We have the numerical solutions for the $\Phi_n(\varphi)$ up to $n = 6$ at hand, see figure 2.1, so we can go ahead and compute the b_n numerically up to $n = 6$ using the formula (2.1.52), and we do so to an accuracy of 10 decimal points:

n	b_n
0	0
1	$0.3177346504 H^2/\sqrt{\lambda}$
2	0
3	$0.0049057183 H^2/\sqrt{\lambda}$
4	0
5	$0.0001126695 H^2/\sqrt{\lambda}$
6	0

Table 2.2: Two-point function coefficients b_n for $n = 0, ..., 6$, computed numerically up to 10 decimal points.

These results will be useful later in this section.

Even though we know what the generic form for the two-point function is, the stochastic formalism also allows us to compute it in the form of a power-series expansion in the time argument around the point $t = 0$. This series expansion of G will be the main point of contact between the stochastic and Euclidean formalisms, so we will spend the remainder of this section studying its properties. For this purpose, it is convenient to make a further choice of the time arguments of G, which still does not lead to any loss of generality, since only the separation between the time argument matters, and we will choose $t_1 = t$, $t_2 = 0$ and write $G(t) \equiv G(t, 0)$ from now on.

The power-series expansion of $G(t)$ in question is simply a Taylor expansion around the point $t = 0$, and as such it reads

$$G(t) = \sum_{n=0}^{\infty} \frac{\mathrm{d}^n G(0)}{\mathrm{d}t^n} \frac{t^n}{n!} \, . \tag{2.1.54}$$

The Taylor coefficients, i.e. the derivatives evaluated at $t = 0$, can be computed analytically, as shown in [60], using the formula

$$\frac{\mathrm{d}^n G(0)}{\mathrm{d}t^n} = \int_{-\infty}^{\infty} \mathrm{d}\varphi \ \varphi \Gamma_\varphi^n [\rho_{1\mathrm{eq}}(\varphi)\varphi] \, , \tag{2.1.55}$$

with the differential operator Γ_φ as defined in equation (2.1.15) containing any potential $V(\varphi)$. Concretely, for the case of interest of a massless, minimally coupled scalar field with quartic potential $V(\varphi) = \frac{\lambda}{4!}\varphi^4$ we find, using the d-dimensional equilibrium distribution (2.1.42) and the d-dimensional version of the Fokker-Planck operator given in (2.1.16):

$$\int_{-\infty}^{\infty} \mathrm{d}\varphi \ \varphi \Gamma_{\varphi,d}^0 (\rho_{1\mathrm{eq}}\varphi) = \langle \bar{\phi}^2 \rangle = \sqrt{\frac{4!}{\lambda V_d}} \frac{\Gamma(\frac{3}{4})}{\Gamma(\frac{1}{4})} \, , \tag{2.1.56}$$

$$\int_{-\infty}^{\infty} \mathrm{d}\varphi\ \varphi\Gamma_{\varphi,d}(\rho_{1\mathrm{eq}}\varphi) = -\frac{1}{H(d-1)V_d}\,, \tag{2.1.57}$$

$$\int_{-\infty}^{\infty} \mathrm{d}\varphi\ \varphi\Gamma^2_{\varphi,d}(\rho_{1\mathrm{eq}}\varphi) = \frac{1}{H^2(d-1)^2V_d}\frac{\lambda}{2}\langle\bar{\phi}^2\rangle\,, \tag{2.1.58}$$

$$\int_{-\infty}^{\infty} \mathrm{d}\varphi\ \varphi\Gamma^3_{\varphi,d}(\rho_{1\mathrm{eq}}\varphi) = -\frac{1}{H^3(d-1)^3V_d}\frac{\lambda^2}{4}\langle\bar{\phi}^4\rangle\,, \tag{2.1.59}$$

$$\int_{-\infty}^{\infty} \mathrm{d}\varphi\ \varphi\Gamma^4_{\varphi,d}(\rho_{1\mathrm{eq}}\varphi) = \frac{1}{H^4(d-1)^4V_d}\left[\frac{\lambda^3}{8}\langle\bar{\phi}^6\rangle + \frac{\lambda^2}{V_d}\langle\bar{\phi}^2\rangle\right], \tag{2.1.60}$$

$$\int_{-\infty}^{\infty} \mathrm{d}\varphi\ \varphi\Gamma^5_{\varphi,d}(\rho_{1\mathrm{eq}}\varphi) = -\frac{1}{H^5(d-1)^5V_d}\left[\frac{\lambda^4}{16}\langle\bar{\phi}^8\rangle + \frac{5\lambda^3\langle\bar{\phi}^4\rangle}{2V_d} + \frac{\lambda^2}{V_d^2}\right], \tag{2.1.61}$$

where we integrated by parts and used the identity (2.1.33) several times, which we reprint here for convenience:

$$\langle V'(\bar{\phi})f(\bar{\phi})\rangle = \frac{1}{V_d}\langle f'(\bar{\phi})\rangle\,. \tag{2.1.62}$$

We can check these results up to $n = 4$ against the ones found in section IV B of [60] in $d = 4$ dimensions, using the relation

$$\frac{\mathrm{d}^n G(0)}{\mathrm{d}t^n} = \frac{3H^{2+n}}{2\pi\sqrt{\lambda}}\left(\frac{\lambda}{144\pi^2}\right)^{\frac{n}{2}}\frac{\mathrm{d}^n g(0)}{\mathrm{d}\tau^n}\,, \tag{2.1.63}$$

and we find

$$G(0) = \frac{3H^2\Gamma(\frac{3}{4})}{\sqrt{\lambda}\pi\Gamma(\frac{1}{4})}\,, \tag{2.1.64}$$

$$\frac{\mathrm{d}G(0)}{\mathrm{d}t} = -\frac{H^3}{8\pi^2}\,, \tag{2.1.65}$$

$$\frac{\mathrm{d}^2G(0)}{\mathrm{d}t^2} = \frac{H^4\sqrt{\lambda}\Gamma(\frac{3}{4})}{16\pi^3\Gamma(\frac{1}{4})}\,, \tag{2.1.66}$$

$$\frac{\mathrm{d}^3G(0)}{\mathrm{d}t^3} = -\frac{H^5\lambda}{128\pi^4}\,, \tag{2.1.67}$$

$$\frac{\mathrm{d}^4G(0)}{\mathrm{d}t^4} = \frac{13H^6\lambda^{\frac{3}{2}}\Gamma(\frac{3}{4})}{768\pi^5\Gamma(\frac{1}{4})}\,. \tag{2.1.68}$$

This agrees with our results above. For $n = 5$, which is not given in [60], the explicit value we find is

$$\frac{\mathrm{d}^5G(0)}{\mathrm{d}t^5} = -\frac{109H^7\lambda^2}{18432\pi^6}\,. \tag{2.1.69}$$

This series expansion turns out to have some interesting properties. In [60] it is remarked that the series expansion (2.1.54) is asymptotic, meaning that it has zero radius of convergence, and we want to prove this statement analytically and check it numerically in the case at hand.

Ratio test

To examine the convergence of the series it is convenient to rewrite it as

$$G(t) \equiv \frac{H^2}{\sqrt{\lambda}}\sum_{n=0}^{\infty}(H\sqrt{\lambda}t)^n G_n \equiv \frac{H^2}{\sqrt{\lambda}}\sum_{n=0}^{\infty}\tau^n G_n\,, \tag{2.1.70}$$

where we defined the rescaled dimensionless time variable $\tau = H\sqrt{\lambda}t$ and the dimensionless coefficients

$$G_n \equiv \frac{1}{H^{2+n}\lambda^{\frac{n-1}{2}}n!}\frac{\mathrm{d}^nG(0)}{\mathrm{d}t^n}$$

$$=\frac{1}{H^{2+n}\lambda^{\frac{n-1}{2}}n!}\int \mathrm{d}\varphi\ \varphi\rho_{1\mathrm{eq}}(\varphi)(\tilde{\Gamma}_{\varphi})^n\varphi \tag{2.1.71}$$

$$=\frac{1}{n!}\int \mathrm{d}\tilde{\varphi}\ \tilde{\varphi}\tilde{\rho}_{1\mathrm{eq}}(\tilde{\varphi})(\hat{\Gamma}_{\tilde{\varphi}})^n\tilde{\varphi} \tag{2.1.72}$$

where to get the second equality we integrated by parts and defined the differential operator

$$\tilde{\Gamma}_{\varphi} \equiv \frac{1}{H(d-1)}\left[-\frac{\lambda}{6}\varphi^3\frac{\partial}{\partial\varphi}+\frac{1}{V_d}\frac{\partial^2}{\partial\varphi^2}\right], \tag{2.1.73}$$

and to get the third equality we introduced the dimensionless quantities

$$\tilde{\varphi} \equiv \frac{\lambda^{\frac{1}{4}}\varphi}{H}, \quad \tilde{\rho}_{1\mathrm{eq}}(\tilde{\varphi}) \equiv \frac{H}{\lambda^{\frac{1}{4}}}\rho_{1\mathrm{eq}}(\tilde{\varphi}), \quad \hat{\Gamma}_{\tilde{\varphi}} \equiv \frac{1}{d-1}\left[-\frac{1}{6}\tilde{\varphi}^3\frac{\partial}{\partial\tilde{\varphi}}+\frac{1}{H^dV_d}\frac{\partial^2}{\partial\tilde{\varphi}^2}\right]. \tag{2.1.74}$$

A good critierion to check whether the series converges is the ratio test, which tells us that for arbitrary fixed $\tau \neq 0$ the series diverges if

$$L \equiv \lim_{n\to\infty}\tau\left|\frac{G_{n+1}}{G_n}\right| > 1\,. \tag{2.1.75}$$

In order to use this we need to determine the leading behaviour of the expression

$$\frac{1}{n!}\int_{-\infty}^{\infty}\mathrm{d}\tilde{\varphi}\ \tilde{\varphi}\tilde{\rho}_{1\mathrm{eq}}(\tilde{\varphi})(\hat{\Gamma}_{\tilde{\varphi}})^n\tilde{\varphi} \tag{2.1.76}$$

as n becomes large. To do so we notice that (2.1.76) will be a sum of the form

$$\sum_{l=0}^{n+1} a_l(n)\lambda^{\frac{l}{2}}\langle\bar{\phi}^{2l}\rangle\,, \tag{2.1.77}$$

where the coefficients will contain powers of n, as well as numbers raised to the n-th power. For the estimate of the asymptotic behaviour of the series, only the former n-dependence is important, since a dependence of the form C^n, with C some real number, will only contribute a multiplicative constant when taking the ratio $|G_{n+1}/G_n|$. Using (2.1.42) we find the following closed formula for the stochastic one-point functions:

$$\langle\bar{\phi}^{2n}\rangle = \left(\frac{4!}{\lambda V_d}\right)^{\frac{n}{2}}\frac{\Gamma(\frac{2n+1}{4})}{\Gamma(\frac{1}{4})}\,. \tag{2.1.78}$$

This formula fixes the n-dependence of the $\langle\bar{\phi}^{2n}\rangle$, so we have to determine how the $a_l(n)$ depend on n. To this end, it is useful to look at how $\tilde{\Gamma}_{\varphi}$ acts on the monomial $\tilde{\varphi}^n$:

$$\hat{\Gamma}_{\tilde{\varphi}}\tilde{\varphi}^n = \frac{1}{d-1}\left[-\frac{n}{6}\tilde{\varphi}^{n+2}+\frac{n(n-1)}{H^dV_d}\tilde{\varphi}^{n-2}\right]. \tag{2.1.79}$$

Therefore, we see that $\hat{\Gamma}_{\tilde{\varphi}}$ acting on any power of $\tilde{\varphi}$ generates two terms containing powers of $\tilde{\varphi}$ increased and decreased by 2, respectively, where the coefficient of the correlator involving the lower power of $\bar{\phi}$ contains one more power of n. This additional power of n is compensated by the fact that

$$\frac{\langle\bar{\phi}^{n+4}\rangle}{\langle\bar{\phi}^{n}\rangle} \sim n\,, \tag{2.1.80}$$

which we can explicitly see from (2.1.78), so

$$\int_{-\infty}^{\infty}\mathrm{d}\tilde{\varphi}\ \tilde{\varphi}\tilde{\rho}_{1\mathrm{eq}}(\tilde{\varphi})\hat{\Gamma}_{\tilde{\varphi}}\tilde{\varphi}^{n-1} \sim n\langle\bar{\phi}^{n+2}\rangle \sim n^2\langle\bar{\phi}^{n-2}\rangle\,, \tag{2.1.81}$$

i.e. it scales homogeneously with n. From this observation, we can conclude that the combination

$$\tilde{\varphi}(\hat{\Gamma}_{\tilde{\varphi}})^n\tilde{\varphi} \tag{2.1.82}$$

will give rise to a polynomial in $\tilde{\varphi}$ which, after being weighted with $\tilde{\rho}_{1\mathrm{eq}}(\tilde{\varphi})$ and integrated, will also scale homogeneously with n. To determine how G_n scales with n, we can thus just pick any one of the terms in (2.1.77) which is simple to compute and determine its n-scaling. We pick the terms which are generated solely by the single-derivative terms to do so:

$$\begin{aligned}
G_n \sim &\frac{1}{n!}\int_{-\infty}^{\infty}\mathrm{d}\tilde{\varphi}\;\tilde{\varphi}\tilde{\rho}_{1\mathrm{eq}}(\tilde{\varphi})\left[\tilde{\varphi}^3\frac{\partial}{\partial\tilde{\varphi}}\right]^n\tilde{\varphi}\\
=&\frac{\lambda^{\frac{n+1}{2}}\langle\bar{\phi}^{2n+2}\rangle}{H^{2n+2}n!}\prod_{m=0}^{n-1}(2m+1)\\
=&\frac{(2n-1)!\,!}{n!}\left(\frac{4!}{V_d}\right)^{n+1}\frac{\Gamma(\frac{2n+3}{4})}{\Gamma(\frac{1}{4})}\,.
\end{aligned} \tag{2.1.83}$$

This fixes the scaling of G_n, which is enough to determine the asymptotic behaviour of the Taylor coefficients only if we can assume that there are no cancellations between the coefficients of the different terms in the polynomial which drastically change the behaviour of the series coefficients. We will see below that this is not the case. Making this assumption, we can approximate for large values of n

$$G_n\Big|_{n\gg 1}\approx A\times C^n\times\frac{(2n-1)!\,!}{n!}\Gamma\left(\frac{2n+3}{4}\right), \tag{2.1.84}$$

where the coefficients A and C are real numbers, and the approximation should improve as n grows and become exact in the limit $n\to\infty$.

We can now use this result in the ratio test:

$$\begin{aligned}
L=&\lim_{n\to\infty}\tau\left|\frac{G_{n+1}}{G_n}\right|\\
=&C\tau\lim_{n\to\infty}\frac{(2n+1)!\,!\,n!}{(2n-1)!\,!\,(n+1)!}\frac{\Gamma(\frac{2n+5}{4})}{\Gamma(\frac{2n+3}{4})}\\
=&C\tau\lim_{n\to\infty}\left[\sqrt{2n}+\mathcal{O}(n^{-\frac{1}{2}})\right].
\end{aligned} \tag{2.1.85}$$

The obtained result naively goes to ∞ like $\sqrt{n}$ for large n for any value of τ, which seems to indicate that the series is indeed asymptotic. We can now check numerically for $d=4$ that, indeed, this is the correct leading asymptotic behaviour of the series coefficients, and we can also determine the coefficients A and C numerically.

Numerical computation of the G_n in $d=4$

We start by inspecting the behaviour of the dimensionless Taylor series coefficients G_n in $d=4$ dimensions, which can be computed in principle to arbitrarily high n using the formula

$$G_n=\frac{1}{n!}\int_{-\infty}^{\infty}\mathrm{d}\tilde{\varphi}\;\tilde{\varphi}\tilde{\rho}_{1,\mathrm{eq}}(\tilde{\varphi})(\hat{\Gamma}_{\tilde{\varphi}})^n\tilde{\varphi}\,. \tag{2.1.86}$$

The dimensionless quantities we defined in (2.1.74) in $d=4$ dimensions read

$$\tilde{\rho}_{1,\mathrm{eq}}(\tilde{\varphi})\equiv\frac{2}{\sqrt{\frac{3}{\pi}}\Gamma(\frac{1}{4})}\exp\left(-\frac{\pi^2}{9}\tilde{\varphi}^4\right), \tag{2.1.87}$$

and

$$\hat{\Gamma}_{\tilde{\varphi}} \equiv -\frac{1}{18}\tilde{\varphi}^3\frac{\partial}{\partial\tilde{\varphi}} + \frac{1}{8\pi^2}\frac{\partial^2}{\partial\tilde{\varphi}^2}\,. \tag{2.1.88}$$

Acting n times with $\hat{\Gamma}_{\tilde{\varphi}}$ on $\tilde{\varphi}$ produces a polynomial of degree $2n+1$, which we then need to multiply by $\tilde{\varphi}$, weight with $\rho_{1,\mathrm{eq}}(\tilde{\varphi})$ and integrate. This procedure can be automated, and we computed the first 2301 coefficients G_n using `Mathematica`, which turn out to be sign-alternating, starting from $G_0 > 0$, a pattern that could already be seen in the first five explicit results (2.1.64)-(2.1.69) and holds true at higher orders, at least to the extent we were able to check. Plotting the absolute value of the G_n agains the order of expansion $n \in [0, 2300]$ we find the plot shown in figure 2.2.

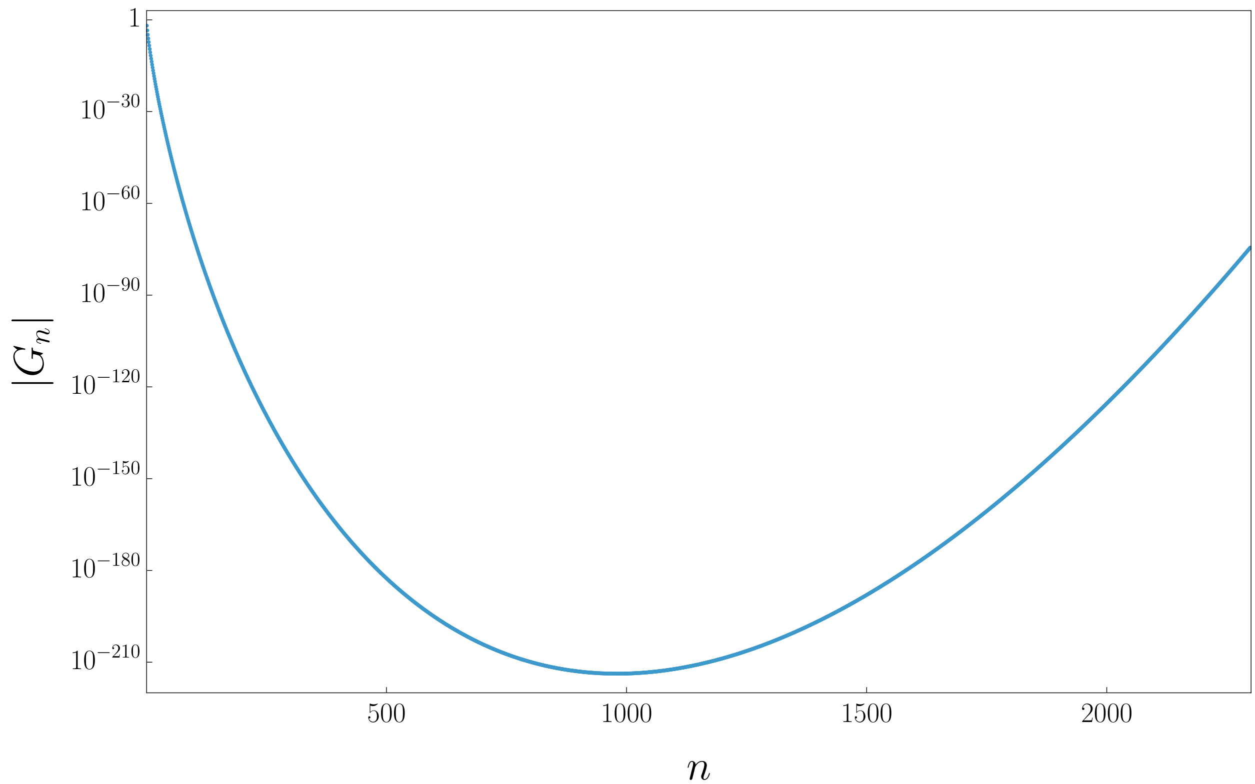

Figure 2.2: Log-linear plot of the absolute value of the dimensionless Taylor coefficients G_n, plotted against $n \in [0, 2300]$. It is clearly visible that the coefficients decrease in magnitude up until around $n \approx 1000$ and then start increasing again, which is the expected behaviour for the coefficients of an asymptotic series.

We thus find the typical pattern of the coefficients of an asymptotic series. The best approximation for small and fixed t would be obtained by truncating the series around $n \approx 1000$, which is however still not useful if we are interested in large values of t.

Above, we derived the following estimate for the asymptotic behaviour of the series coefficients:

$$G_n\Big|_{n\gg 1} \approx A \times C^n \times \frac{(2n-1)!\,!}{n!}\Gamma\left(\frac{2n+3}{4}\right), \tag{2.1.89}$$

which led to the following result for the ratio test:

$$L = C\tau \lim_{n\to\infty}\left[\sqrt{2n} + \mathcal{O}(n^{-\frac{1}{2}})\right]. \tag{2.1.90}$$

By plotting the ratio $|G_{n+1}/G_n|$ and fitting the expected square-root behaviour to it we get the plot shown in figure 2.3.

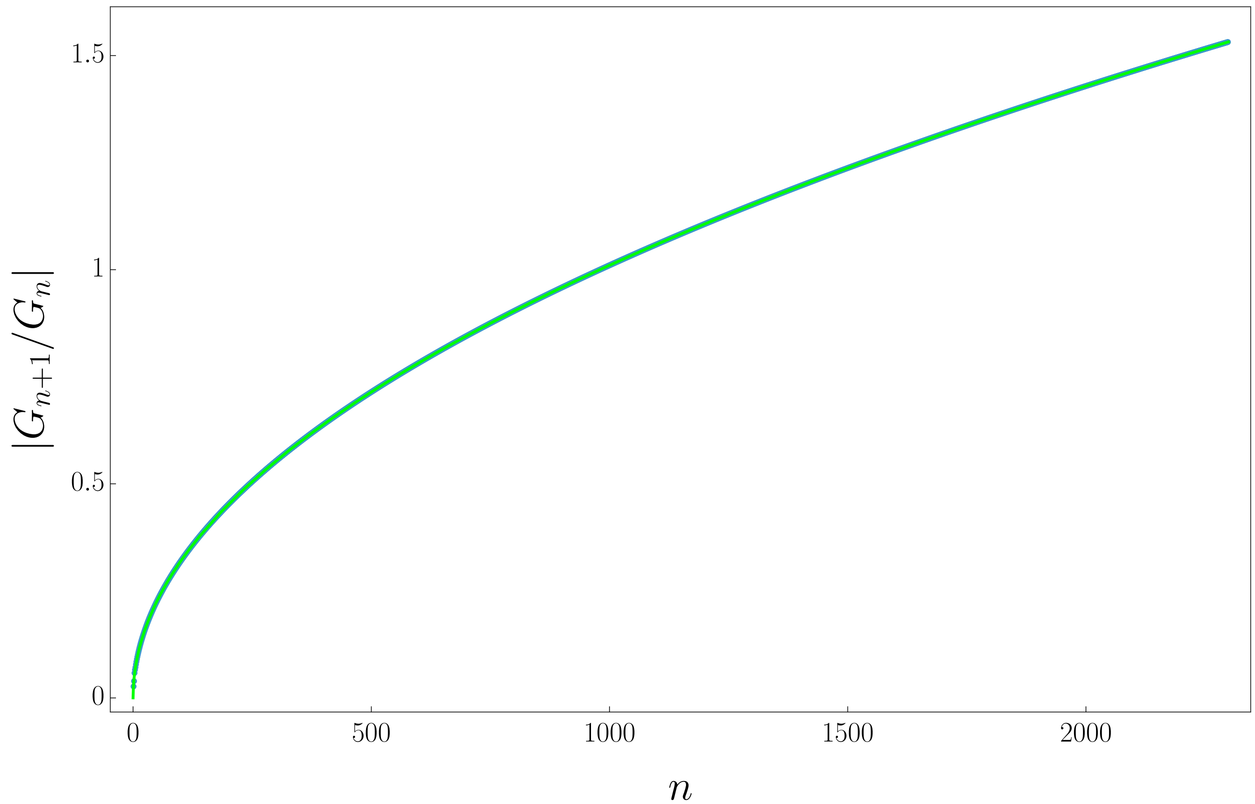

Figure 2.3: Plot of the ratio $|G_{n+1}/G_n|$ (blue dots), plotted against $n \in [0, 2000]$, fitted by a function of the form $\sqrt{n}$ (green curve).

We find that the ratio can be fitted by a function of the form

$$f(n) = (0.03195...)\sqrt{n}\,, \tag{2.1.91}$$

with an error between the two of $\mathcal{O}(10^{-7})$ already starting at $n \approx 200$, and decreasing after that. We therefore find the numerical value

$$C = -\frac{(0.03195...)}{\sqrt{2}}\,, \tag{2.1.92}$$

so we find the following leading asymptotic estimate:

$$G_n\Big|_{n\gg 1} \approx A \times (-1)^n \left(\frac{0.03195...}{\sqrt{2}}\right)^n \frac{(2n-1)!\,!}{n!}\Gamma\left(\frac{2n+3}{4}\right), \tag{2.1.93}$$

where the overall constant A is still undetermined. We can determine it by taking the ratio of the estimated G_n and of the numerically computed true values of G_n and find:

$$A = \frac{G_{n,\text{estimate}}}{G_n}\Bigg|_{n\gg 1} = 2.37511\ldots\,. \tag{2.1.94}$$

We thus find that, indeed, the series expansion of $G(t)$ is an asymptotic one, with a predictable leading divergent behaviour as $n \to \infty$.

It is worthwhile to try to understand why this unusual behaviour arises. We can do so by using the known exact form (2.1.50) and explicitly expanding the exponentials appearing in it, with $t_1 = t$, $t_2 = 0$:

$$G(t) = \sum_{n=1}^{\infty} b_n e^{-\Lambda_n t} = \sum_{n=1}^{\infty} b_n \sum_{m=0}^{\infty} \frac{(-\Lambda_n t)^m}{m!} \,. \tag{2.1.95}$$

Comparing this expression with the generic formula

$$G(t) = \sum_{n=0}^{\infty} \frac{\mathrm{d}^n G(0)}{\mathrm{d}t^n} \frac{t^n}{n!} \tag{2.1.96}$$

leads us to identify the summands as

$$\frac{\mathrm{d}^m G(0)}{\mathrm{d}t^m} = \sum_{n=1}^{\infty} b_n (-\Lambda_n)^m \,. \tag{2.1.97}$$

Notice that we had to interchange the order of the two sums appearing in (2.1.95) to get to this result. Each coefficient of the series is given by an infinite sum over the product of the relaxation Eigenvalues to some power and the coefficients b_n. By expanding the exact result for small t, we scramble the information contained in the relaxation Eigenvalues and the b_n's, which provides a series of decaying exponentials which is well-behaved for large t, and obtain instead an asymptotic series which diverges for any value of t different than zero. The mathematical reason why we end up with such an asymptotic series is that the interchange of sums we carried out does not leave the value of the resulting sum invariant, because the double-sum in (2.1.95) is not absolutely convergent for any $t > 0$. Using the fact that b_n, $\Lambda_n > 0$ we find

$$\sum_{n=1}^{\infty} \sum_{m=0}^{\infty} \left| \frac{b_n(-\Lambda_n t)^m}{m!} \right| = \sum_{n=1}^{\infty} \sum_{m=0}^{\infty} \frac{b_n(\Lambda_n t)^m}{m!} = \sum_{n=1}^{\infty} b_n e^{\Lambda_n t} \to \infty \tag{2.1.98}$$

for any value of $t > 0$, since the Λ_n keep increasing with increasing n, so we are summing over exponentially growing numbers. Physically, the stochastic formalism is describing, by construction, time scales that are of order $t \sim H^{-1}$ or larger [59], such that the point $t = 0$ around which we are expanding is, strictly speaking, outside the regime of validity of the theory. Both of these facts are reflected by the divergence of the Taylor expansion in question. This can be contrasted with the massive non-interacting case, where only $b_1 \neq 0$ [60] and the asymptotic expansion can be univocally summed to the known leading term of the free massive de Sitter two-point function for $t \to \infty$, which in $d = 4$ dimensions reads

$$G(t) = \frac{3H^4}{8\pi^2 m^2} e^{-\frac{m^2}{3H^2} t} \,. \tag{2.1.99}$$

Notice that the form of the series expansion of $G(t)$ we have been considering so far takes the form of an expansion in powers of $t = \ln(a(t))$. In a quantum-field-theoretic context, this type of expansion is what the perturbative treatment of correlation functions of very light fields yields, and the growing powers of t that one finds as one computes higher terms in the series are precisely the secularly growing terms that plague the naive perturbative treatment of these quantities in field theory. In the stochastic formalism this problem is avoided by simply computing the exact form of the two-point function by solving the Fokker-Planck equation, which yields a well-behaved result as $t \to \infty$. This procedure has been regarded in the literature as a way to resum the secular logs, see e.g. [67], drawing a parallel to the summation of large logarithms by means of the renormalization-group equations in standard QFT, which has then led to the interpretation of this procedure as a realization of the idea of the "dynamical renormalization group" [88–91] in de Sitter space.

Motivated by the interpretation of the Fokker-Planck equation effectively resumming the series in $\ln(a(t))$, we can imagine only having access to the asymptotic expansion of $G(t)$, without the knowledge of its exact form, or the ability to compute the relaxation Eigenvalues by means of the Fokker-Planck equation, and ask whether it is still possible to sum this asymptotic series, by means of some other procedure, to get a well behaved result in the limit $t \to \infty$. We will show numerically that the answer to this question is affirmative, and that the asymptotic series can be summed using Padé-Borel resummation, although, of course, we will not be able to reproduce the exact behaviour of $G(t)$, since it involves infinitely many summands. We will see below that this scenario indeed arises in the context of the analytic continuation of the Euclidean two-point function to Lorentzian de Sitter, so studying the viability of this resummation procedure will help us make a more precise and well-founded statement about the meaning of the analytic continuation of the Euclidean result, and its usefulness in a practical sense.

Summation of the asymptotic stochastic series

To show that we can reconstruct the original expression (2.1.50) it will prove convenient to work using the dimensionless time variable τ and series coefficients G_n defined above, in terms of which the expansion of $G(t)$ reads

$$G(\tau) = \frac{H^2}{\sqrt{\lambda}} \sum_{n=0}^{\infty} \tau^n G_n \,. \tag{2.1.100}$$

Our aim will to reproduce the following truncation of the exact result:

$$G_{\text{trunc}}(t) \equiv b_1 e^{-\Lambda_1 t} + b_3 e^{-\Lambda_3 t} + b_5 e^{-\Lambda_5 t} \,, \tag{2.1.101}$$

with our values for the Λ_n and b_n computed above, which we reprint here:

n	Λ_n	b_n
1	$0.0363030441 H\sqrt{\lambda}$	$0.3177346504 H^2/\sqrt{\lambda}$
3	$0.2190951808 H\sqrt{\lambda}$	$0.0049057183 H^2/\sqrt{\lambda}$
5	$0.4736902674 H\sqrt{\lambda}$	$0.0001126695 H^2/\sqrt{\lambda}$

In particular, it is important to have determined the Λ_n to a high degree of accuracy, as $G_{\text{trunc}}(t)$ is exponentially sensitive to them.

The strategy is to compute the Borel transform of $G(\tau)$, which reads

$$B[G](u) \equiv \sum_{n=0}^{\infty} \frac{G_n}{n!} u^n \,, \tag{2.1.102}$$

and we use it compute the Borel sum of the asymptotic series using the formula

$$\tilde{G}(\tau) \equiv \frac{1}{\tau} \int_0^{\infty} \mathrm{d}u \; e^{-\frac{u}{\tau}} B[G](u) \,. \tag{2.1.103}$$

If the series is Borel-summable, then we should find $\tilde{G}(\tau) = G(\tau)$. For this to work, the Borel transform (2.1.102) should converge, which is plausible, since this procedure is known to work for factorially divergent series, and the series under consideration diverges slower than that, as can be seen from our estimate (2.1.93). Further, the series is sign-alternating, which usually leads to poles in the complex u half-plane with $\mathrm{Re}(u) < 0$, such that $B[G](u)$ should have no poles for $u \in [0, \infty)$, which would obstruct the integration contour to compute $\tilde{G}(\tau)$.

Even though we have an analytic formula for the G_n, we are not able to obtain a closed form for the Borel transform, since we would need to know the G_n in closed form, which we do not, and then we would need to evaluate the sum (2.1.102) analytically, since term-by-term integration of $B[G](u)$ in (2.1.103) will just reproduce the summands of the original asymptotic series by construction. In practice, we thus resort to the well-known approximation procedure outlined in [92, 93] to deal with this situation: we truncate the series (2.1.102) at some finite order $n = 2m$ and construct the diagonal (m, m) Padé approximant, which approximates (2.1.102) close to $\tau = 0$. We then plug the obtained Padé approximant into (2.1.103) as an approximation of $B[G](u)$ and perform the integral numerically to as large a value of u as possible. If the result reproduces (2.1.101) to fairly large values of τ, then this is a good indication that the asymptotic series is Borel summable, i.e. that $\tilde{G}(\tau) = G(\tau)$.

We now go through this procedure step by step. We find that the (25, 25) Padé approximant, which we define as

$$R(u) \equiv \frac{\sum_{i=1}^{25} a_i u^i}{1 + \sum_{j=1}^{25} b_j u^j} , \tag{2.1.104}$$

constructed using the truncation at $n = 50$ of the series defining the Borel transform (2.1.102) already reproduces the behaviour of higher truncations of the transform up to $u = 400$ very well, as can be seen in figure 2.4.

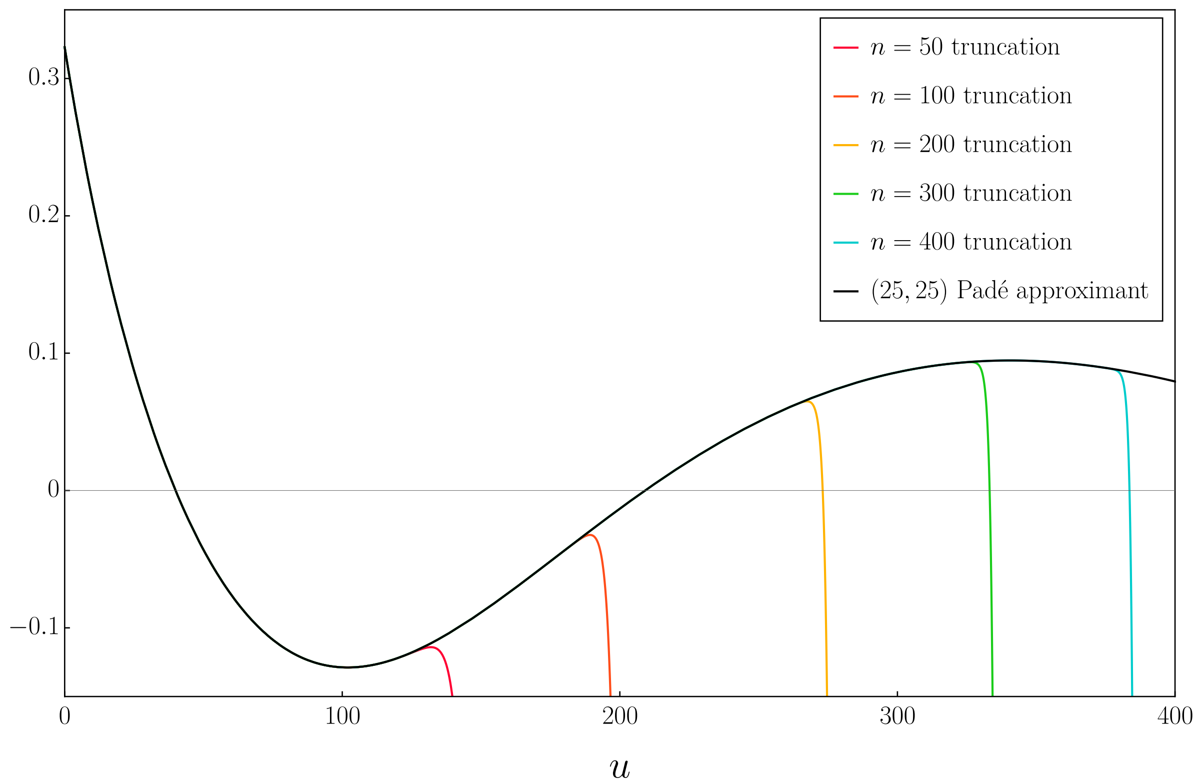

Figure 2.4: Comparison of different Borel truncations (colored lines) with the (25, 25) Padé approximant as a function of the Borel variable u (black line). Up to the point where the different Borel truncations start diverging the lines are indistinguishable from each other, which indicates the faithfulness of the approximation we are using in this range.

Notice the oscillatory behaviour of the approximate form of the Borel transform, which is typical for the transform of sign-alternating series [93].

Finally, we plug the obtained Padé approximant into (2.1.103) and integrate numerically over the range $u \in [0, 10^4]$ while sampling τ-values in the range $\tau \in [1, 150]$ with step size $\Delta\tau = 1$. Doing so, and plotting the result together with the truncation of the exact result (2.1.101), we obtain the following plot shown in figure 2.5.

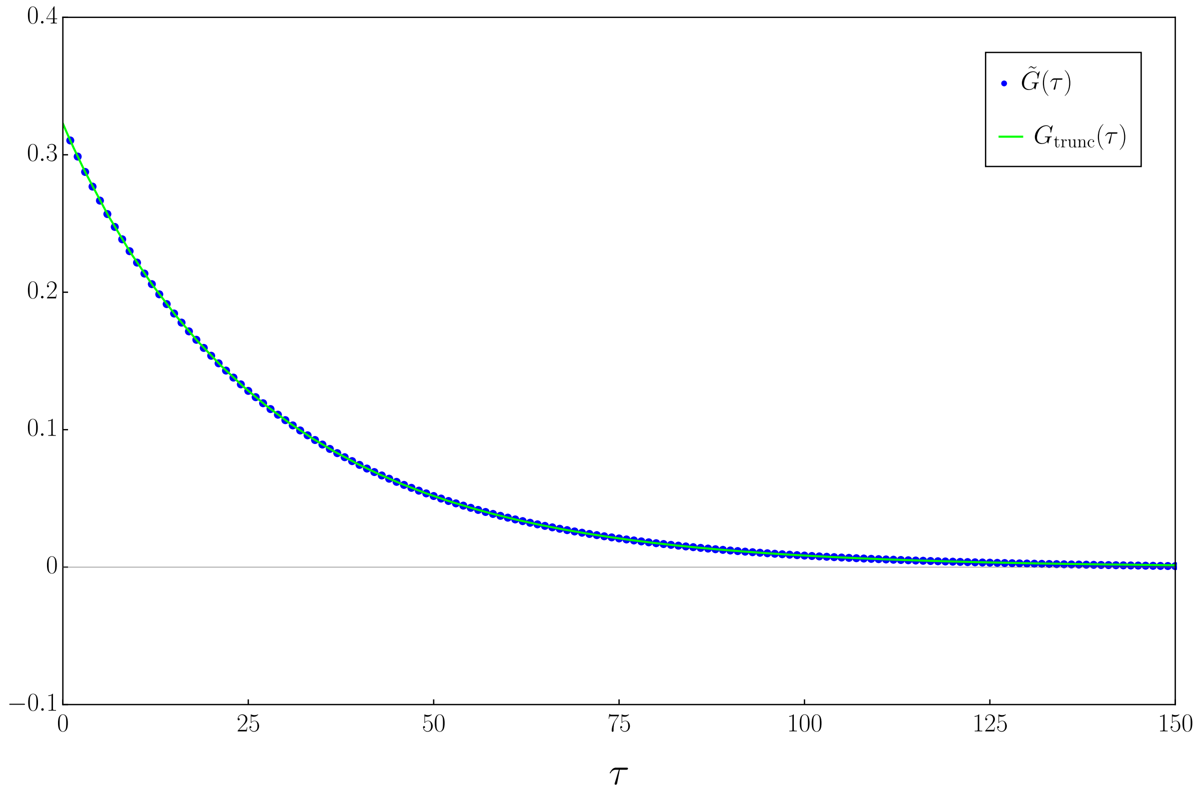

Figure 2.5: Plot of the Borel sum $\tilde{G}(\tau)$, obtained numerically from the $(25, 25)$ Padé approximant (blue dots), overlaid with the truncation of the exact result $G_{\rm trunc}(\tau)$ (green line).

Graphically, the agreement seems very good over the entire considered range of values for τ, where however towards the tail of the plot the Borel sum starts to undershoot the truncation of the exact result. Notice that since $\sqrt{\lambda} \ll 1$ and $\tau = H\sqrt{\lambda}t$ this approximation of the exact result is already a good one up until very large values of Ht, i.e. very large multiples of the Hubble time. We can quantify the goodness of the agreement using the root mean square deviation (RMSD) between the truncated exact result and the Borel sum:

$$\mathrm{RMSD} = \frac{1}{\sqrt{150}}\sqrt{\sum_{n=1}^{150}\Big(G_{\rm trunc}(n\Delta\tau) - \tilde{G}(n\Delta\tau)\Big)^2} = 1.72 \times 10^{-4}\,, \tag{2.1.105}$$

which we can understand as the average difference between any two points of $\tilde{G}(\tau)$ and $G_{\rm trunc}(\tau)$ being $\mathcal{O}(10^{-4})$. The agreement can be improved systematically by using Padé approximants of increasing rank to compute the Borel sum, and eventually also including more terms in the truncation of the exact result (2.1.101). We can expect that the deviations between $\tilde{G}(\tau)$ and $G_{\rm trunc}(\tau)$ are largest close to the origin, where the error due to the truncation of the exact result dominates, and towards the tail of the curve, where the error due to the Padé approximant being constructed using only finitely many G_n dominates.

To conclude this discussion, since we find that already with the used fairly modest approximations we obtain good agreement between the Borel sum and the (truncated) exact result in the considered range of values, the asymptotic expansion of the stochastic two-point function valid for small times appears to be Borel summable to the exact result (2.1.50), which is valid for arbitrarily large times. The Borel summability of the asymptotic expansion of stochastic results was noted also in the recent study [94], where the above procedure was applied to stochastic one-point functions. To the best of our knowledge, the discussion of the summability of the stochastic two-point function has been carried out here for the first time.

Of course, while working within the stochastic formalism, the present discussion is essentially just a mathematical curiosity, since one can always resort to solving the Fokker-Planck equation numerically to get the appropriate form of the desired result at late times. However, since it is known that Stochastic Inflation is equivalent to the full Lorentzian QFT-framework in the leading IR-approximation [64], and the properties of perturbation theory at high orders in QFT are far from trivial, the study of their stochastic counterpart can help to shed some light on them, at least as far as the leading behaviour as $t \to \infty$ is concerned. For our purposes, the discussion of the perturbative expansion of $G(t)$ will help us understand the properties and meaning of the analytic continuation of the analogous quantity computed in Euclidean de Sitter space, to which we now turn.

2.2 Massless, minimally coupled scalar field in Euclidean de Sitter space

We start by reviewing the Euclidean formalism for the treatment of the IR-divergences appearing in correlation functions of massless, minimally coupled scalar fields in de Sitter, with the goal of using it to compute the two-point function of this field in the interacting theory. In particular, we want to study its analytic continuation to Lorentzian de Sitter space and compare the resulting expression to the stochastic results we considered above.

The Euclidean formalism to successfully deal with the IR-divergences in correlation functions of massless scalars was set up in [75] and systematically developed in [76], so we will largely follow their construction. It will prove convenient to work in general spacetime dimension d to leave the possibility for the implementation of dimensional regularization to treat the UV-divergences of the theory open, and also to keep the discussion and the comparison of the Euclidean and stochastic results as general as possible. As we will see below, this will not complicate the discussion with respect to the four-dimensional treatment in any way.

2.2.1 From de Sitter spacetime in global coordinates to the sphere, definition of the observables

The starting point of the construction of the Euclidean formalism is the de Sitter metric in global coordinates, which we discussed in chapter 1, see the discussion in section 1.2.1. We can define it using the line element, which reads

$$\mathrm{d}s^2 = \mathrm{d}t^2 - \frac{1}{H^2}\cosh^2(Ht)\mathrm{d}\Omega_{d-1}\,, \tag{2.2.1}$$

where $\mathrm{d}\Omega_{d-1}$ defines the line element on the unit sphere S^{d-1}. The Euclidean version of this metric is obtained by relating the time variable to a dimensionless angle $\theta \in [0, 2\pi)$ by the defining equation

$$t \equiv -\frac{i}{H}\left(\theta - \frac{\pi}{2}\right), \tag{2.2.2}$$

and for this equation to define a one-to-one mapping between t and θ we must also assume that the time variable has periodicity $2\pi i/H$, where the end points of this interval have to be identified. We are thus compactifying the time variable. In terms of the Euclidean time variable the line element now reads

$$\mathrm{d}s^2 = -\frac{1}{H^2}\left[\mathrm{d}\theta^2 + \sin^2(\theta)\mathrm{d}\Omega_{d-1}\right] = -\frac{1}{H^2}\mathrm{d}\Omega_d\,, \tag{2.2.3}$$

which, up to an overall minus sign, is nothing but the line element of a d-dimensional sphere with radius $1/H$. In this sense, we can say that Euclidean de Sitter space is equivalent to the d-dimensional sphere with radius $1/H$.

Having defined the space in which we wish to work, we now go over to the definition of the observables we wish to study in this setting. We will be interested in studying Euclidean correlation functions of the massless field ϕ. Since in the present setting there is no preferred variable which can play the role of time, these will not be the in-in correlation functions we discussed above in section 1.4, which are the main observables of interest in the Lorentzian setting. We will instead be interested in computing unordered correlation functions of the form

$$\langle\phi(x_1)...\phi(x_n)\rangle = \frac{\int \mathcal{D}[\phi]e^{-S_E}\phi(x_1)...\phi(x_n)}{\int \mathcal{D}[\phi]e^{-S_E}}\,. \tag{2.2.4}$$

Since the above derivation of the Euclidean line element required the compactification of the time variable, it is not obvious that the computation of these objects carried out in the Euclidean spacetime, and then analytically continued to the Lorentzian signature by inverting (2.2.2), will yield results that are valid for the full range of values of the real-valued time variable, $t \in (-\infty, \infty)$. However, in [77] it was shown that for interacting scalar field theories with $m^2 > 0$ the analytic continuation of Euclidean correlators indeed coincides with the Lorentizan result computed in the in-in formalism in the Bunch-Davies vacuum, so these are indeed the physically relevant objects to study.

Of course, we expect to find the same IR-divergent behaviour of the naive perturbative expansion of these correlation functions that is observed in the Lorentzian setting. However, studying this pathological behaviour in the Euclidean setting will allow us to gain further understanding of this effect, and to construct a well-defined, modified perturbative expansion of the correlators on the sphere, following [75, 76].

2.2.2 Free theory: mode functions, two-point function and IR-divergences in the massless theory

A good starting point to understand the origins of IR-divergences in the massless theory is to consider the quantization of the free, massive, minimally coupled, real scalar field, which is defined by the Euclidean version of the action (1.3.1),

$$S_E = \frac{1}{2}\int \mathrm{d}^d x\, \sqrt{g(x)}\Big[g^{\mu\nu}\partial_\mu\phi(x)\partial_\nu\phi(x) + m^2\phi^2(x)\Big]\,. \tag{2.2.5}$$

The Euler-Lagrange equation that one derives from this action is the Euclidean version of (1.3.3), and it reads

$$\left[\frac{1}{\sqrt{g}}\partial_\mu\sqrt{g}g^{\mu\nu}\partial_\nu - m^2\right]\phi(x) = 0\,, \tag{2.2.6}$$

where the differential operator acting on $\phi(x)$ is the Laplace-Beltrami operator, and we will abbreviate it in the following as

$$\Box_x \equiv \frac{1}{\sqrt{g(x)}}\partial^x_\mu\sqrt{g(x)}g^{\mu\nu}(x)\partial^x_\nu\,. \tag{2.2.7}$$

The Green's function associated to this equation of motion is of course the free two-point function of the theory,

$$G_{\text{free}}(x,y) \equiv \langle\phi(x)\phi(y)\rangle\,, \tag{2.2.8}$$

which satisfies the equation

$$\Big[\Box_x - m^2\Big]G_{\text{free}}(x,y) = -\frac{1}{\sqrt{g(x)}}\delta^{(d)}(x-y)\,, \tag{2.2.9}$$

as well as the analogous equation with $x \leftrightarrow y$. The solution to this equation is most simply found by decomposing $G_{\text{free}}(x,y)$ in terms of a set of orthogonal functions on the sphere, and the unique complete set of othonormal Eigenfunctions of the Laplace-Beltrami operator on the d-dimensional unit sphere S^d are the hyperspherical harmonics $Y_{\vec{L}}(x)$ [95]. They are a generalization of the ordinary, two-dimensional spherical harmonics $Y_{lm}(\theta,\varphi)$, and they depend on the d angles we are using to parametrize the surface of the sphere. They are labelled by the vector of angular momenta

$$\vec{L} \equiv (L, L_{d-1}, ..., L_1)\,, \quad L \geq L_{d-1} \geq ... \geq |L_1|\,, \tag{2.2.10}$$

with $L,...,L_2 \in \mathbb{N}_0$ and $L_1 \in \mathbb{Z}$, and they satisfy the eigenvalue equation

$$\Box_x Y_{\vec{L}}(x) = -H^2 L(L+d-1) Y_{\vec{L}}(x)\,. \tag{2.2.11}$$

In our case, since we are working on a sphere with radius $1/H$, they are a complete, *orthogonal* set of functions, satisfying the orthogonality relation

$$\int \mathrm{d}^d x\ \sqrt{g(x)} Y_{\vec{L}}(x) Y^*_{\vec{L}'}(x) = \frac{1}{H^d}\delta_{\vec{L}\vec{L}'} \tag{2.2.12}$$

and the completeness relation

$$\sum_{\vec{L}} Y_{\vec{L}}(x) Y^*_{\vec{L}}(y) = \frac{1}{H^d\sqrt{g(x)}}\delta^{(d)}(x-y)\,. \tag{2.2.13}$$

Since the two-point function is a bi-scalar function on the sphere, a decomposition of it in terms of the hyperspherical harmonics of the form

$$G_{\mathrm{free}}(x,y) = \sum_{\vec{L},\vec{L}'} G_{\vec{L}\vec{L}'} Y_{\vec{L}}(x) Y^*_{\vec{L}'}(y) \tag{2.2.14}$$

must exist, and, using (2.2.11) equation (2.2.9) becomes

$$\sum_{\vec{L},\vec{L}'} [H^2 L(L+d-1)+m^2] G_{\vec{L},\vec{L}'} Y_{\vec{L}}(x) Y^*_{\vec{L}'}(y) = \frac{1}{\sqrt{g(x)}}\delta^{(d)}(x-y)\,. \tag{2.2.15}$$

We see that the expression

$$G_{\vec{L},\vec{L}'} = \frac{H^d \delta_{\vec{L}\vec{L}'}}{H^2 L(L+d-1)+m^2} \tag{2.2.16}$$

together with the completeness relation (2.2.13) satisfies the above equation. We thus find the following representation for the free Euclidean two point function:

$$G_{\mathrm{free}}(x,y) = H^{d-2} \sum_{\vec{L}} \frac{Y_{\vec{L}}(x) Y^*_{\vec{L}}(y)}{L(L+d-1)+m^2/H^2}\,. \tag{2.2.17}$$

This representation is very useful, because it allows us to isolate the source of its IR divergence in the limit $m^2 \to 0$ in the present setting, as was first pointed out in [75]. We can make use of the fact that the lowest hyperspherical harmonic $Y_{\vec{0}}$ is just a constant, and its absolute value squared is

$$|Y_{\vec{0}}|^2 = \frac{1}{V_d H^d}\,, \tag{2.2.18}$$

which can immediately be derived from (2.2.12), to split the sum in (2.2.17) up as

$$G_{\mathrm{free}}(x,y) = \frac{1}{V_d m^2} + H^{d-2} \sum_{\vec{L}\neq 0} \frac{Y_{\vec{L}}(x) Y^*_{\vec{L}}(y)}{L(L+d-1)+m^2/H^2}\,. \tag{2.2.19}$$

In the above equation, and as in the previous section, V_d denotes the volume of Euclidean de Sitter space

$$V_d \equiv \int \mathrm{d}^d x\ \sqrt{g(x)} = \frac{2\pi^{\frac{d+1}{2}}}{\Gamma(\frac{d+1}{2}) H^d}\,. \tag{2.2.20}$$

From (2.2.19) we see that the divergence as $m^2 \to 0$ is caused solely by the term we separated from the sum, which is associated to the mode of the field with vanishing angular momentum, $\vec{L}=0$. In the following, we will refer to this mode as the “zero mode”.

This divergence can be understood at the level of the Euclidean path integral as well, by implementing the following decomposition of the scalar field:

$$\phi(x) = \phi_0 + \hat{\phi}(x)\,. \tag{2.2.21}$$

Here, ϕ_0 denotes the constant part of the field, which is the zero-mode contribution to it, while $\hat{\phi}$ receives contributions from all the other, non-constant modes of the field. In terms of these new variables, the Euclidean action for the free, massive scalar field (2.2.5) becomes

$$S_E = \frac{m^2}{2} V_d \phi_0^2 + \frac{1}{2}\int \mathrm{d}^d x\, \sqrt{g(x)}\Big[g^{\mu\nu}\partial_\mu\hat{\phi}(x)\partial_\nu\hat{\phi}(x) + m^2\hat{\phi}^2(x)\Big]\,, \tag{2.2.22}$$

where we used the fact that ϕ_0 is a constant, as well as the equation (2.2.20). Notice that terms linear in $\hat{\phi}(x)$ have been set to zero, which follows directly from

$$\int \mathrm{d}^d x\, \sqrt{g(x)} Y_{\vec{L}}(x) = 0\,, \tag{2.2.23}$$

which in turn follows from $Y_{\vec{0}} = \text{const.}$ together with the orthogonality relation (2.2.12). Further, in terms of the new field variables defined in (2.2.21), the path integral measure factorizes as follows:

$$\int \mathcal{D}[\phi] = \int_{-\infty}^{\infty} \mathrm{d}\phi_0 \int \mathcal{D}[\hat{\phi}]\,, \tag{2.2.24}$$

where the path integral over ϕ_0 is just an ordinary one-dimensional integral ranging over all possible (real) values of ϕ_0. From (2.2.22) we see that the mass term is the only term that renders the ϕ_0-path integral convergent, since there is no gradient term associated to the zero-mode field. If we let $m^2 \to 0$ this term vanishes, the exponential in the path integral is no longer suppressing the integrand at large values of ϕ_0, and the ϕ_0-integral diverges. This divergence is in one-to-one correspondence with the divergence we observed in $G_{\text{free}}(x, y)$, since we are dealing with a Gaussian theory: by Wick's theorem, any correlation function we would like to compute will reduce to a product of two-point functions.

Therefore, just as in the Lorentzian setting, the conclusion is that the free, massless scalar field theory is ill-defined. However, what we are actually interested in is the interacting theory and, as was argued in [75] and in full analogy to the stochastic story, once we include an interaction term in the action it will have the effect of stabilizing the zero-mode contribution to the path integral, thus removing the pathologies we observed above from the theory. However, the key point is that to get sensible results for the correlation functions we cannot treat the pure zero-mode contribution to the path integral perturbatively. Nevertheless, it is possible to construct a modified, semi-perturbative expansion (borrowing this term from [96]) for the correlation functions of the theory of a massless, self-interacting scalar field which yields well-defined, IR-finite results.

2.2.3 Semi-perturbative expansion of massless Euclidean correlators in the interacting theory

In the previous section the zero mode were identified as the origin of IR divergences in the Euclidean correlators of the massless theory. Building on [75], a modified, systematic perturbative expansion which treats the zero-mode field exactly was developed in [76], which we briefly review in this section.

We start from the Euclidean action of the massless, minimally coupled, quartically self-interacting scalar field,

$$S_E = \int \mathrm{d}^d x\, \sqrt{g(x)}\left[\frac{1}{2} g^{\mu\nu}\partial_\mu\phi(x)\partial_\nu\phi(x) + \frac{\lambda}{4!}\phi^4(x)\right]. \tag{2.2.25}$$

and, as we did above for the free massive field, we implement the field split (2.2.21) in it, which, using (2.2.23) to eliminate terms linear in $\hat{\phi}(x)$, leads us to the following expression:

$$S_E = \frac{V_d\lambda}{4!}\phi_0^4 + \int \mathrm{d}^d x\, \sqrt{g(x)}\left[\frac{1}{2} g^{\mu\nu}\partial_\mu\hat{\phi}(x)\partial_\nu\hat{\phi}(x) + \frac{\lambda}{4!}\Big[6\phi_0^2\hat{\phi}(x)^2 + 4\phi_0\hat{\phi}(x)^3 + \hat{\phi}(x)^4\Big]\right]. \tag{2.2.26}$$

From this result we see that, in the absence of a mass term, the term that ensures the convergence of the path integral over ϕ_0 for large field values is the one $\sim \lambda\phi_0^4$. The naive perturbative treatment of the theory sets this term to zero at lowest order in perturbation theory, which leads to the divergences discussed above. To get a well-defined expression for the correlators, this term must be included in the definition of the lowest-order approximation to any correlator [75], which means that we are expanding the exponential in the path integral around the following "free" action:

$$S_{\text{free}} \equiv \frac{V_d\lambda}{4!}\phi_0^4 + \frac{1}{2}\int \mathrm{d}^d x\, \sqrt{g(x)}g^{\mu\nu}\partial_\mu\hat{\phi}(x)\partial_\nu\hat{\phi}(x)\,, \tag{2.2.27}$$

while all the interaction terms involving non-zero-mode field $\hat{\phi}$ can safely be treated as small perturbations:

$$S_{\text{int}} \equiv \frac{\lambda}{4!}\int \mathrm{d}^d x\, \sqrt{g(x)}\Big[6\phi_0^2\hat{\phi}(x)^2 + 4\phi_0\hat{\phi}(x)^3 + \hat{\phi}(x)^4\Big]\,. \tag{2.2.28}$$

The inclusion of the term $\sim \lambda\phi_0^4$ into the "free" part of the action renders the theory inherently non-Gaussian. However, since the path integral over ϕ_0 is an ordinary, real, one-dimensional integral, the theory is still tractable, and we can compute correlation functions

$$\langle\phi(x_1)...\phi(x_n)\rangle = \frac{\int \mathcal{D}[\phi]e^{-S_E}\phi(x_1)...\phi(x_n)}{\int \mathcal{D}[\phi]e^{-S_E}} \tag{2.2.29}$$

systematically using the following prescription, which was systematically developed in [76]:

- Split every field in the correlation function of interest up as

  $$\phi(x_i) = \phi_0 + \hat{\phi}(x_i)\,, \tag{2.2.30}$$

  which will yield a sum of correlation functions involving products of several ϕ_0 and $\hat{\phi}(x_i)$:

  $$\langle\phi(x_1)...\phi(x_n)\rangle = \sum_{m=0}^{n}\sum_{s\in S(m)}\langle\phi_0^m\hat{\phi}(x_{s(1)})...\hat{\phi}(x_{s(m)})\rangle\,. \tag{2.2.31}$$

  In this formula the innermost sum runs over all elements s of the set of subsets of m numbers of the set $\{1,...,n\}$ which are inequivalent under permutations of their elements, which we denote by $S(m)$. Due to the underlying $\mathbb{Z}_2$-symmetry

  $$\phi_0 \to -\phi_0\,, \quad \hat{\phi}(x) \to -\hat{\phi}(x) \tag{2.2.32}$$

  of the action only correlation functions with an even number of ϕ_0 and $\hat{\phi}(x_i)$, respectively, will not vanish.

- To compute the correlators on the right-hand side of (2.2.31) expand the exponential e^{-S_E} in the path integral around $e^{-S_{\text{free}}}$, and implement the factorization of the path-integral measure (2.2.24):

  $$\int \mathcal{D}[\phi]e^{-S_E} = \int_{-\infty}^{\infty}\mathrm{d}\phi_0\int \mathcal{D}[\hat{\phi}]e^{-S_{\text{free}}}\sum_{n=0}^{\infty}\frac{(-S_{\text{int}})^n}{n!}\,. \tag{2.2.33}$$

  To organize the terms in the perturbative expansion use the following power-counting rules for ϕ_0 and $\hat{\phi}(x)$:

  $$\phi_0 \sim \lambda^{-\frac{1}{4}}\,, \quad \hat{\phi} \sim \lambda^0\,, \tag{2.2.34}$$

  where the non-trivial scaling of ϕ_0 with λ is inherited from (2.2.27). This has as a consequence the following effective power counting for the different interaction terms appearing in (2.2.28):

  $$\frac{\lambda}{4}\phi_0^2\hat{\phi}(x)^2 \sim \sqrt{\lambda}\,, \quad \frac{\lambda}{6}\phi_0\hat{\phi}(x)^3 \sim \lambda^{\frac{3}{4}}\,, \quad \frac{\lambda}{4!}\hat{\phi}(x)^4 \sim \lambda\,. \tag{2.2.35}$$

Since any correlation function must involve an even number of ϕ_0 and $\hat{\phi}$, this implies that the effective expansion parameter of this modified perturbative expansion is $\sqrt{\lambda}$. The scaling $\phi_0 \sim \lambda^{-\frac{1}{4}}$ also implies that the leading contribution to any given correlation function will be given by the summand on the right-hand-side of (2.2.31) which involves only zero-mode fields.

- Carry out the path integral on the right-hand side of (2.2.33). Since the path integral over the non-zero-mode fields is Gaussian, this is done as usual by taking all possible Wick contractions of the appearing $\hat{\phi}$-fields in a given correlator, and integrating over all positions which are associated to interaction vertices. The Wick contractions yield free non-zero-mode two-point functions $\langle\hat{\phi}(x)\hat{\phi}(y)\rangle$. As in standard QFT, this procedure can be represented in terms of Feynman diagrams. To evaluate the path integral over the zero-mode field, we simply collect all powers of ϕ_0 appearing in a given correlation function and compute the resulting pure zero-mode correlator exactly by means of the following formula:
$$\langle\phi_0^{2n}\rangle_0 \equiv N_0 \int_{-\infty}^{\infty} \mathrm{d}\phi_0 \; e^{-\frac{\lambda V_d}{4!}\phi_0^4}\phi_0^{2n} = \left(\frac{4!}{\lambda V_d}\right)^{\frac{n}{2}} \frac{\Gamma(\frac{2n+1}{4})}{\Gamma(\frac{1}{4})}\,, \tag{2.2.36}$$
where we defined the normalization constant
$$N_0^{-1} \equiv \int_{-\infty}^{\infty} \mathrm{d}\phi_0 \; e^{-\frac{\lambda V_d}{4!}\phi_0^4}\,. \tag{2.2.37}$$
Notice the subscript "0" of the correlation function in (2.2.36), which denotes that we are not including non-zero-mode contributions to it.

- An important consequence of the inherent non-Gaussianity of the zero-mode part of the path integral, which implies, for example, that $\langle\phi_0^4\rangle_0 \neq 3\langle\phi_0^2\rangle_0^2$, is that the cancellation of disconnected bubble diagrams between the numerator and denominator of the path integral, see (2.2.29), is not exact, and a remainder is left over. This needs to be taken into account when computing correlation functions in this formalism.

Using this prescription one can compute correlation functions of the massless scalar field on the sphere, in principle to any precision one likes. This formalism solves the problem of IR divergences, however, its application is restricted to the Euclidean setting, since it relies crucially on the mode expansion of the scalar field being discrete, and in particular on the fact that the pathological behaviour of the naive perturbative expansion can be traced back to a single mode, the zero mode. In the Lorentzian setting, which is the physically relevant one, the mode expansion is continuous, and the large IR effects in perturbatively computed correlators are ascribed to the continuum of superhorizon field modes, so the method discussed above is not applicable.

What one can still do, however, is use the present formalism to compute well-defined, finite correlators on the sphere, and then analytically continue the results to Lorentzian signature, by appropriately extending the range of values of the kinematic invariants. This procedure was used in the case of massive scalar fields in [54] to study the properties of massive two-point functions at large invariant distances between the arguments of the fields, and [75] advocated for extending the application of this procedure to the massless case. While there is no technical obstacle in doing so, it is not immediately clear what the physical meaning of the analytic continuation of these results would be. Since there is no vacuum state for the free, massless, minimally coupled scalar field which respects the entire set of de Sitter isometries [56], it is at first unclear even which Lorentzian correlation functions one should compare to the analytically continued Euclidean results. Even if such a vacuum state was selected, to date there is no established and widely accepted quantum-field-theoretic framework in which to carry out this putative computation.

The most solid framework that is able to treat the problem of light and massless scalar fields in Lorentzian signature successfully is the formalism of Stochastic Inflation, which we discussed above. Focussing on the two-point function, the stochastic result we previously considered is the most natural candidate with which we can compare the analytic continuation of the massless two-point function computed on the sphere. The main goal of the remainder of this chapter will be the computation of the massless Euclidean two-point function in the interacting theory, using the framework we set up above, and the comparison to the stochastic result.

2.2.4 Euclidean two-point function in the massless theory and analytic continuation to Lorentzian de Sitter space

We wish to compute the analytic continuation of the massless, interacting Euclidean two-point function,

$$G(x,y) \equiv \langle \phi(x)\phi(y) \rangle \,, \tag{2.2.38}$$

which, in the framework discussed above, is decomposed as follows:

$$G(x,y) = \langle \phi_0 \phi_0 \rangle + \langle \hat{\phi}(x)\hat{\phi}(y) \rangle \,. \tag{2.2.39}$$

The task is therefore to compute the zero-mode and non-zero-mode two-point functions in the interacting theory. Since we are interested in the analytic continuation of the Euclidean result, and in particular in the pieces of the result which will give the leading contribution in the limit of large invariant distances between the arguments of the fields, we only need to focus on these pieces. As we will see in the following, this will simplify the computations tremendously, it will show that the leading pieces in the limit of interest are insensitive to UV-divergences, and it will allow us to compute the relevant parts of the diagrams up to $\mathcal{O}(\lambda^2)$, which is done here for the first time.

Free non-zero-mode two-point function

The basic building block for the computation of the non-zero-mode part of the two-point function, which, at the same time also constitutes the leading term in the expansion of $\langle \hat{\phi}(x)\hat{\phi}(y) \rangle$ in powers of $\sqrt{\lambda}$, is the free non-zero mode propagator

$$\hat{G}(x,y) \equiv \langle \hat{\phi}(x)\hat{\phi}(y) \rangle \Big|_{\mathcal{O}(\lambda^0)} \,. \tag{2.2.40}$$

It is defined by leaving out the $\vec{L} = 0$-contribution to the free two-point function (2.2.17) and taking the limit $m^2 \to 0$ of the resulting (now regular) expression, which gives us

$$\hat{G}(x,y) = H^{d-2} \sum_{\vec{L} \neq 0} \frac{Y_{\vec{L}}(x) Y^*_{\vec{L}}(y)}{L(L+d-1)} \,. \tag{2.2.41}$$

This sum was evaluated in [76] in $d = 4$, and we explicitly show how this can be done leaving d arbitrary in appendix 2.A. The result we find in $d = 4$ reads

$$\hat{G}(x,y) = \frac{H^2}{4\pi^2} \left[\frac{1}{2(1 - Z_{xy})} - \frac{1}{2} \ln\left(\frac{1 - Z_{xy}}{2} \right) - \frac{7}{6} \right] . \tag{2.2.42}$$

In this formula Z_{xy} denotes the embedding distance on the sphere between the points $x = (\theta_x, \vec{x})$ and $y = (\theta_y, \vec{y})$, which is defined as

$$Z_{xy} \equiv \cos(\theta_x)\cos(\theta_y) + \sin(\theta_x)\sin(\theta_y)\vec{x} \cdot \vec{y} \,, \tag{2.2.43}$$

which is restricted to the compact interval $Z_{xy} \in [-1, 1]$ on the sphere. In the following, we will write $Z_{xy} = Z$. Equation (2.2.42) is the same result obtained in [76], making use of the relation between variables

$$y = 2(1 - Z) \,, \tag{2.2.44}$$

up to the constant in the angled bracket, where the authors find -1 instead of $-7/6$. This may be due to a trivial computational error.

We can use (2.2.42) to study the behaviour of $\hat{G}_{\text{free}}$ in the limit of large invariant distances after analytic continuation, which amounts to simply extending the allowed range of values of Z to $(-\infty, \infty)$. Doing so, and taking the limit $Z \to \infty$ we find the leading result

$$\lim_{Z \to \infty} \hat{G}(x,y) = -\frac{H^2}{8\pi^2} \ln(Z) \,. \tag{2.2.45}$$

To get the above result, we used the fact that since we can always write $\ln(aZ) = \ln(a) + \ln(Z)$ any real coefficient multiplying Z in the argument of a logarithm just gives a subleading correction in limit we are considering, so we can simply drop it. We will use this approximation in the following to isolate the leading terms of interest. From the above consideration we see that the analytic continuation of $\hat{G}(x, y)$ exhibits a secular growth for large values of Z. Since $\hat{G}(x, y)$ is the basic building block for any diagram we are going to compute in the Euclidean formalism, its logarithmic dependence on Z will be inherited, and in fact enhanced, by all perturbative corrections to $\langle\hat{\phi}(x)\hat{\phi}(y)\rangle$.

We will now compute higher-order corrections to $\langle\hat{\phi}(x)\hat{\phi}(y)\rangle$ systematically. The $\mathcal{O}(\sqrt{\lambda})$-correction was already computed in [76], and we will push the computation three orders further, up to $\mathcal{O}(\lambda^2)$, for the first time here. Starting from $\mathcal{O}(\lambda^{\frac{3}{2}})$, this would require us to evaluate d-dimensional integrals over combinations of three and four hyperspherical harmonics and their complex conjugates, which can become very complicated very quickly, and eventually intractable, see [54]. However, we are only interested in the leading behaviour of these results as we let $Z \to \infty$ after analytic continuation, so we are not interested in computing the full results. Fortunately, for this purpose, we are able to develop a method based on the differential equation that $\hat{G}_{\text{free}}$ satisfies, and which will allow us to extract the terms which we are interested in from the relevant diagrams, without having to go through the full computation first.

Identification of the relevant diagrams

We start by identifying the relevant diagrams for the computation of $G(x, y)$ up to $\mathcal{O}(\lambda^2)$. Before doing so, a comment about the disconnected bubble diagrams is in order. As mentioned in the last bullet point in section 2.2.3, in the present formalism they do not cancel out between the numerator and denominator of the Euclidean path integral, and they must be taken into account. However, after renormalizing the theory, these diagrams effectively constitute subleading (in $\sqrt{\lambda}$) corrections to the constant multiplying any given connected diagram stemming from the numerator of (2.2.29). Since, in the present discussion, we are only interested in leading-order contributions to $G(x, y)$, we can safely ignore any bubble-diagram contribution, while they must be taken into account if one is interested in studying subleading-order corrections to this (and any other) correlation function.

The leading contribution to $G(x, y)$, which is $\mathcal{O}(\lambda^{-\frac{1}{2}})$ is just the constant zero-mode correlation function

$$\langle\phi_0^2\rangle_0 = \sqrt{\frac{4!}{\lambda V_d}} \frac{\Gamma(\frac{3}{4})}{\Gamma(\frac{1}{4})}\,, \tag{2.2.46}$$

where we used (2.2.36). Because of the non-Gaussianity of the zero-mode sector of the theory, we cannot give a diagrammatic representation to the zero-mode pieces of the correlation function. All of the relevant higher-order contributions will come from the non-zero-mode part $\langle\hat{\phi}(x)\hat{\phi}(y)\rangle$, which can be represented diagrammatically.

At $\mathcal{O}(\lambda^0)$ we have the tree-level expression for $\langle\hat{\phi}(x)\hat{\phi}(y)\rangle$, which is simply $\hat{G}(x, y)$. We can represent it by a solid line connecting the points x and y:

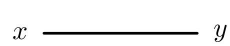

At $\mathcal{O}(\lambda^{\frac{1}{2}})$ we have the first diagram involving an insertion of one of the non-zero-mode vertices, which at this order is the vertex $\sim \phi_0^2\hat{\phi}^2(x)$,

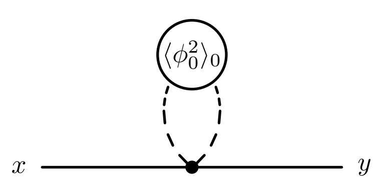

and this diagram corresponds to the expression

$$-\frac{\lambda}{2}\langle\phi_0^2\rangle_0\int_z \hat{G}(x,z)\hat{G}(z,y)\,, \tag{2.2.47}$$

where we introduced the shorthand notation

$$\int_z \equiv \int \mathrm{d}^d z\,\sqrt{g(z)}\,. \tag{2.2.48}$$

In the above diagram, and in all the following diagrams, following [78], we represent pictorially the procedure of collecting all the factors of ϕ_0 appearing in a given diagram and then evaluating the resulting ϕ_0-correlation functions exactly by dashed lines leading from all the $\hat{\phi}$-vertices involving ϕ_0 to a blob containing the resulting ϕ_0-correlator.

At each order in the expansion of $G(x,y)$ in $\sqrt{\lambda}$, we will always have one diagram involving only insertions of the vertex $\sim\phi_0^2\hat{\phi}^2(x)$. We will refer to this type of diagrams as "chain-diagrams", and we will call a diagram involving n insertions of the vertex $\sim\phi_0^2\hat{\phi}^2(x)$ an n-chain. Accordingly, the above diagram is a 1-chain, and $\hat{G}_{\text{free}}(x,y)$ can be regarded as a 0-chain. This class of diagrams is particularly simple, and we will discuss it in more detail below. Since the structure of the integrals which result from the chain-diagrams is always the same, it will prove convenient to define the class of chain integrals

$$I_{n\text{-chain}}(Z) \equiv \int_{z_1,\ldots,z_n} \hat{G}(x,z_1)\cdot\ldots\cdot\hat{G}(z_n,y)\,,\quad n\geq 1\,, \tag{2.2.49}$$

where we anticipated that the result will only depend on the invariant distance Z between x and y. For the special case $n=0$ we define

$$I_{0\text{-chain}}(Z)\equiv\hat{G}(Z)\,. \tag{2.2.50}$$

At $\mathcal{O}(\lambda)$ we have two diagrams: the 2-chain, which has the diagrammatic representation

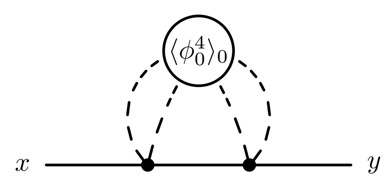

and corresponds to

$$\left(-\frac{\lambda}{2}\right)^2\langle\phi_0^4\rangle_0 I_{2\text{-chain}}(Z)\,, \tag{2.2.51}$$

and the diagram involving the insertion of the vertex $\sim\lambda\hat{\phi}^4(x)$, which gives us a familiar tadpole diagram involving no zero-mode fields at all:

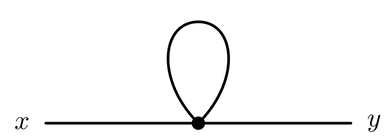

However, since the contribution from the tadpole integral is just a (UV-divergent) constant, and it can be factorized from the rest of the expression, this diagram can simply be reduced to the same diagram as the one appearing at $\mathcal{O}(\lambda^{\frac{1}{2}})$ above, but with an $\mathcal{O}(\lambda)$-coefficient instead. After having been properly renormalized, this diagram can therefore be regarded as a sub-leading correction to the $\mathcal{O}(\lambda^{\frac{1}{2}})$-diagram, suppressed by an additional power of $\sqrt{\lambda}$. In particular, in the large-Z limit after analytic continuation, it will represent a sub-leading correction to the large-Z limit of $G(x,y)$, which we are not interested in in the present discussion. This argument can be run for subdiagrams as well, so from now on we will disregard diagrams involving $\hat{\phi}$-tadpole subgraphs.

Up to this order, no (relevant) diagram involving a $\hat{\phi}$-loop has appeared, which changes for the first time at $\mathcal{O}(\lambda^{\frac{3}{2}})$, where we can insert the vertex $\sim \lambda\phi_0\hat{\phi}^3(x)$ twice to obtain the bubble diagram

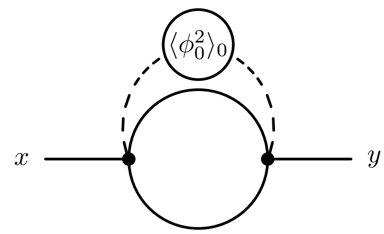

which corresponds to

$$\frac{\lambda^2}{2}\langle\phi_0^2\rangle I_B(Z) \equiv \frac{\lambda^2}{2}\langle\phi_0^2\rangle \int_{z_1,z_2} \hat{G}(x,z_1)\hat{G}^2(z_1,z_2)\hat{G}(z_2,y)\,. \tag{2.2.52}$$

Additionally, at this order we also have the 3-chain

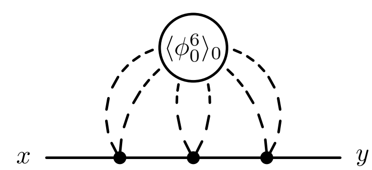

which corresponds to

$$\Big(-\frac{\lambda}{2}\Big)^3 \langle\phi_0^6\rangle_0 I_{\text{3-chain}}(Z)\,. \tag{2.2.53}$$

At the final order we will consider, which is $\mathcal{O}(\lambda^2)$, we have the two-loop sunset diagram

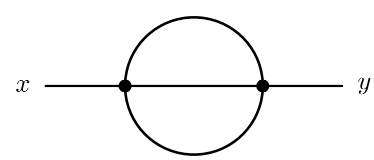

which corresponds to the expression

$$\frac{\lambda^2}{6} I_S(Z) \equiv \frac{\lambda^2}{6} \int_{z_1,z_2} \hat{G}(x,z_1)\hat{G}^3(z_1,z_2)\hat{G}(z_2,y)\,, \tag{2.2.54}$$

the bubble-chain diagram

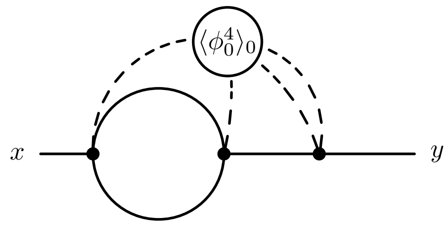

which corresponds to

$$-\frac{\lambda^3}{2}\langle\phi_0^4\rangle I_{BC}(Z) \equiv -\frac{\lambda^3}{2}\langle\phi_0^4\rangle \int_{z_1,z_2,z_3} \hat{G}(x,z_1)\hat{G}^2(z_1,z_2)\hat{G}(z_2,z_3)\hat{G}(z_3,y)\,, \tag{2.2.55}$$

the bubble diagram with a 1-chain insertion

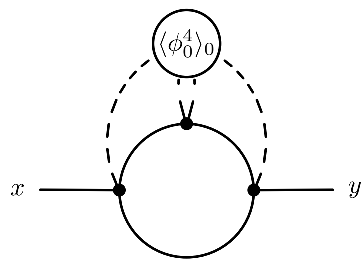

which gives us

$$-\frac{\lambda^3}{2}\langle\phi_0^4\rangle I_{BCI}(Z) = -\frac{\lambda^3}{2}\langle\phi_0^4\rangle \int_{z_1,z_2,z_3} \hat{G}(x,z_1)\hat{G}(z_1,z_2)\hat{G}(z_1,z_3)\hat{G}(z_3,z_2)\hat{G}(z_2,y)\,, \tag{2.2.56}$$

and, finally, the 4-chain

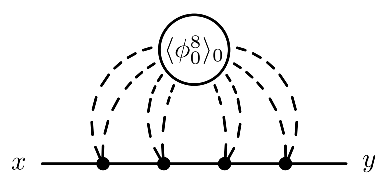

which corresponds to

$$\left(-\frac{\lambda}{2}\right)^4 \langle\phi_0^8\rangle_0 I_{4\text{-chain}}(Z)\,. \tag{2.2.57}$$

We will now extract the leading pieces of each of these diagrams in the limit $Z \to \infty$ after analytic continuation to Lorentzian de Sitter space, starting by examining the chain integrals $I_{n\text{-chain}}(Z)$, and then developing a method to extract the relevant pieces from non-zero-mode loop diagrams.

Chain integrals and their leading large-Z behaviour

To evaluate the contributions from the chain-diagrams we need to evaluate integrals of the form

$$I_{n\text{-chain}}(Z) = \int_{z_1,\ldots,z_n} \hat{G}(x,z_1)\cdot\ldots\cdot\hat{G}(z_n,y)\,. \tag{2.2.58}$$

Using the representation

$$\hat{G}(x,y) = H^{d-2} \sum_{\vec{L}\neq 0} \frac{Y_{\vec{L}}(x) Y^*_{\vec{L}}(y)}{L(L+d-1)} \tag{2.2.59}$$

of $\hat{G}(x,y)$, together with the orthogonality of the hyperspherical harmonics (2.2.12), allows us to reduce the n integrals appearing in (2.2.58) to the following single sum:

$$I_{n\text{-chain}}(Z) = H^{d-2} \sum_{\vec{L}\neq 0} \frac{Y_{\vec{L}}(x) Y^*_{\vec{L}}(y)}{L^{n+1}(L+d-1)^{n+1}} \,. \tag{2.2.60}$$

This sum can be rewritten, by introducing the auxiliary, dimensionless mass-like parameter $\tilde{m}$, as

$$I_{n\text{-chain}}(Z) = H^{d-2} (-1)^n \frac{\partial^n}{\partial \tilde{m}^n}\bigg|_{\tilde{m}=0} \sum_{\vec{L}\neq 0} \frac{Y_{\vec{L}}(x) Y^*_{\vec{L}}(y)}{L(L+d-1)+\tilde{m}} \,, \tag{2.2.61}$$

and we recognize the sum as the free non-zero mode two-point function with mass $m^2 = H^2\tilde{m}$, which we can call $\hat{G}_{\tilde{m}}(Z)$ and write down in closed form as

$$\hat{G}_{\tilde{m}}(Z) = \frac{H^{d-2}}{(4\pi)^{\frac{d}{2}}} \frac{\Gamma(\frac{d-1}{2}+\tilde{\nu})\Gamma(\frac{d-1}{2}-\tilde{\nu})}{\Gamma(\frac{d}{2})} {}_2F_1\left(\frac{d-1}{2}+\tilde{\nu}, \frac{d-1}{2}-\tilde{\nu}; \frac{d}{2}; \frac{1+Z}{2}\right) - \frac{H^{d-2}}{\tilde{m}} \frac{\Gamma(\frac{d+1}{2})}{2\pi^{\frac{d+1}{2}}} \,, \tag{2.2.62}$$

$$\equiv G_{\tilde{m}}(Z) - \frac{H^{d-2}}{\tilde{m}} \frac{\Gamma(\frac{d+1}{2})}{2\pi^{\frac{d+1}{2}}} \,, \tag{2.2.63}$$

with

$$\tilde{\nu} \equiv \sqrt{\left(\frac{d-1}{2}\right)^2 - \tilde{m}} \,. \tag{2.2.64}$$

Any chain integral can therefore be evaluated by taking derivatives of (2.2.62), and then setting $\tilde{m} = 0$. From this, it follows that the chain integral $I_{n\text{-chain}}(Z)$ is related to the coefficient of the n-th term in the Taylor expansion of $\hat{G}_{\tilde{m}}(Z)$ around $\tilde{m} = 0$ as:

$$\hat{G}_{\tilde{m}}(Z) = \sum_{n=0}^{\infty} (-1)^n I_{n\text{-chain}}(Z) \frac{\tilde{m}^n}{n!} \,. \tag{2.2.65}$$

We can now take advantage of this fact by noticing that this equation holds also if we analytically continue it in Z. If we do so, and then take the limit $Z \to \infty$ of (2.2.62), expand the resulting expression in small $\tilde{m}$ and compare coefficients of $\tilde{m}$, this will tell us the large-Z behaviour of any chain integral $I_{n\text{-chain}}$. The leading Lorentzian large-distance limit of the free massive propagator $G_{\tilde{m}}(Z)$ reads

$$\lim_{Z\to\infty} G_{\tilde{m}}(Z) = \frac{H^{d-2}}{(4\pi)^{\frac{d}{2}}} \left[\frac{\Gamma(2\tilde{\nu})\Gamma(\frac{d-1}{2}-\tilde{\nu})}{\Gamma(\frac{1}{2}+\tilde{\nu})} \left(-\frac{Z}{2}\right)^{-\frac{d-1}{2}+\tilde{\nu}} + \frac{\Gamma(-2\tilde{\nu})\Gamma(\frac{d-1}{2}+\tilde{\nu})}{\Gamma(\frac{1}{2}-\tilde{\nu})} \left(-\frac{Z}{2}\right)^{-\frac{d-1}{2}-\tilde{\nu}} \right] \tag{2.2.66}$$

and for $\tilde{m} \ll 1$ the leading term is

$$\lim_{Z\to\infty} G(Z) = \frac{H^{d-2}\Gamma(d)}{(4\pi)^{\frac{d}{2}}\Gamma(\frac{d}{2})\tilde{m}} \left(-\frac{Z}{2}\right)^{-\frac{\tilde{m}}{d-1}} + \mathcal{O}(1) = \frac{1}{V_d H^2 \tilde{m}} \left(-\frac{Z}{2}\right)^{-\frac{\tilde{m}}{d-1}} \,. \tag{2.2.67}$$

Expanding the leading term in (2.2.67) for small $\tilde{m}$ yields, neglecting subleading-logarithmic corrections,

$$\lim_{Z\to\infty} G(Z) = \frac{1}{V_d H^2} \sum_{n=0}^{\infty} \frac{(-1)^n \tilde{m}^{n-1}}{n!} \left(\frac{1}{d-1}\right)^n \ln^n(Z) \,, \tag{2.2.68}$$

which diverges like $\ln^n(Z)$ for large Z if truncated at finite n-th order in $\tilde{m}$. Comparing the coefficient of $\tilde{m}$ in this expression with the ones in (2.2.65) we find the following leading large-Z behaviour for the chain integrals:

$$\lim_{Z\to\infty} I_{n\text{-chain}}(Z) = -\frac{1}{H^{2n+2}V_d(n+1)!}\left(\frac{1}{d-1}\right)^{n+1}\ln^{n+1}(Z) \tag{2.2.69}$$

for any $n \in \mathbb{N}_0$. We can use this result directly to evaluate all leading-logarithmic contributions from the chain diagrams that we listed above at the orders $\mathcal{O}(\lambda^{\frac{1}{2}})$-$\mathcal{O}(\lambda^2)$, and we will do so explicitly below.

Method of differential equations for the extraction of the leading terms from loop diagrams in the $Z \to \infty$ limit

Having determined the behaviour of chain-diagram contributions to the two-point function in the limit of interest, we now still need a way to extract the relevant terms from diagrams involving non-trivial non-zero-mode loops. The naive way is, of course, to compute the diagram in question and then analytically continue the result, but this becomes unfeasible very quickly, due to the complexity of the involved computations. It would thus be desirable to be able to have a procedure to do so which sidesteps the computation of the full diagram, and makes use of the simplification that ensues in the large-Z limit.

The strategy to do so will be to derive a differential equation which the diagrams in question satisfy in this limit, analytically continue the entire differential equation and take the $Z \to \infty$-limit, in which it simplifies, and then solve it. Since the differential equation itself will be simpler in this limit, so will be its solution, and we will thus get access to the result in the limit of interest directly. This can be done using the fact that the free non-zero mode propagator satisfies

$$\Box_x \hat{G}(x,y) \equiv \frac{1}{\sqrt{g(x)}}\partial_\mu^x\left[\sqrt{g(x)}g^{\mu\nu}(x)\partial_\nu^x \hat{G}(x,y)\right] = \frac{1}{V_d} - \frac{1}{\sqrt{g(x)}}\delta^{(d)}(x-y) \tag{2.2.70}$$

and that $\Box_x$ can be rewritten as a differential operator with respect to the de Sitter-invariant distance alone when acting on a function $f(Z_{xy})$ which only depends on Z_{xy} [18],

$$\Box_x f(Z_{xy}) = H^2\left[(1-Z_{xy}^2)\frac{\mathrm{d}^2}{\mathrm{d}Z_{xy}^2} - dZ_{xy}\frac{\mathrm{d}}{\mathrm{d}Z_{xy}}\right]f(Z_{xy})\,, \tag{2.2.71}$$

which is the case for any term in the expansion of the full two-point function, as required by de Sitter-invariance. From now on we will go back to abbreviating $Z_{xy} = Z$. To show how this method works we can apply it to the case of the chain integrals, for which we derived their $Z \to \infty$-behaviour above. For this purpose we will use the 1-chain integral

$$I_{1\text{-chain}}(Z) = \int_z \hat{G}(x,z)\hat{G}(z,y)\,. \tag{2.2.72}$$

Using (2.2.70) and

$$\int_x \hat{G}(x,y) = 0\,, \tag{2.2.73}$$

which follows from (2.2.23), we find

$$\Box_x I_{1\text{-chain}}(Z) = H^2\left[(1-Z^2)\frac{\mathrm{d}^2}{\mathrm{d}Z^2} - dZ\frac{\mathrm{d}}{\mathrm{d}Z}\right]I_{1\text{-chain}}(Z) = -\hat{G}(Z)\,. \tag{2.2.74}$$

In the limit $Z \to \infty$ this equation becomes

$$\left[-Z^2\frac{\mathrm{d}^2}{\mathrm{d}Z^2} - dZ\frac{\mathrm{d}}{\mathrm{d}Z}\right]I_{1\text{-chain},\infty}(Z) = \frac{\ln(Z)}{V_dH^4(d-1)} + \mathcal{O}(1)\,, \tag{2.2.75}$$

where we used the known asymptotic behaviour of $\hat{G}(Z)$ (2.2.69).

The leading piece of the solution of the above differential equation reads

$$I_\infty(Z) = -\frac{\ln^2(Z)}{2V_d H^4(d-1)^2} + \mathcal{O}(\ln(Z))\,, \tag{2.2.76}$$

which reproduces the known leading asymptotic behaviour (2.2.69) for the special case of the considered chain diagram. In particular, since the differential equation we obtain in this manner can be written as a linear differential equation with respect to $\ln(Z)$, the leading part of the result will always be unambiguous, since the integration constants will affect only the subleading parts, which we are not interested in for now.

We now apply this method to the relevant non-zero-mode loop diagrams at $\mathcal{O}(\lambda^{\frac{3}{2}})$ and $\mathcal{O}(\lambda^2)$ we identified in section 2.2.4.

Bubble diagram

We start with the bubble integral I_B, see (2.2.52). We let the operator $\Box_y\Box_x$ act on it and use (2.2.70):

$$\begin{aligned}
\Box_y\Box_x I_B(Z) =& \int_{z_1 z_2} \Box_x \hat{G}(x,z_1)\hat{G}^2(z_1,z_2)\Box_y\hat{G}(z_2,y) \\
=& \frac{1}{V_d}\int_{z_1 z_2} \hat{G}(z_1,z_2)^2\Box_y\hat{G}(z_2,y) - \int_z \hat{G}(x,z)\hat{G}(z,x)\Box_y\hat{G}(z,y) \\
=& \frac{1}{V_d^2}\int_{z_1 z_2} \hat{G}(z_1,z_2)^2 - \frac{2}{V_d}\int_z \hat{G}(x,z)\hat{G}(z,x) + \hat{G}(Z)^2\,.
\end{aligned} \tag{2.2.77}$$

The first two terms in the last equality above are constant and divergent parts, which are expected, since the loop diagram should be UV-divergent. These divergences can, of course, be removed as usual by renormalizing the theory. Further, since these terms are constant with respect to Z, they are subleading compared to the finite part, $\hat{G}(Z)^2$, in the limit of interest. We can therefore simply assume that these divergences have been properly regularized and renormalized, and ignore them for the present discussion, since we are interested only in the leading pieces in the limit $Z \to \infty$, which they are not.

In fact, we will observe this pattern over and over in the following computations, and this tells us that the effects of renormalization are actually irrelevant in the leading-logarithmic approximation as $Z \to \infty$. This is the first sign of a semiclassical picture emerging from the analytic continuation of the Euclidean results in this limit, and it is, of course, compatible with the stochastic framework discussed above, where renormalization also plays no role.

Coming back to the present computation, and keeping only the last term in (2.2.77), we see that we need to solve the differential equation for $I_B(Z)$ in the limit $Z \to \infty$, in which we can write

$$\begin{aligned}
\lim_{Z\to\infty} \Box_x\Box_y =& H^4\left[-Z^2\frac{\mathrm{d}^2}{\mathrm{d}Z^2} - dZ\frac{\mathrm{d}}{\mathrm{d}Z}\right]\left[-Z^2\frac{\mathrm{d}^2}{\mathrm{d}Z^2} - dZ\frac{\mathrm{d}}{\mathrm{d}Z}\right] \\
=& H^4\left[Z^4\frac{\mathrm{d}^4}{\mathrm{d}Z^4} + 2(d+2)Z^3\frac{\mathrm{d}^3}{\mathrm{d}Z^3} + (d^2+4d+2)Z^2\frac{\mathrm{d}^2}{\mathrm{d}Z^2} + d^2 Z\frac{\mathrm{d}}{\mathrm{d}Z}\right],
\end{aligned} \tag{2.2.78}$$

since $I_B(Z)$ must be symmetric in x and y. Notice that dropping the 1's in the $\Box$-operators before or after taking derivatives on them makes no difference, so we can do it right away. We already know the asymptotic behaviour of $\hat{G}(Z)^2$, which is the only term we kept on the right-hand side of (2.2.77), since we know that

$$\lim_{Z\to\infty}\hat{G}(Z) = -\frac{\ln(Z)}{V_d H^2(d-1)} + \mathcal{O}(1)\,. \tag{2.2.79}$$

The differential equation we have to consider is therefore

$$\left[Z^4\frac{\mathrm{d}^4}{\mathrm{d}Z^4} + 2(d+2)Z^3\frac{\mathrm{d}^3}{\mathrm{d}Z^3} + (d^2+4d+2)Z^2\frac{\mathrm{d}^2}{\mathrm{d}Z^2} + d^2 Z\frac{\mathrm{d}}{\mathrm{d}Z}\right] I_{B\infty}(Z) = \frac{\ln^2(Z)}{(d-1)^2 H^8 V_d^2} \tag{2.2.80}$$

and it has the leading solution

$$I_{B\infty}(Z) = \frac{\ln^4(Z)}{12(d-1)^4 H^8 V_d^2} + \mathcal{O}(\ln^3(Z))\,, \tag{2.2.81}$$

so the leading term for $Z \to \infty$ of the bubble diagram reads

$$\frac{\lambda^2}{2}\langle\phi_0^2\rangle I_{B\infty}(Z) = \frac{\lambda^2\langle\phi_0^2\rangle \ln^4(Z)}{4!\,(d-1)^4 H^8 V_d^2}\,. \tag{2.2.82}$$

Sunset diagram

We do the same for the sunset integral, see (2.2.54):

$$\begin{aligned}\Box_y\Box_x I_S(Z) =& \int_{z_1 z_2} \Box_x \hat{G}(x,z_1)\hat{G}^3(z_1,z_2)\Box_y\hat{G}(z_2,y)\\ =&\frac{1}{V_d}\int_{z_1 z_2}\hat{G}(z_1,z_2)^3\Box_y\hat{G}(z_2,y) - \int_z \hat{G}^3(x,z)\Box_y\hat{G}(z,y)\\ =&\frac{1}{V_d^2}\int_{z_1 z_2}\hat{G}(z_1,z_2)^3 - \frac{2}{V_d}\int_z \hat{G}^3(x,z) + \hat{G}(Z)^3\,.\end{aligned} \tag{2.2.83}$$

Again, we find two divergent constant terms, which are irrelevant for the leading large-Z behaviour, and we need to keep $\hat{G}(Z)^3$ on the right-hand side of the above equation. Using (2.2.79) the differential equation we need to solve to find the leading term in the $Z\to\infty$-limit after analytic continuation is

$$\left[Z^4\frac{\mathrm{d}^4}{\mathrm{d}Z^4}+2(d+2)Z^3\frac{\mathrm{d}^3}{\mathrm{d}Z^3}+(d^2+4d+2)Z^2\frac{\mathrm{d}^2}{\mathrm{d}Z^2}+d^2 Z\frac{\mathrm{d}}{\mathrm{d}Z}\right]I_{S\infty}(Z) = -\frac{\ln^3(Z)}{(d-1)^3 H^{10} V_d^3}+\mathcal{O}(\ln^2(Z))\,. \tag{2.2.84}$$

The solution reads

$$I_{S\infty}(Z) = -\frac{\ln^5(Z)}{20(d-1)^5 H^{10} V_d^3} + \mathcal{O}(\ln^4(Z))\,, \tag{2.2.85}$$

so the leading term in the $Z\to\infty$ limit of the analytic continuation of the sunset diagram is

$$\frac{\lambda^2}{6} I_{S\infty}(Z) = -\frac{\lambda^2 \ln^5(Z)}{5!\,(d-1)^5 H^{10} V_d^3}\,. \tag{2.2.86}$$

Bubble-chain diagram

Letting $\Box_y$ act on the bubble-chain integral, see (2.2.55), yields

$$\Box_y I_{BC}(Z) = \frac{1}{V_d}\int_{z_1 z_2 z_3}\hat{G}(x,z_1)\hat{G}^2(z_1,z_2)\hat{G}(z_2,z_3) - I_B(Z)\,. \tag{2.2.87}$$

It is clear that the first term on the right-hand side of the above equation can only contain (possibly divergent) constants, since it depends only on x, and would break de Sitter invariance otherwise. Therefore, since we are only interested in the asymptotic behaviour of this diagram, we can disregard this term. We already know the leading asymptotic behaviour of $I_B(Z)$ from (2.2.81), and plugging this result into the above equation we find that we need to solve

$$\left[-Z^2\frac{\mathrm{d}^2}{\mathrm{d}Z^2} - dZ\frac{\mathrm{d}}{\mathrm{d}Z}\right]I_{BC\infty}(Z) = -\frac{\ln^4(Z)}{12(d-1)^4 H^{10} V_d^2}\,. \tag{2.2.88}$$

It has the leading solution

$$I_{BC\infty}(Z) = \frac{\ln^5(Z)}{60(d-1)^5 H^{10} V_d^2} + \mathcal{O}(\ln^4(Z)) \tag{2.2.89}$$

and the full leading contribution in the $Z\to\infty$ limit of the bubble-chain diagram is then

$$-\frac{\lambda^3}{2}\langle\phi_0^4\rangle I_{BC\infty}(Z) = -\frac{\lambda^3\langle\phi_0^4\rangle \ln^5(Z)}{5!\,(d-1)^5 H^{10} V_d^2}\,. \tag{2.2.90}$$

Bubble-chain-insertion diagram

We let the operator $\Box_y\Box_x$ act on $I_{BCI}(Z)$, see (2.2.56):

$$\begin{aligned}\Box_y\Box_x I_{BCI}(Z) =& \int_{z_1z_2z_3} \Box_x\hat{G}(x,z_1)\hat{G}(z_1,z_2)\hat{G}(z_1,z_3)\hat{G}(z_3,z_2)\Box_y\hat{G}(z_2,y) \\ =&\frac{1}{V_d}\int_{z_1z_2z_3}\hat{G}(z_1,z_2)\hat{G}(z_1,z_3)\hat{G}(z_3,z_2)\Box_y\hat{G}(z_2,y) - \int_{z_1z_2}\hat{G}(x,z_2)\hat{G}(x,z_3)\hat{G}(z_3,z_2)\Box_y\hat{G}(z_2,y) \\ =&\frac{1}{V_d^2}\int_{z_1z_2z_3}\hat{G}(z_1,z_2)\hat{G}(z_1,z_3)\hat{G}(z_3,z_2) - \frac{2}{V_d}\int_{z_1z_2z_3}\hat{G}(z_1,z_2)\hat{G}(z_1,z_3)\hat{G}(z_3,z_2)\hat{G}(z_2,y) \\ &+\hat{G}(Z)\int_z \hat{G}(x,z)\hat{G}(z,y)\,,\end{aligned} \tag{2.2.91}$$

where we only need to take into account the last term in the above equation, which is the product of a 0-chain and a 1-chain, to obtain the leading $Z\to\infty$ limit of $I_{BCI}(Z)$. The leading infrared behaviour of the 1-chain is already known, and it reads

$$\lim_{Z\to\infty}\int_z \hat{G}(x,z)\hat{G}(z,y) = -\frac{\ln^2(Z)}{2V_dH^4(d-1)^2} + \mathcal{O}(\ln(Z))\,, \tag{2.2.92}$$

so the differential equation we need to solve is

$$\left[-Z^2\frac{\mathrm{d}^2}{\mathrm{d}Z^2} - dZ\frac{\mathrm{d}}{\mathrm{d}Z}\right]\left[-Z^2\frac{\mathrm{d}^2}{\mathrm{d}Z^2} - dZ\frac{\mathrm{d}}{\mathrm{d}Z}\right]I_{BCI\infty}(Z) = \frac{\ln^3(Z)}{2(d-1)^3H^{10}V_d^2}\,. \tag{2.2.93}$$

The leading-logarithmic solution reads

$$I_{BCI\infty}(Z) = \frac{\ln^5(Z)}{40H^{10}(d-1)^5V_d^2} + \mathcal{O}(\ln^4(Z)) \tag{2.2.94}$$

and the contribution of the bubble-chain-insertion diagram therefore reads

$$-\frac{\lambda^3}{2}\langle\phi_0^4\rangle I_{BCI\infty}(Z) = -\frac{3}{2}\frac{\lambda^3\langle\phi_0^4\rangle\ln^5(Z)}{5!\,(d-1)^5H^{10}V_d^2}\,. \tag{2.2.95}$$

2.2.5 Summary of the results in the limit $Z\to\infty$ and comparison to the stochastic results

Collecting the results we obtained above for the chain diagrams and the loop diagrams in powers of $\sqrt{\lambda}$, we find the following leading behaviour of the analytically continued Euclidean two-point function, up to $\mathcal{O}(\lambda^2)$:

$$\mathcal{O}(\lambda^{-\frac{1}{2}}):\quad \langle\phi_0^2\rangle_0\,, \tag{2.2.96}$$

$$\mathcal{O}(\lambda^0):\quad -\frac{\ln(Z)}{V_dH^2(d-1)}\,, \tag{2.2.97}$$

$$\mathcal{O}(\lambda^{\frac{1}{2}}):\quad \frac{\lambda}{2}\langle\phi_0^2\rangle_0\frac{\ln^2(Z)}{2!\,V_dH^4(d-1)^2}\,, \tag{2.2.98}$$

$$\mathcal{O}(\lambda):\quad -\frac{\lambda^2}{4}\langle\phi_0^4\rangle_0\frac{\ln^3(Z)}{3!\,V_dH^6(d-1)^3}\,, \tag{2.2.99}$$

$$\mathcal{O}(\lambda^{\frac{3}{2}}):\quad \left[\frac{\lambda^3}{8}\langle\phi_0^6\rangle_0 + \frac{\lambda^2}{V_d}\langle\phi_0^2\rangle_0\right]\frac{\ln^4(Z)}{4!\,(d-1)^4H^8V_d}\,, \tag{2.2.100}$$

$$\mathcal{O}(\lambda^2):\quad -\left[\frac{\lambda^4}{16}\langle\phi_0^8\rangle_0 + \frac{5\lambda^3}{2V_d}\langle\phi_0^4\rangle_0 + \frac{\lambda^2}{V_d^2}\right]\frac{\ln^5(Z)}{5!\,H^{10}(d-1)^5V_d}\,. \tag{2.2.101}$$

We are now in the position to compare these results with their stochastic countertparts. The appropriate stochastic result to compare the above to is the asymptotic expansion of the stochastic two-point function $G(t)$ around $t = 0$, which we wrote above in section 2.1.3 in the form

$$G(t) = \sum_{n=0}^{\infty} \frac{\mathrm{d}^n G(0)}{\mathrm{d}t^n} \frac{t^n}{n!}\,, \tag{2.2.102}$$

and we already computed the Taylor coefficients in d dimensions up to $\mathcal{O}(\lambda^2)$, which we reprint here for convenience:

$$\begin{aligned}
G(0) =&\langle\bar{\phi}^2\rangle\,, && (2.2.103)\\
\frac{\mathrm{d}G(0)}{\mathrm{d}t} =&-\frac{1}{H(d-1)V_d}\,, && (2.2.104)\\
\frac{\mathrm{d}^2G(0)}{\mathrm{d}t^2} =&\frac{1}{H^2(d-1)^2V_d}\frac{\lambda}{2}\langle\bar{\phi}^2\rangle\,, && (2.2.105)\\
\frac{\mathrm{d}^3G(0)}{\mathrm{d}t^3} =&-\frac{1}{H^3(d-1)^3V_d}\frac{\lambda^2}{4}\langle\bar{\phi}^4\rangle\,, && (2.2.106)\\
\frac{\mathrm{d}^4G(0)}{\mathrm{d}t^4} =&\frac{1}{H^4(d-1)^4V_d}\left[\frac{\lambda^3}{8}\langle\bar{\phi}^6\rangle+\frac{\lambda^2}{V_d}\langle\bar{\phi}^2\rangle\right]\,, && (2.2.107)\\
\frac{\mathrm{d}^5G(0)}{\mathrm{d}t^5} =&-\frac{1}{H^5(d-1)^5V_d}\left[\frac{\lambda^4}{16}\langle\bar{\phi}^8\rangle+\frac{5\lambda^3\langle\bar{\phi}^4\rangle}{2V_d}+\frac{\lambda^2}{V_d^2}\right]\,, && (2.2.108)
\end{aligned}$$

The reason why this is the correct object for the comparison is that the invariant distance function in planar coordinates, in which the stochastic formalism is constructed, reads

$$Z_{xy} = \cosh(H(t_x - t_y)) - \frac{e^{H(t_x+t_y)}}{2} H^2|\vec{x}-\vec{y}|^2 \tag{2.2.109}$$

and for large time-like distances, which is the limit we are considering by letting $Z \to \infty$ and which we can explicitly take by letting $\vec{x} = \vec{y}$, $H(t_x - t_y) \to \infty$ this simplifies to

$$Z_{xy} \to \frac{e^{H(t_x-t_y)}}{2}\,. \tag{2.2.110}$$

Taking the logarithm of this expression we see that

$$\ln(Z_{xy}) = H(t_x - t_y) - \ln(2)\,, \tag{2.2.111}$$

and we can neglect the $-\ln(2)$ in this limit. Now setting $t_x = t$, $t_y = 0$, which is the choice we made in section 2.1.3 to derive the stochastic series, and writing again $Z_{xy} = Z$, we get

$$\ln(Z) = Ht\,. \tag{2.2.112}$$

Therefore, the stochastic series can be rewritten as a series in powers of $\sqrt{\lambda}\ln(Z)$, which is exactly the expansion parameter of the analytically continued Euclidean result. Further, in [76] it was noticed for the first time that the d-dimensional stochastic one-point equilibrium PDF $\rho_{1\mathrm{eq}}(\varphi)$, see (2.1.42), and the path-integral weight for the zero-mode part of the full path integral in the Euclidean formalism, agree exactly after replacing $\varphi \leftrightarrow \phi_0$ in either one of them:

$$\frac{2}{\Gamma(\frac{1}{4})}\left(\frac{V_d\lambda}{4!}\right)^{\frac{1}{4}} \exp\left(-\frac{\lambda V_d}{4!}\phi_0^4\right) = \rho_{1\mathrm{eq}}(\phi_0)\,. \tag{2.2.113}$$

From this, it immediately follows that the equilibrium one-point functions computed in the stochastic formalism and the pure zero-mode functions computed in the Euclidean formalism agree:

$$\langle \bar{\phi}^{2n} \rangle = \langle \phi_0^{2n} \rangle_0 \tag{2.2.114}$$

for any n. Using this, as well as (2.2.112) and comparing (2.2.96)-(2.2.101) to (2.2.103)-(2.2.108) we see that the terms in the two series agree order by order in $\sqrt{\lambda}$, which is what we wanted to show.

Discussion of the result

To summarize, we indeed found that, for the case of the two-point function, the perturbative stochastic and Euclidean approaches yield the same result in the limit we are considering. Strikingly, as we let $Z \to \infty$ after analytic continuation, we found that a semiclassical behaviour of the Euclidean theory seems to emerge, since all contributions coming from UV-divergent terms to any given diagram constitute a subleading correction to the leading large-Z behaviour of the diagram in question. In the results we found above, every diagram contributing to the expansion of the two-point function which contains n non-coincident non-zero-mode propagators contributed a leading-logarithmic term after analytic continuation. We can write the following formula for the leading-logarithmic term generated by the above diagrams: a diagram Γ with two external points, m vertices, and n non-coincident non-zero-mode propagators yields the following leading-logarithmic expression after analytic continuation in the $Z \to \infty$-limit:

$$\mathrm{LL}(\Gamma) = \left(- \frac{\ln(Z)}{V_d H^2 (d-1)} \right)^n \times (-V_d)^m \times C(\Gamma) \,, \tag{2.2.115}$$

where the coefficient $C(\Gamma)$ is defined recursively as follows:

$$C(\Gamma) = \frac{1}{n_\Gamma !} \prod_{\gamma_i} C(\gamma_i) \,, \tag{2.2.116}$$

where n_Γ is the number of non-zero mode propagators in the diagram, and the product runs over all subdiagrams γ_i of Γ. This definition can be applied recursively, breaking down the diagram into simpler subdiagrams layer by layer, until there are no more non-trivial subdiagrams than single non-zero mode propagators, at which point $C(\gamma_i) = 1$ and the recursion terminates. If one were able to prove that this formula holds true for any diagram with the described features, to all orders in $\sqrt{\lambda}$, one could read off the leading-logarithmic contribution generated by such a diagram in the limit of interest, without having to go through the explicit computation, but we are not able to do so at the moment of writing.

Presently, we do not know how to prove to all orders in $\sqrt{\lambda}$ that the correspondence between the stochastic and Euclidean results holds, even though it seems plausible that this could be the case. This conjecture is corroborated by the study of the Euclidean two-point function of the $O(N)$-vector model using the large-N approximation in the series of works [78–80], in which the authors of these papers were able to confirm that, to all orders in $\sqrt{\lambda}$ and up to next-to-leading order in $1/N$, the Euclidean results and their stochastic counterparts studied in [81, 82] agree. The diagrammatic analysis we carried out above is likely to be unsuitable to prove (or falsify) such an all-order statement, since, as one proceeds to higher orders in the expansion in $\sqrt{\lambda}$, more and more diagram classes will appear, which might potentially contribute leading-logarithmic terms at the considered order in $\sqrt{\lambda}$. Even if one had a formula such as (2.2.115) to determine the leading-logarithmic contribution from any diagram, one would still need to do so for infinitely many diagram classes, which is not a realistic proposition. However, if one were able to prove that the correspondence holds to all orders, then all the statements we made about the large-order behaviour and Borel summability of the series expansion of G in section 2.1.3 would carry over to the Euclidean leading-logarithmic series. In particular, this would imply that one could extract the relaxation Eigenvalues Λ_n from the divergent series, without having to rely on the Fokker-Planck equation to get them. Indeed, this possibility constituted our main motivation for studying the large-order behaviour of the stochastic series for the two-point function in section 2.1.3: in the absence of the possibility of using the exact solution of Fokker-Planck equation to get the exact form of the two-point function, which is the Euclidean situation, one is still able to access the true late-time behaviour of G by means of Borel resummation, provided that the equality between the Euclidean leading-log series and stochastic series holds to all orders. This would then help to clarify the physical meaning and usefulness of the analytic continuation of the Euclidean result. At this point, however, we are missing the proof of the crucial logical link to be able to run this chain of arguments.

2.3 Conclusion

In this chapter we have introduced and reviewed the formalism of Stochastic Inflation and the Euclidean formulation of the theory of a massless, minimally coupled, self-interacting scalar field. Both approaches are successful in removing the problem of IR-divergences. As an application of the two formalisms we have computed the two-point function of the interacting scalar field (semi-)perturbatively, and we have found that the stochastic and Euclidean results agree in the late-time limit, after the latter have been analytically continued, up to $\mathcal{O}(\lambda^2)$. This is a new result that we showed here for the first time. We have also inspected the high-order behaviour of this series using the stochastic formalism, and shown that it is Borel-summable, at least to the extent we were able to check, which, to the best of our knowledge, has also not been noticed in the literature before.

The agreement of the stochastic and Euclidean results is not wholly unexpected, due to the agreement of the $O(N)$-version of the Euclidean and stochastic two-point functions in the large-Z limit shown by the papers [78–80] and [81,82], respectively, up to next-to-leading order in $1/N$. In fact, at leading order in $1/N$ only the chain-diagrams we have considered above are relevant, the series expansion of $G(x, y)$ in $\sqrt{\lambda}$ converges and can be directly summed to all orders. This simple picture no longer holds starting from next-to-leading order in $1/N$, and additional diagram classes need to be included. This observation is reflected in our computations, since essentially all types of diagrams involving non-zero modes, except for diagrams involving non-zero-mode tadpole subgraphs and disconnected bubble diagrams, contribute a leading-logarithmic contribution after analytic continuation. In particular, in the single-field case we considered here, this means that the partial resummation of chain diagrams proposed in [96] will not substantially ameliorate the behaviour of any truncation of the perturbatively computed Euclidean two-point function after analytic continuation in the limit $Z \to \infty$, since it is still missing relevant contributions from infinitely many diagram classes.

In fact, all our results from the Euclidean computation (2.2.96)-(2.2.101) point to the following conjecture:

Conjecture 1: Every diagram contributing to the expansion of the Euclidean two-point function $G(Z)$ which contains n non-coincident non-zero-mode propagators will contribute a term $\sim \ln^n(Z)$ in the large-Z limit after analytic continuation.

Notably, the renormalization of the Euclidean theory constitutes a subleading correction to the leading-logarithmic results we found above, which is compatible with the semiclassical structure of the stochastic formalism emerging from the Euclidean formalism in the limit of interest.

Further, it appears that we should be able to trade both the zero-mode part of the computation and all of the complicated integrations over hyperspherical harmonics that have to be carried out on the sphere before analytically continuing the result, which in the end just boil down to computing the coefficient in front of the $\ln^n(Z)$ appearing in the diagram in question, for a simple one-dimensional integral of the type

$$\int_{-\infty}^{\infty} \mathrm{d}\varphi \; \rho_{1\mathrm{eq}}(\varphi)\varphi(\hat{\Gamma}_\varphi)^n\varphi \,, \tag{2.3.1}$$

which is computing exactly these coefficients in the cases we were able to check. The difficulty in doing so in practice is that the dramatic simplification of the expressions we observed above only occurs in the limit $Z \to \infty$, and to take this limit we necessarily have to leave the sphere. It is clear how to do this when only considering the correlation functions themselves, but to be able to prove such an all-order statement more control over the theory is needed. In particular, an effective-action description underlying this simpler theory would be highly desirable. Working in Euclidean perturbation theory, even if we had a formula to compute the leading-logarithmic term that any diagram would yield after analytic continuation, we would need to do so for infinitely many classes of diagrams, which is clearly beyond our reach. Since we are interested in a question which cannot be posed directly in the Euclidean setting, it is unclear how to proceed systematically. At the present moment, we can therefore at most make the following conjecture:

Conjecture 2: The analytic continuation of the Euclidean two-point function to the Lorentzian setting yields a well-defined, semi-perturbative expansion of the Lorentzian correlator computed in a non-perturbative vacuum state which respects the full set of de Sitter isometries. The leading-logarithmic terms in the $Z \to \infty$-limit of this result agree with the stochastic expansion of this quantity to all orders, and can be summed using Borel resummation to obtain a well-behaved two-point function at late times.

To conclude, the Euclidean formulation of the theory, while yielding IR-finite and de Sitter-invariant results, is not the optimal setting to examine the late-time limit of correlation functions, since this is a problem which intrinsically requires one to leave the sphere. To address this issue, we have to work directly in Lorentzian spacetime, and, since we are interested in the effective dynamics of the theory at late times, the natural quantum-field-theoretic description of this system should be formulated using effective-field-theoretical methods. This will be the main focus of the remainder of the thesis.

Appendix

2.A Derivation of the free non-zero-mode propagator

In this appendix we show how the sum

$$\hat{G}_{\rm free}(x,y) = H^{d-2} \sum_{\vec{L}\neq 0} \frac{Y_{\vec{L}}(x) Y^*_{\vec{L}}(y)}{L(L+d-1)} \,. \tag{2.A.1}$$

can be evaluated. It can be done in two different ways, both of which make use of results obtained in [54]. In this paper it was shown how to carry out the $\vec{L}$-sum in (2.2.17), and the result reads

$$G^{m^2}_{\rm free}(x,y) = \frac{H^{d-2}}{(4\pi)^{\frac{d}{2}}} \frac{\Gamma(\frac{d-1}{2}+\nu)\Gamma(\frac{d-1}{2}-\nu)}{\Gamma(\frac{d}{2})} {}_2F_1\left(\frac{d-1}{2}+\nu, \frac{d-1}{2}-\nu; \frac{d}{2}; \frac{1+Z_{xy}}{2}\right) . \tag{2.A.2}$$

In the above equation ν denotes the mass parameter

$$\nu \equiv \sqrt{\left(\frac{d-1}{2}\right)^2 - \frac{m^2}{H^2}} \,. \tag{2.A.3}$$

The first way to evaluate (2.A.1) is to subtract the zero-mode piece

$$\frac{1}{V_d m^2} = \frac{H^d}{m^2} \frac{\Gamma(\frac{d+1}{2})}{2\pi^{\frac{d+1}{2}}} \tag{2.A.4}$$

from (2.A.2) and take the limit $m^2 \to 0$ of the difference, which is regular. Doing so, we find the result

$$\hat{G}_{\rm free}(x,y) = \lim_{m\to 0}\left[\frac{H^{d-2}}{(4\pi)^{\frac{d}{2}}} \frac{\Gamma(\frac{d-1}{2}+\nu)\Gamma(\frac{d-1}{2}-\nu)}{\Gamma(\frac{d}{2})} {}_2F_1\left(\frac{d-1}{2}+\nu, \frac{d-1}{2}-\nu; \frac{d}{2}; \frac{1+Z}{4}\right) - \frac{H^d}{m^2}\frac{\Gamma(\frac{d+1}{2})}{2\pi^{\frac{d+1}{2}}}\right] \tag{2.A.5}$$

$$= \frac{H^{d-2}}{(4\pi)^{\frac{d}{2}}} \left[\sum_{n=1}^{\infty} \frac{\Gamma(d-1+n)}{n\Gamma(\frac{d}{2}+n)} \left(\frac{1+Z}{2}\right)^n - \left(\gamma_E + \psi(d-1) + \frac{1}{d-1}\right) \frac{\Gamma(d-1)}{\Gamma(\frac{d}{2})}\right] , \tag{2.A.6}$$

which in $d=4$ evaluates to

$$\hat{G}_{\rm free}(x,y) = \frac{H^2}{4\pi^2} \left[\frac{1}{2(1-Z)} - \frac{1}{2}\ln\left(\frac{1-Z}{2}\right) - \frac{7}{6}\right] . \tag{2.A.7}$$

The second way to derive the above result is to use a Watson-Sommerfeld transformation to explicitly evaluate the sum, as is done in [54] for the massive case and in [96] for the massless case we are considering. Using the summation formula [95]

$$\sum_{\vec{l}} Y_{L\vec{l}}(x) Y^*_{L\vec{l}}(y) = \frac{(2L+d-1)\Gamma(\frac{d-1}{2})}{4\pi^{\frac{d+1}{2}}} C_L^{\frac{d-1}{2}}(Z) \,, \tag{2.A.8}$$

where $C_L^\alpha(z)$ denotes the Gegenbauer polynomials, we can evaluate all the sums over the lower angular momenta in (2.A.1) and find

$$\hat{G}_{\text{free}}(x,y) = \frac{H^{d-2}\Gamma(\frac{d-1}{2})}{4\pi^{\frac{d+1}{2}}} \sum_{L=1}^{\infty} \frac{(2L+d-1)}{L(L+d-1)} C_L^{\frac{d-1}{2}}(Z)\,. \tag{2.A.9}$$

We now wish to turn this sum into a complex contour integral using a Watson-Sommerfeld transformation, which we can do in full analogy to the treatment in [54] and we can write

$$\hat{G}(x,y) = -\frac{H^{d-2}}{(4\pi)^{\frac{d}{2}}\Gamma(\frac{d}{2})} \oint_C \frac{\mathrm{d}L}{2\pi i} \frac{(2L+d-1)\Gamma(-L)\Gamma(L+1)}{L(L+d-1)}\, {}_2F_1\left(-L, L+d-1; \frac{d}{2}; \frac{1+Z}{2}\right). \tag{2.A.10}$$

The only difference between this formula and the one obtained in [54] is that our complex contour C wraps counter-clockwise around the poles at $L \in \mathbb{N}$, while the one in [54] included the pole at $L=0$, since their sum started from $L=0$. To carry out this complex integral we can use the fact that the integrand is symmetric about the point $L = -\frac{d-1}{2}$, just like in the massive case, so if we deform the contour C to a straight line passing at any angle through that point the resulting integral will vanish. By doing so we deform the contour through the double pole at $L=0$, so we pick up the residue there, which is

$$\begin{aligned}
&\operatorname*{Res}_{L=0} \frac{(2L+d-1)\Gamma(-L)\Gamma(L+1)}{L(L+d-1)}\, {}_2F_1\left(-L, L+d-1; \frac{d}{2}; \frac{1+Z}{2}\right) \\
&= \lim_{L\to 0} \frac{\partial}{\partial L} \frac{(2L+d-1)L\Gamma(-L)\Gamma(L+1)}{L+d-1}\, {}_2F_1\left(-L, L+d-1; \frac{d}{2}; \frac{1+Z}{2}\right) \\
&= \Gamma\left(\frac{d}{2}\right)\left[\sum_{n=1}^{\infty} \frac{\Gamma(d-1+n)}{\Gamma(\frac{d}{2}+n)n}\left(\frac{1+Z}{2}\right)^n - \left(\gamma_E + \psi(d-1) + \frac{1}{d-1}\right)\frac{\Gamma(d-1)}{\Gamma(\frac{d}{2})}\right],
\end{aligned} \tag{2.A.11}$$

so we find

$$\hat{G}_{\text{free}}(x,y) = \frac{H^{d-2}}{(4\pi)^{\frac{d}{2}}}\left[\sum_{n=1}^{\infty} \frac{\Gamma(d-1+n)}{n\Gamma(\frac{d}{2}+n)}\left(\frac{1+Z}{2}\right)^n - \left(\gamma_E + \psi(d-1) + \frac{1}{d-1}\right)\frac{\Gamma(d-1)}{\Gamma(\frac{d}{2})}\right], \tag{2.A.12}$$

consistently with (2.A.6).

Chapter 3

Cosmological correlators at late times and the Method of Regions

Motivated by our conclusions in the previous chapter we now leave the Euclidean setting and, for the remainder of the thesis, we will work directly in Lorentzian de Sitter space. This is the setting of physical interest and, importantly for us, the one in which we can access the late-time limit of correlation functions directly. This chapter is dedicated to the computation and study of the properties of equal-time, in-in correlation functions of the massless, minimally coupled, self-interacting scalar field, evaluated at late times:

$$\lim_{-k_i\eta\to 0}\langle\phi(\eta,\vec{k}_1)...\phi(\eta,\vec{k}_n)\rangle\,.$$

In the Lorentzian setting the mode decomposition of the scalar field is continuous, rather than discrete, and the continuum of superhorizon modes is responsible for the infrared divergences occurring in the perturbative expansion of the correlators computed in this theory. In particular, these modes have a non-trivial spacetime-dependence, and, therefore, it is not possible to treat them exactly in the full theory, as we did in the Euclidean theory. In the absence of more powerful methods, we are therefore limited to using perturbation theory in this setting. However, since the late-time limit is directly accessible here, it should be possible to develop a simplified effective description of these modes in the form of an effective field theory (EFT), in which we can hope to understand and tame these infrared divergences. We will see in the next chapter that such a description indeed exists, and we will show how it can be used to solve the issues we see in the IR in the perturbative treatment of the full theory.

However, as discussed below, the EFT in question possesses many couplings which need to be determined by "matching" EFT correlation functions to full-theory ones, and this procedure can be carried out in perturbation theory. This works, even though the full-theory results are ill-defined in the IR by themselves, because these same IR divergences will be faithfully reproduced by the dynamical degrees of freedom of the EFT. These divergences will therefore cancel out in the matching procedure, and the quantities that we are interested in, the matching coefficients, will be IR-insensitive. Thus, the IR-divergent full-theory correlators constitute necessary data to be fed as input to the EFT, in order to then be able to use it to treat the seemingly pathological behaviour of the theory in the infrared. This motivates us to develop computational tools to obtain these results as efficiently as possible, and also to develop an understanding of the way in which the IR divergences manifest themselves in the full theory, and how they can be succesfully regularized.

In this chapter, we will introduce the method of regions [97–99] as a useful tool to simplify the computation of equal-time in-in correlation functions in de Sitter space, with a focus on the real, massless, minimally coupled, self-interacting scalar case. This method was first applied to this setting in [100], and we will show here how to apply it to several cases, some of which go beyond the examples discussed in [100]. This will also give us the opportunity to discuss the UV- and IR-regularization schemes that we are going to use, in order to make the results well-defined and finite, as well as the renormalization procedure to remove the UV divergences. We will also discuss the significance of the renormalized couplings in the full theory. The fully renormalized, but still IR-divergent, results will then be used in the matching procedure in the next chapter, so we will keep referring back to the contents of this chapter in the last part of the thesis.

3.1 Action, UV and IR regulators, renormalization scheme

We start by defining the theory in which we will be working, which means that we need to specify its action, the UV and IR regulators that we will be using, and the renormalization scheme to remove the UV divergences and define the renormalized couplings. As anticipated, we will consider the real, massless, minimally coupled, self-interacting scalar field with a quartic self-interaction, and we will work in the Poincaré patch, using conformal cooordinates:

$$\mathrm{d}s^2 = \frac{1}{(-H\eta)^2}\left[\mathrm{d}\eta^2 - \mathrm{d}\vec{x}^2\right], \tag{3.1.1}$$

where $\eta \in (-\infty, 0)$ denotes the conformal time variable. We will compute equal-time, in-in n-point correlation functions of this field in this spacetime, and we will work in the mixed (conformal-)time-momentum representation of these objects, which we will denote as

$$\langle \phi(\eta, \vec{k}_1)...\phi(\eta, \vec{k}_n)\rangle \,. \tag{3.1.2}$$

To compute these objects, we will use the in-in formalism introduced in section 1.4, which will involve the computation of finite integrals over conformal time and momentum integrations which will, in general, be UV- (and IR-) divergent, so we need to specifiy a regularization and renormalization scheme to properly define the theory. To regularize the UV divergences we will use dimensional regularization (dimreg), by working in a generic spacetime dimension $d = 4 - 2\varepsilon$, where ε is an arbitrary, complex parameter. We will compute the integrals that will appear by assuming ε to be whichever complex number that makes the integrals convergent, and then analytically continue the result to very small values of ε and expand the result in a Laurent series around $\varepsilon = 0$. This scheme by itself is enough to regularize the UV-divergences, which will then manifest themselves as poles in ε after expanding the analytically continued result in question, but it will not regularize the IR-divergences, since the free, massless two-point function is IR-divergent in any spacetime dimension d, as we discussed above in section 1.5. Further, in this scheme we would have to work with the d-dimensional mode functions

$$\phi_{\vec{k}}(\eta) = \sqrt{\frac{\pi}{4H}}\,(-H\eta)^{\frac{d-1}{2}} H_\nu^{(1)}(-k\eta)\,, \quad \nu = \sqrt{\left(\frac{d-1}{2}\right)^2 - \frac{m^2}{H^2}}\,, \tag{3.1.3}$$

with $m = 0$, which would leave the index ν of the Hankel function generic and make the computations very unwieldy. Both of these difficulties can be resolved at once by using the scheme proposed in [101]: we can include a dimension-dependent mass

$$m_d^2 \equiv \frac{H^2(d-4)(d+2)}{4} \tag{3.1.4}$$

in the action, where we recover the massless theory as $\varepsilon \to 0$. The presence of m_d^2 in the action fixes $\nu = 3/2$ for any spacetime dimension d. Since for $\varepsilon \neq 0$ we are now effectively working in a theory with a small mass, this modified version of dimreg is enough to regularize both UV and IR divergences of the theory, which are both represented by poles in ε, and make it well-defined. Further, it simplifies the computations considerably, since the Hankel function appearing in (3.1.3) simplifies to

$$H_{3/2}^{(1)}(-k\eta) = \sqrt{\frac{2}{\pi}}\frac{e^{-ik\eta}(-i + k\eta)}{(-k\eta)^{\frac{3}{2}}} \tag{3.1.5}$$

for any value of d.

In this scheme, the bare action of the regularized theory reads

$$S = \int \frac{\mathrm{d}^d x}{(-H\eta)^d} \left[\frac{(-H\eta)^2}{2} \Big[(\partial_\eta \phi_0)^2 - (\partial_i \phi_0)^2 \Big] - \frac{1}{2} m_0^2 \phi_0^2 - \frac{\kappa_0}{4!} \phi_0^4 \right], \tag{3.1.6}$$

where the subscript 0 denotes bare fields and couplings. We then define the corresponding renormalized quantities as

$$\phi_0(x) = \sqrt{Z_\phi}\, \phi(x)\,, \quad m_0^2 = m_d^2 + \delta m^2\,, \quad \kappa_0 = \tilde{\mu}^{4-d} Z_\kappa \kappa\,. \tag{3.1.7}$$

In the above equation, $\tilde{\mu} = \mu\sqrt{e^{\gamma_E}/4\pi}$ is the 't Hooft-scale of the $\overline{\text{MS}}$ scheme. Introducing this quantity allows us to work with a (mass-)dimensionless d-dimensional renormalized coupling κ. As usual, assuming that the renormalization factors Z_i are of the form $Z_i = 1 + \mathcal{O}(\kappa)$ we can define the counterterms δ_i via

$$\delta_Z \equiv Z_\phi - 1\,, \quad \delta_m \equiv (Z_\phi - 1) m_d^2 + Z_\phi \delta m^2\,, \quad \delta_\kappa \equiv Z_\kappa Z_\phi^2 - 1\,, \tag{3.1.8}$$

which are all assumed to be at least $\mathcal{O}(\kappa)$, and can therefore be treated perturbatively. Expressing the action via the renormalized quantities we find

$$\begin{aligned} S = \int \frac{\mathrm{d}^d x}{(-H\eta)^d} \Bigg[& \frac{(-H\eta)^2}{2} \Big[(\partial_\eta \phi)^2 - (\partial_i \phi)^2 \Big] - \frac{1}{2} m_d^2 \phi^2 - \frac{\kappa \tilde{\mu}^{4-d}}{4!} \phi^4 \\ & + \delta_Z \frac{(-H\eta)^2}{2} \Big[(\partial_\eta \phi)^2 - (\partial_i \phi)^2 \Big] - \frac{1}{2} \delta_m \phi^2 - \delta_\kappa \frac{\kappa \tilde{\mu}^{4-d}}{4!} \phi^4 \Bigg]. \end{aligned} \tag{3.1.9}$$

This version of the theory makes computations simple, because the regularization scheme does not introduce any additional scaleful objects. This, together with the property of dimensional regularization that scaleless integrals are set to zero, makes the computations almost as easy as they can be, given the setting. However, as will be discussed below, this IR-regularization scheme creates some difficulties when matching the results computed using it onto the EFT. For this reason, we will also consider, and use, a different IR-regularization scheme which does introduce an additional scale in the problem, and which, therefore, complicates the computations, but can be very easily implemented in the EFT as well. This IR regulator is introduced by deforming the kinetic terms in the action (3.1.6) as follows:

$$\begin{aligned} S_{\text{kin}} =& \frac{1}{2} \int \frac{\mathrm{d}^d x}{(-H\eta)^d} \Big[(-H\eta)^2 \Big((\partial_\eta \phi)^2 - (\partial_i \phi)^2 \Big) - m_0^2 \phi^2 \Big] \\ \to& \frac{1}{2} \int \frac{\mathrm{d}^d x}{(-H\eta)^d} \Big[(-H\eta)^2 \Big((\partial_\eta \phi)^2 - (\partial_i \phi)^2 + \Lambda_0^2 \phi^2 \Big) - m_0^2 \phi^2 \Big], \end{aligned} \tag{3.1.10}$$

where Λ_0 is a bare parameter that will become the IR regulator in this scheme. The interaction term remains as in (3.1.6). Since we have modified the kinetic term of our theory, we need to determine the new form of the mode functions in this scheme. In the free theory, without interaction terms, we set

$$m_0^2 = m_d^2 = \frac{H^2 (d-4)(d+2)}{4}\,, \quad \Lambda_0^2 = \Lambda^2\,, \tag{3.1.11}$$

where we are still keeping the d-dependent mass term to achieve a similar simplification of the mode functions, regardless of the dimension d, as above, and the modified momentum-space equation of motion for the scalar field mode functions derived from (3.1.10) reads

$$\partial_\eta^2 \phi_{\vec{k}}(\eta) + \frac{H(d-2)}{(-H\eta)} \partial_\eta \phi_{\vec{k}}(\eta) + [k^2 + \Lambda^2] \phi_{\vec{k}}(\eta) + \frac{m_d^2}{(-H\eta)^2} \phi_{\vec{k}}(\eta) = 0\,. \tag{3.1.12}$$

It is solved by the following mode function in the Bunch-Davies vacuum:

$$\phi_{\vec{k}}(\eta) = \sqrt{\frac{\pi}{4H}} (-H\eta)^{\frac{d-1}{2}} H^{(1)}_{3/2} \Big(-\sqrt{k^2 + \Lambda^2}\, \eta \Big), \tag{3.1.13}$$

$$=\frac{(-H\eta)^{\frac{d-1}{2}}}{\sqrt{2H}}\frac{e^{-i\sqrt{k^2+\Lambda^2}\eta}(-i+\sqrt{k^2+\Lambda^2}\eta)}{(-\sqrt{k^2+\Lambda^2}\eta)^{\frac{3}{2}}} \tag{3.1.14}$$

and Λ therefore acts as a comoving IR regulator. We see that in this scheme all of the moduli of comoving momenta appearing in a given expression are replaced by

$$k \to k_\Lambda \equiv \sqrt{\vec{k}^2+\Lambda^2}\,, \tag{3.1.15}$$

where we introduced the shorthand notation that we are going to use in the following for this particular combination. In the early-time limit $\eta \to -\infty$ this mode function reduces to

$$\lim_{\eta\to-\infty}\phi_{\vec{k}}(\eta) = (-H\eta)^{\frac{d-2}{2}}\frac{e^{-ik_\Lambda\eta}}{\sqrt{2k_\Lambda}}\,, \tag{3.1.16}$$

which, up to an overall scale factor, corresponds to a massive flat-space mode function with dispersion relation

$$\omega_{\vec{k}} = \sqrt{k^2+\Lambda^2}\,. \tag{3.1.17}$$

From this observation we see that we can think of Λ as a comoving-"mass" parameter. In the limit $\Lambda \to 0$, $d \to 4$ we recover the standard Bunch-Davies-vacuum result

$$\lim_{\eta\to-\infty}\phi_{\vec{k}}(\eta) = (-H\eta)^{\frac{d-2}{2}}\frac{e^{-ik\eta}}{\sqrt{2k}}\,. \tag{3.1.18}$$

Let us also remark at this point that we can give a physical interpretation to this IR-regularization scheme, to a certain extent: adding the term $\sim (-H\eta)^2\Lambda^2\phi^2$ to the action corresponds to giving the scalar field a naive thermal mass

$$m^2_{\text{th}}(\eta) \sim T^2(\eta) \sim a(\eta)^{-2} \tag{3.1.19}$$

that it would get by coupling to a thermal bath of gauge bosons. This explains the non-trivial scaling with η, which is just the standard redshift factor for the temperature of radiation in de Sitter space. Such a term was briefly discussed in [58], and in [59] it was noticed that it can give an effective IR regularization of the theory. Of course, this interpretation is a loose one, because we are not doing fully-fledged thermal field theory, and actual thermal masses do not need renormalization (at least in flat space).

In the full interacting theory, which in this scheme has the bare action

$$S = \int \frac{\mathrm{d}^d x}{(-H\eta)^d}\left[\frac{(-H\eta)^2}{2}\Big[(\partial_\eta\phi_0)^2-(\partial_i\phi_0)^2+\Lambda_0^2\phi_0^2\Big]-\frac{1}{2}m_0^2\phi_0^2-\frac{\kappa_0}{4!}\phi_0^4\right], \tag{3.1.20}$$

the presence of Λ in the mode functions provides a scale for power-like divergences in loop integrals, which will therefore no longer be set to zero by dimreg. Power divergences in the UV will come from the second term in the numerator of (3.1.14), and since the dimension of the numerator is homogeneous, the positive mass dimension of Λ needs to be compensated by something with negative mass dimension. UV divergences cannot come with inverse powers of momenta, since they have to be local, so they must come with powers of the correlation time η. Just as we renormalize the mass parameter m_0^2 in the action to remove logarithmic divergences proportional to H^2, we should renormalize the IR-regularization parameter Λ_0^2 multiplicatively as

$$\Lambda_0^2 = \Lambda^2(1+\delta\Lambda^2)\,, \tag{3.1.21}$$

to remove UV-divergences proportional to $(-\Lambda\eta)^2$, even if they vanish in the limit $\Lambda \to 0$. The definition of the renormalized mass, field and coupling in this version of the theory is still as in (3.1.7), such that in this scheme we can define the counterterms

$$\delta_Z \equiv Z_\phi - 1\,, \quad \delta_m \equiv (Z_\phi-1)m_d^2 + Z_\phi\delta m^2\,, \quad \delta_\Lambda \equiv \Lambda^2[(Z_\phi-1)+Z_\phi\delta\Lambda^2]\,, \quad \delta_\kappa \equiv Z_\kappa Z_\phi^2 - 1\,, \tag{3.1.22}$$

which can be treated perturbatively, and the action can be expressed via the renormalized quantities as

$$S = \int \frac{\mathrm{d}^d x}{(-H\eta)^d} \left[\frac{(-H\eta)^2}{2} \Big[(\partial_\eta \phi)^2 - (\partial_i \phi)^2 + \Lambda^2 \phi^2 \Big] - \frac{1}{2} m_d^2 \phi^2 - \frac{\kappa \tilde{\mu}^{4-d}}{4!} \phi^4 \right.$$
$$\left. + \delta_Z \frac{(-H\eta)^2}{2} \Big[(\partial_\eta \phi)^2 - (\partial_i \phi)^2 + \Lambda^2 \phi^2 \Big] - \frac{1}{2} \delta_m \phi^2 - \frac{(-H\Lambda\eta)^2}{2} \delta_\Lambda \phi^2 - \delta_\kappa \frac{\kappa \tilde{\mu}^{4-d}}{4!} \phi^4 \right] . \tag{3.1.23}$$

To summarize, explicit computations below will always be carried out using dimreg for the UV-divergeces, while we will switch between using dimreg and the Λ regulator for the IR divergences. For clarity, we will remark at the beginning of each section which scheme we will use by means of the following nomenclature:

- **IR-dimreg scheme**: we use dimreg, together with the dimension-dependent mass m_d^2 defined in (3.1.4), to regulate both UV and IR divergences. In spatial momentum space, which will be the setting we will work in, all of the Schwinger-Keldysh propagators introduced in section 1.4 can be expressed by means of the Wightman function

$$\langle \phi(\eta, \vec{k}) \phi(\eta', \vec{k}') \rangle = (2\pi)^{d-1} \delta^{(d-1)}(\vec{k} + \vec{k}') \frac{\pi}{4H} (-H\eta)^{\frac{d-1}{2}} (-H\eta')^{\frac{d-1}{2}} H^{(1)}_{3/2}(-k\eta) H^{(1)*}_{3/2}(-k\eta') . \tag{3.1.24}$$

  After computing all appearing integrals in an expression, we expand the result in a Laurent series in the limit $\varepsilon \to 0$, and both UV and IR divergences will manifest themselves as poles in ε. The poles associated with UV divergences are subtracted by means of the set of counterterms (3.1.8), while the poles associated to IR divergences remain in the renormalized result.

- **k_Λ-scheme**: we use dimreg, together with the dimension-dependent mass m_d^2 defined in (3.1.4), to regularize the UV divergences, while the IR divergences are regulated by means of the Λ regulator, which is introduced via the mode functions (3.1.14). This amounts to replacing $k \to k_\Lambda$ for all the moduli of the momenta appearing in any given diagram. In this scheme, all momentum-space propagators can be expressed by means of the Wightman function

$$\langle \phi(\eta, \vec{k}) \phi(\eta', \vec{k}') \rangle_\Lambda = (2\pi)^{d-1} \delta^{(d-1)}(\vec{k} + \vec{k}') \frac{\pi}{4H} (-H\eta)^{\frac{d-1}{2}} (-H\eta')^{\frac{d-1}{2}} H^{(1)}_{3/2}(-k_\Lambda\eta) H^{(1)*}_{3/2}(-k_\Lambda\eta') . \tag{3.1.25}$$

  Notice the subscript Λ. After computing all appearing integrals in an expression, we expand the result in a double Laurent series in the limit $\varepsilon \to 0$ and $\Lambda \to 0$. The order of the expansion does not matter. In this scheme, only the poles in ε are associated with UV divergences, which are then are subtracted by means of the set of counterterms (3.1.22). The inverse powers and logarithms of Λ which we will find in this scheme are associated to IR-divergences, and they remain in the renormalized result.

Notice that, taking the limit $\Lambda \to 0$ before carrying out any loop integrals, the k_Λ-scheme reduces to the IR-dimreg scheme, which still yields UV- and IR-regular expressions. This will play an important role in the region decomposition of loop diagrams computed in the k_Λ-scheme.

We have set up the formalism for perturbative renormalization in both schemes by defining the sets of counterterms (3.1.8) and (3.1.22), and the renormalized actions (3.1.9) and (3.1.23), respectively, but we still have to define the renormalization conditions in order to determine the counterterms δ_i. In doing so, we distinguish the renormalization of the field, mass and coupling, which are all associated to physical properties of the theory, and the renormalization of the Λ-parameter, which is simply a feature of the k_Λ-scheme and has no physical meaning by itself. As mentioned above, UV divergences will manifest themselves as poles in ε in both the IR-dimreg scheme and the k_Λ-scheme, and in the first scheme one must be careful to distinguish them from IR divergences, since these will also be represented by poles in ε. Clearly, the counterterms must subtract these UV poles, and since we are working with the 't Hooft-scale $\tilde{\mu}$ of the $\overline{\mathrm{MS}}$ scheme this will automatically involve the subtraction of the finite combination $\gamma_E - \ln(4\pi)$ along with every pole, which will prove convenient. To fully fix the renormalization scheme we would also need to specify the UV-finite term that each counterterm should subtract, which could be done, for example, by requiring the two- and four-point functions to assume a certain finite, fixed value at a certain kinematic point. This would constitute the analogue of an "on-shell" renormalization scheme in conventional quantum field theory [34, 35]. However, if we tried to do that, we would run into the following difficulty: since we are computing perturbatively IR-divergent correlation functions, requiring them to have any finite value to fix the renormalization scheme would necessitate the counterterms to absorb the IR divergences present in the correlation function in question. This would clearly not be a sensible result, since the counterterms should be IR-insensitive. The way out of this predicament is to realize that, since the perturbatively computed correlators are IR-divergent, they do not constitute sensible physical observables that can be used to define any meaningful renormalization scheme. What should rather be used for this purpose is a version of these correlators that is computed non-perturbatively, and, as such, free of IR divergences, as is the case e.g. in the stochastic formalism we discussed above in chapter 2. In the present treatment, these IR-finite quantities are precisely what the EFT description of the theory we are discussing is built to compute, so any sensible renormalization condition should be imposed using the non-perturbative version of the correlators computed in that context. Our strategy to renormalize the theory will therefore be the following:

- For the renormalization of the field, mass and coupling we will allow for the presence of a finite part of each of the counterterms δ_i, and we leave it undetermined for now. Since the perturbative correlation functions that we are going to compute in this chapter will constitute the input to determine the matching coefficients in the EFT in the next chapter, these undetermined finite parts of the counterterms will propagate to it. Eventually, the EFT will be used to compute a non-perturbative, IR-finite version of the correlation functions we will consider in perturbation theory in this chapter, and those will be the quantities that can be used to formulate renormalization conditions that will finally fix the yet-undetermined finite parts of the counterterms.

- Since the Λ regulator in the k_Λ scheme has no physical meaning by itself, we can define the renormalization scheme simply by the requirement that it should yield consistent results in the computations. To that end, it will be necessary to determine the finite part of $\delta\Lambda^2$ at each order in the expansion in κ such that it will subtract any finite terms that are associated to an ε-pole that comes with a factor $(-\Lambda\eta)^2$.

3.1.1 Notation, conventions, and Feynman rules

The above discussion sets the stage for the practical computations we will carry out in this chapter. Before moving on to them, let us introduce the notation, conventions, and diagrammatic rules that we will use to compute momentum-space correlation functions. Since the theory we are considering in any of the schemes defined above respects spatial-momentum conservation, any momentum-space n-point correlation function will involve an overall momentum-conserving delta-distribution. In the following, it will be convenient to strip it off by defining a primed version of the correlator in question as follows:

$$\langle\phi(\eta,\vec{k}_1)...\phi(\eta,\vec{k}_n)\rangle \equiv (2\pi)^{d-1}\delta^{(d-1)}\left(\sum_{i=1}^{n}\vec{k}_i\right)\langle\phi(\eta,\vec{k}_1)...\phi(\eta,\vec{k}_n)\rangle' \,. \tag{3.1.26}$$

It will be useful to represent these momentum-space correlators diagrammatically. The basic building block of any diagram is the free two-point function connecting two fields ϕ, which we will represent by a plain, straight line:

$$\phi(\eta,\vec{k}) \;\; \rule[0.5ex]{3cm}{0.4pt} \;\; \phi(\eta',\vec{k}')$$

In the literature it is common to represent cosmological correlators diagrammatically by means of Witten diagrams, as shown on the left-hand panel in figure 3.1 using the example of the tree-level trispectrum.

We find that this pictorial representation becomes somewhat confusing when the topology of the diagrams becomes more complex, and we will therefore stick to a more common, Feynman-diagrammatic representation of the diagrams in question, as shown on the right-hand panel of figure 3.1.

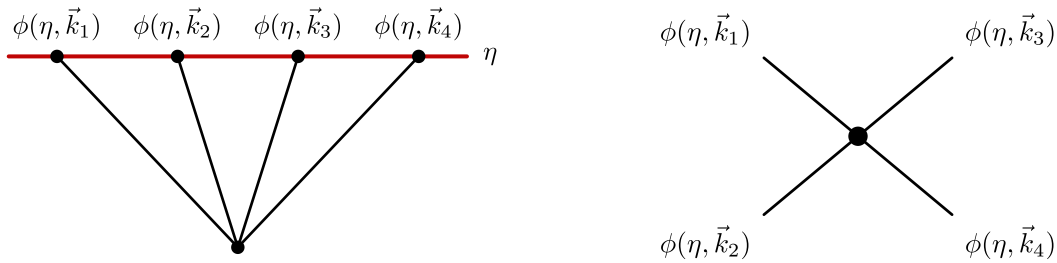

Figure 3.1: Diagrammatic representation of the tree-level trispectrum we are considering as a Witten diagram (left panel) and by the more standard Feynman-diagrammatic depiction (right panel). The red line at the top in the first diagram depicts the late-time boundary at which the correlator is evaluated.

However, the rules of the Schwinger-Keldysh formalism involve two different types of vertices, and for them we will follow the notation of [42] and represent $(+)$- and $(-)$-type vertices by means of full and empty dots, respectively, and draw all diagrams with the various combinations of vertices explicitly. For instance, in a tree-level diagram involving four external legs we would draw the following:

3.2 The method of region for cosmological correlators

Having defined the theory that we will work in, we are now in the position to define the objects we are interested in computing, and to show how the method of regions can be applied to simplify their computation. We will compute the late-time limit of equal-time n-point correlation functions:

$$\lim_{-k_i\eta\to 0}\langle\phi(\eta,\vec{k}_1)...\phi(\eta,\vec{k}_n)\rangle\,,\quad |\vec{k}_1|\sim ...\sim|\vec{k}_n|\,,\tag{3.2.1}$$

where the assumption about all the three-momenta having comparable magnitude, together with the limit we are taking, define what we mean by "late-time" correlators. These are the objects that the EFT, which will be discussed in the next chapter, is built to compute, which motivates our interest in them.

To compute these objects we will work in the Schwinger-Keldysh formalism we introduced in section 1.4, and we will, therefore, have to evaluate multiple nested time- and momentum integrals of the form

$$\int_{-\infty}^{\eta}\frac{\mathrm{d}\eta'}{(-\eta')^d}\int\frac{\mathrm{d}^{d-1}l}{(2\pi)^{d-1}}\tag{3.2.2}$$

over products of mode functions evaluated at different times and momenta. These nested integrations can become notoriously difficult to evaluate [37, 102–104], even at tree-level, once diagrams with multiple vertices are considered, and their evaluation constitutes a major bottleneck in the study of the properties of the correlation functions of interest. While the result of these integrals for general kinematics may be quite complicated, usually the expansion of the result in the limit that we are interested in is vastly simpler. Instead of obtaining this result going through the computation of the full expression first, one may ask if there is a way to simplify the computation at the integrand level, to get more direct access to the desired, simpler result. The method of regions [97–99] was developed just for this purpose. While it was originally conceived with the application to Feynman integrals in mind, the procedure is quite general, and can be applied to the present setting as well. The method works essentially in four steps, which can be applied to any type of integral, as long as at least two external scales, which are widely separated, are involved, and to which the integration variables can be compared. An important caveat, however, is that it is crucial to have a dimensional or analytic regulator in place for the method to work, even if one is trying to compute a finite integral. As discussed above, both schemes we will be working in satisfy this requirement, so we may proceed. The way the method works is as follows:

1) The first step is to identify all of the widely-separated external scales appearing in the integral, which, for us, will be the absolute values of combinations of the external momenta $\vec{k}_i$, which we are assuming to have comparable magnitudes, and the correlation time η. By comparing the magnitude of the integration variables to these external quantities we can define the different regions of the integrals[1]. If a time-integration variable is comparable in magnitude to the external time η, then this defines a "late-time" region. If, instead, it is comparable in magnitude to the inverse of the magnitudes of the external momenta, $1/k_i$, which also implies that it is much larger in magnitude than η, this defines an "early-time" region. Similarly, if a momentum-integration variable is comparable in magnitude to the external momenta $\vec{k}_i$, this defines a "soft-momentum" region, while if it is comparable to $1/|\eta|$, which implies that it is much larger than the magnitudes of the $\vec{k}_i$, this defines a "hard-momentum" region. Since we are dealing with a two-scale problem, the integrals appearing in the quantity of interest will possess two regions each.

2) Having identified all the regions present in the problem, the domain of each integral can be split into pieces in which the associated integration variable can be assumed to have a definite scaling: early ($\eta' \ll \eta$) or late ($\eta' \sim \eta$) for time-integration variables, and hard ($l \gg k_i$) or soft ($l \sim k_i$) for momentum-integration variables. In each of the pieces of the decomposition of the integrals, the combinations of times and momenta appearing in the integrands will have a well-defined scaling, such that we can Taylor-expand the *integrands* in the quantities which are small in each of them, before evaluating the integrals.

3) One can then ignore the restrictions on the integration boundaries that were introduced in the previous step to decompose the integrals into regions, and extend them to the entire integration domain in every region. This is the step that crucially relies on the presence of a dimensional or analytic regulator in the integrals in question. The reason why it works is that extending the regions of integration is equivalent to adding and subtracting scaleless integrals to the region integrals, which are set to zero in dimensional or analytic regularization, and therefore leave the result unchanged. This would not be true in other regularization schemes. Doing so ensures that each region will contribute a series of terms with homogeneous scaling with respect to the external scales. In turn, this implies that each term in the series will contribute to a unique order in the asymptotic expansion resulting from the integrations. The price to pay for this simplification is that, typically, each term in the region decomposition will have additional singularities, which are not present in the full result, and thus must cancel in the sum over the regions. The cancellation of these additional poles serves as a useful consistency check on the computation. Further, as we will see below, these additional singularities are not just a nuisance, but they play a crucial role in reproducing non-analytic terms in the final result.

4) The last step is to compute the integrals appearing in each region and add up the results. The sum of the terms will reproduce the asymptotic expansion of the result of the original integral.

[1] The reason why only the magnitudes of the integration variables are important is because there is no preferred direction singled out by the momenta in the quantities we are interested in computing. This would change if we were to consider special kinematical configurations of the momenta, such as collinear limits.

What the method of regions achieves is the decomposition of complicated, possibly nested, integrals, into sums of simpler, more singular integrals. In doing so, it simplifies the computation of the desired result, and, as an additional benefit, the region structure of an expression gives an important clue as to how such an expression should be reproduced in the context of an EFT description.

Applying this method to the computation of cosmological correlators, we run into the peculiarity that the time integrals have a finite upper boundary, which is a different situation with respect to flat-space computations, where loop integrals always extend over all values of four-momenta. We can understand what the procedure for the region decomposition outlined above implies for the time integrals by considering the simple case of the tree-level four-point function as an example.

3.3 Tree-level trispectrum in the full theory

We start by considering the tree-level trispectrum

$$\langle\phi(\eta,\vec{k}_1)\phi(\eta,\vec{k}_2)\phi(\eta,\vec{k}_3)\phi(\eta,\vec{k}_4)\rangle\,. \tag{3.3.1}$$

The result for the late-time trispectrum in the massless, minimally coupled theory has of course already been computed, and it can be found e.g. in [105]. We will use it in the present setting as a first, simple example for the application of the region decomposition, and also to highlight the fact that, differently than flat-space in-out correlation functions, cosmological corrrelators have a non-trivial region structure already at tree level. This is due to the fact that we cannot get rid of the time integrals associated to the vertices appearing in diagrams, as we did for the spatial integrals by Fourier-transforming our fields, since time translations are not a symmetry of the theory we are considering.

3.3.1 Direct computation

We start by just straightforwardly computing the trispectrum using the in-in Feynman rules and propagators we introduced in section 1.4. The relevant diagrams are

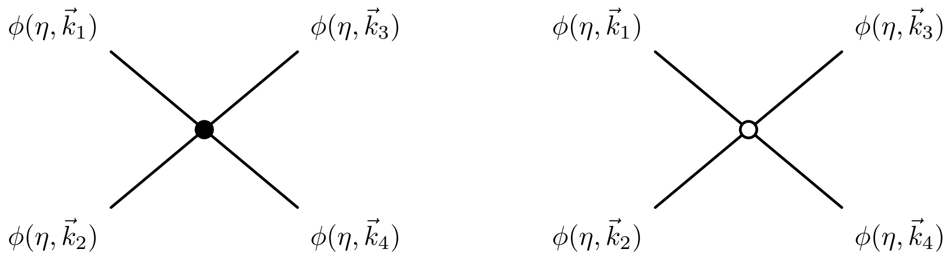

and the correspond to the expression

$$\begin{aligned}
&\langle\phi(\eta,\vec{k}_1)\phi(\eta,\vec{k}_2)\phi(\eta,\vec{k}_3)\phi(\eta,\vec{k}_4)\rangle\\
=&i\tilde{\mu}^{4-d}\kappa\int_{-\infty}^{\eta}\frac{\mathrm{d}\eta'}{(-H\eta')^d}\ \int\left[\prod_{l=1}^{4}\frac{\mathrm{d}^{d-1}p_l}{(2\pi)^{d-1}}\right](2\pi)^{d-1}\delta^{(d-1)}\left(\sum_{l=1}^{4}\vec{p}_l\right)\\
&\times\left[\prod_{i=1}^{4}G_{--}(\eta,\vec{k}_i;\eta',\vec{p}_i)-\prod_{j=1}^{4}G_{++}(\eta,\vec{k}_j;\eta',\vec{p}_j)\right]\\
=&i\tilde{\mu}^{4-d}\kappa(2\pi)^{d-1}\delta^{(d-1)}\left(\sum_{i=1}^{4}\vec{k}_i\right)
\end{aligned}$$

$$\times \int_{-\infty}^{\eta} \frac{\mathrm{d}\eta'}{(-H\eta')^d} \left[\prod_{i=1}^{4} \langle \phi(\eta', \vec{k}_i)\phi(\eta, -\vec{k}_i)\rangle' - \prod_{j=1}^{4} \langle \phi(\eta, \vec{k}_j)\phi(\eta', -\vec{k}_j)\rangle' \right], \tag{3.3.2}$$

where above we are using the Schwinger-Keldysh propagators defined in (1.4.8)-(1.4.11) (using the conformal time variable) and expressing them as Wightman functions, since the ordering of the time arguments is uniquely fixed over the entire integration domain in this case. Further, we have factored out the overall momentum conserving delta-distribution by using the primed notation introduced in (3.1.26). Since the computation will not involve any IR-divergent momentum integrals, both the IR-dimreg scheme and the k_Λ-scheme would yield the same result, and we work in the former scheme for simplicity. Using the Wightman functions (3.1.24) we find the expression

$$\begin{aligned}&\langle \phi(\eta, \vec{k}_1)\phi(\eta, \vec{k}_2)\phi(\eta, \vec{k}_3)\phi(\eta, \vec{k}_4)\rangle' \\ =&\frac{\tilde{\mu}^{4-d}\kappa H^d(-H\eta)^{2d-8}}{8(k_1k_2k_3k_4)^3} \mathrm{Im}\left[\int_{-\infty}^{\eta} \frac{\mathrm{d}\eta'}{(-\eta')^{8-d}} e^{ik_t(\eta'-\eta)} \prod_{j=1}^{4}(-i+k_j\eta)(i+k_j\eta') \right].\end{aligned} \tag{3.3.3}$$

The time integral we have to compute is finite, as long as η is kept finite, and we can therefore safely set $d = 4$ before integrating, which simplifies the computation slightly. The appearing integrals can be computed in terms of exponential integral functions, and taking the late-time limit $-k_i\eta \to 0$ results in [100, 105]

$$\begin{aligned}&\lim_{-k_i\eta\to 0} \langle \phi(\eta, \vec{k}_1)\phi(\eta, \vec{k}_2)\phi(\eta, \vec{k}_3)\phi(\eta, \vec{k}_4)\rangle' \\ =&\frac{\kappa H^4}{8(k_1k_2k_3k_4)^3} \left[\frac{1}{3}\left(\frac{1}{3} + \ln(-e^{\gamma_E}k_t\eta) \right) \sum_{j=1}^{4} k_j^3 - \frac{k_1k_2k_3k_4}{k_t} + k_t \left(\sum_{j<l} k_jk_l - \frac{4}{9}k_t^2 \right) \right],\end{aligned} \tag{3.3.4}$$

where $k_t \equiv k_1 + k_2 + k_3 + k_4$ denotes the sum of the moduli of the external momenta. Before seeing how this result can be reproduced using the method of regions, we note the appearence of the secular logarithm $\ln(-e^{\gamma_E}k_t\eta)$ in the above result, which is the first signal of the IR-singular behaviour of the perturbative expansion of the massless, minimally coupled theory.

3.3.2 Computation using the method of regions

We will now see how this result can be reproduced using the method of regions. We will also use this example as an opportunity to discuss the general procedure to decompose time integrals into their regions, which is slightly different than the conventional region decomposition of momentum integrals in flat space, due to the presence of the non-trivial upper integration boundary.

Identification of the regions of the time integral

To illustrate the general procedure, we abstract the time integration that we carried out in (3.3.3) and write the following integral, evaluated in the late-time limit:

$$\lim_{-k_i\eta\to 0} \int_{-\infty}^{\eta} \mathrm{d}\eta' \, (-\eta')^{-\varepsilon} f(-k_i\eta, -k_i\eta'). \tag{3.3.5}$$

In the above, we are representing the presence of the dimensional regulator by writing the factor $(-\eta')^{-\varepsilon}$ explicitly, while the ε-independent remainder of the integrand of (3.3.3) is represented by f. We now use the method of regions following the steps outlined in section 3.2.

The first step is to identify the regions of the integral in question by using the external scales present in the problem. Since we are assuming the combination $-k_i\eta \ll 1$ to be small, the widely-separated scales are k_i and η. There are then two possibilities: either η' is comparable to the correlation time, $\eta' \sim \eta$, or it is comparable to the inverse magnitude of the momenta, $-\eta' \sim k_i^{-1}$, which then implies $\eta' \ll \eta$. The first possibility defines the late-time region of the time integral, and since we have $\eta' \sim \eta$ the assumption $-k_i\eta \ll 1$ also implies $-k_i\eta' \ll 1$ in this region. We can therefore Taylor-expand the integrand in both of these combinations. On the other hand, the second possibility, which defines the early-time region, has as a consequence that, while $-k_i\eta \ll 1$, we have $-k_i\eta' \sim 1$. In this region, we can therefore only expand the integrand in the small combination $-k_i\eta$, but we have to leave its dependence on $-k_i\eta'$ untouched.

In the next step, we decompose the time integral (3.3.5) into the two regions we identified above. To see how to do this properly, it is useful to extend the domain of integration of the time integral in question to $(-\infty, 0)$ and implement the cutoff at the upper boundary using a θ-distribution as

$$\int_{-\infty}^{\eta} \mathrm{d}\eta' \, (-\eta')^{-\varepsilon} f(-k_i\eta, -k_i\eta') = \int_{-\infty}^{0} \mathrm{d}\eta' \, \theta(\eta - \eta')(-\eta')^{-\varepsilon} f(-k_i\eta, -k_i\eta') \,. \tag{3.3.6}$$

We now split this integral into the regions we identified by introducing the intermediate scale[2] Λ, which separates the two relevant scales as $-k_i^{-1} \ll \Lambda \ll \eta$. The integral (3.3.6) then reads

$$\begin{aligned}
&\lim_{-k_i\eta\to 0} \int_{-\infty}^{0} \mathrm{d}\eta' \, \theta(\eta - \eta')(-\eta')^{-\varepsilon} f(-k_i\eta, -k_i\eta') \\
=& \lim_{-k_i\eta\to 0} \int_{-\infty}^{\Lambda} \mathrm{d}\eta' \, \theta(\eta - \eta')(-\eta')^{-\varepsilon} f(-k_i\eta, -k_i\eta') + \lim_{-k_i\eta\to 0} \int_{\Lambda}^{0} \mathrm{d}\eta' \, \theta(\eta - \eta')(-\eta')^{-\varepsilon} f(-k_i\eta, -k_i\eta') \\
\equiv& I_{\text{early}} + I_{\text{late}} \,.
\end{aligned} \tag{3.3.7}$$

The two pieces in which we have split the integral have the following physical interpretation: they represent the periods of subhorizon ($-k_i\eta' \sim 1$) and superhorizon ($-k\eta' < 1$) evolution of the field modes contributing to the late-time correlation function we are computing. This is made particularly clear by including the intermediate scale Λ in the definition of I_{early} and I_{late}. However, if kept, the presence of this new intermediate scale, which will drop out when we sum up our results for the individual regions, would complicate the computation of the integrals[3]. We will now see how it can be removed altogether, by making use of the properties of dimreg, without changing the final result.

We start by considering I_{early}, which corresponds to the early-time region, in which $\eta' \sim -1/k_i \ll \eta$. In this region, we can expand the integrand in the quantity $-k_i\eta \ll 1$, but we must keep the full dependence on $-k_i\eta'$. Additionally, we can expand the θ-distribution in a distributional sense as

$$\theta(\eta - \eta') = \theta(-\eta') + \eta \, \delta(-\eta') + \mathcal{O}(\eta^2) \,, \tag{3.3.8}$$

and we only need to keep the first term if we are interested in the leading-order term of the asymptotic expansion as $\eta \to 0$. The early-time integral can therefore be rewritten as

$$I_{\text{early}} = \int_{-\infty}^{\Lambda} \mathrm{d}\eta' \, \theta(-\eta')(-\eta')^{-\varepsilon} f(-k_i\eta, -k_i\eta') \Big|_{\substack{-k_i\eta' \sim 1 \\ -k_i\eta \ll 1}} \,, \tag{3.3.9}$$

Notice that the θ-distribution no longer imposes any restriction on the boundaries of the time integral, since the argument is always positive for all possible values of η'. This implies that the result of I_{early} will be time-independent.

Analogously, the integral I_{late} corresponds to the late-time region, in which $\eta' \sim \eta$. Since the argument of $\theta(\eta - \eta')$ scales homogeneously, we leave it untouched, and we expand the remainder of the integrand in the small quantities, which are both $-k_i\eta$ and $-k_i\eta'$ in this region. The late-time integral we obtain in this manner reads

$$I_{\text{late}} = \int_{\Lambda}^{0} \mathrm{d}\eta' \, \theta(\eta - \eta')(-\eta')^{-\varepsilon} f(-k_i\eta, -k_i\eta') \Big|_{\substack{-k_i\eta' \ll 1 \\ -k_i\eta \ll 1}} \,. \tag{3.3.10}$$

[2]This scale should not be confused with the IR regulator of the k_Λ scheme.

[3]However, see [106] for an approach that keeps the dependence on this scale.

In the third step we remove the intermediate scale Λ we introduced above, and extend the integration range to the full one in I_{early}, by letting $\Lambda \to 0$, as well as in I_{late}, by letting $\Lambda \to -\infty$. As remarked in 3.2, this operation corresponds to adding and subtracting scaleless integrals of the form

$$\int_{-\infty}^{0} \mathrm{d}\eta' \, (-\eta')^{n-\varepsilon} = 0 \,, \quad n \in \mathbb{Z} \,, \tag{3.3.11}$$

where the equality only holds because we have our dimensional regulator in place, even though we are trying to reproduce a finite result. By implementing the restriction on the domain of integration imposed by the θ-distributions in the integrands, we find

$$\begin{aligned} &\lim_{-k_i\eta \to 0} \int_{-\infty}^{0} \mathrm{d}\eta' \, \theta(\eta - \eta')(-\eta')^{-\varepsilon} f(-k_i\eta, -k_i\eta') \\ &= \int_{-\infty}^{0} \mathrm{d}\eta' \, (-\eta')^{-\varepsilon} f(-k_i\eta, -k_i\eta')\Big|_{\substack{-k_i\eta' \sim 1 \\ -k_i\eta \ll 1}} + \int_{-\infty}^{\eta} \mathrm{d}\eta' \, (-\eta')^{-\varepsilon} f(-k_i\eta, -k_i\eta')\Big|_{\substack{-k_i\eta' \ll 1 \\ -k_i\eta \ll 1}} . \end{aligned} \tag{3.3.12}$$

As anticipated above, for the early-time integral, the integration domain is now the full range of possible values of η'. This is a generic feature of the early-time regions of the time integrals we will consider in the remainder of this thesis.

We have therefore decomposed the original integral into the sum of two simpler integrals, due to the Taylor expansion of the integrands. Moreover, the results of both integrals will scale homogeneously with respect to the external scales we are considering, which is ensured by the elimination of the fictitious intermediate scale Λ. However, as we will see below, both region integrals will now contain a divergence, in the form of a pole in ε, as a consequence of extending the ranges of integration. Indeed, the divergence of I_{early} comes from the limit $\eta' \to 0$, which can be identified as an IR pole, while the divergence of I_{late} comes from $\eta' \to -\infty$, which can be identified as a UV pole. Since we are computing a finite quantity, these divergences must cancel in the sum after expanding the result of both integrals for small ε. We will see below that these singularities play a crucial role in generating the logarithmic term in (3.3.4).

Let us now compute the two regions of (3.3.4) explicitly.

Late-time region

In this region we expand the integrand of (3.3.3) assuming both $-k_i\eta'$ and $-k_i\eta$ to be small, and we must keep all terms up to $\mathcal{O}((-k_i\eta')^3)$ and $\mathcal{O}((-k_i\eta)^3)$ to capture all terms in the expansion of (3.3.3) which do not yield a vanishing contribution in the limit we are considering. Doing so we find

$$\begin{aligned} &\langle \phi(\eta, \vec{k}_1)\phi(\eta, \vec{k}_2)\phi(\eta, \vec{k}_3)\phi(\eta, \vec{k}_4)\rangle' \Big|_{\text{late } \eta'} \\ =& \frac{\tilde{\mu}^{4-d}\kappa H^d(-H\eta)^{2d-8}}{8(k_1k_2k_3k_4)^3} \lim_{\eta \to 0} \mathrm{Im}\Bigg[\Bigg(1 + \frac{\eta^2}{2}\sum_{i=1}^{4} k_i^2 - \frac{i\eta^3}{3}\sum_{i=1}^{4} k_i^3 + \mathcal{O}\Big((-k_i\eta)^4\Big)\Bigg) \\ &\times \int_{-\infty}^{\eta} \frac{\mathrm{d}\eta'}{(-\eta')^{8-d}} \Bigg(1 + \frac{(-\eta')^2}{2}\sum_{i=1}^{4} k_i^2 - \frac{i(-\eta')^3}{3}\sum_{i=1}^{4} k_i^3 + \mathcal{O}\Big((-k_i\eta')^4\Big)\Bigg)\Bigg] . \end{aligned} \tag{3.3.13}$$

Notice that the expanded integrand only involves integrals of the form

$$\int_{-\infty}^{\eta} \frac{\mathrm{d}\eta'}{(-\eta')^a} = \frac{(-\eta)^{1-a}}{a-1} \,, \tag{3.3.14}$$

which clearly have a homogeneous scaling with η. Importantly, when evaluating this type of integrals we are still assuming the efficacy of the $i\varepsilon$-prescription in damping the contribution from $\eta' \to -\infty$, irrespective of the value of a. In this simple case it is possible to determine the full non-analytic dependence on η of the result without actually carrying out any of the integrals, since it will simply be given by an overall factor $(-\eta)^{-2\varepsilon}$. This is guaranteed by the fact that we have Taylor-expanded the integral in both quantities involving the external momenta, which therefore only appear in integer powers. From this observation, we can also anticipate that the ε-expansion of the result will generate the time-dependent piece of the secular logarithm appearing in (3.3.4).

Computing the integrals appearing in (3.3.13) we find

$$
\begin{aligned}
&\langle\phi(\eta,\vec{k}_1)\phi(\eta,\vec{k}_2)\phi(\eta,\vec{k}_3)\phi(\eta,\vec{k}_4)\rangle'\Big|_{\text{late }\eta'} \\
=&-\frac{\kappa H^{4+2\varepsilon}(-H\eta)^{-4\varepsilon}}{8(k_1k_2k_3k_4)^3}\left(-\frac{H^2\eta}{\tilde{\mu}}\right)^{-2\varepsilon}\frac{1}{2\varepsilon(3+2\varepsilon)}\sum_{j=1}^{4}k_j^3 \\
=&\frac{\kappa H^{4+2\varepsilon}(-H\eta)^{-4\varepsilon}}{24(k_1k_2k_3k_4)^3}\left[-\frac{1}{2\varepsilon}+\frac{1}{3}+\ln\left(-\frac{H^2\eta}{\tilde{\mu}}\right)\right]\sum_{j=1}^{4}k_j^3+\mathcal{O}(\varepsilon)\,,
\end{aligned}
\tag{3.3.15}
$$

which is the leading-order result for the late-time region in powers of $-k_i\eta$. Notice that when expanding the result in ε to get the last equality we only expanded the combination $(-H^2\eta/\tilde{\mu})^{-2\varepsilon}$, since the remaining ε-dependent pieces of the expression are common to both regions, and if we expanded them as well their contributions would just drop out in the sum of the regions, together with the poles.

We see that in the logarithm appearing in (3.3.15) $\tilde{\mu}$ takes the role of the factorisation scale. By rewriting the logarithm in qeustion as

$$
\ln\left(-\frac{H^2\eta}{\tilde{\mu}}\right)=\ln\left(\frac{H}{a(\eta)\tilde{\mu}}\right)\,,
\tag{3.3.16}
$$

we can read off the typical value of $\tilde{\mu}$ for which this logarithm is small, which is $\tilde{\mu}\sim -H^2\eta = H/a(\eta)$. This choice corresponds to the natural scale associated with the late-time region, in which the physical momenta of the superhorizon modes satisfy $k_i/a(t)\ll H$. In this setting, the $\tilde{\mu}$-dependence also tracks the η- (or equivalently, $a(t)$-) dependence of the tree-level trispectrum. We will see in the next chapter that something quite analogous will happen in the EFT, and it will eventually allow us to control and resum these logarithms to all orders.

Early-time region

We now turn to the computation of the early-time region. In this region, the quantity $-k_i\eta$ is small, so we expand the integrand of (3.3.3) in it, but since we have $-k_i\eta'\sim 1$ we must keep the full dependence of the integrand it. Following our discussion above, we must also push the upper integration boundary to 0. This results in

$$
\begin{aligned}
&\langle\phi(\eta,\vec{k}_1)\phi(\eta,\vec{k}_2)\phi(\eta,\vec{k}_3)\phi(\eta,\vec{k}_4)\rangle'\Big|_{\text{early }\eta'} \\
=&\frac{\tilde{\mu}^{4-d}\kappa H^d(-H\eta)^{2d-8}}{8(k_1k_2k_3k_4)^3}\,\mathrm{Im}\left[\int_{-\infty}^{0}\frac{\mathrm{d}\eta'}{(-\eta')^{8-d}}e^{ik_t\eta'}\prod_{j=1}^{4}(i+k_j\eta')\right].
\end{aligned}
\tag{3.3.17}
$$

As we anticipated above, the early-time region of the trispectrum is time-independent, except for the overall factor $(-H\eta)^{2d-8}$, which will become irrelevant as $d\to 4$. Similarly to the case of the late-time region, we have to compute single-scale integrals of the form

$$
\int_{-\infty}^{0}\frac{\mathrm{d}\eta'}{(-\eta')^{a}}\,e^{ik_t\eta'}=(ik_t)^{a-1}\Gamma(1-a)\,,
\tag{3.3.18}
$$

which have a homogenous scaling in the only remaining external scale k_t. The ε-expansion of the result of these integrals will generate logs of k_t, and will therefore give us the missing time-independent piece of the logarithm appearing in (3.3.4). Evaluating the expression (3.3.17) we find the result

$$
\langle\phi(\eta,\vec{k}_1)\phi(\eta,\vec{k}_2)\phi(\eta,\vec{k}_3)\phi(\eta,\vec{k}_4)\rangle'\Big|_{\text{early }\eta'}
$$

$$
\begin{aligned}
=&\frac{\kappa H^{4+2\varepsilon}(-H\eta)^{-4\varepsilon}}{8(k_1k_2k_3k_4)^3}\Gamma(-3-2\varepsilon)\left(\frac{k_t\tilde{\mu}}{H^2}\right)^{2\varepsilon}\Bigg\{2\sum_{j=1}^4 k_j^3+\varepsilon\Bigg[\frac{22}{3}\sum_{j=1}^4 k_j^3\\
&-12\left(\frac{k_1k_2k_3k_4}{k_t}-k_t\left(\sum_{j<l}k_jk_l-\frac{4}{9}k_t^2\right)\right)\Bigg]+\mathcal{O}(\varepsilon^2)\Bigg\}\,.
\end{aligned}
\tag{3.3.19}
$$

The expected divergence is generated by the factor $\Gamma(-3-2\varepsilon)$, and the ε-expansion of this result reads

$$
\begin{aligned}
&\langle\phi(\eta,\vec{k}_1)\phi(\eta,\vec{k}_2)\phi(\eta,\vec{k}_3)\phi(\eta,\vec{k}_4)\rangle'\Big|_{\text{early }\eta'}\\
=&\frac{\kappa H^{4+2\varepsilon}(-\eta H)^{-4\varepsilon}}{8(k_1k_2k_3k_4)^3}\Bigg\{\frac{1}{3}\left[\frac{1}{2\varepsilon}+\ln\left(\frac{e^{\gamma_E}k_t\tilde{\mu}}{H^2}\right)\right]\sum_{j=1}^4 k_j^3-\frac{k_1k_2k_3k_4}{k_t}\\
&+k_t\left(\sum_{j<l}k_jk_l-\frac{4}{9}k_t^2\right)\Bigg\}\,.
\end{aligned}
\tag{3.3.20}
$$

We find the logarithm

$$
\ln\left(\frac{e^{\gamma_E}k_t\tilde{\mu}}{H^2}\right)
\tag{3.3.21}
$$

in this expression and, as in (3.3.15), the scale $\tilde{\mu}$ plays the role of the factorization scale. Instead of a conformal-time factor we now have the quantity k_t appearing in it. However, we can identify it as $k_t\sim-\eta_{\mathrm{cr},k_t}^{-1}=[a(t_{\mathrm{cr},k_t})H]^{-1}$, which is the time when the quantity k_t crosses the horizon. Using this relation to convert k_t into a time variable, we recognize that the found logarithm has the same form as in (3.3.15), with the replacement $\eta\to\eta_{\mathrm{cr},k_t}$. Consequently, the natural scale associated to this logarithm, for which it becomes small, is $\tilde{\mu}\sim-H^2\eta_{\mathrm{cr},k_t}=H/a(\eta_{\mathrm{cr},k_t})$.

Sum of the regions

Having computed both regions of the time integral, we can sum them up to find

$$
\begin{aligned}
&\langle\phi(\eta,\vec{k}_1)\phi(\eta,\vec{k}_2)\phi(\eta,\vec{k}_3)\phi(\eta,\vec{k}_4)\rangle'\Big|_{\text{early }\eta'}+\langle\phi(\eta,\vec{k}_1)\phi(\eta,\vec{k}_2)\phi(\eta,\vec{k}_3)\phi(\eta,\vec{k}_4)\rangle'\Big|_{\text{late }\eta'}\\
&=\frac{\kappa H^4}{8(k_1k_2k_3k_4)^3}\left[\frac{1}{3}\left(\frac{1}{3}+\ln(-e^{\gamma_E}k_t\eta)\right)\sum_{j=1}^4 k_j^3-\frac{k_1k_2k_3k_4}{k_t}+k_t\left(\sum_{j<l}k_jk_l-\frac{4}{9}k_t^2\right)\right].
\end{aligned}
\tag{3.3.22}
$$

The poles in ε appearing in (3.3.15) and (3.3.20) cancel, as it should be, and the associated logarithms combine to reproduce the one we found in (3.3.4). Since the poles are gone, we can let $\varepsilon\to0$ in the overall coefficients we found in (3.3.15) and (3.3.20) as well, which therefore just go to 1. Further, the time-independent terms match the ones in (3.3.4) as well, so we succesfully reproduce the whole expression.

In this simple example the region decomposition was in fact more laborious than simply computing the full expression and taking the late-time limit to find the desired result. Nonetheless, it served as a useful example to illustrate the region decomposition for time integrals, which is slightly different than the usual procedure for momentum integrals. The true power of the method of regions becomes apparent when starting to compute non-trivial loop diagrams, as we will see in the following sections.

3.4 One-loop power spectrum

In this section we compute the first and simplest loop diagram in the theory we are considering, which is the $\mathcal{O}(\kappa)$-contribution to the power spectrum

$$
\langle\phi(\eta,\vec{k})\phi(\eta,\vec{k}')\rangle\,.
\tag{3.4.1}
$$

At this order in the perturbative expansion we have two distinct diagram topologies to consider. The first follows from the insertion of the quartic vertex $\sim \kappa\phi^4$, which leads to the diagrams

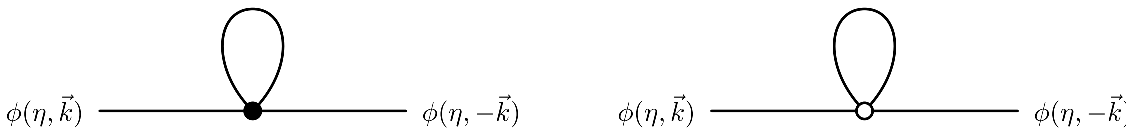

and the second from the insertion of the mass counterterm δm^2, which leads to the diagrams

where we are denoting the insertion of δm^2 by a square. The mass counterterm is present in both the IR-dimreg scheme and the k_Λ-scheme, and in the latter we also have to consider the insertion of the counterterm $\delta\Lambda^2$, which leads to analogous diagrams as the insertion of the mass counterterm.

We will find that the momentum integral associated to the loop diagram will be both UV- and IR-divergent, and we will compute the result using the two different regularization schemes introduced in section 3.1. Since in this case the momentum integration factorizes from the time integration, this example does not yet showcase the full complexity of a non-trivial one-loop computation in de Sitter space, but is in fact closer to a single-vertex, tree-level diagram. For this reason, as was the case for the trispectrum we considered in section 3.3, the computation of this quantity using the method of regions will be more laborious than the direct computation. However, the region decomposition itself is still interesting to consider, since it will instruct us on what we should expect when we will reproduce this result using the EFT in the next chapter, so we will consider in the main text. The concrete computation of the single region integrals, which is the less interesting part, is relegated to appendix 3.A.

3.4.1 Computation in the k_Λ-scheme

We start by computing the one-loop power spectrum in the k_Λ-scheme. This scheme is not exactly the same that was used in [100], since there only the momentum appearing in the denominator of the Hankel function $H^{(1)}_{3/2}(-k\eta)$ was modified. However, for the present computation the differences between the two schemes turn out to be irrelevant, so we will still find the same result as [100]. The present discussion of the renormalization of the IR regulator Λ itself, however, goes beyond what is discussed in the mentioned reference, and will be very important later on in this chapter.

Vertex-insertion diagram

Using the in-in Feynman rules outlined in section 1.4 the vertex-insertion diagrams depicted above lead to the following expression:

$$\begin{aligned}
&\langle\phi(\eta,\vec{k})\phi(\eta,-\vec{k})\rangle'\Big|_\kappa \\
=&\frac{i\kappa\tilde{\mu}^{4-d}}{2}\int_{-\infty}^{\eta}\frac{\mathrm{d}\eta'}{(-H\eta')^d}\int\frac{\mathrm{d}^{d-1}l}{(2\pi)^{d-1}}\left[\langle\bar{T}\{\phi(\eta,\vec{k})\phi(\eta',-\vec{k})\}\rangle_\Lambda'^{\,2}-\langle T\{\phi(\eta,\vec{k})\phi(\eta',-\vec{k})\}\rangle_\Lambda'^{\,2}\right] \\
&\times\langle\phi(\eta',\vec{l})\phi(\eta',-\vec{l})\rangle_\Lambda \\
=&\frac{\tilde{\mu}^{4-d}\kappa H^{d-2}}{8}(-H\eta)^{d-4}\mathrm{Im}\left[\int_{-\infty}^{\eta}\frac{\mathrm{d}\eta'}{(-\eta')^{8-d}}\frac{e^{2ik_\Lambda(\eta'-\eta)}(i-k_\Lambda\eta)^2(i+k_\Lambda\eta')^2}{k_\Lambda^6}\right]
\end{aligned} \tag{3.4.2}$$

$$\times \int \frac{\mathrm{d}^{d-1}l}{(2\pi)^{d-1}} \frac{1 + l_\Lambda^2 \eta'^2}{l_\Lambda^3} \,. \tag{3.4.3}$$

We have used the fact that $\eta' < \eta$ for all values of η' to fix the (anti-)time-ordering, and the k_Λ-scheme Wightman function (3.1.25) to obtain the last equality. As anticipated, we see that the time and momentum integrals are factorized from each other, so we can consider them individually. The loop integral reads, after writing out the explicit form of l_Λ,

$$I(\eta') \equiv \tilde{\mu}^{2\varepsilon} \int \frac{\mathrm{d}^{d-1}l}{(2\pi)^{d-1}} \frac{1 + (l^2 + \Lambda^2)\eta'^2}{[l^2 + \Lambda^2]^{\frac{3}{2}}} = \frac{1}{4\pi^2} \left(\frac{\Lambda}{\mu}\right)^{-2\varepsilon} e^{\varepsilon\gamma_E} \Gamma(\varepsilon) \left[1 - \frac{(\Lambda\eta')^2}{2(1-\varepsilon)}\right] . \tag{3.4.4}$$

We notice that we have two types of UV-divergent terms, coming from the logarithmic divergence and quadratic divergences in the integral, respectively. Since Λ is the only scale appearing in the integral in question, the quadratic divergence is necessarily proportional to Λ^2, which then combines with η'^2 to give a dimensionless quantity. The fact that this divergence is time-dependent signals the explicit breaking of the de Sitter-invariance of this result, which is to be expected, since we deformed the theory in a non-de Sitter-invariant way in order to introduce the IR regulator. Both of these divergences need to be subtracted by means of appropriate counterterms, even though the divergence proportional to Λ will vanish as we let $\Lambda \to 0$.

Even though we need to keep in mind the presence of the $\mathcal{O}(\Lambda^2)$ pieces for the choice of the counterterms later on in this section, they become irrelevant if we are only interested in the regularized result, expanded up to $\mathcal{O}(\Lambda^0, \varepsilon^0)$, in the late-time limit, which reads

$$\begin{aligned}
&\langle \phi(\eta, \vec{k})\phi(\eta, -\vec{k})\rangle' \Big|_\kappa \\
=&\frac{\kappa H^2}{24\pi^2 k^3}(-H\eta)^{-4\varepsilon}\left(\frac{\mu}{\Lambda}\right)^{2\varepsilon}\left[-\frac{1}{2\varepsilon}\Big[2 - \ln(-2e^{\gamma_E}k\eta)\Big] + \frac{1}{2}\ln^2(-2e^{\gamma_E}k\eta) - \frac{7}{3}\ln(-2e^{\gamma_E}k\eta) + \frac{8}{3} - \frac{\pi^2}{24}\right] .
\end{aligned} \tag{3.4.5}$$

Notice the absence of the coefficient e^{γ_E} in front of μ in the above equation, which was erroneously included in the analogous equation in [100], as well as the missing factor of $a(\eta)$ associated to Λ, which was introduced by hand in the mentioned reference. We have left an overall ε-dependent factor unexpanded, in order to avoid cluttering the expression.

Counterterm diagrams

As we discussed above in section 3.1, the action of our theory, expressed in terms of renormalized quantities, contains the following counterterms:

$$S \supset -\frac{1}{2} \int \frac{\mathrm{d}^d x}{(-H\eta)^d} \left[\delta m^2 \phi(\eta, \vec{x})^2 + (-H\eta)^2 \delta\Lambda^2 \phi(\eta, \vec{x})^2\right] . \tag{3.4.6}$$

We will need them both in order to remove the UV divergences due to the loop integral (3.4.4).

The mass-counterterm diagrams we drew above lead to the following expression:

$$\begin{aligned}
\langle \phi(\eta, \vec{k})\phi(\eta, -\vec{k})\rangle' \Big|_{\delta m^2} =& i \int_{-\infty}^{\eta} \frac{\mathrm{d}\eta'}{(-H\eta')^d} \left[\langle \bar{T}\{\phi(\eta, \vec{k})\phi(\eta', -\vec{k})\}\rangle_\Lambda'^{\,2} - \langle T\{\phi(\eta, \vec{k})\phi(\eta', -\vec{k})\}\rangle_\Lambda'^{\,2}\right] \delta m^2 \\
=& \frac{\delta m^2}{2}(-H\eta)^{d-4} \mathrm{Im}\left[\int_{-\infty}^{\eta} \frac{\mathrm{d}\eta'}{(-\eta')^4} \frac{e^{2ik_\Lambda(\eta'-\eta)}(i - k_\Lambda\eta)^2(i + k_\Lambda\eta')^2}{k_\Lambda^6}\right] .
\end{aligned} \tag{3.4.7}$$

Notice that the time integral which we find is independent of the spacetime dimension d. This is a peculiarity of the regularization scheme we are using, and it only happens when considering insertions of operators that are quadratic in ϕ. However, since the integral in question is finite, it poses no problem in the present context, and we can just proceed with the computation. Comparing the above result to (3.4.3), we see that the mass counterterm is multiplying the same time integral as the loop integral in (3.4.3), up to $\mathcal{O}(\varepsilon)$ terms. For this reason, we can read off the pole term that δm^2 needs to subtract simply from the ε-expansion of the result of the loop integral (3.4.4), and we find that the appropriate expression is

$$\delta m^2 = \frac{\kappa H^2}{8\pi^2}\left[-\frac{1}{2\varepsilon}+\delta\hat{m}^2_{\text{fin}}\right]+\mathcal{O}(\kappa^2)\,. \tag{3.4.8}$$

As we discussed in section 3.1, we are not yet in a position to determine the finite part of the mass counterterm $\delta\hat{m}^2_{\text{fin}}$, which we have rewritten as a dimensionless quantity here, in a physically meaningful way, so we leave it undetermined for now.

The insertion of the Λ-counterterm leads to diagrams with the same topology as in the case of the mass counterterm, and the corresponding expression reads

$$\begin{aligned}\langle\phi(\eta,\vec{k})\phi(\eta,-\vec{k})\rangle'\Big|_{\delta\Lambda^2} =& i\int_{-\infty}^{\eta}\frac{\mathrm{d}\eta'}{(-H\eta')^d}\left[\langle\bar{T}\{\phi(\eta,\vec{k})\phi(\eta',-\vec{k})\}\rangle_\Lambda'^{\,2}-\langle T\{\phi(\eta,\vec{k})\phi(\eta',-\vec{k})\}\rangle_\Lambda'^{\,2}\right]\delta\Lambda^2(-H\Lambda\eta')^2\\ =&\frac{H^2\delta\Lambda^2}{2}(-H\eta)^{d-4}\mathrm{Im}\left[\int_{-\infty}^{\eta}\frac{\mathrm{d}\eta'}{(-\eta')^4}\frac{e^{2ik_\Lambda(\eta'-\eta)}(i-k_\Lambda\eta)^2(i+k_\Lambda\eta')^2}{k_\Lambda^6}(-\Lambda\eta')^2\right].\end{aligned} \tag{3.4.9}$$

Comparing this expression again to (3.4.3), we see that it has the appropriate structure to subtract the UV divergence proportional to $(-\Lambda\eta')^2$ generated by the momentum integral (3.4.4). As we discussed above, while the divergent part of the counterterm is unambiguous, we make the choice to fix its finite part to subtract the finite $\mathcal{O}(\Lambda^2)$ terms which stem from the ε-expansion of the integral (3.4.4) as well, and find

$$\delta\Lambda^2 = \frac{\kappa}{32\pi^2}\left[\frac{1}{\varepsilon}+1\right]+\mathcal{O}(\kappa^2)\,. \tag{3.4.10}$$

However, as already mentioned, for the present computation the $\mathcal{O}(\Lambda^2)$ term does not contribute, so and we find the following result for the contribution from the mass- and Λ-counterterms to the one-loop power spectrum:

$$\langle\phi(\eta,\vec{k})\phi(\eta,-\vec{k})\rangle'\Big|_{\delta m^2+\delta\Lambda^2} = \frac{\kappa H^2}{24\pi^2k^3}(-H\eta)^{-2\varepsilon}\left[\frac{1}{2\varepsilon}-\delta\hat{m}^2_{\text{fin}}\right]\Big[2-\ln(-2e^{\gamma_E}k\eta)\Big]\,. \tag{3.4.11}$$

Renormalized result

Summing (3.4.5) and (3.4.11) and expanding the ε-dependent factors which the two expressions do not have in common we find

$$\begin{aligned}\langle\phi(\eta,\vec{k})\phi(\eta,-\vec{k})\rangle'\Big|_{\mathcal{O}(\kappa)} =& \frac{\kappa H^2}{24\pi^2k^3}\bigg\{\Big[2-\ln(-2e^{\gamma_E}k\eta)\Big]\left[\ln\left(-\frac{H\Lambda\eta}{\mu}\right)-\delta\hat{m}^2_{\text{fin}}\right]+\frac{1}{2}\ln^2(-2e^{\gamma_E}k\eta)\\ &-\frac{7}{3}\ln(-2e^{\gamma_E}k\eta)+\frac{8}{3}-\frac{\pi^2}{24}\bigg\}\,.\end{aligned} \tag{3.4.12}$$

Notice the logarithmic dependence on Λ of this result, which is how the logarithmic IR-divergence of the momentum integral (3.4.4) manifests itself in this scheme.

Region decomposition of the one-loop power spectrum

Before repeating the computation we did above in the IR-dimreg scheme, we study the region decomposition of the expressions contributing to the one-loop power spectrum in the present scheme. As we will see below, the present discussion will also be applicable to the IR-dimreg scheme with virtually no changes.

Since we are considering a time- and a momentum integral in the computation of the one-loop power spectrum, one might think that this leads to a more complicated region structure than the one we encountered in the case of the tree-level trispectrum in section 3.3. That is true for a generic one-loop integral in de Sitter space, however, here it is not, for the following reasons: since the time- and momentum integrals factorize, there is no non-trivial interplay between the two integration variables. Further, the momentum integral

$$I(\eta') = \int \frac{\mathrm{d}^{d-1}l}{(2\pi)^{d-1}} \frac{1+(l^2+\Lambda^2)\eta'^2}{[l^2+\Lambda^2]^{\frac{3}{2}}} \tag{3.4.13}$$

would be scaleless in the absence of the IR regulator Λ. This tells us that it has a trivial region structure, i.e. only one non-vanishing region, which is the one in which the magnitude of the loop momentum is $l \sim \Lambda$, and the computation of this region is the same computation as for the full integral. Further, we saw above that the $\mathcal{O}(\eta'^2)$ piece of this integral is irrelevant if we are strictly interested in computing the part of the regularized result which survives in the limit $\Lambda \to 0$. Therefore, for our present purpose, we can replace the loop integral by

$$I(\Lambda) = \int \frac{\mathrm{d}^{d-1}l}{(2\pi)^{d-1}} \frac{1}{[l^2+\Lambda^2]^{\frac{3}{2}}}\,, \tag{3.4.14}$$

which is just a constant, and consider the following expression:

$$\langle\phi(\eta,\vec{k})\phi(\eta,-\vec{k})\rangle'\Big|_{\kappa} = \frac{\tilde{\mu}^{4-d}\kappa H^{d-2}}{8}(-H\eta)^{d-4}\mathrm{Im}\left[\int_{-\infty}^{\eta}\frac{\mathrm{d}\eta'}{(-\eta')^{8-d}}\frac{e^{2ik(\eta'-\eta)}(i-k\eta)^2(i+k\eta')^2}{k^6}\right]I(\Lambda)\,. \tag{3.4.15}$$

The widely separated scales appearing in the time integral are k and η, since we are assuming the limit $-k\eta \to 0$, so, as in section 3.3, the time integral has two regions.

The same consideration also applies to the mass-counterterm contribution (3.4.11), which also just features a single time integral, with the same widely separated scales, k and η. The difference with respect to (3.4.15) is that, in the scheme we are working in, the d-dependence completely drops out of the time integral. This was not problematic for its straightforward evaluation, since it is finite, however, we need to have a dimensional or analytic regulator in place in order to be able to decompose this expression into regions. We therefore introduce the combination

$$(-\nu\eta')^{-2\delta} \tag{3.4.16}$$

as an analytic regulator by hand into the time integral, where ν is a comoving quantity with mass dimension one. This regulator is clearly not de Sitter-invariant, however, any additional invariance-breaking terms which are generated in the single regions by the presence of this additional regulator will cancel out once we sum up all the regions, since the overall δ-dependence, as well as all associated terms, will disappear. The modified counterterm contribution reads

$$\langle\phi(\eta,\vec{k})\phi(\eta,-\vec{k})\rangle'\Big|_{\delta m^2} = \frac{\delta m^2}{2}(-H\eta)^{d-4}\nu^{-2\delta}\mathrm{Im}\left[\int_{-\infty}^{\eta}\frac{\mathrm{d}\eta'}{(-\eta')^{4+2\delta}}\frac{e^{2ik(\eta'-\eta)}(i-k\eta)^2(i+k\eta')^2}{k^6}\right], \tag{3.4.17}$$

and we see that its is simply the same integral as the one in (3.4.15) with the replacement $\varepsilon \to \delta$. Exactly the same discussion would apply to the region decomposition of the $\delta\Lambda^2$-contribution to the power spectrum, but, since it turned out to give a vanishing contribution to the renormalized power spectrum, we will not discuss it explicitly here.

The explicit computation of the above integrals is given in appendix 3.A. Once the regions of (3.4.15) and (3.4.17) are summed, we recover the results (3.4.5) and (3.4.11) and, using the mass counterterm (3.4.8) and summing these two expressions, we recover the renormalized result (3.4.12), as we should.

3.4.2 Computation in the IR-dimreg scheme

We repeat the computation we did above, this time using the IR-dimreg scheme. This simply amounts to setting $\Lambda \to 0$ in the integrands of the above expressions, which makes the computation essentially trivial.

Vertex-insertion diagram

To redo the computation of the vertex-insertion diagrams, we can recycle the integral we wrote down in (3.4.3) and set $\Lambda = 0$ in it. We find

$$\begin{aligned}\langle\phi(\eta,\vec{k})\phi(\eta,-\vec{k})\rangle'\Big|_{\kappa} =&\frac{\tilde{\mu}^{4-d}\kappa H^{d-2}}{8}(-H\eta)^{d-4}\mathrm{Im}\Bigg[\int_{-\infty}^{\eta}\frac{\mathrm{d}\eta'}{(-\eta')^{8-d}}\frac{e^{2ik(\eta'-\eta)}(i-k\eta)^2(i+k\eta')^2}{k^6}\Bigg]\\ &\times\int\frac{\mathrm{d}^{d-1}l}{(2\pi)^{d-1}}\frac{1+l^2{\eta'}^2}{l^3}\\ =&0\,,\end{aligned}\tag{3.4.18}$$

where the last equality follows from the fact that scaleless integrals are set to zero by dimreg. Therefore, the result for these diagrams in this scheme simply vanishes.

Let us elaborate a little more on what is happening in the above result, focussing on the momentum integral

$$\int\frac{\mathrm{d}^{d-1}l}{(2\pi)^{d-1}}\frac{1+l^2{\eta'}^2}{l^3}\,.\tag{3.4.19}$$

As before, it is the sum of a logarithmically (both UV- and IR-) divergent integral, and a quadratically UV-divergent integral, which are both scaleless. The latter is set identically to zero by dimreg, since any non-vanishing result would have to be proportional to some object with mass dimension two, just by naive mass-dimension counting in the integrand, and we have no such scale available in the problem. For the logarithmically divergent integral this line of reasoning does not go through, since the integral as a whole is dimensionless. What is in fact happening is that the UV- and IR-divergences of this integral, which on their own would both manifest as poles in ε, are being set equal and opposite by dimreg, such that their sum cancels:

$$\int\frac{\mathrm{d}^{d-1}l}{(2\pi)^{d-1}}\frac{1}{l^3}=\frac{\Omega_{d-2}}{(2\pi)^{d-1}}\left[\frac{1}{\varepsilon_{\mathrm{UV}}}-\frac{1}{\varepsilon_{\mathrm{IR}}}\right]=0\,,\tag{3.4.20}$$

where in the above equation Ω_{d-2} denotes the volume of the unit hypersphere S^{d-2}. This cancellation was lifted by the presence of the dedicated IR regulator in the computation using the k_Λ-scheme, which also provided a scale for the quadratically divergent integral, which is why above we did not find a vanishing result for the quantity we are considering. In particular, since we were using dimreg to regularize the UV-divergences in the k_Λ-scheme as well, the UV pole of this integral coincides with the corresponding term in (3.4.4), and it needs to be removed by an appropriate counterterm.

Mass-counterterm diagram

In this scheme, we only have the mass counterterm to take into account. The computation is unchanged with respect to the one in the previous scheme, so also here the mass counterterm diagram contributes the expression

$$\langle\phi(\eta,\vec{k})\phi(\eta,-\vec{k})\rangle'\Big|_{\delta m^2}=\frac{\delta m^2}{2}(-H\eta)^{d-4}\mathrm{Im}\Bigg[\int_{-\infty}^{\eta}\frac{\mathrm{d}\eta'}{(-\eta')^4}\frac{e^{2ik(\eta'-\eta)}(i-k\eta)^2(i+k\eta')^2}{k^6}\Bigg]\,.\tag{3.4.21}$$

As in the previous section, the purpose of δm^2 is to remove the UV divergence of the logarithmically divergent momentum integral (3.4.20), which yields the same UV pole as in the previous computation, so the result for the mass counterterm is unchanged:

$$\delta m^2=\frac{\kappa H^2}{8\pi^2}\left[-\frac{1}{2\varepsilon}+\delta\hat{m}^2_{\mathrm{fin}}\right]+\mathcal{O}(\kappa^2)\,.\tag{3.4.22}$$

The time integral is unchanged as well, so the result is precisely the same as in the previous section:

$$\langle\phi(\eta,\vec{k})\phi(\eta,-\vec{k})\rangle'\Big|_{\delta m^2}=\frac{\kappa H^2}{24\pi^2k^3}(-H\eta)^{-2\varepsilon}\left[\frac{1}{2\varepsilon}-\delta\hat{m}^2_{\mathrm{fin}}\right]\Big[2-\ln(-2e^{\gamma_E}k\eta)\Big]\,.\tag{3.4.23}$$

Renormalized result

Since in this scheme the regularized result for the vertex-insertion diagram (3.4.18) is simply zero, the renormalized result is the same as the mass-counterterm contribution (3.4.23), so we find

$$\langle\phi(\eta,\vec{k})\phi(\eta,-\vec{k})\rangle'\Big|_{\mathcal{O}(\kappa)} = \frac{\kappa H^2}{24\pi^2 k^3}(-H\eta)^{-2\varepsilon}\left[\frac{1}{2\varepsilon} - \delta\hat{m}^2_{\rm fin}\right]\Big[2 - \ln(-2e^{\gamma_E}k\eta)\Big]\,. \tag{3.4.24}$$

However, notice that the leftover pole in this result should be interpreted as the IR pole of the momentum integral (3.4.20), since the UV pole has been subtracted by means of δm^2. Contrarily to the k_Λ-scheme, since ε is regularizing the IR divergence in this diagram as well, we cannot set ε exactly to zero, which is the reason why we have left the coefficient $(-H\eta)^{-2\varepsilon}$ not expanded.

Comparing this result to the one we found in the k_Λ-scheme (3.4.12), we see that the coefficient of the logarithmic IR divergence is the same in both schemes. However, in (3.4.12) we also found several finite terms, two of which are secularly divergent logarithms, which are absent in the present scheme. This tells us that the choice of IR regularization does not just affect the form of the IR divergences themselves, but it can also dramatically change the form of the finite terms, which therefore must be sensitive to the presence of IR divergences as well.

Region decomposition of the one-loop power spectrum

Since the only difference between the present scheme and the k_Λ-scheme is that we have set $\Lambda \to 0$, which only affects the momentum integral, which in this case has a trivial region structure, the discussion is exactly the same as the one we have already carried out in section 3.4.1. There is therefore no need to repeat it here.

3.5 Late-time limit of the one-loop bispectrum of the composite operator ϕ^2 in the IR-dimreg scheme

As a first example of a non-trivial one-loop diagram in de Sitter space, we will consider the composite-operator correlation function

$$\langle\phi^2(\eta,\vec{q})\phi(\eta,\vec{k}_1)\phi(\eta,\vec{k}_2)\rangle\,, \tag{3.5.1}$$

computed in the IR-dimreg scheme and evaluated in the late-time limit. The result that we will discuss in this section, as well as some of the figures we will show, were presented in [100], and we will follow the presentation in this reference. In this case, the method of regions will prove instrumental in order to simplify the computation, and make it much more tractable.

The above correlation function receives, at $\mathcal{O}(\kappa)$, two contributions, which we can classify as one-particle-irreducible (1PI), corresponding to diagrams with topology

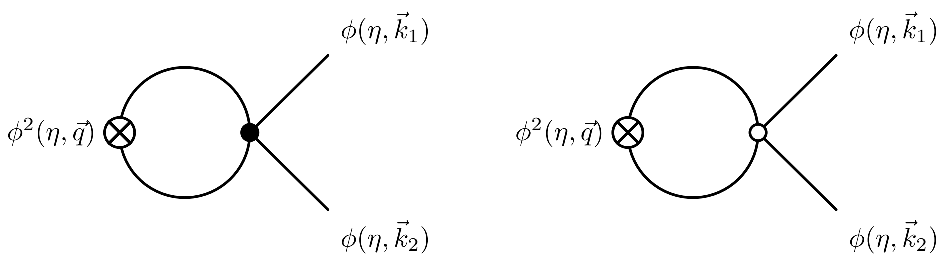

and one-particle-reducible (1PR), corresponding to diagrams with topology

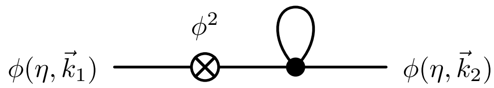

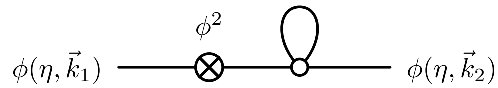

and

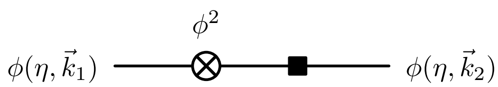

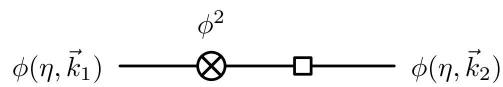

as well as the mirrored copy of the latter two pairs of diagrams. In the above diagrams, we are depicting the insertion of $\phi^2(\eta,\vec{q})$ by means of a crossed circle. The 1PR contribution to the correlator we are considering simply factorizes into a product of power spectra as follows:

$$\langle\phi^2(\eta,\vec{q})\phi(\eta,\vec{k}_1)\phi(\eta,\vec{k}_2)\rangle'\Big|_{\mathcal{O}(\kappa),\ \text{1PR}} = 2\langle\phi(\eta,\vec{k}_1)\phi(\eta,-\vec{k}_1)\rangle'\Big|_{\mathcal{O}(\kappa^0)} \times \langle\phi(\eta,\vec{k}_2)\phi(\eta,-\vec{k}_2)\rangle'\Big|_{\mathcal{O}(\kappa)}\,, \tag{3.5.2}$$

where we used the primed notation to extract an overall momentum-conserving delta distribution. Both of these factors are already known, since we already computed them above. Therefore, in this section we will focus on the 1PI part of the correlation function, which is the truly new object. Beyond it being the simplest non-trivial one-loop computation in the theory we are considering, the motivation to study this quantity also comes from its relevance in the context of SdSET, as is discussed in [107], and as we will also discuss below.

We can define the 1PI part of the momentum-space correlation function (3.5.1) as the Fourier-transform of its position-space version as follows:

$$\begin{aligned}
&\langle\phi^2(\eta,\vec{q})\phi(\eta,\vec{k}_1)\phi(\eta,\vec{k}_2)\rangle\\
\equiv&\int \mathrm{d}^{d-1}x\; e^{-i\vec{q}\cdot\vec{x}}\int\left[\prod_{j=1}^{2}\frac{\mathrm{d}^{d-1}l_j}{(2\pi)^{d-1}}e^{i\vec{l}_j\cdot\vec{x}}\right]\langle\phi(\eta,\vec{l}_1)\phi(\eta,\vec{l}_2)\phi(\eta,\vec{k}_2)\phi(\eta,\vec{k}_2)\rangle\\
=&(2\pi)^{d-1}\delta^{(d-1)}(\vec{q}+\vec{k}_1+\vec{k}_2)\int\frac{\mathrm{d}^{d-1}l}{(2\pi)^{d-1}}\langle\phi(\eta,\vec{l})\phi(\eta,-\vec{l}-\vec{k}_1-\vec{k}_2)\phi(\eta,\vec{k}_1)\phi(\eta,\vec{k}_2)\rangle'\,,
\end{aligned}\tag{3.5.3}$$

where we pulled out the overall momentum-conserving delta distribution by employing the primed notation (3.1.26) in the last step. From this equation we see that to evaluate the correlation function of interest at $\mathcal{O}(\kappa)$ we need to plug into the integral the tree-level trispectrum we already considered above in (3.3.3), and so we find

$$\begin{aligned}
&\langle\phi^2(\eta,\vec{q})\phi(\eta,\vec{k}_1)\phi(\eta,\vec{k}_2)\rangle'\Big|_{\mathcal{O}(\kappa)}\\
=&\frac{\mu^{4-d}\kappa H^d(-H\eta)^{2d-8}}{8(k_1k_2)^3}\mathrm{Im}\left[\int_{-\infty}^{\eta}\frac{\mathrm{d}\eta'}{(-\eta')^{8-d}}\int\frac{\mathrm{d}^{d-1}l}{(2\pi)^{d-1}}\frac{e^{ik_l(\eta'-\eta)}}{l^3|\vec{l}-\vec{q}|^3}(-i+l\eta)(i+l\eta')\right.\\
&\left.\times(-i+|\vec{l}-\vec{q}|\eta)(i+|\vec{l}-\vec{q}|\eta')\prod_{j=1}^{2}(-i+k_j\eta)(i+k_j\eta')\right]\,,
\end{aligned}\tag{3.5.4}$$

where we defined the mombination $k_l \equiv k_1+k_2+l+|\vec{l}-\vec{q}|$ in the exponential. In the following, we will omit the subscript $\mathcal{O}(\kappa)$ of the above correlator to avoid clutter, since no risk of confusion can arise, as we will only consider this order in the expansion in κ in this section.

The direct evaluation of the appearing integrals is quite involved and, to the best of our knowledge, the full result is not available in the literature. However, since we are only interested in the late-time limit of the result, we can apply the method of regions to simplify the computation, in which case the integrals become quite tractable.

3.5.1 Poles of the full result

Before constructing the region expansion and computing the quantities that follow from it, it is instructive to analyze the pole structure of the expression (3.5.4), leaving it as it is. We expect that both UV- and IR divergences will be present in this correlation function, both of which will manifest as ε-poles in the scheme we are currently using. As we have already seen above, the single regions will contain additional divergences, which will generate the pieces of the desired expression that are non-analytic in the limit $-k_i\eta \to 0$ we are considering. Once we sum up all the non-vanishing regions, these additional divergences will cancel, and only the poles of the full expression will be left over. Therefore, computing these poles and comparing them to the ones that survive in the region sum will constitute a consistency check on our result.

By inspecting the form of the integrand in (3.5.4) we can recognize that the time integration will yield no divergences, but the momentum integration will yield a UV divergence, coming from the limit $l \to \infty$, as well as IR divergences coming from the limits $\vec{l} \to \vec{0}$ and $\vec{l} \to \vec{q}$. To see how we can extract these poles, we first write the integrand as

$$\frac{g(l, |\vec{l} - \vec{q}|, k_1, k_2)}{l^3 |\vec{l} - \vec{q}|^3}\,, \tag{3.5.5}$$

where we summarized the numerator of the integrand appearing in (3.5.4) by defining the function $g(l, |\vec{l} - \vec{q}|, k_1, k_2)$ as

$$\begin{aligned} g(l, |\vec{l} - \vec{q}|, k_1, k_2) \equiv\, & e^{ik_t(\eta' - \eta)}(-i + l\eta)(i + l\eta')(-i + |\vec{l} - \vec{q}|\eta)(i + |\vec{l} - \vec{q}|\eta') \\ & \times \prod_{j=1}^{2}(-i + k_j\eta)(i + k_j\eta')\,. \end{aligned} \tag{3.5.6}$$

Having identified the limits of the integration variable which lead to the divergent behaviour of the integral, we can add and subtract the integrand expanded in these limits to the full expression as follows:

$$\begin{aligned} \frac{g(l, |\vec{l} - \vec{q}|, k_1, k_2)}{l^3 |\vec{l} - \vec{q}|^3} = & \underbrace{\left[\frac{g(l, |\vec{l} - \vec{q}|, k_1, k_2)}{l^3 |\vec{l} - \vec{q}|^3} - \frac{g(l, l, k_1, k_2)}{l^6}\bigg|_{l \gg k_{1,2}} - 2\,\frac{g(l, q, k_1, k_2)}{l^3 q^3}\bigg|_{l \ll k_{1,2}} \right]}_{\text{UV- and IR-finite}} \\ & + \frac{g(l, l, k_1, k_2)}{l^6}\bigg|_{l \gg k_{1,2}} + 2\,\frac{g(l, q, k_1, k_2)}{l^3 q^3}\bigg|_{l \ll k_{1,2}}\,. \end{aligned} \tag{3.5.7}$$

The first line of the above equation defines a quantity which is both UV- and IR-finite when integrated, and we can therefore conclude that the poles that we are seeking will be generated solely by the two terms in the second line of (3.5.7). These terms represent the expansion of the integrand in the two singular limits $l \gg k_{1,2}$, which leads to the UV divergence, and $l \ll k_{1,2}$, which leads to the IR divergences. They are simpler than the full expression, and can therefore be straightforwardly integrated. We relegate the details of this computation to appendix 3.B, and using those results we find the following poles:

$$\begin{aligned} & \langle \phi^2(\eta, \vec{q}) \phi(\eta, \vec{k}_1) \phi(\eta, \vec{k}_2) \rangle' \Big|_{\text{poles}} \\ = & \frac{\kappa H^4}{48\pi^2 (k_1 k_2)^3} \left\{ -\frac{3}{4\varepsilon_{\text{UV}}} + \frac{1}{\varepsilon_{\text{IR}}} \left[\left(1 + \frac{k_1^3 + k_2^3}{q^3}\right) \left(1 - \ln\Big(-e^{\gamma_E}(k_1 + k_2 + q)\eta\Big)\right) - f(k_1, k_2, q) \right] \right\}, \end{aligned} \tag{3.5.8}$$

where we defined the function

$$f(k_1, k_2, q) \equiv \frac{4 k_1 k_2}{q^2} - \frac{(k_1 + k_2 + q)[k_1(k_2 + q) + k_2 q]}{q^3}\,. \tag{3.5.9}$$

In the above equation, we pointed out the origin of the various pole terms by means of a subscript, but, as previously discussed, since we are working in dimreg, they are in fact both expressed using the same ε.

3.5.2 Decomposition of the full expression into regions

We now turn to the computation of the late-time correlation function, and we start by discussing its region decomposition. As in the previous two examples we considered, the widely-separated external scales are the momenta $\vec{k}_{1,2}$ and the correlation time η. We are integrating over the loop momentum $\vec{l}$ and the correlation time η', and in this case both integrals will have a non-trivial region structure. To identify the regions, it is natural to compare the vertex time to the correlation time, and the modulus of the loop momentum to the moduli of the external momenta. Analogously to the tree-level trispectrum and the one-loop power spectrum, we can split the time integral into and early- and late-time region, defined by

$$\eta' \ll \eta \;\; (\text{early}) \,, \qquad \eta' \sim \eta \;\; (\text{late}) \,. \tag{3.5.10}$$

Similarly, the momentum integral can be split into a hard- and soft-momentum region, which are defined by

$$l \gg k_{1,}; \; (\text{hard}) \,, \qquad l \sim k_{1,2} \;\; (\text{soft}) \,. \tag{3.5.11}$$

We therefore expect a grand total of four regions that we will need to consider in the computation, which we represent as four sectors in figure 3.2.

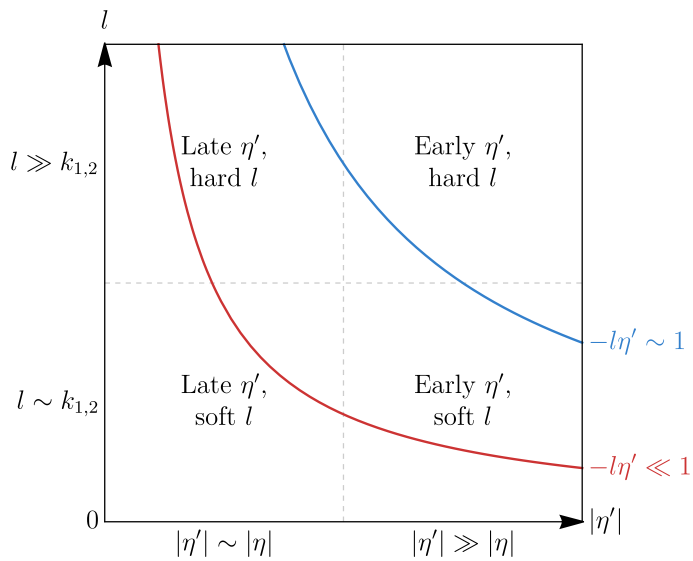

Figure 3.2: Schematic representation of the four relevant regions for the present computation. Additionally, we are representing examples of modes which are subhorizon (blue hyperbola) and superhorizon (red hyperbola) at time η'.

To organize the computation, we choose to group the regions as two late-time regions and two early-time regions. We now analyze these two pairs of regions more closely, in order to determine how to compute them.

1) In the case of the late-time regions we assume the scaling $\eta' \sim \eta$ of the time-integration variable, which tells us that $-k_{1,2}\eta^{(\prime)} \ll 1$ as well. As we argued above, we can then split the momentum integral into its hard and soft regions, in which the products $-l\eta^{(\prime)}$, which are the combinations that appear in the integrand, scale as $-l\eta^{(\prime)} \sim 1$ and $-l\eta^{(\prime)} \ll 1$, respectively:

$$\begin{aligned} &\int_{-\infty}^{\eta} \mathrm{d}\eta' \int \mathrm{d}^{d-1} l \Big|_{\text{late time}} \\ &= \underbrace{\int_{-\infty}^{\eta} \mathrm{d}\eta' \Big|_{-k_{1,2}\eta^{(\prime)} \ll 1} \int \mathrm{d}^{d-1} l \Big|_{-l\eta^{(\prime)} \sim 1}}_{\text{late } \eta',\text{ hard } l} + \underbrace{\int_{-\infty}^{\eta} \mathrm{d}\eta' \Big|_{-k_{1,2}\eta^{(\prime)} \ll 1} \int \mathrm{d}^{d-1} l \Big|_{-l\eta^{(\prime)} \ll 1}}_{\text{late } \eta',\text{ soft } l} . \end{aligned} \tag{3.5.12}$$

The integrands of the two summands on the right-hand side of the above equation are assumed to be Taylor-expanded in the quantities which are small, while the full functional dependence on the quantities which are $\mathcal{O}(1)$ is kept. This defines the integrals that need to be evaluated to compute the late-time regions of the correlation function we are considering.

2) In the case of the early-time regions we assume the scaling $\eta' \ll \eta$ of the time-integration variable, which then tells us that $-k_{1,2}\eta' \sim 1$. As we did in the case of the late-time regions, we split the momentum integration into its hard and soft regions, and the products $-l\eta^{(\prime)}$ scale like $-l\eta' \gg 1$ and $-l\eta' \sim 1$, respectively. As we explained above in section 3.3.2, in the case of the early-time regions we must extend the integration range of η' to $(-\infty, 0)$, while the integral over $\vec{l}$ extends over the full range of values:

$$\begin{aligned}
&\int_{-\infty}^{\eta} \mathrm{d}\eta' \int \mathrm{d}^{d-1}l\Big|_{\text{early time}} \\
&= \underbrace{\int_{-\infty}^{0} \mathrm{d}\eta'\Big|_{\substack{-k_{1,2}\eta'\sim 1\\ -k_{1,2}\eta\ll 1}} \int \mathrm{d}^{d-1}l\Big|_{-l\eta^{(\prime)}\gg 1}}_{\text{early } \eta',\text{ hard } l} + \underbrace{\int_{-\infty}^{0} \mathrm{d}\eta'\Big|_{\substack{-k_{1,2}\eta'\sim 1\\ -k_{1,2}\eta\ll 1}} \int \mathrm{d}^{d-1}l\Big|_{\substack{-l\eta'\sim 1\\ -l\eta\ll 1}}}_{\text{early } \eta',\text{ soft } l} .
\end{aligned} \tag{3.5.13}$$

As was the case in the late-time regions, the integrands of the two summands on the right-hand side of the above equation are assumed to be Taylor-expanded in the quantities which can be considered small.

Each of the four regions describes a specific range of field modes which contribute to the final result for the correlation function, which can be identified by means of their physical three-momentum. Let us start with the two regions associated with late vertex-times $\eta' \sim \eta$. These two regions describe the superhorizon time-evolution of the modes of the external operators $\phi(\eta, \vec{k}_{1,2})$ and $\phi^2(\eta, \vec{q})$, which, however, are interacting with each other by exchanging virtual modes which can be classified as subhorizon ($-l\eta' \sim 1$) and superhorizon ($-l\eta' \ll 1$), with respect to both times η' and η. These are described, respectively, by the hard- and soft-momentum regions associated to late vertex-times. Since the hard-momentum region describes the exchange of virtual modes with large physical three-momenta, and a small associated physical wavelength, compared to the external fields, we expect that this region will give rise to terms that are spatially local, even though they may still depend non-locally on the correlation time. On the other hand, since the modes being described by the soft-momentum region have comparable physical three-momenta to the ones of the external fields, we expect that the contribution from this region will depend non-locally on all external scales. It can therefore be thought of being generated dynamically by the propagation of the field modes which survive until late times. Moving on to the regions associated with early vertex-times $\eta' \ll \eta$ we see that they both describe field modes which would be considered subhorizon at the correlation time η. The soft-momentum region describes the subhorizon evolution of both the modes of the external fields, and the virtual modes circulating in the loop, since in this region $-l\eta' \sim -k_{1,2}\eta' \sim 1$. Since the comoving three-momenta of the virtual modes are comparable to the external ones, we expect the result of this region to depend non-locally on the external momenta, but it should be local in the correlation time η. Indeed, this is guaranteed by the prescription we outlined above. Finally, the hard-momentum region associated to early vertex-times describes modes which have physical momenta which are blueshifted into the deep ultraviolet of the theory, higher than the scale of any physical process we are considering. Since they are associated to comoving momenta and conformal times that are both very much larger in magnitude than the analogous external scales, we expect that this region will simply yield a vanishing result, as we can expand all external scales out of the integrand, which will thus yield a scaleless integral.

Notice that the prescription to decompose the full expression into regions is formulated in terms of comoving quantities. This is, of course, the natural way to formulate it, since the path-integral formalism we are using is built using an action, which is defined as the integral over comoving times and positions of the Lagrangian of the theory. However, the physically meaningful quantities are the physical momenta, which are the product of comoving momenta and conformal time $-k_i\eta$. In particular, there are infinitely many combinations of comoving momenta and conformal times which will yield the same number when taking their product. This is exemplified by the two hyperbolae drawn in figure 3.2, and, indeed, this is realized by the late-time, hard-momentum and early-time, soft-momentum regions we defined above. In both regions we have the combination $-l\eta' \sim 1$, but for different reasons: in the first region we have a large value of l, but a small value of η', while in the other region it is the other way around. This case is represented by the blue hyperbola in figure 3.2. These regions are therefore degenerate from this point of view, and, in particular, the dimensional regulator we are using is only sensitive to the combination $-l\eta'$, and is therefore not able to differentiate between them. In practice, this phenomenon will manifest itself in the integrals associated to the regions we are discussing as divergences which are not regularized by dimreg. To deal with this issue, we will therefore resort to introducing the same analytic regulator

$$(-\nu\eta')^{-2\delta} \tag{3.5.14}$$

in (3.5.4) that we used to decompose the time integral of the one-loop power spectrum into regions in section 3.4.1. This regulator is necessarily not de Sitter-invariant, since it needs to be sensitive to a comoving quantity in order to be able to tell the different regions apart. We could just as well have picked a regulator using the comoving loop momentum l instead of η', but the above choice turns out to be more convenient in the following computations. The divergences which are not regularized by dimreg will then be represented by poles in δ, when we expand the results of the region integrals for δ, $\varepsilon \to 0$. These poles, and all associated terms generated by the δ-expansion, must cancel when we sum up all the regions. This means that any de Sitter-breaking terms that are induced by the presence of this regulator in the different regions will cancel out of the final result. In particular, the order in which we are going to expand these results in δ and ε will matter, in general, so we need to specify it. We can understand which order is the appropriate one by noticing that the direct computation of the full result would not need this additional regulator: we have already analyzed the divergences of the full expression in 3.5.1 and found that they are all regulated by dimreg. Therefore, if we were handed (3.5.4) with the regulator (3.5.14) included in the integrand, we would simply let $\delta \to 0$ right away, compute the integral, expand the result in ε at the end of the computation, and obtain something regular. This fixes the following order of expansion in the region integrals: we expand the results first in δ and then in ε.

Let us also highlight the fact that the need to introduce this additional regulator in the present case is very different than in section 3.4.1: in the latter case, the dependence on the spacetime dimension dropped out of the time integral due to a peculiar, and accidental, cancellation in the regularization scheme we are using. If we used a different scheme, such as a more naive analytic regularization of the physical three-momenta of the fields, this would not have happened. On the other hand, in the present case it is the degeneracy of the physical three-momenta of modes belonging to different regions which leads to unregulated integrals, and this would persist if we used a different regularization scheme which would still only be sensitive to physical three-momenta. Therefore, in the present case, we can conclude that the appearence of unregulated integrals has a physical origin, whereas it was purely accidental in the case of the one-loop power spectrum. In fact, the present situation is similar to the phenomenon of rapidity divergences in the context of collider physics, which was first observed in Soft-Collinear Effective Theory (SCET), which is the effective theory describing soft and collinear modes of energetic particles, typically quarks and gluons, and in particular in $\mathrm{SCET_{II}}$ [108, 109]. In this context, the culprit for the unregulated divergences are the so-called soft and collinear modes of the fields, which have the same virtuality, which is the analogue of physical momentum in our case, but different rapidities, which are the analogue of our comoving quantities. Since dimensional regularization, which is also routinely used in this context, is only sensitive to differences in virtuality, but not in rapidity, it is not able to differentiate between these modes, and this results in unregulated integrals in this case as well. In order to cure this problem, a dedicated rapidity regulator must be introduced [108], which is the analogue of our $(-\nu\eta')^{-2\delta}$. This additional regulator must necessarily break manifest Lorentz invariance, since it needs to distinguish modes with different rapidities, which is again analogous to our situation. Nevertheless, in the final result, after all the contributions from the different modes to a given process are added up, the singularities due to the rapidity divergences cancel out and Lorentz-invariance is recovered. The formalism for the treatment of these divergences in $\mathrm{SCET_{II}}$ has been developed and presented in [110].

We will now proceed with the explicit computation of the expressions associated to each region, and we will pay particular attention to the structure of UV and IR divergences, and to the associated logarithms that will be generated by them. This will be instructive, because it will start to give us an intuition for the typical physical scales that are associated to each region, and will inform our physical picture for the effective description of such processes.

3.5.3 Late-time regions

We consider the late-time regions first. Once the result is obtained, we will study its pole structure and identify whether the poles are of UV or IR origin. Further, we will identify which of the poles will contribute to the poles of the full result, and which are the additional poles that are generated by the region decomposition. The latter are the ones that are most interesting for our purposes here, since they generate the logarithms that we eventually wish to control using the SdSET, and that contain information about the physics being described by this region as well.

Soft momentum integral

We assume that all physical momenta appearing in the integrand are small, so we can Taylor expand it in all of its arguments. Analogously to the tree-level trispectrum we considered in section 3.3, we need to expand the integrand of (3.5.4) to $\mathcal{O}((\eta^{(\prime)})^3)$ (not counting the factors of η' associated to the integration measure) in order to take into account all terms that will contribute to the result at $\mathcal{O}(\eta^0)$ after integrating over time and momentum. We find the following expression after expanding the integrand:

$$\begin{aligned}&\langle\phi^2(\eta,\vec{q})\phi(\eta,\vec{k}_1)\phi(\eta,\vec{k}_2)\rangle'\Big|_{\text{late }\eta',\,\text{soft }l}\\ &=-\frac{\tilde{\mu}^{4-d}\kappa H^d(-H\eta)^{2d-8}}{24(k_1k_2)^3}\nu^{-2\delta}\int_{-\infty}^{\eta}\frac{\mathrm{d}\eta'}{(-\eta')^{8-d+2\delta}}\Big[\eta^3+(-\eta')^3\Big]\int\frac{\mathrm{d}^{d-1}l}{(2\pi)^{d-1}}\frac{l^3+|\vec{l}-\vec{q}|^3+k_1^3+k_2^3}{l^3|\vec{l}-\vec{q}|^3}\,. \quad (3.5.15)\end{aligned}$$

In this particular region the analytic regulator is not necessary, since all appearing integrals are successfully regularized just by using dimreg. We can therefore let $\delta\to 0$ before integrating, which simplifies the structure of the integrand slightly. The time integrals can be carried out right away using (3.3.14), and the leftover expression then reads

$$\begin{aligned}&\langle\phi^2(\eta,\vec{q})\phi(\eta,\vec{k}_1)\phi(\eta,\vec{k}_2)\rangle'\Big|_{\text{late }\eta',\,\text{soft }l}\\ &=-\frac{\tilde{\mu}^{4-d}\kappa H^d(-H\eta)^{2d-8}}{8(k_1k_2)^3}\frac{(-\eta)^{-2\varepsilon}}{2\varepsilon(3+2\varepsilon)}\left[2\int\frac{\mathrm{d}^{d-1}l}{(2\pi)^{d-1}}\frac{1}{l^3}+[k_1^3+k_2^3]\int\frac{\mathrm{d}^{d-1}l}{(2\pi)^{d-1}}\frac{1}{l^3|\vec{l}-\vec{q}|^3}\right]. \quad (3.5.16)\end{aligned}$$

Notice that the time integration generated a pole, which multiplies the whole expression. Since this divergence is associated to the lower integration boundary $\eta'\to-\infty$ of the time integral, we identify it as a UV pole.

We see that the integral appearing in the first summand of (3.5.16) is just scaleless, so it is set to zero by dimensional regularization. Notice, however, that it is logarithmically divergent, and therefore contributes both a UV and an IR divergence, which cancel, but which we need to take into account to properly interpret the pole structure of this expression. The second integral appearing above is UV-finite but cubically IR-divergent. It can be thought of as a bubble integral with two massless propagators raised to half-integer powers, so it can be evaluated in a standard way, e.g. by introducing a Feynman parameter [34], and we find the result

$$\tilde{\mu}^{2\varepsilon}\int\frac{\mathrm{d}^{d-1}l}{(2\pi)^{d-1}}\frac{1}{(l^2)^{\frac{a}{2}}[(\vec{l}-\vec{q})^2]^{\frac{b}{2}}}=\frac{(e^{\gamma_E}\mu)^{2\varepsilon}}{8\pi^{\frac{3}{2}}}\frac{\Gamma(\frac{a+b-3}{2}+\varepsilon)\Gamma(\frac{3-a}{2}-\varepsilon)\Gamma(\frac{3-b}{2}-\varepsilon)}{\Gamma(\frac{a}{2})\Gamma(\frac{b}{2})\Gamma(3-\frac{a+b}{2}-2\varepsilon)}q^{3-a-b-2\varepsilon} \quad (3.5.17)$$

for arbitrary "propagator" powers. Plugging this result into (3.5.16) and expanding for $\varepsilon\to 0$ yields

$$\langle\phi^2(\eta,\vec{q})\phi(\eta,\vec{k}_1)\phi(\eta,\vec{k}_2)\rangle'\Big|_{\text{late }\eta',\,\text{soft }l}$$

$$=\frac{\kappa H^4(-H\eta)^{-4\varepsilon}}{96\pi^2(k_1k_2)^3}\left(\frac{e^{\gamma_E}\mu}{H}\right)^{2\varepsilon}(-2e^{\gamma_E}q\eta)^{-2\varepsilon}\frac{k_1^3+k_2^3}{q^3}\left[\frac{1}{\varepsilon^2}+\frac{4}{3\varepsilon}+\frac{\pi^2}{12}-\frac{8}{9}\right]. \tag{3.5.18}$$

Notice that we have left some factors in front of the pole terms unexpanded, in order to more transparently display the divergence structure.

As we anticipated when discussing the various regions, this result depends non-locally on all external scales. We find that it contains both double- and single-poles, which are a product of UV poles from the time integral and IR poles from the momentum integral, while the full result only contains single-poles, as we found above in (3.5.8). Since this region is generated purely by the dynamics of modes that are superhorizon at time η, as we discussed above, it should be faithfully reproducing the infrared structure of the original full integral, and we therefore expect the IR single-poles of this expression to be reproducing part of those found in (3.5.8). The remaining divergences should then be identifiable as additional UV divergences which are absent in the full result, and that will cancel in the region sum. By carefully tracking the origin of the various pole terms, differentiating UV and IR poles by means of a subscript, and expanding the factors we left unexpanded in (3.5.18) to collect all terms up to $\mathcal{O}(\varepsilon^{-1})$ we can write the resulting expression as

$$-\frac{\kappa H^4(-H\eta)^{-4\varepsilon}}{96\pi^2(k_1k_2)^3}\left(\frac{e^{\gamma_E}\mu}{H}\right)^{2\varepsilon}\left[\frac{1}{\varepsilon_{\mathrm{UV}}}-\frac{2}{3}-2\ln(-2e^{\gamma_E}q\eta)\right]\left[\frac{1}{\varepsilon_{\mathrm{UV}}}-\frac{1}{\varepsilon_{\mathrm{IR}}}-\frac{k_1^3+k_2^3}{q^3}\left(\frac{1}{\varepsilon_{\mathrm{IR}}}+2\right)\right]. \tag{3.5.19}$$

Notice that we have made the cancellation of the UV and IR pole occurring in the scaleless integral in (3.5.16) manifest. We have also left the coefficient $(-H\eta)^{-4\varepsilon}(e^{\gamma_E}\mu/H)^{2\varepsilon}$ not expanded, since it will be common to all the regions we are going to compute, and the pole structure is most transparent when leaving this factor out of the ε-expansion. However, if we are interested in the logarithms that are generated by the additional poles in this region, we do have to expand the factor $(e^{\gamma_E}\mu/H)^{2\varepsilon}$ out, and we then find that logarithms of the form

$$\ln\left(-\frac{\mu}{2q\eta H}\right)=\ln\left(\frac{a(\eta)\mu}{2q}\right) \tag{3.5.20}$$

are generated, and their coefficients are tied to the ε-pole terms. The additional poles themselves will drop out of the region sum, but the logarithms that they generated in each region will combine to something non-vanishing and, indeed, reproduce the secular logarithms of the full expression. We see that, analogously to the case of the tree-level trispectrum, μ plays the role of the factorization scale, and it can be used to track the η-dependence. To make the logarithms of the type appearing in (3.5.20) small we would have to choose $\mu\sim q/a(\eta)\ll H$, which can therefore be interpreted as the natural scale choice for this region. As expected, this tells us that this region is associated with superhorizon physics only.

Hard momentum region

We move on to the computation of the late-time, hard-momentum region. Here we assume the scalings $-k_{1,2}\eta\sim -k_{1,2}\eta'\ll 1$, so these are the small variables we can Taylor-expand the integrand in. However, we also have $-l\eta\sim -l\eta'\sim 1$, and we must keep the full dependence on these combinations. We thus find the following integral:

$$\begin{aligned}&\langle\phi^2(\eta,\vec{q})\phi(\eta,\vec{k}_1)\phi(\eta,\vec{k}_2)\rangle'\Big|_{\text{late }\eta',\text{ hard }l}\\ =&\frac{\tilde{\mu}^{4-d}\kappa H^d(-H\eta)^{2d-8}}{8(k_1k_2)^3}\nu^{-2\delta}\mathrm{Im}\left[\int_{-\infty}^{\eta}\frac{\mathrm{d}\eta'}{(-\eta')^{8-d+2\delta}}\int\frac{\mathrm{d}^{d-1}l}{(2\pi)^{d-1}}\frac{e^{2il(\eta'-\eta)}(-i+l\eta)^2(i+l\eta')^2}{l^6}\right].\end{aligned} \tag{3.5.21}$$

We see that we can trace back all integrals we have to evaluate to the following, single "master integral"

$$I(a,b)\equiv\int_{-\infty}^{\eta}\frac{\mathrm{d}\eta'}{(-\eta')^a}\int\frac{\mathrm{d}^{d-1}l}{(2\pi)^{d-1}}\frac{e^{2il(\eta'-\eta)}}{l^b} \tag{3.5.22}$$

$$=\frac{i(4\pi)^{\varepsilon}(2i)^{b+2\varepsilon}\Gamma(3-b-2\varepsilon)\Gamma(b-2+2\varepsilon)\Gamma(2+a-b-2\varepsilon)}{32\pi^{\frac{3}{2}}\Gamma(\frac{3}{2}-\varepsilon)\Gamma(a)}(-\eta)^{b-a-2+2\varepsilon}. \tag{3.5.23}$$

By expanding the integrand of (3.5.21) and collecting powers of l and η' we could write the result of the integration as a linear combination of various $I(a,b)$ with different values of a and b, and simplify the result as much as possible. However, a less brute-force and more elegant way to compute the result is to use the fact that the above master integral satisfies the following integration-by-parts relations:

$$I(a,b) = \frac{2i\eta}{2+a-b-2\varepsilon} I(a,b-1)\,, \tag{3.5.24}$$

$$I(a,b) = \frac{1+a-b-2\varepsilon}{\eta(1-a)} I(a-1,b)\,, \tag{3.5.25}$$

which can be directly checked using the explicit expression (3.5.23). We can use these relations to reduce all of the integrals appearing in (3.5.21) to a single representative, multiplied by a rational function of δ, ε, and η. Doing so, we find the following result:

$$\begin{aligned}
&\langle \phi^2(\eta,\vec{q})\phi(\eta,\vec{k}_1)\phi(\eta,\vec{k}_2)\rangle'\Big|_{\text{late } \eta',\ \text{hard } l} \\
=&\frac{\tilde{\mu}^{4-d}\kappa H^d(-H\eta)^{2d-8}}{8(k_1k_2)^3}\nu^{-2\delta}\frac{(4+2\delta)[2(\delta+\varepsilon)-1]\eta^2}{2\delta[3+2(\delta+\varepsilon)]} I\Big(2+2(\delta+\varepsilon),2\Big) \\
=&\frac{\kappa H^4(-H\eta)^{-4\varepsilon}}{96\pi^2(k_1k_2)^3}\left(\frac{e^{\gamma_E}\mu}{H}\right)^{2\varepsilon}(-\nu\eta)^{-2\delta}\left[\frac{1}{\delta}\left(\frac{1}{\varepsilon}-\frac{8}{3}\right)-\frac{13}{6\varepsilon}+\frac{56}{9}-\frac{2\pi^2}{3}\right].
\end{aligned} \tag{3.5.26}$$

As anticipated, we see the appearance of explicit δ-poles in the result. Of course, the brute-force computation would have given us the same result, but we stress that making use of such identities goes a long way in improving the efficiency of the computation. It will pay off especially when considering more complicated integrals, or integrals involving a large number of terms.

The found result of the loop integral is completely independent of the external momenta, and we find a spatially local result, as we anticipated above. Indeed, it is already clear from (3.5.21) that this must be the case, since all of the external momenta are negligible with respect to the loop momentum. However, the result has a non-analytic dependence on η, due to the factor $(-\nu\eta)^{-2\delta}$, which will generate logarithms of $-\nu\eta$ after expanding the result in δ. This feature was also anticipated above, since the modes running in the loop that we are describing in this region probe times that are comparable in magnitude to the correlation time.

We can now identify where the poles originate from. We can start by noticing that the expansion of the integrand in this region is essentially the same expansion that we performed in (3.5.7) to isolate the UV-divergent terms of the full expression. The only difference is that in that case we kept the polynomial terms proportional to $k_{1,2}$ in the numerator of the integrand, while here we dropped them. However, the UV divergence of (3.5.7) is local, and therefore the presence or absence of these terms is immaterial, as far as this term is concerned. Therefore, the UV behaviour of the present expression is the same as the term in (3.5.7) we just mentioned, and we can therefore conclude that this region contains the UV pole of the full result. The remaining poles that we find will therefore drop out in the region sum, and are generated by the decomposition into regions. As such, they must be of IR origin, because in this region we modified the behaviour of the integrand for small values of loop momenta. Expanding the integrand up to $\mathcal{O}(\delta^{-1},\varepsilon^{-1})$ and labeling the poles according to their origin we find

$$\begin{aligned}
&\frac{\kappa H^4(-H\eta)^{-4\varepsilon}}{96\pi^2(k_1k_2)^3}\left(\frac{e^{\gamma_E}\mu}{H}\right)^{2\varepsilon}\left\{\left[\frac{1}{\delta}-2\ln(-\nu\eta)\right]\left[\frac{1}{\varepsilon}-\frac{8}{3}\right]-\frac{13}{6\varepsilon}\right\} \\
=&\frac{\kappa H^4(-H\eta)^{-4\varepsilon}}{96\pi^2(k_1k_2)^3}\left(\frac{e^{\gamma_E}\mu}{H}\right)^{2\varepsilon}\left\{\frac{1}{\delta_{\text{IR}}\varepsilon_{\text{IR}}}-\frac{3}{2\varepsilon_{\text{UV}}}-\frac{8}{3\delta_{\text{IR}}}-\frac{2}{\varepsilon_{\text{IR}}}\left[\frac{1}{3}+\ln(-\nu\eta)\right]+\mathcal{O}(\delta^0,\varepsilon^0)\right\}.
\end{aligned} \tag{3.5.27}$$

As we anticipated above, the expansion of the result for small δ generates logarithms of the form

$$\ln(-\nu\eta) = \ln\left(\frac{\nu}{a(\eta)H}\right) \tag{3.5.28}$$

and the expansion for small ε generates logarithms of the form

$$\ln\left(\frac{e^{\gamma_E}\mu}{H}\right). \tag{3.5.29}$$

The poles in δ, and the associated ν-dependence, that we found in this region will drop out completely in the final result, but, as we are considering this specific region, we can use the scale ν to control the appearing logarithm of η. In particular, the natural scale choice to make logarithms such as the one in (3.5.28) small corresponds to $\nu \sim -1/\eta$, which reflects the fact that this region is encapsulating a late-time contribution to the full answer. However, notice that if we were to interpret ν as a scale associated to some comoving momentum, it would count as hard in our classification, since $-\nu\eta \sim 1$ (by construction). Following the same logic, logarithms such as the one appearing in (3.5.29) are small when we choose $\mu \sim H$, which can be associated to the large values of loop momenta contributing to this region.

3.5.4 Early-time regions

We now go over to the computation of the early-time regions, where $|\eta'| \sim 1/k_{1,2}$ holds. This will be the technically most involved part of the present computation.

Soft-momentum region

In this region we assume that $l \sim k_{1,2}$, which combined with $|\eta'| \sim 1/k_{1,2}$ implies the scalings $-k_{1,2}\eta \ll -k_{1,2}\eta' \sim 1$, $-l\eta \ll -l\eta' \sim 1$. Expanding the integrand in the small quantities that are present, and extending the upper integration boundary of the time integral all the way to zero we find the expression

$$\begin{aligned}&\langle\phi^2(\eta,\vec{q})\phi(\eta,\vec{k}_1)\phi(\eta,\vec{k}_2)\rangle'\Big|_{\text{early }\eta',\text{ soft }l}\\ =&\frac{\kappa\tilde{\mu}^{4-d}H^d(-H\eta)^{2d-8}}{8(k_1k_2)^3}\nu^{-2\delta}\mathrm{Im}\left[\int_{-\infty}^{0}\frac{\mathrm{d}\eta'}{(-\eta')^{8-d+2\delta}}\int\frac{\mathrm{d}^{d-1}l}{(2\pi)^{d-1}}\,\frac{e^{ik_l\eta'}(i+l\eta')(i+|\vec{l}-\vec{q}|\eta')}{l^3|\vec{l}-\vec{q}|^3}\prod_{j=1}^{2}(i+k_j\eta')\right].\end{aligned} \tag{3.5.30}$$

We can lead all the integrals that appear in (3.5.30) back to a single "master integral", which reads

$$I(a) \equiv \int_{-\infty}^{0}\frac{\mathrm{d}\eta'}{(-\eta')^{8-d+a}}e^{iK\eta'}\int\frac{\mathrm{d}^{d-1}l}{(2\pi)^{d-1}}\frac{e^{i(l+|\vec{l}-\vec{q}|)\eta'}(i+l\eta')(i+|\vec{l}-\vec{q}|\eta')}{l^3|\vec{l}-\vec{q}|^3}\,, \tag{3.5.31}$$

where we defined the combination of absolute values $K \equiv k_1 + k_2$. The evaluation of this integral is carried out in appendix 3.C, and we find the result

$$\begin{aligned}I(a) = &\frac{e^{\frac{i\pi a}{2}}(e^{2i\pi\varepsilon}-1)\Gamma(-\varepsilon)}{4^{1-\varepsilon}\pi^{\frac{5}{2}-\varepsilon}}K^a\left[\frac{2\Gamma(1+2\varepsilon)\Gamma(-3-a-2\varepsilon)\Gamma(-\varepsilon)}{\Gamma(-\frac{1}{2}-\varepsilon)}\left(\frac{K}{q}\right)^{3+2\varepsilon}\right.\\ &\left.\times\,{}_2F_1\left(-\frac{3+a}{2}-\varepsilon,-1-\frac{a}{2}-\varepsilon;-\frac{1}{2}-\varepsilon;\frac{q^2}{K^2}\right)+\frac{\sqrt{\pi}\Gamma(-a)\csc(\pi\varepsilon)}{(3+2\varepsilon)(1+2\varepsilon)}{}_2F_1\left(\frac{1-a}{2},-\frac{a}{2};\frac{5}{2}+\varepsilon;\frac{q^2}{K^2}\right)\right].\end{aligned} \tag{3.5.32}$$

This integral satisfies the differential equation

$$\frac{\partial}{\partial K}I(a) = -iI(a-1)\,, \tag{3.5.33}$$

which is most easily seen from (3.5.31), and we can use this property to write (3.5.30) as the single integral $I(2\delta)$ with derivatives acting on it. The integral $I(2\delta)$ can then be expanded first in $\delta \to 0$ and then in $\varepsilon \to 0$, since these expansions commute with the derivatives with respect to K. The explicit result for this expansion can be found in appendix 3.C, and we do not display it again here. The result after taking the appropriate derivatives with respect to K reads

$$
\begin{aligned}
&\langle\phi^2(\eta,\vec{q})\phi(\eta,\vec{k}_1)\phi(\eta,\vec{k}_2)\rangle'\Big|_{\text{early }\eta',\text{ soft }l}\\
=&\frac{\kappa\tilde{\mu}^{4-d}H^d(-H\eta)^{2d-8}}{8(k_1k_2)^3}\nu^{-2\delta}\mathrm{Im}\left[\left(-1+K\frac{\partial}{\partial K}-k_1k_2\frac{\partial^2}{\partial K^2}\right)I(2\delta)\right]\Big|_{K=k_1+k_2} \qquad (3.5.34)\\
=&\frac{H^4(-H\eta)^{-4\varepsilon}}{96\pi^2(k_1k_2)^3}\left(\frac{e^{\gamma_E}\mu}{H}\right)^{2\varepsilon}\left(\frac{2e^{\gamma_E}q}{\nu}\right)^{2\delta}\Bigg\{-\frac{1}{\varepsilon^2}\frac{k_1^3+k_2^3}{q^3}-\frac{1}{\delta}\left[\frac{1}{\varepsilon}-\frac{8}{3}\right]\\
&+\frac{2}{\varepsilon}\left[\left(1+\frac{k_1^3+k_2^3}{q^3}\right)\left(\frac{1}{3}-\ln\left(\frac{k_1+k_2+q}{2q}\right)\right)+1-f(k_1,k_2,q)\right]\\
&+\frac{\pi^2}{12}\left[14-\frac{k_1^3+k_2^3}{q^3}\right]-\frac{4}{9}\left[26+\frac{12(k_1+k_2)}{q}+\frac{3(4k_1^2-k_1k_2+4k_2^2)}{q^2}+\frac{(k_1+k_2)^3}{q^3}\right]\\
&+\frac{4}{3}\left[4+\frac{3(k_1+k_2)}{q}+\frac{(k_1+k_2)^3}{q^3}\right]\ln\left(\frac{k_1+k_2+q}{2q}\right)\\
&-\Bigg[\left(1+\frac{k_1^3+k_2^3}{q^3}\right)\ln^2\left(\frac{k_1+k_2+q}{2q}\right)\\
&\qquad+\left(1-\frac{k_1^3+k_2^3}{q^3}\right)\ln\left(\frac{k_1+k_2}{q}\right)\ln\left(\frac{4(k_1+k_2)q}{(k_1+k_2-q)^2}\right)\Bigg]\\
&+2\left(\frac{k_1^3+k_2^3}{q^3}-1\right)\left[\mathrm{Li}_2\left(\frac{q}{k_1+k_2}\right)-\mathrm{Li}_2\left(-\frac{q}{k_1+k_2}\right)+\mathrm{Li}_2\left(\frac{1}{2}-\frac{q}{2(k_1+k_2)}\right)\right]\Bigg\}, \qquad (3.5.35)
\end{aligned}
$$

where we used the same function $f(k_1,k_2,q)$ we already defined in (3.5.9), and $\mathrm{Li}_2(z)$ denotes the dilogarithm function. Notice that we left some δ- and ε-dependent prefactors unexpanded, to make the pole structure of the result as transparent as possible. It is noteworthy that the integral $I(2\delta)$, which generates the (di-)logarithms through the δ- and ε-expansions, depends on the moduli k_1, k_2 only through the combination $K=k_1+k_2$. All of the dependence on k_1 and k_2 which is not of this form comes about due to the explicit factor k_1k_2 which multiplies the second derivative with respect to K appearing in (3.5.34).

As we did for the other regions we already computed, we now inspect the origin of the various poles appearing in the result. To this end, we find it easiest to start from (3.5.30), evaluate the time integral, which generates an IR divergence from its upper integration boundary $\eta'\to 0$, and then investigate the behaviour of the obtained integrand as l is varied. The divergences which will appear for values of $\vec{l}$ which have small magnitudes, $\vec{l}\to\vec{0}$ and $\vec{l}\to\vec{q}$, can then be identified as IR divergences, while the ones that are due to $l\to\infty$ can be identified as UV divergences. The limit which requires the additional analytic regulator is then found to be $l\to\infty$, so we can identify all the δ-poles which appear in the final result as UV poles. Labeling all the poles that we find in this manner according to their origin we find the following expression:

$$
\begin{aligned}
&\frac{H^4(-H\eta)^{-4\varepsilon}}{96\pi^2(k_1k_2)^3}\left(\frac{e^{\gamma_E}\mu}{H}\right)^{2\varepsilon}\Bigg\{-\frac{1}{\varepsilon^2}\frac{k_1^3+k_2^3}{q^3}-\left[\frac{1}{\delta}+2\ln\left(\frac{2e^{\gamma_E}q}{\nu}\right)\right]\left[\frac{1}{\varepsilon}-\frac{8}{3}\right]\\
&+\frac{2}{\varepsilon}\left[\left(1+\frac{k_1^3+k_2^3}{q^3}\right)\left(\frac{1}{3}-\ln\left(\frac{k_1+k_2+q}{2q}\right)\right)+1-f(k_1,k_2,q)\right]\Bigg\}\\
=&\frac{H^4(-H\eta)^{-4\varepsilon}}{96\pi^2(k_1k_2)^3}\left(\frac{e^{\gamma_E}\mu}{H}\right)^{2\varepsilon}\Bigg\{\frac{1}{\varepsilon_{\mathrm{IR}}}\left[\frac{1}{\varepsilon_{\mathrm{UV}}}-\frac{1}{\varepsilon_{\mathrm{IR}}}\left(1+\frac{k_1^3+k_2^3}{q^3}\right)\right]-\frac{1}{\delta_{\mathrm{UV}}\varepsilon_{\mathrm{IR}}}+\frac{8}{3\delta_{\mathrm{UV}}}\\
&-\frac{2}{\varepsilon_{\mathrm{IR}}}\left[\frac{k_1^3+k_2^3}{q^3}+\ln\left(\frac{2e^{\gamma_E}q}{\nu}\right)\right]\\
&+\frac{2}{\varepsilon_{\mathrm{IR}}}\left[\left(1+\frac{k_1^3+k_2^3}{q^3}\right)\left(\frac{4}{3}-\ln\left(\frac{k_1+k_2+q}{2q}\right)\right)-f(k_1,k_2,q)\right]+\mathcal{O}(\delta^0,\varepsilon^0)\Bigg\} \qquad (3.5.36)
\end{aligned}
$$

From the δ- and ε-dependent prefactor that we left unexpanded in (3.5.35) it is clear that the δ-expansion generates logarithms of the form

$$\ln\left(\frac{2e^{\gamma_E}q}{\nu}\right), \tag{3.5.37}$$

and, since we only have single-poles in δ, only single logarithms will be generated. By the same token, the expansion in ε generates the single- and double-logarithms

$$\ln\left(\frac{e^{\gamma_E}\mu}{H}\right), \tag{3.5.38}$$

since we have both single- and double-poles in ε. As before, the choice of the scales μ and ν for which the above logarithms are small defines the natural values for these scales in this region, which are $\nu \sim q$ and $\mu \sim H$, corresponding to the magnitues of the typical external comoving momenta, reflecting the fact that we are considering soft loop momenta, and the Hubble scale, reflecting the fact that we are considering early times.

Hard-momentum region

In this last region we assume that $l \gg k_{1,2}$, which then implies the scalings $-k_{1,2}\eta \ll -k_{1,2}\eta' \sim 1$, $-l\eta \ll -l\eta' \sim 1$. Since the integration variables $\vec{l}$, η' have much larger magnitudes than their external counterparts, we can expand the integrand completely in the external quantities, which will therefore make it scaleless, and therefore vanishing. The expression we find reads

$$\begin{aligned}&\langle\phi^2(\eta,\vec{q})\phi(\eta,\vec{k}_1)\phi(\eta,\vec{k}_2)\rangle'\Big|_{\text{early }\eta',\text{ hard }l}\\ =&\frac{\kappa\tilde{\mu}^{4-d}H^d(-H\eta)^{2d-8}}{8(k_1k_2)^3}\nu^{-2\delta}\,\mathrm{Im}\left[\int\frac{\mathrm{d}^{d-1}l}{(2\pi)^{d-1}}\int_{-\infty}^{0}\frac{\mathrm{d}\eta'}{(-\eta')^{8-d+2\delta}}\,\frac{e^{2il\eta'}(i+l\eta')^2}{l^6}\prod_{j=1}^{2}(i+k_j\eta')\right],\end{aligned} \tag{3.5.39}$$

and we see that to evaluate it we have to compute integrals belonging to the following family:

$$I(a,b) = \int\frac{\mathrm{d}^{d-1}l}{(2\pi)^{d-1}}\int_{-\infty}^{0}\frac{\mathrm{d}\eta'}{(-\eta')^a}\,\frac{e^{2il\eta'}}{l^b}\,. \tag{3.5.40}$$

The evaluation of the time integral appearing in $I(a,b)$ is immediate:

$$\int_{-\infty}^{0}\frac{\mathrm{d}\eta'}{(-\eta')^a}\,e^{2il\eta'} = (2il)^{a-1}\Gamma(1-a)\,, \tag{3.5.41}$$

and this leaves the momentum integration:

$$I(a,b) = (2i)^{a-1}\Gamma(1-a)\int\frac{\mathrm{d}^{d-1}l}{(2\pi)^{d-1}}\frac{1}{l^{b-a+1}}\,. \tag{3.5.42}$$

In this form, it is now clear that these integrals are indeed scaleless, and vanish due to the presence of our analytic regulator, which aligns with our expectations.

Even though we get a vanishing result, it is interesting to determine whether there are any logarithmically divergent integrals contributing to this region. The reason why is that, even though their UV and IR poles cancel each other, they are important to ascribe the correct the physical meaning to the additional poles we found in the other regions. We can determine whether we have any logarithmically divergent integrals among the ones appearing in (3.5.39) by splitting (3.5.42) into two integrals, which capture the UV and IR divergences of the integral in question, respectively, by means an intermediate scale Λ as

$$I(a,b) = (2i)^{a-1}\Gamma(1-a)\frac{\Omega_{d-2}}{(2\pi)^{d-1}}\left[\int_0^{\Lambda}\mathrm{d}l\; l^{d-2+a-b-1} + \int_{\Lambda}^{\infty}\mathrm{d}l\; l^{d-2+a-b-1}\right], \tag{3.5.43}$$

where now our analytic regulator is regularizing the IR ($l \to 0$) of the first integral and the UV ($l \to \infty$) of the first one, which will therefore manifest themselves as poles in δ. Any poles stemming from logarithmically divergent integrals can then be singled out by counting the mass dimension of their coefficient, which should be zero. Plugging the modified "master integral" (3.5.43) into (3.5.39), evaluating the resulting expression and singling out the terms which are generated by logarithmic divergences we find

$$\begin{aligned}
&\langle \phi^2(\eta,\vec{q})\phi(\eta,\vec{k}_1)\phi(\eta,\vec{k}_2)\rangle'\Big|_{\text{early }\eta',\text{ hard }l} \\
&= -\frac{\kappa H^4(-H\eta)^{-4\varepsilon}}{96\pi^2(k_1k_2)^3}\left(\frac{e^{\gamma_E}\mu}{H}\right)^{2\varepsilon}\left[\frac{\nu_{\text{UV}}^{-2\delta_{\text{UV}}}}{\delta_{\text{UV}}}-\frac{\nu_{\text{IR}}^{-2\delta_{\text{IR}}}}{\delta_{\text{IR}}}\right]\left[\frac{1}{\varepsilon_{\text{IR}}}-\frac{8}{3}\right],
\end{aligned} \tag{3.5.44}$$

where we are now denoting the origin of the single poles, and their associated scale ν, by means of subscripts. Indeed, the expression (3.5.39) contains a logarithmic divergence. This result, of course, still vanishes when we identify $\delta_{\text{UV}} = \delta_{\text{IR}}$ and $\nu_{\text{UV}} = \nu_{\text{IR}}$. Furthermore, the factorized structure of the result reflects the fact that the ε-pole is entirely due to the time integration, while the δ-poles are generated by the momentum integration. We notice at this point that the pole structure in (3.5.44) is in one-to-one correspondence with the δ-poles in the late-time, hard-momentum region (3.5.27) and in the early-time, soft-momentum region (3.5.36), respectively. This will become important when we combine the results from all the regions and interpret the physical origin of the various additional poles generated by the region decomposition.

3.5.5 Sum of the regions, renormalization of the operator ϕ^2

Finally, we are in the position to sum the results we found in the previous subsections to obtain the main result of this section. We find

$$\begin{aligned}
&\langle \phi^2(\eta,\vec{q})\phi(\eta,\vec{k}_1)\phi(\eta,\vec{k}_2)\rangle'\Big|_{\text{late }\eta',\text{ soft }l}+\langle \phi^2(\eta,\vec{q})\phi(\eta,\vec{k}_1)\phi(\eta,\vec{k}_2)\rangle'\Big|_{\text{late }\eta',\text{ hard }l} \\
&+\langle \phi^2(\eta,\vec{q})\phi(\eta,\vec{k}_1)\phi(\eta,\vec{k}_2)\rangle'\Big|_{\text{early }\eta',\text{ soft }l}+\langle \phi^2(\eta,\vec{q})\phi(\eta,\vec{k}_1)\phi(\eta,\vec{k}_2)\rangle'\Big|_{\text{early }\eta',\text{ hard }l} \\
=&\frac{H^4(-H\eta)^{-4\varepsilon}}{96\pi^2(k_1k_2)^3}\left(\frac{e^{\gamma_E}\mu}{H}\right)^{2\varepsilon} \\
&\times\Bigg\{\frac{2}{\varepsilon}\left[\left(1+\frac{k_1^3+k_2^3}{q^3}\right)\left(1-\ln\Big(-e^{\gamma_E}(k_1+k_2+q)\eta\Big)\right)-f(k_1,k_2,q)-\frac{3}{4}\right] \\
&+\frac{8}{3}\left[2-\frac{k_1^3+k_2^3}{q^3}\right]\ln(-2e^{\gamma_E}q\eta)+2\frac{k_1^3+k_2^3}{q^3}\ln^2(-2e^{\gamma_E}q\eta) \\
&+\frac{\pi^2}{2}-\frac{4}{9}\left[12+\frac{12(k_1+k_2)}{q}+\frac{3(4k_1^2-k_1k_2+4k_2^2)}{q^2}+3\frac{k_1^3+k_1^2k_2+k_1k_2^2+k_2^3}{q^3}\right] \\
&+\frac{4}{3}\left[4+\frac{3(k_1+k_2)}{q}+\frac{(k_1+k_2)^3}{q^3}\right]\ln\left(\frac{k_1+k_2+q}{2q}\right) \\
&-\Bigg[\left(1+\frac{k_1^3+k_2^3}{q^3}\right)\ln^2\left(\frac{k_1+k_2+q}{2q}\right) \\
&\qquad+\left(1-\frac{k_1^3+k_2^3}{q^3}\right)\ln\left(\frac{k_1+k_2}{q}\right)\ln\left(\frac{4(k_1+k_2)q}{(k_1+k_2-q)^2}\right)\Bigg] \\
&+2\left(\frac{k_1^3+k_2^3}{q^3}-1\right)\left[\text{Li}_2\left(\frac{q}{k_1+k_2}\right)-\text{Li}_2\left(-\frac{q}{k_1+k_2}\right)+\text{Li}_2\left(\frac{1}{2}-\frac{q}{2(k_1+k_2)}\right)\right]\Bigg\}.
\end{aligned} \tag{3.5.45}$$

We see that all of the double-poles in ε, as well as the poles in $\delta\varepsilon$ and the single-poles in δ cancel, and the only leftover poles are the ones we found in (3.5.8). The fact that this happens constitutes a consistency check on our results.

The UV pole we find in this result can be removed in the standard way by renormalizing the correlation function. Even though we are working in renormalized perturbation theory, we see that new divergences are generated at one-loop order when considering correlation functions involving composite operators. This phenomenon is well known, and we interpret it as signaling necessity of renormalizing the composite operators ϕ^n themselves. To do so, we follow the formalism and notation of [111]. We write the following d-dimensional renormalization equation for ϕ^2:

$$\tilde{\mu}^{2\varepsilon}\phi^2(t,\vec{x}) = \tilde{\mu}^{2\varepsilon} Z^{\phi}_{22}[\phi^2](t,\vec{x}) + H^2 Z^{\phi}_{20}\mathbb{1} + \text{operators involving higher powers of } \phi\,. \tag{3.5.46}$$

In the above equation, we are using the only two dimensionful quantities that we have at our disposal, which are μ and H, to balance the mass dimensions of the various quantities appearing on both the left- and right-hand-sides of the equation. To slightly simplify the discussion of the renormalization of the composite operators, we will not us the same renormalization procedure as for the action, where the finite parts of the counterterms where left undetermined, and we will instead use the $\overline{\text{MS}}$ scheme, which is also why we formulated the renormalization equation directly using the rescaled 't Hooft scale $\tilde{\mu}$. This will be enough for our purposes, since these correlation functions will only be needed to study the matching procedure of the analogous objects in the SdSET onto the full-theory correlators. If needed, the results obtained in this scheme can be modified by including a finite part for the Z-factors, analogously to how we proceeded for the renormalization of the full-theory couplings, to translate them to a different scheme. The renormalization equation for ϕ^2 that we set up involves more operators than $[\phi^2]$ because we are anticipating the phenomenon of operator mixing [111], which will become evident below in section 3.7, where we consider the one-point function $\langle\phi^2(t,\vec{x})\rangle$ at two-loop order. For our purposes, we will not need to consider renormalized operators $[\phi^n]$ with $n > 2$, so we do not include them explicitly in (3.5.46), but they must be considered eventually.

Examining the coefficient of the UV pole in (3.5.45), we see that it has the structure of the following tree-level, momentum-space correlation function in the late-time limit:

$$\lim_{\eta\to 0}\langle\phi^2(\eta,\vec{q})\phi(\eta,\vec{k}_1)\phi(\eta,\vec{k}_2)\rangle' = \frac{1}{2k_1^3k_2^3} + \mathcal{O}(\eta)\,, \tag{3.5.47}$$

which can be represented diagrammatically as

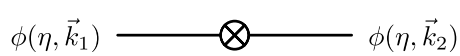

and we are again representing the composite operator ϕ^2 by means of the symbol $\otimes$. Therefore, the appropriate renormalization factor appearing in the renormalization equation (3.5.46) is Z^{ϕ}_{22}, and by picking

$$Z^{\phi}_{22} = 1 - \frac{\kappa}{32\pi^2\varepsilon} + \mathcal{O}(\kappa^2) \tag{3.5.48}$$

we can succesfully remove the UV divergence. We can understand this structure diagrammatically as the loop appearing in the diagrams corresponding to the correlator $\langle\phi^2(\eta,\vec{q})\phi(\eta,\vec{k}_1)\phi(\eta,\vec{k}_2)\rangle|_{\mathcal{O}(\kappa)}$ being shrunk to a point when taking the deep-UV limit for the loop momentum. This reduced the loop diagram to the tree-level ϕ^2-insertion diagram we drew above, multiplied my a local, UV-divergent coefficient, which is nothing but the renormalization factor Z^{ϕ}_{22}.

3.5.6 Discussion of the additional poles appearing in the regions

It is instructive to track how exactly the cancellation of the additional divergences comes about. We can do so by collecting the pole terms we found in (3.5.19), (3.5.27), and (3.5.36), and this time highlighting by a subscript only the poles that survive the sum of all terms to reproduce the ones we found in (3.5.8):

- Late-time, soft-momentum:

$$\frac{\kappa H^4(-H\eta)^{-4\varepsilon}}{96\pi^2(k_1k_2)^3}\left(\frac{e^{\gamma_E}\mu}{H}\right)^{2\varepsilon}\left\{\frac{1}{\varepsilon^2}\frac{k_1^3+k_2^3}{q^3} + \frac{2}{\varepsilon}\left[\frac{1}{3} + \frac{k_1^3+k_2^3}{q^3} + \ln(-2e^{\gamma_E}q\eta)\right]\right.$$

$$
- \frac{2}{\varepsilon_{\text{IR}}} \left[\frac{1}{3} + \ln(-2e^{\gamma_E} q\eta) \right] \left[1 + \frac{k_1^3 + k_2^3}{q^3} \right] \Bigg\} , \tag{3.5.49}
$$

- Late-time, hard-momentum:

$$
\frac{\kappa H^4 (-H\eta)^{-4\varepsilon}}{96\pi^2 (k_1 k_2)^3} \left(\frac{e^{\gamma_E} \mu}{H} \right)^{2\varepsilon} \left\{ \frac{1}{\delta\varepsilon} - \frac{3}{2\varepsilon_{\text{UV}}} - \frac{8}{3\delta} - \frac{2}{\varepsilon} \left[\frac{1}{3} + \ln(-\nu\eta) \right] \right\} , \tag{3.5.50}
$$

- Early-time, soft-momentum:

$$
\begin{aligned}
&\frac{H^4 (-H\eta)^{-4\varepsilon}}{96\pi^2 (k_1 k_2)^3} \left(\frac{e^{\gamma_E} \mu}{H} \right)^{2\varepsilon} \left\{ -\frac{1}{\varepsilon^2} \frac{k_1^3 + k_2^3}{q^3} - \frac{1}{\delta\varepsilon} + \frac{8}{3\delta} - \frac{2}{\varepsilon} \left[\frac{k_1^3 + k_2^3}{q^3} + \ln\!\left(\frac{2e^{\gamma_E} q}{\nu} \right) \right] \right. \\
&\left. + \frac{2}{\varepsilon_{\text{IR}}} \left[\left(1 + \frac{k_1^3 + k_2^3}{q^3} \right) \left(\frac{4}{3} - \ln\!\left(\frac{k_1 + k_2 + q}{2q} \right) \right) - f(k_1, k_2, q) \right] \right\} .
\end{aligned} \tag{3.5.51}
$$

We see that the cancellation of the double-ε-pole occurs between the late-time and early-time soft-momentum regions, since one of the poles in the product is generated by the UV- and IR-divergent time integral in each region, respectively, and therefore they have opposite sign. The second pole in the product is due to an IR divergence in the momentum integration in each region, which is evident due to the non-locality of the pole. The cancellation of poles between the two different regions of the time integral will be a phenomenon that is directly reflected by the structure of the SdSET. On the other hand, we see that the cancellation of the δ-poles seems to happen between the late-time, hard-momentum and early-time, soft-momentum regions. In the former region we identified the δ-poles as being of IR origin, while in the latter they were identified as being of UV origin, while in both cases the pole in ε was identified as an IR divergence. However, this is where our analysis of the divergences in the scaleless integrals in the early-time, hard-momentum region comes in: there we found exactly the combination of δ and ε poles we are currently discussing, where the UV and IR poles in δ cancelled each other. The presence of this divergence structure in this region should therefore be interpreted as follows: the IR pole in δ appearing in the early-time, hard-momentum region cancels its UV counterpart in the early-time, soft-momentum region, leaving the UV-δ pole of the early-time, hard-momentum region over. This cancellation effectively lifts the scale ν originally associated to the UV-δ pole of the early-time, soft momentum region, which has a natural value $\nu \sim q$ and is therefore associated to superhorizon physics, to the scale associated to the UV-δ pole of the early-time, hard-momentum region, which is instead associated to physics close to, or inside, the horizon. The final cancellation then happens between the IR-δ pole of the late-time, hard-momentum region and the UV-δ pole of the early-time, hard-momentum region. This fits with the natural value of ν associated to the UV-δ-pole of the late-time, hard-momentum region, where we found its associated natural value to be $\nu \sim -1/\eta$: when interpreted as a comoving momentum-scale, it is also associated to (sub-)horizon physics.

This computation served as a first example of how a non-trivial one-loop correlation function in de Sitter space can be evaluated in the late-time limit using the method of regions. This allowed us to simplify the computation considerably, and, further, to get a first idea of the relevant physical scales that contribute to its regions by studying the pole structure, and associated logarithms, of said regions. However, for the matching computations of full-theory correlators onto SdSET ones in the next chapter we will work in the k_Λ-scheme, so the remainder of the computations in this chapter will be carried out in this scheme.

3.6 Late-time limit of the one-loop bispectrum of the composite operator $\phi^2(t, \vec{x})$ in the k_Λ-scheme, $\vec{q} = 0$

In this section we will repeat the computation we did in above, but this time using the k_Λ-scheme. We will also consider a special kinematic configuration, where the momenta of the two single fields ϕ appearing in the correlation function are back-to-back, such that $\vec{q} = 0$. We thus compute the correlation function

$$
\langle \phi^2(\eta, \vec{0}) \phi(\eta, \vec{k}) \phi(\eta, -\vec{k}) \rangle' \Big|_{\mathcal{O}(\kappa)} . \tag{3.6.1}
$$

It corresponds to the diagrams

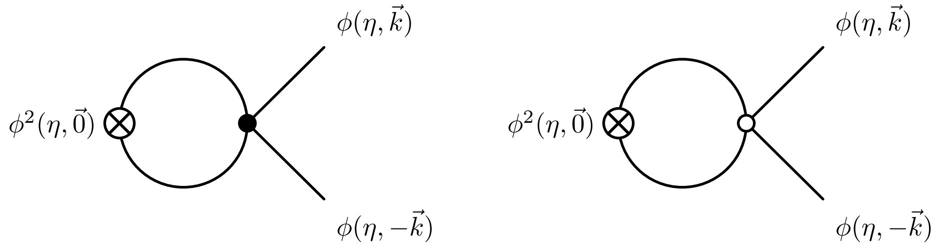

and it is the one that we will use for the matching procedure onto the SdSET in the next chapter. The mentioned kinematic choice is made to simplify the computations that we will need to carry out, while still preserving the information that we will need to extract through the matching computation. The region structure stays the same as in the previous section, and the same discussion applies, so we focus on the practical computation itself in this section. The more complex denominator structure of the integrals with respect to the previous section will lead us to introduce and discuss Mellin-Barnes integrals as a useful computational tool, which we will use in the next chapter as well.

3.6.1 Late-time regions

We follow the same structure of the computation as in the previous section, so we start by computing the late-time regions.

Soft-momentum region

The relevant integrals can be obtained by taking the expression (3.5.16), setting $\vec{k}_1 = -\vec{k}_2 = \vec{k}$, $\vec{q} = 0$ and replacing $k_i \to k_{i\Lambda}$ for all leftover momenta. Doing so we find

$$\begin{aligned}
&\langle \phi^2(\eta,\vec{0})\phi(\eta,\vec{k})\phi(\eta,-\vec{k})\rangle' \Big|_{\mathcal{O}(\kappa),\,\text{late }\eta,\,\text{soft }l} \\
&= -\frac{\tilde{\mu}^{4-d}\kappa H^d(-H\eta)^{2d-8}}{8k_\Lambda^6}\frac{(-\eta)^{-2\varepsilon}}{2\varepsilon(3+2\varepsilon)}\left[2\int\frac{\mathrm{d}^{d-1}l}{(2\pi)^{d-1}}\frac{1}{l_\Lambda^3} + 2k_\Lambda^3\int\frac{\mathrm{d}^{d-1}l}{(2\pi)^{d-1}}\frac{1}{l_\Lambda^6}\right] \\
&= -\frac{\kappa H^4(-H\eta)^{-4\varepsilon}}{96\pi^2 k_\Lambda^6}\left(\frac{e^{\gamma_E}\mu}{H}\right)^{2\varepsilon}(-e^{\gamma_E}\Lambda\eta)^{-2\varepsilon}\left[\frac{1}{\varepsilon^2}-\frac{2}{3\varepsilon}+\frac{4}{9}+\frac{\pi^2}{12}+\frac{\pi k_\Lambda^3}{\Lambda^3}\left(\frac{1}{8\varepsilon}+\frac{1}{6}-\frac{1}{4}\ln(2)\right)\right]. \qquad (3.6.2)
\end{aligned}$$

To obtain the last equality, we expanded the results of the integrals in ε, and dropped the terms that vanish as $\Lambda \to 0$. The UV divergences are now given in terms of ε poles, while the IR-divergences, which are both power-like and logarithmic, are represented by the Λ-dependence of the result, which is singular as $\Lambda \to 0$. Since we have inverse powers of Λ appearing in the result, the expansion of k_Λ in Λ would generate additional, non-vanishing terms as $\Lambda \to 0$. However, since the full k- and Λ-dependence must be reproduced by the EFT, these additional terms will drop out of the matching equation, and would thus simply clutter our equations if we wrote them out explicitly. Even though they are still present, we will therefore simply replace $k_\Lambda \to k$ at the end of the computations in the following equations.

Hard-momentum region

The relevant integrals for this region can be obtained by applying the same modifications described above to the expression (3.5.21). However, since in this region we are assuming $l \gg k$, this also implies that $l \gg \Lambda$, and we therefore let $\Lambda \to 0$ in the integrand. The only leftover Λ-dependence would thus be in the external momenta, but, as we discussed above, we do not need to write this one out explicitly in the final result. The late-time, hard-momentum region is therefore unchanged with respect to the previous computation, and the result still reads

$$
\begin{aligned}
&\langle\phi^2(t,\vec{0})\phi(t,\vec{k})\phi(t,-\vec{k})\rangle'\Big|_{\mathcal{O}(\kappa),\text{ late }\eta,\text{ hard }l}\\
=&\frac{\tilde{\mu}^{4-d}\kappa H^d(-H\eta)^{2d-8}}{8k_\Lambda^6}\nu^{2\delta}\mathrm{Im}\left[\int_{-\infty}^{\eta}\frac{\mathrm{d}\eta'}{(-\eta')^{8-d+2\delta}}\int\frac{\mathrm{d}^{d-1}l}{(2\pi)^{d-1}}\frac{e^{2il(\eta'-\eta)}(-i+l\eta)^2(i+l\eta')^2}{l^6}\right]\\
=&\frac{\kappa H^4(-H\eta)^{-4\varepsilon}}{96\pi^2k^6}\left(\frac{e^{\gamma_E}\mu}{H}\right)^{2\varepsilon}\left(\frac{\nu}{-\eta}\right)^{2\delta}\left[\frac{1}{\delta}\left(\frac{1}{\varepsilon}-\frac{8}{3}\right)-\frac{13}{6\varepsilon}+\frac{56}{9}-\frac{2\pi^2}{3}\right].
\end{aligned}
\tag{3.6.3}
$$

Since we have set $\Lambda\to 0$ before integrating, the IR is being regularized by the presence of δ and ε, as in the previous section.

3.6.2 Early-time regions

We now turn to the early-time regions.

Soft-momentum region

To obtain the expression that we need to compute in this region, we can recycle (3.5.30) and apply to it the changes we described above. The early-time, soft-momentum region now reads

$$
\begin{aligned}
&\langle\phi^2(\eta,\vec{0})\phi(\eta,\vec{k})\phi(\eta,-\vec{k})\rangle'\Big|_{\mathcal{O}(\kappa),\text{ early }\eta,\text{ soft }l}\\
=&\frac{\kappa\mu^{4-d}H^d(-H\eta)^{2d-8}}{8k_\Lambda^6}\nu^{2\delta}\mathrm{Im}\left[\int\frac{\mathrm{d}^{d-1}l}{(2\pi)^{d-1}}\frac{1}{l_\Lambda^6}\int_{-\infty}^{0}\frac{\mathrm{d}\eta'}{(-\eta')^{8-d+2\delta}}\,e^{2i(k_\Lambda+l_\Lambda)\eta'}(i+l_\Lambda\eta')^2(i+k_\Lambda\eta')^2\right].
\end{aligned}
\tag{3.6.4}
$$

To compute this expression we will apply a similar strategy as in the previous section: since we have the identity

$$\frac{1}{2i}\frac{\partial}{\partial k_\Lambda}e^{2i(k_\Lambda+l_\Lambda)\eta'}=\eta' e^{2i(k_\Lambda+l_\Lambda)\eta'}\tag{3.6.5}$$

we can generate any integral of the form

$$\int\frac{\mathrm{d}^{d-1}l}{(2\pi)^{d-1}}\int_{-\infty}^{0}\frac{\mathrm{d}\eta'}{(-\eta')^{8-d+2\delta}}\frac{\eta'^n e^{2i(k_\Lambda+l_\Lambda)\eta'}}{l_\Lambda^{2a}},\quad n\in\mathbb{N}\tag{3.6.6}$$

by acting n times with the differential operator $(2i)^{-1}\partial/\partial k_\Lambda$ on the integral with $n=0$. We will therefore only need to compute integrals of the form

$$\int\frac{\mathrm{d}^{d-1}l}{(2\pi)^{d-1}}\int_{-\infty}^{0}\frac{\mathrm{d}\eta'}{(-\eta')^{8-d+2\delta}}\frac{e^{2i(k_\Lambda+l_\Lambda)\eta'}}{l_\Lambda^{6-2n}},\tag{3.6.7}$$

with $n=0,1,2$. We can fist evaluate the η'-integral, which yields the result

$$\int_{-\infty}^{0}\frac{\mathrm{d}\eta'}{(-\eta')^{8-d+2\delta}}\,e^{2i(k_\Lambda+l_\Lambda)\eta'}=-\frac{i2^{7-d+2\delta}e^{i\pi(4-\frac{d}{2}+\delta)}}{(k_\Lambda+l_\Lambda)^{d-7-2\delta}}\Gamma(d-7-2\delta)\tag{3.6.8}$$

for all integrals of interest.

As this point, we have to face the fact that the $\vec{l}$-integration is complicated with respect to the previous section by the presence of the Λ-regulator. To deal with this, we can make use of the following Mellin-Barnes identity [112]:

$$\frac{1}{(X+Y)^\lambda}=\frac{1}{\Gamma(\lambda)}\frac{1}{2\pi i}\int_{-i\infty}^{i\infty}\mathrm{d}z\,\Gamma(\lambda+z)\Gamma(-z)\frac{X^z}{Y^{\lambda+z}}.\tag{3.6.9}$$

The complex contour of integration is defined somewhat implicitly by the requirement that the full series of poles of the function $\Gamma(\lambda+z)$ is located to the left of the contour, while the full series of poles of $\Gamma(-z)$ is located to the right of it. For $\mathrm{Re}(\lambda)>0$ this can be achieved by means of a contour that runs parallel to the imaginary axis in the z-plane, while the appropriate contour may look more complicated if this is not the case. For a more in-depth discussion of these integrals, and their application to the evaluation of Feynman integrals, see [112]. In practice, the way one uses (4.5.20) in the evaluation of loop integrals is to exchange the order of the z- and momentum integrals, evaluating the latter first, which are reduced to simple tadpole-like integrals, such as what we considered above already, due to the decomposition of the denominators using (4.5.20). Their result can therefore typically be written as a fraction involving products of gamma functions. Then, to evaluate the complex z-integral, one can close the complex contour either in the left or right complex half-plane, and use the residue theorem to rewrite the integral as a sum over residues of the gamma functions appearing in the integrand that have poles enclosed in the integration contour. As is discussed in [112,113], the crucial feature of this procedure, which is the main source of simplification in the computations, is that it grants direct access to the ε-expansion of the result, since the analytic continuation of the result of the $\vec{l}$-integral for $\varepsilon\to 0$ can be performed before evaluating the z-integral, which then typically simpifies the final complex integration(s) quite a bit. The process of analytic continuation in ε of the integrand of the Mellin-Barnes integrals is algorithmic in nature, and has been implemented in the `Mathematica` package `MB` [113], which we used to check our results.

In our case, the appropriate Mellin-Barnes representation reads

$$\frac{1}{(k_\Lambda+l_\Lambda)^{d-7-2\delta}}=\frac{1}{\Gamma(d-7-2\delta)}\frac{1}{2\pi i}\int_{-i\infty}^{i\infty}\mathrm{d}z\,\Gamma(d-7-2\delta+z)\Gamma(-z)\frac{l_\Lambda^z}{k_\Lambda^{d-7-2\delta+z}}\,. \tag{3.6.10}$$

The real part of z has to be chosen such that the series of poles of $\Gamma(-z)$ is completely to the right of the integration contour, while the series of poles of $\Gamma(-3-2\varepsilon-2\delta+z)$ is completely to the left of the integration contour. If we assume that both ε and δ are real and negative, this can be achieved by a vertical contour parallel to the imaginary axis, with

$$3+2\varepsilon+2\delta<\mathrm{Re}(z)<0\,. \tag{3.6.11}$$

After that, we evaluate the leftover Mellin-Barnes integral by means of the residue theorem, and we pick up only the residues which will give terms which do not vanish as we let $\Lambda\to 0$. The explicit results for the relevant integrals are given in appendix 3.D. Using these results we find

$$\begin{aligned}&\langle\phi^2(\eta,\vec{0})\phi(\eta,\vec{k})\phi(\eta,-\vec{k})\rangle'\Big|_{\mathcal{O}(\kappa),\text{ early }\eta,\text{ soft }l}\\ =&\frac{\kappa H^4(-H\eta)^{-4\varepsilon}}{96\pi^2k^6}\left(\frac{e^{\gamma_E}\mu}{H}\right)^{2\varepsilon}(e^{\gamma_E}\Lambda\nu)^{2\delta}\left\{\frac{1}{\varepsilon^2}-\frac{1}{\delta}\left[\frac{1}{\varepsilon}-\frac{8}{3}\right]+\frac{1}{\varepsilon}\frac{\pi k^3}{8\Lambda^3}-\frac{\pi k^3}{4\Lambda^3}\left[\frac{4}{3}-\ln\left(\frac{k}{\Lambda}\right)\right]-\frac{9\pi k}{4\Lambda}\right.\\ &\left.+\ln\left(\frac{2k}{\Lambda}\right)\left[2\ln\left(\frac{2k}{\Lambda}\right)+\frac{1}{3}\right]-\frac{17}{3}+\frac{11\pi^2}{12}\right\}.\end{aligned} \tag{3.6.12}$$

Hard-momentum region

Analogously to the late-time, hard-momentum region, the fact that $l\gg k$ here means that we should let $\Lambda\to 0$ in the integrand in this region. We therefore get the same starting expression as in the analogous region we considered in section 3.5 back, which vanishes.

3.6.3 Sum of the regions, renormalization of the operator ϕ^2

Summing up what we found above we find the result

$$\langle\phi^2(\eta,\vec{0})\phi(\eta,\vec{k})\phi(\eta,-\vec{k})\rangle'\Big|_{\mathcal{O}(\kappa)}$$

$$
\begin{aligned}
=&\frac{\kappa H^4(-H\eta)^{-4\varepsilon}}{96\pi^2k^6}\left(\frac{e^{\gamma_E}\mu}{H}\right)^{2\varepsilon}\bigg\{-\frac{3}{2\varepsilon}+2\ln(-2e^{\gamma_E}k\eta)\bigg[-\ln(-2e^{\gamma_E}k\eta)+2\ln\left(\frac{2k}{\Lambda}\right)+2\bigg]-\frac{11}{3}\ln\left(\frac{2k}{\Lambda}\right)\\
&-\frac{\pi k^3}{4\Lambda^2}\bigg[2-\ln(-2e^{\gamma_E}k\eta)\bigg]-\frac{9\pi k}{4\Lambda}+\frac{1}{9}+\frac{\pi^2}{6}\bigg\}\,.
\end{aligned}
\tag{3.6.13}
$$

We see that the only leftover pole in ε, which comes from the UV divergences of this correlation function, matches the UV divergence we found in the previous section, while the IR divergences are now all captured by the Λ-dependence of the result. This is expected, since we are using a regularization scheme which only affects the IR structure of the correlators.

To remove the UV divergence and define the renormalized correlation function we follow the same logic discussed in section 3.5.5, and define the renormalized operator $[\phi^2](\eta,\vec{x})$ via

$$
\tilde{\mu}^{2\varepsilon}\phi^2(\eta,\vec{x})=Z^{\phi}_{22}\tilde{\mu}^{2\varepsilon}[\phi^2](\eta,\vec{x})+H^2Z^{\phi}_{20}\mathbb{1}+\text{ higher powers of }\phi
\tag{3.6.14}
$$

and we need to pick

$$
Z_{22}=1-\frac{\kappa}{48\pi^2}\frac{3}{2\varepsilon}+\mathcal{O}(\kappa^2)\,.
\tag{3.6.15}
$$

This then defines the four-dimensional renormalized correlator

$$
\begin{aligned}
&\langle[\phi^2](\eta,\vec{0})\phi(\eta,\vec{k})\phi(\eta,-\vec{k})\rangle'\Big|_{\mathcal{O}(\kappa)}\\
=&\frac{\kappa H^4}{96\pi^2k^6}\bigg\{-3\ln\left(\frac{e^{\gamma_E}\mu}{H}\right)+2\ln(-2e^{\gamma_E}k\eta)\bigg[-\ln(-2e^{\gamma_E}k\eta)+2\ln\left(\frac{2k}{\Lambda}\right)+2\bigg]-\frac{11}{3}\ln\left(\frac{2k}{\Lambda}\right)\\
&-\frac{\pi k^3}{4\Lambda^2}\bigg[2-\ln(-2e^{\gamma_E}k\eta)\bigg]-\frac{9\pi k}{4\Lambda}+\frac{1}{9}+\frac{\pi^2}{6}\bigg\}\,,
\end{aligned}
\tag{3.6.16}
$$

which now explicitly depends on μ.

Before moving on, let us make the following remark on operator renormalization in the k_Λ-scheme. In principle, there is the following difference in the scheme we are currently using with respect to the IR dimreg scheme we were using previously: we have introduced the additional dimensionful quantity Λ, which therefore could also appear explicitly in the renormalization equation. However, since it is a comoving quantity, it should be combined with another comoving quantity to yield something physical, and the only possible combination would then be $-\Lambda\eta$, raised to some integer power, multiplying a renormalized operator $[\phi^n]$. Since we are computing late-time correlation functions, the only way such a term could survive is if it was multiplied by an inverse power of $-\Lambda\eta$. Inverse powers of Λ can be, and are, generated by IR divergences in correlation functions of the renormalized operators, but not inverse powers of η, since they would represent exponentially divergent terms in cosmic time t, as we let $\eta\to 0$ ($t\to\infty$). Therefore, we do not need to include such terms in (3.6.14).

3.7 Computation of the one-point function of the operator ϕ^2 in the k_Λ-scheme

We now turn to the last computation that we will carry out in this chapter, which is the one-point function of the operator $\phi^2(t,\vec{x})$ at $\mathcal{O}(\kappa)$. We define it via the following momentum integral over the power spectrum of ϕ:

$$
\begin{aligned}
\langle\phi^2(\eta,\vec{x})\rangle&=\int\frac{\mathrm{d}^{d-1}l_1\mathrm{d}^{d-1}l_2}{(2\pi)^{2d-2}}e^{i(\vec{l}_1+\vec{l}_2)\cdot\vec{x}}\langle\phi(\eta,\vec{l}_1)\phi(\eta,\vec{l}_1)\rangle\\
&=\int\frac{\mathrm{d}^{d-1}l}{(2\pi)^{d-1}}\langle\phi(\eta,\vec{l})\phi(\eta,-\vec{l})\rangle'\,.
\end{aligned}
\tag{3.7.1}
$$

In the absence of the IR regulator Λ, and if regulated using dimreg or another analytic regulator, the one-point function $\langle \phi^2(\eta, \vec{x}) \rangle$ would vanish to all orders in κ, since the integral appearing in (3.7.1) would be scaleless. However, since in the massless theory this integral is both UV- and IR-divergent, the one-point function of the renormalized operator $[\phi^2]$ would no longer be vanishing, and, instead, it would be given by the IR poles, and all terms that are generated by them, after the UV divergences have been removed. In the k_Λ-scheme the IR regulator provides a scale in (3.7.1), and therefore the regularized one-point function $\langle \phi^2(\eta, \vec{x}) \rangle$ will be non-vanishing. Since we will be able to clearly distinguish UV and IR divergences in this scheme, this computation will allow us to renormalize the composite operator ϕ^2 using the same operator renormalization equation (3.5.46) we set up above, and define the renormalized one-point function $\langle [\phi^2](t, \vec{x}) \rangle$. This computation also provides an example of operator mixing in the full theory, since we will see that the appropriate counterterm to subtract the UV poles is Z^ϕ_{20}.

3.7.1 $\langle \phi^2(\eta, \vec{x}) \rangle$ in the free theory

At $\mathcal{O}(\kappa^0)$, without inserting any interaction term, (3.7.1) corresponds to the following one-loop diagram:

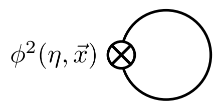

where we are denoting the composite operator ϕ^2 by means of the symbol $\otimes$. It corresponds to the same tadpole integral we already considered in section 3.4.1, up to some additional coefficients:

$$\tilde{\mu}^{2\varepsilon} \langle \phi^2(\eta, \vec{x}) \rangle = \frac{H^2(-H\eta)^{-2\varepsilon} \tilde{\mu}^{2\varepsilon}}{2} \int \frac{\mathrm{d}^{d-1} l}{(2\pi)^{d-1}} \frac{1 + l_\Lambda^2 \eta^2}{l_\Lambda^3} = \frac{H^2}{8\pi^2} \left(\frac{-\Lambda H \eta}{\mu} \right)^{-2\varepsilon} e^{\varepsilon \gamma_E} \Gamma(\varepsilon) \left[1 - \frac{(-\Lambda\eta)^2}{2(1-\varepsilon)} \right] . \quad (3.7.2)$$

Just like in that case, we find a logarithmically UV- and IR-divergent term, and a quadratically UV-divergent one, which is proportional to $(-\Lambda\eta)^2$. As we already discussed, the latter term can be safely ignored, since we are letting $\eta \to 0$, and we are only left with the pole term stemming from the logarithmic divergence. Taking the expectation value of the operator renormalization equation (3.5.46) and neglecting the terms involving higher powers of ϕ, we find the equation

$$\tilde{\mu}^{2\varepsilon} \langle \phi^2(\eta, \vec{x}) \rangle = Z^\phi_{22} \tilde{\mu}^{2\varepsilon} \langle [\phi^2](\eta, \vec{x}) \rangle + H^2 Z^\phi_{20} \,, \quad (3.7.3)$$

which needs to be evaluated at $\mathcal{O}(\kappa^0)$. Above, we found that at this order we simply have $Z^{\phi,(\kappa^0)}_{22} = 1$, which allows us to define the renormalized one-point function as

$$\langle [\phi^2](\eta, \vec{x}) \rangle \Big|_{\mathcal{O}(\kappa^0)} = \tilde{\mu}^{2\varepsilon} \langle \phi^2(\eta, \vec{x}) \rangle \Big|_{\mathcal{O}(\kappa^0)} - H^2 Z^{\phi,(\kappa^0)}_{20} \,, \quad (3.7.4)$$

where we dropped the factor $\tilde{\mu}^{2\varepsilon}$ on the left-hand side, since, by assumption, the correlation function is UV-finite and the limit $\varepsilon \to 0$ can be taken safely. As anticipated, we see that the appropriate counterterm to absorb the UV poles is Z^ϕ_{20}. Choosing

$$Z^\phi_{20} = \frac{1}{8\pi^2 \varepsilon} + \mathcal{O}(\kappa) \quad (3.7.5)$$

we find the renormalized one-point function

$$\begin{aligned} \langle [\phi^2](\eta, \vec{x}) \rangle \Big|_{\mathcal{O}(\kappa^0)} &= \frac{H^2}{8\pi^2} \left[\left(\frac{-\Lambda H \eta}{\mu} \right)^{-2\varepsilon} e^{\varepsilon \gamma_E} \Gamma(\varepsilon) - \frac{1}{\varepsilon} \right] \quad (3.7.6) \\ &= - \frac{H^2}{4\pi^2} \ln \left(\frac{-\Lambda H \eta}{\mu} \right) + \mathcal{O}(\varepsilon) \,. \quad (3.7.7) \end{aligned}$$

For now we can drop the higher-order terms on ε, but they will become important as we go to $\mathcal{O}(\kappa)$.

Thus, we find that already in the free theory, the composite operators ϕ^n require a non-trivial renormalization and, furthermore, they mix non-trivially among each other because of this. We also notice that (3.7.7) has an explicit time-dependence, which in this scheme is generated by the UV pole. All of these properties will carry over to the SdSET, and have profound consequences for the effective dynamics of the late-time correlators in the massless theory. Since in the free theory we already had to compute a one-loop diagram, the computation of $\langle\phi^2(\eta,\vec{x})\rangle$ at $\mathcal{O}(\kappa)$ gives us a chance to study a simple, but still non-trivial, two-loop example of operator renormalization in the massless theory. In the next chapter, this result will be useful to study the matching procedure in the SdSET at two-loop order.

3.7.2 Relevant diagrams and regions at $\mathcal{O}(\kappa)$

We now turn on the interactions and compute $\langle\phi^2(\eta,\vec{x})\rangle$ at $\mathcal{O}(\kappa)$. The correlation function receives contributions from the insertion of the quartic vertex, which corresponds to the two diagrams

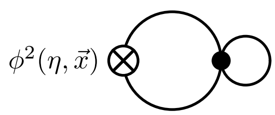

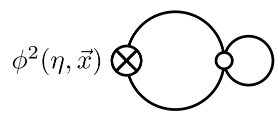

and from the two counterterms δm^2 and $\delta\Lambda^2$, which both lead to the diagrams with topology

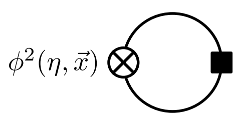

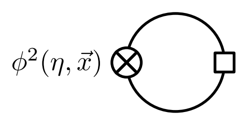

These diagrams can be thought of as the diagrams we considered for the one-loop power spectrum in section 3.4.1 with the coincident limit of their external points taken.

Using the known Feynman rules, we find that we have to evaluate the following correlation function:

$$\begin{aligned}\langle\phi^2(\eta,\vec{x})\rangle\Big|_{\mathcal{O}(\kappa)} =&(-H\eta)^{d-4}\int\frac{\mathrm{d}^{d-1}k}{(2\pi)^{d-1}}\Bigg\{\frac{\tilde{\mu}^{4-d}\kappa H^{d-2}}{8}\mathrm{Im}\Bigg[\int_{-\infty}^{\eta}\frac{\mathrm{d}\eta'}{(-\eta')^{8-d}}\frac{e^{2ik_\Lambda(\eta'-\eta)}(i-k_\Lambda\eta)^2(i+k_\Lambda\eta')^2}{k_\Lambda^6}\Bigg]\\ &\times\int\frac{\mathrm{d}^{d-1}l}{(2\pi)^{d-1}}\frac{1+l_\Lambda^2\eta'^2}{l_\Lambda^3}\\ &+\frac{1}{2}\mathrm{Im}\Bigg[\int_{-\infty}^{\eta}\frac{\mathrm{d}\eta'}{(-\eta')^4}\frac{e^{2ik_\Lambda(\eta'-\eta)}(i-k_\Lambda\eta)^2(i+k_\Lambda\eta')^2}{k_\Lambda^6}\Big[\delta m^2+(-H\eta')^2\delta\Lambda^2\Big]\Bigg]\Bigg\}. \end{aligned} \tag{3.7.8}$$

We have already determined the relevant counterterms at $\mathcal{O}(\kappa)$ in section 3.4.1, and we reprint the results here for convenience:

$$\delta m^2 =\frac{\kappa H^2}{8\pi^2}\left[-\frac{1}{2\varepsilon}+\delta\hat{m}^2_{\mathrm{fin}}\right], \tag{3.7.9}$$

$$\delta\Lambda^2 =\frac{\kappa\Lambda^2}{32\pi^2}\left[\frac{1}{\varepsilon}+1\right]. \tag{3.7.10}$$

In the computation of the one-loop power spectrum the $\delta\Lambda^2$ counterterm was irrelevant, but in this computation it will become important.

We now proceed with the computation, and we make use of the method of regions to simplify it. As in the case of the power spectrum, the factorized one-loop integral has only one region, and we keep it as it is. We can therefore evaluate it immediately, and find

$$I(\eta') \equiv \tilde{\mu}^{2\varepsilon} \int \frac{\mathrm{d}^{d-1}l}{(2\pi)^{d-1}} \frac{1+l_\Lambda^2 \eta'^2}{l_\Lambda^3} = \frac{1}{4\pi^2}\left(\frac{\Lambda}{\mu}\right)^{-2\varepsilon} e^{\varepsilon\gamma_E}\Gamma(\varepsilon)\left[1-\frac{(\Lambda\eta')^2}{2(1-\varepsilon)}\right]. \tag{3.7.11}$$

However, differently than in the case of the power spectrum, the $\mathcal{O}(\Lambda^2)$-piece of this integral cannot be simply dropped at this point in the computation, since it might combine with an $\mathcal{O}(\Lambda^{-2})$ term generated by the remaining time- and momentum integrations to give a finite remainder when we let $\Lambda \to 0$ at the end of the computation. Indeed, we will see that this happens in one of the regions below. For the same reason, the counterterm $\delta\Lambda^2$ is important, since it serves to consistently subtract the $\mathcal{O}(\Lambda^2)$-subdivergence of this integral, and it has to be considered.

To proceed, we need to find the regions of the following integrals:

$$\langle\phi^2(\eta,\vec{x})\rangle\Big|_\kappa = \frac{\tilde{\mu}^{4-d}\kappa H^{d-2}}{8}(-H\eta)^{d-4}\mathrm{Im}\left[\int \frac{\mathrm{d}^{d-1}k}{(2\pi)^{d-1}} \int_{-\infty}^{\eta} \frac{\mathrm{d}\eta'}{(-\eta')^{8-d}} \frac{e^{2ik_\Lambda(\eta'-\eta)}(i-k_\Lambda\eta)^2(i+k_\Lambda\eta')^2}{k_\Lambda^6} I(\eta')\right], \tag{3.7.12}$$

and

$$\langle\phi^2(\eta,\vec{x})\rangle\Big|_{\text{c.t.}} = \frac{1}{2}(-H\eta)^{d-4}\mathrm{Im}\left[\int \frac{\mathrm{d}^{d-1}k}{(2\pi)^{d-1}} \int_{-\infty}^{\eta} \frac{\mathrm{d}\eta'}{(-\eta')^4} \frac{e^{2ik_\Lambda(\eta'-\eta)}(i-k_\Lambda\eta)^2(i+k_\Lambda\eta')^2}{k_\Lambda^6}\left[\delta m^2+(-H\eta')^2\delta\Lambda^2\right]\right] \tag{3.7.13}$$

To decompose the $\vec{k}$- and η'-integrals we only have one external reference scale to do so, which is the late correlation time η. We have the two regions

$$\eta' \ll \eta \quad (\text{early})\,, \qquad \eta' \sim \eta \quad (\text{late}) \tag{3.7.14}$$

for η', and

$$k \sim -\frac{1}{\eta} \quad (\text{hard})\,, \qquad k \ll -\frac{1}{\eta} \quad (\text{soft}) \tag{3.7.15}$$

for $\vec{k}$. As we did above, we treat Λ as being a quantity that scales like a soft comoving momentum. For the decomposition into regions, as was the case for the one-loop power spectrum in section 3.4.1 and the bispectrum of ϕ^2 in the sections 3.5 and 3.6, we will find integrals that are not regularized by the regulators we already have in place. The origin of these unregulated divergences is twofold. The first one is the fact that the time integral for the counterterm-insertion diagrams is d-independent, which is the accidental cancellation that we already observed in section 3.4.1. The second one is the fact that both in the late-time, hard-momentum region and the early-time, soft-momentum region the combination $-k\eta'$ scales like $-k\eta' \sim 1$ for two different reasons, which, as we already discussed in section 3.5, leads to unregulated divergences. Therefore, as we did in the above sections, also in this case we need to introduce the analytic regulator

$$(-\nu\eta')^{-2\delta} \tag{3.7.16}$$

in both integrands above. After carrying out all the integrations we will take the limits $\delta \to 0$, $\varepsilon \to 0$, in this order, as well as the limit $\Lambda \to 0$. We expect the appearence of poles in δ in the mentioned regions, which will then cancel when we evaluate the region sum at the end. All of the appearing integrals can be evaluated directly using `Mathematica`.

3.7.3 Late-time regions

We start by considering the late-time regions.

Soft-momentum region

In this region we have

$$-k\eta \sim -k\eta' \ll 1 \tag{3.7.17}$$

and we can therefore expand the numerator of the remaining integral as

$$e^{2ik_\Lambda(\eta'-\eta)}(i-k_\Lambda\eta)^2(i+k_\Lambda\eta')^2 = 1 + k_\Lambda^2(\eta^2+\eta'^2) + \frac{2ik_\Lambda^3}{3}(\eta'^3-\eta^3) + \mathcal{O}(k_\Lambda^4)\,. \tag{3.7.18}$$

We can truncate the expansion after the $\mathcal{O}(k_\Lambda^3)$-terms, since they will yield terms that are proportional to positive powers of Λ after integration, which will vanish as we let $\Lambda \to 0$ at the end. We find the following results:

$$\begin{aligned}
&\tilde{\mu}^{2\varepsilon}\langle\phi^2(\eta,\vec{x})\rangle\Big|_{\kappa,\text{ late-}\eta,\text{ soft-}k} \\
=&\frac{\tilde{\mu}^{2\varepsilon}\kappa H^{2-2\varepsilon}}{8}(-H\eta)^{-2\varepsilon}\mathrm{Im}\bigg[\int\frac{\mathrm{d}^{d-1}k}{(2\pi)^{d-1}}\int_{-\infty}^{\eta}\frac{\mathrm{d}\eta'}{(-\eta')^{8-d}}\frac{(-\nu\eta')^{-2\delta}}{k_\Lambda^6}\bigg(1+k_\Lambda^2(\eta^2+\eta'^2)+\frac{2ik_\Lambda^3}{3}(\eta'^3-\eta^3)\bigg)I(\eta')\bigg] \qquad (3.7.19) \\
=&-\frac{\kappa H^2}{384\pi^4}\left(\frac{\mu}{H}\right)^{4\varepsilon}e^{2\varepsilon\gamma_E}(-\Lambda\eta)^{-2\varepsilon}(-e^{\gamma_E}\Lambda\eta)^{-2\varepsilon}\left[\frac{1}{\varepsilon^3}-\frac{2}{3\varepsilon^2}+\frac{1}{\varepsilon}\left(\frac{4}{9}+\frac{\pi^2}{6}\right)-\frac{8}{27}-\frac{\pi^2}{9}-\frac{2\zeta(3)}{3}\right] \qquad (3.7.20)
\end{aligned}$$

for the vertex-insertion diagram, where $\zeta(n)$ denotes the Riemann zeta function, and

$$\begin{aligned}
&\tilde{\mu}^{2\varepsilon}\langle\phi^2(\eta,\vec{x})\rangle\Big|_{\text{c.t., late-}\eta,\text{ soft-}k} \\
=&\frac{\tilde{\mu}^{2\varepsilon}}{2}(-H\eta)^{-2\varepsilon}\mathrm{Im}\bigg[\int\frac{\mathrm{d}^{d-1}k}{(2\pi)^{d-1}}\int_{-\infty}^{\eta}\frac{\mathrm{d}\eta'}{(-\eta')^{4}}\frac{(-\nu\eta')^{-2\delta}}{k_\Lambda^6}\bigg(1+k_\Lambda^2(\eta^2+\eta'^2)+\frac{2ik_\Lambda^3}{3}(\eta'^3-\eta^3)\bigg) \\
&\times\Big[\delta m^2+(-H\eta')^2\delta\Lambda^2\Big]\bigg] \qquad (3.7.21) \\
=&-\frac{\kappa H^2}{192\pi^4}\left(\frac{\mu}{H}\right)^{2\varepsilon}(-\Lambda\eta)^{-2\varepsilon}(-\nu\eta)^{-2\delta}\left\{-\frac{1}{\varepsilon^2}\left[\frac{1}{2\delta}-\frac{1}{3}\right]+\frac{\delta\hat{m}^2_{\text{fin}}}{\varepsilon}\left[\frac{1}{\delta}-\frac{2}{3}\right]-\frac{\pi^2}{24\delta}+\frac{\pi^2}{36}\right\} \qquad (3.7.22)
\end{aligned}$$

for the counterterm diagrams. The presence of poles in δ in the latter result signals the necessity of the analytic regulator $(-\nu\eta')^{-2\delta}$, due to the d-independence of the time integral, while for the former result it is not needed, and we could have let $\delta \to 0$ already before evaluating the integrals. For both of these terms, the $\mathcal{O}(\Lambda^2)$-pieces of the tadpole integral and counterterms, respectively, are irrelevant, since they remain $\mathcal{O}(\Lambda^2)$ after the integration, and they vanish as we expand the result in the limit $\Lambda \to 0$.

Hard-momentum region

In this region we have

$$-k\eta \sim -k\eta' \sim 1 \tag{3.7.23}$$

so the numerators of the integrands stay unchanged. However, since we have $k \gg \Lambda$, we must set $\Lambda \to 0$ in the integrands, and in this region any occurring divergences are regularized by dimensional regularization and the analytic regulator. We find the results

$$\begin{aligned}
&\tilde{\mu}^{2\varepsilon}\langle\phi^2(\eta,\vec{x})\rangle\Big|_{\kappa,\text{ late-}\eta,\text{ hard-}k} \\
=&\frac{\tilde{\mu}^{2\varepsilon}\kappa H^{2-2\varepsilon}}{8}(-H\eta)^{-2\varepsilon}\mathrm{Im}\bigg[\int\frac{\mathrm{d}^{d-1}k}{(2\pi)^{d-1}}\int_{-\infty}^{\eta}\frac{\mathrm{d}\eta'}{(-\eta')^{8-d}}(-\nu\eta')^{-2\delta}\frac{e^{2ik(\eta'-\eta)}(i-k\eta)^2(i+k\eta')^2}{k^6}I(\eta')\bigg] \qquad (3.7.24)
\end{aligned}$$

$$
\begin{aligned}
=&\frac{\kappa H^2}{384\pi^4}\left(\frac{\mu}{H}\right)^{4\varepsilon} e^{2\varepsilon\gamma_E}(-\Lambda\eta)^{-2\varepsilon}(-\nu\eta)^{-2\delta}\left\{\frac{1}{\varepsilon^2}\left[\frac{1}{\delta}-\frac{13}{6}\right]+\frac{1}{\varepsilon}\left[-\frac{8}{3\delta}+\frac{56}{9}-\frac{2\pi^2}{3}\right]\right.\\
&\left.+\frac{1}{\delta}\left[\frac{52}{9}-\frac{\pi^2}{3}\right]-30+\frac{5\pi^2}{2}+8\zeta(3)\right\}
\end{aligned}
\tag{3.7.25}
$$

for the vertex-insertion diagram, and

$$
\begin{aligned}
&\tilde{\mu}^{2\varepsilon}\langle\phi^2(\eta,\vec{x})\rangle\Big|_{\text{c.t., late-}\eta,\text{ hard-}k}\\
=&\frac{\tilde{\mu}^{2\varepsilon}}{2}(-H\eta)^{-2\varepsilon}\mathrm{Im}\left[\int\frac{\mathrm{d}^{d-1}k}{(2\pi)^{d-1}}\int_{-\infty}^{\eta}\frac{\mathrm{d}\eta'}{(-\eta')^4}(-\nu\eta')^{-2\delta}\frac{e^{2ik(\eta'-\eta)}(i-k\eta)^2(i+k\eta')^2}{k^6}\left[\delta m^2+(-H\eta')^2\delta\Lambda^2\right]\right]
\end{aligned}
\tag{3.7.26}
$$

$$
\begin{aligned}
=&\frac{\kappa H^2}{192\pi^4}\left(\frac{\mu}{H}\right)^{2\varepsilon}(-\Lambda\eta)^{-2\varepsilon}(-e^{\gamma_E}\Lambda\eta)^{2\varepsilon}\left\{\frac{1}{2\varepsilon^3}-\frac{1}{\varepsilon^2}\left[\frac{1}{4}+\delta\hat{m}^2_{\text{fin}}\right]+\frac{1}{2\varepsilon}\left[\frac{\pi^2}{4}+\delta\hat{m}^2_{\text{fin}}\right]\right.\\
&\left.-\frac{\pi^2}{4}\left[\frac{1}{4}+\delta\hat{m}^2_{\text{fin}}\right]+\frac{\zeta(3)}{6}\right\}
\end{aligned}
\tag{3.7.27}
$$

for the counterterm diagrams. Notice the absence of the subscript Λ in both integrands. Also for these terms, the $\mathcal{O}(\Lambda^2)$-pieces of the tadpole and counterterm, respectively, remain $\mathcal{O}(\Lambda^2)$ after the integration, and thus their contribution vanishes. The appearance of the δ-poles in the vertex-insertion contribution is expected for the reasons discussed above, however, curiously, we find no δ-poles in the counterterm-insertion contribution, even though, naively, we would have expected them. Nevertheless, the cancellation of all pole terms that we will observe below will be a check of this result.

3.7.4 Early-time regions

We now move on to the computation of the early-time regions.

Soft-momentum region

In this region we have

$$
-k\eta\ll 1\,,\quad -k\eta'\sim 1\,,
\tag{3.7.28}
$$

so we can approximate the numerators of the integrands as

$$
e^{2ik_\Lambda(\eta'-\eta)}(i-k_\Lambda\eta)^2(i+k_\Lambda\eta')^2=-e^{2ik_\Lambda\eta'}(i+k_\Lambda\eta')^2+\mathcal{O}\left(\frac{\eta}{\eta'}\right)
\tag{3.7.29}
$$

and we extend the domain of integration to the entire range of values $\eta'\in(-\infty,0)$. We find

$$
\begin{aligned}
&\tilde{\mu}^{2\varepsilon}\langle\phi^2(\eta,\vec{x})\rangle\Big|_{\kappa,\text{ early-}\eta,\text{ soft-}k}\\
=&\frac{\tilde{\mu}^{2\varepsilon}\kappa H^{2-2\varepsilon}}{8}(-H\eta)^{-2\varepsilon}\mathrm{Im}\left[\int\frac{\mathrm{d}^{d-1}k}{(2\pi)^{d-1}}\int_{-\infty}^{0}\frac{\mathrm{d}\eta'}{(-\eta')^{8-d}}(-\nu\eta')^{-2\delta}\frac{e^{2ik_\Lambda\eta'}(i+k_\Lambda\eta')^2}{k_\Lambda^6}I(\eta')\right]
\end{aligned}
\tag{3.7.30}
$$

$$
\begin{aligned}
=&\frac{\kappa H^2}{384\pi^4}\left(\frac{\mu}{H}\right)^{4\varepsilon}e^{2\varepsilon\gamma_E}(-\Lambda\eta)^{-2\varepsilon}\left(\frac{\nu}{e^{\gamma_E}\Lambda}\right)^{-2\delta}\left\{\frac{1}{\varepsilon^3}-\frac{1}{\delta\varepsilon^2}+\frac{1}{\varepsilon}\left[\frac{8}{3\delta}-\frac{72}{18}+\frac{\pi^2}{2}\right]-\frac{1}{\delta}\left[\frac{52}{9}-\frac{\pi^2}{3}\right]\right.\\
&\left.+\frac{1361}{54}-\frac{20\pi^2}{9}-\zeta(3)\right\}
\end{aligned}
\tag{3.7.31}
$$

for the vertex-insertion diagram, and

$$
\tilde{\mu}^{2\varepsilon}\langle\phi^2(\eta,\vec{x})\rangle\Big|_{\text{c.t., early-}\eta,\text{ soft-}k}
$$

$$=\frac{\tilde{\mu}^{2\varepsilon}}{2}(-H\eta)^{-2\varepsilon}\mathrm{Im}\Big[\int\frac{\mathrm{d}^{d-1}k}{(2\pi)^{d-1}}\int_{-\infty}^{0}\frac{\mathrm{d}\eta'}{(-\eta')^4}(-\nu\eta')^{-2\delta}\frac{e^{2ik_\Lambda\eta'}(i+k_\Lambda\eta')^2}{k_\Lambda^6}\Big[\delta m^2+(-H\eta')^2\delta\Lambda^2\Big]\Big] \tag{3.7.32}$$

$$\begin{aligned}=&\frac{\kappa H^2}{192\pi^4}\left(\frac{\mu}{H}\right)^{2\varepsilon}(-\Lambda\eta)^{-2\varepsilon}\left(\frac{\nu}{e^{\gamma_E}\Lambda}\right)^{-2\delta}\Big\{-\frac{1}{2\varepsilon^3}+\frac{1}{\varepsilon^2}\Big[-\frac{1}{2\delta}+\frac{4}{3}+\delta\hat{m}^2_{\mathrm{fin}}\Big]\\&-\frac{1}{\varepsilon}\Big[\frac{\delta\hat{m}^2_{\mathrm{fin}}}{\delta}-\frac{3}{4}+\frac{\pi^2}{24}-\frac{8}{3}\delta\hat{m}^2_{\mathrm{fin}}\Big]-\frac{\pi^2}{24\pi^2\delta}-\frac{3}{4}+\frac{\pi^2}{9}-\frac{\zeta(3)}{3}-\frac{\pi^2}{12}\delta\hat{m}^2_{\mathrm{fin}}\Big\}\end{aligned} \tag{3.7.33}$$

for the counterterm diagrams. For both of these expressions, the $\mathcal{O}(\Lambda^2)$-pieces of $I(\eta')$ and $\delta\Lambda^2$ are important, since the time integral generates IR-divergent $\mathcal{O}(\Lambda^{-2})$ terms, which promote these contributions to be $\mathcal{O}(\Lambda^0)$, and hence they survive the limit $\Lambda\to 0$ we are taking at the end of the computation. The presence of the $\mathcal{O}(\Lambda^2)$-term in the mass counterterm ensures that these terms get subtracted consistently, and, in particular, that they do not get erroneously identified as purely UV poles associated with the renormalization of the composite operator, since they stem from two overlapping UV and IR divergences. In practice, the presence or absence of these terms will impact the coefficient of the $\ln(\Lambda)$-term in the final, renormalized result, so to ensure that we are finding the correct IR-divergent structure of the renormalized correlator it is crucial to take this point into account. Furthermore, we observe the prensence of δ-poles in both results, which, again, were expected from the discussion above.

Hard-momentum region

In this region we have

$$-k\eta\sim 1\,,\quad -k\eta'\gg 1 \tag{3.7.34}$$

and we can therefore replace the integrands with

$$\frac{e^{2ik_\Lambda(\eta'-\eta)}(i-k_\Lambda\eta)^2(i+k_\Lambda\eta')^2}{k_\Lambda^6}\to\frac{e^{2ik\eta'}(k\eta')^2}{k^6}\,. \tag{3.7.35}$$

Therefore, the integrals become scaleless, and they vanish. This region therefore makes no contribution to the final result.

3.7.5 Sum of the regions, renormalization of the operator ϕ^2

Summing up the three non-vanishing regions for each contribution to the one-point function we find

$$\begin{aligned}\tilde{\mu}^{2\varepsilon}\langle\phi^2(\eta,\vec{x})\rangle\Big|_\kappa=&\frac{\kappa H^2}{384\pi^4}\left(\frac{e^{\gamma_E}\mu}{H}\right)^{4\varepsilon}(-e^{\gamma_E}\Lambda\eta)^{-2\varepsilon}\Big\{-\frac{3}{2\varepsilon^2}+\frac{1}{\varepsilon}\Big[-2\ln^2(-e^{\gamma_E}\Lambda\eta)+4\ln(-e^{\gamma_E}\Lambda\eta)+\frac{3}{2}-\frac{\pi^2}{3}\Big]\\&+\frac{4}{3}\ln^3(-e^{\gamma_E}\Lambda\eta)+\frac{4}{3}\ln^2(-e^{\gamma_E}\Lambda\eta)-\left(\frac{32}{3}+\pi^2\right)\ln(-e^{\gamma_E}\Lambda\eta)-\frac{9}{2}+\frac{7\pi^2}{18}+\frac{23\zeta(3)}{3}\Big\}\end{aligned} \tag{3.7.36}$$

for the vertex-insertion contribution, and

$$\begin{aligned}\tilde{\mu}^{2\varepsilon}\langle\phi^2(\eta,\vec{x})\rangle\Big|_{\mathrm{c.t.}}=&\frac{\kappa H^2}{384\pi^4}\left(\frac{e^{\gamma_E}\mu}{H}\right)^{2\varepsilon}(-e^{\gamma_E}\Lambda\eta)^{-2\varepsilon}\Big\{\frac{3}{2\varepsilon^2}+\frac{1}{\varepsilon}\Big[2\ln^2(-e^{\gamma_E}\Lambda\eta)-\ln(-e^{\gamma_E}\Lambda\eta)-\frac{3}{2}+\frac{\pi^2}{3}-3\delta\hat{m}^2_{\mathrm{fin}}\Big]\\&+\frac{4}{3}\ln^3(-e^{\gamma_E}\Lambda\eta)-(1+4\delta\hat{m}^2_{\mathrm{fin}})\ln^2(-e^{\gamma_E}\Lambda\eta)+\left(\frac{\pi^2}{3}+2\delta\hat{m}^2_{\mathrm{fin}}\right)\ln(-e^{\gamma_E}\Lambda\eta)\\&-\frac{3}{2}+\frac{\pi^2}{24}-\frac{2\pi^2}{3}\delta\hat{m}^2_{\mathrm{fin}}-\frac{\zeta(3)}{3}\Big\}\end{aligned} \tag{3.7.37}$$

for the contribution from the counterterms. Notice that all δ-poles cancelled in both results, which is precisely what should happen, since the additional regulator would not be needed if we were to just straightforwardly evaluate the relevant integrals. Notice also that both results involve double and single poles in ε, which are both of UV origin and stem from the subdivergences of the tadpole integral $I(\eta')$ and counterterms, respectively, and the additional UV divergence generated by the momentum integral in (3.7.1) on top of them. Summing the contributions from the vertex and the counterterms, and collecting logarithms of Λ in the result, we find the expression

$$\begin{aligned}
&\tilde{\mu}^{2\varepsilon}\Big[\langle\phi^2(\eta,\vec{x})\rangle\Big|_{\kappa}+\langle\phi^2(\eta,\vec{x})\rangle\Big|_{\text{c.t.}}\Big]\\
=&\frac{\kappa H^2}{384\pi^4}\left(\frac{e^{\gamma_E}\mu}{H}\right)^{2\varepsilon}(-e^{\gamma_E}\Lambda\eta)^{-2\varepsilon}\Bigg\{\frac{3}{\varepsilon}\Bigg[-\delta\hat{m}^2_{\text{fin}}+\ln\left(-\frac{\Lambda H\eta}{\mu}\right)\Bigg]+\frac{8}{3}\ln^3(-e^{\gamma_E}\Lambda\eta)\\
&+\Bigg[\frac{1}{3}-4\delta\hat{m}^2_{\text{fin}}-4\ln\left(\frac{e^{\gamma_E}\mu}{H}\right)\Bigg]\ln^2(-e^{\gamma_E}\Lambda\eta)+2\Bigg[-\frac{16}{3}+\delta\hat{m}^2_{\text{fin}}+\frac{2\pi^2}{3}\\
&+4\ln\left(\frac{e^{\gamma_E}\mu}{H}\right)\Bigg]\ln(-e^{\gamma_E}\Lambda\eta)-3\ln^2\left(\frac{e^{\gamma_E}\mu}{H}\right)+\Bigg[3-\frac{2\pi^2}{3}\Bigg]\ln\left(\frac{e^{\gamma_E}\mu}{H}\right)\\
&-6+\frac{31\pi^2}{72}-\frac{2\pi^2}{3}\delta\hat{m}^2_{\text{fin}}+\frac{22}{3}\zeta(3)\Bigg\}\,.
\end{aligned}\tag{3.7.38}$$

Only a single pole is left over, which is due to the consistent cancellation of the subdivergences, and only the new UV divergence associated to the renormalization of ϕ^2 remains.

The pole contains a term proportional to $\ln(-\Lambda\eta H/\mu)$. This term is expected, since operator mixing is taking place, and it can be understood by inspecting the renormalization equation for this one-point function, which we already wrote down above and reprint here for convenience:

$$\tilde{\mu}^{2\varepsilon}\langle\phi^2(\eta,\vec{x})\rangle=\tilde{\mu}^{2\varepsilon}Z^{\phi}_{22}\langle[\phi^2](\eta,\vec{x})\rangle+H^2Z^{\phi}_{20}\,.\tag{3.7.39}$$

Previously we only considered this equation at $\mathcal{O}(\kappa^0)$, while now we need to consider its $\mathcal{O}(\kappa)$ pieces, which read

$$\tilde{\mu}^{2\varepsilon}\langle\phi^2(\eta,\vec{x})\rangle\Big|_{\mathcal{O}(\kappa)}=\tilde{\mu}^{2\varepsilon}\Big[Z^{\phi,(\kappa^0)}_{22}\langle[\phi^2](\eta,\vec{x})\rangle\Big|_{\mathcal{O}(\kappa)}+Z^{\phi,(\kappa)}_{22}\langle[\phi^2](\eta,\vec{x})\rangle\Big|_{\mathcal{O}(\kappa^0)}\Big]+H^2Z^{\phi,(\kappa)}_{20}\,.\tag{3.7.40}$$

It is still consistent to ignore any contribution from renormalized operators involving higher powers of ϕ, since they would all be at least $\mathcal{O}(\kappa^2)$. In the previous two sections we already determined the renormalization factor

$$\begin{aligned}
Z^{\phi}_{22}\equiv&Z^{\phi,(\kappa^0)}_{22}+Z^{\phi,(\kappa)}_{22}+\mathcal{O}(\kappa^2) &(3.7.41)\\
=&1-\frac{\kappa}{32\pi^2\varepsilon}\,, &(3.7.42)
\end{aligned}$$

and we can therefore define the renormalized one-point function at $\mathcal{O}(\kappa)$ as

$$\langle[\phi^2](\eta,\vec{x})\rangle\Big|_{\mathcal{O}(\kappa)}=\tilde{\mu}^{2\varepsilon}\Big[\langle\phi^2(\eta,\vec{x})\rangle\Big|_{\mathcal{O}(\kappa)}-Z^{\phi,(\kappa)}_{22}\langle[\phi^2](\eta,\vec{x})\rangle\Big|_{\mathcal{O}(\kappa^0)}\Big]-H^2Z^{\phi}_{20}\Big|_{\mathcal{O}(\kappa)}\,,\tag{3.7.43}$$

where we took the limit $\varepsilon\to 0$ on the left-hand side of the equation. We already determined the free-theory result for $\langle[\phi^2](\eta,\vec{x})\rangle$ in equation (3.7.6). There, we were able to neglect the $\mathcal{O}(\varepsilon)$ terms in the ε-expansion, however, since in (3.7.39) the one-point function now appears multiplied by a quantity which has an ε-pole, these terms will matter. Expanding the result (3.7.6) up to $\mathcal{O}(\varepsilon)$ we find

$$\begin{aligned}
\langle[\phi^2](\eta,\vec{x})\rangle\Big|_{\mathcal{O}(\kappa^0)}=&\frac{H^2}{8\pi^2}\Bigg[\left(-\frac{\Lambda H\eta}{\mu}\right)^{-2\varepsilon}e^{\varepsilon\gamma_E}\Gamma(\varepsilon)-\frac{1}{\varepsilon}\Bigg] &(3.7.44)\\
=&\frac{H^2}{4\pi^2}\Bigg\{-\ln\left(-\frac{\Lambda H\eta}{\mu}\right)+\varepsilon\Bigg[\ln^2\left(-\frac{\Lambda H\eta}{\mu}\right)+\frac{\pi^2}{24}\Bigg]\Bigg\}\,, &(3.7.45)
\end{aligned}$$

and with the above results we find that the product

$$Z_{22}^{\phi,(\kappa)}\Big|_{\mathcal{O}(\kappa)}\langle[\phi^2](\eta,\vec{x})\rangle\Big|_{\mathcal{O}(\kappa^0)} = \frac{\kappa H^2}{128\pi^4}\left\{\frac{1}{\varepsilon}\ln\left(-\frac{\Lambda\eta H}{\mu}\right) - \left[\ln^2\left(-\frac{\Lambda\eta H}{\mu}\right) + \frac{\pi^2}{24}\right]\right\} \tag{3.7.46}$$

correctly subtracts the pole term proportional to the logarithm when plugged into (3.7.43). The remaining pole term is local, and can therefore be consistently subtracted by means of a local renormalization factor, and the appropriate one is $Z_{20}^{\phi,(\kappa)}$. By choosing

$$Z_{20}^{\phi,(\kappa)} = \frac{\kappa}{128\pi^4\varepsilon}\left[-\delta\hat{m}^2_{\text{fin}}\right]. \tag{3.7.47}$$

we find the following renormalized one-point function at $\mathcal{O}(\kappa)$:

$$\begin{aligned}\langle[\phi^2](\eta,\vec{x})\rangle\Big|_{\mathcal{O}(\kappa)} =& \frac{\kappa H^2}{384\pi^4}\left\{\frac{8}{3}\ln^3(-e^{\gamma_E}\Lambda\eta) - 4\left[\frac{2}{3} + \delta\hat{m}^2_{\text{fin}} + \ln\left(\frac{e^{\gamma_E}\mu}{H}\right)\right]\ln^2(-e^{\gamma_E}\Lambda\eta)\right.\\ &+ 2\left[-\frac{16}{3} + \frac{2\pi^2}{3} + 4\delta\hat{m}^2_{\text{fin}} + 7\ln\left(\frac{e^{\gamma_E}\mu}{H}\right)\right]\ln(-e^{\gamma_E}\Lambda\eta)\\ &+ \left[3 - \frac{2\pi^2}{3} - 6\delta\hat{m}^2_{\text{fin}} - 6\ln\left(\frac{e^{\gamma_E}\mu}{H}\right)\right]\ln\left(\frac{e^{\gamma_E}\mu}{H}\right)\\ &\left. - 6 + \frac{5\pi^2}{9} - \frac{2\pi^3}{3}\delta\hat{m}^2_{\text{fin}} + \frac{22}{3}\zeta(3)\right\}.\end{aligned} \tag{3.7.48}$$

3.7.6 Discussion of the result

The result we obtained is UV-finite, but still IR-divergent and secularly growing, as can be seen explicitly by means of the logarithmic dependence on the combination $-\Lambda\eta$, like all the correlation functions we computed in this chapter. Taken as it is, it is thus unsuitable to be interpreted as a physically meaningful quantity. Nevertheless, it will still be useful for us in the next chapter.

At this point, we can use this result to make contact with the literature about Stochastic Inflation, and in particular with its discussion as a means of "resumming" the IR divergent terms of correlation functions in de Sitter space. Collecting the leading-logarithmic terms with argument $-\Lambda\eta$ of the renormalized results (3.7.7) and (3.7.48) we find

$$\langle[\phi^2](\eta,\vec{x})\rangle\Big|_{\text{LL}} = -\frac{H^2}{4\pi^2}\ln(-\Lambda\eta) + \frac{\kappa H^2}{144\pi^4}\ln^3(-\Lambda\eta) + \mathcal{O}(\kappa^2). \tag{3.7.49}$$

This result agrees with the one obtained by perturbatively solving the Fokker-Planck equation, as is done e.g. in the references [47, 114], after plugging in $\eta = -1/(a(t)H)$. Since the exact equilibrium solution $\rho_{1\text{eq}}$ of the Fokker-Planck equation, which we discussed above in chapter 2, generates a result for the late-time limit of $\langle[\phi^2](\eta,\vec{x})\rangle$ via the equation

$$\langle[\phi^2](\eta,\vec{x})\rangle = \int_{-\infty}^{\infty}\mathrm{d}\varphi\;\rho_{1\text{eq}}(\varphi)\varphi^2 \tag{3.7.50}$$

which is IR-finite and time-independent, the procedure of solving the Fokker-Planck equation for the probability distribution function, and using it to compute the correlators, is interpreted in the literature as a way to effectively "resum" the IR-divergent logarithms, which also includes their time-dependence. For correlation functions computed in this way the IR regularization is therefore unnecessary, and can be removed, which in our case would correspond to letting $\Lambda \to 0$, which then also removes the de Sitter-breaking time dependence of these one-point functions. The coefficients of the leading-logarithmic terms (3.7.49) are independent of the chosen regularization and renormalization schemes, as long as UV and IR divergences are kept distinct from each other, which is the case for the scheme we are using. This is not so for the subleading-logarithmic terms in $-\Lambda\eta$, as can be explicitly seen in (3.7.48), since their coefficients depend both on logarithms of the renormalization scale μ and on the finite part of the mass counterterm $\delta\hat{m}^2_{\text{fin}}$, which both depend on the renormalization scheme that one is using. This observation matches the statement that a semiclassical picture emerges in the late-time limit of correlation functions in de Sitter space derived in [58–60], which was also our finding in the case of the late-time limit of the analytic continuation of the Euclidean two-point function in chapter 2. From our $\mathcal{O}(\kappa)$ result (3.7.48), we explicitly see that the first point at which the effects of quantum corrections enter the coefficients of these logarithms is at next-to-leading-logarithmic order. This was also observed in [71, 72].

3.8 Conclusion

In this chapter, we have shown how the method of regions [97] can be applied to simplify the computation of late-time correlation functions in de Sitter space, which was shown in [100] for the first time. We have applied this procedure to several examples, all of which involve the real, massless, minimally coupled scalar field with a quartic self-interaction. All of the computations in this chapter were carried out in perturbation theory, and, therefore, all the results we found display secularly growing terms, which appear already at tree level, and when moving on to loop level the results start to display explicit IR divergences on top of the secular growth. This, therefore, required us to specify regularization schemes for both the UV and IR of the theory, which we discussed and implemented in the examples above. Furthermore, we also discussed the renormalization of correlation functions involving elementary fields, as well as composite operators.

Even though none of the results we derived in this chapter qualify, as they are, as physical quantities that can be related to observables, they are far from being meaningless or useless. They constitute valuable theoretical data that we will use in the next chapter as input for the determination of the unknown effective couplings and initial conditions in the Soft de Sitter Effective Theory by carrying out matching computations. This will make it possible for us to discuss how the EFT can be used as the appropriate tool to treat the infrared pathologies that we have observed while working in perturbation theory in this chapter, and to eventually obtain physically meaningful results for the correlation functions of the massless, minimally coupled scalar field.

Appendix

3.A Results for the regions of the one-loop power spectrum

In this appendix we give the explicit computation of the region integrals discussed in section 3.4.1. The following results were presented in [100].

The late-time region of the vertex-insertion diagram, in which we assume the scaling $\eta' \sim \eta$ for the time-integration variable, which has as a consequence that $-k\eta' \sim -k\eta \ll 1$, reads

$$\begin{aligned}\langle\phi(t,\vec{k})\phi(t,-\vec{k})\rangle'\Big|_{\kappa,\ \mathrm{late}\ \eta'} =& \frac{\tilde{\mu}^{4-d}\kappa H^{d-2}}{8}(-H\eta)^{d-4}\ \mathrm{Im}\left[\left(1+(k\eta)^2+\frac{2i}{3}(k\eta)^3\right)\right.\\ &\left.\times\int_{-\infty}^{\eta}\frac{\mathrm{d}\eta'}{(-\eta')^{8-d}}\left(1+(-k\eta')^2+\frac{2i}{3}(-k\eta')^3\right)\right]I(\Lambda)\\ =& \frac{\kappa H^2}{8k^3}(-H\eta)^{-2\varepsilon}\left(-\frac{H^2\eta}{\tilde{\mu}}\right)^{-2\varepsilon}\left[-\frac{1}{3\varepsilon}+\frac{2}{9}-\frac{4\varepsilon}{27}\right]H^{2\varepsilon}I(\Lambda)\,.\end{aligned} \tag{3.A.1}$$

The factor $H^{2\varepsilon}$ combines with the factor $\Lambda^{-2\varepsilon}$ which stems from the momentum integral $I(\Lambda)$. Similarly to the case of the trispectrum, the late-time region of the time integral has a UV-pole, which stems from the lower integration boundary, and the ε-expansion of this result will generate the time-dependent piece of the secular logarithm of the time integral in (3.4.15).

Similarly, for the late-time region of the mass-counterterm diagram we find

$$\langle\phi(t,\vec{k})\phi(t,-\vec{k})\rangle'\Big|_{\delta m^2,\ \mathrm{late}\ \eta'} = \frac{\delta m^2}{3k^3}(-\nu\eta)^{-2\delta}\left[-\frac{1}{2\delta}+\frac{1}{3}\right]. \tag{3.A.2}$$

Notice the δ-pole in the above expression, which makes the necessity of introducing the analytic regulator clear.

For the early-time region of the vertex-insertion diagram we have to evaluate

$$\begin{aligned}\langle\phi(\eta,\vec{k})\phi(\eta,-\vec{k})\rangle'\Big|_{\kappa,\ \mathrm{early}\ \eta'} =& -\frac{\tilde{\mu}^{4-d}\kappa H^{d-2}}{8}(-H\eta)^{d-4}\mathrm{Im}\left[\int_{-\infty}^{0}\frac{\mathrm{d}\eta'}{(-\eta')^{8-d}}\frac{e^{2ik\eta'}(i+k\eta')^2}{k^6}\right]I[a(\eta)\Lambda]\\ =& \frac{\kappa H^2}{8k^3}(-H\eta)^{-2\varepsilon}\left(\frac{2e^{\gamma_E}k\tilde{\mu}}{H^2}\right)^{2\varepsilon}\left[\frac{1}{3\varepsilon}-\frac{14}{9}+\varepsilon\left(\frac{100}{27}-\frac{\pi^2}{18}\right)\right]H^{2\varepsilon}I(\Lambda)\,.\end{aligned} \tag{3.A.3}$$

Comparing the pole terms in this expression with the ones in (3.A.1) we can already see that they will cancel each other. However, since the two expressions differ by overall ε-dependent factors, which therefore generate different logarithms in the ε-expansion, the sum of the two regions will contain a leftover logarithm, the time-dependent part of which is generated by the late-time region, while the early-time region contributes the remaining time-independent part. An analogous computation for the mass-counterterm diagram yields

$$\langle\phi(\eta,\vec{k})\phi(\eta,-\vec{k})\rangle'\Big|_{\delta m^2,\ \mathrm{early}\ \eta} = \frac{\delta m^2}{3k^3}(-H\eta)^{-2\varepsilon}\left(\frac{2e^{\gamma_E}k}{\nu}\right)^{2\delta}\left[\frac{1}{2\delta}-\frac{7}{3}\right]. \tag{3.A.4}$$

Comparing the δ-pole appearing in this expression with the one in (3.A.2), we see that they cancel as well.

3.B Computation of the pole-terms of the one-loop bispectrum of the composite operator ϕ^2 in the IR-dimreg scheme

In this appendix collect the details of the computations that lead to the pole terms (3.5.8). The following results were presented in [100].

3.B.1 UV-pole

As we explained in the main text, the UV-pole given in (3.5.8) follows from the integration of the integrand (3.5.4) expanded in the limit $l \gg k_{1,2}$, which reads

$$\begin{aligned} &\langle \phi^2(\eta,\vec{q})\phi(\eta,\vec{k}_1)\phi(\eta,\vec{k}_2)\rangle'\Big|_{\text{UV-pole}} \\ &= \frac{\mu^{4-d}\kappa H^d(-H\eta)^{2d-8}}{8(k_1k_2)^3}\mathrm{Im}\Bigg[\int_{-\infty}^{\eta}\frac{\mathrm{d}\eta'}{(-\eta')^{8-d}}\int\frac{\mathrm{d}^{d-1}l}{(2\pi)^{d-1}}\frac{e^{2il(\eta'-\eta)}}{l^6}(-i+l\eta)^2(i+l\eta')^2 \\ &\quad\times\prod_{j=1}^{2}(-i+k_j\eta)(i+k_j\eta')\Bigg|_{l\gg k_{1,2}}\Bigg]\,. \end{aligned} \tag{3.B.1}$$

We have already identified the momentum integration as the origin of the UV-divergence, while the time integral is finite. Since we are only interested in the pole-term generated by the above expression, we can therefore replace $(-\eta')^{d-8} \to (-\eta')^{-4}$ to simplify the computation slightly. Furthermore, since in the present scheme the only divergence we will see is the logarithmic one, we can expand the integrand in the limit $l \to \infty$ and pick out the term that scales like $\mathcal{O}(\eta^0, l^3)$, since this is the one that will yield the pole we are seeking:

$$\lim_{l\to\infty}\int_{-\infty}^{\eta}\frac{\mathrm{d}\eta'}{(-\eta')^4}e^{2il(\eta'-\eta)}(-i+l\eta)^2(i+l\eta')^2\prod_{j=1}^{2}(-i+k_j\eta)(i+k_j\eta')\Bigg|_{\mathcal{O}(\eta^0,l^3)} = -\frac{il^3}{2}\,. \tag{3.B.2}$$

With these simplifications applied to (3.B.1) we see that we need to compute

$$\langle \phi^2(\eta,\vec{q})\phi(\eta,\vec{k}_1)\phi(\eta,\vec{k}_2)\rangle'\Big|_{\text{UV-pole}} = -\frac{\mu^{4-d}\kappa H^d(-H\eta)^{2d-8}}{16(k_1k_2)^3}\int\frac{\mathrm{d}^{d-1}l}{(2\pi)^{d-1}}\frac{1}{l^3}\,. \tag{3.B.3}$$

As it is, this integral would be scaleless and be set to zero, which is of course just a consequence of the drastic simplifications we undertook here to isolate the relevant term, and is not the case in the full computation. As we already discussed in section 3.4.2, this is due to the cancellation of the UV- and IR-poles of this integral, which are identified by dimreg. To pick out the UV-pole, we can therefore just introduce an ad-hoc IR-regulator in the integral as follows:

$$\int\frac{\mathrm{d}^{d-1}l}{(2\pi)^{d-1}}\frac{1}{l^3} \to \int\frac{\mathrm{d}^{d-1}l}{(2\pi)^{d-1}}\frac{1}{[l^2+\Lambda^2]^{\frac{3}{2}}} = \frac{\Gamma(\varepsilon)}{4\pi^2}\left(\frac{4\pi}{\Lambda^2}\right)^{\varepsilon}. \tag{3.B.4}$$

The modified integral is no longer vanishing, and its UV-pole coincides with the one we are after. We find the result

$$\langle \phi^2(\eta,\vec{q})\phi(\eta,\vec{k}_1)\phi(\eta,\vec{k}_2)\rangle'\Big|_{\text{UV-pole}} = \frac{\kappa H^4}{64\pi^2(k_1k_2)^3}\left(-\frac{1}{\varepsilon_{\text{UV}}}\right), \tag{3.B.5}$$

which is the UV-pole given in (3.5.8).

3.B.2 IR-pole

The procedure to extract the IR-poles is analogous to the one we used above to obtain the UV-pole. We expand the integrand of (3.5.4) in the limit $l \ll k_{1,2}$, and we therefore have to compute

$$\langle \phi^2(\eta,\vec{q})\phi(\eta,\vec{k}_1)\phi(\eta,\vec{k}_2)\rangle'\Big|_{\text{IR-pole}}$$

$$=\frac{\mu^{4-d}\kappa H^d(-H\eta)^{2d-8}}{4(k_1k_2)^3}\mathrm{Im}\bigg[\int_{-\infty}^{\eta}\frac{\mathrm{d}\eta'}{(-\eta')^{8-d}}\int\frac{\mathrm{d}^{d-1}l}{(2\pi)^{d-1}}\frac{e^{i(k_1+k_2+q)(\eta'-\eta)}}{l^3q^3}(-i+l\eta)(i+l\eta')$$
$$\times(-i+q\eta)(i+q\eta')\prod_{j=1}^{2}(-i+k_j\eta)(i+k_j\eta')\bigg]. \tag{3.B.6}$$

We observe that the expansion of the integrand leads the time- and momentum integrals to factorize, and we can consider them separately. As before, the time integral is finite, and we can set $d=4$ in it to simplify the computation, since we are only interested in the pole term of the above expression, which comes from the momentum integral. As in the case of the UV-divergence, we just need to pick out the term which yields the logarithmically divergent integral in the above sum of terms, which is the $\mathcal{O}(l^0,\eta^0)$-term:

$$\mathrm{Im}\bigg[\int_{-\infty}^{\eta}\frac{\mathrm{d}\eta'}{(-\eta')^4}\,e^{i(k_1+k_2+q)(\eta'-\eta)}(-i+l\eta)(i+l\eta')(-i+q\eta)(i+q\eta')$$
$$\times\prod_{j=1}^{2}(-i+k_j\eta)(i+k_j\eta')\bigg]\bigg|_{\mathcal{O}(l^0,\eta^0)}$$
$$=\frac{1}{3}\bigg[\Big[k_1^3+k_2^3+q^3\Big]\Big[\ln\Big(-e^{\gamma_E}(k_1+k_2+q)\eta\Big)-1\Big]+q^3f(k_1,k_2,q)\bigg], \tag{3.B.7}$$

where we introduced the function

$$f(k_1,k_2,q)\equiv\frac{4k_1k_2}{q^2}-\frac{(k_1+k_2+q)[k_1(k_2+q)+k_2q]}{q^3}. \tag{3.B.8}$$

As for the case of the computation of the UV-pole, the simplifications we used lead to a scaleless, logarithmically divergent momentum integral. Since it vanishes because the UV- and IR-pole are identified, to extract its IR-divergence we can just use the same trick we used in (3.B.4) and flip the sign of the pole term that we obtain from the ε-expansion of the result. Doing so, we find

$$\langle\phi^2(\eta,\vec{q})\phi(\eta,\vec{k}_1)\phi(\eta,\vec{k}_2)\rangle'\Big|_{\text{IR-pole}}$$
$$=\frac{\kappa H^4}{48\pi^2(k_1k_2)^3}\frac{1}{\varepsilon_{\text{IR}}}\left\{\left[1+\frac{k_1^3+k_2^3}{q^3}\right]\Big[1-\ln\Big(-e^{\gamma_E}(k_1+k_2+q)\eta\Big)\Big]-f(k_1,k_2,q)\right\}, \tag{3.B.9}$$

which is the result for the IR-pole given in (3.5.8).

3.C Computation of the integral $I(a)$

In this appendix we show how to solve the "master integral"

$$I(a)\equiv\int_{-\infty}^{0}\frac{\mathrm{d}\eta'}{(-\eta')^{8-d+a}}e^{iK\eta'}\int\frac{\mathrm{d}^{d-1}l}{(2\pi)^{d-1}}\frac{e^{il\eta'}(i+l\eta')e^{i|\vec{l}-\vec{q}|\eta'}(i+|\vec{l}-\vec{q}|\eta')}{l^3|\vec{l}-\vec{q}|^3}, \tag{3.C.1}$$

where $K\equiv k_1+k_2$, following the presentation in [100].

The method is borrowed from the reference [115], which is based on the convolution theorem. The starting point is to notice that the integrand of the momentum integral appearing in (3.C.1) can be regarded as the convolution of the function

$$f(\eta',\vec{l})\equiv\frac{e^{il\eta'}(i+l\eta')}{l^3} \tag{3.C.2}$$

with itself. The convolution theorem states, in general, that

$$\int\frac{\mathrm{d}^{d-1}l}{(2\pi)^{d-1}}f(\eta',\vec{l})f(\eta',\vec{q}-\vec{l})=\int\mathrm{d}^{d-1}x\;e^{i\vec{q}\cdot\vec{x}}f(\eta',\vec{x})f(\eta',-\vec{x}), \tag{3.C.3}$$

where $f(\eta', \vec{x})$ is the inverse Fourier-transform of $f(\eta', \vec{l})$ to position space. It turns out that, in our case, it is simpler to compute the integral appearing on the right-hand side of (3.C.3) than the one on the left-hand side, so that is what we will do. The starting point is, of course, to compute

$$
\begin{aligned}
f(\eta', \vec{x}) =& \int \frac{\mathrm{d}^{d-1}p}{(2\pi)^{d-1}}\, e^{i\vec{p}\cdot\vec{x}} \frac{e^{ip\eta'}(i+p\eta')}{p^3} \\
=& \frac{\Omega_{d-3}}{(2\pi)^{d-1}} \int_{-1}^{1} \mathrm{d}\cos\theta\, (1-\cos^2\theta)^{\frac{d-4}{2}} \int_0^\infty \mathrm{d}p\, p^{d-2} e^{ipx\cos\theta} \frac{e^{ip\eta'}(i+p\eta')}{p^3}\,,
\end{aligned}
\tag{3.C.4}
$$

where we defined $\theta \equiv \angle(\vec{p}, \vec{x})$ and introduced the d-dimensional solid angle

$$
\Omega_d \equiv \frac{2\pi^{\frac{d+1}{2}}}{\Gamma(\frac{d+1}{2})}
\tag{3.C.5}
$$

to evaluate the $d-3$ trivial angular integrations. The integral over $\cos\theta$ gives us the expression

$$
\int_{-1}^{1} \mathrm{d}\cos\theta\, (1-\cos^2\theta)^{\frac{d-4}{2}} e^{ipx\cos\theta} = 2^{\frac{d-3}{2}} \sqrt{\pi} (px)^{\frac{3-d}{2}} \Gamma\left(\frac{d}{2}-1\right) J_{\frac{d-3}{2}}(px)\,,
\tag{3.C.6}
$$

where $J_\nu(z)$ denotes the Bessel function of the first kind. We then find

$$
\begin{aligned}
f(\eta', \vec{x}) =& \frac{\Omega_{d-3}}{(2\pi)^{d-1}} 2^{\frac{d-3}{2}} \sqrt{\pi} x^{\frac{3-d}{2}} \Gamma\left(\frac{d}{2}-1\right) \int_0^\infty \mathrm{d}p\, p^{\frac{d-7}{2}} e^{ip\eta'} (i+p\eta') J_{\frac{d-3}{2}}(px) \\
=& \frac{i}{4\pi^{\frac{d}{2}}} \Gamma\left(\frac{d}{2}-2\right) (x^2-\eta'^2)^{2-\frac{d}{2}}\,,
\end{aligned}
\tag{3.C.7}
$$

which is a remarkably simple expression. In particular, it is far simpler than the inverse Fourier transform of the two summands which make up $f(\eta', \vec{l})$ on their own, and this simplification is the essential reason why this method of computation is successful in solving the integral we are considering.

A way to see why the two summands that make up $f(\eta', \vec{l})$ lead to a simpler result that might at first have been guessed top the inverse Fourier transform is to repeat the computation of $f(\eta', \vec{x})$ by first Wick-rotating $t = i\eta'$ and using the following dispersive representation:

$$
\frac{e^{pt}(1-pt)}{p^3} = 4 \int \frac{\mathrm{d}\omega}{2\pi} e^{i\omega t} \frac{1}{(\omega^2+p^2)^2}\,.
\tag{3.C.8}
$$

The simplicity of this representation can be viewed as the root of the simplicity of the final result for $f(\eta', \vec{x})$. We then compute

$$
\begin{aligned}
f(\eta', \vec{x}) &= \int \frac{\mathrm{d}^{d-1}p}{(2\pi)^{d-1}} e^{i\vec{p}\cdot\vec{x}} \frac{e^{ip\eta'}(i+p\eta')}{p^3} = i \int \frac{\mathrm{d}^{d-1}p}{(2\pi)^{d-1}} e^{i\vec{p}\cdot\vec{x}+pt} \frac{(1-pt)}{p^3} \\
&= 4i \int \frac{\mathrm{d}^d P}{(2\pi)^d} e^{iP\cdot X} \frac{1}{P^4} = \frac{i}{4\pi^{\frac{d}{2}}} \Gamma\left(\frac{d}{2}-2\right) |X|^{4-d}\,,
\end{aligned}
\tag{3.C.9}
$$

where we defined the "momentum" and "position" variables $P \equiv (\omega, \vec{p})$, $X \equiv (t, \vec{x})$. Either way, the result is the same, of course.

Plugging the obtained result for $f(\eta', \vec{x})$ into (3.C.3) we find the result

$$
\begin{aligned}
&\int \mathrm{d}^{d-1}x\, e^{i\vec{q}\cdot\vec{x}} f(\eta', \vec{x}) f(\eta', -\vec{x}) \\
=& -\frac{e^{-2\pi i d}}{16\pi^d} \Gamma\left(\frac{d}{2}-2\right)^2 \Omega_{d-3} \int_{-1}^{1} \mathrm{d}\cos\theta\, (1-\cos^2\theta)^{\frac{d-4}{2}} \int_0^\infty \mathrm{d}x\, e^{iqx\cos\theta} x^{d-2} (x^2-\eta'^2)^{4-d}
\end{aligned}
$$

$$=(1-e^{-i\pi d})(2\pi)^{-\frac{d+1}{2}}\Gamma(5-d)\Gamma\left(\frac{d}{2}-2\right)^2\left(-\frac{q}{\eta}\right)^{\frac{d-7}{2}}\left[ie^{\frac{i\pi d}{2}}J_{\frac{7-d}{2}}(q\eta)-J_{\frac{d-7}{2}}(q\eta)\right]. \tag{3.C.10}$$

Therefore, by means of the convolution theorem (3.C.3) we have found that

$$\begin{aligned}&\int\frac{\mathrm{d}^{d-1}l}{(2\pi)^{d-1}}\frac{e^{il\eta'}(i+l\eta')e^{i|\vec{l}-\vec{q}|\eta'}(i+|\vec{l}-\vec{q}|\eta')}{l^3|\vec{l}-\vec{q}|^3}\\&=(1-e^{-i\pi d})(2\pi)^{-\frac{d+1}{2}}\Gamma(5-d)\Gamma\left(\frac{d}{2}-2\right)^2\left(-\frac{q}{\eta'}\right)^{\frac{d-7}{2}}\left[ie^{\frac{i\pi d}{2}}J_{\frac{7-d}{2}}(q\eta')-J_{\frac{d-7}{2}}(q\eta')\right].\end{aligned} \tag{3.C.11}$$

To get to the final result for $I(a)$ we need to plug this expression into (3.C.1) and integrate over η', which gives us the result given in the main text:

$$\begin{aligned}I(a)=&\frac{e^{\frac{i\pi a}{2}}(e^{2i\pi\varepsilon}-1)\Gamma(-\varepsilon)}{4^{1-\varepsilon}\pi^{\frac{5}{2}-\varepsilon}}K^a\left[\frac{2\Gamma(1+2\varepsilon)\Gamma(-3-a-2\varepsilon)\Gamma(-\varepsilon)}{\Gamma(-\frac{1}{2}-\varepsilon)}\left(\frac{K}{q}\right)^{3+2\varepsilon}\right.\\&\left.\times\,{}_2F_1\left(-\frac{3+a}{2}-\varepsilon,-1-\frac{a}{2}-\varepsilon;-\frac{1}{2}-\varepsilon;\frac{q^2}{K^2}\right)+\frac{\sqrt{\pi}\Gamma(-a)\csc(\pi\varepsilon)}{(3+2\varepsilon)(1+2\varepsilon)}{}_2F_1\left(\frac{1-a}{2},-\frac{a}{2};\frac{5}{2}+\varepsilon;\frac{q^2}{K^2}\right)\right].\end{aligned} \tag{3.C.12}$$

In the above expression we have already plugged in $d=4-2\varepsilon$.

The expansion of $\mathrm{Im}[I(2\delta)]$ first in δ and then in ε can be found using the `Mathematica` package `HypExp 2.0` [116], and the result reads

$$\begin{aligned}\mathrm{Im}[I(2\delta)]=&\frac{(4\pi e^{\gamma_E})^\varepsilon(2e^{\gamma_E}q)^{2\delta}}{12\pi^2}\left\{-\frac{1}{\varepsilon^2}\frac{K[K^2-3q^2]}{q^3}+\frac{1}{\delta}\left[\frac{1}{\varepsilon}-\frac{8}{3}\right]\right.\\&+\frac{1}{\varepsilon}\left[-\frac{(K+q)^2(K-2q)}{q^3}\ln\left(\frac{K+q}{2q}\right)-\frac{8}{3}-\frac{7K}{2q}+\frac{K^2}{q^2}+\frac{5K^3}{6q^3}\right]\\&-\frac{\pi^2}{24}\left[28+\frac{K^3}{q^3}-\frac{3K}{q}\right]+\frac{104}{9}+\frac{41K}{6q}-\frac{11K^2}{3q^2}-\frac{19K^3}{18q^3}\\&-\left[\frac{16}{3}+\frac{7K}{q}-\frac{5K^3}{3q^3}\right]\ln\left(\frac{K+q}{2q}\right)\\&-\frac{(K+q)^2(K-2q)}{2q^3}\ln^2\left(\frac{K+q}{2q}\right)-\frac{(K-q)^2(K+2q)}{2q^3}\ln\left(\frac{K}{q}\right)\ln\left(\frac{(K-q)^2}{4Kq}\right)\\&\left.+\frac{(K-q)^2(K+2q)}{q^3}\left[\mathrm{Li}_2\left(\frac{q}{K}\right)-\mathrm{Li}_2\left(-\frac{q}{K}\right)+\mathrm{Li}_2\left(\frac{K-q}{2K}\right)\right]\right\}.\end{aligned} \tag{3.C.13}$$

3.D Integrals for the computation of $\langle\phi^2(\eta,\vec{0})\phi(\eta,\vec{k})\phi(\eta,-\vec{k})\rangle'$ in the k_Λ scheme

In this appendix we collect the explicit results for the integrals relevant for the computation of the early-time, soft-momentum region of the correlator considered in section 3.6, following the procedure discussed there. The Mellin-Barnes integration was carried out by hand and checked using the `Mathematica` package `MB`. The relevant results read:

$$\begin{aligned}&\mathrm{Im}\left[\int\frac{\mathrm{d}^{d-1}l}{(2\pi)^{d-1}}\int_{-\infty}^0\frac{\mathrm{d}\eta'}{(-\eta')^{8-d+2\delta}}\frac{e^{2i(k_\Lambda+l_\Lambda)\eta'}}{l_\Lambda^6}\right]\\&=\frac{1}{6\pi^2}\left\{-\frac{1}{\varepsilon^2}+\frac{1}{\varepsilon}\left[\frac{1}{\delta}-\frac{3\pi k}{2\Lambda}-\frac{2k^2}{\Lambda^2}-\frac{\pi k^3}{8\Lambda^3}\right]-\frac{5}{3\delta}-2\ln^2\left(\frac{2k}{\Lambda}\right)-\frac{10}{3}\ln\left(\frac{2k}{\Lambda}\right)-\frac{11\pi^2}{12}\right.\end{aligned}$$

$$
+\frac{3\pi k}{\Lambda}\left[1-\ln\left(\frac{k}{\Lambda}\right)\right]+\frac{2k^2}{\Lambda^2}\left[3-2\ln\left(\frac{2k}{\Lambda}\right)\right]+\frac{\pi k^3}{24\Lambda^3}\left[5-6\ln\left(\frac{k}{\Lambda}\right)\right]\Bigg\}, \tag{3.D.1}
$$

$$
\begin{aligned}
&\mathrm{Im}\bigg[\int\frac{\mathrm{d}^{d-1}l}{(2\pi)^{d-1}}\int_{-\infty}^{0}\frac{\mathrm{d}\eta'}{(-\eta')^{8-d+2\delta}}\frac{e^{2i(k_\Lambda+l_\Lambda)\eta'}}{l_\Lambda^5}\bigg]\\
=&\frac{k}{2\pi^2}\bigg\{-\frac{1}{\varepsilon^2}+\frac{1}{\varepsilon}\left[\frac{1}{\delta}-\frac{\pi k}{2\Lambda}-\frac{2k^2}{9\Lambda^2}\right]-\frac{1}{\delta}-2\ln^2\left(\frac{2k}{\Lambda}\right)+2\ln\left(\frac{2k}{\Lambda}\right)-2-\frac{11\pi^2}{12}+\frac{\pi k}{2\Lambda}\left[3-2\ln\left(\frac{k}{\Lambda}\right)\right]\\
&+\frac{2k^2}{27\Lambda^2}\left[11-6\ln\left(\frac{2k}{\Lambda}\right)\right]\bigg\},
\end{aligned} \tag{3.D.2}
$$

$$
\begin{aligned}
&\mathrm{Im}\bigg[\int\frac{\mathrm{d}^{d-1}l}{(2\pi)^{d-1}}\int_{-\infty}^{0}\frac{\mathrm{d}\eta'}{(-\eta')^{8-d+2\delta}}\frac{e^{2i(k_\Lambda+l_\Lambda)\eta'}}{l_\Lambda^4}\bigg]\\
=&\frac{k^2}{2\pi^2}\bigg\{-\frac{1}{\varepsilon^2}+\frac{1}{\varepsilon}\left[\frac{1}{\delta}-\frac{\pi k}{6\Lambda}\right]-2\ln^2\left(\frac{2k}{\Lambda}\right)+6\ln\left(\frac{2k}{\Lambda}\right)-7-\frac{11\pi^2}{12}+\frac{\pi k}{18\Lambda}\left[11-6\ln\left(\frac{k}{\Lambda}\right)\right]\bigg\},
\end{aligned} \tag{3.D.3}
$$

where we only display the imaginary parts of the integrals, since they are the ones that are relevant for the final result given in section 3.6.

Chapter 4

Soft de Sitter Effective Theory

We now come to the final topic that is discussed in this thesis, which is the Soft de Sitter Effective Theory (SdSET). It is an EFT constructed to describe the dynamics of the superhorizon modes of quantum fields evolving in a rigid de Sitter space background. As such, it can be regarded as a modern incarnation of Starobinsky's original construction that became the formalism of Stochastic Inflation [58–60]. The SdSET was originally introduced in [105], and further developed in [107], to describe the superhorizon dynamics of real scalar fields, and, in particular, to tackle the description of the massless, minimally coupled, self-interacting scalar field. Later, it was also applied to the description of scalar perturbations in a framework closer to a realistic inflationary scenario in [117], and, more recently, to the case of heavy scalar fields in [118] and to the tensor modes of the metric evolving in a quasi-de Sitter background in [119].

Being an EFT which is formulated in the Schwinger-Keldysh formalism, the SdSET has very unique and interesting properties that are foreign to more conventional EFTs formulated in flat space. Beyond this, the most interesting aspect of the SdSET for us is that, in the case of the massless, minimally coupled scalar field, it seems a very promising framework to handle the effectively strongly-coupled dynamics of the superhorizon modes of the field in a systematic manner that goes beyond perturbation theory. The first exploration in this direction was carried out in [105, 107]. The reference [105] pointed out that the SdSET can be used to reproduce the results of the formalism of Stochastic Inflation at leading order in the expansion in the effective coupling. In the context of the EFT the effective stochastic description is a consequence of composite-operator mixing under renormalization, and this phenomenon was interpreted as a concrete realization of the idea of the "dynamical renormalization group" [88–90] in de Sitter space [91]. The follow-up work [107] leveraged this insight, together with the fact that in the EFT one has the advantage of having a well-defined power-counting scheme, which allows one to systematically organize the expansion of observables in the late-time limit, and thus to go beyond the leading-order approximation. In this reference, the authors focussed on the study of the effective dynamics of EFT one-point functions, which are governed by a Kramers-Moyal equation. The building blocks that make up the coefficients of this equation were identified as the effective couplings and the anomalous dimensions of composite operators built out of the elementary SdSET-fields, which where then computed using the EFT up to next-to-next-to-leading order in powers of the full-theory coupling, while remaining at leading-order in the power-counting parameter.

While the basic formalism of the SdSET was established in the two papers [105, 107], some important structural aspects of the EFT where left unexplored in the literature. The three most central ones, for our purposes, are the systematic implementation of non-Gaussian initial conditions in the SdSET path integral, the formulation of a consistent regularization and renormalization scheme for the EFT, and the rigorous derivation of the Kramers-Moyal equation governing the non-perturbative dynamics of EFT one-point functions. We regard it as imperative for these open points to be cleared up in order to be able to reliably apply the machinery of the SdSET to more complicated observables, and, eventually, theories, than what was already considered in the literature. Our purpose in this chapter will be to fill these gaps to the best of our abilities, and to then use the obtained formalism to extend the application of the SdSET beyond what has been done so far. We will do so in a constructive manner, by first presenting general and abstract arguments about the field-theoretic structure of the EFT, and then illustrate and test them by carrying out explicit matching computations. For this purpose, we will use the explicit results for full-theory correlation functions that we derived in chapter 3. This will also give us the chance to highlight the parallels between the region decomposition of the full-theory quantities, and the quantities in the EFT which are involved in the matching, which will help us build our intuition about why the SdSET is the way it is.

4.1 Physical picture for the SdSET

Before we dive into the technicalities of the construction of the SdSET as a quantum field theory we wish to present the physical picture for this EFT, which will help us develop much of our intuition about its structure.

The SdSET is built to reproduce the late-time limit of equal-time, in-in correlation functions, which we can formulate using momentum-space fields as[1]

$$\lim_{k_i/(a(t)H)\to 0}\langle \phi(t,\vec{k}_1)...\phi(t,\vec{k}_n)\rangle\,. \tag{4.1.1}$$

For the remainder of this chapter, we will make the additional assumption that all the three-momenta of the fields appearing in the above correlator have comparable magnitudes,

$$k_1 \sim ... \sim k_n\,, \tag{4.1.2}$$

and, furthermore, that they are in an otherwise generic kinematic configuration, such that there are no preferred directions. This is a simplifying assumption that we make, because this way we will be essentially dealing with a two-scale problem, the two scales being the typical magnitude of the physical momenta of the fields at late times, $k_i/a(t)$, and the Hubble parameter, H, which, by assumption satisfy $k_i/a(t) \ll H$. Assuming strong hierarchies between, or particular kinematic configurations of, the external momenta in a given correlation function would simply add more scales to the problem. These scales would then need to be disentangled from each other by formulating several versions of the SdSET, each appropriate for describing one of the several relevant regimes, and these EFTs would then need to be matched onto one another. This would be a technically more challenging problem, however, conceptually it would not pose any additional difficulties compared to what we are going to consider. Furthermore, the additional structure would not be directly related to the large IR effects that we wish to understand using the SdSET, which is our primary motivation here. We therefore leave these more complicated scenarios for potential future investigation, and press on with the simpler setup described above.

One can draw a simple picture to visualize the time-evolution of an in-in correlation function with the properties described above, which we represent in figure 4.1. The fields appearing in the correlator (4.1.1) start their time-evolution at $t = -\infty$, where we assume that the fields only have Gaussian correlations, and their three-momenta get redshifted by the expansion of the spacetime, while they evolve forward in time and start interacting with each other. The time t_H at which the three-momenta of the fields satisfy

$$\frac{k_i}{a(t_H)H} \sim 1 \tag{4.1.3}$$

is called the time of "horizon-crossing", since at this moment in time the typical wavelength of the quanta associated with the fields is of comparable size to the radius of the event horizon of de Sitter space, which is $r_H = 1/H$. This equal-time slice is depicted as the blue surface in figure 4.1. Since we are assuming (4.1.2), we have a unique value for t_H. Accordingly, we will call modes with $k_i/(a(t)H) > 1$ subhorizon, and modes with $k_i/(a(t)H) < 1$ superhorizon modes. After crossing the horizon, the three-momenta of the fields get redshifted further, until the correlation time t is reached, where we compute the correlation properties of the fields. This equal-time slice is depicted as the red surface in figure 4.1

[1] The field ϕ here does not necessarily have to be an elementary, or scalar, field, even though we will restrict ourselves to discussing real scalar fields below.

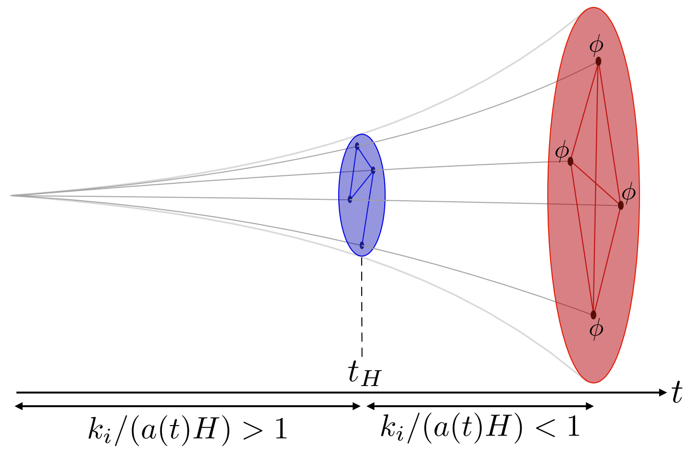

Figure 4.1: Schematic representation of the time-evolution of an equal-time correlation function, in this case a trispectrum, with fields with three-momenta of comparable magnitudes. The regime of validity of the SdSET is located between the two colored surfaces.

The SdSET can, by construction, only describe the dynamics of fields with superhorizon momenta, and so its regime of validity is after the time t_H, and on physical length scales larger than the Hubble horizon. All of the information about physical processes which are associated to physical length scales of order $1/H$ or smaller, or to times before t_H, which of course make an important contribution to the late-time full-theory correlation functions, must therefore be provided as additional input. The contributions from short-distance physics are associated to the exchange of virtual quanta with large physical momenta between the fields appearing in the correlation function, which can happen at any point during their time-evolution, while the contributions from early times are associated to the entire subhorizon evolution of the full-theory fields. Since the full-theory fields can still exchange large-momentum modes after having crossed the horizon, this has the effect of generating effective interactions between the long-wavelength modes, which can be accounted for in the EFT by writing down all possible local, and in general non-renormalizable, interaction vertices. This situation is fully analogous to the flat-space case, and it leads to the necessity of determining these unspecified effective couplings by matching the SdSET onto the full theory. A much less familiar feature of this EFT comes from the fact that we have integrated out the entire non-trivial subhorizon evolution of the full-theory fields, which led to the development of non-Gaussian correlations among them by the time that they cross the horizon. Since the time-slice at t_H is the initial-time slice for the SdSET, the effective fields will start their life directly with these non-trivial correlations among them, which must be specified in terms of non-Gaussian initial conditions. These need to be determined by means of matching computations as well.

These considerations, based on the simple physical picture represented in figure 4.1, already provide us with a rough picture of which elements the SdSET should involve, in order to faithfully capture the various physical processes that are encoded in the late-time correlation functions. Let us now see how this physical picture for the SdSET can be implemented in practice as a quantum field theory.

4.2 Derivation of the free action for the SdSET fields

As the starting point of our discussion we review and extend the derivation of the action describing the late-time dynamics of free-field modes given in [105]. We will derive this result using a method which is valid in arbitrary numbers of dimensions by means of a non-local field redefinition of the full field inspired by the discussion of the non-relativistic scalar field in Minkowski space presented in [120]. This sets the stage for the implementation of dimreg for the regularization of UV divergences in the EFT. Since the discussion in [120] plays an essential role for the development of both our physical intuition for the effective fields, and the theoretical framework that we will use to derive the effective action we are seeking, the appendix 4.A is dedicated to its detailed presentation. The discussion in the main text is fully dedicated to the de Sitter case.

4.2.1 Identification, and basic properties, of the effective fields in the late-time limit

To provide the motivation for the following construction we review and adapt the discussion of the late-time limit of the mode functions of the free, massive scalar field presented in [105]. Since this first section is meant to build the physical intuition to motivate the more technical manipulations that will follow, we restrict the discussion to four spacetime dimensions, which is the physically relevant case, and we work using cosmic time t instead of conformal time η, which is the more physically intuitive variable. Whenever it will be more convenient to use η, we will relate it to t by means of $\eta = \eta(t) = -1/(a(t)H)$, and suppress its argument.

Late-time limit of the free, massive scalar field in de Sitter space and emergence of the effective degrees of freedom

We consider the field operator in the free, massive theory, which reads

$$\phi(t, \vec{x}) = \int \frac{\mathrm{d}^3 k}{(2\pi)^3} \Big[e^{i\vec{k}\cdot\vec{x}} \phi_{\vec{k}}(t) a_{\vec{k}} + e^{-i\vec{k}\cdot\vec{x}} \phi^*_{\vec{k}}(t) a^\dagger_{\vec{k}} \Big] . \tag{4.2.1}$$

For the creation and annihilation operators $a_{\vec{k}}$, $a^\dagger_{\vec{k}}$ appearing in the above equation we use the following commutation relations:

$$[a_{\vec{p}}, a_{\vec{k}}] = [a^\dagger_{\vec{p}}, a^\dagger_{\vec{k}}] = 0 \,, \quad [a_{\vec{p}}, a^\dagger_{\vec{k}}] = (2\pi)^3 \delta^{(3)}(\vec{p} - \vec{k}) \,. \tag{4.2.2}$$

The mode functions $\phi_{\vec{k}}(t)$ appearing in (4.2.1) solve the equation of motion

$$\Big[\partial_t^2 + 3H\partial_t - \frac{\vec{k}^2}{a(t)^2} + \frac{m^2}{H^2} \Big] \phi_{\vec{k}}(t) = 0 \,, \tag{4.2.3}$$

and, in the Bunch-Davies vacuum, the explicit solution reads, up to an irrelevant, k-independent phase, [30]

$$\phi_{\vec{k}}(t) = \frac{\sqrt{\pi} H (-\eta)^{\frac{3}{2}}}{2} H^{(1)}_\nu(-k\eta) \,, \tag{4.2.4}$$

where $H^{(1)}_\nu(z)$ denotes the Hankel function of the first kind, which we define via the Bessel functions of the first and second kind, $J_\nu(z)$ and $Y_\nu(z)$, as

$$H^{(1)}_\nu(z) = J_\nu(z) + iY_\nu(z) \,, \tag{4.2.5}$$

and ν denotes the mass parameter, which is defined as

$$\nu \equiv \sqrt{\frac{9}{4} - \frac{m^2}{H^2}} \,. \tag{4.2.6}$$

We now study the late-time behaviour of $\phi_{\vec{k}}(t)$, by which we mean letting

$$\frac{k}{a(t)H} = -k\eta \to 0 \,. \tag{4.2.7}$$

Taking this limit, the leading expression of the mode function reads

$$\lim_{k/(a(t)H)\to 0} \phi_{\vec{k}}(t) = H \Bigg[\frac{(a(t)H)^{-\frac{3}{2}+\nu}}{k^\nu} \Bigg(-\frac{i2^{\nu-1}\Gamma(\nu)}{\sqrt{\pi}} + \mathcal{O}\Bigg(\frac{k^2}{(a(t)H)^2} \Bigg) \Bigg)$$

$$+\frac{(a(t)H)^{-\frac{3}{2}-\nu}}{k^{-\nu}}\bigg(\frac{2^{-\nu-1}\sqrt{\pi}(1+i\cot(\nu\pi))}{\Gamma(1+\nu)}+\mathcal{O}\bigg(\frac{k^2}{(a(t)H)^2}\bigg)\bigg)\bigg]\,. \tag{4.2.8}$$

We thus find that in this limit the mode function $\phi_{\vec{k}}(t)$ decomposes as

$$\lim_{k/(a(t)H)\to 0}\phi_{\vec{k}}(t)=H\Big[(a(t)H)^{-\alpha}\varphi_{+,\vec{k}}(t)+(a(t)H)^{-\beta}\varphi_{-,\vec{k}}(t)\Big]\,, \tag{4.2.9}$$

where we defined

$$\alpha\equiv\frac{3}{2}-\nu\,,\quad \beta=\frac{3}{2}+\nu\,, \tag{4.2.10}$$

and the functions $\varphi_{\pm,\vec{k}}(t)$ then have the form

$$\varphi_{+,\vec{k}}(t)=-\frac{i2^{\nu-1}\Gamma(\nu)}{\sqrt{\pi}k^{\nu}}+\mathcal{O}\bigg(\frac{k^2}{(a(t)H)^2}\bigg)\,, \tag{4.2.11}$$

$$\varphi_{-,\vec{k}}(t)=\frac{2^{-\nu-1}\sqrt{\pi}(1+i\cot(\nu\pi))}{\Gamma(1+\nu)k^{-\nu}}+\mathcal{O}\bigg(\frac{k^2}{(a(t)H)^2}\bigg)\,. \tag{4.2.12}$$

Notice that they are time-independent at leading power in the gradient terms. The two summands in (4.2.9) have a characteristic time-dependence associated to them, and it reflects the fact that the generally covariant field $\phi(t,\vec{x})$ is describing two different degrees of freedom, or field modes, which in flat spacetime would be associated to particles and antiparticles. The functions $\varphi_{\pm,\vec{k}}(t)$ we defined in (4.2.9) can then be interpreted as the mode functions associated to these two degrees of freedom in the limit we are considering.

The behaviour (4.2.9) is precisely the one we already mentioned above in section 1.3 when discussing the framework of the Cosmological Bootstrap, in which α and β are identified as scaling dimensions $\Delta_\pm$ of primary fields living at the future spatial boundary of de Sitter space. The associated modes, which we are writing as $\varphi_{+,\vec{k}}(t)$ and $\varphi_{-,\vec{k}}(t)$, are referred to in the literature as "growing" and "decaying" modes, respectively, even tough for $0\leq\nu<3/2$ they are both decaying exponentially, albeit one more slowly than the other. The key idea behind the SdSET is to elevate the behaviour of the mode functions (4.2.9) to a statement about the late-time behaviour of the field itself. The claim is that we can write, at leading power in the expansion in $k/(a(t)H)$,

$$\lim_{k/(a(t)H)\to 0}\phi(t,\vec{k})=H\Big[(a(t)H)^{-\alpha}\varphi_{+}(t,\vec{k})+(a(t)H)^{-\beta}\varphi_{-}(t,\vec{k})\Big]\,, \tag{4.2.13}$$

where we have now introduced the (momentum-space) effective fields $\varphi_\pm(t,\vec{k})$. This equation can be Fourier-transformed, and its position-space version then reads simply

$$\phi(t,\vec{x})=H\Big[(a(t)H)^{-\alpha}\varphi_{+}(t,\vec{x})+(a(t)H)^{-\beta}\varphi_{-}(t,\vec{x})\Big]\,, \tag{4.2.14}$$

where now the late-time limit, as defined above, is implied on the left-hand side of the equation. The physical motivation behind this field decomposition is that it achieves the factorization of the leading time dependence, which is given by $(a(t)H)^{-\frac{3}{2}\pm\nu}$, from the residual time dependence, which always appears in the combination $k/(a(t)H)$, as we see from (4.2.9). These two time-dependent terms are associated to different quantities: one is the inverse comoving horizon radius $a(t)H$, about which we are making no assumptions, and therefore have to treat as being an $\mathcal{O}(1)$-quantity, while the second one is associated to the physical momentum of the field in Hubble units $k/(a(t)H)$, which, by assumption, is small. We want the effective fields $\varphi_\pm$ to describe physical processes associated to physical time- and (inverse-) length scales of typical magnitude comparable to the small quantity $k/(a(t)H)$ dynamically. The leading part of the time-evolution lies outside of the regime of dynamical description of the EFT, and, therefore, has to be stripped off.

The combinations $a(t)H$ and $k/(a(t)H)$ naturally organize the expansion of the mode functions in the late-time limit, and the latter provides the definition of the power-counting parameter of this EFT:

$$\lambda\sim\frac{k}{a(t)H}\,, \tag{4.2.15}$$

where the time variable t is the time at which the correlation functions we wish to describe are evaluated. For late-time correlators, this quantity is small by definition, and can therefore be used as a perturbative parameter to organize their expansion in this limit. By associating a definite scaling in powers of λ to the $\varphi_\pm$, we can then systematize the expansion of a given late-time correlator in terms of correlation functions made up of effective fields, and we will see how this can be done below. The combination $a(t)H$ can be regarded as the comoving UV scale of the SdSET:

$$\Lambda_{\rm UV}(t) \sim a(t)H\,, \tag{4.2.16}$$

while also determining the leading time-evolution associated to $\varphi_\pm$ in the expansion of ϕ. At first glance, it looks difficult to work with an EFT which has a time-dependent UV scale. However, as long as we are not varying the correlation time t, this scale is just a constant. Therefore, the correlation time t can be taken as an external kinematic variable which enters the definition of the SdSET.

Before moving on, let us remark that the above construction follows the same logic as the construction of the EFT describing the dynamics of a non-relativistic (heavy) scalar field in Minkowski space [120]. In that case, one is considering observables expanded in the limit $k/m \to 0$, where m is the mass of the field, and the full-theory field is expanded as

$$\phi(t,\vec{x}) = \frac{1}{\sqrt{2m}}\Big[e^{-imt}\psi(t,\vec{x}) + e^{imt}\psi^*(t,\vec{x})\Big]\,, \tag{4.2.17}$$

where ψ and ψ^* are the effective fields describing the residual time-evolution after the leading piece, $e^{\pm imt}$, has been factored out. This field decomposition mirrors precisely (4.2.14), where the role of the factors $e^{\pm imt}$ is played by $(a(t)H)^{-\frac{3}{2}\pm\nu}$. In fact, since the scale factor has an exponential form as well, $a(t) = e^{Ht}$, the field decomposition (4.2.14) for $m^2 \leq 9H^2/4$ can be regarded as a version of (4.2.17) with an imaginary mass, such that instead of oscillating exponentials we get decaying ones. For $m^2 > 9H^2/4$ the factors $(a(t)H)^{-\frac{3}{2}\pm\nu}$ are complex exponentials as well, in which case the analogy is even closer than before, and in the infinite-mass limit the analogy becomes exact, since then one has $a(t) \to e^{imt} + \mathcal{O}(m/H)$. In the following, it will prove fruitful to keep drawing analogies between this example and the de Sitter-case we are studying. As we will see, the parallels between the two theories run fairly deep.

Symmetries of the effective fields

To start to characterize the effective fields $\varphi_\pm$ that we wish to work with, and the underlying field theory that describes their dynamics, we can work out the implications of the full-theory symmetries for them.

As we discussed in section 1.2.3, the metric of d-dimensional de Sitter space is invariant under the action of elements of the symmetry group $\mathrm{SO}(1,d)$, which is the Lorentz group in $d+1$-dimensions. It contains spatial translations and rotations, dilatations and special conformal transformations, and, in conformal coordinates, its generators read

$$P_i = \partial_i\,, \qquad R^i{}_j = x^i\partial_j - x_j\partial^i\,, \tag{4.2.18}$$

$$D = -\,\eta\partial_\eta - x^i\partial_i\,, \quad K^i = 2x^i\eta\partial_\eta + 2x^ix^j\partial_j + (\eta^2 - \vec{x}^2)\partial^i\,. \tag{4.2.19}$$

The elements of the de Sitter group are obtained from these generators by contracting them with a tensor of parameters of the appropriate rank and exponentiating the resulting object. By expanding this exponential to linear order, we can derive how infinitesimal transformations act on the position vector $x^\mu = (\eta, \vec{x})$.

The action of translations and rotations is of course the standard one. Infinitesimal dilations act homogeneously on x^μ, which can be seen as follows:

$$x^\mu \to x'^\mu = (1+\delta D)x^\mu\,, \tag{4.2.20}$$

where $\delta \ll 1$ parametrizes the transformation, which can be written in components as

$$\eta \to \eta' = (1-\delta)\eta\,, \tag{4.2.21}$$

$$\vec{x} \to \vec{x}' = (1-\delta)\vec{x}\,. \tag{4.2.22}$$

The transformation behaviour of η directly implies

$$a(\eta) \to a(\eta') = (1+\delta)a(\eta) \tag{4.2.23}$$

for the scale factor. Below, we will often find it convenient to work with the macroscopic version of the dilatation transformation, which amounts to just replacing $(1\pm\delta) \to \xi^{\pm 1}$ in the above equations, where ξ denotes the macroscopic dilatation factor.

The action of special conformal transformations is more complicated. They act inhomogeneously on the components of x^μ, which we can see as follows:

$$x^\mu \to x'^\mu = (1+\vec{b}\cdot\vec{K})x^\mu\,, \tag{4.2.24}$$

where $\vec{b}$ is a three-vector which parametrizes the transformation, and we can write this equation in components as

$$\eta \to \eta' = (1+2\vec{b}\cdot\vec{x})\eta\,, \tag{4.2.25}$$

$$\vec{x} \to \vec{x}' = \vec{x} + 2(\vec{b}\cdot\vec{x})\vec{x} + (\eta^2 - \vec{x}^2)\vec{b}\,. \tag{4.2.26}$$

We see that under special conformal transformations the temporal and spatial components of the vector x^μ get mixed, similarly to Lorentz boosts in Minkowski space.

The full-theory field is a scalar under the action of the tranformations generated by these operators, which means that

$$\phi'(\eta',\vec{x}') = \phi(\eta,\vec{x})\,. \tag{4.2.27}$$

From this equation, and the leading-power field-decomposition, which for our purposes here is most conveniently written using η,

$$\phi(\eta,\vec{x}) = H^{\frac{d}{2}-1}\Big[(-\eta)^\alpha\varphi_+(\eta,\vec{x}) + (-\eta)^\beta\varphi_-(\eta,\vec{x})\Big]\,, \tag{4.2.28}$$

we can derive the transformation behaviour of the effective fields $\varphi_\pm$ under the de Sitter isometries. Since the field decomposition involves explicit powers of η, which are not invariant under the action of dilatations and special conformal transformations, it is clear that the EFT fields must transform non-trivially as well to compensate for this. By the same token, since η is left invariant by spatial translations and rotations, we can conclude that the $\varphi_\pm$ are scalars under these types of transformations. By plugging the field decomposition (4.2.28) into both sides of the equation (4.2.27), using the transformation behaviour of η, see (4.2.21) and (4.2.25), and comparing powers of η in the resulting equation we find the following transformation behaviour for the SdSET fields:

$$\text{spatial translations and rotations:}\quad \varphi_\pm(\eta,\vec{x}) \to \varphi'_\pm(\eta',\vec{x}') = \varphi_\pm(\eta,\vec{x})\,, \tag{4.2.29}$$

$$\text{dilatations:}\quad \varphi_\pm(\eta,\vec{x}) \to \varphi'_\pm(\eta',\vec{x}') = \left[1 + \left(\frac{3}{2}\mp\nu\right)\delta\right]\varphi_\pm(\eta,\vec{x})\,, \tag{4.2.30}$$

$$\text{special conformal transformations:}\quad \varphi_\pm(\eta,\vec{x}) \to \varphi'_\pm(\eta',\vec{x}') = \Big[1 - (3\mp 2\nu)\vec{b}\cdot\vec{x}\Big]\varphi_\pm(\eta,\vec{x})\,. \tag{4.2.31}$$

The above equations tell us how the effective fields and their arguments transform simultaneously. However, it is also useful to know how the field $\varphi_\pm$ transforms by itself, i.e. how $\varphi'_\pm(\eta,\vec{x})$ and $\varphi_\pm(\eta,\vec{x})$ are related to each other. This is also known as the active transformation behaviour of the effective fields. We can do so by first expanding the fields $\varphi'_\pm(\eta',\vec{x}')$ in a Taylor series up to linear order as

$$\varphi'_\pm(\eta',\vec{x}') = \varphi'_\pm(\eta,\vec{x}) + (x'^\mu - x^\mu)\partial_\mu\varphi'_\pm(\eta,\vec{x}) + \mathcal{O}(\partial^2\varphi'_\pm)\,. \tag{4.2.32}$$

We can then plug in the found expressions for $\varphi'_\pm(\eta',\vec{x}')$ and invert the resulting equation for $\varphi'_\pm(\eta,\vec{x})$ perturbatively in powers of the infinitesimal parameters of the transformations. This effectively just amounts to replacing $(x'^{\mu} - x^{\mu})\partial_\mu \varphi'_\pm \to (x'^{\mu} - x^{\mu})\partial_\mu \varphi_\pm$, since any higher-order corrections to this replacement would be quadratic in the parameters, and we are working only at linear order. Doing so, we find the infinitesimal transformation behaviour

$$\varphi'_\pm(\eta, \vec{x}) = \left[1 + \left(\frac{3}{2} \mp \nu\right)\delta + \delta\left[\eta\partial_\eta + \vec{x}\cdot\vec{\partial}\right]\right]\varphi_\pm(\eta, \vec{x}) \,, \tag{4.2.33}$$

$$\varphi'_\pm(\eta, \vec{x}) = \left[1 - (3 \mp 2\nu)\vec{b}\cdot\vec{x} - 2(\vec{b}\cdot\vec{x})\eta\partial_\eta - \left(2(\vec{b}\cdot\vec{x})\vec{x} + (\eta^2 - \vec{x}^2)\vec{b}\right)\cdot\vec{\partial}\right]\varphi_\pm(\eta, \vec{x}) \tag{4.2.34}$$

under dilatations and special conformal transformations, respectively. The second equation agrees with the finding of [105], after using $\eta\partial_\eta = -\partial_t$.

Another important symmetry of the effective fields is an internal one, which follows from the the "one-to-many" field decomposition (4.2.14), and is called "reparametrization invariance" (RPI) of ϕ under transformations of the form [105]

$$\varphi_+ \to \varphi_+ + \iota (a(t)H)^{\alpha-\beta}\varphi_- \,, \quad \varphi_- \to (1-\iota)\varphi_- \,, \tag{4.2.35}$$

where ι is an infinitesimal parameter. Clearly, such a transformation leaves the decomposition of ϕ in terms of $\varphi_\pm$ invariant, even though it mixes the effective fields among each other. Since ϕ is left invariant by this transformation, its correlation functions will be left invariant, too, and since the SdSET is constructed to reproduce precisely these correlators, this transformation must be a symmetry of the EFT. Requiring that the SdSET as a whole is left invariant by reparametrization transformations will enforce non-trivial relations on the terms which will appear in the SdSET-action, linking terms at different orders in the power-counting parameter λ. This will help us constrain its form below.

Commutation relations of the effective fields

We can directly infer the decomposition of the effective fields $\varphi_\pm(t, \vec{x})$ in creation and annihilation operators using the late-time limit of the full-theory mode functions (4.2.9). Plugging this equation into (4.2.1) we get the expression

$$\begin{aligned}\phi(t, \vec{x}) = H \int \frac{\mathrm{d}^3k}{(2\pi)^3} \Big[&(a(t)H)^{-\alpha}\Big(e^{i\vec{k}\cdot\vec{x}}\varphi_{+,\vec{k}}(t)a_{\vec{k}} + e^{-i\vec{k}\cdot\vec{x}}\varphi^*_{+,\vec{k}}(t)a^\dagger_{\vec{k}}\Big) \\ &+ (a(t)H)^{-\beta}\Big(e^{i\vec{k}\cdot\vec{x}}\varphi_{-,\vec{k}}(t)a_{\vec{k}} + e^{-i\vec{k}\cdot\vec{x}}\varphi^*_{-,\vec{k}}(t)a^\dagger_{\vec{k}}\Big)\Big] \,.\end{aligned} \tag{4.2.36}$$

Comparing the coefficients of the factors $(a(t)H)^{-\alpha}$ and $(a(t)H)^{-\beta}$ with (4.2.14) leads us to define the following mode decomposition for the free effective fields using the full-theory operators $a_{\vec{k}}$ and $a^\dagger_{\vec{k}}$:

$$\varphi_+(t, \vec{x}) \equiv \int \frac{\mathrm{d}^3k}{(2\pi)^3}\left[e^{i\vec{k}\cdot\vec{x}}\varphi_{+,\vec{k}}(t)a_{\vec{k}} + e^{-i\vec{k}\cdot\vec{x}}\varphi^*_{+,\vec{k}}(t)a^\dagger_{\vec{k}}\right] , \tag{4.2.37}$$

$$\varphi_-(t, \vec{x}) \equiv \int \frac{\mathrm{d}^3k}{(2\pi)^3}\left[e^{i\vec{k}\cdot\vec{x}}\varphi_{-,\vec{k}}(t)a_{\vec{k}} + e^{-i\vec{k}\cdot\vec{x}}\varphi^*_{-,\vec{k}}(t)a^\dagger_{\vec{k}}\right] , \tag{4.2.38}$$

The commutation relations of $\varphi_\pm$ among themselves now follow from the defining expressions, from the commutation relations for $a_{\vec{k}}$ and $a^\dagger_{\vec{k}}$ (4.2.2) and from the form of the effective mode functions (4.2.11), (4.2.12). Since the $\varphi_{\pm,\vec{k}}(t)$ depend only on the magnitudes of their momenta, one finds

$$\begin{aligned}[\varphi_+(t, \vec{x}), \varphi_+(t, \vec{y})] &= \int \frac{\mathrm{d}^3p\mathrm{d}^3k}{(2\pi)^6}\left[e^{i(\vec{k}\cdot\vec{x} - \vec{p}\cdot\vec{y})}\varphi_{+,\vec{k}}(t)\varphi^*_{+,\vec{p}}(t)[a_{\vec{k}}, a^\dagger_{\vec{p}}] - e^{-i\vec{k}\cdot\vec{x} + i\vec{p}\cdot\vec{y}}\varphi^*_{+,\vec{k}}(t)\varphi_{+,\vec{p}}(t)[a_{\vec{p}}, a^\dagger_{\vec{k}}]\right] \\ &= \int \frac{\mathrm{d}^3k}{(2\pi)^3}\left[e^{i\vec{k}\cdot(\vec{x}-\vec{y})}\varphi_{+,\vec{k}}(t)\varphi^*_{+,\vec{k}}(t) - e^{-i\vec{k}\cdot(\vec{x}-\vec{y})}\varphi^*_{+,\vec{k}}(t)\varphi_{+,\vec{k}}(t)\right]\end{aligned}$$

$$
\begin{aligned}
&= \int \frac{\mathrm{d}^3 k}{(2\pi)^3}\, e^{i\vec{k}\cdot(\vec{x}-\vec{y})} \left[\varphi_{+,\vec{k}}(t)\varphi^*_{+,\vec{k}}(t) - \varphi^*_{+,-\vec{k}}(t)\varphi_{+,-\vec{k}}(t)\right] \\
&= 0\,, \qquad (4.2.39)
\end{aligned}
$$

and analogously for the equal-commutator $[\varphi_-(t,\vec{x}), \varphi_-(t,\vec{y})]$. Pairs of effective fields φ_+ and pairs of φ_- thus have vanishing equal-commutation relations. This is no longer true if we consider the equal-time commutator of a φ_+- and a φ_--field. By the analogous manipulations as above we get

$$
[\varphi_+(t,\vec{x}), \varphi_-(t,\vec{y})] = \int \frac{\mathrm{d}^3 k}{(2\pi)^3}\, e^{i\vec{k}\cdot(\vec{x}-\vec{y})} \left[\varphi_{+,\vec{k}}\varphi^*_{-,\vec{k}} - \varphi^*_{+,\vec{k}}\varphi_{-,\vec{k}}\right], \tag{4.2.40}
$$

and plugging in the leading-power expression for the mode functions (4.2.11), (4.2.12) one finds

$$
[\varphi_+(t,\vec{x}), \varphi_-(t,\vec{y})] = -\int \frac{\mathrm{d}^3 k}{(2\pi)^3}\, e^{i\vec{k}\cdot(\vec{x}-\vec{y})} \frac{i}{2\nu} = -\frac{i}{2\nu}\delta^{(3)}(\vec{x}-\vec{y})\,. \tag{4.2.41}
$$

Collecting the above results, we derived the canonical commutation relations for the free SdSET fields:

$$
[\varphi_+(t,\vec{x}), \varphi_+(t,\vec{y})] = [\varphi_-(t,\vec{x}), \varphi_-(t,\vec{y})] = 0\,, \tag{4.2.42}
$$

$$
[\varphi_+(t,\vec{x}), \varphi_-(t,\vec{y})] = -\frac{i}{2\nu}\delta^{(3)}(\vec{x}-\vec{y})\,. \tag{4.2.43}
$$

These commutation relations allow us to interpret φ_+ and φ_- as a pair of (not canonically normalized) canonically conjugated variables, which was also observed in [105]. Since we will be mostly concerned with studying the properties of φ_+, which will give us the leading contributions when matching the EFT onto the full theory, it is most convenient to regard φ_+ as the fundamental field variable and φ_- as its conjugated momentum variable. Again, at this point we can draw a parallel to the non-relativistic scalar field in Minkowski space, where the effective fields ψ and ψ^* have the same relationship to each other as $\varphi_\pm$.

4.2.2 Construction of the free SdSET action

In the previous section, we have identified the fundamental field variables to construct the SdSET, their relationship to the full-theory field, and what they describe physically. Importantly, we found that the pair of fields φ_+ and $-2\nu\varphi_-$ behave like canonically conjugated variables to each other. Using what we have learned above about the effective fields, we are now in the position to construct the free action describing their dynamics, starting from the action of the free, massive, real scalar field ϕ in de Sitter space. The desired action, which was obtained in [105], should have the following two properties, which follow from our observations in the previous section:

1) It should yield equations of motion which are first-order in time for $\varphi_\pm$. This reflects the fact that the effective fields each describe only one degree of freedom of the two that are contained in the full, generally covariant field ϕ.

2) The equations of motion for $\varphi_\pm$ should be decoupled from each other in the absence of interactions. This is because the two effective fields are associated to two different branches of time-evolution of the full field ϕ in the late-time limit, see (4.2.14), which can also be thought of as displaying the emergence of two operators with different scaling dimensions in the late-time limit.

In practice, this boils down to constructing the canonical transformation to switch from the canonical variables of the full theory, which are ϕ and its conjugated momentum, to the canonical pair $\{\varphi_+, -2\nu\varphi_-\}$, which are the appropriate variables to construct the effective description we are seeking. It will prove fruitful to follow the logic and methods applied in [120], which we reproduce and extend in appendix 4.A, while generalizing the procedure used in this reference to accommodate the fact that we are working in a time-dependent background geometry. This will yield a rigorous top-down derivation of the free SdSET action. For the bottom-up construction, we refer to [105].

First steps using the leading-power decomposition of ϕ

The starting point for the top-down derivation of the free SdSET-action is the action for the free, massive scalar field in de Sitter space in four dimensions, which reads

$$S \equiv \int \mathrm{d}^3x\mathrm{d}\hat{t}\; \mathcal{L}(\phi, \dot{\phi}) \tag{4.2.44}$$

$$= \frac{1}{2}\int \mathrm{d}^3x\mathrm{d}\hat{t}\; a(\hat{t})^3 H\left[\dot{\phi}^2 - \frac{(\partial_i\phi)^2}{(a(\hat{t})H)^2} - \frac{m^2}{H^2}\phi^2\right], \tag{4.2.45}$$

where the first equation defines our convention for what we call the Lagrangian density $\mathcal{L}$, we defined the dimensionless time variable $\hat{t} \equiv Ht$, denoted as $\mathtt{t}$ in [105], and we introduced the shorthand notation

$$\dot{\phi} \equiv \frac{\partial\phi}{\partial\hat{t}}\,. \tag{4.2.46}$$

For the sake of compactness of the notation, we will write $a(\hat{t}) = a$ from now on, since the time arguments of the quantities we consider will always be unique. Plugging the leading-power field decomposition (4.2.14) into (4.2.45) we find

$$\begin{aligned} S = \frac{1}{2}\int \mathrm{d}^3x\mathrm{d}\hat{t}\Big[&(aH)^{2\nu}\dot{\varphi}_+^2 + (aH)^{-2\nu}\dot{\varphi}_-^2 + 2\dot{\varphi}_+\dot{\varphi}_- - 2\nu(\dot{\varphi}_+\varphi_- - \varphi_+\dot{\varphi}_-) \\ &- (aH)^{2\nu-2}(\partial_i\varphi_+)^2 - (aH)^{-2\nu-2}(\partial_i\varphi_-)^2 - 2(aH)^{-2}\partial_i\varphi_+\partial_i\varphi_-\Big]\,. \end{aligned} \tag{4.2.47}$$

The Euler-Lagrange equations that we obtain by taking the variation of this action with respect to φ_+ and φ_-, respectively, read:

$$\varphi_+ : \quad (aH)^{2\nu}(\ddot{\varphi}_+ + 2\nu\dot{\varphi}_+) + \ddot{\varphi}_- - 2\nu\dot{\varphi}_- - (aH)^{2\nu-2}\partial_i^2\varphi_+ - (aH)^{-2}\partial_i^2\varphi_- = 0\,, \tag{4.2.48}$$

$$\varphi_- : \quad (aH)^{-2\nu}(\ddot{\varphi}_- - 2\nu\dot{\varphi}_-) + \ddot{\varphi}_+ + 2\nu\dot{\varphi}_+ - (aH)^{-2\nu-2}\partial_i^2\varphi_- - (aH)^{-2}\partial_i^2\varphi_+ = 0\,, \tag{4.2.49}$$

which is just the same equation twice:

$$\ddot{\varphi}_+ + 2\nu\dot{\varphi}_+ + (aH)^{-2\nu}(\ddot{\varphi}_- - 2\nu\dot{\varphi}_-) - (aH)^{-2}[(aH)^{-2\nu}\partial_i^2\varphi_- + \partial_i^2\varphi_+] = 0\,. \tag{4.2.50}$$

Some comments about this result are in order. The fact that we obtain the same equation of motion by taking the variation with respect to φ_+ and φ_- is a reflection of the fact that we used two a-priori independent fields, $\varphi_\pm$, to describe a single field ϕ, thereby introducing a redundancy which we need to remove. The equation involves both second- and first-order derivatives in time, which tells us that the two degrees of freedom of the full field ϕ have not yet been properly distributed among the effective fields $\varphi_\pm$. For the same reason, the fields $\varphi_\pm$ are still coupled to each other via their equation of motion, and, in particular, they are coupled via terms that are proportional to factors of aH, as well as gradient terms. The latter terms are small in the limit we are interested in, so we might argue that we can just drop them. However, we do not have any parametric argument to discuss away the former terms, so we need to take a different approach to get rid of them. These features tell us that we have not yet identified the appropriate mapping from the full field ϕ to $\varphi_\pm$.

All the problematic properties of the action (4.2.47) that we observe here were also observed in its flat-space analogue discussed in [120], when following the same naive procedure to obtain the EFT action from the full one that we pursued thus far. The reference shows that the key to remove the redundancy we observed above is to relate the fields $\varphi_\pm$ to a second variable that is independent of ϕ. The natural quantity to use is the canonically conjugated momentum to ϕ, which we will call π. In the Hamiltonian formulation of the theory, the two variables are introduced independently of each other, and are then related by means of the Hamilton equations. This suggests that the canonical formalism is more appropriate for our purposes than the Lagrangian one, so at this point we switch to it. Once this has been done, the way to fully decouple the equations of motion for $\varphi_\pm$ is to construct a field redefinition which generalizes (4.2.14).

We can compute π from the definitions (4.2.44) and (4.2.45). It reads

$$\pi \equiv \frac{\partial}{\partial \dot{\phi}} \mathcal{L}(\phi, \dot{\phi}) = a^3 H \dot{\phi} \tag{4.2.51}$$

and satisfies

$$\dot{\pi} = a^3 H \left(\frac{\partial_i^2}{(aH)^2} \phi - \frac{m^2}{H^2} \phi \right). \tag{4.2.52}$$

The Hamiltonian density $\tilde{\mathcal{H}}$ of this theory is obtained by performing a Legendre transformation of the Lagrangian density $\mathcal{L}$:

$$\begin{aligned} \tilde{\mathcal{H}} &= \pi \dot{\phi}(\phi, \pi) - \mathcal{L}(\phi, \pi) &(4.2.53)\\ &= \frac{1}{2} \left[\frac{1}{a^3 H} \pi^2 + a^3 H \frac{(\partial_i \phi)^2}{(aH)^2} + \frac{a^3 m^2}{H} \phi^2 \right]. &(4.2.54) \end{aligned}$$

We are now in the appropriate setting to eliminate the redundancy introduced by relating the single field ϕ to both $\varphi_\pm$. Proceeding by analogy to the flat-space case, we start by defining the following two relations between the canonical pairs $\{\phi, \pi\}$ and $\{\varphi_+, -2\nu\varphi_-\}$:

$$\begin{aligned} \phi &\equiv H[(aH)^{-\alpha} \varphi_+ + (aH)^{-\beta} \varphi_-], &(4.2.55)\\ \pi &\equiv -a^3 H^2 [\alpha (aH)^{-\alpha} \varphi_+ + \beta (aH)^{-\beta} \varphi_-]. &(4.2.56) \end{aligned}$$

This implies the constraint equation

$$(aH)^{\nu} \dot{\varphi}_+ + (aH)^{-\nu} \dot{\varphi}_- = 0, \tag{4.2.57}$$

which eliminates the redundancy we observed above. Further, enforcing (4.2.52), gives us the following equation:

$$\dot{\varphi}_\pm = \pm \frac{1}{2\nu} \frac{\partial_i^2}{(aH)^2} \Big[\varphi_\pm + (aH)^{\mp 2\nu} \varphi_\mp \Big]. \tag{4.2.58}$$

Comparing this equation with (4.2.50), we see that it contains far fewer terms, and, in particular, all terms involving second time derivatives have vanished. This is a positive consequence of specifying the two independent equations (4.2.55), (4.2.56), both involving the fields $\varphi_\pm$, which therefore eliminated the redundancy present in the single equation (4.2.55). However, it appears that these equations are missing some terms in order to also achieve the decoupling of the equations of motion for $\varphi_\pm$, and in particular to remove the term

$$\pm \frac{1}{2\nu} \frac{\partial_i^2}{(aH)^2} (aH)^{\mp 2\nu} \varphi_\mp \tag{4.2.59}$$

from (4.2.58). This suggests that the missing terms should be related in some way to the gradient terms $\partial_i^2/(aH)^2$ acting on the effective fields. Again, this is analogous to the flat-space discussion in [120], so we can apply the same procedure to make progress.

Rigorous field redefinition in d dimensions

The discussion carried out in the previous section made it clear that we need to follow a slightly generalized procedure to the one used in [120] to find the correct generalization of the field redefinitions (4.2.55), (4.2.56) relating the canonical pair $\{\phi, \pi\}$ to $\{\varphi_+, -2\nu\varphi_-\}$. The necessity for generalization comes from the fact that we need to rearrange the gradient terms $\partial_i^2/(aH)^2$, which still couple the effective fields via the equation of motion (4.2.58), and they involve an explicit time-dependence due to the scale factor. This property, in turn, is clearly inherited from the fact that we are working in a time-dependent background spacetime. We will construct the appropriate field redefinitions by also generalizing the spacetime dimension from four to d dimensions, which, as we will see, will not involve any additional complications. The benefit of doing so is that we will obtain the d-dimensional form of the free effective action, which will be the starting point for the implementation of dimreg as a regulator for the UV divergences appearing in the SdSET.

We start by considering the free, d-dimensional full-theory action, which reads

$$S \equiv \frac{1}{2} \int \mathrm{d}^{d-1}x \mathrm{d}\hat{t} \; Ha(\hat{t})^{d-1} \left[\dot{\phi}^2 - \frac{(\partial_i \phi)^2}{(aH)^2} - \frac{m^2}{H^2}\phi^2 \right], \tag{4.2.60}$$

In the following we will always work with the dimensionless time variable $\hat{t}$, so we will drop the hat.

The canonically conjugated momentum to ϕ, following the conventions of [30] regarding factors of the metric determinant, reads

$$\pi = Ha^{d-1}\dot{\phi}, \tag{4.2.61}$$

and we get the Hamiltonian density $\tilde{\mathcal{H}}$ by Legendre-transforming the Lagrangian density:

$$\begin{aligned} \tilde{\mathcal{H}} &= \pi\dot{\phi} - \mathcal{L} && (4.2.62)\\ &= \frac{Ha^{d-1}}{2}\left[\frac{1}{H^2 a^{2d-2}}\pi^2 + \frac{(\partial_i \phi)^2}{(aH)^2} + \frac{m^2}{H^2}\phi^2 \right]. && (4.2.63) \end{aligned}$$

The starting ansatz for the decomposition of the field and its canonically conjugated momentum in terms of $\varphi_\pm$ is

$$\phi = H^{\frac{d}{2}-1}\left[(aH)^{-\alpha} D_\nu\left(\frac{\partial_i^2}{(aH)^2} \right)\varphi_+ + (aH)^{-\beta} D_{-\nu}\left(\frac{\partial_i^2}{(aH)^2} \right)\varphi_- \right], \tag{4.2.64}$$

$$\pi = -a^{d-1}H^{\frac{d}{2}}\left[\alpha(aH)^{-\alpha} P_\nu\left(\frac{\partial_i^2}{(aH)^2} \right)\varphi_+ + \beta(aH)^{-\beta} P_{-\nu}\left(\frac{\partial_i^2}{(aH)^2} \right)\varphi_- \right], \tag{4.2.65}$$

where we now have the generalized expressions

$$\alpha = \frac{d-1}{2} - \nu, \quad \beta = \frac{d-1}{2} + \nu, \quad \nu = \sqrt{\left(\frac{d-1}{2}\right)^2 - \frac{m^2}{H^2}}. \tag{4.2.66}$$

This ansatz still factors the leading time-dependence $(aH)^{-\alpha}$, $(aH)^{-\beta}$ out of the effective fields, while $D_{\pm\nu}$ and $P_{\pm\nu}$ are assumed to be analytic functions of the differential operator $\partial_i^2/(aH)^2$. We assume that they can be defined via a series expansion as follows:

$$D_{\pm\nu}(X) = \sum_{n=0}^{\infty} d_{n,\pm\nu}X^n, \quad d_{0,\pm\nu} = 1, \tag{4.2.67}$$

$$P_{\pm\nu}(X) = \sum_{n=0}^{\infty} p_{n,\pm\nu}X^n, \quad p_{0,\pm\nu} = 1, \tag{4.2.68}$$

where we introduced

$$X \equiv \sqrt{\frac{\partial_i^2}{(aH)^2}}. \tag{4.2.69}$$

In the following we will suppress the argument of these differential operators and abbreviate them as $D_\pm$, $P_\pm$. From this construction we see that the equations (4.2.55), (4.2.56) are recovered by replacing the operators $D_\pm$ and $P_\pm$ by their leading-power terms.

The equal-time canonical commutation relations for the pairs $\{\phi, \pi\}$ and $\{\varphi_+, -2\nu\varphi_-\}$ are

$$[\phi(t,\vec{x}), \pi(t,\vec{y})] = i\delta^{(d-1)}(\vec{x}-\vec{y}), \tag{4.2.70}$$

$$-2\nu[\varphi_+(t,\vec{x}), \varphi_-(t,\vec{y})] = i\delta^{(d-1)}(\vec{x}-\vec{y}), \tag{4.2.71}$$

from which we can derive the following constraint equation on $D_\pm$ and $P_\pm$:

$$\beta P_- D_+ - \alpha P_+ D_- = 2\nu\,. \tag{4.2.72}$$

It will also prove useful to use the above equation in its form after taking a single time-derivative, which reads

$$\beta \dot{P}_- D_+ - \alpha P_+ \dot{D}_- = \alpha \dot{P}_+ D_- - \beta P_- \dot{D}_+\,. \tag{4.2.73}$$

The change of variables from $\{\phi, \pi\}$ to $\{\varphi_+, -2\nu\varphi_-\}$ is achieved by means of a canonical transformation, which we carry out following [121]. As a first step π and φ_- need to be expressed only in terms of ϕ and φ_+ by inverting (4.2.64) and (4.2.65), and we find

$$\varphi_- = \frac{(aH)^\beta}{H^{\frac{d}{2}-1}D_-}\phi - \frac{(aH)^{2\nu}D_+}{D_-}\varphi_+\,, \tag{4.2.74}$$

$$\pi = a^{d-1}H^{\frac{d}{2}}\left[\frac{2\nu(aH)^{-\alpha}}{D_-}\varphi_+ - \frac{\beta P_-}{H^{\frac{d}{2}-1}D_-}\phi\right]. \tag{4.2.75}$$

The generating functional $F[\phi, \varphi_+, t]$ of the canonical transformation has to satisfy[2]

$$\pi[\phi, \varphi_+] = \frac{\partial F}{\partial \phi}\,, \quad -2\nu\varphi_-[\phi, \varphi_+] = -\frac{\partial F}{\partial \varphi_+}\,, \tag{4.2.76}$$

and we find the solution

$$F[\phi, \varphi_+, t] = -a^{d-1}\phi\frac{H\beta P_-}{2D_-}\phi + 2\nu\varphi_+\frac{(aH)^\beta}{H^{\frac{d}{2}-1}D_-}\phi - \nu\varphi_+\frac{(aH)^{2\nu}D_+}{D_-}\varphi_+\,. \tag{4.2.77}$$

Its partial time derivative, which only acts on the explicit time-dependence in $a(t)$ and $D_\pm$, $P_\pm$, but not on the implicit one of the fields ϕ and φ_+, reads

$$\begin{aligned}\frac{\partial F}{\partial t} = &-\frac{\alpha(aH)^{2\nu}}{2}\varphi_+\Big[(d-1)P_+D_+ + \dot{P}_+D_+ - P_+\dot{D}_+\Big]\varphi_+ - \frac{1}{2}\varphi_+\Big[(d-1)\Big(\alpha P_+D_- \\ &+ \beta P_-D_+\Big) + \alpha\Big(\dot{P}_+D_- - P_+\dot{D}_-\Big) + \beta\Big(\dot{P}_-D_+ - P_-\dot{D}_+\Big) - 4\nu^2\Big]\varphi_- \\ &- \frac{\beta(aH)^{-2\nu}}{2}\varphi_-\Big[(d-1)P_-D_- + \dot{P}_-D_- - P_-\dot{D}_-\Big]\varphi_-\,,\end{aligned} \tag{4.2.78}$$

where we used (4.2.72), (4.2.73) to bring this expression in a form that is manifestly symmetric under $\nu \to -\nu$. With this result, and using again (4.2.72), (4.2.73), we find the following canonically transformed Hamiltonian density expressed only in terms of $\varphi_\pm$:

$$\begin{aligned}\mathcal{H} &= \tilde{\mathcal{H}} + \frac{\partial F}{\partial t} \qquad (4.2.79)\\ &= \frac{1}{2}\Bigg\{(aH)^{2\nu}\varphi_+\Bigg[\alpha^2P_+^2 - D_+^2\Bigg(\frac{\partial_i^2}{(aH)^2} + \nu^2 - \Big(\frac{d-1}{2}\Big)^2\Bigg) - \alpha\Big[(d-1)P_+D_+ + \dot{P}_+D_+ \\ &\quad - P_+\dot{D}_+\Big]\Bigg]\varphi_+ + (aH)^{-2\nu}\varphi_-\Bigg[\beta^2P_-^2 - D_-^2\Bigg(\frac{\partial_i^2}{(aH)^2} + \nu^2 - \Big(\frac{d-1}{2}\Big)^2\Bigg) - \beta\Big[(d-1)P_-D_- \\ &\quad + \dot{P}_-D_- - P_-\dot{D}_-\Big]\Bigg]\varphi_- + 2\varphi_+\Bigg[\alpha\beta P_+P_- - D_+D_-\Bigg(\frac{\partial_i^2}{(aH)^2} + \nu^2 - \Big(\frac{d-1}{2}\Big)^2\Bigg) + 2\nu^2\end{aligned}$$

[2] From this point on we will be slightly sloppy with the notation, since F is a functional, so it should be defined as an integral over products of fields and operators, and we should be taking functional derivatives of it with respect to ϕ and φ_+. However, for the present manipulations this distinction is immaterial, and we can write F as a product of fields and operators and treat the fields as if they were one-dimensional variables to avoid cluttering our expressions, as long as we are careful about preserving the order of operators and fields.

$$-\frac{\alpha}{2}\Big((d-1)P_+D_- + \dot{P}_+D_- - P_+\dot{D}_-\Big) - \frac{\beta}{2}\Big((d-1)P_-D_+ + \dot{P}_-D_+ - P_-\dot{D}_+\Big)\Big]\varphi_-\Big\}\,. \tag{4.2.80}$$

By assumption $\mathcal{H}$ satisfies the following canonical equations:

$$\dot{\varphi}_+ = \frac{1}{2\nu}\frac{\partial\mathcal{H}}{\partial\varphi_-}\,, \quad -2\nu\dot{\varphi}_- = -\frac{\partial\mathcal{H}}{\partial\varphi_+}\,, \tag{4.2.81}$$

and one equation can be obtained from the other by means of the replacements $\varphi_+ \leftrightarrow \varphi_-$, $\nu \to -\nu$. Since we want the equations of motion for $\varphi_\pm$ to be first order in time and decoupled from each other, which we can write abstractly as

$$\dot{\varphi}_\pm = \text{const.} \times E\varphi_\pm \tag{4.2.82}$$

with E an undetermined operator containing no time derivatives, it follows that the desired form of the Hamiltonian for $\varphi_\pm$ is

$$\mathcal{H} = \varphi_+ E\varphi_-\,. \tag{4.2.83}$$

This means that we need to require that the terms quadratic in $\varphi_\pm$ in (4.2.80) vanish, which implies the differential equations

$$f_\pm^2 + (d-1)f_\pm + \dot{f}_\pm - \left[\frac{\partial_i^2}{(aH)^2} + \nu^2 - \left(\frac{d-1}{2}\right)^2\right] = 0\,, \tag{4.2.84}$$

where we defined

$$f_\pm \equiv -\left(\frac{d-1}{2} \mp \nu\right)\frac{P_\pm}{D_\pm}\,. \tag{4.2.85}$$

Assuming that (4.2.72) and (4.2.84) hold the Hamiltonian can be greatly simplified to

$$\mathcal{H} = \varphi_+\left[2\nu^2\left(1 - \frac{1}{D_+D_-}\right) + \nu\frac{\dot{D}_+D_- - D_+\dot{D}_-}{D_+D_-}\right]\varphi_-\,. \tag{4.2.86}$$

This is the first point where the more general nature of our setting manifests itself: we will not be able to reduce the differential equation (4.2.84) to an algebraic one, which happens in the flat-space case, see the discussion in appendix 4.A.

From equations (4.2.67), (4.2.68) it follows that we should solve the differential equations (4.2.84) with the boundary conditions

$$\lim_{X\to 0} f_\pm(X) = -\left(\frac{d-1}{2} \mp \nu\right) + \mathcal{O}(X)\,. \tag{4.2.87}$$

The solutions read

$$f_+(X) = \frac{X}{2\nu}\frac{\alpha I_{-\nu-1}(X) - \beta I_{-\nu+1}(X)}{I_{-\nu}(X)}\,, \tag{4.2.88}$$

$$f_-(X) = -\frac{X}{2\nu}\frac{\beta I_{\nu-1}(X) - \alpha I_{\nu+1}(X)}{I_\nu(X)}\,, \tag{4.2.89}$$

where $I_\nu(z)$ is the modified Bessel function of the first kind. Combining this result with (4.2.72) we further find the following relations:

$$D_+D_- = \Gamma(1-\nu)\Gamma(1+\nu)I_\nu(X)I_{-\nu}(X)\,, \tag{4.2.90}$$

$$\alpha\beta P_+P_- = \left(\frac{X}{2}\right)^2\Gamma(\nu)\Gamma(-\nu)[\alpha I_{-\nu-1}(X) - \beta I_{-\nu+1}(X)][\beta I_{\nu-1}(X) - \alpha I_{\nu+1}(X)]\,. \tag{4.2.91}$$

At this point we have exhausted the constraints on $D_\pm$ and $P_\pm$, but only the products D_+D_- and P_+P_- are uniquely determined, not the operators $D_\pm$ and $P_\pm$ themselves. We can factorize our residual ignorance about these operators by redefining

$$D_\pm(X) = g_\pm(X)\check{D}_\pm(X)\,, \quad P_\pm(X) = g_\pm(X)\check{P}_\pm(X)\,, \tag{4.2.92}$$

where the function $g_\pm$ absorbs any residual freedom left in the choice of $D_\pm$ and $P_\pm$. We must require that both $g_\pm$ and $\check{D}_\pm$, $\check{P}_\pm$ be 1 at leading power in the expansion in X, and further that

$$g_+ g_- = 1\,, \tag{4.2.93}$$

in order to still satisfy the above constraints. This tells us that we can write the $g_\pm$ as exponentials:

$$g_\pm(X) = \exp\Big[\pm\nu\gamma(X)\Big]\,, \quad \gamma(X) = 0 + \mathcal{O}(X)\,, \tag{4.2.94}$$

with γ an even function under $\nu \to -\nu$. Once we choose $\check{D}_\pm$, the $\check{P}_\pm$ are fixed by the above equations, or vice-versa. Following this procedure we get the results

$$\check{D}_\pm(X) = {}_0F_1\left(1\mp\nu; \frac{X^2}{4}\right)\,, \tag{4.2.95}$$

$$\check{P}_\pm(X) = {}_0F_1\left(\mp\nu; \frac{X^2}{4}\right) + \frac{\beta X^2}{4\alpha\nu(\nu\mp 1)}\,{}_0F_1\left(2\mp\nu; \frac{X^2}{4}\right)\,, \tag{4.2.96}$$

where ${}_0F_1(a;z)$ is a confluent hypergeometric function, defined by the series expansion

$${}_0F_1(a;z) \equiv \sum_{k=0}^{\infty}\frac{z^k}{(a)_k k!}\,, \quad (a)_n \equiv \prod_{k=0}^{n-1}(a-k) \tag{4.2.97}$$

for $|z|< 1$, and by analytic continuation otherwise [51]. By plugging the exact expressions for $D_\pm$ in (4.2.86) we find that all that is left is

$$\mathcal{H} = 2\nu^2\varphi_+\dot{\gamma}\left(\frac{\partial_i^2}{(aH)^2}\right)\varphi_-\,. \tag{4.2.98}$$

To write the action as the integral of a Lagrangian density we eliminate the canonically conjugated momentum $-2\nu\varphi_-$ in favor of $\dot{\varphi}_+$ by means of an inverse Legendre transformation, and get

$$S = \int \mathrm{d}^{d-1}x\mathrm{d}t\Big[-2\nu\dot{\varphi}_+\varphi_- - \mathcal{H}\Big] \tag{4.2.99}$$

$$= -\nu\int \mathrm{d}^{d-1}x\mathrm{d}t\left[\dot{\varphi}_+\varphi_- - \varphi_+\dot{\varphi}_- + 2\nu\varphi_+\dot{\gamma}\left(\frac{\partial_i^2}{(aH)^2}\right)\varphi_-\right]. \tag{4.2.100}$$

The equations of motion of $\varphi_\pm$ are thus fully determined by the form of γ:

$$\dot{\varphi}_\pm = \mp\nu\dot{\gamma}\left(\frac{\partial_i^2}{(aH)^2}\right)\varphi_\pm\,. \tag{4.2.101}$$

We should therefore understand which further constraints the function γ must obey. In appendix 4.A we observed that the flat-space version of γ can only depend linearly on the time variable, as a consequence of energy conservation. This is the second point where the present curved-spacetime discussion differs majorly from its flat-space counterpart, since energy is not conserved in de Sitter space, which means that

$$\frac{\partial\mathcal{H}}{\partial t} \neq 0\,. \tag{4.2.102}$$

Therefore, we cannot further constrain the functional form of γ beyond what we have already used above, which leaves a considerable amount of freedom. However, we can select the form of γ that is most suited for our purposes by the following physical argument, which we already alluded to above: by taking the limit $m/H \to \infty$ we should recover the free action for the heavy scalar field in Minkowski space, with the replacement $\partial_i \to \partial_i/a(t)$. This is because in this limit the effects stemming from spacetime curvature are negligibly small and the superhorizon modes approach the non-relativistic modes in flat space. In this limit, the parameter ν goes to

$$\lim_{\frac{m}{H}\to\infty} \nu = \lim_{\frac{m}{H}\to\infty} \sqrt{\left(\frac{d-1}{2}\right)^2 - \frac{m^2}{H^2}} \to \frac{im}{H} \,. \tag{4.2.103}$$

We can take this limit by analytically continuing the results obtained above to complex ν. If we insist that our modes should still be superhorizon, such that the above construction is still valid, for a finite mass $m > H$ we also have

$$\frac{k}{am} < \frac{k}{aH} \ll 1 \,, \tag{4.2.104}$$

which corroborates our expectation. Choosing

$$\gamma(X) = \frac{1}{2\sqrt{1+\frac{X^2}{\nu^2}}}\left[\sqrt{1+\frac{X^2}{\nu^2}} - 1 - \frac{X^2}{2\nu^2}\right], \tag{4.2.105}$$

where the square root of the operator X^2 is defined by its series expansion, gives us the free SdSET action

$$S = -\nu \int \mathrm{d}^{d-1}x\mathrm{d}t \left\{\dot{\varphi}_+\varphi_- - \varphi_+\dot{\varphi}_- + 2\nu\varphi_+\left[1 - \sqrt{1+\frac{\partial_i^2}{(\nu a H)^2}}\right]\varphi_-\right\}, \tag{4.2.106}$$

which leads to the equations of motion

$$\dot{\varphi}_\pm = \mp\nu\left[1 - \sqrt{1+\frac{\partial_i^2}{(\nu a(t) H)^2}}\right]\varphi_\pm \,. \tag{4.2.107}$$

This is the form of the action that agrees with the result in [105] once we expand the square root to first order in the gradient terms and set $d = 4$.

Summarizing our results, the exact field redefinitions with the choice (4.2.105) read

$$\begin{aligned}\phi(t,\vec{x}) = {}& H^{\frac{d}{2}-\alpha-1}{}_0F_1\left(1-\nu;\frac{X^2}{4}\right)e^{-\alpha t+\nu\gamma(X^2)}\varphi_+(t,\vec{x}) \\ &+ H^{\frac{d}{2}-\beta-1}{}_0F_1\left(1+\nu;\frac{X^2}{4}\right)e^{-\beta t-\nu\gamma(X^2)}\varphi_-(t,\vec{x})\,,\end{aligned} \tag{4.2.108}$$

$$\begin{aligned}\pi(t,\vec{x}) = {}& - H^{\frac{d}{2}-\alpha}\left[{}_0F_1\left(-\nu;\frac{X^2}{4}\right) + \frac{\beta X^2}{4\alpha\nu(\nu-1)}{}_0F_1\left(2-\nu;\frac{X^2}{4}\right)\right]e^{\beta t+\nu\gamma(X^2)}\varphi_+(t,\vec{x}) \\ &- H^{\frac{d}{2}-\beta}\left[{}_0F_1\left(\nu;\frac{X^2}{4}\right) + \frac{\alpha X^2}{4\beta\nu(\nu+1)}{}_0F_1\left(2+\nu;\frac{X^2}{4}\right)\right]e^{\alpha t-\nu\gamma(X^2)}\varphi_-(t,\vec{x})\,.\end{aligned} \tag{4.2.109}$$

Comparing the leading time dependence in the exponentials in the exact redefinitions (4.2.108), (4.2.109) to the equations (7a) and (7b) presented in [120] in the limit (4.2.103) we see that the modes $\varphi_\pm$ take on the roles of the non-relativistic flat space modes ψ, ψ^* as follows:

$$\varphi_- \to \psi\,, \quad \varphi_+ \to \psi^*\,. \tag{4.2.110}$$

Finally, taking the limit $m/H \to \infty$ in (4.2.107), we see that we indeed recover the form of the equations of motion presented in [120] with $\partial_i \to \partial_i/a(t)$ and $\varphi_\pm$ playing the expected roles:

$$\lim_{\frac{m}{H}\to\infty} i\frac{\partial\varphi_\pm}{\partial t} = \lim_{\frac{m}{H}\to\infty} \mp iH\nu\left[1 - \sqrt{1+\frac{\partial_i^2}{(\nu a(t)H)^2}}\right]\varphi_\pm \to \mp m\left[\sqrt{1-\frac{\partial_i^2}{(a(t)m)^2}} - 1\right]\varphi_\pm\,. \tag{4.2.111}$$

This analogy however breaks down in the massless case $m = 0$, since we cannot take the limit $m/H \to \infty$ in the first place. The field redefinitions (4.2.108), (4.2.109) themselves are nevertheless still well-defined and valid.

To conclude this section, we provided an alternative derivation of the free SdSET action presented in [105] by means of a canonical transformation valid in any spacetime dimension d, which takes the form of the concrete field redefinitions (4.2.108), (4.2.109) relating $\{\phi, \pi\}$ to $\{\varphi_+, -2\nu\varphi_-\}$. In the limit in which the EFT is valid, i.e. where all gradient terms are small, we recover the simple equations

$$\phi(t,\vec{x}) = H^{\frac{d}{2}-1}[(aH)^{-\alpha}\varphi_+(t,\vec{x}) + (aH)^{-\beta}\varphi_-(t,\vec{x})]\,, \tag{4.2.112}$$

$$\pi(t,\vec{x}) = -\,a^{d-1}H^{\frac{d}{2}}[\alpha(aH)^{-\alpha}\varphi_+(t,\vec{x}) + \beta(aH)^{-\beta}\varphi_-(t,\vec{x})] \tag{4.2.113}$$

at leading power in the gradient expansion of (4.2.108), (4.2.109), but now the equations of motion for the effective fields have the desired form (4.2.107). This tells us that we have identified the correct effective fields $\varphi_\pm$ by means of the above procedure. Further, it became clear that the analogy to the non-relativistic scalar field in flat space is not merely superficial, but extends to all orders in the gradient expansion. This provided us with useful physical insight, and was ultimately instrumental in motivating the choice for the function γ. As an added benefit, we already know all gradient corrections to the leading-power equations of motion.

4.2.3 Choice of Gaussian initial conditions, definition of the power-counting scheme for the effective fields and matching scheme for correlation functions

In the previous section we constructed the form of the effective action that we are going to use, and found that the free effective fields satisfy the equation of motion

$$\dot{\varphi}_\pm(t,\vec{x}) = \mp\nu\left[1 - \sqrt{1 + \frac{\partial_i^2}{(\nu a(t)H)^2}}\right]\varphi_\pm(t,\vec{x})\,. \tag{4.2.114}$$

Both of these equations involve analytic functions of the gradient term $\partial_i^2/(a(t)H)^2$, which make formal sense because these terms, when acting on the effective fields, are small, and can therefore be expanded in a power series in a sensible way. In (4.2.15) we introduced the concept of a small power-counting parameter

$$\lambda \sim \frac{k}{a(t)H} \ll 1\,, \tag{4.2.115}$$

making precise what we mean when we say that a given term appearing in the EFT is "small". So far, the construction of the effective action used no arguments relying on the smallness of λ, and we will show now how we can use it to organize the infinite series of terms which we introduced above. This discussion goes hand-in-hand with the characterization of the leading correlation properties of the $\varphi_\pm$.

By definition, the gradient term $\partial_i^2/(a(t)H)^2$ acting on the effective fields counts as $\mathcal{O}(\lambda^2)$. We can therefore expand the square root appearing in the equations of motion for $\varphi_\pm$, as well as the one in the free effective action (4.2.106). Doing so, at leading power in λ the equation of motion reduces to

$$\dot{\varphi}_\pm(t,\vec{x}) = 0 + \mathcal{O}(\lambda^2)\,. \tag{4.2.116}$$

The above equation implies that the leading expression for the effective fields is constant in time, which agrees with our findings about the four-dimensional effective mode functions in equations (4.2.11), (4.2.12), but it provides no information about their dependence on position, or momentum in the case of the Fourier-transformed fields. Once this is known, it will then also determine which power counting in λ we should assign to the effective fields, which we have not yet done. As stated in [105], this information must be provided as additional input to the EFT[3].

[3] Notice that the overall k-dependence of the mode functions of the effective fields can be inferred from their transformation behaviour under dilatations and special conformal transformations we discussed in section 4.2.1. However, this leaves the numerical coefficient multiplying the power of k undetermined, and a matching computation is still needed to fix it.

One can, of course, just study the late-time limit of the d-dimensional full-theory mode functions, analogously to what we did above, which is also the route taken in [105]. However, here we will give an alternative, but equivalent, way of determining the free-theory mode functions, which is more in line with the general matching methodology that we will apply later in this chapter to fix the free parameters in the EFT. Determining the free-EFT mode functions at leading power in λ is equivalent to matching the correlation functions of the EFT in the Gaussian approximation to those of the free full theory at leading power in λ. By Wick's theorem, this just amounts to matching the two-point functions of φ_+ and φ_- to those of ϕ, which can be done directly in d dimensions for any value of the mass parameter ν. Using the d-dimensional form of the scalar-field mode functions,

$$\phi_{\vec{k}}(\eta) = \sqrt{\frac{\pi}{4H}}(-H\eta)^{\frac{d-1}{2}} H_\nu^{(1)}(-k\eta)\,, \tag{4.2.117}$$

we find that the leading-power expression of the late-time, full-theory two-point function reads

$$\lim_{k/(a(t)H)\to 0} \langle \phi(t,\vec{k})\phi(t,-\vec{k})\rangle' = H^{d-2}\Big[(a(t)H)^{-2\alpha}\frac{C_\nu}{k^{2\nu}} - (a(t)H)^{1-d}\frac{\cot(\pi\nu)}{2\nu} + (a(t)H)^{-2\beta}\frac{C_{-\nu}}{k^{-2\nu}}\Big]\,, \tag{4.2.118}$$

where we have collected the contributions according to the unsuppressed time-dependence, which is given by the factors of $a(t)H$, and kept only the leading terms in $k/(a(t)H)$ in all three pieces. We also used the quantities

$$\alpha = \frac{d-1}{2} - \nu\,, \quad \beta = \frac{d-1}{2} + \nu\,, \quad C_\nu \equiv \frac{4^{\nu-1}e^{4\pi i\nu}\Gamma(\nu)^2}{\pi}\,, \tag{4.2.119}$$

and stripped off an overall momentum-conserving delta distribution using the primed notation, see (3.1.26). Plugging the leading-power field decomposition (4.2.112) for the Fourier-transformed field $\phi(t,\vec{k})$ into the left-hand side of (4.2.118), we find

$$\begin{aligned}\langle \phi(t,\vec{k})\phi(t,-\vec{k})\rangle' = H^{d-2}\Big[&(a(t)H)^{-2\alpha}\langle \varphi_+(t,\vec{k})\varphi_+(t,-\vec{k})\rangle' + (a(t)H)^{-2\beta}\langle \varphi_-(t,\vec{k})\varphi_-(t,-\vec{k})\rangle' \\ &+ (a(t)H)^{1-d}\Big(\langle \varphi_+(t,\vec{k})\varphi_-(t,-\vec{k})\rangle' + \langle \varphi_-(t,\vec{k})\varphi_+(t,-\vec{k})\rangle'\Big)\Big]\,.\end{aligned} \tag{4.2.120}$$

Comparing the coefficients of $a(t)H$ appearing in this result to the ones in (4.2.118), we find the following power spectra for the EFT fields:

$$\langle \varphi_+(t,\vec{k})\varphi_+(t,-\vec{k})\rangle' = \frac{C_\nu}{k^{2\nu}}\,, \tag{4.2.121}$$

$$\langle \varphi_-(t,\vec{k})\varphi_-(t,-\vec{k})\rangle' = \frac{C_{-\nu}}{k^{-2\nu}}\,, \tag{4.2.122}$$

as well as the following constraint equation:

$$\langle \varphi_+(t,\vec{k})\varphi_-(t,-\vec{k})\rangle' + \langle \varphi_-(t,\vec{k})\varphi_+(t,-\vec{k})\rangle' = -\frac{\cot(\pi\nu)}{2\nu}\,. \tag{4.2.123}$$

Equations (4.2.121) and (4.2.122) define the power spectra of $\varphi_\pm$ at leading power in the gradient expansion, and they agree with the ones given in [105] for $d = 4$, up to a different phase convention used for the mode functions of the scalar field in the reference. This difference in phase will drop out when computing correlators, and is therefore not relevant. One could use (4.2.123), together with the expectation value of the Fourier-transformed equal-time commutation relation (4.2.43),

$$\langle [\varphi_+(t,\vec{k}), \varphi_-(t,-\vec{k})]\rangle' = -\frac{i}{2\nu} \tag{4.2.124}$$

to determine the mixed two-point function $\langle \varphi_+(t,\vec{k})\varphi_-(t,-\vec{k})\rangle'$, which is then related to $\langle \varphi_-(t,\vec{k})\varphi_+(t,-\vec{k})\rangle'$ by complex conjugation. However, this is not necessary, since the field decomposition (4.2.112) ensures that the mixed EFT-correlators always appear in a symmetric combination when matching onto their full-theory counterparts. Moreover, as we will see below, when computing the correlation functions relevant for the matching in the interacting EFT, Weinberg's multiple commutator formula [37], see (1.4.6), will guarantee that all of the φ_- appearing in a given correlation function can be eliminated by using the canonical commutation relation (4.2.43)[4].

We can now use the EFT-power spectra, (4.2.121) and (4.2.122), to fix the power counting of the position-space fields $\varphi_\pm(t,\vec{x})$. From the Fourier representation of the two-point functions

$$\langle\varphi_\pm(t,\vec{x})\varphi_\pm(t,\vec{y})\rangle = \int \frac{\mathrm{d}^{d-1}k}{(2\pi)^{d-1}} e^{i\vec{k}\cdot(\vec{x}-\vec{y})}\langle\varphi_\pm(t,\vec{k})\varphi_\pm(t,-\vec{k})\rangle' \tag{4.2.125}$$

one infers

$$\varphi_+ \sim \lambda^\alpha\,, \quad \varphi_- \sim \lambda^\beta\,, \tag{4.2.126}$$

simply by counting powers of k in the integrands, including the integration measure, which, of course, is the result found in [105]. Notice that, with this power-counting assignment to the effective fields, the leading-power term in the free effective action (4.2.106), which is the one involving no gradient terms, satisfies

$$S_{\text{kin, lead}} = -\nu\int \mathrm{d}^{d-1}x\mathrm{d}t\,(\dot{\varphi}_+\varphi_- - \varphi_+\dot{\varphi}_-) \sim \lambda^0\,. \tag{4.2.127}$$

This follows using that $\vec{x}\sim\lambda^{-1}$, which follows from (4.2.15) and the fact that $\vec{x}$ is the canonically conjugated variable to $\vec{k}$, that $t\sim\lambda^0$ and $\alpha+\beta=d-1$. Further, the field redefinition obtained in section 4.2.2 is consistent with these power-counting rules, since all corrections to (4.2.112) are suppressed by powers of gradients. Both these results are crucial self-consistency properties of the framework.

As a last remark on the power counting of the effective fields, we also notice that their power-counting dimension coincides with their mass dimension,

$$[\varphi_+] = \alpha\,, \quad [\varphi_-] = \beta\,, \tag{4.2.128}$$

which constitutes a further analogy between SdSET and the non-relativistic EFT in flat space, as well as with their scaling dimension.

We have now gathered enough information about the fundamental properties of the SdSET-fields, and their relation to the full-theory field ϕ, to formulate the basic matching strategy between full-theory and EFT correlators, which is essentially a straightforward generalization of the procedure we already used above to determine the form of the EFT two-point functions. To match an n-point correlation functions

$$\langle\phi(t,\vec{x}_1)...\phi(t,\vec{x}_n)\rangle \tag{4.2.129}$$

using the SdSET all we need to do is plug into it the decomposition of ϕ in terms of $\varphi_\pm$, which, in the free theory, is given by (4.2.108), expand it into a sum of EFT correlation functions and collect the terms according to the power counting in λ. For values of the mass parameter $0<\nu\leq 3/2$ we have $\alpha<\beta$, such that the leading contribution to the resulting matching equation is obtained by simply replacing $\phi\to\varphi_+$ in (4.2.129). The subleading terms then involve correlation functions containing φ_--fields, as well gradient terms acting on the effective fields, which can appear both explicitly in the matching equation, due to the gradient terms featured in the exact field redefinition (4.2.108), as well as implicitly, due to insertions of the gradients contained in the free effective action (4.2.106), which can be treated as power-suppressed bilinear interaction terms when evaluating the EFT correlation functions in perturbation theory.

Even though we have formulated the matching procedure in the free effective theory, it will persist in the full, interacting SdSET. However, the presence of interaction terms will induce a more complicated relation between ϕ and the EFT-fields $\varphi_\pm$, which we will study in detail in the next section.

[4]Note also that the correlators $\langle\varphi_+(t,\vec{x})\varphi_-(t,\vec{y})\rangle$ and $\langle\varphi_-(t,\vec{x})\varphi_+(t,\vec{y})\rangle$ are complex-valued and can therefore never appear on their own when matching onto the real-valued full-theory correlators.

4.3 Interaction terms, non-Gaussian initial conditions, and regularization and renormalization in the SdSET

In the previous section we derived the form of the free SdSET action, and defined the two-point functions of the effective fields by means of Gaussian initial conditions. We will now turn on the interactions in the SdSET and study which form they can take, as well as their implications for the matching procedure between full and effective theories. As we discussed in section 4.1, an important new feature of the SdSET is that to correctly match the late-time limit of correlation functions computed in the full interacting theory, it is not enough to use just local interaction terms, but we must also allow for the presence of non-Gaussian initial conditions in the SdSET path integral. For the following discussion, we will restrict ourselves to working at leading power in the EFT power-counting parameter λ. We will also work directly in d dimensions, which will enable us to introduce the regularization and renormalization scheme for the EFT in direct connection to the discussion of the types of interactions appearing in the SdSET.

4.3.1 Local interaction terms at leading power in λ and power counting in the interacting SdSET

Let us start the discussion from the more conventional local interaction terms in the SdSET. We can construct them using products of effective fields $\varphi_\pm$ with both time- and spatial derivatives acting on them. However, it is immediately clear that spatial derivatives acting on the effective fields count as power-suppressed terms, since gradient terms are directly proprtional to λ. Similarly, time derivatives can be rewritten as gradient terms by means of the free equation of motion of the EFT-fields (4.2.107)[5], which in its expanded form reads

$$\dot{\varphi}_\pm = \left[\pm \frac{1}{2\nu}\frac{(\partial_i)^2}{(a(t)H)^2} + \mathcal{O}(\lambda^4)\right]\varphi_\pm\,. \tag{4.3.1}$$

Therefore, it is clear that the least-suppressed interaction terms that we can construct are those involving no derivatives at all, and thus take the form of a potential constructed out of products of $\varphi_\pm$. We can therefore make the following ansatz for the interaction terms appearing in the SdSET action:

$$S_{\text{int}} \sim \int \mathrm{d}^{d-1}x\mathrm{d}t\, \sum_{n=0}^{\infty}\sum_{m=0}^{n} c_{n-m,m}\varphi_+^{n-m}(t,\vec{x})\varphi_-^m(t,\vec{x})\,, \tag{4.3.2}$$

where we introduced the couplings $c_{n-m,m}$. However, we can further constrain the form of the above interaction terms, and make the construction more precise. The first constraint on these terms comes from the requirement that the SdSET action should be invariant under the de Sitter isometries, as discussed above in section 4.2.1. Under dilatations the coordinates and fields appearing in the above ansatz for S_{int} transform as follows:

$$t\to t\,,\quad \vec{x}\to\vec{x}/\xi\,,\quad a(t)\to\xi a(t)\,,\quad \varphi_+(t,\vec{x})\to\xi^\alpha\varphi_+(t,\vec{x})\,,\quad \varphi_-(t,\vec{x})\to\xi^\beta\varphi_-(t,\vec{x})\,. \tag{4.3.3}$$

Since the effective fields $\varphi_\pm$ are scalars under translations and rotations we cannot use any function of $\vec{x}$ to make up for their non-trivial transformation behaviour, since the resulting interaction terms would then no longer be invariant under spatial translations and rotations. This leaves us with factors of $a(t)$ being the only viable option, and we find

$$S_{\text{int}} = -\int \mathrm{d}^{d-1}x\mathrm{d}t\, \sum_{n=1}^{\infty}\sum_{m=0}^{n} a(t)^{d-1-(n-m)\alpha-m\beta}\frac{c^0_{n-m,m}}{(n-m)!\,m!}\varphi_{+,0}^{n-m}(t,\vec{x})\varphi_{-,0}^m(t,\vec{x})\,, \tag{4.3.4}$$

[5] This statement is somewhat imprecise, since the rigorous way to eliminate these terms is to apply a field redefinitoon to $\varphi_\pm$ which gets rid of them. However, as long as one is only working at leading power in λ, this yields the same results as simply using the (classical) equations of motion for the effective fields to rewrite these terms. For a discussion on this topic, see [122].

where we also defined the effective couplings $c^0_{n-m,m}$ including an explicit factor $((n-m)!\,m!\,)^{-1}$ for later convenience. This form of the action is indeed invariant under (4.3.3). Furthermore, it is also automatically invariant under special conformal transformations as well. This can be recognized most easily by noticing that we can distribute the powers of $a(t)$ appearing in it as follows. We can group $a(t)^{d-1}$ together with the integration measure $\mathrm{d}^{d-1}x\mathrm{d}t$, which then simply results in the de Sitter-invariant integration measure $\mathrm{d}^dx\,\sqrt{-g}$. The remaining factors of $a(t)$ can be grouped with all the appearing EFT fields in each summand, and we know from the discussion above that the $\varphi_\pm$ transform in such a way as to make the combinations $a(t)^{-\frac{3}{2}\mp\nu}\varphi_\pm(t,\vec{x})$ invariant under all de Sitter isometries by themselves.

This form of the action is the same form found in [105] in four dimensions, up to powers of H. We will come to these in a moment. Interaction terms with the same field content as any of the terms we wrote above, but involving additional derivatives acting on the fields, can be regarded as subleading-power corrections to these terms. In (4.3.4) we have now denoted both the effective fields and couplings with a superscript "0", to make clear that they are bare quantities, and will need to be renormalized once we start computing loop diagrams in the SdSET. The mass dimension of the d-dimensional bare couplings is

$$[c^0_{n-m,m}] = d-1-(n-m)\alpha - m\beta\,, \tag{4.3.5}$$

which follows from straightforward mass-dimension counting of the terms appearing in the integrand of $S_{\rm int}$, using the mass dimensions of the effective fields (4.2.128) and remembering that we are working with a dimensionless time variable in Hubble units. The reference [105] chose to work with dimensionless couplings, by pulling out factors of H to account for their mass dimension. We will go a slightly different route, and we postpone its systematic discussion to the section dedicated to the renormalization of the effective action below. However, at this point we can note that not all bare couplings $c^0_{n-m,m}$ are independent of each other. Due to the RPI-relation between effective fields (4.2.35), which we reprint here for convenience,

$$\varphi_+ \to \varphi_+ + \iota(a(t)H)^{\alpha-\beta}\varphi_-\,, \quad \varphi_- \to (1-\iota)\varphi_-\,, \tag{4.3.6}$$

we find the following relation between "nearest-neighbour" couplings, which multiply operators built out of the same number of effective fields but differing by one power of φ_+ (or φ_-):

$$c^0_{n-m,m}H^{\alpha-\beta} = c^0_{n-m+1,m-1}\,. \tag{4.3.7}$$

Using this, one can relate all the couplings of operators built out of n effective fields to each other, for any n, such that only one representative of these "families" of effective couplings is truly unknown. This coupling (or, rather, its renormalized counterpart), must be determined by an appropriate matching computation. Through the above argument, we also see that H naturally appears to account for at least part of the mass dimension of the bare couplings.

The discussion so far has been quite general. To start making it more concrete, from this point on we will specialize it to the case that we will be interested in. We will be matching the SdSET onto the theory we considered in chapter 3, the real, massless, minimally coupled scalar field with a quartic self-interaction, regularized in the infrared by the k_Λ-scheme. Several properties of this theory, which must be inherited by the SdSET, can be implemented before carrying out any matching computations to simplify its structure. Since there is only one interaction type in the full theory, with (renormalized) coupling κ, it is clear that all the effective couplings will be related to this single coupling. Furthermore, since the underlying theory is invariant under $\phi\to-\phi$, the form of the possible interaction terms in the SdSET is restricted to

$$S_{\rm int} = -\int \mathrm{d}^{d-1}x\mathrm{d}t\,\sum_{n=1}^{\infty}\sum_{m=0}^{2n} a(t)^{d-1-(2n-m)\alpha-m\beta}\,\frac{c^0_{2n-m,m}}{(2n-m)!\,m!}\,\varphi^{2n-m}_{+,0}(t,\vec{x})\varphi^m_{-,0}(t,\vec{x})\,, \tag{4.3.8}$$

i.e. only interaction terms involving an even number of EFT fields can appear. Finally, the presence of the evanescent mass term in the full theory, which fixed the value $\nu=3/2$ in any dimension, implies that in the SdSET we can fix

$$\alpha = \frac{d-4}{2}\,, \quad \beta = \frac{d+2}{2} \tag{4.3.9}$$

for any d, and, in particular, in $d = 4$ dimensions we have $\alpha = 0$, $\beta = 3$. The combinations

$$\alpha + \beta = d - 1\,, \quad \alpha - \beta = -3 \tag{4.3.10}$$

will also appear often, so it is useful to keep them in mind.

We wish to work at leading power in λ, so we need to identify the interaction terms which will give us the leading contributions to a given correlation function, and we can ignore the rest. Since in our setting we have $\alpha < \beta$, and given the power-counting rules for the effective fields (4.2.126), we should minimize the number of φ_--fields appearing in a given interaction term in (4.3.4). Naively, we would then conclude that the only relevant interaction terms are the ones involving φ_+-fields alone. However, since the φ_+-fields commute with each other, such interaction terms will always vanish when inserted into EFT-correlation functions involving only φ_+-fields, as can be seen most easily by using the multiple-commutator formula (1.4.6). These SdSET correlators are the ones that should give us the leading-power terms when matching full-theory correlators using the SdSET, and since the φ_+^n-terms appearing in (4.3.4) cannot give contribute to them, one might suspect that these terms are, in fact, redundant, and should be removed from the interaction terms. However, this is not the end of the story. These terms make a non-vanishing contribution for the first time in SdSET correlation functions involving at least one φ_--field, which can also be directly seen from (1.4.6), since the commutator $[\varphi_+, \varphi_-]$ does not vanish. According to the rules (4.2.126), such correlation functions should be power-suppressed with respect to correlators involving only φ_+-fields. However, once an interaction term of the form φ_+^n is inserted into them, they will yield a result which power-counts like a correlation function involving only φ_+-fields into which an interaction term of the form $\varphi_+^{n-1}\varphi_-$ has been inserted, which can be seen immediately:

$$\langle \varphi_+(t,\vec{x}_1)...\varphi_+(t,\vec{x}_m)\varphi_+^{n-1}(t',\vec{x})\varphi_-(t',\vec{x})\rangle \sim \langle \varphi_+(t,\vec{x}_1)...\varphi_+(t,\vec{x}_{m-1})\varphi_-(t,\vec{x}_m)\varphi_+^{n}(t',\vec{x})\rangle \sim \lambda^{\alpha(m+n-1)+\beta}\,. \tag{4.3.11}$$

For the above argument it is, of course, not important at which spacetime point the field φ_- is evaluated. The presence of interaction terms proportional to φ_+^n therefore leads to a non-manifest power-counting for the EFT correlation functions. While this is not technically inconsistent, and one could in principle still work with such a theory, it would be a highly undesirable feature of the EFT if such terms were kept. After all, we wish to use the SdSET to be able to organize the expansion of the full-theory correlators in the late-time limit in a systematic and clear way.

The way out of this predicament is to get rid of these interaction terms by means of a field-redefinition of the bare φ_--fields of the form

$$\varphi_{-,0} \to \varphi_{-,0} + \sum_{n=0}^{\infty} a(t)^{(4-d)n+3} r_n \varphi_{+,0}^{2n+1}\,, \tag{4.3.12}$$

which was already done in [107]. At first it seems to be inconsistent to apply such a field redefinition to φ_-, since, assuming the power-counting rules $\varphi_+ \sim \lambda^\alpha$ and $\varphi_- \sim \lambda^\beta$, such a redefinition would turn the φ_--field into an $\mathcal{O}(\lambda^\alpha)$-quantity. However, we have already noticed that before eliminating these terms from the effective action the power-counting rules for $\varphi_\pm$ we established in the free theory do not reflect the factual power counting of the correlation functions in the interacting theory. Furthermore, we have not yet made use of the power-counting rules (4.2.126), which we eventually wish to assign to the effective fields based on the matching of their power spectra, at any point in our derivation. Therefore, we are still free to use field redefinitons of the form (4.3.13) without running into any logical conteradictions. The observation of the non-manifest power counting of the EFT correlators in the interacting theory as a consequence of the presence of the φ_+^n interactions is just telling us that to implement the desired power-counting rules for $\varphi_\pm$ in the interacting theory we should first find a suitable field basis, in which these interaction terms are have been removed. Only then will the power-counting rules for $\varphi_\pm$ and their correlation functions match up.

The appropriate field redefiniton of φ_- reads

$$\varphi_{-,0} \to \varphi_{-,0} + (a(t)H)^3\left[\frac{c_{1,1}^0}{9}\varphi_{+,0} + \frac{c_{3,1}^0 a(t)^{4-d}}{18(7-d)}\varphi_{+,0}^3 + \frac{2a(t)^{2(4-d)}}{11-2d}\left[\frac{c_{5,1}^0}{6!} + \frac{(c_{3,1}^0)^2}{108(7-d)}\right]\varphi_{+,0}^5\right] + \mathcal{O}(\varphi_{+,0}^7)\,, \tag{4.3.13}$$

and it is derived in appendix 4.B. As is explained there, this redefinition only takes into account the leading-power expression for the effective couplings in powers of the (renormalized) full-theory coupling κ, since it is all that we consider in this chapter. Once subleading-power corrections to the EFT couplings are included, the above redefinition needs to be corrected accordingly, in order to ensure consistent matching onto the full theory. The d-dimensional, interacting full-theory and EFT-fields are then related as

$$\begin{aligned}\phi(t,\vec{x}) =& H^{\frac{d}{2}-1}\Bigg\{(a(t)H)^{-\frac{d-4}{2}}\left[\left(1+\frac{c^0_{1,1}}{9}\right)\varphi_{+,0}(t,\vec{x})+\frac{c^0_{3,1}a(t)^{4-d}}{18(7-d)}\varphi^3_{+,0}(t,\vec{x})\right.\\ &\left.+\frac{2a(t)^{2(4-d)}}{11-2d}\left[\frac{c^0_{5,1}}{6!}+\frac{(c^0_{3,1})^2}{108(7-d)}\right]\varphi^5_{+,0}(t,\vec{x})\right]+(a(t)H)^{-\frac{d+2}{2}}\varphi_{-,0}(t,\vec{x})\Bigg\}\,. \end{aligned} \tag{4.3.14}$$

Thus, we see that the terms we are removing from the action will still give us a non-vanishing contribution when matching a full-theory correlation function using the EFT, which was already noticed in [107]. Because of the non-linear relationship between the full-theory and EFT fields, to correctly match a full-theory correlation function at leading power in λ it is not enough to compute the same correlation function with the replacement $\phi \to \varphi_+$ using the EFT, but we must instead consider several EFT correlators, according to the field decomposition (4.3.14). We will see how this works in practice in several examples below.

4.3.2 Non-Gaussian initial conditions

As already anticipated, to correctly match the full-theory correlation functions using the SdSET we need to include non-Gaussian initial conditions in the SdSET path integral. We will use the formalism presented in [49], reviewed in section 1.4, and adapt it to our setting. The initial time-slice for the SdSET is located at a finite time, which we will call t_*, which, physically, should be thought of being located close to the time of horizon crossing of the modes described by the EFT-fields, $t_* \sim t_H$. Therefore, this is where our initial-condition functional $F[\varphi_\pm]$ for the SdSET should be localized, and we make the following ansatz for it:

$$F[\varphi_\pm] \equiv \sum_{n=1}^{\infty}\int\left[\prod_{j=1}^{2n}\mathrm{d}^{d-1}x_j a_*^{d-1}\right]\sum_{m=0}^{2n}\frac{a_*^{-(2n-m)\alpha-m\beta}}{(2n-m)!\,m!}\Xi^{\sigma_1,\dots,\sigma_{2n}}_{2n-m,m;0}(\vec{x}_1,\dots,\vec{x}_{2n})\prod_{k=0}^{2n-m}\varphi^{\sigma_k}_{+,0}(t_*,\vec{x}_k)\prod_{l=0}^{m}\varphi^{\sigma_l}_{-,0}(t_*,\vec{x}_l)\,, \tag{4.3.15}$$

where, similarly to the case of the EFT couplings, we have included the subscript "0" in the definition of the bare functions $\Xi^{\sigma_1,\dots,\sigma_{2n}}_{2n-m,m;0}$, since we expect that they will need to be renormalized. In the above definition we directly implemented the restrictions implied by the symmetry under $\phi \to -\phi$ of the full theory. Even though $F[\varphi_\pm]$ depends explicitly on t_*, the dependence on this quantity must drop out in the matching, since the full-theory correlation functions do not depend on it. We will make extensive use of this fact further below.

Notice that the definition (4.3.15) assumes total symmetry of the functions $\Xi^{\sigma_1,\dots,\sigma_n}_{n-m,m;0}(\vec{x}_1,\dots,\vec{x}_n)$ in their arguments. The factors of a_* which we already included in the above terms can be motivated in full analogy to the factors of $a(t)$ we included in the vertices in section 4.3.1, since we want $F[\varphi_\pm]$ to be invariant under the full set of de Sitter isometries, and we have already observed above that the combinations $a(t)^{-\frac{3}{2}\mp\nu}\varphi_\pm(t,\vec{x})$ are de Sitter-invariant by themselves. The factors of a_* then fully compensate for the transformation behaviour of all other objects appearing in the integrals, provided that the initial-condition functions $\Xi^{\sigma_1,\dots,\sigma_n}_{n-m,m;0}$ are left invariant under the action of the de Sitter isometries. This also directly implies that they scale like x^0. Notice also that, differently than the case of the vertex terms, here we have several position variables involved in each term. Since the transformation of the scale factor under special conformal transformations involves an explicit position argument, see (4.2.25), each factor of $a_*^{-\frac{3}{2}\mp\nu}$ should be directly associated to one of the $\varphi_\pm$, such that it is clear which position argument should appear as it transforms.

Under the assumption that the initial condition functions $\Xi^{\sigma_1,\dots,\sigma_n}_{n-m,m;0}$ are parametrizing a Hermitean density matrix describing the initial state of the theory, which we will assume from now on, they must satisfy [49]

$$i\Xi^{\sigma_1,\dots,\sigma_n}_{n-m,m;0}(\vec{x}_1,\dots,\vec{x}_n) = \left[i\Xi^{-\sigma_1,\dots,-\sigma_n}_{n-m,m;0}(\vec{x}_1,\dots,\vec{x}_n)\right]^*\,. \tag{4.3.16}$$

At first, all possible combinations of CTP-indices σ_i are allowed. However, since we will use this formalism in an effective theory which stems from an underlying theory which, by construction, only involves interactions with all-plus or all-minus fields, and is furthermore conservative, it will be enough to restrict ourselves to initial-condition functions involving all-plus and all-minus CTP-indices only, which therefore can be summarized by a single index σ. We therefore write

$$\Xi^{\sigma_1,\dots,\sigma_n}_{n-m,m;0}(\vec{x}_1,\dots,\vec{x}_n) = \left[\prod_{i=1}^{n} \delta_{\sigma_i\sigma}\right] \Xi^{\sigma}_{n-m,m;0}(\vec{x}_1,\dots,\vec{x}_n)\,. \tag{4.3.17}$$

Since they should be real-valued functions of the position arguments, equation (4.3.16) then implies that they flip their sign with σ:

$$\Xi^{+}_{n-m,m;0}(\vec{x}_1,\dots,\vec{x}_n) = -\Xi^{-}_{n-m,m;0}(\vec{x}_1,\dots,\vec{x}_n)\,. \tag{4.3.18}$$

Furthermore, since the theory needs to be invariant under the reparametrization transformation (4.2.35), which at time t_* reads

$$\varphi_+(t_*,\vec{x}) \to \varphi_+(t_*,\vec{x}) + \iota (a_* H)^{\alpha-\beta}\varphi_-(t_*,\vec{x})\,, \quad \varphi_-(t_*,\vec{x}) \to (1-\iota)\varphi_-(t_*,\vec{x})\,, \tag{4.3.19}$$

we get an analogous constraint on the initial-conditions functions as we did for the EFT-couplings in (4.3.7):

$$\Xi^{\sigma}_{n-m,m;0}(\vec{x}_1,\dots,\vec{x}_n) H^{\alpha-\beta} = \Xi^{\sigma}_{n-m-1,m+1;0}(\vec{x}_1,\dots,\vec{x}_n)\,. \tag{4.3.20}$$

Notice, however, that these equations have a more restricting effect on the initial-condition functions for a fixed n than they did on the effective couplings, since they imply that they must all have the same functional form. This statement is also compatible with the requirement that all the initial-condition functions have the same overall scaling.

For practical calculations, we will find it most convenient to represent the initial-condition function $\Xi^{\sigma}_{n-m,m;0}$ in momentum space, and, since we are assuming them to be translationally invariant, one finds [49]

$$\Xi^{\sigma}_{n-m,m;0}(\vec{x}_1,\dots,\vec{x}_n) = \int \left[\prod_{i=1}^{n} \frac{\mathrm{d}^{d-1}k_i}{(2\pi a_*)^{d-1}}\right] \exp\left[i\sum_{j=1}^{n} \vec{k}_j\cdot\vec{x}_j\right] (2\pi a_*)^{d-1}\delta^{(d-1)}\left(\sum_{l=1}^{n}\vec{k}_l\right) \Xi^{\sigma}_{n-m,m;0}(\vec{k}_1,\dots,\vec{k}_n)\,, \tag{4.3.21}$$

where the powers of a_* appearing in the above equation ensure the de Sitter-invariance of the various components that make up the right-hand side of it, which then implies that $\Xi^{\sigma}_{n-m,m;0}(\vec{k}_1,\dots,\vec{k}_n)$ should be de Sitter-invariant as well. The momentum-space representation of $F[\varphi_\pm]$ then reads

$$\begin{aligned} F[\varphi_\pm] = &\sum_{n=1}^{\infty} \int \left[\prod_{j=1}^{2n} \frac{\mathrm{d}^{d-1}k_j}{(2\pi)^{d-1}}\right] \sum_{m=0}^{2n} \frac{a_*^{d-1-(2n-m)\alpha-m\beta}}{(2n-m)!\,m!} \Xi^{\sigma}_{2n-m,m;0}(\vec{k}_1,\dots,\vec{k}_{2n}) \prod_{l=0}^{2n-m} \varphi^{\sigma}_{+,0}(t_*,\vec{k}_l) \prod_{q=0}^{m} \varphi^{\sigma}_{-,0}(t_*,\vec{k}_q) \\ &\times (2\pi)^{d-1}\delta^{(d-1)}\left(\sum_{l=1}^{2n}\vec{k}_l\right)\,, \end{aligned} \tag{4.3.22}$$

and from this expression we see that the non-Gaussian initial conditions can be treated as non-local, momentum-conserving "vertices".

Analogously to the case of the effective couplings, the renormalized versions of the non-Gaussian initial conditions functions must be determined by carrying out matching computations. Allowing for the presence of non-vanishing initial condition functions $\Xi^{\sigma}_{2n,0;0}$ would lead, again analogously to the effective couplings, to a non-manifest power counting of the SdSET correlation functions. We have seen above how to construct the suitable effective field basis in which this is not the case, which led to the elimination of the couplings $c^{0}_{2n,0}$, and, when carrying out matching computations, we will always assume that we are working in that particular basis. In particular, in this basis, the functions $\Xi^{\sigma}_{2n,0;0}$ must be absent as well, so the leading-power functions that we will need to determine below are the renormalized version of $\Xi^{\sigma}_{2n+1,1;0}(\vec{k}_1,\dots,\vec{k}_{2n+2})$.

4.3.3 Regularization and renormalization in the SdSET

Having introduced the formalism that we will use to carry out computations in the interacting SdSET, we now discuss the regularization of UV and IR divergences that we will encounter in the EFT, and the renormalization of the former divergences.

Regularization scheme

We have already set up the theory in such a way as to be able to regularize the UV divergences using dimensional regularization, together with the same evanescent mass term that we used in the full theory, such that the parameter ν is fixed to $\nu = 3/2$ in any dimension The SdSET has the peculiarity that the time integrals associated with vertices in diagrams generate UV divergences, which is not the case in the full theory. This is essentially due to the fact that the two-point functions of EFT fields are time-independent, and in the absence of any regulator we would be evaluating a time integral over a constant function in the interval $(-\infty, t]$ for each vertex appearing in an EFT diagram. In particular, this implies that we will have to renormalize the theory already at tree level, which is a very unusual feature. Once we move on to computing quantum corrections in the EFT, we will additionally start encountering, in general, both UV- and IR-divergent momentum integrals, which is rather standard and in line with what we observed in the full-theory computations in chapter 3. At leading power in λ the interaction terms in the SdSET read

$$S_{\text{int}} = -\int \mathrm{d}^{d-1}x\mathrm{d}t \, \sum_{n=0}^{\infty} a(t)^{(4-d)n} \frac{c^0_{2n+1,1}}{(2n+1)!} \varphi^{2n+1}_{+,0}(t,\vec{x})\varphi_{-,0}(t,\vec{x}) \,, \tag{4.3.23}$$

where we used

$$\alpha = \frac{d-4}{2} \,, \quad \beta = \frac{d+2}{2} \tag{4.3.24}$$

to simplify the exponent of $a(t)$ in the integrand. We see that all summands, except for the very first one with $n = 0$, feature $a(t)$ with a dimension-dependent exponent which can be used to regularize the divergent time integrals by defining [105]

$$\int_{-\infty}^{t} \mathrm{d}t' \; a(t')^{p+\varepsilon} \equiv \frac{a(t)^{p+\varepsilon}}{p+\varepsilon} \tag{4.3.25}$$

for any value of p, as long as the dimreg-parameter ε does not drop out of the exponent. Since the summand with $n = 0$ in (4.3.23) has no factor of $a(t)$ in it, the associated time integral is not regularized. This is the same accidental cancellation of the dimension-dependent terms in the mass-counterterm-insertion diagrams that we observed in in section 3.4.1 while studying the one-loop power spectrum, which we identified as a peculiarity of the version of dimreg that we are using. This forces us to introduce an additional analytic regulator

$$(a(t)\nu)^{2\delta} \tag{4.3.26}$$

in the bilinear interaction term appearing in (4.3.27), such that S_{int} becomes

$$S_{\text{int}} = -\int \mathrm{d}^{d-1}x\mathrm{d}t \, \left[c^0_{1,1}(a(t)\nu)^{2\delta}\varphi_{+,0}(t,\vec{x})\varphi_{-,0}(t,\vec{x}) + \sum_{n=1}^{\infty} a(t)^{(4-d)n} \frac{c^0_{2n+1,1}}{(2n+1)!} \varphi^{2n+1}_{+,0}(t,\vec{x})\varphi_{-,0}(t,\vec{x}) \right] , \tag{4.3.27}$$

and all integrals appearing in it are now well-defined: the explicit powers of $a(t)$ regularize the time integrals, while the d-dependence of the spatial integration measure regularizes the loop integrals.

Similarly, the leading-power initial-condition functional reads, written in terms of momentum-space fields,

$$\begin{aligned} F[\varphi_\pm] = &\sum_{n=0}^{\infty} \int \left[\prod_{j=1}^{2n+2} \frac{\mathrm{d}^{d-1}k_j}{(2\pi)^{d-1}} \right] \frac{a_*^{(4-d)n}}{(2n+1)!} \Xi^\sigma_{2n+1,1;0}(\vec{k}_1, ..., \vec{k}_{2n+2}) \left[\prod_{l=1}^{2n+1} \varphi^\sigma_{+,0}(t_*, \vec{k}_l) \right] \varphi^\sigma_{-,0}(t_*, \vec{k}_{2n+2}) \\ &\times (2\pi)^{d-1} \delta^{(d-1)}\left(\sum_{l=1}^{2n+2} \vec{k}_l \right) , \end{aligned} \tag{4.3.28}$$

and the d-dependence of the momentum integration measure regularizes the loop integrals into which the initial-conditions functions are inserted. It will prove convenient to mirror the addition of the analytic regulator (4.3.26) in the bilinear term of the initial-condition functional, by multiplying it with $(a_*\nu)^{2\delta}$, so we will use the following, modified form of $F[\varphi_\pm]$ for the explicit computations below:

$$
\begin{aligned}
F[\varphi_\pm] = \int \frac{\mathrm{d}^{d-1}k}{(2\pi)^{d-1}}\, (a_*\nu)^{2\delta}\Xi^\sigma_{1,1;0}(\vec{k},-\vec{k})\varphi_{+,0}(t_*,\vec{k})\varphi_{-,0}(t_*,-\vec{k}) \\
+ \sum_{n=1}^{\infty}\int\left[\prod_{j=1}^{2n+2}\frac{\mathrm{d}^{d-1}k_j}{(2\pi)^{d-1}}\right]\frac{a_*^{(4-d)n}}{(2n+1)!}\Xi^\sigma_{2n+1,1;0}(\vec{k}_1,...,\vec{k}_{2n+2})\left[\prod_{l=1}^{2n+1}\varphi^\sigma_{+,0}(t_*,\vec{k}_l)\right]\varphi^\sigma_{-,0}(t_*,\vec{k}_{2n+2}) \\
\times (2\pi)^{d-1}\delta^{(d-1)}\left(\sum_{l=1}^{2n+2}\vec{k}_l\right),
\end{aligned}
\tag{4.3.29}
$$

We have effectively implemented the same UV-regularization scheme as in the full-theory in the SdSET, even though this is not a requirement: we might just as well have implemented a very different UV-regularization scheme in the EFT, since the difference between the two schemes used in the full and effective theories can always be compensated by the matching coefficients that will be determined through explicit computations. We just followed this route because it will turn out to be the most convenient, as far as the technical aspects of the computations are concerned.

For the IR regularization, however, we must use the same scheme in the full and effective theories. The reason for this is the following: the SdSET is constructed to faithfully reproduce the infrared structure of the full theory, and this includes all of the IR-divergent terms that we found in the previous chapter while computing correlation functions of massless, minimally coupled scalar fields perturbatively. Since the divergent terms appear on both sides of the matching equations between full-theory and EFT correlators, they will cancel out in the matching. The difference of the two sides of the equations will determine the matching coefficients and non-Gaussian initial conditions of the SdSET, which will thus be free of any pathologies that are generated by carrying out the matching procedure perturbatively. This is what validates our strategy to determine the short-distance and early-time information that must be fed into the EFT using perturbation theory, even though it is ill-defined for the massless, minimally coupled scalar field. For the cancellation of all IR-sensitive terms in a given correlator to work out exactly, however, it is imperative that the same IR-regularization schemes are implemented in both theories.

In the full theory we defined the k_Λ-scheme by introducing a mass in the action which acted like a "comoving mass" term, see the discussion in section 3.1. The effect of this "comoving mass" in the full theory is completely reproduced in the EFT by the replacement

$$\vec{k}^2 \to \vec{k}^2 + \Lambda^2 \tag{4.3.30}$$

in every k-dependent function that we will encounter in the EFT. This is the very same effect that this type of IR regulator had in the full theory, as we saw above. The power spectrum of φ_+ that we found in (4.2.121) for arbitrary values of the mass of the field is therefore modified to

$$\langle\varphi_+(t,\vec{k})\varphi_+(t,\vec{k}')\rangle = (2\pi)^{d-1}\delta^{(d-1)}(\vec{k}+\vec{k}')\frac{1}{2[\vec{k}^2+\Lambda^2]^{\frac{3}{2}}}\,, \tag{4.3.31}$$

where we used that $\nu = 3/2$ for any d, and this is the "propagator" that we will use in all of the following computations. The power spectrum of φ_- that we found in (4.2.122) gets modified accordingly, but we will never need it in the following, so we do not write it out explicitly here. Importantly, the canonical commutation relations

$$[\varphi_+(t,\vec{k}),\varphi_-(t,\vec{k}')] = -\frac{i}{3}\delta^{(d-1)}(\vec{k}+\vec{k}') \tag{4.3.32}$$

are left unchanged in this scheme. To keep the notation as transparent as possible, we will abbreviate

$$k_\Lambda \equiv \sqrt{\vec{k}^2+\Lambda^2} \tag{4.3.33}$$

in the following, as we did in the full theory.

Renormalization scheme, renormalization-group equations of the SdSET couplings and initial conditions

Both classes of UV divergences that we discussed above, coming from time- and momentum integrals in the SdSET, need to be removed by renormalizing the effective fields, couplings and the non-Gaussian initial-condition functions.

Let us start by discussing the renormalization of the effective fields. We follow the standard procedure, and define the renormalized fields $\varphi_\pm$ as

$$\varphi_{\pm,0} = \sqrt{Z_\varphi}\varphi_\pm \,, \tag{4.3.34}$$

where the wave-function renormalization factors Z_φ for the two effective fields must be equal due to RPI (4.2.35). To use Z_φ to subtract divergences in perturbation theory we would define the associated counterterm δ_φ as

$$Z_\varphi = 1 + \delta_\varphi \,. \tag{4.3.35}$$

We can directly make the following simplifying observation about this renormalization factor: when working at leading power in λ, meaning that the gradient terms in the effective action can be neglected, the kinetic term (4.2.106), expressed in terms of renormalized fields, reduces to

$$S_{\text{kin}} = -\frac{3}{2}\int \mathrm{d}^{d-1}x\mathrm{d}t \; Z_\varphi(\dot{\varphi}_+\varphi_- - \varphi_+\dot{\varphi}_-) \,. \tag{4.3.36}$$

Here, we assumed that Z_φ is time-independent, and therefore that it commutes with the time derivatives. Working in perturbation theory we would consider $\delta_\varphi(\dot{\varphi}_+\varphi_- - \varphi_+\dot{\varphi}_-)$ to be a perturbative quantity, and treat it as a vertex to be inserted in diagrams. However, the leading-power equations of motion derived from the full SdSET action imply that this term is degenerate with the interaction terms, since we could replace the insertion of terms involving effective fields with time derivatives acting on them in correlation functions by means of interaction terms. Thus, any effect that this vertex would have can be absorbed into the renormalization of the effective couplings when working at leading power in λ. Therefore, we can conclude

$$Z_\varphi = 1 + \mathcal{O}(\lambda^2) \,, \tag{4.3.37}$$

and we do not need to consider its presence further for the remainder of this chapter. We can therefore identify directly $\varphi_{\pm,0} = \varphi_\pm$ in all the following expressions.

We now turn to the renormalization of the effective couplings, for which we can follow the standard approach that is familiar from renormalization in flat-space QFT. In $d = 4-2\varepsilon$ dimensions the bare couplings have non-vanishing mass dimension, which we find using the general formula (4.3.5) to be

$$[c^0_{2n+1,1}] = 2\varepsilon n \,. \tag{4.3.38}$$

This coincides with the scaling dimension of the operators associated to these couplings, see (4.3.27), which is no surprise, since the scaling and mass dimension of all objects appearing in the action coincide. Notice also that the coupling with $n = 0$ is dimensionless in every dimension, which reflects the fact that the bilinear term $\sim \varphi_+\varphi_-$ in the action is independent of d. As we already discussed in the full theory in chapter 3, it is most convenient to work with dimensionless couplings in any dimensions, so we rewrite the bare, d-dimensional couplings by means of bare, dimensionless couplings $\hat{c}^0_{2n+1,1}$ by introducing the 't Hooft-scale $\tilde{\mu} = \sqrt{e^{\gamma_E}/(4\pi)}\mu$ of the $\overline{\text{MS}}$ scheme, as

$$c^0_{2n+1,1} = \tilde{\mu}^{2\varepsilon n}\hat{c}^0_{2n+1,1} \,, \tag{4.3.39}$$

and we wish to express the $\hat{c}^0_{2n+1,1}$ in terms of renormalized, dimensionless couplings and renormalization factors, as usual. Since in four dimensions all operators appearing in S_{int} have vanishing mass dimension, we expect that the couplings will mix under renormalization, which is a common situation whenever multiple operators with the same mass dimension are present in a theory [111]. Since we have infinitely many effective couplings with the same mass dimension, we need to introduce an "$\infty\times\infty$"-matrix of renormalization factors Z^c, and write

$$c^0_{2n+1,1} = \tilde{\mu}^{2\varepsilon n} \sum_{m=0}^{\infty} Z^c_{nm} c_{2m+1,1} \,, \tag{4.3.40}$$

where $c_{2n+1,1}$ denotes the renormalized couplings. The matrix elements of Z^c must have the structure

$$Z^c_{nm} = \delta_{nm} + \mathcal{O}(c_{2n+1,1}) \,, \tag{4.3.41}$$

since at lowest order the effective couplings are determined by means of tree-level matching computations, and therefore must be finite. Even though Z^c has infinitely many entries, there will always be only finitely many contributing at each order in the perturbative expansion of correlation functions in powers of the renormalized full-theory coupling κ, which makes the problem tractable. To renormalize the EFT couplings we will subtract the ε-pole terms that appear in a given correlation function using the renormalization factors, and leave the finite parts of the couplings undetermined. These parts are then determined by matching the renormalized SdSET correlation functions onto the renormalized full-theory correlators.

The renormalization of the effective couplings will induce an implicit dependence on the scale μ, which can be captured by means of a renormalization-group equation (RGE) for the couplings. It can be derived from (4.3.40) using the fact that the bare couplings do not depend on μ. Taking the logarithmic derivative with respect to μ on both sides of the equation we then find

$$\frac{\mathrm{d}c_{2n+1,1}}{\mathrm{d}\ln(\mu)} = -\sum_{k,l=0}^{\infty} Z^{-1}_{nk} \left[2\varepsilon k Z^c_{kl} + \frac{\mathrm{d}Z^c_{kl}}{\mathrm{d}\ln(\mu)}\right] c_{2l+1,1} \tag{4.3.42}$$

$$\equiv \sum_{l=0}^{\infty} \beta_{nl} c_{2l+1,1} \,, \tag{4.3.43}$$

where we defined the beta-function matrix

$$\beta_{nm} = -\sum_{k=0}^{\infty} Z^{-1}_{nk} \left[2\varepsilon k Z^c_{km} + \frac{\mathrm{d}Z^c_{km}}{\mathrm{d}\ln(\mu)}\right] . \tag{4.3.44}$$

The above discussion can be repeated analogously for the couplings multiplying power-suppressed terms in S_{int}, which we will not have to deal with in this thesis. In general, it is expected that all the couplings $c_{n,l}$ for a certain fixed l and arbitrary n will mix among each other, since the effective field φ_- is dimensionful, while φ_+ is not.

Finally, let us discuss the renormalization of the initial-condition functions $\Xi^\sigma_{2n+1,1;0}$. In momentum space, they have the same mass dimension as the effective couplings,

$$\left[\Xi^\sigma_{2n+1,1;0}(\vec{k}_1, ..., \vec{k}_{2n+2})\right] = 2\varepsilon n \,. \tag{4.3.45}$$

We can therefore proceed analogously and define a (mass-)dimensionless version of the bare initial-condition functions $\hat{\Xi}^\sigma_{2n+1,1;0}$ by extracting a factor $\tilde{\mu}^{n(4-d)}$, and then split the bare, dimensionless functions into initial-condition counterterms $\xi^\sigma_{2n+1,1}$ and renormalized initial-condition functions $\Xi^\sigma_{2n+1,1}$. In particular, the counterterms have to subtract (time-independent) UV divergences in SdSET correlators, and must therefore be local and momentum-independent. We find:

$$\Xi^\sigma_{2n+1,1;0}(\vec{k}_1, ..., \vec{k}_{2n+2}) = \tilde{\mu}^{2\varepsilon n} \hat{\Xi}^\sigma_{2n+1,1;0}(\vec{k}_1, ..., \vec{k}_{2n+2}) \tag{4.3.46}$$

$$= \tilde{\mu}^{2\varepsilon n} \left[\xi^\sigma_{2n+1,1} + \Xi^\sigma_{2n+1,1}(\vec{k}_1, ..., \vec{k}_{2n+2})\right] . \tag{4.3.47}$$

Differently than the case of the effective couplings, the renormalization of the non-Gaussian initial-condition functions starts already at tree level, and the counterterms $\xi^\sigma_{2n+1,1}$ will be used to remove the UV poles generated by the time integrals associated with the vertices of the EFT we alluded to above. This tells us immediately that the renormalization structure of these objects is additive, rather than multiplicative, which motivates our ansatz above. Once we go to loop level, the $\xi^{\sigma}_{2n+1,1}$ will also be used to remove UV divergences generated by momentum integrations, in addition to to the UV poles of the time integrals in the EFT.

As far as we know, and to date, there is no general theory of perturbative renormalization of the non-Gaussian initial-condition functions that we can build on, so we will refrain from the attempt of making general statements about their all-order renormalization or mixing structure, beyond what we have already stated above. For our purposes in this thesis, the equation (4.3.47) will suffice. For a study initiating the exploration of this topic in the context of super-renormalizable theories, see [123].

The renormalized initial-condition functions satisfy two sets of RGEs, one with respect to the 't Hooft-scale μ, and one with respect to the reference scale factor a_*. Let us start their discussion with the former. As for the effective couplings, we can obtain an RGE for the renormalized initial-condition functions by using the fact that the bare functions are independent of μ. Taking the logarithmic derivative of both sides of the equation (4.3.47) we find

$$\frac{\mathrm{d}}{\mathrm{d}\ln(\mu)}\Xi^{\sigma}_{2n+1,1}(\vec{k}_1,...,\vec{k}_{2n+2}) = -2\varepsilon n\Big[\xi^{\sigma}_{2n+1,1} + \Xi^{\sigma}_{2n+1,1}(\vec{k}_1,...,\vec{k}_{2n+2})\Big] - \frac{\mathrm{d}\xi^{\sigma}_{2n+1,1}}{\mathrm{d}\ln(\mu)}\,. \tag{4.3.48}$$

Notice that this equation includes the case $n = 0$, since it is mass-dimensionless in every dimension, so no factors of μ need to be introduced to write $\Xi^{\sigma}_{1,1;0}$ in terms of a bare, dimensionless function. Since the counterterms $\xi^{\sigma}_{2n+1,1}$ will depend explicitly on the renormalized couplings $c_{2n+1,1}$, their running behaviour will contribute to the running of the renormalized initial-condition functions, as we will see in the explicit results below.

To derive the RGEs in a_*, the starting point is to notice, by inspecting the momentum-space representation of the functional $F[\varphi_\pm]$ (4.3.29), that the combinations

$$a_*^{2\delta}\,\Xi^{\sigma}_{1,1;0}(\vec{k},-\vec{k}) \tag{4.3.49}$$

and

$$a_*^{2\varepsilon n}\,\Xi^{\sigma}_{2n+1,1;0}(\vec{k}_1,...,\vec{k}_{2n+2}) \tag{4.3.50}$$

for $n \geq 1$ must be independent of a_*, since the logarithmic a_*-dependence generated by the coefficients $a_*^{2\delta}$ and $a_*^{2\varepsilon n}$, respectively, combined with the pole terms contained in the counterterms $\xi^{\sigma}_{2n+1,1}$ must be cancelled by the finite functions $\Xi^{\sigma}_{2n+1,1}(\vec{k}_1,...,\vec{k}_{2n+2})$. Plugging the decomposition (4.3.47) into the above equation and taking the logarithmic derivative with respect to a_* we then find

$$\frac{\mathrm{d}}{\mathrm{d}\ln(a_*)}\Xi^{\sigma}_{1,1}(\vec{k},-\vec{k}) = -\,2\varepsilon n\Big[\xi^{\sigma}_{1,1} + \Xi^{\sigma}_{1,1}(\vec{k}-\vec{k})\Big] - \frac{\mathrm{d}\xi^{\sigma}_{1,1}}{\mathrm{d}\ln(a_*)}\,, \tag{4.3.51}$$

$$\frac{\mathrm{d}}{\mathrm{d}\ln(a_*)}\Xi^{\sigma}_{2n+1,1}(\vec{k}_1,...,\vec{k}_{2n+2}) = -\,2\varepsilon n\Big[\xi^{\sigma}_{2n+1,1} + \Xi^{\sigma}_{2n+1,1}(\vec{k}_1,...,\vec{k}_{2n+2})\Big] - \frac{\mathrm{d}\xi^{\sigma}_{2n+1,1}}{\mathrm{d}\ln(a_*)}\,, \quad n \geq 1\,. \tag{4.3.52}$$

Since we expect that the renormalized couplings will not run with a_*, the above equation will receive contributions only from the explicit a_*-dependence of the renormalized initial-condition functions, and from the implicit a_*-dependence that the initial-condition counterterms will receive at loop level, once they are used to subtract UV poles that are gnerated by the insertion of the $\Xi^{\sigma}_{2n+1,1}$ in loop diagrams. Again, we will see how this happens below using explicit results from computations.

4.3.4 Feynman rules of the SdSET

The last ingredient we need to start carrying out explicit computations in the SdSET is the specification of the Feynman rules of this theory. As we did in the full theory, we will represent correlation functions in the EFT diagrammatically by a representation that is closer to flat-space Feynman diagrams. In particular we will not place the ends of all the external legs on a horizontal line at the top of the diagrams, as is done for

Witten diagrams, since this representation will get cumbersome when we start to consider more complicated diagrams. We will, however, follow the notation of [42] and represent (+)- and (−)-type vertices by means of full and empty dots, respectively, and draw all diagrams with the various combinations of vertices explicitly. For instance, in a tree-level diagram involving four external legs we would draw the following digrams:

For the non-Gaussian initial conditions we will follow the notation of [49] and draw their insertions in diagrams as polygons with as many corners as they have fields multiplying them in the functional $F[\varphi_\pm]$. The initial-condition counterterms $\xi^{\sigma}_{2n+1,1}$ will be drawn as small polygons, and since they carry a CTP-index as well, we will draw (+)- and (−)-type vertices by means of full and empty polygons, following the notation for the vertices. For instance, in a tree-level diagram involving four external legs we would draw the following diagrams:

Finally, for the insertion of the finite part of the non-Gaussian initial conditions $\Xi^{\sigma}_{2n+1,1}$ we will draw larger versions of the same polygons as for their associated counterterms, such as:

As we saw above, the effective fields have non-vanishing two-point functions involving all combinations of $\varphi_\pm$ inserted into them. We will use the following three types of lines to represent them:

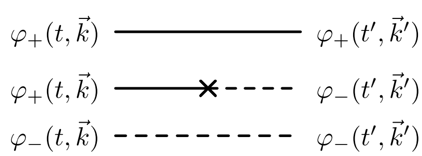

Since we will work in the standard interaction picture, all correlation functions of fields appearing in a particular diagram will be evaluated using the free-field two-point functions, which are all time-independent. Therefore, we can generalize the results found in the previous sections for equal-time two-point functions to unequal-time ones. Working in the k_Λ scheme the solid line in the above figure then represents

$$\langle \varphi_+(t,\vec{k})\varphi_+(t',\vec{k}')\rangle = (2\pi)^{d-1}\delta^{(d-1)}(\vec{k}+\vec{k}')\frac{1}{2k_\Lambda^3}\,. \tag{4.3.53}$$

The $\varphi_+\varphi_-$-propagators will always organize themselves in such a way that they can be written either in symmetric or antisymmetric combinations, which can be evaluated using the formulas

$$\langle[\varphi_+(t,\vec{k}),\varphi_-(t',\vec{k}')]\rangle = -\,(2\pi)^{d-1}\delta^{(d-1)}(\vec{k}+\vec{k}')\frac{i}{3}\,, \tag{4.3.54}$$

$$\langle\varphi_+(t,\vec{k})\varphi_-(t',\vec{k}')\rangle + \langle\varphi_-(t,\vec{k})\varphi_+(t',\vec{k}')\rangle = -\,(2\pi)^{d-1}\delta^{(d-1)}(\vec{k}+\vec{k}')\frac{\cot(\pi\nu)}{2\nu}\,, \tag{4.3.55}$$

but it will still be useful to have the above diagrammatic notation for a single propagator available. Finally, since we will work at leading power, we will never encounter the two-point function $\langle\varphi_-\varphi_-\rangle$, as it counts as λ^3 and is therefore heavily power-suppressed.

We now have all the necessary tools at our disposal to start carrying out practical computations in the SdSET. Before doing so, let us remark that to organize the perturbative expansion in powers of the effective couplings, as well as initial conditions, in a simple way, we will organize it using the scaling of both types of quantities in powers of the full-theory coupling κ.

4.4 Matching the tree-level trispectrum onto SdSET

This section is dedicated to the matching of the tree-level trispectrum of the full theory, which we computed in the previous chapter, onto SdSET. In section 3.3 we found the four-dimensional result

$$\begin{aligned}
&\lim_{-k_i\eta\to 0}\langle\phi(t,\vec{k}_1)\phi(t,\vec{k}_2)\phi(t,\vec{k}_3)\phi(t,\vec{k}_4)\rangle' \\
&= \frac{\kappa H^4}{8(k_1k_2k_3k_4)^3}\left\{\frac{1}{3}\left[\frac{1}{3}+\ln\left(\frac{e^{\gamma_E}k_t}{a(t)H}\right)\right]\sum_{j=1}^{4}k_j^3 - \frac{k_1k_2k_3k_4}{k_t} + k_t\left(\sum_{j<l}k_jk_l - \frac{4}{9}k_t^2\right)\right\},
\end{aligned} \tag{4.4.1}$$

which we aim to reproduce.

The matching equation between full-theory and SdSET correlators is most easily and transparently formulated in position space, even though for practical computations it will be most convenient to switch to momentum space afterwards. Due to the non-linear relation between ϕ and φ_+ (4.3.14), which up to $\mathcal{O}(\kappa)$ reads

$$\phi(t,\vec{x}) = H^{\frac{d}{2}-1}\left\{(a(t)H)^{-\frac{d-4}{2}}\left[\left(1+\frac{c_{1,1}^0}{9}\right)\varphi_+(t,\vec{x}) + \frac{c_{3,1}^0 a(t)^{4-d}}{18(7-d)}\varphi_+^3(t,\vec{x})\right] + (a(t)H)^{-\frac{d+2}{2}}\varphi_{-,0}(t,\vec{x})\right\}, \tag{4.4.2}$$

to match the full-theory tree-level correlator (4.4.1) at leading power correctly we need to consider the following combination of EFT-correlators in $d=4$ dimensions:

$$\begin{aligned}
&\langle\phi(t,\vec{x}_1)\phi(t,\vec{x}_2)\phi(t,\vec{x}_3)\phi(t,\vec{x}_4)\rangle\Big|_{\mathcal{O}(\kappa)} \\
=&H^4\bigg\{\langle\varphi_+(t,\vec{x}_1)\varphi_+(t,\vec{x}_2)\varphi_+(t,\vec{x}_3)\varphi_+(t,\vec{x}_4)\rangle\Big|_{\mathcal{O}(\kappa)} + \frac{c_{3,1}}{54}\Big[\langle\varphi_+^3(t,\vec{x}_1)\varphi_+(t,\vec{x}_2)\varphi_+(t,\vec{x}_3)\varphi_+(t,\vec{x}_4)\rangle\Big|_{\mathcal{O}(\kappa^0)} \\
&+\langle\varphi_+(t,\vec{x}_1)\varphi_+^3(t,\vec{x}_2)\varphi_+(t,\vec{x}_3)\varphi_+(t,\vec{x}_4)\rangle\Big|_{\mathcal{O}(\kappa^0)} + \langle\varphi_+(t,\vec{x}_1)\varphi_+(t,\vec{x}_2)\varphi_+^3(t,\vec{x}_3)\varphi_+(t,\vec{x}_4)\rangle\Big|_{\mathcal{O}(\kappa^0)} \\
&+\langle\varphi_+(t,\vec{x}_1)\varphi_+(t,\vec{x}_2)\varphi_+(t,\vec{x}_3)\varphi_+^3(t,\vec{x}_4)\rangle\Big|_{\mathcal{O}(\kappa^0)}\Big]\bigg\} + \text{terms that are subleading in } \lambda \text{ and } \kappa\,.
\end{aligned} \tag{4.4.3}$$

In the above equation we have also substituted the bare coupling $c_{3,1}^0$ for its tree-level value, which is finite and coincides with the renormalized coupling $c_{3,1}$, up to higher-order corrections in powers of the full-theory coupling κ, which do not contribute here. Notice that we have only taken into account the terms $\sim c_{3,1}\varphi_+^3$ appearing in the field redefinition, since we are interested in matching the connected components of the full-theory correlation function, and the term $\sim c_{1,1}^0\varphi_+$ only contributes to the disconnected components.

The momentum-space version of the above matching equation can then be written as

$$
\begin{aligned}
&\langle\phi(t,\vec{k}_1)\phi(t,\vec{k}_2)\phi(t,\vec{k}_3)\phi(t,\vec{k}_4)\rangle'\Big|_{\mathcal{O}(\kappa)} \\
&= H^4\Bigg\{\langle\varphi_+(t,\vec{k}_1)\varphi_+(t,\vec{k}_2)\varphi_+(t,\vec{k}_3)\varphi_+(t,\vec{k}_4)\rangle'\Big|_{\mathcal{O}(\kappa)} + \frac{c_{3,1}}{54}\Big[\langle\varphi_+^3(t,\vec{k}_1)\varphi_+(t,\vec{k}_2)\varphi_+(t,\vec{k}_3)\varphi_+(t,\vec{k}_4)\rangle'\Big|_{\mathcal{O}(\kappa^0)} \\
&\quad + \langle\varphi_+(t,\vec{k}_1)\varphi_+^3(t,\vec{k}_2)\varphi_+(t,\vec{k}_3)\varphi_+(t,\vec{k}_4)\rangle'\Big|_{\mathcal{O}(\kappa^0)} + \langle\varphi_+(t,\vec{k}_1)\varphi_+(t,\vec{k}_2)\varphi_+^3(t,\vec{k}_3)\varphi_+(t,\vec{k}_4)\rangle'\Big|_{\mathcal{O}(\kappa^0)} \\
&\quad + \langle\varphi_+(t,\vec{k}_1)\varphi_+(t,\vec{k}_2)\varphi_+(t,\vec{k}_3)\varphi_+^3(t,\vec{k}_4)\rangle'\Big|_{\mathcal{O}(\kappa^0)}\Big]\Bigg\}\,,
\end{aligned}
\tag{4.4.4}
$$

where we defined the spatial (inverse) Fourier-transform of the local composite operator $\varphi_+^n(t,\vec{x})$ (in d dimensions) as

$$
\varphi_+^n(t,\vec{k}) \equiv \int \mathrm{d}^{d-1}x\; e^{-i\vec{k}\cdot\vec{x}}\varphi_+^n(t,\vec{x})\,. \tag{4.4.5}
$$

The subscripts of the various EFT correlation functions denote at which order in the perturbative expansion in effective couplings and initial conditions they should be evaluated. The correlator involving only single fields will receive contributions from the leading-power quartic EFT vertex $\sim \varphi_+^3\varphi_-$, as well as from the non-Gaussian initial conditions. On the other hand, the correlators involving the composite operator φ_+^3 get multiplied by $c_{3,1}$, so we just need to evaluate their connected component in the Gaussian approximation, without inserting any additional interaction terms. Since we are computing tree-level correlation functions, the IR regulator is not needed, and we can let $\Lambda \to 0$ already at the start of the computation and drop the subscript "Λ" for the absolute values of momenta, which will also avoid unnecessary clutter.

Since this is the first set of computations we carry out in the EFT, it will give us a chance to see how the various rules for the SdSET that we introduced in the previous section work in practice, and we will explicitly refer to the equations that we use in each step, which we will no longer do in the next sections. As we make our way through the computation, we will also highlight the parallels between it and the region decomposition of the full-theory trispectrum we discussed previously in section 3.3.

4.4.1 Computation of the tree-level SdSET trispectrum

We start by computing the tree-level SdSET trispectrum

$$
\langle\varphi_+(t,\vec{k}_1)\varphi_+(t,\vec{k}_2)\varphi_+(t,\vec{k}_3)\varphi_+(t,\vec{k}_4)\rangle'\,, \tag{4.4.6}
$$

which receives contributions from the quartic EFT vertex $\sim c_{3,1}$, the initial-condition counterterm $\xi^\sigma_{3,1}$ and the finite initial-condition function $\Xi^\sigma_{3,1}$. We now go through these contributions one by one.

Contribution from the leading-power quartic vertex

The first contribution to the SdSET trispectrum comes from the insertion of the leading-power quartic interaction term, which reads

$$
-\frac{ic_{3,1}}{3!}\int \mathrm{d}^{d-1}x\mathrm{d}t\;(a(t)\tilde{\mu})^{4-d}\varphi_+^3(t,\vec{x})\varphi_-(t,\vec{x})\,, \tag{4.4.7}
$$

with $d = 4-2\varepsilon$. When inserted into the four-point function of φ_+ fields it leads to Schwinger-Keldysh diagrams with the following topology:

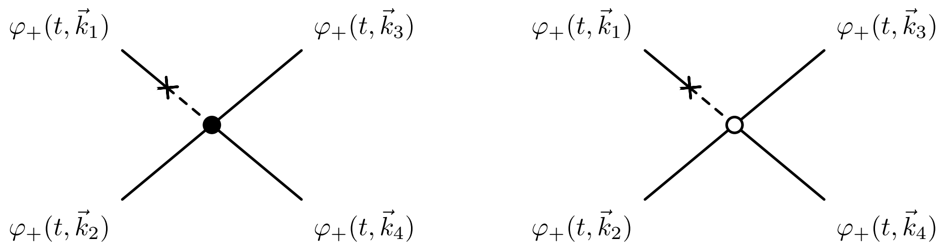

In this computation, and in the following ones in this section as well, we need to consider all four topologies where the $\langle\varphi_+\varphi_-\rangle$-propagator attaches to all four external φ_+-fields, and we just drew one exemplary topology above. Summing over all contributing diagrams we find the expression

$$
\begin{aligned}
&\langle\varphi_+(t,\vec{k}_1)\varphi_+(t,\vec{k}_2)\varphi_+(t,\vec{k}_3)\varphi_+(t,\vec{k}_4)\rangle'\Big|_{c_{3,1}} \\
&= \frac{3!\,ic_{3,1}}{3!}\int_{-\infty}^{t}\mathrm{d}t'\;(a(t')\tilde{\mu})^{2\varepsilon}\sum_{i=1}^{4}\Bigg[\langle\overline{T}\{\varphi_+(t,\vec{k}_i)\varphi_-(t',-\vec{k}_i)\}\rangle'\prod_{\substack{j=1\\ j\neq i}}^{4}\langle\overline{T}\{\varphi_+(t,\vec{k}_j)\varphi_+(t',-\vec{k}_j)\}\rangle' \\
&\quad-\langle T\{\varphi_+(t,\vec{k}_i)\varphi_-(t',-\vec{k}_i)\}\rangle'\prod_{\substack{j=1\\ j\neq i}}^{4}\langle T\{\varphi_+(t,\vec{k}_j)\varphi_+(t',-\vec{k}_j)\}\rangle'\Bigg] \\
&= -\,ic_{3,1}\tilde{\mu}^{2\varepsilon}\int_{-\infty}^{t}\mathrm{d}t'\;a(t')^{2\varepsilon}\sum_{i=1}^{4}\langle[\varphi_+(t,\vec{k}_i),\varphi_-(t',-\vec{k}_i)]\rangle'\prod_{\substack{j=1\\ j\neq i}}^{4}\langle\varphi_+(t',\vec{k}_j)\varphi_+(t,\vec{k}_j)\rangle'\,, \qquad (4.4.8)
\end{aligned}
$$

where we have stripped off an overall momentum-conserving delta distribution using the primed notation (3.1.26). Using the EFT two-point functions (4.3.53) and (4.3.54), which are both time-independent, we see that the only term which gets integrated over time is $a(t')^{2\varepsilon}$, and using the formula (4.3.25) to evaluate this integral we find the result

$$
\begin{aligned}
\langle\varphi_+(t,\vec{k}_1)\varphi_+(t,\vec{k}_2)\varphi_+(t,\vec{k}_3)\varphi_+(t,\vec{k}_4)\rangle'\Big|_{c_{3,1}} &= ic_{3,1}\frac{i}{3}\frac{1}{8(k_1k_2k_3k_4)^3}\frac{(a(t)\tilde{\mu})^{2\varepsilon}}{2\varepsilon}\sum_{j=1}^{4}k_j^3 \\
&= \frac{\tilde{\mu}^{2\varepsilon}c_{3,1}}{24(k_1k_2k_3k_4)^3}\left[-\frac{1}{2\varepsilon}+\ln\left(\frac{1}{a(t)}\right)+\mathcal{O}(\varepsilon)\right]\sum_{j=1}^{4}k_j^3\,. \qquad (4.4.9)
\end{aligned}
$$

We observe the first instance of a pole term being generated by a time integral in the SdSET already at tree level. It comes from the lower integration boundary of the time integral, and as such we classify it as a UV pole. The ε-expansion of the divergent result generates the time-dependent part of the secular logarithm that appears in the full result, and this parallels exactly what happened in the region decomposition of the time integral of the full-theory result. In the above equation we have left the factor $\tilde{\mu}^{2\varepsilon}$ unexpanded, since it will appear as a common factor in all other contributions to the SdSET trispectrum as well, so any terms that would be generated by its ε-expansion would just drop out as we subtract the pole term.

Insertion of $\xi^{\sigma}_{3,1}$, renormalization of the tree-level SdSET trispectrum

We saw that the insertion of the quartic interaction vertex led to the appearence of a UV pole, which needs to be renormalized by an appropriate counterterm, which is the initial-condition counterterm $\xi^{\sigma}_{3,1}$. It appears in the SdSET path integral through the term

$$i\frac{a_*^{4-d}}{3!}\xi^{\sigma}_{3,1}\int\left[\prod_{j=1}^{4}\frac{\mathrm{d}^{d-1}k_j}{(2\pi)^{d-1}}\right]\varphi^{\sigma}_{+}(t_*,\vec{k}_1)\varphi^{\sigma}_{+}(t_*,\vec{k}_1)\varphi^{\sigma}_{+}(t_*,\vec{k}_2)\varphi^{\sigma}_{+}(t_*,\vec{k}_3)\varphi^{\sigma}_{-}(t_*,\vec{k}_4)(2\pi)^{d-1}\delta^{(d-1)}\left(\sum_{l=1}^{4}\vec{k}_l\right) \tag{4.4.10}$$

and its insertion into the trispectrum leads to diagrams with topology

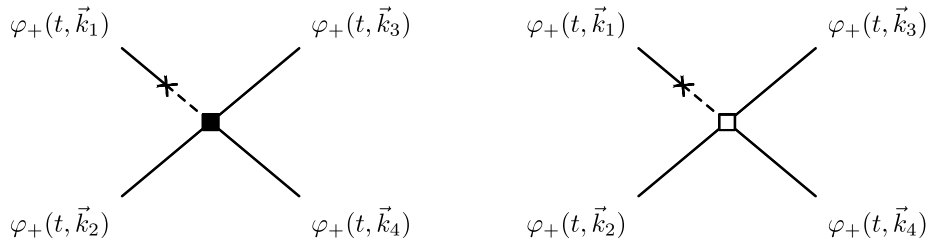

These diagrams are fully analogous to the ones we found while considering the vertex insertion, and the computation that follows from them is analogous as well:

$$\begin{aligned}
&\langle\varphi_+(t,\vec{k}_1)\varphi_+(t,\vec{k}_2)\varphi_+(t,\vec{k}_3)\varphi_+(t,\vec{k}_4)\rangle'\Big|_{\xi^{\sigma}_{3,1}}\\
&=\frac{3!}{3!}i(a_*\tilde{\mu})^{2\varepsilon}\sum_{i=1}^{4}\Bigg\{\xi^{+}_{3,1}\Bigg[\langle\overline{T}\{\varphi_+(t,\vec{k}_i)\varphi_-(t_*,-\vec{k}_i)\}\rangle'\prod_{\substack{j=1\\ j\neq i}}^{4}\langle\overline{T}\{\varphi_+(t,\vec{k}_j)\varphi_+(t_*,-\vec{k}_j)\}\rangle'\Bigg]\\
&\quad+\xi^{-}_{3,1}\langle T\{\varphi_+(t,\vec{k}_i)\varphi_-(t_*,-\vec{k}_i)\}\rangle'\Bigg[\prod_{\substack{j=1\\ j\neq i}}^{4}\langle T\{\varphi_+(t,\vec{k}_j)\varphi_+(t_*,-\vec{k}_j)\}\rangle'\Bigg]\Bigg\}\\
&=-\,i(a_*\tilde{\mu})^{2\varepsilon}\xi^{+}_{3,1}\sum_{i=1}^{4}\langle[\varphi_+(t,\vec{k}_i),\varphi_-(t_*,-\vec{k}_i)]\rangle'\prod_{\substack{j=1\\ j\neq i}}^{4}\langle\varphi_+(t_*,\vec{k}_j)\varphi_+(t,\vec{k}_j)\rangle'\\
&=-\,\frac{(a_*\tilde{\mu})^{2\varepsilon}}{24(k_1k_2k_3k_4)^3}\xi^{+}_{3,1}\sum_{j=1}^{4}k_j^3\,,
\end{aligned} \tag{4.4.11}$$

where we used the relation (4.3.18) in order to express the result only in terms of $\xi^{+}_{3,1}$. Comparing this result to (4.4.9), we see that the momentum structure of the two results matches. In order to subtract the pole from the time integral when summing the two contributions to the SdSET trispectrum we need to choose

$$\xi^{\sigma}_{3,1}=-\frac{\sigma c_{3,1}}{2\varepsilon}\,. \tag{4.4.12}$$

Notice that the counterterm is fully determined within the EFT, without the need of any input from matching. This pole term coincides with the late-time pole that was generated by the time integral appearing in the early-time region of the full-theory trispectrum in section 3.3.

Expanding the resulting contribution to the trispectrum in ε and letting $\varepsilon\to 0$ after the pole has been subtracted we find the following renormalized EFT result:

$$\begin{aligned}
&\langle\varphi_+(t,\vec{k}_1)\varphi_+(t,\vec{k}_2)\varphi_+(t,\vec{k}_3)\varphi_+(t,\vec{k}_4)\rangle'\Big|_{c_{3,1}}+\langle\varphi_+(t,\vec{k}_1)\varphi_+(t,\vec{k}_2)\varphi_+(t,\vec{k}_3)\varphi_+(t,\vec{k}_4)\rangle'\Big|_{\xi_{3,1}}\\
&=\frac{c_{3,1}}{24(k_1k_2k_3k_4)^3}\ln\left(\frac{a_*}{a(t)}\right)\sum_{j=1}^{4}k_j^3\,.
\end{aligned} \tag{4.4.13}$$

We see that the result is now finite, but it depends on the reference scale factor a_*. Therefore, a_* plays the role of the factorization scale in this result, and tracks its time-dependence.

Insertion of $\Xi^\sigma_{3,1}$

The final contribution to the SdSET trispectrum comes from the insertion of the finite part of the four-point initial condition $\Xi^\sigma_{3,1}$, which appears in the SdSET path integral in the term

$$i\frac{a_*^{4-d}}{3!}\int\left[\prod_{j=1}^{4}\frac{\mathrm{d}^{d-1}k_j}{(2\pi)^{d-1}}\right]\Xi^\sigma_{3,1}(\vec{k}_1,\vec{k}_2,\vec{k}_3,\vec{k}_4)\varphi^\sigma_+(t_*,\vec{k}_1)\varphi^\sigma_+(t_*,\vec{k}_1)\varphi^\sigma_+(t_*,\vec{k}_2)\varphi^\sigma_+(t_*,\vec{k}_3)\varphi^\sigma_-(t_*,\vec{k}_4)$$
$$\times(2\pi)^{d-1}\delta^{(d-1)}\left(\sum_{l=1}^{4}\vec{k}_l\right). \tag{4.4.14}$$

It represents the finite piece of the early-time region of the full-theory trispectrum we considered above. Its insertion leads to diagrams with topology

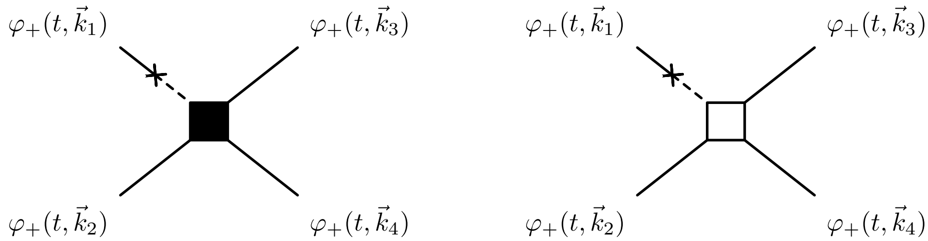

A completely analogous computation to the case of the initial-condition counterterm $\xi^\sigma_{3,1}$ leads to the result

$$\langle\varphi_+(t,\vec{k}_1)\varphi_+(t,\vec{k}_2)\varphi_+(t,\vec{k}_3)\varphi_+(t,\vec{k}_4)\rangle'\Big|_{\Xi_{3,1}} = -\frac{(a_*\tilde{\mu})^{2\varepsilon}}{24(k_1k_2k_3k_4)^3}\Xi^+_{3,1}(\vec{k}_1,\vec{k}_2,\vec{k}_3,\vec{k}_4)\sum_{j=1}^{4}k_j^3\,. \tag{4.4.15}$$

Letting $\varepsilon\to 0$, since $\Xi^+_{3,1}(\vec{k}_1,\vec{k}_2,\vec{k}_3,\vec{k}_4)$ is finite by definition, and summing this contribution to the EFT trispectrum with the other two we found above, we get the final expression for the renormalized SdSET trispectrum:

$$\begin{aligned}&\langle\varphi_+(t,\vec{k}_1)\varphi_+(t,\vec{k}_2)\varphi_+(t,\vec{k}_3)\varphi_+(t,\vec{k}_4)\rangle'\Big|_{c_{3,1}}+\langle\varphi_+(t,\vec{k}_1)\varphi_+(t,\vec{k}_2)\varphi_+(t,\vec{k}_3)\varphi_+(t,\vec{k}_4)\rangle'\Big|_{\xi_{3,1}}\\&+\langle\varphi_+(t,\vec{k}_1)\varphi_+(t,\vec{k}_2)\varphi_+(t,\vec{k}_3)\varphi_+(t,\vec{k}_4)\rangle'\Big|_{\Xi_{3,1}}\\=&\frac{1}{24(k_1k_2k_3k_4)^3}\left\{c_{3,1}\ln\left(\frac{a_*}{a(t)}\right)-\Xi^+_{3,1}(\vec{k}_1,\vec{k}_2,\vec{k}_3,\vec{k}_4)\right\}\sum_{j=1}^{4}k_j^3\,.\end{aligned} \tag{4.4.16}$$

As we anticipated from the general considerations in the previous section, this result contains two unknown quantities, $c_{3,1}$ and $\Xi^+_{3,1}$, both of which need to be determined by matching onto the full-theory result (4.4.1). Before doing so, however, we need to compute the contributions from the other four correlators appearing in (4.4.4).

4.4.2 Correlators following from the φ_--field redefinition

We evaluate the four correlation functions involving the composite operator φ_+^3 appearing in (4.4.4) in the Gaussian approximation. We are only interested in the connected components of these correlators, which are obtained by taking the Wick contraction of the single field appearing in it with the three fields that φ_+^3 is made up of. Exemplarily, we find

$$\langle\varphi_+^3(t,\vec{x}_1)\varphi_+(t,\vec{x}_2)\varphi_+(t,\vec{x}_3)\varphi_+(t,\vec{x}_4)\rangle = 3!\,\langle\varphi_+(t,\vec{x}_1)\varphi_+(t,\vec{x}_2)\rangle\langle\varphi_+(t,\vec{x}_1)\varphi_+(t,\vec{x}_3)\rangle\langle\varphi_+(t,\vec{x}_1)\varphi_+(t,\vec{x}_4)\rangle\,, \tag{4.4.17}$$

and the Fourier-transform of the above equation, using the notation introduced in (4.4.5), reads

$$\langle\varphi_+^3(t,\vec{k}_1)\varphi_+(t,\vec{k}_2)\varphi_+(t,\vec{k}_3)\varphi_+(t,\vec{k}_4)\rangle' = \frac{3}{4(k_2k_3k_4)^3}\,. \tag{4.4.18}$$

The result for the remaining three correlators can be obtained from the above equation, by just taking permutations of the labels of the momenta. We then find the following momentum-space result for the sum of these four correlation functions, multiplied by $c_{3,1}/54$ according to equation (4.4.4):

$$\begin{aligned}
&\langle\varphi_+(t,\vec{k}_1)\varphi_+(t,\vec{k}_2)\varphi_+(t,\vec{k}_3)\varphi_+(t,\vec{k}_4)\rangle'\Big|_{\text{redef.}}\\
\equiv&\frac{c_{3,1}}{54}\Big[\langle\varphi_+^3(t,\vec{k}_1)\varphi_+(t,\vec{k}_2)\varphi_+(t,\vec{k}_3)\varphi_+(t,\vec{k}_4)\rangle' + \langle\varphi_+(t,\vec{k}_1)\varphi_+^3(t,\vec{k}_2)\varphi_+(t,\vec{k}_3)\varphi_+(t,\vec{k}_4)\rangle'\\
&+\langle\varphi_+(t,\vec{k}_1)\varphi_+(t,\vec{k}_2)\varphi_+^3(t,\vec{k}_3)\varphi_+(t,\vec{k}_4)\rangle' + \langle\varphi_+(t,\vec{k}_1)\varphi_+(t,\vec{k}_2)\varphi_+(t,\vec{k}_3)\varphi_+^3(t,\vec{k}_4)\rangle'\Big] && (4.4.19)\\
=&\frac{c_{3,1}}{24(k_1k_2k_3k_4)^3}\frac{1}{3}\sum_{j=1}^4 k_j^3\,. && (4.4.20)
\end{aligned}$$

In the above equation, we are denoting the entire combination by means of the correlation function defined above for conciseness.

4.4.3 Complete EFT result, matching of $c_{3,1}$ and $\Xi^\sigma_{3,1}$

Adding up what we found previously we get the full, renormalized EFT result in $d = 4$ dimensions:

$$\begin{aligned}
&\langle\varphi_+(t,\vec{k}_1)\varphi_+(t,\vec{k}_2)\varphi_+(t,\vec{k}_3)\varphi_+(t,\vec{k}_4)\rangle'\Big|_{c_{3,1}} + \langle\varphi_+(t,\vec{k}_1)\varphi_+(t,\vec{k}_2)\varphi_+(t,\vec{k}_3)\varphi_+(t,\vec{k}_4)\rangle'\Big|_{\xi_{3,1}}\\
&+\langle\varphi_+(t,\vec{k}_1)\varphi_+(t,\vec{k}_2)\varphi_+(t,\vec{k}_3)\varphi_+(t,\vec{k}_4)\rangle'\Big|_{\Xi_{3,1}} + \langle\varphi_+(t,\vec{k}_1)\varphi_+(t,\vec{k}_2)\varphi_+(t,\vec{k}_3)\varphi_+(t,\vec{k}_4)\rangle'\Big|_{\text{redef.}}\\
=&\frac{1}{24(k_1k_2k_3k_4)^3}\left\{c_{3,1}\left[\ln\left(\frac{a_*}{a(t)}\right)+\frac{1}{3}\right] - \Xi^+_{3,1}(\vec{k}_1,\vec{k}_2,\vec{k}_3,\vec{k}_4)\right\}\sum_{j=1}^4 k_j^3\,. && (4.4.21)
\end{aligned}$$

We can now match this renormalized result onto the full-theory result (4.4.1), which we reprint here for convenience,

$$\begin{aligned}
&\lim_{-k_i\eta\to0}\langle\phi(t,\vec{k}_1)\phi(t,\vec{k}_2)\phi(t,\vec{k}_3)\phi(t,\vec{k}_4)\rangle'\\
=&\frac{\kappa H^4}{8(k_1k_2k_3k_4)^3}\left\{\frac{1}{3}\left[\frac{1}{3}+\ln\left(\frac{e^{\gamma_E}k_t}{a(t)H}\right)\right]\sum_{j=1}^4 k_j^3 - \frac{k_1k_2k_3k_4}{k_t} + k_t\left(\sum_{j<l}k_jk_l - \frac{4}{9}k_t^2\right)\right\}, && (4.4.22)
\end{aligned}$$

by means of the matching equation (4.4.4). The effective coupling $c_{3,1}$ is uniquely determined by comparing the coefficients of the time-dependent logarithm, and at this order in the perturbative expansion it is simply

$$c_{3,1} = \kappa\,. \tag{4.4.23}$$

We anticipate that this result will receive higher-order corrections in the full-theory coupling. The initial-condition function $\Xi^+_{3,1}(\vec{k}_1,\vec{k}_2,\vec{k}_3,\vec{k}_4)$ then needs to reproduce the remaining, time-independent terms, and to compensate the dependence of the EFT-result on a_*. We find

$$\Xi^\sigma_{3,1}(\vec{k}_1, \vec{k}_2, \vec{k}_3, \vec{k}_4) = -3\sigma\kappa \left\{ \frac{1}{3} \ln\left(\frac{e^{\gamma_E} k_t}{a_* H}\right) + \left(\sum_{j=1}^{4} k_j^3\right)^{-1} \left[-\frac{k_1 k_2 k_3 k_4}{k_t} + k_t \left(\sum_{j<l} k_j k_l - \frac{4}{9} k_t^2\right)\right]\right\}, \quad (4.4.24)$$

which will also receive higher-order corrections in powers of the full-theory coupling.

4.4.4 Renormalization-group evolution of $c_{3,1}$ and $\Xi^\sigma_{3,1}$

We can now use these first explicit results for $c_{3,1}$ and $\Xi^\sigma_{3,1}$ to study their running behaviour with μ and a_*, applying the general formalism we set up in section 4.3.3.

Running with μ

At tree level, the renormalization-factor matrix for the couplings is just $Z^c_{nm} = \delta_{nm}$, so the RGE for the couplings (4.3.42) for the case of $c_{3,1}$ implies simply

$$\frac{\mathrm{d}c_{3,1}}{\mathrm{d}\ln(\mu)} = -2\varepsilon c_{3,1} \,. \quad (4.4.25)$$

As $\varepsilon \to 0$ the right-hand side of this equation vanishes. However, this "tree-level running" of $c_{3,1}$ will play an extremely important role below, when we start discussing results from loop diagrams, since as the $\mathcal{O}(\varepsilon)$-term hits a pole term it can leave a finite remainder in the limit $\varepsilon \to 0$. In fact, this is the mechanism by means of which all beta-function and anomalous-dimension terms are generated in the formalism that we are using.

The μ-RGE for $\Xi^\sigma_{3,1}$ that follows from the general formula (4.3.48) reads

$$\frac{\mathrm{d}}{\mathrm{d}\ln(\mu)} \Xi^\sigma_{3,1}(\vec{k}_1, \vec{k}_2, \vec{k}_3, \vec{k}_4) = -2\varepsilon \Big[\xi^\sigma_{3,1} + \Xi^\sigma_{3,1}(\vec{k}_1, \vec{k}_2, \vec{k}_3, \vec{k}_4)\Big] - \frac{\mathrm{d}\xi^\sigma_{3,1}}{\mathrm{d}\ln(\mu)} \,. \quad (4.4.26)$$

By renormalizing the tree-level trispectrum we found that

$$\xi^\sigma_{3,1} = -\frac{\sigma c_{3,1}}{2\varepsilon} \,, \quad (4.4.27)$$

and, using the tree-level running of $c_{3,1}$ (4.4.25) the result for the $\ln(\mu)$-derivative of $\xi^\sigma_{3,1}$ reads

$$\frac{\mathrm{d}\xi^\sigma_{3,1}}{\mathrm{d}\ln(\mu)} = \sigma c_{3,1} \,. \quad (4.4.28)$$

Plugging this expression in the above equation, we find the following tree-level RGE for $\Xi^\sigma_{3,1}$:

$$\frac{\mathrm{d}}{\mathrm{d}\ln(\mu)} \Xi^\sigma_{3,1}(\vec{k}_1, \vec{k}_2, \vec{k}_3, \vec{k}_4) = -2\varepsilon \Xi^\sigma_{3,1}(\vec{k}_1, \vec{k}_2, \vec{k}_3, \vec{k}_4) \,, \quad (4.4.29)$$

which is analogous to the one for $c_{3,1}$. As is the case for the running couplings, the tree-level running of $\Xi^\sigma_{3,1}$ becomes crucial when discussing the results of loop diagrams, since it can generate a finite remainder when it hits a UV pole, and we must therefore keep track of it. Since at this order in the expansion the running behaviour of $\Xi^\sigma_{3,1}$ is very simple, just being multiplicative, it can be implemented by letting the coupling multiplying the found result for $\Xi^\sigma_{3,1}$, see equation (4.4.24), run according to (4.4.29), analogously to $c_{3,1}$. We can get some more precise information about this coupling by studying the a_*-running of $\Xi^\sigma_{3,1}$.

Running with a_*

We now inspect the running behaviour of the matched quantities with the scale a_*.

The effective coupling $c_{3,1}$ that we have defined and matched above does not depend on the scale a_* explicitly nor implicitly, so, at least at this order in the expansion, we have

$$\frac{\mathrm{d}c_{3,1}}{\mathrm{d}\ln(a_*)} = 0\,. \tag{4.4.30}$$

On the other hand, the a_*-dependence of the renormalized initial-condition function $\Xi^{\sigma}_{3,1}$ is controlled by (4.3.52), which in this case reads

$$\frac{\mathrm{d}}{\mathrm{d}\ln(a_*)}\Xi^{\sigma}_{3,1}(\vec{k}_1,\vec{k}_2,\vec{k}_3,\vec{k}_4) = -2\varepsilon\Big[\xi^{\sigma}_{3,1} + \Xi^{\sigma}_{3,1}(\vec{k}_1,\vec{k}_2,\vec{k}_3,\vec{k}_4)\Big] - \frac{\mathrm{d}\xi^{\sigma}_{3,1}}{\mathrm{d}\ln(a_*)}\,. \tag{4.4.31}$$

Using the tree-level result for $\xi^{\sigma}_{3,1}$, as well as (4.4.30), it follows that at this order in the expansion we have

$$\frac{\mathrm{d}\xi^{\sigma}_{3,1}}{\mathrm{d}\ln(a_*)} = 0\,, \tag{4.4.32}$$

and, therefore, we get the result

$$\frac{\mathrm{d}}{\mathrm{d}\ln(a_*)}\Xi^{\sigma}_{3,1}(\vec{k}_1,\vec{k}_2,\vec{k}_3,\vec{k}_4) = \sigma c_{3,1} - 2\varepsilon\Xi^{\sigma}_{3,1}(\vec{k}_1,\vec{k}_2,\vec{k}_3,\vec{k}_4)\,. \tag{4.4.33}$$

Both the running in μ and a_* can be implemented by interpreting the factor of κ appearing in (4.4.24) as being a new coupling $g_{3,1}$, which gives us the expression

$$\Xi^{\sigma}_{3,1}(\mu;\vec{k}_1,\vec{k}_2,\vec{k}_3,\vec{k}_4) = -3\sigma g_{3,1}\left\{\frac{1}{3}\ln\left(\frac{e^{\gamma_E}k_t}{a_*H}\right) + \left(\sum_{j=1}^{4}k_j^3\right)^{-1}\left[-\frac{k_1k_2k_3k_4}{k_t} + k_t\left(\sum_{j<l}k_jk_l - \frac{4}{9}k_t^2\right)\right]\right\}. \tag{4.4.34}$$

The coupling $g_{3,1}$ can be used as a bookkeeping device to track the contributions from the running of $\Xi^{\sigma}_{3,1}$ in results from loop diagrams. From the above equations, it follows that it should have the same value as $c_{3,1}$ at tree level, but the tree-level running

$$\frac{\mathrm{d}g_{3,1}}{\mathrm{d}\ln(\mu)} = \frac{\mathrm{d}g_{3,1}}{\mathrm{d}\ln(a_*)} = -2\varepsilon g_{3,1} = -2\varepsilon c_{3,1}\,, \tag{4.4.35}$$

which differs from the found running of $c_{3,1}$. With the introduction of $g_{3,1}$, we see that the inhomogeneous term on the right-hand side of of (4.4.33) is reproduced by the explicitly appearing $\ln(a_*)$, while the homogeneous term is reproduced by the running of $g_{3,1}$.

4.5 Matching the one-loop power spectrum onto SdSET

Having determined the tree-level values of the quartic EFT coupling $c_{3,1}$ and four-point initial condition $\Xi^{\sigma}_{3,1}$, we now turn to our first loop-level computation in SdSET, which is the one-loop power spectrum. Since we will be dealing with both UV- and IR-divergent quantities, we now have to keep the full d- and Λ-dependence of the quantities we will consider in the EFT intact. In section 3.4.1 we found the following renormalized result for the one-loop power spectrum, working in the k_Λ-scheme:

$$\begin{aligned}\langle\phi(t,\vec{k})\phi(t,-\vec{k})\rangle'\Big|_{\mathcal{O}(\kappa)} =& \frac{\kappa H^2}{24\pi^2k^3}\left\{\left[2-\ln\left(\frac{2e^{\gamma_E}k}{a(t)H}\right)\right]\left[\ln\left(\frac{\Lambda}{a(t)\mu}\right) - \delta\hat{m}^2_{\text{fin}}\right] + \frac{1}{2}\ln^2\left(\frac{2e^{\gamma_E}k}{a(t)H}\right)\right.\\ &\left. - \frac{7}{3}\ln\left(\frac{2e^{\gamma_E}k}{a(t)H}\right) + \frac{8}{3} - \frac{\pi^2}{24}\right\},\end{aligned} \tag{4.5.1}$$

and in this section we will reproduce it using the SdSET. The computation will serve as a first example of how UV divergences from momentum integrals can be renormalized consistently within the EFT, and it will allow us to determine the values of the renormalized SdSET coupling $c_{1,1}$ and initial condition $\Xi^{\sigma}_{1,1}$.

The non-linear relation between full-theory and EFT fields

$$\phi(t,\vec{x}) = H^{\frac{d}{2}-1}\left\{(a(t)H)^{-\frac{d-4}{2}}\left[\left(1+\frac{c^0_{1,1}}{9}\right)\varphi_+(t,\vec{x}) + \frac{c^0_{3,1}a(t)^{4-d}}{18(7-d)}\varphi_+^3(t,\vec{x})\right] + (a(t)H)^{-\frac{d+2}{2}}\varphi_{-,0}(t,\vec{x})\right\} \tag{4.5.2}$$

implies the following $d = 4-2\varepsilon$-dimensional momentum-space matching equation between full-theory and EFT correlators, at $\mathcal{O}(\kappa)$:

$$\begin{aligned}\langle\phi(t,\vec{k})\phi(t,-\vec{k})\rangle'\Big|_{\mathcal{O}(\kappa)} =& H^2 a(t)^{2\varepsilon}\Bigg[\langle\varphi_+(t,\vec{k})\varphi_+(t,-\vec{k})\rangle'\Big|_{\mathcal{O}(\kappa)} + \frac{2c^0_{1,1}}{9}\langle\varphi_+(t,\vec{k})\varphi_+(t,-\vec{k})\rangle'\Big|_{\mathcal{O}(\kappa^0)} \\ &+ \frac{c^0_{3,1}a(t)^{2\varepsilon}}{18(3+2\varepsilon)}\Big(\langle\varphi_+^3(t,\vec{k})\varphi_+(t,-\vec{k})\rangle'\Big|_{\mathcal{O}(\kappa^0)} + \langle\varphi_+(t,\vec{k})\varphi_+^3(t,-\vec{k})\rangle'\Big|_{\mathcal{O}(\kappa^0)}\Big)\Bigg].\end{aligned} \tag{4.5.3}$$

We are again using the notation (4.4.5) for the Fourier transforms of the composite operators φ_+^n. We will find below that the combination of EFT correlation functions in the angled brackets appearing in (4.5.3) is finite, so we can just set the overall coefficient $a(t)^{2\varepsilon}$ to one. The subscripts of the EFT correlation functions denote at which order in the perturbative expansion in the couplings and initial conditions they should be evaluated.

4.5.1 One-loop SdSET power spectrum

We start by evaluating the correlation function

$$\langle\varphi_+(t,\vec{k})\varphi_+(t,-\vec{k})\rangle'\Big|_{\mathcal{O}(\kappa)}, \tag{4.5.4}$$

which receives contributions from the insertions of the quartic vertex $c_{3,1}$, the initial-condition counterterm $\xi^{\sigma}_{3,1}$ and the finite initial-condition function $\Xi^{\sigma}_{3,1}$, which have all been determined at tree level, meaning at $\mathcal{O}(\kappa)$, in the previous section. In addition to these already-known quantities, the insertions of the bare vertex $c^0_{1,1}$ and bare initial condition $\Xi^{\sigma}_{1,1;0}$ also contribute. They will be decomposed into counterterms and finite parts, respectively, and we will then use the counterterms to remove all UV divergences appearing in the EFT results, while the finite parts will be determined at the end of the computation by matching onto the full-theory result.

Insertions of the leading-power quartic vertex and $\xi^{\sigma}_{3,1}$

We start by considering the contributions to the one-loop power spectrum coming from the insertions of the quartic EFT vertex $\sim c_{3,1}$, see (4.4.7), and initial-condition counterterm $\sim \xi^{\sigma}_{3,1}$, see (4.4.10). It will prove convenient to consider their sum directly, which will become evident shortly.

When inserted into the power spectrum, the quartic vertex leads to diagrams with the following topology:

Similarly to the diagrams we considered in the previous section, in addition to the above topologies we need to consider the diagrams where the $\langle\varphi_+\varphi_-\rangle$ propagator attaches to the external field $\varphi_+(t,-\vec{k})$ as well. Their sum then correspond to the mathematical expression

$$\begin{aligned}\langle\varphi_+(t,\vec{k})\varphi_+(t,-\vec{k})\rangle'\Big|_{c_{3,1}} =& i\tilde{\mu}^{2\varepsilon}c_{3,1}\frac{i}{3}\frac{1}{4k_\Lambda^3}\int_{-\infty}^{t}\mathrm{d}t'\ (a(t'))^{2\varepsilon}\int\frac{\mathrm{d}^{d-1}l}{(2\pi)^{d-1}}\frac{1}{l_\Lambda^3}\\ =& -\frac{c_{3,1}}{12k^3}\frac{1}{2\varepsilon}\frac{1}{4\pi^2}\left(\frac{\Lambda^2}{4\pi a(t)^2\tilde{\mu}^2}\right)^{-\varepsilon}\Gamma(\varepsilon)\,,\end{aligned} \tag{4.5.5}$$

where we replaced $k_\Lambda \to k$ for the external momentum after computing the loop integral, since the result of the loop integration does not involve any inverse powers of Λ, and therefore the expansion of the result as $\Lambda \to 0$ is simply equivalent to dropping the subscript for the external momentum. We will do so also in the remaining terms that we compute in this section.

Notice that we are not considering diagrams with topology

because they simply give a vanishing result: we are connecting the propagator $\langle\varphi_+\varphi_-\rangle$ to the same point, so we use the unordered Wightman function for it, and since the φ_+-fields commute the two diagrams have the same $\langle\varphi_+\varphi_+\rangle$-propagators attaching the vertex to the external points as well. Therefore, because of the relative minus sign between the two diagrams, we are subtracting two copies of the same diagram from each other, and get zero. This is a general observation that will hold also for all following SdSET diagrams we will consider: diagrams containing a $\langle\varphi_+\varphi_-\rangle$-line attaching to the same vertex will drop out once we sum over CTP indices. We will therefore ignore them in the following. This can be understood from the multiple-commutator formula (1.4.6) as well, since diagrams like this would correspond to exchanging the order of field operators appearing in the quartic vertex $\varphi_+^3\varphi_-$, which never occurs in the prescription given by (1.4.6) to compute in-in correlation functions. Thus, these terms should be absent in the diagrammatic approach as well, and indeed we find that they are.

The result (4.5.5) could be expanded in ε, which would generate double- and single-poles in ε. However, it is more convenient to first compute the contribution to the power spectrum coming from the insertion of $\xi^\sigma_{3,1}$, and expand the sum of the two, since the double-pole terms will drop out by construction and the expansion of the sum will be simpler than the expansion of the individual results. The insertion of the initial-condition counterterm in the power spectrum leads to diagrams with topology

which then yield the expression

$$\begin{aligned}\langle\varphi_+(t,\vec{k})\varphi_+(t,-\vec{k})\rangle'\Big|_{\xi_{3,1}} =& -\frac{1}{3}\frac{(a_*\tilde{\mu})^{2\varepsilon}\xi^+_{3,1}}{4k_\Lambda^3}\int\frac{\mathrm{d}^{d-1}l}{(2\pi)^{d-1}}\frac{1}{l_\Lambda^3}\\ =& \frac{(a_*\tilde{\mu})^{2\varepsilon}}{12k^3}\frac{c_{3,1}}{2\varepsilon}\frac{1}{4\pi^2}\left(\frac{\Lambda^2}{4\pi a(t)^2\tilde{\mu}^2}\right)^{-\varepsilon}\Gamma(\varepsilon)\,,\end{aligned} \tag{4.5.6}$$

where we plugged in the value

$$\xi^{+}_{3,1} = -\frac{c_{3,1}}{2\varepsilon} \tag{4.5.7}$$

obtained in the previous section. Summing the two contributions that we found, and expanding the result in ε, we get

$$\begin{aligned}\langle \varphi_+(t,\vec{k})\varphi_+(t,-\vec{k})\rangle'\Big|_{c_{3,1}} + \langle \varphi_+(t,\vec{k})\varphi_+(t,-\vec{k})\rangle'\Big|_{\xi_{3,1}} =& \frac{c_{3,1}}{12k^3}\frac{a_*^{2\varepsilon}-a(t)^{2\varepsilon}}{2\varepsilon}\left(\frac{\Lambda^2}{4\pi a(t)^2\tilde{\mu}^2}\right)^{-\varepsilon}\Gamma(\varepsilon) && (4.5.8)\\ =& \frac{c_{3,1}}{48\pi^2 k^3}\left(\frac{\Lambda}{a(t)\mu}\right)^{-2\varepsilon}\ln\left(\frac{a_*}{a(t)}\right)\left[\frac{1}{\varepsilon}+\ln\left(\frac{a_*}{a(t)}\right)\right], && (4.5.9)\end{aligned}$$

where we used $\tilde{\mu} = \mu\sqrt{e^{\gamma_E}/(4\pi)}$. As anticipated, the result only contains single-pole terms, as a result of the partial cancellation occurring between the two contributions. This pole term should be interpreted asthe UV pole stemming from the momentum integral alone, since only the finite piece of the combination $[a_*^{2\varepsilon}-a(t)^{2\varepsilon}]/(2\varepsilon)$ survives the ε-expansion. It should be subtracted by an appropriate counterterm, which, since it needs to come with a time-dependent factor, should be contained in one of the EFT vertices. As we will now see, the vertex $\sim c^0_{1,1}$ fulfills all the necessary requirements.

Insertion of the mass counterterm, determination of the divergent part of $c^0_{1,1}$

The next contribution to the power spectrum we consider comes from the insertion of the bilinear vertex

$$-\int \mathrm{d}^{d-1}x\mathrm{d}t\,(a(t)\nu)^{2\delta}c^0_{1,1}\varphi_+(t,\vec{x})\varphi_-(t,\vec{x}), \tag{4.5.10}$$

which is featured in this computation for the first time. The coupling $c^0_{1,1}$ is also the first EFT coupling that we need to renormalize. It will play the role of a mass counterterm in the SdSET, and we therefore refer to it as such from now.

When inserted into the power spectrum it leads to diagrams with topology

corresponding to the expression

$$\begin{aligned}\langle \varphi_+(t,\vec{k})\varphi_+(t,-\vec{k})\rangle'\Big|_{c_{1,1}} =& 2ic^0_{1,1}\frac{i}{3}\frac{\nu^{2\delta}}{2k_\Lambda^3}\int_{-\infty}^{t}\mathrm{d}t'\,a(t')^{2\delta}\\ =& -\frac{c^0_{1,1}(a_*\nu)^{2\delta}}{3k^3}\left[\frac{1}{2\delta}-\ln\left(\frac{a_*}{a(t)}\right)\right]. && (4.5.11)\end{aligned}$$

From the δ-pole featured in this result, which is a UV pole, we explicitly see the necessity of introducing the analytic regulator $a(t)^{2\delta}$ in the SdSET action. To write the result expanded in δ as we did above, we multiplied and divided it by a factor $a_*^{2\delta}$, since this proves to be the most convenient representation for the manipulations that follow.

Summing up what we found so far, we get

$$\begin{aligned}&\langle \varphi_+(t,\vec{k})\varphi_+(t,-\vec{k})\rangle'\Big|_{c_{3,1}} + \langle \varphi_+(t,\vec{k})\varphi_+(t,-\vec{k})\rangle'\Big|_{\xi_{3,1}} + \langle \varphi_+(t,\vec{k})\varphi_+(t,-\vec{k})\rangle'\Big|_{c_{1,1}}\\ =& \frac{c_{3,1}}{48\pi^2k^3}\left(\frac{\Lambda}{a(t)\mu}\right)^{-2\varepsilon}\ln\left(\frac{a_*}{a(t)}\right)\left[\frac{1}{\varepsilon}+\ln\left(\frac{a_*}{a(t)}\right)\right] - \frac{c^0_{1,1}(a_*\nu)^{2\delta}}{3k^3}\left[\frac{1}{2\delta}-\ln\left(\frac{a_*}{a(t)}\right)\right]. && (4.5.12)\end{aligned}$$

We see that the pole in ε can now be subtracted consistently by means of $c^0_{1,1}$, since it appears multiplied by the correct time-dependent factor, by choosing

$$c^0_{1,1} = -\frac{c_{3,1}}{16\pi^2\varepsilon} + c_{1,1} \tag{4.5.13}$$

$$= \frac{c_{3,1}}{8\pi^2}\left[-\frac{1}{2\varepsilon} + \hat{c}_{1,1}\right]. \tag{4.5.14}$$

In the above expressions $c_{1,1}$ denotes the still-unknown finite part of the bare coefficient $c^0_{1,1}$, which will be determined below by matching onto the full-theory result. For later convenience, we have also introduced its rescaled version $\hat{c}_{1,1}$.

With this choice, the combination (4.5.12) is still not UV-finite,

$$\begin{aligned}&\langle\varphi_+(t,\vec{k})\varphi_+(t,-\vec{k})\rangle'\Big|_{c_{3,1}} + \langle\varphi_+(t,\vec{k})\varphi_+(t,-\vec{k})\rangle'\Big|_{\xi_{3,1}} + \langle\varphi_+(t,\vec{k})\varphi_+(t,-\vec{k})\rangle'\Big|_{c_{1,1}} \\ =&\frac{c_{3,1}}{24\pi^2k^3}\left\{\frac{1}{2}\ln\left(\frac{a_*}{a(t)}\right)\left[\ln\left(\frac{a_*}{a(t)}\right) - 2\ln\left(\frac{\Lambda}{a(t)\mu}\right) + 2\hat{c}_{1,1}\right] + \frac{(a_*\nu)^{2\delta}}{2\delta}\left(\frac{1}{2\varepsilon} - \hat{c}_{1,1}\right)\right\}.\end{aligned} \tag{4.5.15}$$

since the δ- and $\delta\varepsilon$-poles are left over. However, we are also still missing some contributions to the SdSET power spectrum, so we postpone the treatment of these leftover poles to later in this section.

Insertion of the initial condition $\Xi^\sigma_{3,1}$

We now come to the most technically challenging part of the present computation, which are the diagrams resulting from inserting the finite initial condition $\Xi^\sigma_{3,1}$ into the power spectrum. In the previous section we found the result

$$\Xi^\sigma_{3,1}(\vec{k}_1,\vec{k}_2,\vec{k}_3,\vec{k}_4) = -3\sigma g_{3,1}\left\{\frac{1}{3}\ln\left(\frac{e^{\gamma_E}k_t}{a_*H}\right) + \left(\sum_{j=1}^{4}k_j^3\right)^{-1}\left[-\frac{k_1k_2k_3k_4}{k_t} + k_t\left(\sum_{j<l}k_jk_l - \frac{4}{9}k_t^2\right)\right]\right\}, \tag{4.5.16}$$

where the value of the coupling $g_{3,1}$ is equal to the tree-level value of $c_{3,1}$. We will keep track of this coupling up to the end of the section, when we discuss the matching procedure, since it will be relevant for the following dicussion.

Since we are working in the k_Λ-scheme, we also need to replace all absolute values of momenta appearing in $\Xi^\sigma_{3,1}$ by

$$k_i \to k_{i\Lambda}\,, \quad i = 1,...,4\,. \tag{4.5.17}$$

The relevant diagrams we need to consider have the topology

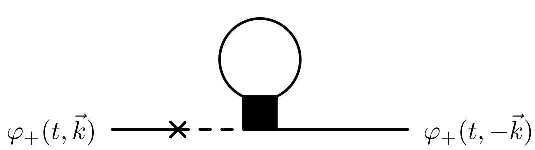

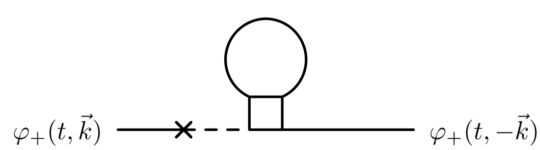

and we have to compute

$$\begin{aligned}\langle\varphi_+(t,\vec{k})\varphi_+(t,-\vec{k})\rangle'\Big|_{\Xi^\sigma_{3,1}} =& \frac{i(a_*\tilde{\mu})^{2\varepsilon}}{4k_\Lambda^3}\frac{i}{3}\int\frac{\mathrm{d}^{d-1}l}{(2\pi)^{d-1}}\,\frac{1}{l_\Lambda^3}\Xi^+_{3,1}(\vec{k},-\vec{k},\vec{l},-\vec{l}) \\ =& \frac{g_{3,1}(a_*\tilde{\mu})^{2\varepsilon}}{8k_\Lambda^3}\int\frac{\mathrm{d}^{d-1}l}{(2\pi)^{d-1}}\,\frac{1}{l_\Lambda^3}\left\{\frac{2}{3}\ln\left(\frac{2e^{\gamma_E}(k_\Lambda+l_\Lambda)}{a_*H}\right)\right. \\ &\left.-\frac{1}{k_\Lambda^3+l_\Lambda^3}\left[\frac{k_\Lambda^2l_\Lambda^2}{2(k_\Lambda+l_\Lambda)} + \frac{2}{9}(7k_\Lambda^3+3k_\Lambda^2l_\Lambda+3k_\Lambda l_\Lambda^2+7l_\Lambda^3)\right]\right\}.\end{aligned} \tag{4.5.18}$$

The rational part of the integrand can be simplified by observing that we can rewrite

$$\frac{1}{k_\Lambda^3+l_\Lambda^3}\left[\frac{k_\Lambda^2 l_\Lambda^2}{2(k_\Lambda+l_\Lambda)}+\frac{2}{9}(7k_\Lambda^3+3k_\Lambda^2 l_\Lambda+3k_\Lambda l_\Lambda^2+7l_\Lambda^3)\right]=\frac{14}{9}+\frac{k_\Lambda^2}{6(k_\Lambda+l_\Lambda)^2}+\frac{k_\Lambda(-k_\Lambda^2+6k_\Lambda l_\Lambda+4l_\Lambda^2)}{6(k_\Lambda^3+l_\Lambda^3)}\,, \quad (4.5.19)$$

which leads to a simpler denominator structure. This will make the integrations that we need to perform considerably easier.

We thus have three classes of integrals to evaluate: one class involving a logarithm of $k_\Lambda + l_\Lambda$, one class involving the denominator $(k_\Lambda + l_\Lambda)^2$ and one class involving the denominator $k_\Lambda^3 + l_\Lambda^3$. All of these integrals can be evaluated by making use of the Mellin-Barnes identity [112]

$$\frac{1}{(X+Y)^\lambda}=\frac{1}{\Gamma(\lambda)}\frac{1}{2\pi i}\int_{-i\infty}^{i\infty}\mathrm{d}z\;\Gamma(\lambda+z)\Gamma(-z)\frac{X^z}{Y^{\lambda+z}}\,, \quad (4.5.20)$$

and the details of the computation are collected in appendix 4.C.

Evaluating the loop integrals, and keeping only the terms in the result which do not vanish as $\Lambda \to 0$, we get

$$\begin{aligned}\langle\varphi_+(t,\vec{k})\varphi_+(t,-\vec{k})\rangle'\Big|_{\Xi_{3,1}} =&\frac{g_{3,1}}{96\pi^2k^3}\left(\frac{\Lambda}{a_*\mu}\right)^{-2\varepsilon}\left\{\frac{1}{\varepsilon^2}-\frac{2}{\varepsilon}\left[\frac{4}{3}-\ln\left(\frac{e^{\gamma_E}\Lambda}{a_*H}\right)\right]+2\ln^2\left(\frac{2k}{\Lambda}\right)-4\ln\left(\frac{2k}{\Lambda}\right)\right.\\ &\left.+5-\frac{20\pi}{3\sqrt{3}}+\frac{5\pi^2}{12}\right\}. \end{aligned} \quad (4.5.21)$$

We find both double- and single-UV poles, which are generated by the logarithmic term appearing in the integrand. The single-pole term we wrote above seems troublesome, since it is proportional to $\ln(\Lambda)$, which is an IR-divergent term, and is therefore incompatible with the interpretation of this pole as being purely UV and removable using a local counterterm. However, after expanding this result completely in ε, this term will cancel. Notice also the very unusual finite term proportional to $\pi/\sqrt{3}$, which stems from the denominator structure $k_\Lambda^3 + l_\Lambda^3$.

Insertion of $\xi^\sigma_{1,1}$, renormalization of the remaining UV-divergences

The last two contributions to the SdSET power spectrum both come from the bare initial-condition function $\Xi_{1,1;0}$, which we split into a counterterm and a finite part, and we consider the insertion of the former first. It enters the SdSET path integral via the term

$$i(a_*\nu)^{2\delta}\xi^\sigma_{1,1}\int\frac{\mathrm{d}^{d-1}k}{(2\pi)^{d-1}}\;\varphi^\sigma_+(t_*,\vec{k})\varphi^\sigma_+(t_*,-\vec{k})\,, \quad (4.5.22)$$

which, when inserted into the EFT power spectrum, yields

$$\begin{aligned}\langle\varphi_+(t,\vec{k})\varphi_+(t,-\vec{k})\rangle'\Big|_{\xi_{1,1}} =&\frac{i}{2k^3}\frac{i}{3}(a_*\nu)^{2\delta}\xi^+_{1,1}\\ =&-\frac{(a_*\nu)^{2\delta}\xi^+_{1,1}}{6k^3}\,, \end{aligned} \quad (4.5.23)$$

where we have already let $\Lambda \to 0$. Since this is the last counterterm that we have at our disposal for the present computation, we must require the sum

$$\begin{aligned}&\langle\varphi_+(t,\vec{k})\varphi_+(t,-\vec{k})\rangle'\Big|_{c_{3,1}}+\langle\varphi_+(t,\vec{k})\varphi_+(t,-\vec{k})\rangle'\Big|_{\xi_{3,1}}+\langle\varphi_+(t,\vec{k})\varphi_+(t,-\vec{k})\rangle'\Big|_{c_{1,1}}+\langle\varphi_+(t,\vec{k})\varphi_+(t,-\vec{k})\rangle'\Big|_{\Xi_{3,1}}\\ &+\langle\varphi_+(t,\vec{k})\varphi_+(t,-\vec{k})\rangle'\Big|_{\xi_{1,1}}\end{aligned}$$

$$
\begin{aligned}
=&\frac{c_{3,1}}{24\pi^2k^3}\left\{\frac{1}{2}\ln\left(\frac{a_*}{a(t)}\right)\left[\ln\left(\frac{a_*}{a(t)}\right)-2\ln\left(\frac{\Lambda}{a(t)\mu}\right)+2\hat{c}_{1,1}\right]+\frac{(a_*\nu)^{2\delta}}{2\delta}\left(\frac{1}{2\varepsilon}-\hat{c}_{1,1}\right)\right\}\\
&+\frac{g_{3,1}}{96\pi^2k^3}\left\{\frac{1}{\varepsilon^2}-\frac{2}{\varepsilon}\left[\frac{4}{3}-\ln\left(\frac{e^{\gamma_E}\mu}{H}\right)\right]-2\ln^2\left(\frac{\Lambda}{a_*\mu}\right)+4\left[\frac{4}{3}-\ln\left(\frac{e^{\gamma_E}\mu}{H}\right)\right]\ln\left(\frac{\Lambda}{a_*\mu}\right)\right.\\
&\left.+2\ln^2\left(\frac{2k}{\Lambda}\right)-4\ln\left(\frac{2k}{\Lambda}\right)+5-\frac{20\pi}{3\sqrt{3}}+\frac{5\pi^2}{12}\right\}-\frac{(a_*\nu)^{2\delta}\xi^+_{1,1}}{6k^3}
\end{aligned}\tag{4.5.24}
$$

to be finite. We see that this can be ensured by picking

$$
\xi^\sigma_{1,1}=\frac{\sigma g_{3,1}}{16\pi^2}\left\{\frac{1}{\varepsilon^2}-\frac{2}{\varepsilon}\left[\frac{4}{3}-\ln\left(\frac{e^{\gamma_E}\mu}{H}\right)\right]\right\}+\frac{\sigma c_{3,1}}{8\pi^2\delta}\left[\frac{1}{2\varepsilon}-\hat{c}_{1,1}\right],\tag{4.5.25}
$$

and we can then send $\delta\to 0$ without generating any additional terms from the expansion of the coefficients $(a_*\nu)^{2\delta}$, since in (4.5.24) they appear in front of both δ-poles, so they cancel exactly.

For the result (4.5.25), and its later applications, it is very important to distinguish $g_{3,1}$ and $c_{3,1}$, since their running behaviour is different. However, for the use of the renormalized result in the matching computation the difference is immaterial, since the two couplings have the same value. To start simplifying the found expression, we therefore set $c_{3,1}=g_{3,1}$ in it, and find

$$
\begin{aligned}
&\langle\varphi_+(t,\vec{k})\varphi_+(t,-\vec{k})\rangle'\Big|_{c_{3,1}}+\langle\varphi_+(t,\vec{k})\varphi_+(t,-\vec{k})\rangle'\Big|_{\xi_{3,1}}+\langle\varphi_+(t,\vec{k})\varphi_+(t,-\vec{k})\rangle'\Big|_{c_{1,1}}+\langle\varphi_+(t,\vec{k})\varphi_+(t,-\vec{k})\rangle'\Big|_{\Xi_{3,1}}\\
&+\langle\varphi_+(t,\vec{k})\varphi_+(t,-\vec{k})\rangle'\Big|_{\xi_{1,1}}\\
=&\frac{c_{3,1}}{24\pi^2k^3}\left\{\left[\frac{7}{3}-\ln\left(\frac{2e^{\gamma_E}k}{a(t)H}\right)\right]\ln\left(\frac{\Lambda}{a(t)\mu}\right)+\ln\left(\frac{2e^{\gamma_E}k}{a(t)H}\right)\left[\frac{1}{2}\ln\left(\frac{2e^{\gamma_E}k}{a(t)H}\right)-\ln\left(\frac{e^{\gamma_E}\mu}{H}\right)-1\right]\right.\\
&\left.-\left[\frac{4}{3}-\ln\left(\frac{e^{\gamma_E}\mu}{H}\right)-\hat{c}_{1,1}\right]\ln\left(\frac{a_*}{a(t)}\right)+\ln\left(\frac{e^{\gamma_E}\mu}{H}\right)\left[\frac{1}{2}\ln\left(\frac{e^{\gamma_E}\mu}{H}\right)+1\right]+\frac{5}{4}-\frac{5\pi}{3\sqrt{3}}+\frac{5\pi^2}{48}\right\}.
\end{aligned}\tag{4.5.26}
$$

Insertion of $\Xi^\sigma_{1,1}$

Finally, we compute the contribution coming from the insertion of $\Xi^\sigma_{1,1}$, which enters through the term

$$
i(a_*\nu)^{2\delta}\int\frac{\mathrm{d}^{d-1}k}{(2\pi)^{d-1}}\,\Xi^\sigma_{1,1}(\vec{k})\varphi^\sigma_+(t_*,\vec{k})\varphi^\sigma_+(t_*,-\vec{k}),\tag{4.5.27}
$$

and, in full analogy to the case of $\xi^\sigma_{1,1}$, it leads to the expression

$$
\langle\varphi_+(t,\vec{k})\varphi_+(t,-\vec{k})\rangle'\Big|_{\Xi_{1,1}}=-\frac{(a_*\nu)^{2\delta}\Xi^+_{1,1}(\vec{k})}{6k^3}.\tag{4.5.28}
$$

We can directly let $\delta\to 0$ in it, since the function $\Xi^+_{1,1}(\vec{k})$ is finite by construction. The full expression for the renormalized SdSET power spectrum, at this order in the perturbative expansion, thus reads

$$
\begin{aligned}
&\langle\varphi_+(t,\vec{k})\varphi_+(t,-\vec{k})\rangle'\Big|_{\mathcal{O}(\kappa)}\\
=&\langle\varphi_+(t,\vec{k})\varphi_+(t,-\vec{k})\rangle'\Big|_{c_{3,1}}+\langle\varphi_+(t,\vec{k})\varphi_+(t,-\vec{k})\rangle'\Big|_{\xi_{3,1}}+\langle\varphi_+(t,\vec{k})\varphi_+(t,-\vec{k})\rangle'\Big|_{c_{1,1}}+\langle\varphi_+(t,\vec{k})\varphi_+(t,-\vec{k})\rangle'\Big|_{\Xi_{3,1}}\\
&+\langle\varphi_+(t,\vec{k})\varphi_+(t,-\vec{k})\rangle'\Big|_{\xi_{1,1}}+\langle\varphi_+(t,\vec{k})\varphi_+(t,-\vec{k})\rangle'\Big|_{\Xi_{1,1}}\\
=&\frac{c_{3,1}}{24\pi^2k^3}\left\{\left[\frac{7}{3}-\ln\left(\frac{2e^{\gamma_E}k}{a(t)H}\right)\right]\ln\left(\frac{\Lambda}{a(t)\mu}\right)+\ln\left(\frac{2e^{\gamma_E}k}{a(t)H}\right)\left[\frac{1}{2}\ln\left(\frac{2e^{\gamma_E}k}{a(t)H}\right)-\ln\left(\frac{e^{\gamma_E}\mu}{H}\right)-1\right]\right.\\
&\left.-\left[\frac{4}{3}-\ln\left(\frac{e^{\gamma_E}\mu}{H}\right)-\hat{c}_{1,1}\right]\ln\left(\frac{a_*}{a(t)}\right)+\ln\left(\frac{e^{\gamma_E}\mu}{H}\right)\left[\frac{1}{2}\ln\left(\frac{e^{\gamma_E}\mu}{H}\right)+1\right]+\frac{5}{4}-\frac{5\pi}{3\sqrt{3}}+\frac{5\pi^2}{48}\right\}
\end{aligned}
$$

$$- \frac{\Xi^{+}_{1,1}(\vec{k})}{6k^3} \,. \tag{4.5.29}$$

We see that it contains two unknown quantities, $\hat{c}_{1,1}$ and $\Xi^{+}_{1,1}(\vec{k})$, which both need to be determined by matching the above expression to the full-theory result. However, before being able to do so, we need the last missing pieces entering the matching equation (4.5.3), which are the correlation functions generated by the non-linear relation between full and effective fields.

4.5.2 Correlators following from the φ_--field redefinition

We need to compute the following combination of correlators and bare couplings:

$$\begin{aligned}&\langle\varphi_+(t,\vec{k})\varphi_+(t,-\vec{k})\rangle'\Big|_{\text{redef.}}\\ \equiv&\frac{2c^0_{1,1}}{9}\langle\varphi_+(t,\vec{k})\varphi_+(t,-\vec{k})\rangle'\Big|_{\mathcal{O}(\kappa^0)}+\frac{c^0_{3,1}a(t)^{2\varepsilon}}{18(3+2\varepsilon)}\Big(\langle\varphi^3_+(t,\vec{k})\varphi_+(t,-\vec{k})\rangle'\Big|_{\mathcal{O}(\kappa^0)}+\langle\varphi_+(t,\vec{k})\varphi^3_+(t,-\vec{k})\rangle'\Big|_{\mathcal{O}(\kappa^0)}\Big)\,.\end{aligned} \tag{4.5.30}$$

Since both $c^0_{1,1}$ and $c^0_{3,1}$ are both $\mathcal{O}(\kappa)$, we evaluate the correlators appearing in the bracket in the Gaussian approximation. Therefore, the correlation function that multiplies $c^0_{1,1}$ is simply the Gaussian power spectrum,

$$\langle\varphi_+(t,\vec{k})\varphi_+(t,-\vec{k})\rangle'\Big|_{\mathcal{O}(\kappa^0)}=\frac{1}{2k^3_\Lambda}\,. \tag{4.5.31}$$

To understand the correlators that multiply $c^0_{3,1}$ it is most convenient to start by inspecting their position-space version, which reads

$$\langle\varphi^3_+(t,\vec{x})\varphi_+(t,\vec{y})\rangle=3\langle\varphi_+(t,\vec{x})\varphi_+(t,\vec{y})\rangle\langle\varphi^2_+(t,\vec{x})\rangle \tag{4.5.32}$$

for $\langle\varphi^3_+(t,\vec{k})\varphi_+(t,-\vec{k})\rangle'|_{\mathcal{O}(\kappa^0)}$, and the analogous expression with $\vec{x}\leftrightarrow\vec{y}$ for $\langle\varphi_+(t,\vec{k})\varphi^3_+(t,-\vec{k})\rangle'|_{\mathcal{O}(\kappa^0)}$. Since

$$\langle\varphi^2_+(t,\vec{x})\rangle=\frac{1}{2}\int\frac{\mathrm{d}^{d-1}l}{(2\pi)^{d-1}}\frac{1}{l^3_\Lambda} \tag{4.5.33}$$

is just a (divergent) constant, the Fourier transform of the product appearing in (4.5.32) is also just proportional to the Gaussian power spectrum. Putting the pieces together we thus find

$$\begin{aligned}\langle\varphi_+(t,\vec{k})\varphi_+(t,-\vec{k})\rangle'\Big|_{\text{redef.}}=&\frac{c^0_{1,1}}{9k^3_\Lambda}\frac{1}{2k^3}+\frac{\tilde{\mu}^{2\varepsilon}c_{3,1}}{(3+2\varepsilon)}\frac{a(t)^{2\varepsilon}}{2k^3}\int\frac{\mathrm{d}^{d-1}l}{(2\pi)^{d-1}}\frac{1}{l^3_\Lambda}\\ =&\frac{c^0_{1,1}}{9k^3}+\frac{c_{3,1}}{2k^3(3+2\varepsilon)}\left(\frac{\Lambda}{a(t)\mu}\right)^{-2\varepsilon}\frac{e^{\varepsilon\gamma_E}}{4\pi^2}\Gamma(\varepsilon)\\ =&\frac{c^0_{1,1}}{9k^3}+\frac{c_{3,1}}{12\pi^2k^3}\left[\frac{1}{2\varepsilon}-\ln\left(\frac{\Lambda}{a(t)\mu}\right)-\frac{1}{3}\right]\,.\end{aligned} \tag{4.5.34}$$

Now, plugging in the result we obtained above for the mass counterterm $c^0_{1,1}$, see (4.5.14), we find the finite result

$$\langle\varphi_+(t,\vec{k})\varphi_+(t,-\vec{k})\rangle'\Big|_{\text{redef.}}=\frac{c_{3,1}}{24\pi^2k^3}\left[-2\ln\left(\frac{\Lambda}{a(t)\mu}\right)+\frac{\hat{c}_{1,1}}{3}-\frac{2}{3}\right]\,. \tag{4.5.35}$$

Thus, we observe that, even though the single terms generated by the field redefinition are divergent, their sum is finite. In fact, this must be the case for our procedure to be consistent, since we are matching renormalized EFT correlators onto renormalized full-theory ones, and no UV divergences on either side of the matching equation can be left over.

4.5.3 Complete EFT result, matching of $\hat{c}_{1,1}$ and $\Xi^{\sigma}_{1,1}$

We now have all the necessary pieces together to carry out the matching procedure. Summing what we found above and plugging in the known value $c_{3,1} = \kappa$ we get the result

$$\begin{aligned}
&\langle\varphi_+(t,\vec{k})\varphi_+(t,-\vec{k})\rangle'\Big|_{\mathcal{O}(\kappa)} + \langle\varphi_+(t,\vec{k})\varphi_+(t,-\vec{k})\rangle'\Big|_{\text{redef.}} \\
=&\frac{\kappa}{24\pi^2k^3}\Bigg\{\left[2-\ln\left(\frac{2e^{\gamma_E}k}{a(t)H}\right)\right]\left[\ln\left(\frac{\Lambda}{a(t)\mu}\right)-\hat{c}_{1,1}\right]+\frac{1}{2}\ln^2\left(\frac{2e^{\gamma_E}k}{a(t)H}\right)-\frac{7}{3}\ln\left(\frac{2e^{\gamma_E}k}{a(t)H}\right) \\
&+\left[\frac{4}{3}-\hat{c}_{1,1}\right]\ln\left(\frac{2e^{\gamma_E}k}{a_*H}\right)+\left[1+\frac{1}{2}\ln\left(\frac{e^{\gamma_E}\mu}{H}\right)\right]\ln\left(\frac{e^{\gamma_E}\mu}{H}\right)+\frac{7\hat{c}_{1,1}}{3}+\frac{41}{36}-\frac{5\pi}{3\sqrt{3}}+\frac{5\pi^2}{48}\Bigg\} \\
&-\frac{\Xi^{+}_{1,1}(\vec{k})}{6k^3}\,.
\end{aligned} \tag{4.5.36}$$

This combination of terms, multiplied by an overall factor of H^2, needs to reproduce the renormalized full-theory result in $d = 4$ dimensions,

$$\begin{aligned}
\langle\phi(t,\vec{k})\phi(t,-\vec{k})\rangle'\Big|_{\mathcal{O}(\kappa)} =&\frac{\kappa H^2}{24\pi^2k^3}\Bigg\{\left[2-\ln\left(\frac{2e^{\gamma_E}k}{a(t)H}\right)\right]\left[\ln\left(\frac{\Lambda}{a(t)\mu}\right)-\delta\hat{m}^2_{\text{fin}}\right]+\frac{1}{2}\ln^2\left(\frac{2e^{\gamma_E}k}{a(t)H}\right) \\
&-\frac{7}{3}\ln\left(\frac{2e^{\gamma_E}k}{a(t)H}\right)+\frac{8}{3}-\frac{\pi^2}{24}\Bigg\}\,,
\end{aligned} \tag{4.5.37}$$

and the matching equation (4.5.3) fixes both the finite part of the EFT mass counterterm $\hat{c}_{1,1}$ and the one-loop result for $\Xi_{1,1}(\vec{k})$. It follows that we must pick

$$\hat{c}_{1,1} = \delta\hat{m}^2_{\text{fin}} \tag{4.5.38}$$

and

$$\begin{aligned}
\Xi^{\sigma}_{1,1}(\vec{k}) =&\frac{\sigma\kappa}{4\pi^2}\Bigg\{\left[\frac{4}{3}-\ln\left(\frac{e^{\gamma_E}\mu}{H}\right)-\delta\hat{m}^2_{\text{fin}}\right]\ln\left(\frac{2e^{\gamma_E}k}{a_*H}\right)+\left[1+\frac{1}{2}\ln\left(\frac{e^{\gamma_E}\mu}{H}\right)\right]\ln\left(\frac{e^{\gamma_E}\mu}{H}\right) \\
&+\frac{7\delta\hat{m}^2_{\text{fin}}}{3}-\frac{55}{36}-\frac{5\pi}{3\sqrt{3}}+\frac{7\pi^2}{48}\Bigg\}\,.
\end{aligned} \tag{4.5.39}$$

Both these results will receive higher-order corrections in powers of κ as higher orders in the perturbative expansion are reached.

At this point, we recall that the (rescaled) finite part of the full-theory mass counterterm $\delta\hat{m}^2_{\text{fin}}$ is still undetermined, because we cannot formulate a physically meaningful renormalization scheme based on perturbative results in the full theory, see the discussion in section 3.1. Instead, we postponed the formulation of a renormalization scheme to after having obtained an IR-finite, non-perturbative version of the correlation functions using the EFT, mentioning that the undetermined finite parts of the full-theory counterterms would be featured in the matching coefficients of the SdSET, and thus, ultimatively, in the non-perturbatively computed correlation functions. Here we can see one example of the first step of this program being realized in practice, since both $\hat{c}_{1,1}$ and $\Xi^{\sigma}_{1,1}(\vec{k})$ feature the still-unknown constant $\delta\hat{m}^2_{\text{fin}}$.

4.5.4 Renormalization-group evolution of $\hat{c}_{1,1}$ and $\Xi^{\sigma}_{1,1}$

To close this section we inspect the running behaviour of the newly matched coefficients.

Running of $\hat{c}_{1,1}$ with μ

To obtain the running of the finite part of the mass counterterm we use the fact that the combination

$$c^0_{1,1} = \frac{c_{3,1}}{8\pi^2}\left[-\frac{1}{2\varepsilon}+\hat{c}_{1,1}\right] \tag{4.5.40}$$

should have no running, since it is a bare quantity. Using the tree-level running of $c_{3,1}$

$$\frac{\mathrm{d}c_{3,1}}{\mathrm{d}\ln(\mu)} = -2\varepsilon c_{3,1}\,, \tag{4.5.41}$$

we derive the one-loop running of the combination

$$\frac{\mathrm{d}}{\mathrm{d}\ln(\mu)}\left[\frac{c_{3,1}}{8\pi^2}\hat{c}_{1,1}\right] = -\frac{c_{3,1}}{8\pi^2}\,. \tag{4.5.42}$$

From this equation the running of $\hat{c}_{1,1}$ could be derived in its own right, but since by construction it is always the combination $c_{1,1} = c_{3,1}\hat{c}_{1,1}/(8\pi^2)$ that will appear in SdSET correlation functions, the above equation is sufficient.

This is the first example of the phenomenon of effective couplings mixing under renormalization, which we discussed in general in section 4.3.3. The RGE (4.5.42) can be rewritten in the notation introduced in that section by identifying the one-loop beta-function matrix element

$$\beta_{01} = -\frac{1}{8\pi^2}\,. \tag{4.5.43}$$

Running of $\Xi^\sigma_{1,1}$ with μ

Requiring that the combination

$$\Xi^\sigma_{1,1;0}(\vec{x}_1,\vec{x}_2) = (a_*\nu)^{2\delta}\Big[\xi^\sigma_{1,1}(\vec{x}_1,\vec{x}_2) + \Xi^\sigma_{1,1}(\vec{x}_1,\vec{x}_2)\Big] \tag{4.5.44}$$

does not run with μ implies the equation

$$\frac{\mathrm{d}\Xi^\sigma_{1,1}}{\mathrm{d}\ln(\mu)} = -\frac{\mathrm{d}\xi^\sigma_{1,1}}{\mathrm{d}\ln(\mu)}\,. \tag{4.5.45}$$

As in the case of the coupling $c_{1,1}$, this is also just a special case of the general discussion about the renormalization of initial conditions we led in section 4.3.3. Using the result

$$\xi^\sigma_{1,1} = \frac{\sigma g_{3,1}}{16\pi^2}\left\{\frac{1}{\varepsilon^2} - \frac{2}{\varepsilon}\left[\frac{4}{3} - \ln\left(\frac{e^{\gamma_E}\mu}{H}\right)\right]\right\} + \frac{\sigma c_{3,1}}{8\pi^2\delta}\left[\frac{1}{2\varepsilon} - \hat{c}_{1,1}\right], \tag{4.5.46}$$

together with the tree-level running of $g_{3,1}$ and $c_{3,1}$ and the found running of $\hat{c}_{1,1}$ we get

$$\frac{\mathrm{d}\xi^\sigma_{1,1}}{\mathrm{d}\ln(\mu)} = \frac{\sigma g_{3,1}}{4\pi^2}\left[\frac{4}{3} - \ln\left(\frac{e^{\gamma_E}\mu}{H}\right)\right], \tag{4.5.47}$$

from which it then follows that

$$\frac{\mathrm{d}\Xi^\sigma_{1,1}(\mu)}{\mathrm{d}\ln(\mu)} = -\frac{\sigma g_{3,1}}{4\pi^2}\left[\frac{4}{3} - \ln\left(\frac{e^{\gamma_E}\mu}{H}\right)\right]. \tag{4.5.48}$$

The explicit result that we found for $\Xi^\sigma_{1,1}$ in (4.5.39) with κ replaced by $g_{1,1}$ and $\delta\hat{m}^2_{\text{fin}}$ replaced by $\hat{c}_{1,1}$ reads

$$\begin{aligned}\Xi^\sigma_{1,1}(\vec{k}) =& \frac{\sigma g_{1,1}}{4\pi^2}\left\{\left[\frac{4}{3} - \ln\left(\frac{e^{\gamma_E}\mu}{H}\right) - \hat{c}_{1,1}\right]\ln\left(\frac{2e^{\gamma_E}k}{a_*H}\right) + \left[1 + \frac{1}{2}\ln\left(\frac{e^{\gamma_E}\mu}{H}\right)\right]\ln\left(\frac{e^{\gamma_E}\mu}{H}\right)\right.\\ &\left. + \frac{7\hat{c}_{1,1}}{3} - \frac{55}{36} - \frac{5\pi}{3\sqrt{3}} + \frac{7\pi^2}{48}\right\}.\end{aligned} \tag{4.5.49}$$

It has the correct running behaviour at this order in the expansion, provided that $g_{1,1}$ does not run at this order in the expansion:

$$\frac{\mathrm{d}g_{1,1}}{\mathrm{d}\ln(\mu)} = 0\,. \tag{4.5.50}$$

Running of $\Xi^\sigma_{1,1}$ with a_*

Lastly, we can also compute the a_*-running of $\Xi^\sigma_{1,1}$ with the obtained results. By taking the $\ln(a_*)$-derivative of both sides of the equation (4.5.44) we obtain

$$\frac{\mathrm{d}}{\mathrm{d}\ln(a_*)}\Big[\xi^\sigma_{1,1}(\vec{x}_1,\vec{x}_2)+\Xi^\sigma_{1,1}(\vec{x}_1,\vec{x}_2)\Big] = -2\delta\Big[\xi^\sigma_{1,1}(\vec{x}_1,\vec{x}_2)+\Xi^\sigma_{1,1}(\vec{x}_1,\vec{x}_2)\Big]\,. \tag{4.5.51}$$

To obtain the running of $\Xi^\sigma_{1,1}$ alone we can first compute the $\ln(a_*)$-derivative of $\xi^\sigma_{1,1}$. Using that the $c^0_{1,1}$ does not run with a_*, i.e.

$$\frac{\mathrm{d}}{\mathrm{d}\ln(a_*)}\left[\frac{c_{3,1}}{8\pi^2}\left(-\frac{1}{2\varepsilon}+\hat{c}_{1,1}\right)\right]=0\,, \tag{4.5.52}$$

whereas

$$\frac{\mathrm{d}g_{3,1}}{\mathrm{d}\ln(a_*)} = -2\varepsilon g_{3,1}\,, \tag{4.5.53}$$

we find

$$\frac{\mathrm{d}\xi^\sigma_{1,1}}{\mathrm{d}\ln(a_*)} = -\frac{\sigma g_{3,1}}{8\pi^2}\left\{\frac{1}{\varepsilon}-2\left[\frac{4}{3}-\ln\left(\frac{e^{\gamma_E}\mu}{H}\right)\right]\right\}. \tag{4.5.54}$$

Plugging this result into (4.5.51) and solving for $\mathrm{d}\Xi_{1,1}/\mathrm{d}\ln(a_*)$ we get

$$\frac{\mathrm{d}\Xi^\sigma_{1,1}}{\mathrm{d}\ln(a_*)} = \frac{\sigma g_{3,1}}{4\pi^2}\left[\hat{c}_{1,1}+\ln\left(\frac{e^{\gamma_E}\mu}{H}\right)-\frac{4}{3}\right], \tag{4.5.55}$$

where we neglected terms that vanish as we let $\delta\to 0$, which includes the ε-poles contained in $\xi^\sigma_{1,1}$, since we let $\delta\to 0$ before $\varepsilon\to 0$. Comparing with the matched result (4.5.39), we see that the explicitly appearing $\ln(a_*)$-terms reproduce the obtained derivative, so we can interpret this result as an absence of the running of the coupling $g_{1,1}$ we introduced in (4.5.49) with a_* at this order in the perturbative expansion, as was the case for its μ-running:

$$\frac{\mathrm{d}g_{1,1}}{\mathrm{d}\ln(a_*)} = 0\,. \tag{4.5.56}$$

4.6 Composite operators in SdSET: renormalization, mixing and matching

In the remainder of this chapter, we will study the properties of composite operators of the form φ^n_+, which we will do primarily by computing SdSET correlation functions containing them, alongside other elementary fields. We will also see how to use such correlators to match analogous full-theory correlation functions involving composite operators of the form ϕ^n, which will give us insight into how renormalized full-theory and effective composite operators are related to each other. Developing a rigorous understanding of the problem of composite-operator renormalization and matching in the SdSET will prove crucial for working towards our ultimate goal of understanding the non-perturbative dynamics of full-theory correlators in the late-time limit. Therefore, this section is dedicated to introducing the basic framework that we will use to deal with this problem.

4.6.1 Renormalization of composite operators φ^n_+, definition of operator anomalous dimensions

In the following we will be interested in studying operators built out of renormalized SdSET fields of the form

$$\varphi^n_+(t,\vec{x})\,. \tag{4.6.1}$$

Importantly, we will assume for the present discussion that the effective fields and action have already been fully renormalized, and so the operator φ^n_+ is built out of the renormalized effective field φ_+. When operators of this form are inserted into correlation functions they will, in general, generate divergences which are not removed by renormalizing the effective action alone. Therefore, these composite operators necessitate a separate renormalization procedure to define renormalized composite operators[6] $[\varphi_+^n]$, in order to then consistently define UV-finite correlation functions involving them. Furthermore, since in $d = 4$ the effective field φ_+ is dimensionless, and so is any power of it, we expect that all renormalized operators $[\varphi_+^n]$ will mix among each other due to the renormalization procedure, analogously to the situation that one is facing when renormalizing the effective coupllings we discussed in section 4.3.3. Following [65], we will therefore need to set up an operator renormalization equation of the form

$$\varphi_+^n \sim \sum_{m=0}^{\infty} Z_{nm}[\varphi_+^m]\,, \tag{4.6.2}$$

where Z_{nm} denotes the matrix of operator renormalization factors. Since both the left- and right-hand sides of this equation generate UV-divergences when inserted into correlation functions, it is only well-defined for $\varepsilon \neq 0$, so all quantities appearing in it should be treated as being d-dimensional. Both the bare, regularized operator φ_+^n, as well as its renormalized counterpart $[\varphi_+^n]$, have mass dimension $n(d-4)/2$, so if we want to describe the phenomenon of operator mixing, we need to compensate the mass-dimensional mismatch by appropriate factors of the renormalization scale μ. Further, in section 4.2.1 we found that the effective fields transform non-trivially under infinitesimal dilatations and special conformal transformations as

$$\varphi_\pm(\eta,\vec{x}) \to \varphi'_\pm(\eta',\vec{x}') = \left[1 + \left(\frac{3}{2} \pm \nu\right)\delta\right]\varphi_\pm(\eta,\vec{x})\,, \tag{4.6.3}$$

$$\varphi_\pm(\eta,\vec{x}) \to \varphi'_\pm(\eta',\vec{x}') = \left[1 - (3 \pm 2\nu)\vec{b}\cdot\vec{x}\right]\varphi_\pm(\eta,\vec{x})\,, \tag{4.6.4}$$

respectively, so there is again a mismatch between the transformation behaviour of operators involving a different number of fields. Both of these mismatches can be compensated by including appropriate factors of $a(t)$ in front of the operators. Similarly to the discussion of the renormalization of the effective couplings, adding powers of the scale factor is the only possible option here, since the renormalization equation should be local in space and time, so we only have quantities evaluated at the spacetime point $(t,\vec{x})$ to work with. Since φ_+^n is a scalar under spatial translations and rotations, a function of $\vec{x}$ is not an option, and we are left with a function of $a(t)$.

We therefore make the following ansatz for the operator renormalization equation:

$$\varphi_+^n(t,\vec{x}) = (a(t)\tilde{\mu})^{n\frac{d-4}{2}} \sum_{m=0}^{\infty} (a(t)\tilde{\mu})^{-m\frac{d-4}{2}} Z_{nm}[\varphi_+^m](t,\vec{x})\,, \tag{4.6.5}$$

with $d = 4-2\varepsilon$, and we have formulated it using the rescaled renormalization scale $\tilde{\mu}$. We did so because we will use the $\overline{\text{MS}}$ scheme for the renormalization of the φ_+^n, as we did for the renormalization of the composite operators ϕ^n in the full theory. The bare operator φ_+^n is both a_*- and μ-independent, while, in general, the Z_{nm} and renormalized operators $[\varphi_+^n]$ are not. From (4.6.5), it then follows that their respective dependence on these two scales must be such that it cancels out when they are plugged into the renormalization equation. This fact can be used to derive the following RGEs for the renormalized operators:

$$\frac{\mathrm{d}[\varphi_+^n]}{\mathrm{d}\ln(\mu)} = -\,n\varepsilon[\varphi_+^n] + (a(t)\tilde{\mu})^{n\varepsilon} \sum_{m=0}^{\infty}\left[\sum_{l=0}^{\infty} Z_{nl}^{-1}\left(l\varepsilon Z_{lm} - \frac{\mathrm{d}Z_{lm}}{\mathrm{d}\ln(\mu)}\right)\right](a(t)\tilde{\mu})^{-m\varepsilon}[\varphi_+^m]\,, \tag{4.6.6}$$

$$\frac{\mathrm{d}[\varphi_+^n]}{\mathrm{d}\ln(a_*)} = -\,(a(t)\tilde{\mu})^{n\varepsilon} \sum_{m=0}^{\infty}\left[\sum_{l=0}^{\infty} Z_{nl}^{-1}\frac{\mathrm{d}Z_{lm}}{\mathrm{d}\ln(a_*)}\right](a(t)\tilde{\mu})^{-m\varepsilon}[\varphi_+^m]\,. \tag{4.6.7}$$

These equations suggest the definition of the two anomalous dimension matrices (ADMs) γ^μ and γ^{a_*} via

$$\gamma^\mu_{nm} \equiv -\,n\varepsilon\delta_{nm} + \sum_{l=0}^{\infty} Z_{nl}^{-1}\left[l\varepsilon Z_{lm} - \frac{\mathrm{d}Z_{lm}}{\mathrm{d}\ln(\mu)}\right]\,, \tag{4.6.8}$$

[6]We follow the notation in [65] and use angled brackets to define the renormalized version of composite operators.

$$\gamma_{nm}^{a_*} \equiv -\sum_{l=0}^{\infty} Z_{nl}^{-1} \frac{\mathrm{d}Z_{lm}}{\mathrm{d}\ln(a_*)}\,, \tag{4.6.9}$$

which must be finite (which is however not at all obvious from their definition), and we can therefore let $\varepsilon \to 0$ in the above equations. We can then write the two sets of RGEs as

$$\frac{\mathrm{d}[\varphi_+^n](t,\vec{x})}{\mathrm{d}\ln(\mu, a_*)} = \sum_{m=0}^{\infty} \gamma_{nm}^{\mu,a_*}[\varphi_+^m](t,\vec{x})\,. \tag{4.6.10}$$

In practice, we will renormalize the composite operators in perturbation theory, by inserting them into correlation functions and computing the resulting UV poles. Since all EFT couplings are ultimatively related to the full-theory coupling κ, the renormalization factors can be organized in an expansion in powers of κ as well. The ADMs then inherit this property, and their matrix elements will have the form

$$\gamma_{nm}^{\mu,a_*} = \sum_{l=0}^{\infty} \kappa^l \gamma_{nm}^{\mu,a_*(\kappa^l)}\,. \tag{4.6.11}$$

4.6.2 Properties of the renormalization factors

Before seeing how the renormalization procedure for the φ_+^n works in practice, it is useful to reflect on the general properties that the Z_{nm} must have, which will then inform what we expect when carrying out practical computations. Since any power of φ_+ can mix with any other power of φ_+, the renormalization-factor matrix is an "$\infty \times \infty$"-matrix. In the $\overline{\mathrm{MS}}$ scheme, its matrix elements will, in general, be given in terms of infinite series in powers of $1/\varepsilon$, as follows:

$$n < m: \quad Z_{nm} = \sum_{l=1}^{\infty} \varepsilon^{-l} \sum_{k=\frac{m-n}{2}+1}^{\infty} z_{nm}^{(k,l)}\,, \tag{4.6.12}$$

$$n = m: \quad Z_{nn} = 1 + \sum_{l=1}^{\infty} \varepsilon^{-l} \sum_{k=1}^{\infty} z_{nn}^{(k,l)}\,, \tag{4.6.13}$$

$$n > m: \quad Z_{nm} = \sum_{l=\frac{n-m}{2}}^{\infty} \varepsilon^{-l} \sum_{k=0}^{\infty} z_{nm}^{(k,l)}\,, \tag{4.6.14}$$

where the coefficients of the ε-poles scale like

$$z_{nm}^{(k,l)} \sim \kappa^k\,. \tag{4.6.15}$$

Notice that the ratio $(n-m)/2$ appearing in the above equations is an integer since, due to the underlying symmetry of the theory under $\varphi_\pm \to -\varphi_\pm$, the difference between the powers of φ_+ that are mixing among each other must be an integer multiple of 2, so $n-m$ is even. If $n-m$ is odd, the corresponding renormalization-factor matrix element Z_{nm} simply vanishes. Equation (4.6.12) reflects the simple fact that for an operator φ_+^n to mix with a higher power of φ_+ it needs to do so via interaction terms, and the first type of diagram which can generate a divergence is a one-loop diagram with insertions of the quartic vertex $\sim c_{3,1} \sim \kappa$ and quartic initial condition $\Xi_{3,1}^{\sigma} \sim \kappa$, which gives rise to the given lowest possible κ-scaling. Equation (4.6.13) expresses the fact that at tree level bare and renormalized operators are equivalent, and therefore at leading power in κ Z_{nn} is unity. The most unusual feature of the Z_{nm} is captured by (4.6.14), which expresses the fact that to let an operator φ_+^n mix with a lower number of fields we can arrange it by simply tying pairs of fields together in "elementary" loops, e.g.

$$(a(t)\tilde{\mu})^{2\varepsilon}\langle\varphi_+^2(t,\vec{x})\rangle = \frac{(a(t)\tilde{\mu})^{2\varepsilon}}{2}\int \frac{\mathrm{d}^{d-1}l}{(2\pi)^{d-1}}\frac{1}{l_\Lambda^3}$$

$$
\begin{aligned}
&= \frac{1}{8\pi^2}\left(\frac{\Lambda^2}{4\pi a(t)^2\tilde{\mu}^2}\right)^{-\varepsilon}\Gamma(\varepsilon) \\
&= \frac{1}{8\pi^2}\left[\frac{1}{\varepsilon} - 2\ln\left(\frac{\Lambda}{a(t)\mu}\right)\right], \qquad (4.6.16)
\end{aligned}
$$

without having to pay a price in powers of κ. Therefore, the Z_{nm} with $n > m$ already start with $\mathcal{O}(\kappa^0)$ pole terms. Since one elementary loop contributes a factor $1/\varepsilon$ in our regularization scheme, the renormalization factor must absorb one inverse power of ε per pair of fields tied together in a loop, which gives rise to the sum given above. This is a consequence of the dimensionlessness of the φ_+ in the massless SdSET, and it will have profound consequences for the effective dynamics of the correlation functions. What this tells us is that, differently than the discussion of the renormalization of the couplings, already in the free theory we have to deal with a non-trivial, infinite-dimensional renormalization problem, and the matrix Z already contains infinitely many non-vanishing entries before starting to consider the interacting SdSET. As we will see in a moment, the free-theory Z-matrix has a lower-triangular structure, which makes the problem tractable, even in the absence of a perturbative parameter.

Let us now look more closely at the entries of Z_{nm}. We can immediately conclude that it contains two trivial rows with only one non-zero entry, to all orders in κ, namely

$$
\begin{aligned}
Z_{0n} &= \delta_{0n}, \qquad (4.6.17) \\
Z_{1n} &= \delta_{1n}, \qquad (4.6.18)
\end{aligned}
$$

since the unit operator $\varphi_+^0 = \mathbb{1}$ requires no renormalization, and we assume that the elementary effective field $\varphi_+^1 = \varphi_+$ has already been fully renormalized. From (4.6.12)-(4.6.14) we see that turning the coupling κ off the "$\infty \times \infty$"-matrix Z reduces to a lower-triangular form with 1 on the diagonal entries:

$$
\begin{aligned}
n < m: &\quad Z_{nm} = 0, \qquad (4.6.19) \\
n = m: &\quad Z_{nn} = 1, \qquad (4.6.20) \\
n > m: &\quad Z_{nm} = \frac{z_{nm}^{(0,\frac{n-m}{2})}}{\varepsilon^{\frac{n-m}{2}}}. \qquad (4.6.21)
\end{aligned}
$$

This means that the inverse matrix Z^{-1} will also be of lower-triangular form with entries of 1 on the diagonal:

$$
\begin{aligned}
n < m: &\quad Z^{-1}_{nm} = 0, \qquad (4.6.22) \\
n = m: &\quad Z^{-1}_{nn} = 1, \qquad (4.6.23) \\
n > m: &\quad Z^{-1}_{nm} = \frac{\zeta_{nm}^{(0,\frac{n-m}{2})}}{\varepsilon^{\frac{n-m}{2}}}, \qquad (4.6.24)
\end{aligned}
$$

where we are denoting the coefficients of the ε-poles appearing in the inverse matrix by ζ. Since we are working with a perturbative coupling, once we switch κ back on, the same structure above will persist at leading power in κ, and only receive perturbative corrections.

4.6.3 Mixing in the free effective theory

To get a better intuition for the structure of the Z-factors we start by computing some of them in the free theory. This will also already allow us to compute the leading-power piece of some μ-anomalous dimensions, which here are simply given by

$$
\gamma_{nm}^{\mu(\kappa^0)} = -n\varepsilon\delta_{nm} + \varepsilon\sum_{l=0}^{\infty} Z^{-1}_{nl}\, l Z_{lm}. \qquad (4.6.25)
$$

The a_*-anomalous dimensions, on the other hand, are all vanishing in the free theory, since the a_*-dependence of the renormalized operators enters via the non-Gaussian initial conditions, which are all set to zero in the free theory, because it is Gaussian:

$$
\gamma_{nm}^{a_*(\kappa^0)} = 0. \qquad (4.6.26)
$$

Since we will only consider the μ-anomalous dimension here we will suppress the label μ in the following.

We know that both Z_{nm} and Z_{nm}^{-1} here are lower-triangular matrices, so the only summands in (4.6.25) which do not vanish identically are those for which the summation index l satisfies

$$m \leq l \leq n \tag{4.6.27}$$

simultaneously, so we only have a finite sum to consider:

$$\gamma_{nm}^{(\kappa^0)} = -n\varepsilon\delta_{nm} + \varepsilon\sum_{l=m}^{n} Z_{nl}^{-1} l Z_{lm}\,. \tag{4.6.28}$$

This immediately implies that

$$\gamma_{nm}^{(\kappa^0)} = 0 \quad \text{for } n < m\,. \tag{4.6.29}$$

Further, in the boundary case $m = n$ we also have

$$\gamma_{nn}^{(\kappa^0)} = 0\,, \tag{4.6.30}$$

since in the free theory $Z_{nn} = Z_{nn}^{-1} = 1$.

To develop some intuition about the renormalization procedure of the φ_+^n, it will prove useful to keep drawing diagrams associated to correlation functions containing them. In these diagrams, we will denote the insertion of any $\varphi_+^n(t,\vec{x})$ by the symbol $\otimes$, and we omit any labeling of the symbol in this section, since the inserted operator will always be at the point $(t,\vec{x})$. The exponent can then be inferred by the number of legs radiating from this simbol.

Mixing of $\varphi_+^2 \to \mathbb{1}$

The mixing of φ_+^2 with the unit operator is the simplest possible process we can consider, and it is extracted from the diagram

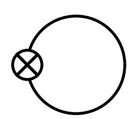

Above, we already evaluated

$$\begin{aligned}(a(t)\tilde{\mu})^{2\varepsilon}\langle\varphi_+^2(t,\vec{x})\rangle =& \frac{(a(t)\tilde{\mu})^{2\varepsilon}}{2}\int\frac{\mathrm{d}^{d-1}l}{(2\pi)^{d-1}}\frac{1}{l_\Lambda^3} \\ =& \frac{1}{8\pi^2}\left[\frac{1}{\varepsilon} - 2\ln\left(\frac{\Lambda}{a(t)\mu}\right) + \mathcal{O}(\varepsilon)\right]\,,\end{aligned} \tag{4.6.31}$$

and we can drop the higher-order terms in ε for now. Using the equation (4.6.5) and the properties of the free-theory matrix Z we collected above, see (4.6.12)-(4.6.14), we find the operator-renormalization equation

$$(a(t)\tilde{\mu})^{2\varepsilon}\varphi_+^2(t,\vec{x}) = (a(t)\tilde{\mu})^{2\varepsilon} Z_{22}[\varphi_+^2](t,\vec{x}) + Z_{20}\mathbb{1}\,, \tag{4.6.32}$$

and $Z_{22} = 1$ in the free theory. The divergent piece in (4.6.31) can be subtracted by choosing

$$Z_{20} = \frac{1}{8\pi^2\varepsilon}\,, \tag{4.6.33}$$

which then defines the renormalized-operator correlation function in $d = 4$ dimensions as

$$\langle[\varphi_+^2](t,\vec{x})\rangle = -\frac{1}{4\pi^2}\ln\left(\frac{\Lambda}{a(t)\mu}\right)\,. \tag{4.6.34}$$

Using this result we can already compute the anomalous dimension $\gamma_{20}^{(0)}$. Using (4.6.25) we have

$$\gamma_{20}^{(0)} = \varepsilon \sum_{l=0}^{2} Z_{2l}^{-1} l Z_{l0} \tag{4.6.35}$$

and plugging in the found values for the relevant Z_{nm} we find

$$\gamma_{20}^{(0)} = 2\varepsilon \frac{1}{8\pi^2 \varepsilon} = \frac{1}{4\pi^2} \,. \tag{4.6.36}$$

We can now safely take the limit $\varepsilon \to 0$ and get the finite result

$$\gamma_{20}^{(\kappa^0)} = \frac{1}{4\pi^2} \,. \tag{4.6.37}$$

Mixing of $\varphi_+^3 \to \varphi_+$

This case is almost identical to the previous one, since we need to compute

$$\langle \varphi_+^3(t,\vec{x})\varphi_+(t,\vec{x}_1)\rangle = 3\langle \varphi_+^2(t,\vec{x})\rangle\langle \varphi_+(t,\vec{x})\varphi_+(t,\vec{x}_1)\rangle \,, \tag{4.6.38}$$

which corresponds to the diagram

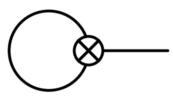

Using the results from the previous subsubsection we find simply

$$(a(t)\tilde{\mu})^{2\varepsilon} \langle \varphi_+^3(t,\vec{x})\varphi_+(t,\vec{x}_1)\rangle = \frac{3}{8\pi^2}\left[\frac{1}{\varepsilon} - 2\ln\left(\frac{\Lambda}{a(t)\mu}\right) + \mathcal{O}(\varepsilon)\right]\langle \varphi_+(t,\vec{x})\varphi_+(t,\vec{x}_1)\rangle \,. \tag{4.6.39}$$

The renormalized operator $[\varphi_+^3]$ is defined by the equation

$$(a(t)\tilde{\mu})^{3\varepsilon}\varphi_+^3(t,\vec{x}) = (a(t)\tilde{\mu})^{3\varepsilon} Z_{33}[\varphi_+^3](t,\vec{x}) + (a(t)\tilde{\mu})^{\varepsilon} Z_{31}\varphi_+(t,\vec{x}) \,, \tag{4.6.40}$$

and we can use that $Z_{33} = 1$ in the free theory. We can absorb the divergence by choosing

$$Z_{31} = \frac{3}{8\pi^2\varepsilon} = 3Z_{20} \,, \tag{4.6.41}$$

which defines, in $d = 4$,

$$\langle [\varphi_+^3](t,\vec{x})\varphi_+(t,\vec{x}_1)\rangle = -\frac{3}{4\pi^2}\ln\left(\frac{\Lambda}{a(t)\mu}\right)\langle \varphi_+(t,\vec{x})\varphi_+(t,\vec{x}_1)\rangle \,. \tag{4.6.42}$$

We can now compute the anomalous dimension $\gamma_{31}^{(\kappa^0)}$, which is given by

$$\gamma_{31}^{(\kappa^0)} = \varepsilon \sum_{l=1}^{3} Z_{3l}^{-1} l Z_{l1} = \varepsilon\Big[Z_{31}^{-1} Z_{11} + 3Z_{33}^{-1} Z_{31}\Big] \,. \tag{4.6.43}$$

Up to now we have determined the upper 4×4-block of Z, which is

$$Z\Big|_{\text{upper } 4\times 4} = \begin{pmatrix} 1 & 0 & 0 & 0 \\ 0 & 1 & 0 & 0 \\ Z_{20} & 0 & 1 & 0 \\ 0 & Z_{31} & 0 & 1 \end{pmatrix} \tag{4.6.44}$$

and this block is enough to renormalize the set of operators $\{\mathbb{1}, \varphi_+, \varphi_+^2, \varphi_+^3\}$, so we can consider it in its own right and compute its inverse,

$$Z^{-1}\Big|_{\text{upper } 4\times 4} = \begin{pmatrix} 1 & 0 & 0 & 0 \\ 0 & 1 & 0 & 0 \\ -Z_{20} & 0 & 1 & 0 \\ 0 & -Z_{31} & 0 & 1 \end{pmatrix} . \tag{4.6.45}$$

Since the matrix is lower triangular, the upper 4×4-block of the inverse will stay unchanged once we determine more and more entries and invert the matrix.

Using the above result we can compute

$$\gamma_{31}^{(\kappa^0)} = \varepsilon\left[-\frac{3}{8\pi^2\varepsilon} + \frac{9}{8\pi^2\varepsilon}\right] = \frac{3}{4\pi^2} = 3\gamma_{20}^{(\kappa^0)} \tag{4.6.46}$$

and also here we can take the limit $\varepsilon \to 0$ safely and get

$$\gamma_{31}^{(\kappa^0)} = \frac{3}{4\pi^2} . \tag{4.6.47}$$

Mixing of $\varphi_+^4 \to \mathbb{1}$

We go one step further and compute the mixing of φ_+^4 with the unit operator, which is determined from the correlator

$$\begin{aligned} &(a(t)\tilde{\mu})^{4\varepsilon}\langle\varphi_+^4(t,\vec{x})\rangle = 3(a(t)\tilde{\mu})^{4\varepsilon}\langle\varphi_+^2(t,\vec{x})\rangle^2 \\ =&\frac{3}{64\pi^4}\left(\frac{\Lambda^2}{4\pi a(t)^2\tilde{\mu}^2}\right)^{-2\varepsilon}\Gamma(\varepsilon)^2 \\ =&\frac{3}{64\pi^4}\left\{\frac{1}{\varepsilon^2} - \frac{4}{\varepsilon}\ln\left(\frac{\Lambda}{a(t)\mu}\right) + \frac{\pi^2}{6} + 8\ln^2\left(\frac{\Lambda}{a(t)\mu}\right) + \mathcal{O}(\varepsilon)\right\} , \end{aligned} \tag{4.6.48}$$

corresponding to the diagram

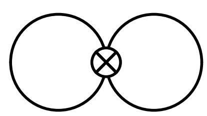

The result found in (4.6.48) seems problematic at first, since it involves a pole term with a Λ-dependent coefficient. However, we will now see that this poses no issue, and it is simply a manifestation of operator mixing.

The renormalized operator $[\varphi_+^4]$ is defined via (4.6.5) as

$$(a(t)\tilde{\mu})^{4\varepsilon}\varphi_+^4(t,\vec{x}) = (a(t)\tilde{\mu})^{4\varepsilon}Z_{44}[\varphi_+^4](t,\vec{x}) + (a(t)\tilde{\mu})^{2\varepsilon}Z_{42}[\varphi_+^2](t,\vec{x}) + Z_{40}\mathbb{1} \tag{4.6.49}$$

and, using that $Z_{44} = 1$ in the free theory and using the renormalized result (4.6.34), which contains an explicit factor of $\ln(\Lambda/(a(t)\mu))$, we see that we need to pick

$$Z_{40} = \frac{3}{64\pi^4\varepsilon^2} , \tag{4.6.50}$$

$$Z_{42} = \frac{3}{4\pi^2\varepsilon} , \tag{4.6.51}$$

to correctly subtract the pole terms. Then, using the fact that in d dimensions we have

$$\begin{aligned} Z_{42}(a(t)\tilde{\mu})^{2\varepsilon}\langle[\varphi_+^2](t,\vec{x})\rangle =&\frac{3}{4\pi^2\varepsilon}\left[\frac{1}{8\pi^2}\left(\frac{\Lambda}{a(t)\mu}\right)^{-2\varepsilon}e^{\varepsilon\gamma_E}\Gamma(\varepsilon)-\frac{1}{8\pi^2\varepsilon}\right] \\ =&\frac{3}{16\pi^4}\left[-\frac{1}{\varepsilon}\ln\left(\frac{\Lambda}{a(t)\mu}\right)+\ln^2\left(\frac{\Lambda}{a(t)\mu}\right)+\frac{\pi^2}{24}\right], \end{aligned} \tag{4.6.52}$$

we find that (4.6.49) defines the renormalized one-point function

$$\langle[\varphi_+^4](t,\vec{x})\rangle = \frac{3}{16\pi^4}\ln^2\left(\frac{\Lambda}{a(t)\mu}\right). \tag{4.6.53}$$

Thus, we see that it is important to keep in mind that the operator-renormalization equation (4.6.5) is only well-defined in d dimensions, where the correlation functions of renormalized operators still possess non-vanishing terms involving positive powers of ε, which can then generate non-vanishing terms in the limit $\varepsilon \to 0$ when multiplied with the Z-factors. This observation will be especially important when we start computing composite-operator correlation functions in the interacting theory.

We have now determined the upper 5×5-block of the matrix of renormalization factors Z, which reads

$$Z\Big|_{\text{upper }5\times5} = \begin{pmatrix} 1 & 0 & 0 & 0 & 0 \\ 0 & 1 & 0 & 0 & 0 \\ Z_{20} & 0 & 1 & 0 & 0 \\ 0 & Z_{31} & 0 & 1 & 0 \\ Z_{40} & 0 & Z_{42} & 0 & 1 \end{pmatrix}, \tag{4.6.54}$$

and it can be inverted in its own right to yield

$$Z^{-1}\Big|_{\text{upper }5\times5} = \begin{pmatrix} 1 & 0 & 0 & 0 & 0 \\ 0 & 1 & 0 & 0 & 0 \\ -Z_{20} & 0 & 1 & 0 & 0 \\ 0 & -Z_{31} & 0 & 1 & 0 \\ -Z_{40}+Z_{20}Z_{42} & 0 & -Z_{42} & 0 & 1 \end{pmatrix}. \tag{4.6.55}$$

Using these results we can compute the anomalous dimension $\gamma_{40}^{(\kappa^0)}$, which is given by

$$\gamma_{40}^{(\kappa^0)} = \varepsilon\sum_{l=0}^{4} Z_{4l}^{-1} l Z_{l0} = \varepsilon\Big[2Z_{42}^{-1}Z_{20}+4Z_{44}^{-1}Z_{40}\Big] \tag{4.6.56}$$

and plugging in the results we found above we get

$$\gamma_{40}^{(\kappa^0)} = \varepsilon\left[-2\frac{3}{4\pi^2\varepsilon}\frac{1}{8\pi^2\varepsilon}+4\frac{3}{64\pi^2\varepsilon^2}\right] = 0\,. \tag{4.6.57}$$

This must be the case for the above scheme to be self-consistent, since any non-vanishing result would have been $\mathcal{O}(\varepsilon^{-1})$, and thus ill-defined in the limit $\varepsilon \to 0$. We can also compute $\gamma_{42}^{(0)}$, which is given by

$$\gamma_{42}^{(\kappa^0)} = \varepsilon\sum_{l=2}^{4} Z_{4l}^{-1} l Z_{l2} = \varepsilon\Big[2Z_{42}^{-1}Z_{22}+4Z_{44}^{-1}Z_{42}\Big] = 2\varepsilon\frac{3}{4\pi^2\varepsilon} = \frac{3}{2\pi^2}\,. \tag{4.6.58}$$

In the limit $\varepsilon \to 0$ we thus find

$$\gamma_{40}^{(\kappa^0)} = 0\,, \tag{4.6.59}$$

$$\gamma_{42}^{(\kappa^0)} = \frac{3}{2\pi^2}\,. \tag{4.6.60}$$

Mixing of $\varphi_+^4 \to \varphi_+^2$

As a consistency check with the above result we compute

$$\begin{aligned}
&(a(t)\tilde{\mu})^{2\varepsilon}\langle\varphi_+^4(t,\vec{x})\varphi_+(t,\vec{x}_1)\varphi_+(t,\vec{x}_2)\rangle\Big|_{\text{conn.}}\\
=&12(a(t)\tilde{\mu})^{2\varepsilon}\langle\varphi_+^2(t,\vec{x})\rangle\langle\varphi_+(t,\vec{x})\varphi_+(t,\vec{x}_1)\rangle\langle\varphi_+(t,\vec{x})\varphi_+(t,\vec{x}_2)\rangle\\
=&\frac{3}{2\pi^2}\left[\frac{1}{\varepsilon}-2\ln\left(\frac{\Lambda}{a(t)\mu}\right)\right]\langle\varphi_+(t,\vec{x})\varphi_+(t,\vec{x}_1)\rangle\langle\varphi_+(t,\vec{x})\varphi_+(t,\vec{x}_2)\rangle\,,
\end{aligned} \tag{4.6.61}$$

where by the subscript "conn." we are denoting the connected component of the correlation functions, which is the one that matters for the present discussion. It corresponds to the diagram

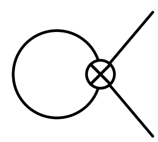

Writing again

$$(a(t)\tilde{\mu})^{4\varepsilon}\varphi_+^4(t,\vec{x}) = (a(t)\tilde{\mu})^{4\varepsilon}[\varphi_+^4](t,\vec{x}) + (a(t)\tilde{\mu})^{2\varepsilon}Z_{42}[\varphi_+^2](t,\vec{x}) + Z_{40}\mathbb{1} \tag{4.6.62}$$

we see that indeed the found counterterm

$$Z_{42} = \frac{3}{4\pi^2\varepsilon} \tag{4.6.63}$$

does absorb the divergence, since at tree level we simply have

$$\langle[\varphi_+^2](t,\vec{x})\varphi_+(t,\vec{x}_1)\varphi_+(t,\vec{x}_2)\rangle = \langle\varphi_+^2(t,\vec{x})\varphi_+(t,\vec{x}_1)\varphi_+(t,\vec{x}_2)\rangle = 2\langle\varphi_+(t,\vec{x})\varphi_+(t,\vec{x}_1)\rangle\langle\varphi_+(t,\vec{x})\varphi_+(t,\vec{x}_2)\rangle\,. \tag{4.6.64}$$

This then leads us to define the renormalized correlator

$$\langle[\varphi_+^4](t,\vec{x})\varphi_+(t,\vec{x}_1)\varphi_+(t,\vec{x}_2)\rangle = -\frac{3}{\pi^2}\ln\left(\frac{\Lambda}{a(t)\mu}\right)\langle\varphi_+(t,\vec{x})\varphi_+(t,\vec{x}_1)\rangle\langle\varphi_+(t,\vec{x})\varphi_+(t,\vec{x}_2)\rangle \tag{4.6.65}$$

$$= -\frac{3}{2\pi^2}\ln\left(\frac{\Lambda}{a(t)\mu}\right)\langle[\varphi_+^2](t,\vec{x})\varphi_+(t,\vec{x}_1)\varphi_+(t,\vec{x}_2)\rangle\,. \tag{4.6.66}$$

General case: mixing of $\varphi_+^n \to \varphi_+^m$ with $n \geq m$ and anomalous dimensions

In all the above computations, we saw that all pole terms appearing in the considered correlation functions where generated by powers of the "elementary" loop $\langle\varphi_+^2(t,\vec{x})\rangle$, and we would keep finding this result if we were to compute more of such free-theory correlators. This allows us to directly generalize the above considerations to determine all Z_{nm} in the free theory in closed form. It is not surprising that this is possible, since the free theory is exactly solvable.

We consider the mixing of φ_+^n with φ_+^m, where we assume that $n-m$ is even to obtain a non-trivial result. We thus consider the correlation function

$$\langle\varphi_+^n(t,\vec{x})\varphi_+(t,\vec{x}_1)...\varphi_+(t,\vec{x}_m)\rangle = \frac{n!}{(n-m)!}\frac{(n-m)!}{2^{\frac{n-m}{2}}(\frac{n-m}{2})!}\langle\varphi_+^2(t,\vec{x})\rangle^{\frac{n-m}{2}}\prod_{j=1}^{n-m}\langle\varphi_+(t,\vec{x})\varphi_+(t,\vec{x}_j)\rangle$$

$$=\frac{n!}{2^{\frac{n-m}{2}}(\frac{n-m}{2})!}\left[\frac{1}{8\pi^2}\left(\frac{\Lambda^2}{4\pi a(t)^2\tilde{\mu}^2}\right)^{-\varepsilon}\Gamma(\varepsilon)\right]^{\frac{n-m}{2}}\prod_{j=1}^{n-m}\langle\varphi_+(t,\vec{x})\varphi_+(t,\vec{x}_j)\rangle\,, \tag{4.6.67}$$

where the combinatorial factor arises as follows: there are $n!/(n-m)!$ ways of contracting m external (distinguishable) fields with n indistinguishable fields at $\vec{x}$, and there are

$$\frac{(2n)!}{2^n n!} \tag{4.6.68}$$

different ways of tying $2n$ indistinguishable fields into n loops.

The pole part of the above correlator is thus

$$\langle\varphi_+^n(t,\vec{x})\varphi_+(t,\vec{x}_1)...\varphi_+(t,\vec{x}_m)\rangle\Big|_{\text{pole}}=\frac{n!}{2^{\frac{n-m}{2}}(\frac{n-m}{2})!}\left(\frac{1}{8\pi^2\varepsilon}\right)^{\frac{n-m}{2}}\prod_{j=1}^{n-m}\langle\varphi_+(t,\vec{x})\varphi_+(t,\vec{x}_j)\rangle \tag{4.6.69}$$

and it needs to be absorbed by the Z-factor defined by

$$\langle\varphi_+^n(t,\vec{x})\varphi_+(t,\vec{x}_1)...\varphi_+(t,\vec{x}_m)\rangle\Big|_{\text{pole}}\equiv Z_{nm}\langle[\varphi_+^m](t,\vec{x})\varphi_+(t,\vec{x}_1)...\varphi_+(t,\vec{x}_m)\rangle\,. \tag{4.6.70}$$

In the free theory we simply have

$$\langle[\varphi_+^m](t,\vec{x})\varphi_+(t,\vec{x}_1)...\varphi_+(t,\vec{x}_m)\rangle=m!\,Z_{nm}\prod_{j=1}^{n-m}\langle\varphi_+(t,\vec{x})\varphi_+(t,\vec{x}_j)\rangle \tag{4.6.71}$$

and comparing the coefficients of the product of m two-point functions we find

$$Z_{nm}=\frac{n!}{2^{\frac{n-m}{2}}m!\,(\frac{n-m}{2})!}\left(\frac{1}{8\pi^2\varepsilon}\right)^{\frac{n-m}{2}} \tag{4.6.72}$$

$$=\frac{n!}{2^{\frac{n-m}{2}}m!\,(\frac{n-m}{2})!}Z_{20}^{\frac{n-m}{2}}\,. \tag{4.6.73}$$

As expected, all of the higher Z_{nm} are related to Z_{20}. This formula reproduces all of the special cases found above, as well as the general case where $n=m$, which just gives

$$Z_{nn}=1\,, \tag{4.6.74}$$

as it should.

In the free theory we thus have, for $n-m$ even,

$$Z_{nm}=0\,,\quad n<m\,, \tag{4.6.75}$$

$$Z_{nm}=\frac{n!}{2^{\frac{n-m}{2}}m!\,(\frac{n-m}{2})!}\left(\frac{1}{8\pi^2\varepsilon}\right)^{\frac{n-m}{2}}\,,\quad n\geq m\,, \tag{4.6.76}$$

and, for $n-m$ odd,

$$Z_{nm}=0\,. \tag{4.6.77}$$

From these results we see that we can decompose the matrix Z as

$$Z=\mathbb{1}+N\,, \tag{4.6.78}$$

where N has zeroes on its diagonal and the lower triangle under the diagonal contains all the non-trivial entries of Z. From this we can write the formal inverse of Z as

$$Z^{-1} = [\mathbb{1} + N]^{-1} = \mathbb{1} + \sum_{l=1}^{\infty}(-1)^l N^l \,. \tag{4.6.79}$$

If Z where a finite-dimensional $n \times n$-matrix, then N would be nilpotent, meaning that $N^n = 0$, and the sum would terminate after $l = n$. However, since Z is an "$\infty \times \infty$"-matrix we would have to raise N to the "infinitieth power" in order for it to vanish, so the concept of nilpotency is somewhat ill-defined here. What remains true in this setting is the fact that the matrix N^m has zeroes on its main diagonal and on its first $m-1$ lower off-diagonals. This means that to determine the entry $Z^{-1}_{n,n-m}$ of Z^{-1} we can truncate the sum after $l = m$, since all the subsequent summands will only contribute zeroes:

$$Z^{-1}_{n,n-m} = \delta_{n,n-m} + \sum_{l=1}^{m}(-1)^l (N^l)_{n,n-m} \,. \tag{4.6.80}$$

This is the essential feature that makes the present problem tractable. Even though the matrix Z has infinitely many entries, the entries above any n-th row, which are always finitely many, can be treated independently of the infinitely many entries below this row, if one is interested in computing the corresponding entries of the inverse matrix. We have also already used this property above, when computing non-trivial entries of Z^{-1}.

From (4.6.80) we find, using (4.6.76)

$$Z^{-1}_{nn} = 1 \,, \tag{4.6.81}$$

$$Z^{-1}_{n,n-2} = - Z_{n,n-2} = -\frac{n(n-1)}{16\pi^2\varepsilon} \,, \tag{4.6.82}$$

$$Z^{-1}_{n,n-4} = - Z_{n,n-4} + Z_{n,n-2}Z_{n-2,n-4} = \frac{n!}{512\pi^4(n-4)!\,\varepsilon^2} \,, \tag{4.6.83}$$

$$\begin{aligned} Z^{-1}_{n,n-6} &= - Z_{n,n-6} + Z_{n,n-4}Z_{n-4,n-6} + Z_{n,n-2}Z_{n-2,n-6} - Z_{n,n-2}Z_{n-2,n-4}Z_{n-4,n-6} \\ &= -\frac{n!}{24576\pi^6(n-6)!\,\varepsilon^3} \,, \end{aligned} \tag{4.6.84}$$

for any n. This now allows us to compute the first three non-trivial off-diagonals of the anomalous dimension matrix using the formula

$$\gamma^{(\kappa^0)}_{nm} = -n\varepsilon\delta_{nm} + \varepsilon\sum_{l=m}^{n} Z^{-1}_{nl}\, l Z_{lm} \,, \tag{4.6.85}$$

and we find

$$\gamma^{(\kappa^0)}_{n,n-2} = \varepsilon\Big[(n-2)Z^{-1}_{n,n-2}Z_{n-2,n-2} + nZ^{-1}_{n,n}Z_{n,n-2}\Big] = \frac{n(n-1)}{8\pi^2} \,, \tag{4.6.86}$$

$$\gamma^{(\kappa^0)}_{n,n-4} = \varepsilon\Big[(n-4)Z^{-1}_{n,n-4}Z_{n-4,n-4} + (n-2)Z^{-1}_{n,n-2}Z_{n-2,n-4} + nZ^{-1}_{n,n}Z_{n,n-4}\Big] = 0 \,, \tag{4.6.87}$$

$$\begin{aligned} \gamma^{(\kappa^0)}_{n,n-6} =& \varepsilon\Big[(n-6)Z^{-1}_{n,n-6}Z_{n-6,n-6} + (n-4)Z^{-1}_{n,n-4}Z_{n-4,n-6} + (n-2)Z^{-1}_{n,n-2}Z_{n-2,n-6} + nZ^{-1}_{n,n}Z_{n,n-6}\Big] \\ =& 0 \,, \end{aligned} \tag{4.6.88}$$

for any n. From (4.6.76), (4.6.80) and (4.6.85) we see that all anomalous dimensions $\gamma^{(\kappa^0)}_{n,n-m}$ with $m \geq 4$ would be proportional to $\varepsilon^{-\frac{m}{2}+1}$ and thus be ill-defined in the limit $\varepsilon \to 0$, so they must all vanish for the above scheme to be self-consistent, which we see explicitly for the cases $m = 4$ and $m = 6$ above. In the free theory we thus must have:

$$\gamma^{(\kappa^0)}_{n,m} = \frac{n(n-1)}{8\pi^2} \,, \tag{4.6.89}$$

$$\gamma^{(\kappa^0)}_{nm} = 0 \quad \text{for } m \neq n-2 \,. \tag{4.6.90}$$

Inversion of Z in the interacting theory

As a last remark on the structure of the matrix Z, we consider how to deal with it once interactions are switched on.

To compute anomalous dimensions in the interacting theory we still need to invert the matrix Z. To do so, we build on the considerations above and write

$$Z = Z_{\text{free}} + \sum_{n=1}^{\infty} \kappa^n Z_{\text{int}}^{(n)} , \tag{4.6.91}$$

where Z_{free} is the counterterm matrix in the free theory and $Z_{\text{int}}^{(n)}$ contains all the $\mathcal{O}(\kappa^n)$-coefficients of the new contributions coming from interaction terms.

To obtain the inverse of Z, we factorize Z_{free} from the remainder, and write Z as

$$Z = Z_{\text{free}} \left[\mathbb{1} + Z_{\text{free}}^{-1} \sum_{n=1}^{\infty} \kappa^n Z_{\text{int}}^{(n)} \right] , \tag{4.6.92}$$

from which we get the formal inverse as

$$Z^{-1} = \left[\mathbb{1} + Z_{\text{free}}^{-1} \sum_{n=1}^{\infty} \kappa^n Z_{\text{int}}^{(n)} \right]^{-1} Z_{\text{free}}^{-1} . \tag{4.6.93}$$

The inverse of the square bracket can then be computed perturbatively in powers of κ. To get Z^{-1} at $\mathcal{O}(\kappa)$ we can truncate the resulting series in κ after the second summand and get

$$Z^{-1} = Z_{\text{free}}^{-1} - \kappa Z_{\text{free}}^{-1} Z_{\text{int}}^{(1)} Z_{\text{free}}^{-1} + \mathcal{O}(\kappa^2) . \tag{4.6.94}$$

We can now use the decomposition of Z_{free} that we found above in (4.6.78), (4.6.79),

$$Z_{\text{free}} = \mathbb{1} + N , \quad Z_{\text{free}}^{-1} = \mathbb{1} + \sum_{l=1}^{\infty} (-1)^l N^l , \tag{4.6.95}$$

with the same matrix N described under (4.6.79), to write

$$Z^{-1} = Z_{\text{free}}^{-1} - \kappa \left[Z_{\text{int}}^{(1)} + \sum_{l=1}^{\infty} (-1)^l N^l Z_{\text{int}}^{(1)} + Z_{\text{int}}^{(1)} \sum_{l=1}^{\infty} (-1)^l N^l + \sum_{l=1}^{\infty} (-1)^l N^l Z_{\text{int}}^{(1)} \sum_{m=1}^{\infty} (-1)^m N^m \right] + \mathcal{O}(\kappa^2) . \tag{4.6.96}$$

Since the matrix N^m is lower triangular, and additionally its main diagonal and first $m-1$ lower diagonals are all vanishing as well, to compute a particular entry of Z^{-1} requires considering only finitely many summands:

$$(Z_{\text{free}}^{-1})_{n,n-m} - \kappa \left[Z_{\text{int}}^{(1)} + \sum_{l=1}^{m} (-1)^l N^l Z_{\text{int}}^{(1)} + Z_{\text{int}}^{(1)} \sum_{l=1}^{m} (-1)^l N^l + \sum_{l=1}^{m} (-1)^l N^l Z_{\text{int}}^{(1)} \sum_{k=1}^{m} (-1)^k N^k \right]_{n,n-m} + \mathcal{O}(\kappa^2) , \tag{4.6.97}$$

which again makes the problem of actually computing its entries tractable, even though we are dealing with an infinite-dimensional Z_{free}.

4.6.4 Composite-operator matching

After studying the renormalization of composite SdSET operators, we now set up the necessary formalism to match renormalized composite operators $[\varphi_+^n]$ in the SdSET to renormalized composite operators $[\phi^n]$ in the full theory.

We would like to write down an equation with the generic form

$$[\phi^n] \sim \sum_m C_{nm}[\varphi_+^m]\,, \tag{4.6.98}$$

where we are anticipating that we will need dedicated operator-matching coefficients C_{nm} to correctly reproduce correlators involving insertions of composite operators in the full theory. The matrix of matching coefficients C has a similar structure to the matrix of renormalization factors Z, and, in particular, we must again assume it to be infinite-dimensional. This is again due to dimensionlessness of the renormalized operators $[\varphi_+^n]$. The C_{nm} should then get contributions from physical processes which are outside of the regime of dynamical description of the SdSET, and we have to determine them through matching computations. At this point, we can make use of the intuition about the region structure of full-theory correlation functions that we developed from the computations we carried out in chapter 3, and anticipate that the C_{nm} will typically receive contributions from the hard-momentum regions of the full-theory correlation functions. They should therefore be spatially local, and thus independent of any position arguments. However, since these regions can have a non-trivial late-time subregion, the C_{nm} do not necessarily need to be time-independent. We therefore make the following ansatz for the d-dimensional matching equation in terms of bare quantities in the EFT:

$$[\phi^n](t,\vec{x}) = H^n \sum_{m=0}^{\infty} C^0_{nm}(t)(a(t)\tilde{\mu})^{m\frac{4-d}{2}}\varphi_+^m(t,\vec{x})\,, \tag{4.6.99}$$

where C^0_{nm} denotes the bare matching coefficient. The overall factor H^n appearing in the above matching equation is motivated by the known relation between ϕ and φ_+, while the powers of $a(t)$ are again dictated by the non-trivial transformation behaviour of the EFT fields under dilatations and special conformal transformations, see (4.6.3) and (4.6.4), while the full-theory field transforms as a scalar under them.

The fact that the poles generated by the composite operators φ_+^n need to be cancelled by the bare Wilson coefficients C^0_{nm} means that they must renormalize with the inverse of the same matrix of Z-factors that renormalizes the φ_+^n:

$$C^0_{nm}(t) = \sum_{k=0}^{\infty} C_{nk}(t) Z^{-1}_{km}\,, \tag{4.6.100}$$

and we can then write the matching equation directly in terms of renormalized quantities:

$$[\phi^n](t,\vec{x}) = H^n \sum_{m=0}^{\infty} C_{nm}(t)(a(t)\tilde{\mu})^{m\frac{4-d}{2}}[\varphi_+^m](t,\vec{x})\,. \tag{4.6.101}$$

In practice, we will determine the renormalized C_{nm} in perturbation theory, so, like the Z-factors and the anomalous dimensions, they will be computed as power series in the full-theory coupling κ. The analogous considerations that we made above to infer the general structure of the Z_{nm} applies here as well, and the matching coefficients C_{nm} will, in general, have the following structure as power series in κ:

$$n < m: \quad C_{nm} = \sum_{k=\frac{m-n}{2}+1}^{\infty} \kappa^k C^{(k)}_{nm}\,, \tag{4.6.102}$$

$$n = m: \quad C_{nn} = 1 + \sum_{k=1}^{\infty} \kappa^k C^{(k)}_{nn}\,, \tag{4.6.103}$$

$$n > m: \quad C_{nm} = \sum_{k=0}^{\infty} \kappa^k C^{(k)}_{nm}\,, \tag{4.6.104}$$

which mirrors the structure of the Z_{nm}, see (4.6.12)-(4.6.14).

The renormalization structure of the bare matching coefficients, see (4.6.100), also has a direct implication for the dependence of the renormalized coefficients on the factorization scales of the EFT, which are μ and

a_*. Both of these scales appear in renormalized SdSET correlation functions, but they do not appear in the full-theory ones (once we are careful about the distinction of the renormalization scale of the full theory and the factorization scale of the EFT, which, up to now, we both called μ). This means that the dependence of the renormalized operators $[\varphi_+^n]$ on these scales must be exactly compensated by the dependence of the renormalized C_{nm} on them. But this is exactly what (4.6.100) is implying, since we know that the μ- and a_*-dependence of the $[\varphi_+^n]$ is introduced by the renormalization procedure. In general, both the renormalized full-theory and EFT-operators depend logarithmically on two different scales, which we can call μ_{full} and μ_{eff}, and the matching coefficients will depend on ratios of the two scales in such a way as to compensate the dependence of the $[\varphi_+^n]$ on μ_{eff}, since the $[\phi^n]$ do not depend on it. Furthermore, the EFT operators also depend on the scale a_*, which does not exist in the full theory, so this dependence must be cancelled by the C_{nm} as well:

$$[\phi^n](\mu_{\text{full}}; t, \vec{x}) = H^n \sum_{m=0}^{\infty} C_{nm}(\mu_{\text{full}}/\mu_{\text{eff}}, a_*/a(t))[\varphi_+^m](\mu_{\text{eff}}, a_*; t, \vec{x}) \,. \tag{4.6.105}$$

The requirement that the dependence on μ_{eff} and a_* cancels between the C_{nm} and the $[\varphi_+^n]$ implies the following RGEs for the renormalized EFT-operators:

$$\frac{\mathrm{d}[\varphi_+^n]}{\mathrm{d}\ln(\mu_{\text{eff}}, a_*)} = -\sum_{m=0}^{\infty}\left[\sum_{l=0}^{\infty} C_{nl}^{-1}\frac{\mathrm{d}C_{lm}}{\mathrm{d}\ln(\mu_{\text{eff}}, a_*)}\right][\varphi_+^m] \,. \tag{4.6.106}$$

But these must coincide with the already derived RGEs in $\mu = \mu_{\text{eff}}$ and a_* for the EFT-operators, see (4.6.6) and (4.6.7), and the coefficients of the $[\varphi_+^m]$ appearing on the right-hand-side of the above equation must be the same as the already known anomalous dimension matrices we defined above:

$$\gamma_{nm}^{\mu, a_*} = -\sum_{l=0}^{\infty} C_{nl}^{-1}\frac{\mathrm{d}C_{lm}}{\mathrm{d}\ln(\mu_{\text{eff}}, a_*)} \,. \tag{4.6.107}$$

This is the standard situation [124]. Since we can compute the γ_{nm}^{μ, a_*} using only the Z-factors for the EFT-operators, see equations (4.6.8) and (4.6.9), we can use this equation to run a consistency check on the explicit results we will find for the matching coefficients.

For practical matching computations, we must choose a particular scale at which to evaluate both the left-hand side and the right-hand side of the (expectation values of the) matching equation. In particular, we will usually choose $\mu_{\text{full}} = \mu_{\text{eff}} = \mu$, and leave μ arbitrary. However, for the purpose of running the consistency check on the found results for the C_{nm} we must leave μ_{full} and μ_{eff} distinct from each other.

Matching coefficients in the free theory

As a first application of the general framework we set up above, we can consider the matching procedure in the free full and effective theories. Due to the non-trivial operator mixing taking place in both theories, the matching of the full theory onto the EFT can already be non-trivial, depending on the choice of scales at which we carry out the matching. In the free theory, the scale a_* does not enter, so the matching coefficients will not depend on it. Turning to their μ-dependence, if we choose to carry out the matching at a common scale $\mu_{\text{full}} = \mu_{\text{eff}} = \mu$, which would be the physically motivated procedure, then the correlation functions of $[\phi^n]$ and $[\varphi_+^n]$ will immediately agree by construction, and we will simply find for the matching coefficients in the free theory

$$C_{nm} = \delta_{nm} \,. \tag{4.6.108}$$

However, this is not strictly necessary: if we leave μ_{full} and μ_{eff} distinct from each other, then the C_{nm} will differ from the above result by logs of the ratio $\mu_{\text{full}}/\mu_{\text{eff}}$, and the matching still works. This must be the case in order to derive the non-trivial anomalous dimensions

$$\gamma_{nm}^{\mu} = \frac{n(n-1)}{8\pi^2}\delta_{n-2,m} \tag{4.6.109}$$

from the equation (4.6.107). To illustrate this, we can consider a few simple free-theory examples, recycling the free-theory computations we already carried out in section 4.6.3. In the free theory, the results for the correlation functions of the full theory and the EFT differ only by powers of H and the replacement $\mu_{\rm full} \leftrightarrow \mu_{\rm eff}$.

According to the matching equation (4.6.105) the following equality must hold:

$$\langle[\phi^2](t,\vec{x})\rangle = H^2\Big[C_{22}\langle[\varphi_+^2](t,\vec{x})\rangle + C_{20}\Big]\,. \tag{4.6.110}$$

Using the results of section 4.6.3 we find the following results for the two correlators appearing in the above equation:

$$\begin{aligned}\langle[\phi^2](t,\vec{x})\rangle =& -\frac{H^2}{4\pi^2}\ln\left(\frac{\Lambda}{a(t)\mu_{\rm full}}\right)\,, &(4.6.111)\\ \langle[\varphi_+^2](t,\vec{x})\rangle =& -\frac{1}{4\pi^2}\ln\left(\frac{\Lambda}{a(t)\mu_{\rm eff}}\right)\,, &(4.6.112)\end{aligned}$$

such that, plugging these results into the matching equation, we get

$$-\frac{H^2}{4\pi^2}\ln\left(\frac{\Lambda}{a(t)\mu_{\rm full}}\right) = -C_{22}\frac{H^2}{4\pi^2}\ln\left(\frac{\Lambda}{a(t)\mu_{\rm eff}}\right) + H^2C_{20}\,. \tag{4.6.113}$$

This equation then fixes

$$\begin{aligned}C_{22} =& 1\,, &(4.6.114)\\ C_{20} =& -\frac{1}{4\pi^2}\ln\left(\frac{\mu_{\rm eff}}{\mu_{\rm full}}\right)\,, &(4.6.115)\end{aligned}$$

which is the structure that we expected to find from the above considerations.

Next, we look at the following matching equation:

$$[\phi^3](t,\vec{x}) = H^3\Big[C_{33}[\varphi_+^3](t,\vec{x}) + C_{31}\varphi_+(t,\vec{x})\Big]\,, \tag{4.6.116}$$

which, at the level of correlation functions, implies

$$\langle[\phi^3](t,\vec{x})\phi(t,\vec{x}_1)\rangle = H^4\Big[C_{33}\langle[\varphi_+^3](t,\vec{x})\varphi_+(t,\vec{x}_1)\rangle + C_{31}\langle\varphi_+(t,\vec{x})\varphi_+(t,\vec{x}_1)\rangle\Big]\,. \tag{4.6.117}$$

Using again the results that we ovtained above for the free SdSET, we find the following results for the correlators of interest:

$$\begin{aligned}\langle[\phi^3](t,\vec{x})\phi(t,\vec{x}_1)\rangle =& -\frac{3H^2}{4\pi^2}\ln\left(\frac{\Lambda}{a(t)\mu_{\rm full}}\right)\langle\phi(t,\vec{x})\phi(t,\vec{x}_1)\rangle\,, &(4.6.118)\\ \langle[\varphi_+^3](t,\vec{x})\varphi_+(t,\vec{x}_1)\rangle =& -\frac{3}{4\pi^2}\ln\left(\frac{\Lambda}{a(t)\mu_{\rm eff}}\right)\langle\varphi_+(t,\vec{x})\varphi_+(t,\vec{x}_1)\rangle\,, &(4.6.119)\end{aligned}$$

and the matching equation then reads

$$\begin{aligned}&-\frac{3H^2}{4\pi^2}\ln\left(\frac{\Lambda}{a(t)\mu_{\rm full}}\right)\langle\phi(t,\vec{x})\phi(t,\vec{x}_1)\rangle\\ =&H^4\Big[-C_{33}\frac{3}{4\pi^2}\ln\left(\frac{\Lambda}{a(t)\mu_{\rm eff}}\right)\langle\varphi_+(t,\vec{x})\varphi_+(t,\vec{x}_1)\rangle + C_{31}\langle\varphi_+(t,\vec{x})\varphi_+(t,\vec{x}_1)\rangle\Big]\,. &(4.6.120)\end{aligned}$$

Using the fact that

$$\langle\phi(t,\vec{x})\phi(t,\vec{x}_1)\rangle = H^2\langle\varphi_+(t,\vec{x})\varphi_+(t,\vec{x}_1)\rangle \tag{4.6.121}$$

we get

$$C_{33} =1\,, \tag{4.6.122}$$

$$C_{31} =-\frac{3}{4\pi^2}\ln\left(\frac{\mu_{\rm eff}}{\mu_{\rm full}}\right). \tag{4.6.123}$$

Similarly, from the matching equation

$$[\phi^4](t,\vec{x}) = H^4\Big[C_{44}[\varphi_+^4](t,\vec{x})+C_{42}[\varphi_+^2](t,\vec{x})+C_{40}\mathbb{1}\Big] \tag{4.6.124}$$

we find the equation

$$\begin{aligned}&\langle[\phi^4](t,\vec{x})\phi(t,\vec{x}_1)\phi(t,\vec{x}_2)\rangle\\ =&H^6\Big[C_{44}\langle[\varphi_+^4](t,\vec{x})\varphi_+(t,\vec{x}_1)\varphi_+(t,\vec{x}_2)\rangle+C_{42}\langle[\varphi_+^2](t,\vec{x})\varphi_+(t,\vec{x}_1)\varphi_+(t,\vec{x}_2)\rangle+C_{40}\langle\varphi_+(t,\vec{x}_1)\varphi_+(t,\vec{x}_2)\rangle\Big]\,.\end{aligned} \tag{4.6.125}$$

To match the connected part of these correlators, we consider the equation

$$\begin{aligned}&-\frac{3H^2}{2\pi^2}\ln\left(\frac{\Lambda}{a(t)\mu_{\rm full}}\right)\langle[\phi^2](t,\vec{x})\phi(t,\vec{x}_1)\phi(t,\vec{x}_2)\rangle\\ =&H^6\Big[-\frac{3C_{44}}{2\pi^2}\ln\left(\frac{\Lambda}{a(t)\mu_{\rm eff}}\right)+C_{42}\Big]\langle[\varphi_+^2](t,\vec{x})\varphi_+(t,\vec{x}_1)\varphi_+(t,\vec{x}_2)\rangle\,,\end{aligned} \tag{4.6.126}$$

and, using the fact that

$$\langle[\phi^2](t,\vec{x})\phi(t,\vec{x}_1)\phi(t,\vec{x}_2)\rangle = H^4\langle[\varphi_+^2](t,\vec{x})\varphi_+(t,\vec{x}_1)\varphi_+(t,\vec{x}_2)\rangle\,, \tag{4.6.127}$$

we find

$$C_{44} =1\,, \tag{4.6.128}$$

$$C_{42} =-\frac{3}{2\pi^2}\ln\left(\frac{\mu_{\rm eff}}{\mu_{\rm full}}\right). \tag{4.6.129}$$

From the same matching equation we get

$$\langle[\phi^4](t,\vec{x})\rangle = H^4\Big[C_{44}\langle[\varphi_+^4](t,\vec{x})\rangle+C_{42}\langle[\varphi_+^2](t,\vec{x})\rangle+C_{40}\Big]\,. \tag{4.6.130}$$

Using

$$\langle[\phi^4](t,\vec{x})\rangle =\frac{3H^4}{16\pi^4}\ln^2\left(\frac{\Lambda}{a(t)\mu_{\rm full}}\right), \tag{4.6.131}$$

$$\langle[\varphi_+^4](t,\vec{x})\rangle =\frac{3}{16\pi^4}\ln^2\left(\frac{\Lambda}{a(t)\mu_{\rm eff}}\right) \tag{4.6.132}$$

and the found results for C_{44} and C_{42} we get

$$C_{40} =H^{-4}\langle[\phi^4](t,\vec{x})\rangle-\langle[\varphi_+^4](t,\vec{x})\rangle+\frac{3}{2\pi^2}\ln\left(\frac{\mu_{\rm eff}}{\mu_{\rm full}}\right)\langle[\varphi_+^2](t,\vec{x})\rangle \tag{4.6.133}$$

$$=\frac{3}{16\pi^4}\ln^2\left(\frac{\mu_{\rm eff}}{\mu_{\rm full}}\right). \tag{4.6.134}$$

To summarize the above considerations, we have determined the upper 5×5-block of the infinite-dimensional matrix C, which reads

$$C\Big|_{\text{upper }5\times 5} = \begin{pmatrix} 1 & 0 & 0 & 0 & 0 \\ 0 & 1 & 0 & 0 & 0 \\ -\frac{L}{4\pi^2} & 0 & 1 & 0 & 0 \\ 0 & -\frac{3L}{4\pi^2} & 0 & 1 & 0 \\ \frac{3L^2}{16\pi^4} & 0 & -\frac{3L}{2\pi^2} & 0 & 1 \end{pmatrix}, \tag{4.6.135}$$

where we abbreviated

$$L \equiv \ln\left(\frac{\mu_{\text{eff}}}{\mu_{\text{full}}}\right). \tag{4.6.136}$$

Since this is a lower-triangular matrix, it can be inverted in its own right, and we find

$$C^{-1}\Big|_{\text{upper }5\times 5} = \begin{pmatrix} 1 & 0 & 0 & 0 & 0 \\ 0 & 1 & 0 & 0 & 0 \\ \frac{L}{4\pi^2} & 0 & 1 & 0 & 0 \\ 0 & \frac{3L}{4\pi^2} & 0 & 1 & 0 \\ \frac{3L^2}{16\pi^4} & 0 & \frac{3L}{2\pi^2} & 0 & 1 \end{pmatrix}. \tag{4.6.137}$$

Using these results in the formula (4.6.106) we can now check that, indeed, we get the already known results for the anomalous dimensions back, as it must be:

$$\gamma_{20}^{\mu,(\kappa^0)} = -\sum_{l=0}^{\infty} C^{-1}_{2l}\frac{\mathrm{d}C_{l0}}{\mathrm{d}\ln(\mu_{\text{eff}})} = \frac{1}{4\pi^2}, \tag{4.6.138}$$

$$\gamma_{31}^{\mu,(\kappa^0)} = -\sum_{l=0}^{\infty} C^{-1}_{3l}\frac{\mathrm{d}C_{l1}}{\mathrm{d}\ln(\mu_{\text{eff}})} = \frac{3}{4\pi^2}, \tag{4.6.139}$$

$$\gamma_{42}^{\mu,(\kappa^0)} = -\sum_{l=0}^{\infty} C^{-1}_{4l}\frac{\mathrm{d}C_{l2}}{\mathrm{d}\ln(\mu_{\text{eff}})} = \frac{3}{2\pi^2}, \tag{4.6.140}$$

$$\gamma_{40}^{\mu,(\kappa^0)} = -\sum_{l=0}^{\infty} C^{-1}_{4l}\frac{\mathrm{d}C_{l0}}{\mathrm{d}\ln(\mu_{\text{eff}})} = 0. \tag{4.6.141}$$

With the necessary formalism set up, we can start to match interacting SdSET correlation functions involving composite operators to their full-theory counterparts. We will show how to do this in practice in the next two sections by making use of the results we obtained in sections 3.6 and 3.7.

4.7 Matching the one-loop bispectrum of the composite operator ϕ^2 with $\vec{q} = 0$ onto SdSET

As a first example of the matching procedure for correlation functions involving composite operators we are going to match the one-loop bispectrum of the composite operator ϕ^2 in the k_Λ-scheme in the late-time limit we computed in section 3.6. There, we found the following renormalized result for the 1PI contribution to the correlation function:

$$\begin{aligned}&\langle[\phi^2](t,\vec{0})\phi(t,\vec{k})\phi(t,-\vec{k})\rangle'\Big|_{\mathcal{O}(\kappa),\text{ 1PI}} \\ =&\frac{\kappa H^4}{96\pi^2 k^6}\Bigg\{-3\ln\left(\frac{e^{\gamma_E}\mu}{H}\right) + 2\ln\left(\frac{2e^{\gamma_E}k}{a(t)H}\right)\left[-\ln\left(\frac{2e^{\gamma_E}k}{a(t)H}\right) + 2\ln\left(\frac{2k}{\Lambda}\right) + 2\right] - \frac{11}{3}\ln\left(\frac{2k}{\Lambda}\right) \\ &-\frac{\pi k^3}{4\Lambda^2}\left[2 - \ln\left(\frac{2e^{\gamma_E}k}{a(t)H}\right)\right] - \frac{9\pi k}{4\Lambda} + \frac{1}{9} + \frac{\pi^2}{6}\Bigg\},\end{aligned} \tag{4.7.1}$$

where we switched back to using coordinate time t, since in the SdSET it is more convenient to work with this variable, instead of conformal time η. The special kinematic configuration of this correlation function will simplify the computations that will follow, while still allowing us to extract the relevant subhorizon physics linking full-theory and EFT composite operators, which is encoded in the operator matching coefficients appearing in (4.6.101).

4.7.1 Setup of the matching computation: 1PR and 1PI components of the correlator of interest, operator-matching equation

As we already discussed above, at $\mathcal{O}(\kappa)$ the full-theory correlator we want to match has a one-particle reducible (1PR) component, coming from diagrams with topology

and

which simply factorize into products of a free-theory and a one-loop power spectrum, which we both already computed above, and a one-particle-irreducible (1PI) component, which comes from the diagrams

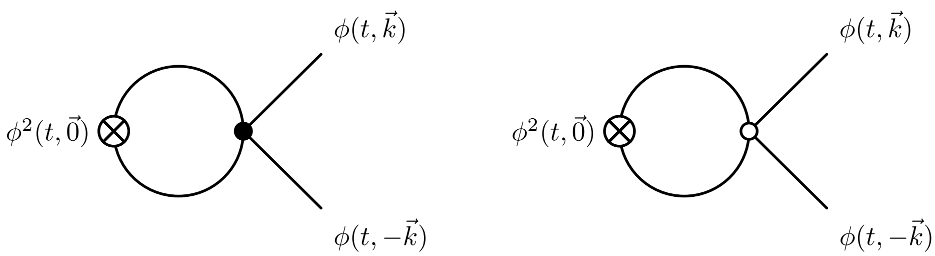

Both components are relevant for the matching, and need to be reproduced by the SdSET. Usually, in flat-space matching computations, the 1PR- and 1PI-parts of correlation functions (or scattering amplitudes) can be matched separately, since they do not mix with each other, and one then usually focusses on 1PI correlators only, since they are the basic building blocks for the 1PR-ones. Below, we will see that, due to the non-linear relation between ϕ and φ_+, these two types of contributions to the full-theory correlation functions are reproduced by the EFT in a way that does not make it possible to completely disentangle them from each other, and, in particular, we cannot disregard the 1PR components. We still find it useful to distinguish them, but, in the end, for the matching computation we will be forced to consider the full connected component of the correlation functions we will be studying.

The goal of this section (as well as the next) will be to relate the renormalized full-theory operator $[\phi^2]$ to renormalized composite operators $[\varphi_+^n]$ in the SdSET. To identify the relevant terms in the general matching equation (4.6.101) between these objects up to $\mathcal{O}(\kappa)$ it is useful to recall that we previously set up the following non-linear relation between full-theory and EFT-fields up to $\mathcal{O}(\kappa)$ and at leading power in λ:

$$\phi(t,\vec{x}) = H^{\frac{d}{2}-1}a(t)^{\frac{4-d}{2}}\left[\left(1+\frac{c^0_{1,1}}{9}\right)\varphi_+(t,\vec{x}) + \frac{c^0_{3,1}a(t)^{4-d}}{18(7-d)}\varphi_+^3(t,\vec{x}) + \mathcal{O}(\kappa^2)\right] + \mathcal{O}(\lambda^{d-1})\,. \tag{4.7.2}$$

This equation tells us that, at $\mathcal{O}(\kappa)$, the operator $[\phi^2]$ will not only be related to $[\varphi_+^2]$, which would be the first guess, but also to $[\varphi_+^4]$, due to the term $\sim \varphi_+^3$ in (4.7.2). Further, having studied the renormalization of the one-point function $\langle \phi^2(t,\vec{x})\rangle$ at $\mathcal{O}(\kappa)$ in section 3.7, and having observed that it necessitates a counterterm proportional to the unit operator, we anticipate that to match $[\phi^2]$ we will need to include this operator in the matching equation at $\mathcal{O}(\kappa)$ as well. We therefore make the following ansatz:

$$[\phi^2](t,\vec{x}) = H^2\Big[C_{20}\mathbb{1} + C_{22}[\varphi_+^2](t,\vec{x}) + C_{24}[\varphi_+^4](t,\vec{x}) + \mathcal{O}(\kappa^2)\Big]\,, \tag{4.7.3}$$

where we anticipate that

$$C_{20} = \mathcal{O}(\kappa)\,, \quad C_{22} = 1+\mathcal{O}(\kappa)\,, \quad C_{24} = \mathcal{O}(\kappa)\,. \tag{4.7.4}$$

Before carrying out any matching computation, we can also anticipate what value of C_{24} we expect to find at $\mathcal{O}(\kappa)$, by simply squaring both sides of (4.7.2) and inspecting the resulting coefficient of the operator φ_+^4 in four dimensions, with $c^0_{3,1} = \kappa + \mathcal{O}(\kappa^2)$ plugged in. Doing so, we find that the coefficient should be

$$C_{24} = \frac{\kappa}{27} + \mathcal{O}(\kappa^2)\,. \tag{4.7.5}$$

Below, we will see that, indeed, this expectation will be confirmed.

The matching equation between connected momentum-space correlation functions, up to $\mathcal{O}(\kappa)$, then reads

$$\begin{aligned}
&\langle[\phi^2](t,\vec{0})\phi(t,\vec{k})\phi(t,-\vec{k})\rangle'\Big|_{\mathcal{O}(\kappa)} \\
=&H^4\Bigg\{\bigg[C_{22}\langle[\varphi_+^2](t,\vec{0})\varphi_+(t,\vec{k})\varphi_+(t,-\vec{k})\rangle' + C_{24}\langle[\varphi_+^4](t,\vec{0})\varphi_+(t,\vec{k})\varphi_+(t,-\vec{k})\rangle'\bigg]\bigg|_{\mathcal{O}(\kappa)} \\
&+\frac{2c^0_{1,1}}{9}\langle[\varphi_+^2](t,\vec{0})\varphi_+(t,\vec{k})\varphi_+(t,-\vec{k})\rangle'\Big|_{\mathcal{O}(\kappa^0)} + \frac{c^0_{3,1}a(t)^{2\varepsilon}}{18(7-d)}\Big[\langle[\varphi_+^2](t,\vec{0})\varphi_+^3(t,\vec{k})\varphi_+(t,-\vec{k})\rangle' \\
&+\langle[\varphi_+^2](t,\vec{0})\varphi_+(t,\vec{k})\varphi_+^3(t,-\vec{k})\rangle'\Big]\Big|_{\mathcal{O}(\kappa^0)}\Bigg\}\,,
\end{aligned} \tag{4.7.6}$$

where, as we already did above, we are using the following definition for the momentum-space composite operators:

$$\varphi_+^n(t,\vec{k}) \equiv \int \mathrm{d}^{d-1}x\; e^{-i\vec{k}\cdot\vec{x}}\varphi_+^n(t,\vec{x})\,. \tag{4.7.7}$$

The last three terms in (4.7.6) come from the non-linear relation (4.7.2) applied to the single fields appearing in the correlation function on the left-hand side of the equation. Notice that the matching equation is formulated in terms of correlation functions of renormalized effective operators, which therefore will not generate any UV divergences, and bare effective couplings, which do contain explicit UV divergences. Since the left-hand side of the equation is UV-finite, we expect that all the explicit UV divergences entering the right-hand side of the equation via the $c^0_{n,m}$ will cancel, once we put the pieces together, and we will see below that it is indeed so. No term proportional to C_{20} appears in (4.7.6), since such a term would only contribute to the disconnected component of the correlation function, which we will not consider here. However, the Wilson coefficient C_{20} will become relevant in the next section.

The main task in this section will be to compute the various SdSET correlation functions appearing in (4.7.6), some of which are already known from the above sections. The most technically challenging part of the computation will be to determine the first correlator on the right-hand side of the equation, which is defined by

$$\langle\varphi_+^2(t,\vec{q})\varphi_+(t,\vec{k}_1)\varphi_+(t,\vec{k}_2)\rangle$$

$$\equiv \int \mathrm{d}^{d-1}x e^{-i\vec{q}\cdot\vec{x}} \int \left[\prod_{j=1}^{2} \frac{\mathrm{d}^{d-1}l_j}{(2\pi)^{d-1}}\right] e^{i\vec{x}\cdot(\vec{l}_1+\vec{l}_2)} \langle \varphi_+(t,\vec{l}_1)\varphi_+(t,\vec{l}_2)\varphi_+(t,\vec{k}_1)\varphi_+(t,\vec{k}_2)\rangle \tag{4.7.8}$$

with the kinematic choice $\vec{k}_1 = -\vec{k}_2 = \vec{k}$. The renormalization of this correlation function will also give us a first chance to discuss operator renormalization in the interacting SdSET. Once this has been done, the results can be plugged into the matching equation (4.7.6), which we will then use to determine the matching coefficients C_{22} and C_{24} at $\mathcal{O}(\kappa)$. We will expand the results we obtain both in small ε and Λ, and keep only the non-vanishing terms in the double limit $\varepsilon \to 0$ and $\Lambda \to 0$. As was the case in the previous sections, since the dependence on the external momentum $\vec{k}$ of the full-theory result needs to be reproduced exactly by the EFT, it is not necessary to expand its deformation in Λ, so we will just write k instead of k_Λ in the final results.

4.7.2 1PI contribution to the correlation function, renormalization of φ_+^2

We start by computing the contributions coming from the 1PI diagram topologies. They will feature UV-divergent terms, which we will remove by renormalizing the operator φ_+^2.

EFT-vertex and initial-condition-counterterm insertion contributions

As was the case for the matching of the one-loop power spectrum, it is most convenient to consider the contributions coming from the insertion of the quartic EFT vertex $\sim c_{3,1}$ and of the initial-condition counterterm $\sim \xi^{\sigma}_{3,1}$ together, since, by construction, a partial cancellation between the two will occur when considering their sum. The insertion of the quartic EFT vertex leads to diagrams with topology

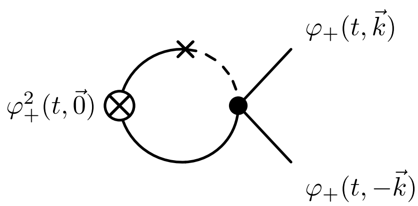

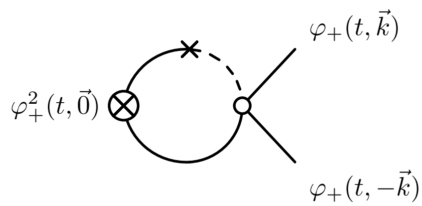

and

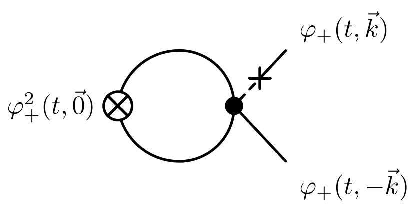

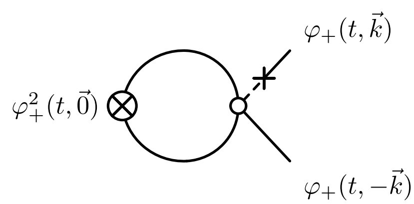

while the insertion of the initial-condition counterterm leads to diagrams with topology

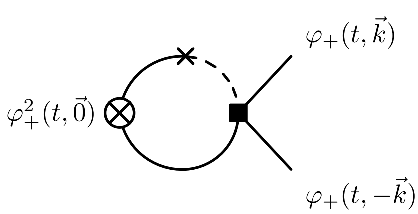

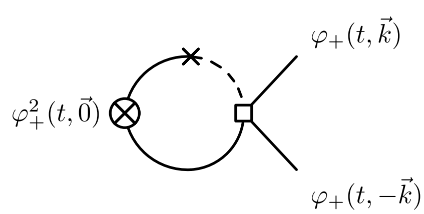

and

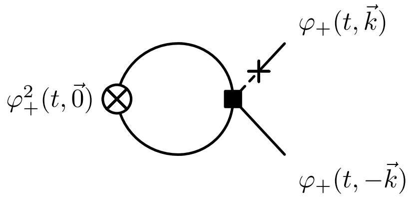

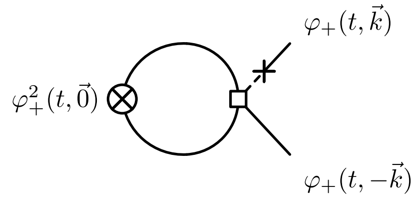

For all of the above diagrams, we must consider all permutations of the occurring lines, as usual. The result for the sum of the correlation functions with the insertion of these terms then reads

$$\begin{aligned}&\langle\varphi_+^2(t,\vec{0})\varphi_+(t,\vec{k})\varphi_+(t,-\vec{k})\rangle'\Big|_{c_{3,1}}+\langle\varphi_+^2(t,\vec{0})\varphi_+(t,\vec{k})\varphi_+(t,-\vec{k})\rangle'\Big|_{\xi_{3,1}}\\ =&-\frac{\tilde{\mu}^{2\varepsilon}\kappa}{24k_\Lambda^6}\frac{a(t)^{2\varepsilon}-a_*^{2\varepsilon}}{2\varepsilon}\left[2\int\frac{\mathrm{d}^{d-1}l}{(2\pi)^{d-1}}\frac{1}{l_\Lambda^3}+2k^3\int\frac{\mathrm{d}^{d-1}l}{(2\pi)^{d-1}}\frac{1}{l_\Lambda^6}\right]\\ =&\frac{\kappa}{96\pi^2k^6}\left(\frac{\Lambda}{a(t)\mu}\right)^{-2\varepsilon}\ln\left(\frac{a_*}{a(t)}\right)\left[\frac{2}{\varepsilon}+2\ln\left(\frac{a_*}{a(t)}\right)+\frac{\pi k^3}{4\Lambda^3}\right],\end{aligned}\tag{4.7.9}$$

where we did not yet expand this result out completely in ε.

The result that we find is both UV- and IR-divergent. As expected, the ε pole stemming from the time integration in the EFT-vertex-insertion diagrams is cancelled by $\xi_{3,1}^\sigma$, and only the UV divergence generated by the momentum integrals remains. Two types of such integrals appear: one which is logarithmically UV- and IR-divergent, which comes from the diagrams with a $\langle\varphi_+\varphi_-\rangle$-line connecting the external operator φ_+^2 to the vertex, and a UV-finite but IR-power-divergent integral, which comes from the diagrams where the $\langle\varphi_+\varphi_-\rangle$-line connects the vertex to the single external fields.

Initial-condition insertion

The last contribution to the 1PI part of the correlation function we are considering comes from the insertion of the finite part of the four-point initial condition $\Xi_{3,1}^\sigma$, for which we previously found the result

$$\Xi_{3,1}^\sigma(\vec{k}_1,\vec{k}_2,\vec{k}_3,\vec{k}_4)=-3\sigma g_{3,1}\left\{\frac{1}{3}\ln\left(\frac{e^{\gamma_E}k_t}{a_*H}\right)+\left(\sum_{j=1}^4k_j^3\right)^{-1}\left[-\frac{k_1k_2k_3k_4}{k_t}+k_t\left(\sum_{j<l}k_jk_l-\frac{4}{9}k_t^2\right)\right]\right\}.\tag{4.7.10}$$

Its insertion into the correlation function that we are considering leads to diagrams with topology

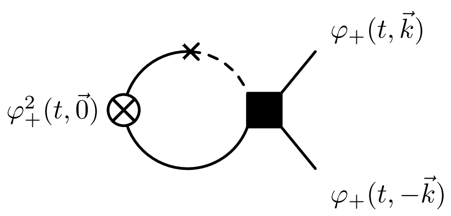

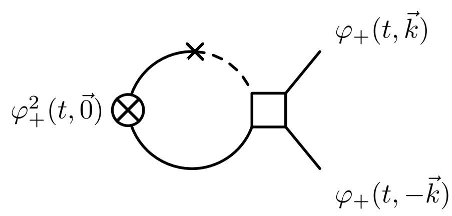

and

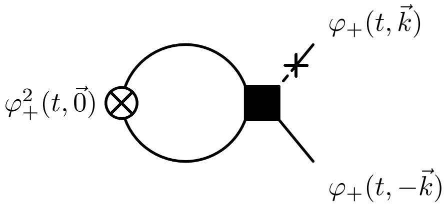

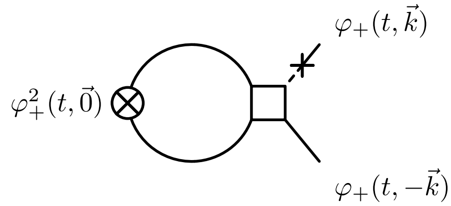

which lead to the following integrals:

$$
\begin{aligned}
&\langle\varphi_+^2(t,\vec{0})\varphi_+(t,\vec{k})\varphi_+(t,-\vec{k})\rangle'\Big|_{\Xi_{3,1}}\\
=&\frac{i(a_*\tilde{\mu})^{2\varepsilon}}{8}\int\frac{\mathrm{d}^{d-1}l}{(2\pi)^{d-1}}\frac{2(k_\Lambda^3+l_\Lambda^3)}{k_\Lambda^6 l_\Lambda^6}\frac{i}{3}\Xi_{3,1}^+(\vec{k},-\vec{k},\vec{l},-\vec{l})\\
=&\frac{g_{3,1}(a_*\tilde{\mu})^{2\varepsilon}}{8k_\Lambda^6}\int\frac{\mathrm{d}^{d-1}l}{(2\pi)^{d-1}}\frac{1}{l_\Lambda^6}\left[\frac{2(l_\Lambda^3+k_\Lambda^3)}{3}\ln\left(\frac{2e^{\gamma_E}(l_\Lambda+k_\Lambda)}{a_*H}\right)-\frac{l_\Lambda^2k_\Lambda^2}{2(l_\Lambda+k_\Lambda)}\right.\\
&\left.-\frac{2}{9}\Big[7k_\Lambda^3+3k_\Lambda^2l_\Lambda+3k_\Lambda l_\Lambda^2+7l_\Lambda^3\Big]\right]. \qquad (4.7.11)
\end{aligned}
$$

We find that we need to evaluate four tadpole-like integrals, which are readily evaluated using `Mathematica`, and two non-trivial types of integrals, one involving a logarithm of the combination $(l_\Lambda+k_\Lambda)$, and the other featuring the same combination in the denominator. The details for the evaluation of these integrals are relegated to appendix 4.D.

Evaluating all of the integrals appearing above leads to the result

$$
\begin{aligned}
&\langle\varphi_+^2(t,\vec{0})\varphi_+(t,\vec{k})\varphi_+(t,-\vec{k})\rangle'\Big|_{\Xi_{3,1}}\\
=&\frac{g_{3,1}}{96\pi^2k^6}\left(\frac{\Lambda}{a_*\mu}\right)^{-2\varepsilon}\left\{\frac{1}{\varepsilon^2}-\frac{2}{\varepsilon}\left[\frac{4}{3}-\ln\left(\frac{e^{\gamma_E}\Lambda}{a_*H}\right)\right]+\ln\left(\frac{2k}{\Lambda}\right)\left[2\ln\left(\frac{2k}{\Lambda}\right)+\frac{1}{3}\right]+\frac{1}{9}+\frac{5\pi^2}{12}\right.\\
&\left.-\frac{9\pi k}{4\Lambda}-\frac{\pi k^3}{4\Lambda^3}\left[\frac{7}{3}-\ln\left(\frac{2e^{\gamma_E}k}{a_*H}\right)\right]\right\}, \qquad (4.7.12)
\end{aligned}
$$

where we also left an ε-dependent coefficient unexpanded, to write the result as transparently as possible. Notice that the result features a double pole, even though we only evaluated a one-loop integral, and this double pole comes from the integral containing the logarithm. One of the UV single-poles appears to have a Λ-dependent coefficient, but the Λ-dependence will drop out once the expression is expanded out completely in ε, leaving only local, Λ-independent poles.

Sum of the terms, renormalization of φ_+^2

In the above results we found UV poles which need to be removed by renormalizing the composite operator φ_+^2, and we can proceed analogously to the renormalization of ϕ^2 that we discussed above in section 3.6. Collecting the pole terms of the results, and expanding the remaining ε-dependent coefficients, we get

$$
\begin{aligned}
&\Big[\langle\varphi_+^2(t,\vec{0})\varphi_+(t,\vec{k})\varphi_+(t,-\vec{k})\rangle'\Big|_{c_{3,1}}+\langle\varphi_+^2(t,\vec{0})\varphi_+(t,\vec{k})\varphi_+(t,-\vec{k})\rangle'\Big|_{\xi_{3,1}}\\
&+\langle\varphi_+^2(t,\vec{0})\varphi_+(t,\vec{k})\varphi_+(t,-\vec{k})\rangle'\Big|_{\Xi_{3,1}}\Big]\Big|_{\text{poles}}\\
=&\frac{g_{3,1}}{96\pi^2k^6}\left\{\frac{1}{\varepsilon^2}+\frac{2}{\varepsilon}\left[\ln\left(\frac{e^{\gamma_E}\mu}{H}\right)-\frac{4}{3}\right]\right\}+\frac{c_{3,1}}{48\pi^2k^6}\frac{1}{\varepsilon}\ln\left(\frac{a_*}{a(t)}\right). \qquad (4.7.13)
\end{aligned}
$$

To renormalize the operator φ_+^2 we use the equation

$$(a(t)\tilde{\mu})^{2\varepsilon}\varphi_+^2(t,\vec{x}) = \sum_{n=0}^{\infty}(a(t)\tilde{\mu})^{n\varepsilon} Z_{2n}[\varphi_+^n](t,\vec{x})\,, \tag{4.7.14}$$

which is just a special case of (4.6.5). The k-dependence of the pole terms matches the structure of the tree-level correlation function

$$\langle[\varphi_+^2](t,\vec{0})\varphi_+(t,\vec{k})\varphi_+(t,-\vec{k})\rangle'\Big|_{\mathcal{O}(\kappa^0)} = \frac{1}{2k^6}\,, \tag{4.7.15}$$

and, from this, we can infer that the appropriate renormalization factor to absorb the UV poles is Z_{22}:

$$Z_{22} = 1 + \frac{g_{3,1}}{48\pi^2}\left\{\frac{1}{\varepsilon^2} + \frac{2}{\varepsilon}\left[\ln\left(\frac{e^{\gamma_E}\mu}{H}\right) - \frac{4}{3}\right]\right\} + \frac{c_{3,1}}{24\pi^2}\frac{1}{\varepsilon}\ln\left(\frac{a_*}{a(t)}\right) + \mathcal{O}(\kappa^2)\,. \tag{4.7.16}$$

The difference between $c_{3,1}$ and $g_{3,1}$ is in their running behaviour, which, for our purposes, is important to distinguish in the Z-factors, but less so in the final, renormalized result. Therefore, to simplify our expressions, at this point we can plug in the matched values for $c_{3,1}$ and $g_{3,1}$, which are both equal to κ up to higher-order corrections, and get the renormalized 1PI component of the correlation function we are studying:

$$\begin{aligned}
&\langle[\varphi_+^2](t,\vec{0})\varphi_+(t,\vec{k})\varphi_+(t,-\vec{k})\rangle'\Big|_{c_{3,1}} + \langle[\varphi_+^2](t,\vec{0})\varphi_+(t,\vec{k})\varphi_+(t,-\vec{k})\rangle'\Big|_{\xi_{3,1}} + \langle[\varphi_+^2](t,\vec{0})\varphi_+(t,\vec{k})\varphi_+(t,-\vec{k})\rangle'\Big|_{\Xi_{3,1}} \\
=&\frac{\kappa}{96\pi^2k^6}\Bigg\{2\ln\left(\frac{e^{\gamma_E}\mu}{H}\right)\left[\ln\left(\frac{e^{\gamma_E}\mu}{H}\right) + 2\ln\left(\frac{a_*}{a(t)}\right) - \frac{8}{3}\right] + 2\ln\left(\frac{2e^{\gamma_E}k}{a(t)H}\right)\Bigg[\ln\left(\frac{2e^{\gamma_E}k}{a(t)H}\right) \\
&- 2\ln\left(\frac{e^{\gamma_E}\Lambda}{a(t)H}\right) - 2\ln\left(\frac{a_*}{a(t)}\right) - \frac{4}{3}\Bigg] + \frac{28}{9} + \frac{5\pi^2}{12} - \frac{3\pi k}{\Lambda} - \frac{\pi k^3}{4\Lambda^3}\left[\frac{7}{3} - \ln\left(\frac{2e^{\gamma_E}k}{a(t)H}\right)\right]\Bigg\}\,.
\end{aligned} \tag{4.7.17}$$

4.7.3 1PR contribution to the correlation function

The 1PR component of the SdSET correlation function we are considering reads

$$\langle\varphi_+^2(t,\vec{0})\varphi_+(t,\vec{k})\varphi_+(t,-\vec{k})\rangle'\Big|_{\mathcal{O}(\kappa),\ \mathrm{1PR}} = 2\langle\varphi_+(t,\vec{k})\varphi_+(t,-\vec{k})\rangle'\Big|_{\mathcal{O}(\kappa^0)} \times \langle\varphi_+(t,\vec{k})\varphi_+(t,-\vec{k})\rangle'\Big|_{\mathcal{O}(\kappa)} \tag{4.7.18}$$

$$\begin{aligned}
=&\frac{c_{3,1}}{24\pi^2k^6}\Bigg\{-\ln\left(\frac{2e^{\gamma_E}k}{a(t)H}\right)\left[\ln\left(\frac{\Lambda}{a(t)\mu}\right) - \hat{c}_{1,1}\right] + 4\ln\left(\frac{\Lambda}{a(t)\mu}\right) \\
&+ \frac{5\hat{c}_{1,1}}{3} + \frac{1}{2}\ln^2\left(\frac{2e^{\gamma_E}k}{a(t)H}\right) - \frac{7}{3}\ln\left(\frac{2e^{\gamma_E}k}{a(t)H}\right) + \frac{10}{3} - \frac{\pi^2}{24}\Bigg\}\,,
\end{aligned} \tag{4.7.19}$$

where we used the results found in section 4.5 for the one-loop SdSET power spectrum. For comparison, the 1PR-part of the full-theory correlator is

$$\langle\phi^2(t,\vec{0})\phi(t,\vec{k})\phi(t,-\vec{k})\rangle'\Big|_{\mathcal{O}(\kappa),\ \mathrm{1PR}} = 2\langle\phi(t,\vec{k})\phi(t,-\vec{k})\rangle'\Big|_{\mathcal{O}(\kappa^0)} \times \langle\phi(t,\vec{k})\phi(t,-\vec{k})\rangle'\Big|_{\mathcal{O}(\kappa)} \tag{4.7.20}$$

$$\begin{aligned}
=&\frac{\kappa H^4}{24\pi^2k^6}\Bigg\{\left[2 - \ln\left(\frac{2e^{\gamma_E}k}{a(t)H}\right)\right]\left[\ln\left(\frac{\Lambda}{a(t)\mu}\right) - \delta\hat{m}^2_{\mathrm{fin}}\right] + \frac{1}{2}\ln^2\left(\frac{2e^{\gamma_E}k}{a(t)H}\right) \\
&- \frac{7}{3}\ln\left(\frac{2e^{\gamma_E}k}{a(t)H}\right) + \frac{8}{3} - \frac{\pi^2}{24}\Bigg\}\,.
\end{aligned} \tag{4.7.21}$$

Plugging in the known values $c_{3,1} = \kappa$ and $\hat{c}_{1,1} = \delta\hat{m}^2_{\mathrm{fin}}$ we see that there is a mismatch between the two results, and, from the discussion in section 4.5, we know that the mismatch comes from the terms generated by the non-linear relation between ϕ and φ_+ (4.7.2), which we did not yet take into account. In the matching equation (4.7.6), the terms

$$\begin{aligned}&\frac{2c^0_{1,1}}{9}\langle[\varphi_+^2](t,\vec{0})\varphi_+(t,\vec{k})\varphi_+(t,-\vec{k})\rangle\Big|_{\mathcal{O}(\kappa^0)}\\&+\frac{c^0_{3,1}a(t)^{2\varepsilon}}{9(7-d)}\Big[\langle[\varphi_+^2](t,\vec{0})\varphi_+^3(t,\vec{k})\varphi_+(t,-\vec{k})\rangle+\langle[\varphi_+^2](t,\vec{0})\varphi_+(t,\vec{k})\varphi_+^3(t,-\vec{k})\rangle\Big]\Big|_{\mathcal{O}(\kappa^0)}\end{aligned}\tag{4.7.22}$$

appearing on the right-hand side only account for the redefinition-terms associated to the external fields, but not for the ones associated to the renormalized operator $[\phi^2]$. They need to be reproduced by appropriately choosing the Wilson coefficient C_{22}, which will therefore receive contributions coming from both the 1PR- and 1PI-components of the correlation function. For later convenience, we split C_{22} up as follows:

$$C_{22}^{(\kappa)}=C_{22}^{\rm 1PR}+C_{22}^{\rm 1PI}\,,\tag{4.7.23}$$

and both pieces will be determined below. Before being able to do so, however, we still need to compute the remaining SdSET correlation functions appearing on the right-hand side of (4.7.6).

4.7.4 Contributions from the field-redefinition terms

In this subsection we compute the contributions coming from the terms in the third and fourth line of the matching equation (4.7.6), which we reprint here for convenience:

$$\begin{aligned}&\langle[\phi^2](t,\vec{0})\phi(t,\vec{k})\phi(t,-\vec{k})\rangle'\Big|_{\mathcal{O}(\kappa)}\\=&H^4\bigg\{\Big[C_{22}\langle[\varphi_+^2](t,\vec{0})\varphi_+(t,\vec{k})\varphi_+(t,-\vec{k})\rangle+C_{24}\langle[\varphi_+^4](t,\vec{0})\varphi_+(t,\vec{k})\varphi_+(t,-\vec{k})\rangle'\Big]\Big|_{\mathcal{O}(\kappa)}\\&+\frac{2c^0_{1,1}}{9}\langle[\varphi_+^2](t,\vec{0})\varphi_+(t,\vec{k})\varphi_+(t,-\vec{k})\rangle'\Big|_{\mathcal{O}(\kappa^0)}+\frac{c^0_{3,1}a(t)^{2\varepsilon}}{18(7-d)}\Big[\langle[\varphi_+^2](t,\vec{0})\varphi_+^3(t,\vec{k})\varphi_+(t,-\vec{k})\rangle'\\&+\langle[\varphi_+^2](t,\vec{0})\varphi_+(t,\vec{k})\varphi_+^3(t,-\vec{k})\rangle\Big]\Big|_{\mathcal{O}(\kappa^0)}\bigg\}\,.\end{aligned}\tag{4.7.24}$$

Since these SdSET correlation functions do not have as illuminating a diagrammatic interpretation as the ones we considered thus far, we will have to identify the results in this section as contributions to the matching of the 1PR- and 1PI-parts of the full-theory correlation function by hand, in order to find the correct results for the matching coefficients below. Notice that we could also have proceeded differently than we did, without distinguishing 1PI and 1PR contributions to the correlation functions, and simply computed all possible contributions to the connected part of the correlation functions appearing on both sides of the matching equation (4.7.6), and we would still find the same results that we are going to find below. There is therefore no arbitrariness introduced by the assignment that we will carry out, as we are simply distributing all contributions to the connected parts of the correlators in a specific way.

Contribution from $[\varphi_+^4](t,\vec{x})$

In section 4.6.3 above we already defined the renormalized position-space correlator

$$\langle[\varphi_+^4](t,\vec{x})\varphi_+(t,\vec{x}_1)\varphi_+(t,\vec{x}_2)\rangle=-\frac{3}{2\pi^2}\ln\left(\frac{\Lambda}{a(t)\mu}\right)\langle[\varphi_+^2](t,\vec{x})\varphi_+(t,\vec{x}_1)\varphi_+(t,\vec{x}_2)\rangle\,,\tag{4.7.25}$$

which, in momentum space, translates to (setting $\vec{k}_1=-\vec{k}_2=\vec{k}$)

$$\langle[\varphi_+^4](t,\vec{0})\varphi_+(t,\vec{k})\varphi_+(t,-\vec{k})\rangle'=-\frac{3}{4\pi^2k^6}\ln\left(\frac{\Lambda}{a(t)\mu}\right)\,.\tag{4.7.26}$$

The contribution (4.7.26) needs to be split in two equal pieces, and one half is identified as a contribution to the 1PI topology, the other to the 1PR topology:

$$\langle[\varphi_+^4](t,\vec{0})\varphi_+(t,\vec{k})\varphi_+(t,-\vec{k})\rangle'\Big|_{\text{1PR}} = -\frac{3}{8\pi^2k^6}\ln\left(\frac{\Lambda}{a(t)\mu}\right), \tag{4.7.27}$$

$$\langle[\varphi_+^4](t,\vec{0})\varphi_+(t,\vec{k})\varphi_+(t,-\vec{k})\rangle'\Big|_{\text{1PI}} = -\frac{3}{8\pi^2k^6}\ln\left(\frac{\Lambda}{a(t)\mu}\right). \tag{4.7.28}$$

Contributions from external fields

We also have to consider the correlator

$$\begin{aligned}&\langle\varphi_+^2(t,\vec{q})\varphi_+^3(t,\vec{k}_1)\varphi_+(t,\vec{k}_2)\rangle\\ =&6(2\pi)^{d-1}\delta^{(d-1)}(\vec{k}_1+\vec{k}_2+\vec{q})\frac{1}{2k_{2\Lambda}^3}\int\frac{\mathrm{d}^{d-1}l}{(2\pi)^{d-1}}\left[\frac{1}{4l_\Lambda^3|\vec{l}-\vec{q}|_\Lambda^3}+\frac{1}{4k_{1\Lambda}^3l_\Lambda^3}\right],\end{aligned} \tag{4.7.29}$$

with the kinematic configuration $\vec{k}_1=-\vec{k}_2=\vec{k}$, as well as the correlator with φ_+^3 and φ_+ exchanged. It will be sufficient to compute the above correlation function, and the other one will then simply be equal.

Also in this case, we need to split this correlator up into its 1PI-part,

$$\begin{aligned}\langle\varphi_+^2(t,\vec{0})\varphi_+^3(t,\vec{k})\varphi_+(t,-\vec{k})\rangle'\Big|_{\text{1PI}} =&\frac{3}{4k_\Lambda^3}\int\frac{\mathrm{d}^{d-1}l}{(2\pi)^{d-1}}\frac{1}{l_\Lambda^6}\\ =&\frac{3}{4k^3}\frac{1}{32\pi\Lambda^3},\end{aligned} \tag{4.7.30}$$

which is UV-finite, and 1PR-part,

$$\begin{aligned}\langle\varphi_+^2(t,\vec{0})\varphi_+^3(t,\vec{k})\varphi_+(t,-\vec{k})\rangle'\Big|_{\text{1PR}} =&\frac{3}{4k_\Lambda^6}\int\frac{\mathrm{d}^{d-1}l}{(2\pi)^{d-1}}\frac{1}{l_\Lambda^3}\\ =&\frac{3}{16\pi^2k^6}\left(\frac{e^{\gamma_E}\Lambda^2}{4\pi}\right)^{-\varepsilon}\frac{1}{\varepsilon},\end{aligned} \tag{4.7.31}$$

which is UV- and IR-divergent. From this result, the following expressions follow immediately:

$$\langle\varphi_+^2(t,\vec{0})\varphi_+(t,\vec{k})\varphi_+^3(t,-\vec{k})\rangle'\Big|_{\text{1PI}} =\frac{3}{4k^3}\frac{1}{32\pi\Lambda^3}, \tag{4.7.32}$$

$$\langle\varphi_+^2(t,\vec{0})\varphi_+(t,\vec{k})\varphi_+^3(t,-\vec{k})\rangle'\Big|_{\text{1PR}} =\frac{3}{16\pi^2k^6}\left(\frac{e^{\gamma_E}\Lambda^2}{4\pi}\right)^{-\varepsilon}\frac{1}{\varepsilon}. \tag{4.7.33}$$

Finally, we have the tree-level correlator

$$\langle[\varphi_+^2](t,\vec{0})\varphi_+(t,\vec{k})\varphi_+(t,-\vec{k})\rangle'\Big|_{\mathcal{O}(\kappa^0)} = \frac{1}{2k^6}, \tag{4.7.34}$$

which we already considered above. Putting the pieces together in (4.7.6), and using the known d-dimensional results for the effective couplings

$$c_{1,1}^0 =\frac{c_{3,1}}{8\pi^2}\left[-\frac{1}{2\varepsilon}+\hat{c}_{1,1}\right]+\mathcal{O}(\kappa^2), \tag{4.7.35}$$

$$c_{3,1}^0 =\tilde{\mu}^{2\varepsilon}c_{3,1}+\mathcal{O}(\kappa^2), \tag{4.7.36}$$

we find the following result for the relevant combination of 1PR components

$$\frac{2c_{1,1}^0}{9}\langle[\varphi_+^2](t,\vec{0})\varphi_+(t,\vec{k})\varphi_+(t,-\vec{k})\rangle'\Big|_{\mathcal{O}(\kappa^0)}+\frac{c_{3,1}^0a(t)^{2\varepsilon}}{18(3+2\varepsilon)}\Bigg[\langle\varphi_+^2(t,\vec{0})\varphi_+^3(t,\vec{k})\varphi_+(t,-\vec{k})\rangle'\Big|_{\mathcal{O}(\kappa^0),\text{ 1PR}}$$

$$+\langle\varphi_+^2(t,\vec{0})\varphi_+(t,\vec{k})\varphi_+^3(t,-\vec{k})\rangle'\Big|_{\mathcal{O}(\kappa^0),\ \text{1PR}}\Bigg]$$
$$=\frac{c_{3,1}}{96\pi^2k^6}\frac{4}{3}\left[\hat{c}_{1,1}-\frac{1}{3}-\ln\left(\frac{\Lambda}{a(t)\mu}\right)\right], \tag{4.7.37}$$

and 1PI components

$$\frac{c^0_{3,1}a(t)^{2\varepsilon}}{18(3+2\varepsilon)}\left[\langle\varphi_+^2(t,\vec{0})\varphi_+^3(t,\vec{k})\varphi_+(t,-\vec{k})\rangle'\Big|_{\mathcal{O}(\kappa^0),\ \text{1PI}}+\langle\varphi_+^2(t,\vec{0})\varphi_+(t,\vec{k})\varphi_+^3(t,-\vec{k})\rangle'\Big|_{\mathcal{O}(\kappa^0),\ \text{1PI}}\right]=\frac{c_{3,1}}{96\pi^2k^6}\frac{\pi k^3}{12\Lambda^3} \tag{4.7.38}$$

of the correlation functions. Notice that, as we anticipated above, even though these combinations involve bare effective couplings, they are UV-finite once all terms are plugged in.

4.7.5 Matching the correlators

We now have all the pieces we need to carry out the matching computation of both the 1PR and 1PI components of the correlator of interest. The relevant terms of the operator matching equation (4.7.3) up to $\mathcal{O}(\kappa)$ are

$$[\phi^2](t,\vec{x})=H^2\left[\left(1+C_{22}^{(\kappa)}\right)[\varphi_+^2](t,\vec{x})+C_{24}^{(\kappa)}[\varphi_+^4](t,\vec{x})+\mathcal{O}(\kappa^2)\right], \tag{4.7.39}$$

and we employ the split of the Wilson coefficient

$$C_{22}^{(\kappa)}=C_{22}^{\text{1PR}}+C_{22}^{\text{1PI}} \tag{4.7.40}$$

we motivated above.

1PI-components

The matching equation for these components reads

$$\langle[\phi^2](t,\vec{0})\phi(t,\vec{k})\phi(t,-\vec{k})\rangle'\Big|_{\mathcal{O}(\kappa),\ \text{1PI}}$$
$$=H^4\Bigg\{\langle[\varphi_+^2](t,\vec{0})\varphi_+(t,\vec{k})\varphi_+(t,-\vec{k})\rangle'\Big|_{\mathcal{O}(\kappa),\ \text{1PI}}+C_{22}^{\text{1PI}}\langle[\varphi_+^2](t,\vec{0})\varphi_+(t,\vec{k})\varphi_+(t,-\vec{k})\rangle'\Big|_{\mathcal{O}(\kappa^0)}$$
$$+C_{24}^{(\kappa)}\langle[\varphi_+^4](t,\vec{0})\varphi_+(t,\vec{k})\varphi_+(t,-\vec{k})\rangle'\Big|_{\mathcal{O}(\kappa^0),\ \text{1PI}}+\frac{c^0_{3,1}a(t)^{2\varepsilon}}{18(3+2\varepsilon)}\Bigg[\langle[\varphi_+^2](t,\vec{0})\varphi_+^3(t,\vec{k})\varphi_+(t,-\vec{k})\rangle'\Big|_{\mathcal{O}(\kappa^0),\ \text{1PI}}$$
$$+\langle[\varphi_+^2](t,\vec{0})\varphi_+(t,\vec{k})\varphi_+^3(t,-\vec{k})\rangle'\Big|_{\mathcal{O}(\kappa^0),\ \text{1PI}}\Bigg]\Bigg\}. \tag{4.7.41}$$

The goal is now to determine the matching coefficients C_{22}^{1PI} and C_{24} at $\mathcal{O}(\kappa)$. The renormalized full-theory correlator is

$$\langle[\phi^2](t,\vec{0})\phi(t,\vec{k})\phi(t,-\vec{k})\rangle'\Big|_{\mathcal{O}(\kappa),\ \text{1PI}}$$
$$=\frac{\kappa H^4}{96\pi^2k^6}\Bigg\{-3\ln\left(\frac{e^{\gamma_E}\mu}{H}\right)+2\ln\left(\frac{2e^{\gamma_E}k}{a(t)H}\right)\left[-\ln\left(\frac{2e^{\gamma_E}k}{a(t)H}\right)+2\ln\left(\frac{2k}{\Lambda}\right)+2\right]-\frac{11}{3}\ln\left(\frac{2k}{\Lambda}\right)$$
$$-\frac{\pi k^3}{4\Lambda^2}\left[2-\ln\left(\frac{2e^{\gamma_E}k}{a(t)H}\right)\right]-\frac{9\pi k}{4\Lambda}+\frac{1}{9}+\frac{\pi^2}{6}\Bigg\}, \tag{4.7.42}$$

and above we found the results

$$\langle[\varphi_+^4](t,\vec{0})\varphi_+(t,\vec{k})\varphi_+(t,-\vec{k})\rangle'\Big|_{\mathcal{O}(\kappa^0),\ \text{1PI}}=-\frac{3}{8\pi^2k^6}\ln\left(\frac{\Lambda}{a(t)\mu}\right) \tag{4.7.43}$$

$$\langle\varphi_+^2(t,\vec{0})\varphi_+^3(t,\vec{k})\varphi_+(t,-\vec{k})\rangle'\Big|_{\mathcal{O}(\kappa^0),\ \mathrm{1PI}} = \langle\varphi_+^2(t,\vec{0})\varphi_+(t,\vec{k})\varphi_+^3(t,-\vec{k})\rangle\Big|'_{\mathcal{O}(\kappa^0),\ \mathrm{1PI}} = \frac{3}{4k^3}\frac{1}{32\pi\Lambda^3}\,. \tag{4.7.44}$$

Using them in (4.7.41), and plugging the known value $c_{3,1} = \kappa + \mathcal{O}(\kappa^2)$ in this equation as well, we get the following relation:

$$\begin{aligned}
&C_{22}^{\mathrm{1PI}}\langle[\varphi_+^2](t,\vec{0})\varphi_+(t,\vec{k})\varphi_+(t,-\vec{k})\rangle'\Big|_{\mathcal{O}(\kappa^0)} + C_{24}^{(\kappa)}\langle[\varphi_+^4](t,\vec{0})\varphi_+(t,\vec{k})\varphi_+(t,-\vec{k})\rangle'\Big|_{\mathcal{O}(\kappa^0)}\\
=&H^{-4}\langle[\phi^2](t,\vec{0})\phi(t,\vec{k})\phi(t,-\vec{k})\rangle'\Big|_{\mathcal{O}(\kappa),\ \mathrm{1PI}} - \Bigg[\langle[\varphi_+^2](t,\vec{0})\varphi_+(t,\vec{k})\varphi_+(t,-\vec{k})\rangle'\Big|_{\mathcal{O}(\kappa),\ \mathrm{1PI}}\\
&+\frac{c_{3,1}^0 a(t)^{2\varepsilon}}{18(3+2\varepsilon)}\bigg(\langle[\varphi_+^2](t,\vec{0})\varphi_+^3(t,\vec{k})\varphi_+(t,-\vec{k})\rangle'\Big|_{\mathcal{O}(\kappa^0),\ \mathrm{1PI}} + \langle[\varphi_+^2](t,\vec{0})\varphi_+(t,\vec{k})\varphi_+^3(t,-\vec{k})\rangle'\Big|_{\mathcal{O}(\kappa^0),\ \mathrm{1PI}}\bigg)\Bigg]\\
=&\frac{\kappa}{96\pi^2k^6}\left\{\ln\left(\frac{e^{\gamma_E}\mu}{H}\right)\left[\frac{7}{3} - 4\ln\left(\frac{a_*}{a(t)}\right) - 2\ln\left(\frac{e^{\gamma_E}\mu}{H}\right)\right] + 4\ln\left(\frac{a_*}{a(t)}\right) - \frac{4}{3}\ln\left(\frac{e^{\gamma_E}\Lambda}{a_*H}\right) - \frac{\pi^2}{4}\right\}.
\end{aligned} \tag{4.7.45}$$

From (4.7.26) we see that we can match the $\ln(\Lambda)$-term by picking

$$C_{24}^{(\kappa)} = \frac{\kappa}{27}\,, \tag{4.7.46}$$

which is the expected result from the non-linear relation between ϕ and φ_+ we discussed above. Bringing this now-known term to the other side of (4.7.41) the terms that are then left over read

$$\begin{aligned}
&C_{22}^{\mathrm{1PI}}\langle[\varphi_+^2](t,\vec{0})\varphi_+(t,\vec{k})\varphi_+(t,-\vec{k})\rangle'\Big|_{\mathcal{O}(\kappa^0)}\\
=&\frac{\kappa}{96\pi^2k^6}\left\{\ln\left(\frac{e^{\gamma_E}\mu}{H}\right)\left[1 - 2\ln\left(\frac{e^{\gamma_E}a_*^2\mu}{a(t)^2H}\right)\right] + \frac{16}{3}\ln\left(\frac{a_*}{a(t)}\right) - \frac{\pi^2}{4}\right\}.
\end{aligned} \tag{4.7.47}$$

Using that

$$\langle[\varphi_+^2](t,\vec{0})\varphi_+(t,\vec{k})\varphi_+(t,-\vec{k})\rangle'\Big|_{\mathcal{O}(\kappa^0)} = \frac{1}{2k^6} \tag{4.7.48}$$

we can reproduce the right-hand-side of the equation by fixing

$$C_{22}^{\mathrm{1PI}} = \frac{\kappa}{48\pi^2}\left[\ln\left(\frac{e^{\gamma_E}\mu}{H}\right)\left[1 - 2\ln\left(\frac{e^{\gamma_E}a_*^2\mu}{a(t)^2H}\right)\right] + \frac{16}{3}\ln\left(\frac{a_*}{a(t)}\right) - \frac{\pi^2}{4}\right] + \mathcal{O}(\kappa^2)\,. \tag{4.7.49}$$

1PR-components

We are now only missing the 1PR-part of the matching. The matching equation for these components of the correlators reads

$$\begin{aligned}
&H^{-4}\langle[\phi^2](t,\vec{0})\phi(t,\vec{k})\phi(t,-\vec{k})\rangle'\Big|_{\mathcal{O}(\kappa),\ \mathrm{1PR}}\\
=&\Bigg[\langle[\varphi_+^2](t,\vec{0})\varphi_+(t,\vec{k})\varphi_+(t,-\vec{k})\rangle'\Big|_{\mathcal{O}(\kappa),\ \mathrm{1PR}} + C_{22}^{\mathrm{1PR}}\langle[\varphi_+^2](t,\vec{0})\varphi_+(t,\vec{k})\varphi_+(t,-\vec{k})\rangle'\Big|_{\mathcal{O}(\kappa^0)}\\
&+\frac{\kappa}{27}\langle[\varphi_+^4](t,\vec{0})\varphi_+(t,\vec{k})\varphi_+(t,-\vec{k})\rangle'\Big|_{\mathcal{O}(\kappa),\ \mathrm{1PR}}\Bigg]\\
&+\frac{2c_{1,1}^0}{9}\langle[\varphi_+^2](t,\vec{0})\varphi_+(t,\vec{k})\varphi_+(t,-\vec{k})\rangle'\Big|_{\mathcal{O}(\kappa^0)} + \frac{c_{3,1}^0 a(t)^{2\varepsilon}}{18(3+2\varepsilon)}\Bigg[\langle[\varphi_+^2](t,\vec{0})\varphi_+^3(t,\vec{k})\varphi_+(t,-\vec{k})\rangle'\Big|_{\mathcal{O}(\kappa^0),\ \mathrm{1PR}}\\
&+\langle[\varphi_+^2](t,\vec{0})\varphi_+(t,\vec{k})\varphi_+^3(t,-\vec{k})\rangle'\Big|_{\mathcal{O}(\kappa^0),\ \mathrm{1PR}}\Bigg],
\end{aligned} \tag{4.7.50}$$

where we plugged in the determined value for C_{24}. As we discussed above in section 4.7.3, the mismatch between the 1PR-components of the full-theory and EFT-correlators is simply the one stemming from the field-redefiniton terms applied to the two fields making up the composite operator ϕ^2, which reads

$$\begin{aligned}&\frac{\kappa}{36\pi^2 k^6}\left[\delta\hat{m}^2_{\text{fin}} - \ln\left(\frac{\Lambda}{a(t)\mu}\right) - \frac{1}{3}\right]\\ =&H^{-4}\langle[\phi^2](t,\vec{0})\phi(t,\vec{k})\phi(t,-\vec{k})\rangle'\Big|_{\mathcal{O}(\kappa),\ \text{1PR}} - \langle[\varphi_+^2](t,\vec{0})\varphi_+(t,\vec{k})\varphi_+(t,-\vec{k})\rangle'\Big|_{\mathcal{O}(\kappa),\ \text{1PR}}\,,\end{aligned} \tag{4.7.51}$$

so this difference needs to be reproduced by the remaining terms appearing on the right-hand side of the matching equation (4.7.50). We already found above that the combination

$$\begin{aligned}&\frac{2c^0_{1,1}}{9}\langle[\varphi_+^2](t,\vec{0})\varphi_+(t,\vec{k})\varphi_+(t,-\vec{k})\rangle'\Big|_{\mathcal{O}(\kappa^0)} + \frac{c^0_{3,1}a(t)^{2\varepsilon}}{18(3+2\varepsilon)}\Big[\langle\varphi_+^2(t,\vec{0})\varphi_+^3(t,\vec{k})\varphi_+(t,-\vec{k})\rangle'\Big|_{\mathcal{O}(\kappa^0),\ \text{1PR}}\\ &+\langle\varphi_+^2(t,\vec{0})\varphi_+(t,\vec{k})\varphi_+^3(t,-\vec{k})\rangle'\Big|_{\mathcal{O}(\kappa^0),\ \text{1PR}}\Big]\\ =&\frac{c_{3,1}}{72\pi^2 k^6}\left[\hat{c}^{\text{fin}}_{1,1} - \frac{1}{3} - \ln\left(\frac{\Lambda}{a(t)\mu}\right)\right]\end{aligned} \tag{4.7.52}$$

is finite, and we also obtained the result

$$\frac{\kappa}{27}\langle[\varphi_+^4](t,\vec{0})\varphi_+(t,\vec{k})\varphi_+(t,-\vec{k})\rangle'\Big|_{\mathcal{O}(\kappa^0),\ \text{1PR}} = -\frac{\kappa}{72\pi^2 k^6}\ln\left(\frac{\Lambda}{a(t)\mu}\right). \tag{4.7.53}$$

Combining these expressions, and using (4.7.48), as well as the known values for $c_{3,1}$ and $\hat{c}_{1,1}$, we get

$$\begin{aligned}&\frac{\kappa}{27}\langle[\varphi_+^4](t,\vec{0})\varphi_+(t,\vec{k})\varphi_+(t,-\vec{k})\rangle'\Big|_{\mathcal{O}(\kappa),\ \text{1PR}} + \frac{2c^0_{1,1}}{9}\langle[\varphi_+^2](t,\vec{0})\varphi_+(t,\vec{k})\varphi_+(t,-\vec{k})\rangle'\Big|_{\mathcal{O}(\kappa^0)}\\ &+\frac{c^0_{3,1}a(t)^{2\varepsilon}}{18(3+2\varepsilon)}\Big[\langle[\varphi_+^2](t,\vec{0})\varphi_+^3(t,\vec{k})\varphi_+(t,-\vec{k})\rangle'\Big|_{\mathcal{O}(\kappa^0),\ \text{1PR}} + \langle[\varphi_+^2](t,\vec{0})\varphi_+(t,\vec{k})\varphi_+^3(t,-\vec{k})\rangle'\Big|_{\mathcal{O}(\kappa^0),\ \text{1PR}}\Big]\\ &+C_{22}^{\text{1PR}}\langle[\varphi_+^2](t,\vec{0})\varphi_+(t,\vec{k})\varphi_+(t,-\vec{k})\rangle'\Big|_{\mathcal{O}(\kappa^0)}\\ =&\frac{\kappa}{72\pi^2 k^6}\left[\delta\hat{m}^2_{\text{fin}} - \frac{1}{3} - 2\ln\left(\frac{\Lambda}{a(t)\mu}\right)\right] + \frac{C_{22}^{\text{1PR}}}{2k^6}\,.\end{aligned} \tag{4.7.54}$$

Comparing this combination of terms to (4.7.51), we see that the logarithmic term is correctly reproduced, while the missing constant terms need to be made up by C_{22}^{1PR}, so we fix

$$C_{22}^{\text{1PR}} = \frac{\kappa}{36\pi^2}\left[\delta\hat{m}^2_{\text{fin}} - \frac{1}{3}\right] + \mathcal{O}(\kappa^2)\,. \tag{4.7.55}$$

4.7.6 Main results of the matching computation

Let us summarize our findings from this computation. The main result has been the determination of the matching coefficients C_{22} and C_{24}, which up to $\mathcal{O}(\kappa)$ read

$$C_{22} = 1 + \frac{\kappa}{48\pi^2}\left[\ln\left(\frac{e^{\gamma_E}\mu}{H}\right)\left[1 - 2\ln\left(\frac{e^{\gamma_E}a_*^2\mu}{a(t)^2 H}\right)\right] + \frac{16}{3}\ln\left(\frac{a_*}{a(t)}\right) + \frac{4}{3}\delta\hat{m}^2_{\text{fin}} - \frac{4}{9} - \frac{\pi^2}{4}\right] + \mathcal{O}(\kappa^2) \tag{4.7.56}$$

and

$$C_{24} = \frac{\kappa}{27} + \mathcal{O}(\kappa^2)\,. \tag{4.7.57}$$

Along the way, we also carried out the first renormalization of an SdSET composite operator in the interacting theory, and determined the renormalization factor

$$Z_{22} = 1 + \frac{g_{3,1}}{48\pi^2}\left\{\frac{1}{\varepsilon^2} + \frac{2}{\varepsilon}\left[\ln\left(\frac{e^{\gamma_E}\mu}{H}\right) - \frac{4}{3}\right]\right\} + \frac{c_{3,1}}{24\pi^2}\frac{1}{\varepsilon}\ln\left(\frac{a_*}{a(t)}\right) + \mathcal{O}(\kappa^2)\,. \tag{4.7.58}$$

Both Z_{22} and C_{22} are local in position, but they display a non-trivial dependence on the scale μ, as well as on the scale factors a_* and $a(t)$. Notably, the dependence on the last two quantities drops out if we pick $a_* = a(t)$, which will become relevant later in this chapter.

The fact that we were able to reproduce the complete Λ- and k-dependence of the full-theory correlation function by matching the local coefficients C_{22} and C_{24} constitutes a non-trivial consistency check on the general framework of the SdSET, as well as our formulation of it.

4.7.7 Determination of the operator anomalous dimensions γ_{22}^{μ} and $\gamma_{22}^{a_*}$

Having determined both the renormalization factor Z_{22} and the matching coefficient C_{22} at $\mathcal{O}(\kappa)$, we are now in the position to compute the operator anomalous dimensions γ_{22}^{μ} and $\gamma_{22}^{a_*}$ at $\mathcal{O}(\kappa)$. As we discussed above in section 4.6, the anomalous dimensions can be computed from the renormalization factors alone, already before carrying out the matching computation, and for the anomalous dimensions of interest the relevant formulas read

$$\gamma_{22}^{\mu} = -\,2\varepsilon + \sum_{l=0}^{\infty} Z_{2l}^{-1}\left[l\varepsilon Z_{l2} - \frac{\mathrm{d}Z_{l2}}{\mathrm{d}\ln(\mu)}\right], \tag{4.7.59}$$

$$\gamma_{22}^{a_*} = -\sum_{l=0}^{\infty} Z_{2l}^{-1}\frac{\mathrm{d}Z_{l2}}{\mathrm{d}\ln(a_*)}\,. \tag{4.7.60}$$

On the other hand, these same anomalous dimension govern the dependence of the renormalized Wilson coefficients on the factorization scales $\mu = \mu_{\text{eff}}$ and on the reference scale factor a_*, respectively:

$$\gamma_{22}^{\mu} = -\sum_{l=0}^{\infty} C_{2l}^{-1}\frac{\mathrm{d}C_{l2}}{\mathrm{d}\ln(\mu_{\text{eff}})}\,, \tag{4.7.61}$$

$$\gamma_{22}^{a_*} = -\sum_{l=0}^{\infty} C_{2l}^{-1}\frac{\mathrm{d}C_{l2}}{\mathrm{d}\ln(a_*)}\,. \tag{4.7.62}$$

Therefore, we can use the results for these two anomalous dimensions to run a self-consistency check on our framework. In order to get the correct result for γ_{22}^{μ} from C_{22}, it is very important to properly differentiate between the renormalization scale of the full theory, which we will call μ_{full}, and of the EFT, which we will call μ_{eff}, which we set equal above when determining C_{22}, as well as to take into account the fact that already at $\mathcal{O}(\kappa^0)$ the Wilson coefficients have a non-vanishing μ_{eff}-dependence, as we discussed in section 4.6.4.

Computation of γ_{22}^{μ}

At this order in κ, the formula (4.7.59) for the μ-anomalous dimension reduces to

$$\begin{aligned}\gamma_{22}^{\mu} &= -\,\frac{\mathrm{d}Z_{22}^{(\kappa)}}{\mathrm{d}\ln(\mu)} + \mathcal{O}(\kappa^2) &(4.7.63)\\ &= -\,\frac{\kappa}{12\pi^2}\left[\frac{4}{3} - \ln\left(\frac{e^{\gamma_E}a_*\mu}{a(t)H}\right)\right] + \mathcal{O}(\kappa^2)\,, &(4.7.64)\end{aligned}$$

where we used the result (4.7.58) for Z_{22}, as well as the tree-level RGEs

$$\frac{\mathrm{d}c_{3,1}}{\mathrm{d}\ln(\mu)} = -2\varepsilon c_{3,1}\,, \tag{4.7.65}$$

$$\frac{\mathrm{d}g_{3,1}}{\mathrm{d}\ln(\mu)} = -2\varepsilon g_{3,1}\,, \tag{4.7.66}$$

and plugged in the matched values for $c_{3,1} = g_{3,1} = \kappa$ at the end, to simplify the expression.

We can now use this result to check the μ_{eff}-dependence of C_{22}, and to do so correctly we need to identify all terms that are μ_{eff}-dependent. We can do this by explicitly differentiating μ_{full} and μ_{eff}, and reminding ourselves that the term proportional to $\kappa\delta\hat{m}^2_{\text{fin}}$ appearing in the final result (4.7.56) came from $c_{3,1}\hat{c}_{1,1}$, which has a non-trivial running behaviour in four dimensions. It is not necessary to trace κ back to the couplings $c_{3,1}$ and $g_{3,1}$ for all the other terms appearing in C_{22}, since they both have vanishing running in four dimensions at this order in the expansion. Therefore, we rewrite C_{22} as follows:

$$\begin{aligned} C^{(\kappa)}_{22} =& \frac{\kappa}{48\pi^2}\left[2\ln\left(\frac{e^{\gamma_E}\mu_{\text{eff}}}{H}\right)\left[2-\ln\left(\frac{e^{\gamma_E}a_*^2\mu_{\text{eff}}}{a(t)^2H}\right)\right]+\frac{16}{3}\ln\left(\frac{a_*}{a(t)}\right)-3\ln\left(\frac{e^{\gamma_E}\mu_{\text{full}}}{H}\right)\right. \\ &\left.-\frac{4}{9}-\frac{\pi^2}{4}\right]+\frac{c_{3,1}}{36\pi^2}\hat{c}^{\text{fin}}_{1,1}\,. \end{aligned} \tag{4.7.67}$$

At $\mathcal{O}(\kappa)$ the formula (4.7.61) for γ^{μ}_{22} reads

$$\gamma^{\mu}_{22} = -\left[\frac{\mathrm{d}C^{(\kappa)}_{22}}{\mathrm{d}\ln(\mu_{\text{eff}})} - C^{(\kappa)}_{24}\frac{\mathrm{d}C^{(\kappa^0)}_{42}}{\mathrm{d}\ln(\mu_{\text{eff}})}\right]+\mathcal{O}(\kappa^2)\,, \tag{4.7.68}$$

where we used the fact that $C_{02} = 0$ to all orders in κ, and we inverted the matrix of matching coefficients, taking into account the non-trivial $\mathcal{O}(\kappa^0)$-terms we found in section 4.6.4, perturbatively. Using

$$\frac{\mathrm{d}}{\mathrm{d}\ln(\mu_{\text{eff}})}\left[c_{3,1}\hat{c}^{\text{fin}}_{1,1}\right] = -c_{3,1} \tag{4.7.69}$$

and, using the result for $C^{(\kappa^0)}_{42}$ that we obtained in (4.6.129) we get

$$\frac{\mathrm{d}C^{(\kappa^0)}_{42}}{\mathrm{d}\ln(\mu_{\text{eff}})} = -\frac{3}{2\pi^2}\,, \tag{4.7.70}$$

which leads us to the result

$$\gamma^{\mu}_{22} = -\frac{\kappa}{12\pi^2}\left[\frac{4}{3}-\ln\left(\frac{e^{\gamma_E}a_*\mu_{\text{eff}}}{a(t)H}\right)\right]+\mathcal{O}(\kappa^2)\,. \tag{4.7.71}$$

It agrees with (4.7.64) after setting $\mu_{\text{eff}} = \mu$, as it should.

Computation of $\gamma^{a_*}_{22}$

The computation of the a_*-anomalous dimension $\gamma^{a_*}_{22}$ is less involved than the one for γ^{μ}_{22}. The formula (4.7.60) at $\mathcal{O}(\kappa)$ reduces to

$$\begin{aligned} \gamma^{a_*}_{22} &= -\frac{\mathrm{d}Z^{(\kappa)}_{22}}{\mathrm{d}\ln(a_*)}+\mathcal{O}(\kappa^2) \\ &= -\frac{\kappa}{12\pi^2}\left[\frac{4}{3}-\ln\left(\frac{e^{\gamma_E}\mu}{H}\right)\right]+\mathcal{O}(\kappa^2)\,, \end{aligned} \tag{4.7.72}$$

where we used the result (4.7.58) for Z_{22}, as well as the tree-level running

$$\frac{\mathrm{d}g_{3,1}}{\mathrm{d}\ln(a_*)} = -2\varepsilon g_{3,1}\,. \tag{4.7.73}$$

We can cross-check this result using the formula (4.7.62). The Wilson coefficent C_{22} only depends non-trivially on a_* via the explicitly appearing logarithms, so at $\mathcal{O}(\kappa)$ we find:

$$\begin{aligned}\gamma_{22}^{a_*} &= -\frac{\mathrm{d}C_{22}^{(\kappa)}}{\mathrm{d}\ln(a_*)} + \mathcal{O}(\kappa^2) \\ &= -\frac{\kappa}{12\pi^2}\left[\frac{4}{3} - \ln\left(\frac{e^{\gamma_E}\mu}{H}\right)\right] + \mathcal{O}(\kappa^2)\,,\end{aligned} \tag{4.7.74}$$

which agrees with (4.7.72), as it should.

4.8 Matching of the one-point function of the operator ϕ^2 at $\mathcal{O}(\kappa)$ onto SdSET

We now turn to the final matching computation that we will carry out in this chapter, which is the matching of the renormalized full-theory one-point function $\langle[\phi^2](t,\vec{x})\rangle$. In section 3.7 we found the renormalized result

$$\begin{aligned}\langle[\phi^2](t,\vec{x})\rangle\Big|_{\mathcal{O}(\kappa)} =& \frac{\kappa H^2}{384\pi^4}\Bigg\{\frac{8}{3}\ln^3\left(\frac{e^{\gamma_E}\Lambda}{a(t)H}\right) - 4\left[\frac{2}{3} + \delta\hat{m}^2_{\text{fin}} + \ln\left(\frac{e^{\gamma_E}\mu}{H}\right)\right]\ln^2\left(\frac{e^{\gamma_E}\Lambda}{a(t)H}\right) \\ &+ 2\left[-\frac{16}{3} + \frac{2\pi^2}{3} + 4\delta\hat{m}^2_{\text{fin}} + 7\ln\left(\frac{e^{\gamma_E}\mu}{H}\right)\right]\ln\left(\frac{e^{\gamma_E}\Lambda}{a(t)H}\right) \\ &+ \left[3 - \frac{2\pi^2}{3} - 6\delta\hat{m}^2_{\text{fin}} - 6\ln\left(\frac{e^{\gamma_E}\mu}{H}\right)\right]\ln\left(\frac{e^{\gamma_E}\mu}{H}\right) \\ &- 6 + \frac{5\pi^2}{9} - \frac{2\pi^3}{3}\delta\hat{m}^2_{\text{fin}} + \frac{22}{3}\zeta(3)\Bigg\}\,,\end{aligned} \tag{4.8.1}$$

which we will reproduce using the SdSET by simply taking the expectation value of the matching equation between full-theory and SdSET composite operators (4.7.3) we set up above:

$$\langle[\phi^2](t,\vec{x})\rangle\Big|_{\mathcal{O}(\kappa)} = H^2\Big[C_{20} + C_{22}\langle[\varphi_+^2](t,\vec{x})\rangle + C_{24}\langle[\varphi_+^4](t,\vec{x})\rangle\Big]\Big|_{\mathcal{O}(\kappa)}\,. \tag{4.8.2}$$

In the previous section we already determined the matching coefficients C_{22} and C_{24} at $\mathcal{O}(\kappa)$, which means that the SdSET correlation functions which enter the matching equation (4.8.2) are $\langle[\varphi_+^2](t,\vec{x})\rangle$ evaluated at $\mathcal{O}(\kappa)$ and $\langle[\varphi_+^4](t,\vec{x})\rangle$ evaluated at $\mathcal{O}(\kappa^0)$. The latter is already known from the discussion in section 4.6, so the only new contribution we need to compute in this section is the former. This will also give us a chance to further study the renormalization of the operator φ_+^2, as well as the phenomenon of operator mixing, in the interacting SdSET. The main result of the matching computation will then be the determination of the Wilson coefficient C_{20} at $\mathcal{O}(\kappa)$.

4.8.1 Computation of $\langle\varphi_+^2(t,\vec{x})\rangle$ at $\mathcal{O}(\kappa)$, renormalization of φ_+^2

The computation of the one-point function $\langle\varphi_+^2(t,\vec{x})\rangle$ parallels the computation of the one-loop SdSET power spectrum we discussed in section 4.5, since the one-point function we are discussing can be obtained from the power spectrum by taking the coincident limit of its external points. Therefore, all of the effective couplings and initial conditions which contributed there, and that we matched in that section, will appear again here as insertions in loop diagrams.

However, differently than in all the previous sections, because of the many terms that we will encounter in this computation, and to simplify the intermediate results as much as possible, we will refrain from distinguishing the couplings $c_{3,1}$, $g_{3,1}$ and $g_{1,1}$ from each other, and simply plug in their matched value directly, which is κ for all of them. Similarly, we will directly use the matched value $\delta\hat{m}^2_{\text{fin}}$ for the finite part of the EFT mass counterterm $\hat{c}_{1,1}$. When deriving the anomalous dimensions γ_{20}^{μ} and $\gamma_{20}^{a_*}$ from the relevant renormalization factors in this problem, we will still need to take into account the different running behaviour of the various couplings with μ and a_*, and we will do so without writing this out explicitly. Finally, let us mention that we will compute $\langle\varphi_+^2(t,\vec{x})\rangle$ multiplied by a factor $(a(t)\tilde{\mu})^{2\varepsilon}$ to obtain a scaling- and mass-dimensionless result, which will prove convenient for the renormalization of φ_+^2.

Quartic-vertex and $\xi_{3,1}$-insertion contributions

We start by considering the contributions from the insertion of the quartic EFT vertex $\sim c_{3,1}$ and initial-condition-counterterm $\sim \xi^{\sigma}_{3,1}$, which lead to the diagrams

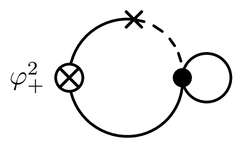

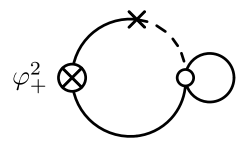

and

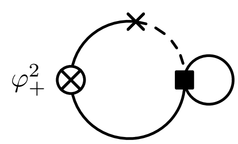

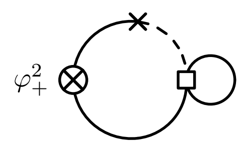

respectively. As we discussed already in section 4.5, we do not need to consider diagrams with topology

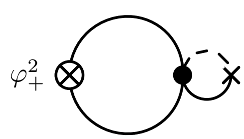

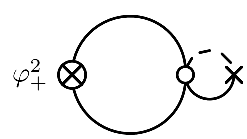

for the insertion of the vertex or the counterterm, since they cancel each other when summed up.

We then get

$$\begin{aligned}
&(a(t)\tilde{\mu})^{2\varepsilon}\Big[\langle\varphi_+^2(t,\vec{x})\rangle\Big|_{c_{3,1}}+\langle\varphi_+^2(t,\vec{x})\rangle\Big|_{\xi_{3,1}}\Big]\\
=&-\frac{\kappa}{12}(a(t)\tilde{\mu})^{2\varepsilon}\frac{(a(t)\tilde{\mu})^{2\varepsilon}-(a_*\tilde{\mu})^{2\varepsilon}}{2\varepsilon}\left[\int\frac{\mathrm{d}^{d-1}l}{(2\pi)^{d-1}}\frac{1}{l_\Lambda^3}\right]^2\\
=&\frac{\kappa}{192\pi^4}\left(\frac{\Lambda}{a(t)\mu}\right)^{-4\varepsilon}\ln\left(\frac{a_*}{a(t)}\right)\left\{\frac{1}{\varepsilon^2}+\frac{1}{\varepsilon}\ln\left(\frac{a_*}{a(t)}\right)+\frac{2}{3}\ln^2\left(\frac{a_*}{a(t)}\right)+\frac{\pi^2}{6}\right\},
\end{aligned}\tag{4.8.3}$$

where we dropped terms that vanish as $\Lambda\to 0$, and left some of the ε-dependent coefficients unexpanded for the sake of transparency of the result.

Mass-counterterm and $\xi_{1,1}$-insertion contributions

Both the insertions of the mass counterterm $\sim c_{1,1}$ and the initial-condition counterterm $\sim \xi^{\sigma}_{1,1}$, which we determined in section 4.5 at $\mathcal{O}(\kappa)$ and found the results

$$c^0_{1,1}=\frac{\kappa}{8\pi^2}\left[-\frac{1}{2\varepsilon}+\delta\hat{m}^2_{\text{fin}}\right]+\mathcal{O}(\kappa^2)\,,\tag{4.8.4}$$

$$\xi_{1,1}^{\sigma} = \frac{\sigma\kappa}{8\pi^2}\left\{\frac{1}{2\varepsilon^2} - \frac{1}{\varepsilon}\left[\frac{4}{3} - \ln\left(\frac{e^{\gamma_E}\mu}{H}\right)\right] + \frac{1}{\delta}\left[\frac{1}{2\varepsilon} - \delta\hat{m}^2_{\mathrm{fin}}\right]\right\} + \mathcal{O}(\kappa^2)\,, \tag{4.8.5}$$

yield diagrams with topology

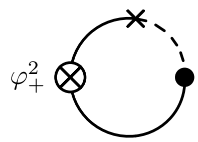

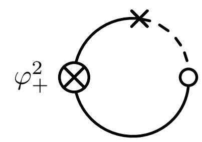

leading to the following expression:

$$\begin{aligned}
&(a(t)\tilde{\mu})^{2\varepsilon}\left[\langle\varphi_+^2(t,\vec{x})\rangle\Big|_{c_{1,1}} + \langle\varphi_+^2(t,\vec{x})\rangle\Big|_{\xi_{1,1}}\right] \\
=& -\frac{\kappa(a(t)\tilde{\mu})^{2\varepsilon}(\nu a(t))^{2\delta}}{24\pi^2}\left\{\frac{1}{2\delta}\left[-\frac{1}{2\varepsilon} + \delta\hat{m}^2_{\mathrm{fin}}\right] + \left(\frac{a_*}{a(t)}\right)^{2\delta}\left[\frac{1}{4\varepsilon^2} - \frac{1}{2\varepsilon}\left(\frac{4}{3} - \ln\left(\frac{e^{\gamma_E}\mu}{H}\right)\right)\right.\right. \\
&\left.\left. + \frac{1}{2\delta}\left(\frac{1}{2\varepsilon} - \delta\hat{m}^2_{\mathrm{fin}}\right)\right]\right\}\int\frac{\mathrm{d}^{d-1}l}{(2\pi)^{d-1}}\frac{1}{l_\Lambda^3} \\
=& \frac{\kappa}{192\pi^4}\left(\frac{\Lambda}{a(t)\mu}\right)^{-2\varepsilon}\left\{-\frac{1}{2\varepsilon^3} + \frac{1}{\varepsilon^2}\left[\frac{4}{3} - \ln\left(\frac{e^{\gamma_E}a_*\mu}{a(t)H}\right)\right] + \frac{1}{\varepsilon}\left[2\delta\hat{m}^2_{\mathrm{fin}}\ln\left(\frac{a_*}{a(t)}\right) - \frac{\pi^2}{24}\right] - \frac{\pi^2}{12}\ln\left(\frac{e^{\gamma_E}a_*\mu}{a(t)H}\right)\right. \\
&\left. + \frac{\pi^2}{9} + \frac{\zeta(3)}{6}\right\}.
\end{aligned} \tag{4.8.6}$$

Notice that, while the intermediate result depends on the analytic regulator δ, the final result does not. This happens by construction, since the explicit δ-poles appearing in $\xi^{\sigma}_{1,1}$ are chosen in order to cancel the ones that are generated by the time integral associated to the vertex $\sim c_{1,1}$. The momentum integral, which appears as a common multiplicative factor in both contributions, only generates poles in ε, so the cancellation of the δ-poles still works out exactly in this case.

$\Xi_{3,1}$-insertion contribution

As was the case for the one-loop power spectrum in section 4.5, for the insertion of the renormalized initial condition $\Xi^{\sigma}_{3,1}$ we only have to consider the diagram topology

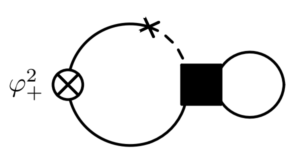

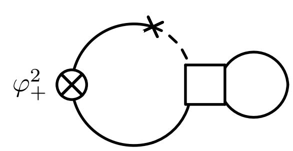

since the diagrams with topology

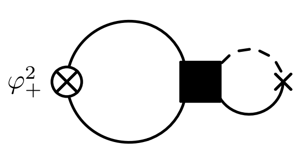

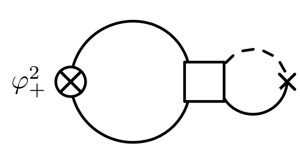

cancel each other when summed. We thus have to evaluate the following expression:

$$
\begin{aligned}
(a(t)\tilde{\mu})^{2\varepsilon}\langle\varphi_+^2(t,\vec{x})\rangle\Big|_{\Xi_{3,1}} =&\frac{\kappa(a(t)\tilde{\mu})^{2\varepsilon}(a_*\tilde{\mu})^{2\varepsilon}}{8}\int\frac{\mathrm{d}^{d-1}l_1\mathrm{d}^{d-1}l_2}{(2\pi)^{2d-2}}\frac{1}{l_{1\Lambda}^3l_{2\Lambda}^3}\bigg\{\frac{2}{3}\ln\left(\frac{2e^{\gamma_E}(l_{1\Lambda}+l_{2\Lambda})}{a_*H}\right)\\
&-\frac{1}{l_{12\Lambda}^3+l_{2\Lambda}^3}\left[\frac{l_{1\Lambda}^2l_{2\Lambda}^2}{2(l_{1\Lambda}+l_{2\Lambda})}+\frac{2}{9}\left[7l_{1\Lambda}^3+3l_{1\Lambda}^2l_{2\Lambda}+3l_{1\Lambda}l_{2\Lambda}^2+7l_{2\Lambda}^3\right]\right]\bigg\}. \qquad (4.8.7)
\end{aligned}
$$

All of the integrals appearing in this expression are in a such a form that they cannot be immediately computed using `Mathematica`. Nevertheless, they can be evaluated, and the details, as well as the explicit results for them, are relegated to appendix 4.E. Using the results we find there we get the following expression for this contribution to the one-point function:

$$
\begin{aligned}
(a(t)\tilde{\mu})^{2\varepsilon}\langle\varphi_+^2(t,\vec{x})\rangle\Big|_{\Xi_{3,1}} =&\frac{\kappa}{192\pi^4}\left(\frac{\Lambda^2}{a(t)a_*\tilde{\mu}^2}\right)^{-2\varepsilon}\bigg\{\frac{3}{4\varepsilon^3}+\frac{1}{\varepsilon^2}\left[\ln\left(\frac{e^{\gamma_E}\Lambda}{a_*H}\right)-\frac{4}{3}\right]+\frac{1}{\varepsilon}\left[\frac{5}{4}-\frac{5\pi}{3\sqrt{3}}+\frac{\pi^2}{8}\right]\\
&+\frac{\pi^2}{6}\ln\left(\frac{e^{\gamma_E}\Lambda}{a_*H}\right)+\frac{5}{2}-\frac{\pi}{\sqrt{3}}\left[2+\frac{2}{3}\ln(2)-\frac{7}{4}\ln(3)\right]-\frac{23\pi^2}{108}-\frac{3}{2}\zeta(3)\\
&+\frac{1}{18}\psi^{(1)}\left(\frac{1}{6}\right)-\frac{1}{9}\psi^{(1)}\left(\frac{1}{3}\right)+\frac{1}{6}\psi^{(1)}\left(\frac{2}{3}\right)-\frac{1}{12}\psi^{(1)}\left(\frac{5}{6}\right)\bigg\}, \qquad (4.8.8)
\end{aligned}
$$

where $\psi^{(1)}(z)$ denotes the polygamma function of order 1.

$\Xi_{1,1}$-insertion contribution

The final contribution to the one-point function we are considering comes from the insertion of the initial condition $\Xi_{1,1}^\sigma$, which we determined at $\mathcal{O}(\kappa)$ in section 4.5, and found the result

$$
\begin{aligned}
\Xi_{1,1}^\sigma(\vec{k}) =&\frac{\sigma\kappa}{4\pi^2}\bigg\{\left[\frac{4}{3}-\ln\left(\frac{e^{\gamma_E}\mu}{H}\right)-\delta\hat{m}_{\text{fin}}^2\right]\ln\left(\frac{2e^{\gamma_E}k}{a_*H}\right)+\left[1+\frac{1}{2}\ln\left(\frac{e^{\gamma_E}\mu}{H}\right)\right]\ln\left(\frac{e^{\gamma_E}\mu}{H}\right)\\
&+\frac{7\delta\hat{m}_{\text{fin}}^2}{3}-\frac{55}{36}-\frac{5\pi}{3\sqrt{3}}+\frac{7\pi^2}{48}\bigg\} \qquad (4.8.9)
\end{aligned}
$$

for it. Its insertion into the one-point function leads to the expression

$$
\begin{aligned}
&(a(t)\tilde{\mu})^{2\varepsilon}\langle\varphi_+^2(t,\vec{x})\rangle\Big|_{\Xi_{1,1}}\\
&=-\frac{(a(t)\tilde{\mu})^{2\varepsilon}}{6}\frac{\kappa}{4\pi^2}\int\frac{\mathrm{d}^{d-1}l}{(2\pi)^{d-1}}\frac{1}{l_\Lambda^3}\bigg\{\left[\frac{4}{3}-\ln\left(\frac{e^{\gamma_E}\mu}{H}\right)-\delta\hat{m}_{\text{fin}}^2\right]\ln\left(\frac{2e^{\gamma_E}l_\Lambda}{a_*H}\right)\\
&+\left[1+\frac{1}{2}\ln\left(\frac{e^{\gamma_E}\mu}{H}\right)\right]\ln\left(\frac{e^{\gamma_E}\mu}{H}\right)+\frac{7\delta\hat{m}_{\text{fin}}^2}{3}-\frac{55}{36}-\frac{5\pi}{3\sqrt{3}}+\frac{7\pi^2}{48}\bigg\}, \qquad (4.8.10)
\end{aligned}
$$

and to compute the integral containing the log we rewrite it as

$$
\ln\left(\frac{2e^{\gamma_E}l_\Lambda}{a_*H}\right)=\frac{\mathrm{d}}{\mathrm{d}u}\bigg|_{u=0}\left(\frac{2e^{\gamma_E}l_\Lambda}{a_*H}\right)^u, \qquad (4.8.11)
$$

which yields an integrand which can be straightforwardly integrated. Doing so, we find the result

$$
\begin{aligned}
&(a(t)\tilde{\mu})^{2\varepsilon}\langle\varphi_+^2(t,\vec{x})\rangle\Big|_{\Xi_{1,1}}\\
=&\frac{\kappa}{192\pi^4}\left(\frac{\Lambda}{a(t)\mu}\right)^{-2\varepsilon}\bigg\{\frac{1}{\varepsilon^2}\left[\ln\left(\frac{e^{\gamma_E}\mu}{H}\right)+\delta\hat{m}_{\text{fin}}^2-\frac{4}{3}\right]+\frac{1}{\varepsilon}\left[2\ln\left(\frac{e^{\gamma_E}\Lambda}{a_*H}\right)\left(\ln\left(\frac{e^{\gamma_E}\mu}{H}\right)+\delta m_{\text{fin}}^2-\frac{4}{3}\right)\right.\\
&\left.-\ln^2\left(\frac{e^{\gamma_E}\mu}{H}\right)-\frac{8}{3}\delta m_{\text{fin}}^2+\frac{7}{18}+\frac{10\pi}{3\sqrt{3}}-\frac{7\pi^2}{24}\right]+\frac{\pi^2}{12}\left[\ln\left(\frac{e^{\gamma_E}\mu}{H}\right)+\delta\hat{m}_{\text{fin}}^2-\frac{4}{3}\right]\bigg\}. \qquad (4.8.12)
\end{aligned}
$$

Sum of all the terms, renormalization of φ_+^2

We finally have all the contributions to $\langle\varphi_+^2(t,\vec{x})\rangle$ together, and we just need to sum them up. Doing so, and expanding out the prefactors we previously left unexpanded, we get

$$
\begin{aligned}
&(a(t)\tilde{\mu})^{2\varepsilon}\Big[\langle\varphi_+^2(t,\vec{x})\rangle\Big|_{c_{3,1}}+\langle\varphi_+^2(t,\vec{x})\rangle\Big|_{\xi_{3,1}}+\langle\varphi_+^2(t,\vec{x})\rangle\Big|_{\Xi_{3,1}}+\langle\varphi_+^2(t,\vec{x})\rangle\Big|_{c_{1,1}}+\langle\varphi_+^2(t,\vec{x})\rangle\Big|_{\xi_{1,1}}+\langle\varphi_+^2(t,\vec{x})\rangle\Big|_{\Xi_{1,1}}\Big]\\
=&\frac{\kappa}{192\pi^4}\left\{\frac{1}{4\varepsilon^3}+\frac{1}{\varepsilon^2}\left[\frac{1}{2}\ln\left(\frac{e^{2\gamma_E}a_*\mu^2}{a(t)H^2}\right)+\delta\hat{m}^2_{\text{fin}}-\frac{4}{3}-\ln\left(\frac{\Lambda}{a(t)\mu}\right)\right)\right]\\
&+\frac{1}{\varepsilon}\left[\ln\left(\frac{\Lambda}{a(t)\mu}\right)\left(\ln\left(\frac{\Lambda}{a(t)\mu}\right)-2\ln\left(\frac{e^{\gamma_E}\mu a_*}{a(t)H}\right)+\frac{8}{3}\right)+\ln\left(\frac{e^{\gamma_E}\mu}{H}\right)\left(\ln\left(\frac{e^{\gamma_E}\mu}{H}\right)+2\delta m^2_{\text{fin}}-\frac{8}{3}\right)\right.\\
&\left.+\frac{1}{2}\ln^2\left(\frac{a_*}{a(t)}\right)-\frac{8\delta m^2_{\text{fin}}}{3}+\frac{59}{36}+\frac{5\pi}{3\sqrt{3}}-\frac{5\pi^2}{24}\right]\\
&+\frac{2}{3}\ln^3\left(\frac{e^{\gamma_E}\Lambda}{a(t)H}\right)+2\left[\ln\left(\frac{e^{\gamma_E}a_*\mu}{a(t)H}\right)-\delta m^2_{\text{fin}}-\frac{8}{3}\right]\ln^2\left(\frac{e^{\gamma_E}\Lambda}{a(t)H}\right)\\
&+\left[8\ln\left(\frac{e^{\gamma_E}\mu}{H}\right)\left(2-\ln\left(\frac{e^{\gamma_E}\mu a_*}{a(t)H}\right)\right)+\frac{16}{3}\ln\left(\frac{a_*}{a(t)}\right)+\frac{16}{3}\delta\hat{m}^2_{\text{fin}}-\frac{52}{9}+\frac{\pi^2}{3}\right]\ln\left(\frac{e^{\gamma_E}\Lambda}{a(t)H}\right)\\
&-\frac{1}{3}\ln^3\left(\frac{a_*}{a(t)}\right)+\left[2\ln\left(\frac{e^{\gamma_E}\mu}{H}\right)-\frac{8}{3}\right]\ln^2\left(\frac{a_*}{a(t)}\right)+\left[\ln\left(\frac{e^{\gamma_E}\mu}{H}\right)\left(6\ln\left(\frac{e^{\gamma_E}\mu}{H}\right)-\frac{16}{3}\right)\right.\\
&\left.+\frac{5}{2}-\frac{10\pi}{3\sqrt{3}}+\frac{\pi^2}{6}\right]\ln\left(\frac{a_*}{a(t)}\right)\\
&+\frac{16}{3}\ln^3\left(\frac{e^{\gamma_E}\mu}{H}\right)-2\left[\frac{16}{3}-\delta\hat{m}^2_{\text{fin}}\right]\ln^2\left(\frac{e^{\gamma_E}\mu}{H}\right)+\left[\frac{52}{9}-\frac{\pi^2}{3}-\frac{16}{3}\delta\hat{m}^2_{\text{fin}}\right]\ln\left(\frac{e^{\gamma_E}\mu}{H}\right)\\
&-\frac{\pi^2}{12}\delta\hat{m}^2_{\text{fin}}+\frac{5}{2}-\frac{\pi}{\sqrt{3}}\left[2+\frac{2}{3}\ln(2)-\frac{7}{4}\ln(3)\right]+\frac{\pi^2}{108}-\frac{4}{3}\zeta(3)+\frac{1}{18}\psi^{(1)}\left(\frac{1}{6}\right)-\frac{1}{9}\psi^{(1)}\left(\frac{1}{3}\right)\\
&+\frac{1}{6}\psi^{(1)}\left(\frac{2}{3}\right)-\frac{1}{12}\psi^{(1)}\left(\frac{5}{6}\right)\right\}, \qquad (4.8.13)
\end{aligned}
$$

where we organized this rather lengthy result as follows: we first collected the pole terms in ε in descending order, then the UV- finite but IR-divergent terms, which are all logarithmic, in descending order, then the finite but time-dependent terms, which are also all logarithmic, in descending order, and then finally the constant terms, collecting powers of logarithms of μ/H in descending order.

As was the case in section 4.7, we can remove the UV-divergent terms by renormalizing the operator φ_+^2. Notice that the ε-poles appearing above involve IR-divergent terms, which, at face value, seem to be telling us that they cannot be subtracted by means of a local counterterm. However, these terms are just a manifestation of the phenomenon of operator mixing, and we will see in a moment that they can be accounted for consistently. We already set up the renormalization equation for φ_+^2 (4.7.14) above, and the relevant terms for the present discussion are

$$(a(t)\tilde{\mu})^{2\varepsilon}\varphi_+^2(t,\vec{x})=(a(t)\tilde{\mu})^{2\varepsilon}Z_{22}[\varphi_+^2](t,\vec{x})+Z_{20}\mathbb{1}\,. \qquad (4.8.14)$$

The renormalization equation for the one-point function can then be obtained from this one by taking its expectation value, and we find

$$(a(t)\tilde{\mu})^{2\varepsilon}\langle\varphi_+^2(t,\vec{x})\rangle\Big|_{\mathcal{O}(\kappa)}=\Big[(a(t)\tilde{\mu})^{2\varepsilon}Z_{22}\langle[\varphi_+^2](t,\vec{x})\rangle+Z_{20}\Big]\Big|_{\mathcal{O}(\kappa)}\,. \qquad (4.8.15)$$

The only unknown quantity in this equation is the $\mathcal{O}(\kappa)$-piece of Z_{20}, which is the appropriate renormalization factor to absorb the UV divergences of the correlation function we are considering, and which we will therefore determine. The result for Z_{22} at $\mathcal{O}(\kappa)$ is known from the previous section, see (4.7.16), and plugging

$c_{3,1} = g_{3,1} = \kappa$ into that result it simplifies to

$$Z_{22} = 1 + \frac{\kappa}{48\pi^2}\left[\frac{1}{\varepsilon^2} + \frac{2}{\varepsilon}\left(\ln\left(\frac{e^{\gamma_E}a_*\mu}{a(t)H}\right) - \frac{4}{3}\right)\right] + \mathcal{O}(\kappa^2)\,. \tag{4.8.16}$$

Using this form of Z_{22} in (4.8.15), we see that the $\mathcal{O}(\kappa)$-piece of Z_{20} in the $\overline{\text{MS}}$ scheme is then defined as follows:

$$Z_{20}^{(\kappa)} = \left[(a(t)\tilde{\mu})^{2\varepsilon}\langle\varphi_+^2(t,\vec{x})\rangle\Big|_{\mathcal{O}(\kappa)} - Z_{22}^{(\kappa)}(a(t)\tilde{\mu})^{2\varepsilon}\langle[\varphi_+^2](t,\vec{x})\rangle\right]\Big|_{\text{poles}}\,. \tag{4.8.17}$$

When discussing operator renormalization and mixing in the free theory in section 4.6.3, we defined the d-dimensional, $\mathcal{O}(\kappa^0)$ renormalized one-point function $\langle[\varphi_+^2](t,\vec{x})\rangle$ via the equation

$$(a(t)\tilde{\mu})^{2\varepsilon}\langle[\varphi_+^2](t,\vec{x})\rangle = \frac{1}{8\pi^2}\left(\frac{\Lambda}{a(t)\mu}\right)^{-2\varepsilon}e^{\varepsilon\gamma_E}\Gamma(\varepsilon) - \frac{1}{8\pi^2\varepsilon} \tag{4.8.18}$$

$$= \frac{1}{4\pi^2}\Bigg\{-\ln\left(\frac{\Lambda}{a(t)\mu}\right) + \varepsilon\left[\frac{\pi^2}{24} + \ln^2\left(\frac{\Lambda}{a(t)\mu}\right)\right] - \frac{\varepsilon^2}{3}\left[2\ln^3\left(\frac{\Lambda}{a(t)\mu}\right) + \frac{\pi^2}{4}\ln\left(\frac{\Lambda}{a(t)\mu}\right) + \frac{\zeta(3)}{2}\right]\Bigg\} + \mathcal{O}(\varepsilon^3)\,. \tag{4.8.19}$$

Using this result, we find the following ε-expansion of the product $Z_{22}^{(\kappa)}(a(t)\tilde{\mu})^{2\varepsilon}\langle[\varphi_+^2](t,\vec{x})\rangle$:

$$\begin{aligned}&Z_{22}^{(\kappa)}(a(t)\tilde{\mu})^{2\varepsilon}\langle[\varphi_+^2](t,\vec{x})\rangle\\ =&\frac{\kappa}{192\pi^4}\Bigg\{-\frac{1}{\varepsilon^2}\ln\left(\frac{\Lambda}{a(t)\mu}\right) + \frac{1}{\varepsilon}\left[\ln^2\left(\frac{\Lambda}{a(t)\mu}\right) - 2\left(\ln\left(\frac{e^{\gamma_E}a_*\mu}{a(t)H}\right) - \frac{4}{3}\right)\ln\left(\frac{\Lambda}{a(t)\mu}\right) + \frac{\pi^2}{24}\right]\\ &- \frac{2}{3}\ln^3\left(\frac{\Lambda}{a(t)\mu}\right) - 2\left[\frac{4}{3} - \ln\left(\frac{e^{\gamma_E}a_*\mu}{a(t)H}\right)\right]\ln^2\left(\frac{\Lambda}{a(t)\mu}\right) - \frac{\pi^2}{12}\ln\left(\frac{\Lambda}{a(t)\mu}\right) - \frac{1}{12}\left[\left(\frac{4}{3} - \ln\left(\frac{e^{\gamma_E}a_*\mu}{a(t)H}\right)\right)\right.\\ &\left.+ 2\zeta(3)\right]\Bigg\}\,.\end{aligned} \tag{4.8.20}$$

Comparing the $\ln(\Lambda)$-terms appearing in the pole terms of this result to the corresponding ones in (4.8.13), we see that they match. Therefore, plugging this result in (4.8.17), we obtain a local result for $Z_{20}^{(\kappa)}$,

$$\begin{aligned}Z_{20}^{(\kappa)} =&\frac{\kappa}{192\pi^4}\Bigg\{\frac{1}{4\varepsilon^3} + \frac{1}{\varepsilon^2}\left[\frac{1}{2}\ln\left(\frac{e^{2\gamma_E}a_*\mu^2}{a(t)H^2}\right) + \delta\hat{m}^2_{\text{fin}} - \frac{4}{3}\right]\\ &+ \frac{1}{\varepsilon}\left[\ln\left(\frac{e^{\gamma_E}\mu}{H}\right)\left(\ln\left(\frac{e^{\gamma_E}\mu}{H}\right) + 2\delta\hat{m}^2_{\text{fin}} - \frac{8}{3}\right) + \frac{1}{2}\ln^2\left(\frac{a_*}{a(t)}\right) - \frac{8\delta\hat{m}^2_{\text{fin}}}{3} + \frac{59}{36} + \frac{5\pi}{3\sqrt{3}} - \frac{\pi^2}{4}\right]\Bigg\}.\end{aligned} \tag{4.8.21}$$

Subtracting this expression from the regularized result and letting $\varepsilon \to 0$ we get the final result for the renormalized one-point function:

$$\begin{aligned}\langle[\varphi_+^2](t,\vec{x})\rangle\Big|_{\mathcal{O}(\kappa)} =&(a(t)\tilde{\mu})^{2\varepsilon}\langle\varphi_+^2(t,\vec{x})\rangle\Big|_{\mathcal{O}(\kappa)} - Z_{22}^{(\kappa)}(a(t)\tilde{\mu})^{2\varepsilon}\langle[\varphi_+^2](t,\vec{x})\rangle\Big|_{\mathcal{O}(\kappa^0)} - Z_{20}^{(\kappa)}\\ =&\frac{\kappa}{192\pi^4}\Bigg\{\frac{4}{3}\ln^3\left(\frac{e^{\gamma_E}\Lambda}{a(t)H}\right) - \left[\frac{8}{3} + 2\delta\hat{m}^2_{\text{fin}} + 2\ln\left(\frac{e^{\gamma_E}\mu}{H}\right)\right]\ln^2\left(\frac{e^{\gamma_E}\Lambda}{a(t)H}\right)\\ &+ \left[\ln\left(\frac{e^{\gamma_E}\mu}{H}\right)\left(\frac{32}{3} - 2\ln\left(\frac{e^{\gamma_E}\mu}{H}\right) - 4\ln\left(\frac{a_*}{a(t)}\right)\right) + \frac{16}{3}\delta\hat{m}^2_{\text{fin}} - \frac{52}{9}\right.\\ &\left.+ \frac{5\pi^2}{12}\right]\ln\left(\frac{e^{\gamma_E}\Lambda}{a(t)H}\right)\end{aligned} \tag{4.8.22}$$

$$
\begin{aligned}
&-\frac{1}{3}\ln^3\left(\frac{a_*}{a(t)}\right)+\left[2\ln\left(\frac{e^{\gamma_E}\mu}{H}\right)-\frac{8}{3}\right]\ln^2\left(\frac{a_*}{a(t)}\right)\\
&+\left[\ln\left(\frac{e^{\gamma_E}\mu}{H}\right)\left(4\ln\left(\frac{2e^{\gamma_E}\mu}{H}\right)-\frac{16}{3}\right)+\frac{5}{2}-\frac{10\pi}{3\sqrt{3}}+\frac{\pi^2}{12}\right]\ln\left(\frac{a_*}{a(t)}\right)\\
&+\frac{8}{3}\ln^3\left(\frac{e^{\gamma_E}\mu}{H}\right)-2\Big[4-\delta\hat{m}^2_{\text{fin}}\Big]\ln^2\left(\frac{e^{\gamma_E}\mu}{H}\right)+\left[\frac{52}{9}-\frac{\pi^2}{2}-\frac{16}{3}\delta\hat{m}^2_{\text{fin}}\right]\ln\left(\frac{e^{\gamma_E}\mu}{H}\right)\\
&-\frac{\pi^2}{12}\delta\hat{m}^2_{\text{fin}}+\frac{5}{2}-\frac{\pi}{\sqrt{3}}\left[2+\frac{2}{3}\ln(2)-\frac{7}{4}\ln(3)\right]+\frac{13\pi^2}{108}-\frac{7}{6}\zeta(3)\\
&+\frac{1}{18}\psi^{(1)}\left(\frac{1}{6}\right)-\frac{1}{9}\psi^{(1)}\left(\frac{1}{3}\right)+\frac{1}{6}\psi^{(1)}\left(\frac{2}{3}\right)-\frac{1}{12}\psi^{(1)}\left(\frac{5}{6}\right)\Bigg\}\,. \qquad (4.8.23)
\end{aligned}
$$

4.8.2 Matching

We can now go ahead and use the renormalized result we found above to match the analogous full-theory quantity:

$$
\begin{aligned}
\langle[\phi^2](t,\vec{x})\rangle\Big|_{\mathcal{O}(\kappa)} =&\frac{\kappa H^2}{192\pi^4}\Bigg\{\frac{4}{3}\ln^3\left(\frac{e^{\gamma_E}\Lambda}{a(t)H}\right)-2\left[\frac{2}{3}+\delta\hat{m}^2_{\text{fin}}+\ln\left(\frac{e^{\gamma_E}\mu}{H}\right)\right]\ln^2\left(\frac{e^{\gamma_E}\Lambda}{a(t)H}\right)\\
&+\left[-\frac{16}{3}+\frac{2\pi^2}{3}+4\delta\hat{m}^2_{\text{fin}}+7\ln\left(\frac{e^{\gamma_E}\mu}{H}\right)\right]\ln\left(\frac{e^{\gamma_E}\Lambda}{a(t)H}\right)\\
&+\left[\frac{3}{2}-\frac{\pi^2}{3}-6\delta\hat{m}^2_{\text{fin}}-3\ln\left(\frac{e^{\gamma_E}\mu}{H}\right)\right]\ln\left(\frac{e^{\gamma_E}\mu}{H}\right)\\
&-3+\frac{5\pi^2}{18}-\frac{\pi^3}{3}\delta\hat{m}^2_{\text{fin}}+\frac{11}{3}\zeta(3)\Bigg\}\,. \qquad (4.8.24)
\end{aligned}
$$

The operator matching equation between $[\phi^2]$ and the renormalized EFT operators $[\varphi_+^n]$ was already set up above in (4.7.3), and the relevant terms for the present discussion read

$$
[\phi^2](t,\vec{x})=H^2\Big[C_{20}\mathbb{1}+C_{22}[\varphi_+^2](t,\vec{x})+C_{24}[\varphi_+^4](t,\vec{x})\Big]\,. \qquad (4.8.25)
$$

The appropriate matching equation between correlation functions is then obtained by taking the expectation value of this equation, and we get

$$
\langle[\phi^2](t,\vec{x})\rangle\Big|_{\mathcal{O}(\kappa)}=H^2\Big[C_{20}+C_{22}\langle[\varphi_+^2](t,\vec{x})\rangle+C_{24}\langle[\varphi_+^4](t,\vec{x})\rangle\Big]\Big|_{\mathcal{O}(\kappa)}\,. \qquad (4.8.26)
$$

From this equation, the Wilson coefficient C_{20} can be determined at $\mathcal{O}(\kappa)$ as

$$
C_{20}^{(\kappa)} =H^{-2}\langle[\phi^2](t,\vec{x})\rangle\Big|_{\mathcal{O}(\kappa)}-\langle[\varphi_+^2](t,\vec{x})\rangle\Big|_{\mathcal{O}(\kappa)}-C_{22}^{(\kappa)}\langle[\varphi_+^2](t,\vec{x})\rangle\Big|_{\mathcal{O}(\kappa^0)}-C_{24}^{(\kappa)}\langle[\varphi_+^4](t,\vec{x})\rangle\Big|_{\mathcal{O}(\kappa^0)}\,. \qquad (4.8.27)
$$

All of the quantities entering this equation are now known: we already determined C_{22} and C_{24} up to $\mathcal{O}(\kappa)$ in section 4.7, and the results read

$$
\begin{aligned}
C_{22} =&1+\frac{\kappa}{48\pi^2}\left[\ln\left(\frac{e^{\gamma_E}\mu}{H}\right)\left[1-2\ln\left(\frac{e^{\gamma_E}a_*^2\mu}{a(t)^2H}\right)\right]+\frac{16}{3}\ln\left(\frac{a_*}{a(t)}\right)+\frac{4}{3}\delta\hat{m}^2_{\text{fin}}-\frac{4}{9}-\frac{\pi^2}{4}\right]+\mathcal{O}(\kappa^2)\,, \qquad (4.8.28)\\
C_{24} =&\frac{\kappa}{27}+\mathcal{O}(\kappa^2)\,. \qquad (4.8.29)
\end{aligned}
$$

We also already determined the necessary renormalized free-theory correlators appearing in (4.8.27) in section 4.6.3:

$$
\langle[\varphi_+^2](t,\vec{x})\rangle\Big|_{\mathcal{O}(\kappa^0)}=-\frac{1}{4\pi^2}\ln\left(\frac{\Lambda}{a(t)\mu}\right)\,, \qquad (4.8.30)
$$

$$\langle[\varphi_+^4](t,\vec{x})\rangle\Big|_{\mathcal{O}(\kappa^0)} = \frac{3}{16\pi^4}\ln^2\left(\frac{\Lambda}{a(t)\mu}\right). \tag{4.8.31}$$

Plugging all these expressions into (4.8.27) we find the following result for C_{20}:

$$\begin{aligned}C_{20} =& \frac{\kappa}{192\pi^4}\Bigg\{\frac{1}{3}\ln^3\left(\frac{a_*}{a(t)}\right) - 2\left[\ln\left(\frac{e^{\gamma_E}\mu}{H}\right) - \frac{4}{3}\right]\ln^2\left(\frac{a_*}{a(t)}\right) - \left[\frac{5}{2} - \frac{10\pi}{3\sqrt{3}} + \frac{\pi^2}{12}\right]\ln\left(\frac{a_*}{a(t)}\right) \\ & - \frac{2}{3}\ln^3\left(\frac{e^{\gamma_E}\mu}{H}\right) + 2\left[\frac{4}{3} - \delta\hat{m}^2_{\rm fin}\right]\ln^2\left(\frac{e^{\gamma_E}\mu}{H}\right) - \left[\frac{23}{6} - \frac{5\pi^2}{12} - \delta\hat{m}^2_{\rm fin}\right]\ln\left(\frac{e^{\gamma_E}\mu}{H}\right) \\ & - \frac{\pi^2}{4}\delta\hat{m}^2_{\rm fin} - \frac{11}{2} + \frac{\pi}{\sqrt{3}}\left[2 + \frac{2}{3}\ln(2) - \frac{7}{4}\ln(3)\right] + \frac{17\pi^2}{108} + \frac{29}{6}\zeta(3) - \frac{1}{18}\psi^{(1)}\left(\frac{1}{6}\right) + \frac{1}{9}\psi^{(1)}\left(\frac{1}{3}\right) \\ & - \frac{1}{6}\psi^{(1)}\left(\frac{2}{3}\right) + \frac{1}{12}\psi^{(1)}\left(\frac{5}{6}\right)\Bigg\} + \mathcal{O}(\kappa^2). \end{aligned} \tag{4.8.32}$$

This expression is spatially local and independent of Λ, as it must be. Thus, the complete Λ-dependence of the full-theory correlator is successfully reproduced by the SdSET-correlators appearing in the matching equation alone, which is a further non-trivial consistency check on the framework we are using.

While being local in space, the found Wilson coefficient still has an explicit $a(t)$-dependence, but it only comes in the combination $a_*/a(t)$. Thus, the coefficient becomes time-independent with the choice $a_* = a(t)$, which will be important below.

4.8.3 Computation of γ_{20}^{μ} and $\gamma_{20}^{a_*}$ at $\mathcal{O}(\kappa)$

Having determined the operator renormalization factor Z_{20} at $\mathcal{O}(\kappa)$, as well as the matching coefficient C_{20} at $\mathcal{O}(\kappa)$, we are now in the position to compute both γ_{20}^{μ} and $\gamma_{20}^{a_*}$ at $\mathcal{O}(\kappa)$. As we discussed in section 4.7.7 in the case of γ_{22}^{μ} and $\gamma_{22}^{a_*}$, we can compute the anomalous dimensions independently using the renormalization factors and the Wilson coefficients, and the results that we find must agree. This will serve as a further consistency check on the present formalism. We will also need these quantities in the discussion of the resummation of the secular logs in the EFT framework below.

Computation of γ_{20}^{μ}

We start by considering γ_{20}^{μ}, which is given to all orders in κ by the formula

$$\gamma_{20}^{\mu} = \sum_{l=0}^{\infty} Z_{2l}^{-1}\left[l\varepsilon Z_{l0} - \frac{\mathrm{d}Z_{l0}}{\mathrm{d}\ln(\mu)}\right]. \tag{4.8.33}$$

We are only interested in this expression up to $\mathcal{O}(\kappa)$, and using the fact that $Z_{2n}^{-2} = \mathcal{O}(\kappa^2)$ for $n \geq 4$ we can truncate the sum after $l = 2$, and we find

$$\gamma_{20}^{\mu} = 2\varepsilon Z_{20}^{(\kappa^0)}\left[Z_{22}^{(\kappa^0)} - Z_{22}^{(\kappa)}\right] + Z_{22}^{(\kappa^0)}\left[2\varepsilon Z_{20}^{(\kappa)} - \frac{\mathrm{d}Z_{20}^{(\kappa)}}{\mathrm{d}\ln(\mu)}\right] + \mathcal{O}(\kappa^2). \tag{4.8.34}$$

To determine $\mathrm{d}Z_{20}/\mathrm{d}\ln(\mu)$ correctly, it is crucial to take into account the running of the couplings and initial conditions, which read

$$\frac{\mathrm{d}c_{3,1}}{\mathrm{d}\ln(\mu)} = -2\varepsilon c_{3,1} + \mathcal{O}(\kappa^2), \tag{4.8.35}$$

$$\frac{\mathrm{d}g_{3,1}}{\mathrm{d}\ln(\mu)} = -2\varepsilon g_{3,1} + \mathcal{O}(\kappa^2), \tag{4.8.36}$$

$$\frac{\mathrm{d}}{\mathrm{d}\ln(\mu)}\left[c_{3,1}\hat{c}_{1,1}\right] = -c_{3,1} + \mathcal{O}(\kappa^2), \tag{4.8.37}$$

$$\frac{\mathrm{d}g_{1,1}}{\mathrm{d}\ln(\mu)} =\frac{c_{3,1}}{4\pi^2}\left[\frac{4}{3}-\ln\left(\frac{e^{\gamma_E}\mu}{H}\right)\right]. \tag{4.8.38}$$

Even though we did not differentiate these couplings explicitly in the above results, for the sake of conciseness, we traced the different pieces making up the renormalization factor Z_{20} to the corresponding couplings, and took the running behaviour written above into account to find

$$\begin{aligned}\frac{\mathrm{d}Z_{20}}{\mathrm{d}\ln(\mu)} =& -\frac{\kappa}{192\pi^4}\Bigg\{\frac{1}{2\varepsilon^2}+\frac{1}{\varepsilon}\left[\ln\left(\frac{a_*}{a(t)}\right)-2\delta\hat{m}^2_{\text{fin}}\right]+\ln\left(\frac{a_*}{a(t)}\right)\left[\ln\left(\frac{a_*}{a(t)}\right)+4\ln\left(\frac{e^{\gamma_E}\mu}{H}\right)-\frac{16}{3}\right]\\ &+\frac{5}{2}-\frac{10\pi}{3\sqrt{3}}+\frac{\pi^2}{12}\Bigg\},\end{aligned} \tag{4.8.39}$$

where we set $c_{3,1}=g_{3,1}=\kappa$. With this result we get the following anomalous dimension:

$$\gamma^{\mu}_{20}=\frac{1}{4\pi^2}+\frac{\kappa}{96\pi^4}\left\{\ln\left(\frac{e^{\gamma_E}a_*\mu}{a(t)H}\right)\left[\ln\left(\frac{e^{\gamma_E}a_*\mu}{a(t)H}\right)-\frac{8}{3}\right]-2\delta\hat{m}^2_{\text{fin}}\left[\frac{4}{3}-\ln\left(\frac{e^{\gamma_E}\mu}{H}\right)\right]+\frac{26}{9}-\frac{5\pi^2}{24}\right\}+\mathcal{O}(\kappa^2), \tag{4.8.40}$$

where we incorporated the $\mathcal{O}(\kappa^0)$-piece of it that we already found in section 4.6.3.

We can compare this result to the one we get using the formula for the anomalous dimension computed in terms of the matching coefficients:

$$\begin{aligned}\gamma^{\mu}_{20} &= -\sum_{l=0}^{\infty}C^{-1}_{2l}\frac{\mathrm{d}C_{l0}}{\mathrm{d}\ln(\mu_{\text{eff}})} \qquad (4.8.41)\\ &= -\left[\frac{\mathrm{d}C^{(\kappa^0)}_{20}}{\mathrm{d}\ln(\mu_{\text{eff}})}+\frac{\mathrm{d}C^{(\kappa)}_{20}}{\mathrm{d}\ln(\mu_{\text{eff}})}-C^{(\kappa)}_{22}\frac{\mathrm{d}C^{(\kappa^0)}_{20}}{\mathrm{d}\ln(\mu_{\text{eff}})}-C^{(\kappa)}_{24}\frac{\mathrm{d}C^{(\kappa^0)}_{40}}{\mathrm{d}\ln(\mu_{\text{eff}})}\right]+\mathcal{O}(\kappa^2). \qquad (4.8.42)\end{aligned}$$

To use this formula correctly, we need to distinguish the μ-dependence inherited from the full-theory result from the one that is generated by the UV divergences in the EFT. In particular, we also need to distinguish the finite part of the full-theory mass-counterterm $\delta\hat{m}^2_{\text{fin}}$ from the analogous quantity in the EFT $\hat{c}^{\text{fin}}_{1,1}$, since the former does not run with with μ_{eff}, while the latter does. Doing so, we find the following expression for the μ_{eff}-dependent part of C_{20}:

$$\begin{aligned}C^{(\kappa)}_{20} =&\frac{\kappa}{192\pi^4}\Bigg\{-\frac{2}{3}\ln^3\left(\frac{e^{\gamma_E}\mu_{\text{eff}}}{H}\right)+2\left[\frac{4}{3}-\frac{c_{3,1}}{\kappa}\hat{c}^{\text{fin}}_{1,1}\right]\ln^2\left(\frac{e^{\gamma_E}\mu_{\text{eff}}}{H}\right)\\ &+\left[3\ln\left(\frac{e^{\gamma_E}\mu_{\text{full}}}{H}\right)-2\ln^2\left(\frac{a_*}{a(t)}\right)+4\hat{c}^{\text{fin}}_{1,1}-\frac{16}{3}+\frac{3\pi^2}{4}\right]\ln\left(\frac{e^{\gamma_E}\mu_{\text{eff}}}{H}\right)+\frac{\pi^2c_{3,1}}{12\kappa}\hat{c}^{\text{fin}}_{1,1}\\ &+\mu_{\text{eff}}\text{-independent}\Bigg\}.\end{aligned} \tag{4.8.43}$$

The $\ln(\mu_{\text{eff}})$-derivative of $C^{(\kappa)}_{22}$ also appears in (4.8.42), so we need to isolate the μ_{eff}-dependent pieces of this Wilson coefficient as well. We already did so in section 4.7.7, and we reprint the result here for convenience:

$$\begin{aligned}C^{(\kappa)}_{22} =&\frac{\kappa}{48\pi^2}\left[2\ln\left(\frac{e^{\gamma_E}\mu_{\text{eff}}}{H}\right)\left[2-\ln\left(\frac{e^{\gamma_E}a^2_*\mu_{\text{eff}}}{a(t)^2H}\right)\right]+\frac{16}{3}\ln\left(\frac{a_*}{a(t)}\right)-3\ln\left(\frac{e^{\gamma_E}\mu_{\text{full}}}{H}\right)\right.\\ &\left.-\frac{4}{9}-\frac{\pi^2}{4}\right]+\frac{c_{3,1}}{36\pi^2}\hat{c}_{1,1}.\end{aligned} \tag{4.8.44}$$

Taking the $\ln(\mu_{\text{eff}})$-derivative of these expressions, while taking into account that

$$\frac{\mathrm{d}}{\mathrm{d}\ln(\mu_{\text{eff}})}\Big[c_{3,1}\hat{c}_{1,1}\Big]=-c_{3,1}, \tag{4.8.45}$$

and plugging the result into (4.8.42) together with the $\mathcal{O}(\kappa^0)$-results

$$\frac{\mathrm{d}C_{20}^{(\kappa^0)}}{\mathrm{d}\ln(\mu_{\text{eff}})} = -\frac{1}{4\pi^2}\,, \tag{4.8.46}$$

$$\frac{\mathrm{d}C_{40}^{(\kappa^0)}}{\mathrm{d}\ln(\mu_{\text{eff}})} = \frac{3}{8\pi^2}\ln\left(\frac{\mu_{\text{eff}}}{\mu_{\text{full}}}\right)\,, \tag{4.8.47}$$

that we already found in section 4.6.3, and finally identifying $\mu_{\text{eff}} = \mu_{\text{full}} = \mu$, we get

$$\gamma_{20}^{\mu} = \frac{1}{4\pi^2} + \frac{\kappa}{96\pi^4}\left\{\ln\left(\frac{e^{\gamma_E}a_*\mu}{a(t)H}\right)\left[\ln\left(\frac{e^{\gamma_E}a_*\mu}{a(t)H}\right) - \frac{8}{3}\right] - 2\delta\hat{m}_{\text{fin}}^2\left[\frac{4}{3} - \ln\left(\frac{e^{\gamma_E}\mu}{H}\right)\right] + \frac{26}{9} - \frac{5\pi^2}{24}\right\} + \mathcal{O}(\kappa^2)\,. \tag{4.8.48}$$

This is the same result we found above in (4.8.40), as it must be.

Computation of $\gamma_{20}^{a_*}$

Analogously to what we did above, we compute $\gamma_{20}^{a_*}$, which is given to all orders in κ by the formula

$$\gamma_{20}^{a_*} = -\sum_{l=0}^{\infty} Z_{2l}^{-1}\frac{\mathrm{d}Z_{l0}}{\mathrm{d}\ln(a_*)}\,. \tag{4.8.49}$$

As in the case of γ_{20}^{μ}, we are interested in the result at $\mathcal{O}(\kappa)$, so we can truncate the sum after $l = 2$.

As it was above, to get the correct result from this formula it is crucial to take into account the running of the couplings and initial conditions with a_*. The renormalized effective couplings $c_{3,1}$, $c_{1,1}$ do not run with a_*, so neither does the tree-level result for $\xi_{3,1}^{\sigma}$ we used in the computation to get Z_{20} at $\mathcal{O}(\kappa)$. For the remaining quantities contributing to the above results we found the following running behaviour:

$$\frac{\mathrm{d}\Xi_{3,1}^{\sigma}}{\mathrm{d}\ln(a_*)} = \sigma c_{3,1} - 2\varepsilon\Xi_{3,1}^{\sigma}\,, \tag{4.8.50}$$

$$\frac{\mathrm{d}\xi_{1,1}^{\sigma}}{\mathrm{d}\ln(a_*)} = -\frac{\sigma c_{3,1}}{8\pi^2}\left\{\frac{1}{\varepsilon} - 2\left[\frac{4}{3} - \ln\left(\frac{e^{\gamma_E}\mu}{H}\right)\right]\right\}\,, \tag{4.8.51}$$

$$\frac{\mathrm{d}\Xi_{1,1}^{\sigma}}{\mathrm{d}\ln(a_*)} = \frac{\sigma c_{3,1}}{4\pi^2}\left[\hat{c}_{1,1} + \ln\left(\frac{e^{\gamma_E}\mu}{H}\right) - \frac{4}{3}\right]\,, \tag{4.8.52}$$

Using these expressions, and the fact that $Z_{22}^{-1} = 1 + \mathcal{O}(\kappa)$, we get

$$\begin{aligned}\gamma_{20}^{a_*} &= -\frac{\mathrm{d}Z_{20}^{(\kappa)}}{\mathrm{d}\ln(a_*)} + \mathcal{O}(\kappa^2)\\ &= \frac{\kappa}{192\pi^4}\left\{\ln\left(\frac{a_*}{a(t)}\right)\left[-\ln\left(\frac{a_*}{a(t)}\right) + 4\ln\left(\frac{e^{\gamma_E}\mu}{H}\right) - \frac{16}{3}\right] + \frac{5}{2} - \frac{10\pi}{3\sqrt{3}} + \frac{\pi^2}{12}\right\} + \mathcal{O}(\kappa^2)\,.\end{aligned} \tag{4.8.53}$$

We can use this result to run a consistency check on the a_*-dependence of the Wilson coefficient C_{20} using the equation

$$\gamma_{20}^{a_*} = -\sum_{l=0}^{\infty} C_{2l}^{-1}\frac{\mathrm{d}C_{l0}}{\mathrm{d}\ln(a_*)} \tag{4.8.54}$$

$$= -\frac{\mathrm{d}C_{20}}{\mathrm{d}\ln(a_*)} + \mathcal{O}(\kappa^2)\,, \tag{4.8.55}$$

where we used that $C_{22}^{-1} = 1 + \mathcal{O}(\kappa)$, and the fact that $C_{n0} = \mathcal{O}(\kappa^2)$ for $n \geq 4$. Since in $d = 4$ dimensions the a_*-running of all the finite parts of the initial conditions that enter the result for C_{20} simply reproduce the explicitly appearing logarithms of a_*, to compute $\gamma_{20}^{a_*}$ we just need to take the derivative of the result (4.8.32) with respect to $\ln(a_*)$, and find

$$\gamma_{20}^{a_*} = \frac{\kappa}{192\pi^4}\left\{ \ln\left(\frac{a_*}{a(t)}\right)\left[-\ln\left(\frac{a_*}{a(t)}\right) + 4\ln\left(\frac{e^{\gamma_E}\mu}{H}\right) - \frac{16}{3}\right] + \frac{5}{2} - \frac{10\pi}{3\sqrt{3}} + \frac{\pi^2}{12}\right\} + \mathcal{O}(\kappa^2)\,. \tag{4.8.56}$$

This is the same result as (4.8.53), as it must be.

4.9 Removing infrared singularities and secular growth from full-theory correlation functions using the SdSET

We now come to the final section of this chapter, where we will discuss how the issue of infrared divergences and secular logarithms, which we kept finding in all the perturbative computations carried out above, can be addressed using the SdSET. In the previous chapters, we showed that renormalized full-theory correlation functions involving both elementary fields ϕ and composite operators $[\phi^n]$ can be faithfully reproduced using the SdSET by making use of leading-power (in λ) matching equations of the form

$$\phi(t,\vec{x}) = H\sum_{n=0}^{\infty} r_{2n+1}\varphi_+^{2n+1}(t,\vec{x})\,, \tag{4.9.1}$$

$$[\phi^n](t,\vec{x}) = H^n\sum_{m=0}^{\infty} C_{nm}[\varphi_+^m](t,\vec{x})\,. \tag{4.9.2}$$

The coefficients r_{2n+1} are determined by the field redefinition of φ_- to eliminate interaction terms $\sim \varphi_+^n$ from the SdSET action, as shown in appendix 4.B, while the operator matching coefficients C_{nm} have to be determined by means of perturbative matching computations. In sections 4.4 and 4.5 we considered the matching procedure of the full-theory tree-level trispectrum and one-loop power spectrum, respectively, to show how correlation functions of elementary full-theory fields can be reproduced using the SdSET, while in sections 4.7 and 4.8 we showed how to match composite-operator correlation functions by determining C_{24}, C_{22} and C_{20} at $\mathcal{O}(\kappa)$, respectively. By doing so we checked that all IR-divergent terms appearing in the full-theory result are generated by the SdSET correlation functions, which ensures that the coefficients of the above matching equations are free of infrared pathologies. Therefore, to remove the IR divergences from the full-theory correlation functions we need to understand how to tame the same divergences in the SdSET correlation functions. Once this is done, and a prescription to compute SdSET correlators in an infrared-safe way has been established, the matching equations between full-theory and EFT correlators that follow from the matching equations at the operator level can be used to obtain IR-finite full-theory results.

The core idea to develop such a prescription is the one presented in [105, 107], namely to derive an equation of motion for the renormalized SdSET correlation functions which holds non-perturbatively, and to solve it self-consistently in the sense of [40]. In the case of the simplest non-trivial correlation functions, namely the one-point functions $\langle\varphi_+^n(t,\vec{x})\rangle$, such an equation of motion should reproduce the results obtained from Stochastic Inflation [58–60], but then allow one to go beyond this known and leading approximation in a systematic and controlled fashion. The papers [105, 107] postulated that this equation can be obtained within the SdSET as an RGE with respect to a physical-momentum reference scale, which was denoted by k_*/a_*, which serves to track the secular logarithms

$$\ln\left(\frac{k_i}{a(t)H}\right), \tag{4.9.3}$$

and therefore the time dependence of the SdSET correlation functions, to all orders in κ. The solution of such an equation should then "resum" these logarithms, yielding an IR-finite, non-secularly growing expression, which is the desired result. This is the essential idea of the dynamical renormalization group [88–90], which was applied to the cosmological context in [91,115]. This RGE picture immediately leads to the interpretation of the coefficients multiplying the operators appearing in such an equation as anomalous dimensions of some kind, which should then be directly related to the coefficients of the UV poles encountered when renormalizing the operators in question. This is the basic intuition that was used in [107] to compute the next-to-next-to-leading order corrections to the Fokker-Planck equation of Stochastic Inflation.

For this picture to work, it must be guaranteed that the reference scale, such as the combination k_*/a_* used in [105, 107], and the argument of the logarithms which one wishes to track, and eventually control, always appear in the same combination, for instance $k_i a_*/(k_* a(t))$. This was shown to happen in the case of a one-loop example computed in the theory of a massless, conformally coupled scalar field in [115], and then again for the same case in [105]. However, no proof for this claim was given for the massless, minimally coupled scalar field, which is most relevant case for the study of this issue. It would therefore be highly desirable to have a systematic way to check that this logic indeed applies.

This will be our goal in this section. To achieve it, in the following we will pursue the opposite strategy with respect to the mentioned references, and proceed as follows: based on what we learned so far about the properties of the renormalized SdSET operators $[\varphi_+^n]$, we will derive an equation of motion which they satisfy at leading power in λ and to all orders in κ. The coefficients of this equation of motion will involve the operator renormalization factors Z_{nm} we introduced in section 4.6, as well as the effective couplings $c_{n,m}$. We will then study the structure of the coefficients of this equation of motion, and discuss how they are linked to the anomalous dimensions γ^{μ}_{nm} and $\gamma^{a_*}_{nm}$ that we introduced and computed in the above sections. Doing so, we will see how the intuition of [105, 107] is realized in our scheme. Finally, we will discuss how the obtained equations can be used in practice to remove the IR pathologies we observed in perturbation theory.

4.9.1 Equation of motion for $[\varphi_+^n]$ for generic values of a_*

We start by deriving the equation of motion for $[\varphi_+^n]$ while keeping the full dependence on both μ and a_* in the EFT. We will see that the resulting equation will still involve time-dependent coefficients, and we will discuss how to consistently remove this remaining time-dependence in the next subsection.

Derivation of the general formula

The starting point for the derivation is the defining equation for the renormalized operators $[\varphi_+^n]$ which we set up above in section 4.6, see (4.6.5):

$$\varphi_+^n(t,\vec{x}) = (a(t)\tilde{\mu})^{n\frac{d-4}{2}} \sum_{m=0}^{\infty} (a(t)\tilde{\mu})^{-m\frac{d-4}{2}} Z_{nm}[\varphi_+^m](t,\vec{x})\,. \tag{4.9.4}$$

Inverting this equation for $[\varphi_+^n]$, and taking the time derivative of both sides, we find

$$\begin{aligned}\frac{\mathrm{d}}{\mathrm{d}t}[\varphi_+^n] =& \frac{\mathrm{d}}{\mathrm{d}t} \sum_{m=0}^{\infty} (a(t)\tilde{\mu})^{(m-n)\frac{4-d}{2}} Z^{-1}_{nm}\varphi_+^m \\ =& \sum_{m=0}^{\infty} (a(t)\tilde{\mu})^{(m-n)\frac{4-d}{2}} \left[(m-n)\frac{4-d}{2} Z^{-1}_{nm}\varphi_+^m + \frac{\mathrm{d}Z^{-1}_{nm}}{\mathrm{d}t}\varphi_+^m + Z^{-1}_{nm}\frac{\mathrm{d}}{\mathrm{d}t}\varphi_+^m\right],\end{aligned} \tag{4.9.5}$$

which involves the derivative of the bare composite operator φ_+^n on the right-hand side. To evaluate this term we can use the following generic formula for the time derivative of any operator $Q(t)$, which holds in the SdSET at leading power in λ:

$$\frac{\mathrm{d}}{\mathrm{d}t}Q(t) = i\int \mathrm{d}^{d-1}x \sum_{l=0}^{\infty} (a(t)\tilde{\mu})^{l(4-d)} \frac{\hat{c}^0_{2l+1,1}}{(2l+1)!}\left[\varphi_+^{2l+1}(t,\vec{x})\varphi_-(t,\vec{x}), Q(t)\right]. \tag{4.9.6}$$

The derivation of this formula can be found in appendix 4.F. Notice the absence of the analytic regulator in this expression, which justified in the same appendix. Plugging in $Q(t) = \varphi_+^n(t,\vec{x})$ we get

$$\frac{\mathrm{d}}{\mathrm{d}t}\varphi_+^n(t,\vec{x}) = i\int \mathrm{d}^{d-1}y\ \sum_{l=0}^{\infty}(a(t)\tilde{\mu})^{l(4-d)}\frac{\hat{c}^0_{2l+1,1}}{(2l+1)!}\Big[\varphi_+^{2l+1}(t,\vec{y})\varphi_-(t,\vec{y}),\varphi_+^n(t,\vec{x})\Big]\,. \tag{4.9.7}$$

The commutator appearing on the right-hand side of the above equation can be evaluated as follows: we know that the free EFT fields $\varphi_{\pm,\mathrm{free}}$ obey the canonical equal-time commutation relations

$$[\varphi_{+,\mathrm{free}}(t,\vec{x}),\varphi_{-,\mathrm{free}}(t,\vec{y})] = -\frac{i}{3}\delta^{(d-1)}(\vec{x}-\vec{y})\,, \tag{4.9.8}$$

$$[\varphi_{\pm,\mathrm{free}}(t,\vec{x}),\varphi_{\pm,\mathrm{free}}(t,\vec{y})] = 0\,. \tag{4.9.9}$$

Since this holds for arbitrary times, we can rewrite $\varphi_{\pm,\mathrm{free}}$ in terms of the interacting fields $\varphi_\pm$ evaluated at time $t=-\infty$, at which we assume all interactions to be switched off and therefore for free and interacting fields to coincide, and we still have

$$[\varphi_+(-\infty,\vec{x}),\varphi_-(-\infty,\vec{y})] = -\frac{i}{3}\delta^{(d-1)}(\vec{x}-\vec{y})\,, \tag{4.9.10}$$

$$[\varphi_\pm(-\infty,\vec{x}),\varphi_\pm(-\infty,\vec{y})] = 0\,. \tag{4.9.11}$$

Now we can time-evolve these equations to arbitrary correlation time t using the time-evolution operator $U(t,-\infty)$ and find

$$\begin{aligned}
&U^\dagger(t,-\infty)[\varphi_+(-\infty,\vec{x}),\varphi_-(-\infty,\vec{y})]U(t,-\infty)\\
=&\Big[U^\dagger(t,-\infty)\varphi_+(-\infty,\vec{x})U(t,-\infty),U^\dagger(t,-\infty)\varphi_-(-\infty,\vec{x})U(t,-\infty)\Big]\\
=&[\varphi_+(t,\vec{x}),\varphi_-(t,\vec{y})] = -\frac{i}{3}\delta^{(d-1)}(\vec{x}-\vec{y})\,.
\end{aligned} \tag{4.9.12}$$

Analogously we get

$$[\varphi_\pm(t,\vec{x}),\varphi_\pm(t,\vec{y})] = 0\,, \tag{4.9.13}$$

so we can conclude that the interacting fields satisfy the same equal-time commutation relations as the free ones. Using these result in (4.9.7) we find

$$\frac{\mathrm{d}}{\mathrm{d}t}\varphi_+^n(t,\vec{x}) = -\frac{n}{3}\sum_{l=0}^{\infty}(a(t)\tilde{\mu})^{l(4-d)}\frac{\hat{c}^0_{2l+1,1}}{(2l+1)!}\varphi_+^{2l+n}(t,\vec{x})\,, \tag{4.9.14}$$

which is, of course, the result that one would naively have expected from the single-field equation of motion

$$\frac{\mathrm{d}}{\mathrm{d}t}\varphi_+(t,\vec{x}) = -\frac{1}{3}\sum_{l=0}^{\infty}(a(t)\tilde{\mu})^{l(4-d)}\frac{\hat{c}^0_{2l+1,1}}{(2l+1)!}\varphi_+^{2l+1}(t,\vec{x})\,. \tag{4.9.15}$$

Plugging (4.9.14) into (4.9.5) yields

$$\begin{aligned}
\frac{\mathrm{d}}{\mathrm{d}t}[\varphi_+^n] =& \sum_{m=0}^{\infty}(a(t)\tilde{\mu})^{(n-m)\frac{d-4}{2}}\left[(m-n)\frac{4-d}{2}Z^{-1}_{nm}\varphi_+^m + \frac{\mathrm{d}Z^{-1}_{nm}}{\mathrm{d}t}\varphi_+^m - \frac{m}{3}Z^{-1}_{nm}\sum_{l=0}^{\infty}(a(t)\tilde{\mu})^{l(4-d)}\frac{\hat{c}^0_{2l+1,1}}{(2l+1)!}\varphi_+^{2l+m}\right]\\
=& \sum_{m,k=0}^{\infty}(a(t)\tilde{\mu})^{(k-n)\varepsilon}\left[m\varepsilon Z^{-1}_{nm}Z_{mk} + \frac{\mathrm{d}Z^{-1}_{nm}}{\mathrm{d}t}Z_{mk} - \frac{m}{3}Z^{-1}_{nm}\sum_{l=0}^{\infty}\frac{\hat{c}^0_{2l+1,1}}{(2l+1)!}Z_{2l+m,k}\right][\varphi_+^k]\\
&- n\varepsilon[\varphi_+^n]\,,
\end{aligned} \tag{4.9.16}$$

where to obtain the final equlity we used (4.9.4) to rewrite the entire equation in terms of renormalized operators $[\varphi_+^n]$, and plugged in $d = 4 - 2\varepsilon$. We can further simplify the equation by using

$$\delta_{nm} = \sum_{l=0}^{\infty} Z_{nl}^{-1} Z_{lm} \,, \tag{4.9.17}$$

from which it follows immediately that

$$0 = \sum_{l=0}^{\infty} \left[\frac{\mathrm{d}Z_{nl}^{-1}}{\mathrm{d}t} Z_{lm} + Z_{nl}^{-1} \frac{\mathrm{d}Z_{lm}}{\mathrm{d}t} \right]. \tag{4.9.18}$$

Using this relation we get

$$\frac{\mathrm{d}}{\mathrm{d}t}[\varphi_+^n] = -\, n\varepsilon[\varphi_+^n] + \sum_{m,k=0}^{\infty} (a(t)\tilde{\mu})^{(k-n)\varepsilon} Z_{nm}^{-1} \left[m\varepsilon Z_{mk} - \frac{\mathrm{d}Z_{mk}}{\mathrm{d}t} - \frac{m}{3} \sum_{l=0}^{\infty} \frac{\hat{c}^0_{2l+1,1}}{(2l+1)!} Z_{2l+m,k} \right] [\varphi_+^k] \tag{4.9.19}$$

$$\equiv \sum_{k=0}^{\infty} (a(t)\tilde{\mu})^{(k-n)\varepsilon} H_{nk} [\varphi_+^k] \,, \tag{4.9.20}$$

where we defined the equation-of-motion coefficients

$$H_{nm} = -n\varepsilon\delta_{nm} + \sum_{k=0}^{\infty} Z_{nk}^{-1} \left[k\varepsilon Z_{km} - \frac{\mathrm{d}Z_{km}}{\mathrm{d}t} - \frac{k}{3} \sum_{l=0}^{\infty} \frac{\hat{c}^0_{2l+1,1}}{(2l+1)!} Z_{2l+k,m} \right]. \tag{4.9.21}$$

So far, we have succeeded in deriving the equation of motion for the operators $[\varphi_+^n]$,

$$\frac{\mathrm{d}}{\mathrm{d}t}[\varphi_+^n] = \sum_{m=0}^{\infty} (a(t)\tilde{\mu})^{(m-n)\varepsilon} H_{nm} [\varphi_+^m] \,, \tag{4.9.22}$$

and, as anticipated, the coefficients H_{nm} involve both the Z_{nm} and the effective couplings. The obtained equation has a similar structure as the RGEs controlling the μ- and a_*-dependence of the $[\varphi_+^n]$, and the formula for the coefficients H_{nm} shares some features with the formulas for the ADM elements γ^{μ}_{nm} and $\gamma^{a_*}_{nm}$. Analogously to them, the H_{nm} must be finite, which is, however, not at all obvious from their definition.

Computation of the matrix elements H_{nm}

To get some intuition for the structure of the coefficients H_{nm} we will compute as many as we can using all the results for the effective couplings and operator renormalization coefficents that we determined in the previous sections. This will also serve as a sanity check on the formula (4.9.21), since we must obtain finite results in the limit $\varepsilon \to 0$. However, before carrying out any explicit computation, we can make the following two general and useful statements about the coefficients by just inspecting the defining equation (4.9.21):

- For the very first entry, which is H_{00}, we see that

  $$H_{00} = 0 \tag{4.9.23}$$

  to all orders in the coupling, since $Z_{0m}^{-1} = \delta_{0m}$ to all orders in the coupling. This is what we expect to find, because the unit operator is time-independent, and it is not affected by the renormalization process in any way.

- At $\mathcal{O}(\kappa^0)$, we observe that the formula (4.9.21) reduces to

  $$H_{nm}^{(\kappa^0)} = -n\varepsilon\delta_{nm} + \sum_{k=0}^{\infty} [Z^{(\kappa^0)}]_{nk}^{-1} k\varepsilon Z_{km}^{(\kappa^0)} \,, \tag{4.9.24}$$

since we can neglect all contributions from the effective couplings, and the operator renormalization factors are all time-independent, so their time derivative vanishes. Comparing this result to the formula for the μ-anomalous dimension we found above in (4.6.25) we see that they agree:

$$H_{nm}^{(\kappa^0)} = \gamma_{nm}^{\mu,(\kappa^0)} = \frac{n(n-2)}{8\pi^2}\delta_{n-2,m}\,. \tag{4.9.25}$$

We used (4.6.89) and (4.6.90) to get the last equality.

We now turn to the practical computation of specific coefficients. To do so, let us first collect all the results for the Z_{nm} that we found in sections 4.6.3, 4.7 and 4.8, as well as for the two dimensionless, bare couplings we matched in sections 4.4 and 4.5:

$$\begin{aligned}
Z_{20} =& \frac{1}{8\pi^2\varepsilon} + \frac{\kappa}{192\pi^4}\Bigg\{\frac{1}{4\varepsilon^3} + \frac{1}{\varepsilon^2}\left[\frac{1}{2}\ln\left(\frac{e^{2\gamma_E}a_*\mu^2}{a(t)H^2}\right) + \delta\hat{m}_{\rm fin}^2 - \frac{4}{3}\right] \\
&+ \frac{1}{\varepsilon}\left[\ln\left(\frac{e^{\gamma_E}\mu}{H}\right)\left(\ln\left(\frac{e^{\gamma_E}\mu}{H}\right) + 2\delta m_{\rm fin}^2 - \frac{8}{3}\right) + \frac{1}{2}\ln^2\left(\frac{a_*}{a(t)}\right) - \frac{8\delta m_{\rm fin}^2}{3} + \frac{59}{36} + \frac{5\pi}{3\sqrt{3}} - \frac{\pi^2}{4}\right]\Bigg\} \\
&+ \mathcal{O}(\kappa^2)\,, \qquad (4.9.26)\\
Z_{22} =& 1 + \frac{\kappa}{48\pi^2}\left[\frac{1}{\varepsilon^2} + \frac{2}{\varepsilon}\left(\ln\left(\frac{e^{\gamma_E}a_*\mu}{a(t)H}\right) - \frac{4}{3}\right)\right] + \mathcal{O}(\kappa^2)\,, \qquad (4.9.27)\\
Z_{40} =& \frac{3}{64\pi^4\varepsilon^2} + \mathcal{O}(\kappa)\,, \qquad (4.9.28)\\
Z_{42} =& \frac{3}{4\pi^4\varepsilon} + \mathcal{O}(\kappa)\,, \qquad (4.9.29)\\
Z_{51} =& \frac{15}{64\pi^4\varepsilon^2} + \mathcal{O}(\kappa)\,, \qquad (4.9.30)\\
\hat{c}_{1,1}^0 =& \frac{\kappa}{8\pi^2}\left[-\frac{1}{2\varepsilon} + \delta\hat{m}_{\rm fin}^2\right] + \mathcal{O}(\kappa^2)\,, \qquad (4.9.31)\\
\hat{c}_{3,1}^0 =& \kappa + \mathcal{O}(\kappa^2)\,. \qquad (4.9.32)
\end{aligned}$$

With these results, we are now in the position to compute the following entries of the infinite-dimensional matrix of coefficients H_{nm}:

- We can start by looking at the non-trivial family of matrix elements H_{1n}, which are given by the formula

$$H_{1n} = -\delta_{1n}\varepsilon + \sum_{m=0}^{\infty} Z_{1m}^{-1}\left[m\varepsilon Z_{mn} - \frac{\mathrm{d}Z_{mn}}{\mathrm{d}t} - \frac{m}{3}\sum_{l=0}^{\infty}\frac{\hat{c}_{2l+1,1}^0}{(2l+1)!}Z_{2l+m,n}\right], \tag{4.9.33}$$

and, using that $Z_{1n} = \delta_{1n}$ to all orders in the coupling, which then also implies $Z_{1n}^{-1} = \delta_{1n}$, the above expression reduces to

$$H_{1n} = -\frac{1}{3}\sum_{l=0}^{\infty}\frac{\hat{c}_{2l+1,1}^0}{(2l+1)!}Z_{2l+1,n}\,. \tag{4.9.34}$$

The first representative of this family that we look at is H_{11}, which up to $\mathcal{O}(\kappa)$ is given by

$$\begin{aligned}
H_{11} =& -\frac{1}{3}\left[\hat{c}_{1,1}^0 Z_{11}^{(\kappa^0)} + \frac{\hat{c}_{3,1}^0}{3!}Z_{31}^{(\kappa^0)}\right] \\
=& -\frac{1}{3}\left[\frac{\kappa}{8\pi^2}\left(-\frac{1}{2\varepsilon} + \delta\hat{m}_{\rm fin}^2\right) + \frac{\kappa}{6}\frac{3}{8\pi^2\varepsilon}\right] + \mathcal{O}(\kappa^2) \\
=& -\frac{\kappa}{24\pi^2}\delta\hat{m}_{\rm fin}^2\,, \qquad (4.9.35)
\end{aligned}$$

where we used the above results, and the fact that $c_{2l+1,1} \sim \kappa^2$ for $l \geq 2$, so we can truncate the series in (4.9.34) after $l = 1$. The result is finite as $\varepsilon \to 0$, as it must be, and we notice that a non-trivial cancellation of ε-poles had to take place in order to ensure the finiteness of the result.

Next, we look at H_{13}, and at $\mathcal{O}(\kappa)$ we find

$$H_{13} = -\frac{\kappa}{18} + \mathcal{O}(\kappa^2)\,, \tag{4.9.36}$$

where we used that $Z_{13} = 0$, and that $Z_{33} = 1 + \mathcal{O}(\kappa)$ and $c_{2l+1,1} \sim \kappa^2$ for $l \geq 2$, so we could truncate the series in (4.9.34) after $l = 1$. This result is trivially finite.

- The next non-trivial entry we can look at is H_{20}, which, using (4.9.21), is defined by

$$H_{20} = \sum_{m=0}^{\infty} Z^{-1}_{2m}\left[m\varepsilon Z_{m0} - \frac{\mathrm{d}Z_{m0}}{\mathrm{d}t} - \frac{m}{3}\sum_{l=0}^{\infty}\frac{\hat{c}^0_{2l+1,1}}{(2l+1)!}Z_{2l+m,0}\right]. \tag{4.9.37}$$

We consider this quantity up to $\mathcal{O}(\kappa)$. Using that

$$Z_{22} = 1 + Z^{(\kappa)}_{22} + \mathcal{O}(\kappa^2)\,, \quad Z^{-1}_{22} = 1 - Z^{(\kappa)}_{22} + \mathcal{O}(\kappa^2)\,, \quad Z^{-1}_{2m} = \mathcal{O}(\kappa^2) \quad \text{for } m > 2\,, \tag{4.9.38}$$

we can truncate the outermost series in (4.9.37) after $m = 2$ and the innermost series after $l = 1$ and get

$$H_{20} = 2\varepsilon\left[Z^{(\kappa^0)}_{20} + Z^{(\kappa)}_{20} - Z^{(\kappa)}_{22}Z^{(\kappa^0)}_{20}\right] - \frac{\mathrm{d}Z^{(\kappa)}_{20}}{\mathrm{d}t} - \frac{2}{3}\left[\hat{c}^0_{1,1}Z^{(\kappa^0)}_{20} + \frac{\hat{c}^0_{3,1}}{3!}Z^{(\kappa^0)}_{40}\right] + \mathcal{O}(\kappa^2)\,. \tag{4.9.39}$$

Using the results listed above for the operator-renormalization factors and bare, dimensionless couplings we find

$$\begin{aligned} H_{20} =& \frac{1}{4\pi^2} + \frac{\kappa}{192\pi^4}\left[\ln^2\left(\frac{a_*}{a(t)}\right) + 2\ln\left(\frac{e^{\gamma_E}\mu}{H}\right)\left(\ln\left(\frac{e^{\gamma_E}\mu}{H}\right) + 2\delta\hat{m}^2_{\text{fin}} - \frac{8}{3}\right)\right. \\ &\left. - \frac{16\delta m^2_{\text{fin}}}{3} + \frac{59}{18} + \frac{10\pi}{3\sqrt{3}} - \frac{\pi^2}{2}\right] + \mathcal{O}(\kappa^2)\,, \end{aligned} \tag{4.9.40}$$

which is finite as $\varepsilon \to 0$. This result constitutes the most non-trivial check that we can carry out for the formula (4.9.21) at the time of writing, and it has two noteworthy features. The first is that, comparing it to the result for Z_{20}, we can notice that it is equal to 2ε times its single-pole part. This observation is suggestive of the standard procedure to extract beta-function and anomalous-dimensions coefficients from the single-pole terms of renormalization factors working in dimensional regularization [111], but we will see shortly that this will not be the case for all H_{nm}. The second is that it features a $\ln^2(a_*/a(t))$, which is the first instance of a residual time-dependence being left over in the coefficients H_{nm} that we anticipated above.

- The next interesting entry which we can look at is H_{22}, which, using (4.9.21), reads

$$\begin{aligned} H_{22} =& -2\varepsilon + \sum_{m=0}^{\infty} Z^{-1}_{2m}\left[m\varepsilon Z_{m2} - \frac{\mathrm{d}Z_{m2}}{\mathrm{d}t} - \frac{m}{3}\sum_{l=0}^{\infty}\frac{c^0_{2l+1,1}}{(2l+1)!}Z_{2l+m,2}\right] \end{aligned} \tag{4.9.41}$$

$$= -\frac{\mathrm{d}Z^{(\kappa)}_{22}}{\mathrm{d}t} - \frac{2}{3}\left[c^0_{1,1} + \frac{c^0_{3,1}}{3!}Z^{(\kappa^0)}_{42}\right] + \mathcal{O}(\kappa^2)\,, \tag{4.9.42}$$

where we used that $Z^{-1}_{24} = \mathcal{O}(\kappa^2)$ to truncate the outer series in (4.9.41) after $m = 2$, and that $c_{2l+1,1} = \mathcal{O}(\kappa^2)$ for $l \geq 2$ to truncate the inner series after $l = 1$. Plugging the known quantities into this formula we find the result

$$H_{22} = -\frac{\kappa}{12\pi^2}\delta\hat{m}^2_{\text{fin}}\,, \tag{4.9.43}$$

which is finite as $\varepsilon \to 0$. Differently than the case of H_{20}, this result is not simply 2ε times Z_{22}.

- Finally, we look at H_{24}, which reads

$$H_{24} = \sum_{m=0}^{\infty} Z_{2m}^{-1}\left[m\varepsilon Z_{m4} - \frac{\mathrm{d}Z_{m4}}{\mathrm{d}t} - \frac{m}{3}\sum_{l=0}^{\infty}\frac{c^0_{2l+1,1}}{(2l+1)!}Z_{2l+m,4}\right] \tag{4.9.44}$$

$$= -\frac{2}{3}\frac{c^0_{3,1}}{3!} + \mathcal{O}(\kappa^2) \tag{4.9.45}$$

$$= -\frac{\kappa}{9} + \mathcal{O}(\kappa^2)\,, \tag{4.9.46}$$

where we used that $Z_{22}^{(\kappa^0)} = Z_{44}^{(\kappa^0)} = 1$, and the fact that $Z_{24} \sim Z_{24}^{-1} \sim \kappa^2$. This result is trivially finite.

Thus, we find that, in the cases we were able to check, the formula (4.9.21) indeed yields finite results in the limit $\varepsilon \to 0$, which constitutes a consistency check on it. The cancellation of the poles in ε, which appear both in the operator-renormalization factors and in the bare couplings, is non-trivial, and the fact that it successfully occurs implies a relation between the poles that are encountered when renormalizing the effective couplings and the ones that are encountered when renormalizing the composite operators φ_+^n, which is not an obvious statement from the outset.

We also confirmed, using the example of H_{20}, that for general values of a_* the coefficients H_{nm} are manifestly time-dependent, via logarithms of the ratio $a_*/a(t)$. Before seeing how this remaining time-dependence can be removed, we can use some of the coefficients H_{nm} we computed above to verify that they indeed faithfully describe the time dependence of the renormalized operators $[\varphi_+^n]$ using an example.

Perturbative solution of the equation of motion for $\langle[\varphi_+^2](t,\vec{x})\rangle$ and comparison to the diagrammatic result

As a further consistency check on the derived equation of motion (4.9.22) we show that its perturbative solution reproduces the renormalized result found in section 4.8 for the one-point function $\langle[\varphi_+^2](t,\vec{x})\rangle$. In the case of $[\varphi_+^2]$ the expectation value of the equation (4.9.22) reads

$$\frac{\mathrm{d}}{\mathrm{d}t}\langle[\varphi_+^2](t,\vec{x})\rangle = \sum_{m=0}^{\infty} H_{2m}\langle[\varphi_+^m](t,\vec{x})\rangle\,. \tag{4.9.47}$$

The above sum can be truncated after $m = 4$, because starting from H_{26} all the coefficients are at least $\mathcal{O}(\kappa^2)$, as the mixing of $[\varphi_+^2]$ with the operator $[\varphi_+^n]$ with $n \geq 6$ would occur via at least two insertions of the quartic EFT coupling. We then have the following equation:

$$\frac{\mathrm{d}}{\mathrm{d}t}\langle[\varphi_+^2](t,\vec{x})\rangle = H_{20}^{(\kappa^0)} + H_{20}^{(\kappa)} + H_{22}^{(\kappa)}\langle[\varphi_+^2](t,\vec{x})\rangle + H_{24}^{(\kappa)}\langle[\varphi_+^4](t,\vec{x})\rangle + \mathcal{O}(\kappa^2)\,, \tag{4.9.48}$$

where the right-hand-side of it involves the two one-point functions $\langle[\varphi_+^2](t,\vec{x})\rangle$ and $\langle[\varphi_+^4](t,\vec{x})\rangle$. To solve this equation perturbatively for the one-point function $\langle[\varphi_+^2](t,\vec{x})\rangle$ in an expansion in powers of κ, we make the ansatz

$$\langle[\varphi_+^n](t,\vec{x})\rangle = \langle[\varphi_+^n](t,\vec{x})\rangle^{(\kappa^0)} + \langle[\varphi_+^n](t,\vec{x})\rangle^{(\kappa)} + \mathcal{O}(\kappa^2) \tag{4.9.49}$$

for $n = 2, 4$. As a first step to solve (4.9.48) we thus need to find the solution for $\langle[\varphi_+^2](t,\vec{x})\rangle$ and $\langle[\varphi_+^4](t,\vec{x})\rangle$ at $\mathcal{O}(\kappa^0)$.

At $\mathcal{O}(\kappa^0)$ the equation (4.9.48) reduces to

$$\frac{\mathrm{d}}{\mathrm{d}t}\langle[\varphi_+^2](t,\vec{x})\rangle^{(\kappa^0)} = H_{20}^{(\kappa^0)} = \frac{1}{4\pi^2}\,. \tag{4.9.50}$$

This equation is solved by

$$\langle[\varphi_+^2](t,\vec{x})\rangle^{(\kappa^0)} = \frac{t}{4\pi^2} + C_2^{(\kappa^0)} = \frac{1}{4\pi^2}\ln(a(t)) + C_2^{(\kappa^0)}\,, \tag{4.9.51}$$

where we used that we are working with the dimensionless time variable t, which is equivalent to $\ln(a(t))$. We still have an undetermined integration constant $C_2^{(\kappa^0)}$ to fix, and to do so we can compare the above result to the $\mathcal{O}(\kappa^0)$-result we found in section 4.6.3 above, in equation (4.6.34),

$$\langle[\varphi_+^2](t,\vec{x})\rangle^{(\kappa^0)} = -\frac{1}{4\pi^2}\ln\left(\frac{\Lambda}{a(t)\mu}\right). \tag{4.9.52}$$

Comparing the two expressions, we see that the the time-dependent part agrees, and that we need to choose the IR-divergent integration constant

$$C_2^{(\kappa^0)} = -\ln\left(\frac{\Lambda}{\mu}\right) \tag{4.9.53}$$

to reach full agreement with the perturbative result.

To find the $\mathcal{O}(\kappa^0)$-expression for $\langle[\varphi_+^4](t,\vec{x})\rangle$, which we will need to find the $\mathcal{O}(\kappa)$-solution of (4.9.48), we take the expectation value of (4.9.22) for the special case of $[\varphi_+^4]$ on its left-hand side, and find

$$\begin{aligned}\frac{\mathrm{d}}{\mathrm{d}t}\langle[\varphi_+^4](t,\vec{x})\rangle &= \sum_{m=0}^{\infty} H_{4m}\langle[\varphi_+^m](t,\vec{x})\rangle \\ &= \gamma_{42}^{\mu,(\kappa^0)}\langle[\varphi_+^2](t,\vec{x})\rangle^{(\kappa^0)} + \mathcal{O}(\kappa) \\ &= \frac{3}{2\pi^2}\langle[\varphi_+^2](t,\vec{x})\rangle^{(\kappa^0)}\,,\end{aligned} \tag{4.9.54}$$

where we used that at $\mathcal{O}(\kappa^0)$ the matrix elements H_{nm} are the same as the ones of the μ-ADM, see (4.9.25). With this result at hand, as well as the result (4.9.52) for $\langle[\varphi_+^2](t,\vec{x})\rangle^{(\kappa^0)}$, the equation of motion for $\langle[\varphi_+^4](t,\vec{x})\rangle$ at $\mathcal{O}(\kappa^0)$ reads

$$\frac{\mathrm{d}}{\mathrm{d}t}\langle[\varphi_+^4](t,\vec{x})\rangle^{(\kappa^0)} = -\frac{3}{8\pi^4}\ln\left(\frac{\Lambda}{a(t)\mu}\right). \tag{4.9.55}$$

It is solved by

$$\langle[\varphi_+^4](t,\vec{x})\rangle^{(\kappa^0)} = \frac{3}{16\pi^4}\ln^2\left(\frac{\Lambda}{a(t)\mu}\right) - \frac{3}{16\pi^4}\ln^2\left(\frac{\Lambda}{\mu}\right) + C_4^{(\kappa^0)}\,, \tag{4.9.56}$$

and, also in this case, we need to fix the constant of integration $C_4^{(\kappa^0)}$, which we can do by comparing the obtained result for $\langle[\varphi_+^4](t,\vec{x})\rangle^{(\kappa^0)}$ to the result we found above section 4.6.3, equation (4.6.53):

$$\langle[\varphi_+^4](t,\vec{x})\rangle^{(\kappa^0)} = \frac{3}{16\pi^4}\ln^2\left(\frac{\Lambda}{a(t)\mu}\right). \tag{4.9.57}$$

Comparing this expression to the perturbative result of the equation of motion, we can see that the time-dependent piece agrees in this case as well, and we need to choose

$$C_4^{(\kappa^0)} = \frac{3}{16\pi^4}\ln^2\left(\frac{\Lambda}{\mu}\right) \tag{4.9.58}$$

to reach full agreement with the perturbative result.

Plugging these results into (4.9.48) we find the $\mathcal{O}(\kappa)$-equation

$$\begin{aligned}\frac{\mathrm{d}}{\mathrm{d}t}\langle[\varphi_+^2](t,\vec{x})\rangle^{(\kappa)} = &\frac{\kappa}{192\pi^4}\Bigg\{-3\ln^2(a(t)) + 2\ln(a(t))\left[4\ln\left(\frac{\Lambda}{\mu}\right) - \ln(a_*) - 2\delta\hat{m}_{\text{fin}}^2\right] \\ &+\ln\left(\frac{e^{\gamma_E}\mu}{H}\right)\left[2\ln\left(\frac{e^{\gamma_E}\mu}{H}\right) - 4\left(\frac{4}{3} - \delta\hat{m}_{\text{fin}}^2\right)\right] + \ln^2(a_*) + \frac{59}{18} - \frac{16}{3}\delta\hat{m}_{\text{fin}}^2 + \frac{10\pi}{3\sqrt{3}} - \frac{\pi^2}{2}\end{aligned}$$

$$- 4\ln^2\left(\frac{\Lambda}{\mu}\right) + 4\delta\hat{m}^2_{\rm fin}\ln\left(\frac{\Lambda}{\mu}\right)\Bigg\}\,, \tag{4.9.59}$$

where we collected all the powers of $\ln(a(t))$ for convenience. This equation is solved by

$$\begin{aligned}\langle[\varphi_+^2](t,\vec{x})\rangle^{(\kappa)} =& \frac{\kappa}{192\pi^4}\Bigg\{-\ln^3(a(t)) + \ln^2(a(t))\left[4\ln\left(\frac{\Lambda}{\mu}\right) - \ln(a_*) - 2\delta\hat{m}^2_{\rm fin}\right] \\ &+ \ln(a(t))\left[\ln\left(\frac{e^{\gamma_E}\mu}{H}\right)\left(2\ln\left(\frac{e^{\gamma_E}\mu}{H}\right) - 4\left(\frac{4}{3} - \delta\hat{m}^2_{\rm fin}\right)\right) + \ln^2(a_*) + \frac{59}{18} - \frac{16}{3}\delta\hat{m}^2_{\rm fin}\right. \\ &\left.+ \frac{10\pi}{3\sqrt{3}} - \frac{\pi^2}{2} - 4\ln^2\left(\frac{\Lambda}{\mu}\right) + 4\delta\hat{m}^2_{\rm fin}\ln\left(\frac{\Lambda}{\mu}\right)\right]\Bigg\} + C_2^{(\kappa)}\,,\end{aligned} \tag{4.9.60}$$

and this expression indeed reproduces all the time-dependent terms of the renormalized one-point function $\langle[\varphi_+^2](t,\vec{x})\rangle$ we found in (4.8.23). By a suitable choice of $C_2^{(\kappa)}$ we can then reproduce the remaining time-independent, finite terms as well.

We were thus able to successfully check, in this case, that the equation of motion for renormalized operators (4.9.22) faithfully reproduces the result we obtained using diagrammatic methods, after fixing suitable integration constants. In particular, the time dependence of the equation-of-motion coefficients H_{nm} plays an important role in making sure that this is the case. At this point, we also notice that the IR-divergent logarithms $\ln(\Lambda)$ enter the perturbative solution of (4.9.22) only via the integration constants C_n, which we picked in the present case in order to match the diagrammatic result. This procedure can be interpreted as choosing particular boundary conditions for the solution of the differential equation in question. Since we know that, perturbatively, the Bunch-Davies vacuum is ill-defined for the free massless, minimally coupled scalar field, we can interpret these IR-divergent constants as being introduced by the ill-defined initial conditions that we are using for the perturbative diagrammatic computation, which we carried out using Bunch-Davies mode functions.

4.9.2 Removing the leftover time dependence from the equation-of-motion coefficients

Above we have derived an equation of motion for the renormalized composite operators $[\varphi_+^n]$, which involves coefficients H_{nm} that can be computed from the operator-renormalization factors Z_{nm} and the bare, dimensionless effective couplings $\hat{c}^0_{n,m}$, in a similar fashion to how the operator anomalous dimensions γ^μ_{nm} and $\gamma^{a_*}_{nm}$ can be computed. We also checked that it consistently reproduces the diagrammatic results using a non-trivial example. By means of some explicit computations to determine the coefficients H_{nm}, we saw that, in general, they are time-dependent due to powers of logarithms of the form $\ln(a_*/a(t))$ appearing in them. While this form of the equation is suitable to just reproduce the results obtained in perturbation theory for SdSET correlation functions, which we exemplified above using the case of the one-point function $\langle[\varphi_+^2](t,\vec{x})\rangle$, it is not yet suited for its use as a tool to remove both IR divergences and secular growth from the EFT correlators, which is what we are interested in. The reason is that if we tried to solve the equation of motion self-consistently, e.g. for the one-point functions $\langle[\varphi_+^n](t,\vec{x})\rangle$, the result would inevitably inherit the logarithmic time-dependence from the H_{nm}, and thus still exhibit secular growth. We will now see how this residual time-dependence can be removed.

The general argument

The formula we derived in section 4.9.1 for the H_{nm} left the reference scale factor a_* arbitrary, and we can identify this as the source of the remaining time dependence of the coefficients. To remove it, we should evolve the scale factor a_* down to its natural value for the problem we are considering, which is $a(t)$. In practice, up to the order of the expansion in the full-theory coupling we are considering, this simply amounts to setting $a_* = a(t)$ and then taking into account the additional time dependence that this choice induces when computing $\mathrm{d}[\varphi_+^n]/\mathrm{d}t$.

This proposition can be motivated as follows: from the point of view of the EFT, $a(t)$ is an external kinematic parameter that enters in the definition of our soft scale and power-counting parameter,

$$\frac{k_i}{a(t)H} \sim \lambda\,, \tag{4.9.61}$$

and a_* is an arbitrary reference scale factor, that can be set to any value, in particular also to $a(t)$. After matching the effective couplings and non-Gaussian initial conditions of the EFT using correlators involving only elementary fields, we are now using the obtained results to compute SdSET correlators involving composite operators, which live at the soft scale. To do this properly, all involved quantities should be evaluated at that scale, and this should be done using the RGEs for the involved scales to evolve them down to the soft one, which is a well-known procedure to resum the large logarithms which would be generated otherwise. However, we found that the a_*-RGEs for the initial conditions we derived in section 4.3.3 and analyzed in the explicit cases of $\Xi^{\sigma}_{3,1}$ and $\Xi^{\sigma}_{1,1}$ in the sections 4.4.4 and 4.5.4, respectively, were trivial up to the considered order in the coupling, in the sense that their solution would just give us the explicitly appearing $\ln(a_*)$ in the matched results back. Therefore, the "evolution" of a_* down to $a(t)$ just amounts to setting directly $a_* = a(t)$ in the SdSET correlators. For the examples we considered thus far, this has the following consequences:

- The contributions from the vertex-insertion diagrams and from the initial-condition-counterterm diagrams cancel exactly, since they are, by construction, equal and opposite, except for the fact that one comes with a factor $a(t)^{n\varepsilon}$ and the other with a factor $a_*^{n\varepsilon}$, which are now set equal. The computation of EFT diagrams reduces to the contributions coming from the finite pieces of the initial conditions.

- The matched finite parts of the non-Gaussian initial conditions now contain logs of $k_i/a(t)$. At tree level, these are nothing but the "classical logarithms" that are accounted for by the classical equation of motion for the elementary effective fields $\varphi_\pm$, but they are also generated at loop level, as we saw in the case of $\Xi^{\sigma}_{1,1}$. The only other source of logarithms of $a(t)$ in the EFT-correlators is from the poles generated by the momentum integrals over the renormalized initial-condition functions (no contributions from time integrals are left, since these only come from the vertex-insertions diagrams, which all get cancelled by the initial-condition counterterms), and this "anomalous" $a(t)$-dependence is tracked by the μ-dependence, since the two quantities always appear together in the combination $(a(t)\tilde{\mu})^{n\varepsilon}$ in front of the renormalized non-Gaussian initial conditions. This time dependence should, therefore, be linked to the μ-anomalous dimensions, which realizes the intuition of [105, 107].

- In the case of one-point functions, which is all we are considering here, the time-dependence in the full theory can only appear in the combination

$$\ln\left(\frac{\Lambda}{a(t)H}\right), \tag{4.9.62}$$

since Λ is the only comoving scale which can ever appear in a given one-point correlator computed in the k_Λ-scheme, and the only available value of the scale factor is $a(t)$. In the EFT one-point functions, the only comoving scale is also Λ, which can be converted into a physical scale by combining it with either a_* or $a(t)$. If we set $a_* = a(t)$, then the only available combination is

$$\ln\left(\frac{\Lambda}{a(t)\mu}\right), \tag{4.9.63}$$

which we explicitly saw in the above results. Therefore, the IR regulator always appears divided by $a(t)$, and if the EFT reproduces the full Λ-dependence, which it must, it also follows that it will reproduce the full time-dependence. In particular, the equation of motion for the composite operators $[\varphi_+^n]$ should then reproduce the Fokker-Planck equation of Stochastic Inflation at leading order, and the equation-of-motion coefficients should no longer contain logarithms of $a_*/a(t)$ at any order, which is what we want.

However, setting $a_* = a(t)$ induces an additional time dependence in composite-operator correlation functions, which must be taken into account to obtain the correct equation of motion for $[\varphi_+^n]$. We can do it as follows: the total time derivative of $[\varphi_+^n]$ with a_* and $a(t)$ set equal can be decomposed in terms of partial derivatives with respect to t and $\ln(a_*)$ as

$$\frac{\mathrm{d}}{\mathrm{d}t}\left[[\varphi_+^n](t,\vec{x})\Big|_{a_*=a(t)}\right] = \left[\frac{\partial}{\partial t}[\varphi_+^n](t,\vec{x}) + \frac{\mathrm{d}}{\mathrm{d}\ln(a_*)}[\varphi_+^n](t,\vec{x})\right]\Bigg|_{a_*=a(t)}. \tag{4.9.64}$$

The first term on the right-hand side of (4.9.64) can be obtained by means of the known equation of motion we derived above for the $[\varphi_+^n]$:

$$\frac{\partial}{\partial t}\left[[\varphi_+^n](t,\vec{x})\Big|_{a_*=a(t)}\right] = \sum_{m=0}^{\infty} H_{nm}[\varphi_+](t,\vec{x})\Big|_{a_*=a(t)}, \tag{4.9.65}$$

since this equation only tracks the $a(t)$-dependence, with a_* left arbitrary, and in particular different than $a(t)$. It is clear that setting $a_* = a(t)$ in the above equation sets all the $\ln(a_*/a(t))$-factors appearing in the H_{nm} which we found above to zero, and the equation-of-motion coefficients just become finite, time-independent constants. The second term on the right-hand side of (4.9.64) is known as well, and it is given by

$$\frac{\mathrm{d}[\varphi_+^n]}{\mathrm{d}\ln(a_*)} = \sum_{m=0}^{\infty} \gamma_{nm}^{a_*}[\varphi_+^m], \tag{4.9.66}$$

where the a_*-anomalous dimensions can be computed from the Z_{nm} using the formula

$$\gamma_{nm}^{a_*} = -\sum_{l=0}^{\infty} Z_{nl}^{-1}\frac{\mathrm{d}Z_{lm}}{\mathrm{d}\ln(a_*)} \tag{4.9.67}$$

we derived above. Analogously to the H_{nm}, any dependence of the a_*-anomalous dimensions on logarithms of the ratio $a_*/a(t)$ is eliminated by setting these two scales equal, so the $\gamma_{nm}^{a_*}$ reduce to finite, time-independent constants as well.

In summary, from the above considerations we found that the equation of motion for the renormalized composite operators evaluated at $a_* = a(t)$, which is the natural value for the reference scale factor a_* when computing SdSET correlation functions, is given by

$$\frac{\mathrm{d}}{\mathrm{d}t}\left[[\varphi_+^n](t,\vec{x})\Big|_{a_*=a(t)}\right] = \sum_{m=0}^{\infty}\left[H_{nm} + \gamma_{nm}^{a_*}\right][\varphi_+^m](t,\vec{x})\Bigg|_{a_*=a(t)}. \tag{4.9.68}$$

The right-hand side of this equation no longer involves any explicit time dependence in any of the coefficients, which makes it suitable for a self-consistent-solution approach to compute SdSET correlation functions involving the $[\varphi_+^n]$ to remove both the IR-singular and secular character of said correlators. Further, both the equation-of-motion coefficients H_{nm} and the anomalous dimensions $\gamma_{nm}^{a_*}$ can be computed using only the effective couplings and the Z_{nm}, which shows that the full time dependence of the renormalized operators $[\varphi_+^n]$, and hence of the full-theory operators $[\phi^n]$, is described within the EFT alone, without having to take contributions from the operator matching coefficients C_{nm} into account.

An explicit check

We can repeat the procedure we followed in section 4.9.1 to check (4.9.68). Taking the expectation value of this equation with $n = 2$ gives

$$\frac{\mathrm{d}}{\mathrm{d}t}\left[\langle[\varphi_+^2](t,\vec{x})\rangle\Big|_{a_*=a(t)}\right] = \sum_{m=0}^{\infty}\left[H_{2m} + \gamma_{2m}^{a_*}\right]\langle[\varphi_+^m](t,\vec{x})\rangle\Bigg|_{a_*=a(t)}. \tag{4.9.69}$$

We will keep only the terms up to $\mathcal{O}(\kappa)$ on both sides of the equation and and compare both sides, which we can determine independently of each other by using some of the results we already obtained above.

To determine the first term on the right-hand side of (4.9.69) we use the general equation of motion for $[\varphi_+^n]$ derived in section 4.9.1, now adapted to the present notation, and find

$$\frac{\partial}{\partial t}\langle[\varphi_+^2](t,\vec{x})\rangle = H_{24}^{(\kappa)}\langle[\varphi_+^4](t,\vec{x})\rangle\Big|_{\mathcal{O}(\kappa^0)} + H_{22}^{(\kappa)}\langle[\varphi_+^2](t,\vec{x})\rangle\Big|_{\mathcal{O}(\kappa^0)} + H_{20}^{(\kappa^0)} + H_{20}^{(\kappa)} + \mathcal{O}(\kappa^2)\,, \tag{4.9.70}$$

with

$$H_{24} = -\frac{\kappa}{9} + \mathcal{O}(\kappa^2)\,, \tag{4.9.71}$$

$$H_{22} = -\frac{\kappa}{12\pi^2}\delta\hat{m}_{\text{fin}}^2 + \mathcal{O}(\kappa^2)\,, \tag{4.9.72}$$

$$\begin{aligned} H_{20} =& \frac{1}{4\pi^2} + \frac{\kappa}{192\pi^4}\left[\ln^2\left(\frac{a_*}{a(t)}\right) + 2\ln\left(\frac{e^{\gamma_E}\mu}{H}\right)\left(\ln\left(\frac{e^{\gamma_E}\mu}{H}\right) + 2\delta\hat{m}_{\text{fin}}^2 - \frac{8}{3}\right)\right. \\ &\left. - \frac{16\delta m_{\text{fin}}^2}{3} + \frac{59}{18} + \frac{10\pi}{3\sqrt{3}} - \frac{\pi^2}{2}\right] + \mathcal{O}(\kappa^2)\,. \end{aligned} \tag{4.9.73}$$

Setting $a_* = a(t)$ leaves H_{24} and H_{22} unchanged, whereas the result for H_{20} reduces to

$$H_{20} = \frac{1}{4\pi^2} + \frac{\kappa}{96\pi^4}\left[\ln\left(\frac{e^{\gamma_E}\mu}{H}\right)\left(\ln\left(\frac{e^{\gamma_E}\mu}{H}\right) + 2\delta\hat{m}_{\text{fin}}^2 - \frac{8}{3}\right) - \frac{8\delta m_{\text{fin}}^2}{3} + \frac{59}{36} + \frac{5\pi}{3\sqrt{3}} - \frac{\pi^2}{4}\right] + \mathcal{O}(\kappa^2)\,. \tag{4.9.74}$$

Plugging these expressions into (4.9.70) we find the following equation:

$$\begin{aligned} \frac{\partial}{\partial t}\langle[\varphi_+^2](t,\vec{x})\rangle\Big|_{a_*=a(t)} =& -\frac{\kappa}{9}\langle[\varphi_+^4](t,\vec{x})\rangle\Big|_{\mathcal{O}(\kappa^0)} - \frac{\kappa}{12\pi^2}\delta\hat{m}_{\text{fin}}^2\langle[\varphi_+^2](t,\vec{x})\rangle\Big|_{\mathcal{O}(\kappa^0)} + \left\{\frac{1}{4\pi^2}\right. \\ &\left. + \frac{\kappa}{96\pi^4}\left[\ln\left(\frac{e^{\gamma_E}\mu}{H}\right)\left(\ln\left(\frac{e^{\gamma_E}\mu}{H}\right) + 2\delta\hat{m}_{\text{fin}}^2 - \frac{8}{3}\right) - \frac{8\delta m_{\text{fin}}^2}{3} + \frac{59}{36} + \frac{5\pi}{3\sqrt{3}} - \frac{\pi^2}{4}\right]\right\}. \end{aligned} \tag{4.9.75}$$

To determine the second summand on the right-hand side of (4.9.69) we use the a_*-RGE of $[\varphi_+^2]$, keeping the relevant terms up to $\mathcal{O}(\kappa)$, and we get

$$\frac{\mathrm{d}}{\mathrm{d}\ln(a_*)}\langle[\varphi_+^2](t,\vec{x})\rangle\Big|_{a_*=a(t)} = \left[\gamma_{22}^{a_*}\langle[\varphi_+^2](t,\vec{x})\rangle\Big|_{\mathcal{O}(\kappa^0)} + \gamma_{20}^{a_*} + \mathcal{O}(\kappa^2)\right]\Big|_{a_*=a(t)} \tag{4.9.76}$$

$$= -\frac{\kappa}{12\pi^2}\left[\frac{4}{3} - \ln\left(\frac{e^{\gamma_E}\mu}{H}\right)\right]\langle[\varphi_+^2](t,\vec{x})\rangle\Big|_{\mathcal{O}(\kappa^0)} + \frac{\kappa}{192\pi^4}\left[\frac{5}{2} - \frac{10\pi}{3\sqrt{3}} + \frac{\pi^2}{12}\right]. \tag{4.9.77}$$

To obtain this result we used the expressions we found above for the relevant $\gamma_{nm}^{a_*}$,

$$\gamma_{22}^{a_*} = -\frac{\kappa}{12\pi^2}\left[\frac{4}{3} - \ln\left(\frac{e^{\gamma_E}\mu}{H}\right)\right], \tag{4.9.78}$$

$$\gamma_{20}^{a_*} = \frac{\kappa}{192\pi^4}\left\{\ln\left(\frac{a_*}{a(t)}\right)\left[-\ln\left(\frac{a_*}{a(t)}\right) + 4\ln\left(\frac{e^{\gamma_E}\mu}{H}\right) - \frac{16}{3}\right] + \frac{5}{2} - \frac{10\pi}{3\sqrt{3}} + \frac{\pi^2}{12}\right\}, \tag{4.9.79}$$

and set $a_* = a(t)$ in them. Plugging the two pieces (4.9.75) and (4.9.77) into (4.9.69), we find the equation

$$\frac{\mathrm{d}}{\mathrm{d}t}\left[\langle[\varphi_+^2](t,\vec{x})\rangle\Big|_{a_*=a(t)}\right] = -\frac{\kappa}{9}\langle[\varphi_+^4](t,\vec{x})\rangle\Big|_{\mathcal{O}(\kappa^0)} - \frac{\kappa}{12\pi^2}\left[\frac{4}{3} - \ln\left(\frac{e^{\gamma_E}\mu}{H}\right) + \delta\hat{m}_{\text{fin}}^2\right]\langle[\varphi_+^2](t,\vec{x})\rangle\Big|_{\mathcal{O}(\kappa^0)} + \left\{\frac{1}{4\pi^2}\right.$$

$$+\frac{\kappa}{96\pi^4}\left[\ln\left(\frac{e^{\gamma_E}\mu}{H}\right)\left(\ln\left(\frac{e^{\gamma_E}\mu}{H}\right)+2\delta\hat{m}^2_{\rm fin}-\frac{8}{3}\right)-\frac{8\delta m^2_{\rm fin}}{3}+\frac{26}{9}-\frac{5\pi^2}{24}\right]\Bigg\}. \tag{4.9.80}$$

Taking the results for $\langle[\varphi_+^2](t,\vec{x})\rangle|_{\mathcal{O}(\kappa^0)}$ and $\langle[\varphi_+^4](t,\vec{x})\rangle|_{\mathcal{O}(\kappa^0)}$ that we obtained in section 4.6.3, which read

$$\langle[\varphi_+^2](t,\vec{x})\rangle\Big|_{\mathcal{O}(\kappa^0)}=-\frac{1}{4\pi^2}\ln\left(\frac{\Lambda}{a(t)\mu}\right), \tag{4.9.81}$$

$$\langle[\varphi_+^4](t,\vec{x})\rangle\Big|_{\mathcal{O}(\kappa^0)}=\frac{3}{16\pi^4}\ln^2\left(\frac{\Lambda}{a(t)\mu}\right), \tag{4.9.82}$$

and plugging them into the right-hand side of (4.9.80) yields

$$\begin{aligned}\frac{\mathrm{d}}{\mathrm{d}t}\left[\langle[\varphi_+^2](t,\vec{x})\rangle\Big|_{a_*=a(t)}\right]=&\frac{1}{4\pi^2}+\frac{\kappa}{96\pi^4}\Bigg\{-2\ln^2\left(\frac{\Lambda}{a(t)\mu}\right)+2\left[\frac{4}{3}-\ln\left(\frac{e^{\gamma_E}\mu}{H}\right)+\delta\hat{m}^2_{\rm fin}\right]\ln\left(\frac{\Lambda}{a(t)\mu}\right)\\&+\left[\ln\left(\frac{e^{\gamma_E}\mu}{H}\right)\left(\ln\left(\frac{e^{\gamma_E}\mu}{H}\right)+2\delta\hat{m}^2_{\rm fin}-\frac{8}{3}\right)-\frac{8\delta\hat{m}^2_{\rm fin}}{3}+\frac{26}{9}-\frac{5\pi^2}{24}\right]\Bigg\}\end{aligned} \tag{4.9.83}$$

$$\begin{aligned}=&-\frac{\kappa}{9}\langle[\varphi_+^4](t,\vec{x})\rangle-\frac{\kappa}{12\pi^2}\left[\frac{4}{3}-\ln\left(\frac{e^{\gamma_E}\mu}{H}\right)+\delta\hat{m}^2_{\rm fin}\right]\langle[\varphi_+^2](t,\vec{x})\rangle+\Bigg\{\frac{1}{4\pi^2}\\&+\frac{\kappa}{96\pi^4}\left[\ln\left(\frac{e^{\gamma_E}\mu}{H}\right)\left(\ln\left(\frac{e^{\gamma_E}\mu}{H}\right)+2\delta\hat{m}^2_{\rm fin}-\frac{8}{3}\right)-\frac{8\delta m^2_{\rm fin}}{3}+\frac{26}{9}-\frac{5\pi^2}{24}\right]\Bigg\}.\end{aligned} \tag{4.9.84}$$

On the other hand, using the result for $\langle[\varphi_+^2](t,\vec{x})\rangle|_{\mathcal{O}(\kappa)}$ that we obtained in section 4.8 and setting $a_*=a(t)$ in it gives

$$\begin{aligned}&\langle[\varphi_+^2](t,\vec{x})\rangle\Big|_{\substack{\mathcal{O}(\kappa)\\a_*=a(t)}}\\=&\frac{\kappa}{192\pi^4}\Bigg\{\frac{4}{3}\ln^3\left(\frac{e^{\gamma_E}\Lambda}{a(t)H}\right)-\left[\frac{8}{3}+2\delta\hat{m}^2_{\rm fin}+2\ln\left(\frac{e^{\gamma_E}\mu}{H}\right)\right]\ln^2\left(\frac{e^{\gamma_E}\Lambda}{a(t)H}\right)\\&+\left[\ln\left(\frac{e^{\gamma_E}\mu}{H}\right)\left(\frac{32}{3}-2\ln\left(\frac{e^{\gamma_E}\mu}{H}\right)-4\ln\left(\frac{a_*}{a(t)}\right)\right)+\frac{16}{3}\delta\hat{m}^2_{\rm fin}-\frac{52}{9}+\frac{5\pi^2}{12}\right]\ln\left(\frac{e^{\gamma_E}\Lambda}{a(t)H}\right)\\&+\frac{8}{3}\ln^3\left(\frac{e^{\gamma_E}\mu}{H}\right)-2\left[4-\delta\hat{m}^2_{\rm fin}\right]\ln^2\left(\frac{e^{\gamma_E}\mu}{H}\right)+\left[\frac{52}{9}-\frac{\pi^2}{2}-\frac{16}{3}\delta\hat{m}^2_{\rm fin}\right]\ln\left(\frac{e^{\gamma_E}\mu}{H}\right)\\&-\frac{\pi^2}{12}\delta\hat{m}^2_{\rm fin}+\frac{5}{2}-\frac{\pi}{\sqrt{3}}\left[2+\frac{2}{3}\ln(2)-\frac{7}{4}\ln(3)\right]+\frac{13\pi^2}{108}-\frac{7}{6}\zeta(3)+\frac{1}{18}\psi^{(1)}\left(\frac{1}{6}\right)-\frac{1}{9}\psi^{(1)}\left(\frac{1}{3}\right)\\&+\frac{1}{6}\psi^{(1)}\left(\frac{2}{3}\right)-\frac{1}{12}\psi^{(1)}\left(\frac{5}{6}\right)\Bigg\}.\end{aligned} \tag{4.9.85}$$

Using this expression, as well as (4.9.81) and taking the time derivative of the sum $\langle[\varphi_+^2](t,\vec{x})\rangle|_{\mathcal{O}(\kappa^0)}+\langle[\varphi_+^2](t,\vec{x})\rangle|_{\mathcal{O}(\kappa)}$ we get

$$\begin{aligned}&\frac{\mathrm{d}}{\mathrm{d}t}\left[\langle[\varphi_+^2](t,\vec{x})\rangle\Big|_{\mathcal{O}(\kappa^0)}+\langle[\varphi_+^2](t,\vec{x})\rangle\Big|_{\substack{\mathcal{O}(\kappa)\\a_*=a(t)}}\right]\\=&\frac{1}{4\pi^2}+\frac{\kappa}{96\pi^4}\Bigg\{-2\ln^2\left(\frac{\Lambda}{a(t)\mu}\right)+2\left[\frac{4}{3}-\ln\left(\frac{e^{\gamma_E}\mu}{H}\right)+\delta\hat{m}^2_{\rm fin}\right]\ln\left(\frac{\Lambda}{a(t)\mu}\right)\\&+\left[\ln\left(\frac{e^{\gamma_E}\mu}{H}\right)\left(\ln\left(\frac{e^{\gamma_E}\mu}{H}\right)+2\delta\hat{m}^2_{\rm fin}-\frac{8}{3}\right)-\frac{8\delta\hat{m}^2_{\rm fin}}{3}+\frac{26}{9}-\frac{5\pi^2}{24}\right]\Bigg\}\\=&-\frac{\kappa}{9}\langle[\varphi_+^4](t,\vec{x})\rangle\Big|_{\mathcal{O}(\kappa^0)}-\frac{\kappa}{12\pi^2}\left[\frac{4}{3}-\ln\left(\frac{e^{\gamma_E}\mu}{H}\right)+\delta\hat{m}^2_{\rm fin}\right]\langle[\varphi_+^2](t,\vec{x})\rangle\Big|_{\mathcal{O}(\kappa^0)}+\Bigg\{\frac{1}{4\pi^2}\end{aligned} \tag{4.9.86}$$

$$+\frac{\kappa}{96\pi^4}\left[\ln\left(\frac{e^{\gamma_E}\mu}{H}\right)\left(\ln\left(\frac{e^{\gamma_E}\mu}{H}\right)+2\delta\hat{m}^2_{\text{fin}}-\frac{8}{3}\right)-\frac{8\delta m^2_{\text{fin}}}{3}+\frac{26}{9}-\frac{5\pi^2}{24}\right]\Bigg\}, \tag{4.9.87}$$

which agrees with the right-hand side of (4.9.84), as it should. This completes the check.

4.9.3 Linking the H_{nm}, $\gamma^{a_*}_{nm}$ and γ^{μ}_{nm} together

In the previous subsection we derived and checked the validity of the equation

$$\frac{\mathrm{d}}{\mathrm{d}t}\left[[\varphi^n_+](t,\vec{x})\Big|_{a_*=a(t)}\right]=\sum_{m=0}^{\infty}\left[H_{nm}+\gamma^{a_*}_{nm}\right][\varphi^m_+](t,\vec{x})\Big|_{a_*=a(t)}, \tag{4.9.88}$$

which allows us to express the time dependence of any composite operator $[\varphi^n_+]$ in terms of time-independent coefficients multiplying the operators $[\varphi^n_+]$ themselves. This equation now has a suitable form to be used as a tool to compute correlation functions involving composite SdSET operators beyond perturbation theory, thereby removing the issue of IR divergences and secularly growing terms.

However, before describing how this can be done in practice, we recall that the argument we ran above in section 4.9.2 led us to the conclusion that the coefficients on the right-hand side of the above equation should be expressible in terms of the anomalous dimensions γ^{μ}_{nm} and renormalized EFT couplings, which is not obvious in its present form. However, we can already see a glimpse of this being the case using (4.9.80), which we used above for the explicit check. Using the two anomalous dimensions

$$\gamma^{\mu}_{22}=-\frac{\kappa}{12\pi^2}\left[\frac{4}{3}-\ln\left(\frac{e^{\gamma_E}\mu a_*}{a(t)H}\right)\right], \tag{4.9.89}$$

$$\gamma^{\mu}_{20}=\frac{1}{4\pi^2}+\frac{\kappa}{96\pi^4}\left\{\ln\left(\frac{e^{\gamma_E}a_*\mu}{a(t)H}\right)\left[\ln\left(\frac{e^{\gamma_E}a_*\mu}{a(t)H}\right)-\frac{8}{3}\right]-2\delta\hat{m}^2_{\text{fin}}\left[\frac{4}{3}-\ln\left(\frac{e^{\gamma_E}\mu}{H}\right)\right]+\frac{26}{9}-\frac{5\pi^2}{24}\right\}, \tag{4.9.90}$$

we found in sections 4.7 and 4.8, respectively, and setting $a_*=a(t)$ in them, we see that we can rewrite (4.9.80) as

$$\frac{\mathrm{d}}{\mathrm{d}t}\left[\langle[\varphi^2_+](t,\vec{x})\rangle\Big|_{a_*=a(t)}\right]=-\frac{c_{3,1}}{9}\langle[\varphi^4_+](t,\vec{x})\rangle\Big|_{\mathcal{O}(\kappa^0)}+\left[\gamma^{\mu}_{22}\Big|_{a_*=a(t)}-\frac{2}{3}c_{1,1}\right]\langle[\varphi^2_+](t,\vec{x})\rangle\Big|_{\mathcal{O}(\kappa^0)}+\gamma^{\mu}_{20}\Big|_{a_*=a(t)}, \tag{4.9.91}$$

where we used that

$$c_{1,1}=\frac{\kappa}{8\pi^2}\delta\hat{m}^2_{\text{fin}}+\mathcal{O}(\kappa^2). \tag{4.9.92}$$

This is precisely the structure of the equation that we expected from the general considerations above. Thus, there indeed seems to be a connection between the sum $H_{nm}+\gamma^{a_*}_{nm}$ evaluated at the point $a_*=a(t)$, the anomalous dimensions γ^{μ}_{nm} evaluated at $a_*=a(t)$, and the renormalized EFT-couplings, which we now make precise.

The general formulae for the three quantities of interest read

$$H_{nm}=-n\varepsilon\delta_{nm}+\sum_{l=0}^{\infty}Z^{-1}_{nl}\left[l\varepsilon Z_{lm}-\frac{\mathrm{d}Z_{lm}}{\mathrm{d}t}-\frac{l}{3}\sum_{k=0}^{\infty}\frac{c^0_{2k+1,1}}{(2k+1)!}Z_{2k+l,m}\right], \tag{4.9.93}$$

$$\gamma^{a_*}_{nm}=-\sum_{l=0}^{\infty}Z^{-1}_{nl}\frac{\mathrm{d}Z_{lm}}{\mathrm{d}\ln(a_*)}, \tag{4.9.94}$$

$$\gamma^{\mu}_{nm}=-n\varepsilon\delta_{nm}+\sum_{l=0}^{\infty}Z^{-1}_{nl}\left[l\varepsilon Z_{lm}-\frac{\mathrm{d}Z_{lm}}{\mathrm{d}\ln(\mu)}\right]. \tag{4.9.95}$$

The sum of interest then reads

$$\left[H_{nm}+\gamma^{a_*}_{nm}\right]\Big|_{a_*=a(t)}=\left\{-n\varepsilon\delta_{nm}+\sum_{l=0}^{\infty}Z^{-1}_{nl}\left[l\varepsilon Z_{lm}-\frac{\mathrm{d}Z_{lm}}{\mathrm{d}t}-\frac{\mathrm{d}Z_{lm}}{\mathrm{d}\ln(a_*)}-\frac{l}{3}\sum_{k=0}^{\infty}\frac{c^0_{2k+1,1}}{(2k+1)!}Z_{2k+l,m}\right]\right\}\Bigg|_{a_*=a(t)}. \tag{4.9.96}$$

To establish the link between this combination of quantities and γ^{μ}_{nm} we need to rewrite the combination

$$\frac{\mathrm{d}Z_{lm}}{\mathrm{d}t} + \frac{\mathrm{d}Z_{lm}}{\mathrm{d}\ln(a_*)} \tag{4.9.97}$$

as $\mathrm{d}Z_{lm}/\mathrm{d}\ln(\mu)$ plus an additional term which can be combined with the contribution from the bare effective couplings to give something finite. We have seen that for $a_* \neq a(t)$ these two scale factors appear in the Z-factors always in the combination $\ln(a_*/a(t))$. From this, it immediately follows that

$$\frac{\mathrm{d}Z_{nm}}{\mathrm{d}t} = -\frac{\partial Z_{nm}}{\partial \ln(a_*)}\,, \tag{4.9.98}$$

where by the partial derivatives we mean that they act only on the explicit dependence of the Z_{nm} on $\ln(a_*)$. Therefore, the explicit dependence on a_* and $a(t)$ cancels out in the sum (4.9.97). The only dependence that is left over is therefore the implicit a_*-dependence of the Z-factors, which stems from the a_*-running of the non-Gaussian initial conditions. This running is due to the overall factor of a_* that we pulled out of the bare initial conditions, which we rewrite here for convenience:

$$a_*^{2\delta}\,\Xi^{\sigma}_{1,1;0}(\vec{k}) = (a_*\nu)^{2\delta}\left[\xi^{\sigma}_{1,1}(\vec{k}) + \Xi^{\sigma}_{1,1}(\vec{k})\right], \tag{4.9.99}$$

$$a_*^{2\varepsilon n}\,\Xi^{\sigma}_{2n+1,1;0}(\vec{k}_1,...,\vec{k}_n) = (a_*\tilde{\mu})^{2\varepsilon n}\left[\xi^{\sigma}_{2n+1,1}(\vec{k}_1,...,\vec{k}_n) + \Xi^{\sigma}_{2n+1,1}(\vec{k}_1,...,\vec{k}_n)\right], \quad n \geq 1\,. \tag{4.9.100}$$

From these equations, we can directly see that this implicit a_*-dependence reflects the implicit ν-dependence for the initial condition with indices $(1,1)$, and the implicit μ-dependence for all other initial conditions, since they always come together in the product. As we explain in appendix 4.F, the δ-poles should never appear in the operator renormalization factors, so we can work under the assumption that the implicit a_*-dependence of the Z_{nm} is only related to their implicit μ-dependence via the initial-condition couplings $g_{2n+1,1}$ with $n \geq 1$, and that the implicit ν-dependence is irrelevant for this matter. We can therefore write:

$$\frac{\mathrm{d}Z_{lm}}{\mathrm{d}t} + \frac{\mathrm{d}Z_{lm}}{\mathrm{d}\ln(a_*)} = \left.\frac{\mathrm{d}}{\mathrm{d}\ln(a_*)}\right|_{\text{implicit through } g_{2n+1,1}} Z_{lm} \tag{4.9.101}$$

$$= \left.\frac{\mathrm{d}}{\mathrm{d}\ln(\mu)}\right|_{\text{implicit through } g_{2n+1,1}} Z_{lm} \tag{4.9.102}$$

$$= \frac{\mathrm{d}Z_{lm}}{\mathrm{d}\ln(\mu)} - \frac{\partial Z_{lm}}{\partial \ln(\mu)} - \left[\left.\frac{\mathrm{d}}{\mathrm{d}\ln(\mu)}\right|_{\text{implicit through } c_{2n+1,1}} Z_{lm}\right]. \tag{4.9.103}$$

To get the last equality we rewrote the implicit μ-dependence of the Z_{lm} induced via the non-Gaussian initial conditions as the total μ-dependence minus the remaining sources of μ-dependence, which are the explicit μ-dependence and the one induced by the running of the effective couplings. We can write the latter one as

$$\left.\frac{\mathrm{d}}{\mathrm{d}\ln(\mu)}\right|_{\text{implicit through } c_{2n+1,1}} Z_{lm} = \sum_{p=0}^{\infty} \frac{\partial Z_{lm}}{\partial c_{2p+1,1}} \frac{\mathrm{d}c_{2p+1,1}}{\mathrm{d}\ln(\mu)} = \sum_{p=0}^{\infty} \frac{\partial Z_{lm}}{\partial c_{2p+1,1}} \sum_{r=0}^{\infty} \beta_{pr} c_{2r+1,1}\,, \tag{4.9.104}$$

where used the beta-function (matrix) of the effective couplings, which is defined as

$$\frac{\mathrm{d}c_{2n+1,1}}{\mathrm{d}\ln(\mu)} = \sum_{l=0}^{\infty} \beta_{nl} c_{2l+1,1}\,. \tag{4.9.105}$$

We therefore found the following relation between derivatives of the operator renormalization coefficients:

$$\frac{\mathrm{d}Z_{lm}}{\mathrm{d}t} + \frac{\mathrm{d}Z_{lm}}{\mathrm{d}\ln(a_*)} = \frac{\mathrm{d}Z_{lm}}{\mathrm{d}\ln(\mu)} - \frac{\partial Z_{lm}}{\partial \ln(\mu)} - \sum_{p=0}^{\infty} \frac{\partial Z_{lm}}{\partial c_{2p+1,1}} \sum_{r=0}^{\infty} \beta_{pr} c_{2r+1,1}\,. \tag{4.9.106}$$

Plugging this equation into (4.9.96), we then find

$$\begin{aligned}
&\Big[H_{nm}+\gamma^{a_*}_{nm}\Big]\Big|_{a_*=a(t)}\\
=&\bigg\{-n\varepsilon\delta_{nm}+\sum_{l=0}^{\infty}Z^{-1}_{nl}\bigg[l\varepsilon Z_{lm}-\frac{\mathrm{d}Z_{lm}}{\mathrm{d}\ln(\mu)}+\frac{\partial Z_{lm}}{\partial\ln(\mu)}+\sum_{p=0}^{\infty}\frac{\partial Z_{lm}}{\partial c_{2p+1,1}}\sum_{r=0}^{\infty}\beta_{pr}c_{2r+1,1}\\
&-\frac{l}{3}\sum_{k=0}^{\infty}\frac{c^0_{2k+1,1}}{(2k+1)!}Z_{2k+l,m}\bigg]\bigg\}\bigg|_{a_*=a(t)} \qquad (4.9.107)\\
=&\bigg\{\gamma^{\mu}_{nm}+\sum_{l=0}^{\infty}Z^{-1}_{nl}\bigg[\frac{\partial Z_{lm}}{\partial\ln(\mu)}+\sum_{p=0}^{\infty}\frac{\partial Z_{lm}}{\partial c_{2p+1,1}}\sum_{r=0}^{\infty}\beta_{pr}c_{2r+1,1}-\frac{l}{3}\sum_{k=0}^{\infty}\frac{c^0_{2k+1,1}}{(2k+1)!}Z_{2k+l,m}\bigg]\bigg\}\bigg|_{a_*=a(t)} \qquad (4.9.108)\\
=&\Big[\gamma^{\mu}_{nm}+V_{nm}\Big]\Big|_{a_*=a(t)}\,, \qquad (4.9.109)
\end{aligned}$$

where we defined the matrix

$$V_{nm}\equiv\sum_{l=0}^{\infty}Z^{-1}_{nl}\bigg[\frac{\partial Z_{lm}}{\partial\ln(\mu)}+\sum_{p=0}^{\infty}\frac{\partial Z_{lm}}{\partial c_{2p+1,1}}\sum_{r=0}^{\infty}\beta_{pr}c_{2r+1,1}-\frac{l}{3}\sum_{k=0}^{\infty}\frac{c^0_{2k+1,1}}{(2k+1)!}Z_{2k+l,m}\bigg]\bigg|_{a_*=a(t)}\,. \qquad (4.9.110)$$

Notice that in the above equation both the bare and renormalized effective couplings appear. We could write the latter in terms of the former using their renormalization equation (4.3.40), which we reprint here for the bare, dimensionless couplings:

$$\hat{c}^0_{2n+1,1}=\sum_{m=0}^{\infty}Z^c_{nm}c_{2m+1,1}\,. \qquad (4.9.111)$$

However, this would not lead to an immediate simplification of (4.9.110), and would instead make it look more complicated, so we refrain from doing so at this point.

We thus found the following linking equation between the quantities H_{nm}, $\gamma^{a_*}_{nm}$ and γ^{μ}_{nm}:

$$\Big[H_{nm}+\gamma^{a_*}_{nm}\Big]\Big|_{a_*=a(t)}=\Big[\gamma^{\mu}_{nm}+V_{nm}\Big]\Big|_{a_*=a(t)}\,, \qquad (4.9.112)$$

which holds only under the condition that the scales a_* and $a(t)$ have been set equal. Combining this equation with (4.9.69), we get

$$\frac{\mathrm{d}}{\mathrm{d}t}\bigg[[\varphi^n_+](t,\vec{x})\Big|_{a_*=a(t)}\bigg]=\sum_{m=0}^{\infty}\Big[\gamma^{\mu}_{nm}+V_{nm}\Big][\varphi^m_+](t,\vec{x})\Big|_{a_*=a(t)}\,, \qquad (4.9.113)$$

which indeed shows that the μ-anomalous dimensions enter the effective equation of motion for the renormalized composite operators $[\varphi^n_+]$, which we anticipated from the general argument we ran in section 4.9.2, and which realizes the intuition of [105, 107]. The same argument leads us to expect that the matrix V_{nm} is directly related to the renormalized effective couplings, since it should contain the information about the "classical" time dependence of the $[\varphi^n_+]$, which is not captured by the anomalous dimensions γ^{μ}_{nm}. While the effective couplings appear in two of the three terms in (4.9.110), it is not obvious at all from this general equation that only the terms associated to the classical equation of motion of the fields, which should basically just be the renormalized effective couplings, will survive when plugging in all the necessary pieces. Indeed, similarly to the case of the anomalous dimensions and the H_{nm}, it is not even obvious that the V_{nm} are finite by just looking at (4.9.110), which, however, must be the case for the equation (4.9.112) to be correct. For both statements to be true, several relations between the operator renormalization factors Z_{nm} and the coupling renormalization factors Z^c_{nm} must exist, and their pole terms must conspire in order to cancel out when plugged into (4.9.110), and leave a finite remainder which should be related to the $c_{n,m}$. We already saw that this happened when computing some explicit examples of the H_{nm} in section 4.9.1, so it is plausible that this will be the case, but we do not have a way of proving this statement to all orders in the expansion of V_{nm} in powers of κ at the time of writing. What we can do, however, is run some checks on the formula (4.9.110) using known results.

Two explicit checks of the formula for the V_{nm}

In (4.9.91) we found the non-trivial results

$$\left[H_{22}+\gamma_{22}^{a_*}\right]\Big|_{a_*=a(t)} =\gamma_{22}^{\mu}\Big|_{a_*=a(t)}-\frac{2}{3}c_{1,1}\,, \tag{4.9.114}$$

$$\left[H_{20}+\gamma_{20}^{a_*}\right]\Big|_{a_*=a(t)} =\gamma_{20}^{\mu}\Big|_{a_*=a(t)}\,, \tag{4.9.115}$$

which make the following prediction for the values of V_{22} and V_{20}:

$$V_{22}=-\frac{2}{3}c_{1,1}+\mathcal{O}(\kappa^2)\,, \tag{4.9.116}$$

$$V_{20}=0+\mathcal{O}(\kappa^2)\,. \tag{4.9.117}$$

We can now check with the known results for the operator-renormalization factors and effective couplings that these predicted results are reproduced by (4.9.110). In order to successfully do so, it is crucial to differentiate correctly the contributions to the Z-factors which come from the effective couplings and from the initial conditions, since we need to take partial derivatives with respect to the former. Let us start with

$$V_{22}=\sum_{l=0}^{\infty}Z_{2l}^{-1}\left[\frac{\partial Z_{l2}}{\partial\ln(\mu)}+\sum_{p=0}^{\infty}\frac{\partial Z_{l2}}{\partial c_{2p+1,1}}\sum_{r=0}^{\infty}\beta_{pr}c_{2r+1,1}-\frac{l}{3}\sum_{k=0}^{\infty}\frac{c^0_{2k+1,1}}{(2k+1)!}Z_{2k+l,2}\right]\Bigg|_{a_*=a(t)} \tag{4.9.118}$$

$$=\left\{\frac{\partial Z^{(\kappa)}_{22}}{\partial\ln(\mu)}+\frac{\partial Z^{(\kappa)}_{22}}{\partial c_{11}}\beta_{13}c_{31}+\frac{\partial Z^{(\kappa)}_{22}}{\partial c_{31}}\beta_{33}c_{31}-\frac{2}{3}\left[c^0_{1,1}+\frac{c^0_{31}}{3!}Z^{(\kappa^0)}_{42}\right]\right\}\Bigg|_{a_*=a(t)}+\mathcal{O}(\kappa^2)\,. \tag{4.9.119}$$

We write the Z-factors of interest as

$$Z_{22}=1+\frac{g_{3,1}}{48\pi^2}\left[\frac{1}{\varepsilon^2}+\frac{2}{\varepsilon}\left(\ln\left(\frac{e^{\gamma_E}\mu}{H}\right)-\frac{4}{3}\right)\right]+\frac{c_{3,1}}{24\pi^2\varepsilon}\ln\left(\frac{a_*}{a(t)}\right), \tag{4.9.120}$$

$$Z_{42}=\frac{3}{4\pi^2\varepsilon}\,, \tag{4.9.121}$$

where we have written Z_{22} in this way to make clear on which quantities the derivatives with respect to the effective couplings should act. At the end we will set $a_*=a(t)$ and use that, as far as their values are concerned, we have $g_{3,1}=c_{3,1}$. We thus find

$$\frac{\partial Z_{22}}{\partial\ln(\mu)}=\frac{g_{3,1}}{24\pi^2\varepsilon}\,, \tag{4.9.122}$$

$$\frac{\partial Z_{22}}{\partial c_{31}}=\frac{1}{24\pi^2}\ln\left(\frac{a_*}{a(t)}\right), \tag{4.9.123}$$

$$\frac{\partial Z_{22}}{\partial c_{11}}=0\,, \tag{4.9.124}$$

and plugging everything into (4.9.119), setting $a_*=a(t)$ in the resulting expression and identifying $g_{3,1}=c_{3,1}$ we find

$$V_{22}=\frac{c_{3,1}}{24\pi^2\varepsilon}-\frac{2}{3}\left[-\frac{c_{3,1}}{16\pi^2\varepsilon}+c_{1,1}+\frac{c_{3,1}}{8\pi^2\varepsilon}\right]=-\frac{2}{3}c_{1,1}\,, \tag{4.9.125}$$

which is indeed what we should find.

We now turn to

$$V_{20}=\sum_{l=0}^{\infty}Z_{2l}^{-1}\left[\frac{\partial Z_{l0}}{\partial\ln(\mu)}+\sum_{p=0}^{\infty}\frac{\partial Z_{l0}}{\partial c_{2p+1,1}}\sum_{r=0}^{\infty}\beta_{pr}c_{2r+1,1}-\frac{l}{3}\sum_{k=0}^{\infty}\frac{c^0_{2k+1,1}}{(2k+1)!}Z_{2k+l,0}\right]\Bigg|_{a_*=a(t)} \tag{4.9.126}$$

$$=\left\{\frac{\partial Z_{20}^{(\kappa)}}{\partial\ln(\mu)}+\frac{\partial Z_{20}^{(\kappa)}}{\partial c_{11}}\beta_{13}c_{3,1}+\frac{\partial Z_{20}^{(\kappa)}}{\partial c_{3,1}}\beta_{33}c_{3,1}-\frac{2}{3}\left[c_{1,1}^{0}Z_{20}^{(\kappa^0)}+\frac{c_{3,1}^{0}}{3!}Z_{40}^{(\kappa^0)}\right]\right\}\bigg|_{a_*=a(t)}+\mathcal{O}(\kappa^2)\,. \tag{4.9.127}$$

Using

$$\begin{aligned}
Z_{20}=&\frac{1}{8\pi^2\varepsilon}+\frac{\kappa}{192\pi^4}\left\{\frac{1}{4\varepsilon^3}+\frac{1}{\varepsilon^2}\left[\frac{1}{2}\ln\left(\frac{e^{2\gamma_E}a_*\mu^2}{a(t)H^2}\right)+\delta\hat{m}_{\rm fin}^2-\frac{4}{3}\right]\right.\\
&\left.+\frac{1}{\varepsilon}\left[\ln\left(\frac{e^{\gamma_E}\mu}{H}\right)\left(\ln\left(\frac{e^{\gamma_E}\mu}{H}\right)+2\delta m_{\rm fin}^2-\frac{8}{3}\right)+\frac{1}{2}\ln^2\left(\frac{a_*}{a(t)}\right)-\frac{8\delta m_{\rm fin}^2}{3}+\frac{59}{36}+\frac{5\pi}{3\sqrt{3}}-\frac{\pi^2}{4}\right]\right\}\\
&+\mathcal{O}(\kappa^2)\,,
\end{aligned} \tag{4.9.128}$$

$$Z_{40}=\frac{3}{64\pi^4\varepsilon^2}+\mathcal{O}(\kappa)\,, \tag{4.9.129}$$

and tracing back the contributions to Z_{20} to the effective couplings and initial conditions we find

$$\frac{\partial Z_{20}}{\partial\ln(\mu)}=\frac{\kappa}{192\pi^4}\left\{\frac{1}{\varepsilon^2}+\frac{2}{\varepsilon}\left[\ln\left(\frac{e^{\gamma_E}\mu}{H}\right)+\delta\hat{m}_{\rm fin}^2-\frac{4}{3}\right]\right\}, \tag{4.9.130}$$

$$\frac{\partial Z_{20}}{\partial c_{31}}=\frac{1}{192\pi^4}\ln\left(\frac{a_*}{a(t)}\right)\frac{1}{\varepsilon}\left[\frac{1}{\varepsilon}+\ln\left(\frac{a_*}{a(t)}\right)\right], \tag{4.9.131}$$

$$\frac{\partial Z_{20}}{\partial c_{11}}=\frac{1}{24\pi^2}\frac{1}{\varepsilon}\left[\frac{1}{\varepsilon}+2\ln\left(\frac{e^{\gamma_E}\mu}{H}\right)-\frac{8}{3}+\ln\left(\frac{a_*}{a(t)}\right)\right]. \tag{4.9.132}$$

Plugging these results in, using

$$\beta_{13}c_{3,1}=-\frac{\kappa}{8\pi^2} \tag{4.9.133}$$

and setting $a_*=a(t)$ yields

$$\begin{aligned}
V_{20}=&\frac{\kappa}{192\pi^4}\left\{\frac{1}{\varepsilon^2}+\frac{2}{\varepsilon}\left[\ln\left(\frac{e^{\gamma_E}\mu}{H}\right)+\delta\hat{m}_{\rm fin}^2-\frac{4}{3}\right]\right\}-\frac{\kappa}{8\pi^2}\frac{1}{24\pi^2}\frac{1}{\varepsilon}\left[\frac{1}{\varepsilon}+2\ln\left(\frac{e^{\gamma_E}\mu}{H}\right)-\frac{8}{3}\right]-\frac{\kappa}{96\pi^4\varepsilon}\delta\hat{m}_{\rm fin}^2\\
=&0\,,
\end{aligned} \tag{4.9.134}$$

which, again, is what we should find. This completes the check.

4.9.4 Discussion of the found results, and their application to the issue of IR divergences

In this section we derived two versions of the effective equation of motion which controls the time dependence of the renormalized composite operators $[\varphi_+^n]$ to all orders in κ and to leading power in λ. They read

$$\frac{\rm d}{{\rm d}t}\left[[\varphi_+^n](t,\vec{x})\Big|_{a_*=a(t)}\right]=\sum_{m=0}^{\infty}\left[H_{nm}+\gamma_{nm}^{a_*}\right][\varphi_+^m](t,\vec{x})\Big|_{a_*=a(t)}\,, \tag{4.9.135}$$

$$\frac{\rm d}{{\rm d}t}\left[[\varphi_+^n](t,\vec{x})\Big|_{a_*=a(t)}\right]=\sum_{m=0}^{\infty}\left[\gamma_{nm}^{\mu}+V_{nm}\right][\varphi_+^m](t,\vec{x})\Big|_{a_*=a(t)}\,, \tag{4.9.136}$$

and the quantities appearing on the right-hand sides of the two equations are defined by the equations

$$\gamma_{nm}^{a_*}=-\sum_{l=0}^{\infty}Z_{nl}^{-1}\frac{{\rm d}Z_{lm}}{{\rm d}\ln(a_*)}\,, \tag{4.9.137}$$

$$\gamma_{nm}^{\mu}=-n\varepsilon\delta_{nm}+\sum_{l=0}^{\infty}Z_{nl}^{-1}\left[l\varepsilon Z_{lm}-\frac{{\rm d}Z_{lm}}{{\rm d}\ln(\mu)}\right], \tag{4.9.138}$$

$$H_{nm} = - n\varepsilon\delta_{nm} + \sum_{l=0}^{\infty} Z^{-1}_{nl}\left[l\varepsilon Z_{lm} - \frac{\mathrm{d}Z_{lm}}{\mathrm{d}t} - \frac{l}{3}\sum_{k=0}^{\infty}\frac{c^{0}_{2k+1,1}}{(2k+1)!}Z_{2k+l,m}\right], \tag{4.9.139}$$

$$V_{nm} = \sum_{l=0}^{\infty} Z^{-1}_{nl}\left[\frac{\partial Z_{lm}}{\partial\ln(\mu)} + \sum_{p=0}^{\infty}\frac{\partial Z_{lm}}{\partial c_{2p+1,1}}\sum_{r=0}^{\infty}\beta_{pr}c_{2r+1,1} - \frac{l}{3}\sum_{k=0}^{\infty}\frac{c^{0}_{2k+1,1}}{(2k+1)!}Z_{2k+l,m}\right]. \tag{4.9.140}$$

Both forms of the equation of motion for $[\varphi^n_+]$ are equivalent, and the coefficients appearing on the right-hand side of both equations are constants. The version (4.9.136) is particularly suggestive, since it represents a realization of the intuition of the original SdSET papers [105, 107], which in turn is informed by the idea of the dynamical renormalization group, that the time-evolution and renormalization-group evolution of operators in the SdSET are closely related. Showing that this is indeed the case in our scheme was one of the goals we set for ourselves in this section. Based on the explicit checks we were able to run, the matrix V_{nm} appearing on the right-hand side of (4.9.136) is related to the renormalized effective couplings, but we are unable, at least at the moment, to prove that it reduces to a combination of just the effective couplings to all orders in its expansion in powers of κ, and that it does not receive contributions from other quantities. Nevertheless, we would like to highlight that both forms of the equation of motion for $[\varphi^n_+]$ (4.9.135) and (4.9.136) are suitable to formulate a self-consistent computation scheme for the SdSET correlation functions. which can then be used to define IR-finite full-theory correlation functions. Let us now discuss how this works in practice for the simplest class of correlation functions, the one-point functions.

This procedure was already laid out for the (renormalized) EFT one-point functions $\langle[\varphi^n_+](t,\vec{x})\rangle$ in [105, 107], and we will follow this logic and extend it slightly. By taking the expectation value of either of the two equations (4.9.135) and (4.9.136) (let us pick the second one for concreteness) we obtain the equation

$$\frac{\mathrm{d}}{\mathrm{d}t}\left[\langle[\varphi^n_+](t,\vec{x})\rangle\Big|_{a_*=a(t)}\right] = \sum_{m=0}^{\infty}\left[\gamma^{\mu}_{nm} + V_{nm}\right]\langle[\varphi^m_+](t,\vec{x})\rangle\Big|_{a_*=a(t)}. \tag{4.9.141}$$

This equation should thought of as the analogue of the Schwinger-Dyson equations [34, 35] familiar from usual flat-space QFT, adapted to the case of the one-point functions $\langle[\varphi^n_+](t,\vec{x})\rangle$ in the present setting. To solve this equation self-consistently, the strategy is to associate a generating function $\rho_1(t,z)$ to the one-point functions $\langle[\varphi^n_+](t,\vec{x})\rangle$ via the defining equation

$$\langle[\varphi^n_+](t,\vec{x})\rangle \equiv \int_{-\infty}^{\infty}\mathrm{d}z\;\rho_1(t,z)z^n\,. \tag{4.9.142}$$

From this point of view, the function $\rho_1(t,z)$ plays the same role as the one-point probability distribution function in the formalism of Stochastic Inflation we discussed in chapter 2. Using (4.9.142) on both sides of (4.9.141), the latter equation can be written as a single partial differential equation for $\rho_1(t,z)$ of the form

$$\frac{\partial}{\partial t}\rho_1(t,z) = \sum_{n=1}^{\infty}\sum_{m=0}^{\infty}\frac{1}{n!\,m!}\frac{\partial^n}{\partial z^n}\left[D_{nm}z^m\rho_1(t,z)\right]. \tag{4.9.143}$$

The coefficients D_{nm} appearing in this equation can be related to the combination $[\gamma^{\mu}_{nm}+V_{nm}]|_{a_*=a(t)}$ in a straightforward way, and they are determined in terms of a power series in κ. The self-consistent approach to solving this equation, in the sense of [40], consists in defining a consistent approximation scheme to truncate the expansion of the D_{nm}, and then solving the resulting equation as it is, either analytically or numerically, for $\rho_1(t,z)$, without resorting to any further approximation. The resulting function can then be used in (4.9.142) to compute a version of the one-point functions $\langle[\varphi^n_+](t,\vec{x})\rangle$ which is free of IR divergences or secularly growing behaviour. These can then be plugged into the expectation value of the matching equation between renormalized full-theory and SdSET operators,

$$\langle[\phi^n](t,\vec{x})\rangle = H^n\sum_{m=0}^{\infty}C_{nm}\langle[\varphi^m_+](t,\vec{x})\rangle\,, \tag{4.9.144}$$

together with the matching coefficients C_{nm}, to obtain a physical result for the late-time limit of the full-theory one-point function $\langle[\phi^n](t,\vec{x})\rangle$.

Reproducing Stochastic Inflation with the SdSET

The equation (4.9.143) has the form of a Kramers-Moyal equation for the function $\rho_1(t,z)$ [61], which reduces to the Fokker-Planck equation in a special case. Indeed, it was already discussed in [105] that using the Gaussian approximation for the anomalous dimensions γ^{μ}_{nm}, in which case, in our notation, they reduce to

$$\gamma^{\mu}_{nm} = \frac{n(n-2)}{8\pi^2}\delta_{m,n-2}\,, \tag{4.9.145}$$

and including only the tree-level quartic interaction term $\sim c_{3,1}$ in the SdSET potential, which in our language amounts to reducing the matrix V_{nm} to

$$V_{nm} = -\frac{n}{3}\frac{\kappa}{3!}\delta_{m,n+2}\,, \tag{4.9.146}$$

the equation (4.9.141) reduces to

$$\frac{\mathrm{d}}{\mathrm{d}t}\langle[\varphi_+^n](t,\vec{x})\rangle = -\frac{\kappa n}{18}\langle[\varphi_+^{n+2}](t,\vec{x})\rangle + \frac{n(n-1)}{8\pi^2}\langle[\varphi_+^{n-2}](t,\vec{x})\rangle\,. \tag{4.9.147}$$

In turn, this leads to the equation

$$\frac{\partial\rho_1(t,z)}{\partial t} = \frac{1}{3}\frac{\partial}{\partial z}\left[\frac{\kappa}{6}z^3\rho_1(t,z)\right] + \frac{1}{8\pi^2}\frac{\partial^2}{\partial z^2}\rho_1(t,z)\,, \tag{4.9.148}$$

which is nothing but the Fokker-Planck equation[7] of Stochastic Inflation [58–60]. As we already discussed in chapter 2, this equation admits a non-perturbative, time-independent equilibrium solution of the form

$$\rho_{1\mathrm{eq}}(z) = \frac{2\kappa^{\frac{1}{4}}}{\sqrt{\frac{3}{\pi}}\Gamma(\frac{1}{4})}\exp\left(-\frac{\kappa\pi^2}{9}z^4\right)\,, \tag{4.9.149}$$

which then gives us the following solution for the SdSET one-point functions involving renormalized operators:

$$\langle[\varphi_+^{2n}](t,\vec{x})\rangle = \left(\frac{3}{8\pi^2\kappa}\right)^{\frac{n}{2}}\frac{\Gamma(\frac{2n+1}{4})}{\Gamma(\frac{1}{4})}\,. \tag{4.9.150}$$

Using that at leading power in the expansion in κ we have $C_{nm} = \delta_{nm}$[8], and that the equation (4.9.144) therefore reduces to

$$\langle[\phi^{2n}](t,\vec{x})\rangle = H^{2n}\langle[\varphi_+^{2n}](t,\vec{x})\rangle\,, \tag{4.9.151}$$

we conclude that the SdSET successfully reproduces the schochastic results.

Next-to-leading, and higher-order corrections

The truncation of (4.9.141) which yields the Fokker-Planck equation defines the lowest-order approximate form of this equation, and the equilibrium solution of the Fokker-Planck equation (4.9.149) defines the true, non-perturbative vacuum state of the massless, minimally coupled scalar field. Looking at the form of the one-point functions that it leads to, equation (4.9.150), we see that we should assign the non-perturbative counting $\varphi_+ \sim \kappa^{-\frac{1}{4}}$ to the leading-power SdSET field, which can then be used to define a consistent approximation scheme to compute corrections to the lowest-order truncation of (4.9.141) systematically. Starting from the next-to-leading order (NLO) corrections, which are $\sqrt{\kappa}$-suppressed with respect to the leading-order ones, both the higher-order coefficients of the equation of motion and the higher-order terms in the operator matching coefficients become relevant to compute the full-theory one-point functions $\langle[\phi^n](t,\vec{x})\rangle$. In fact, we

[7] Notice that powers of H are absent in this equation, since we have scaled all factors of H out of the effective fields.

[8] Here we are assuming that the two scales μ_{full} and μ_{eff} have been set equal in the matching equation,

already computed all the relevant quantities at this order: the matching equation between full-theory and SdSET one-point functions at NLO reads

$$\langle[\phi^{2n}](t,\vec{x})\rangle\Big|_{\rm NLO} = H^{2n}\left[\langle[\varphi_+^{2n}](t,\vec{x})\rangle\Big|_{\rm NLO} + \frac{n\kappa}{27}\langle[\varphi_+^{2n+2}](t,\vec{x})\rangle\Big|_{\rm LO} + \mathcal{O}(\kappa^{-\frac{n}{2}+1})\right], \tag{4.9.152}$$

where we generalized the result

$$C_{24} = \frac{\kappa}{27} + \mathcal{O}(\kappa^2) \tag{4.9.153}$$

we found in section 4.7 to

$$C_{n,n+2} = \frac{n\kappa}{27} + \mathcal{O}(\kappa^2)\,. \tag{4.9.154}$$

The one-point functions on the right-hand side of (4.9.152) need to be computed with the NLO- and LO-truncations of the Kramers-Moyal equation, respectively, as indicated by their subscripts, and the NLO-truncation of the Kramers-Moyal equation reads

$$\frac{\partial\rho_1(t,z)}{\partial t} = \frac{1}{3}\frac{\partial}{\partial z}\left[\left(c_{1,1}z + \frac{c_{3,1}}{3!}z^3 + \frac{c_{5,1}}{5!}z^5\right)\rho_1(t,z)\right] + \frac{1}{2}\frac{\partial^2}{\partial z^2}\left[\gamma_{20}^{\mu,(\kappa^0)} + \gamma_{22}^{\mu,(\kappa)}|_{a_*=a(t)}z^2\right]\rho_1(t,z)\,, \tag{4.9.155}$$

with the quantities

$$\begin{aligned}
c_{1,1} =& \frac{\kappa}{8\pi^2}\delta\hat{m}^2_{\rm fin} + \mathcal{O}(\kappa^2)\,, && (4.9.156)\\
c_{3,1} =& \kappa + \mathcal{O}(\kappa^2)\,, && (4.9.157)\\
c_{5,1} =& \frac{10\kappa^2}{9} + \mathcal{O}(\kappa^2)\,, && (4.9.158)\\
\gamma_{20}^{\mu,(\kappa^0)} =& \frac{1}{4\pi^2}\,, && (4.9.159)\\
\gamma_{22}^{\mu,(\kappa)}|_{a_*=a(t)} =& -\frac{\kappa}{12\pi^2}\left[\frac{4}{3} - \ln\left(\frac{e^{\gamma_E}\mu}{H}\right)\right] && (4.9.160)
\end{aligned}$$

we determined in the previous sections. These results agree with the ones found in [107], after setting $\mu = H$ and $c_{1,1} = 0$, which matches the (implicit) scheme choice used in this reference, and they are compatible with [71, 72], which both find a similar matching equation to (4.9.152)[9], as well as an NLO Kramers-Moyal equation of the form (4.9.155). The result that these references find for what we call $\gamma_{22}^{\mu,(\kappa)}$ is different than ours, which is due to the different regularization scheme that these references are using.

One can then use the approximation scheme we defined here to push the accuracy of the result for $\langle[\phi^{2n}](t,\vec{x})\rangle$ to higher orders in the expansion in powers of the full-theory coupling, which is now an expansion in powers of $\sqrt{\kappa}$. In [107] it was shown how to carry out the computation of the $\langle[\varphi_+^{2n}](t,\vec{x})\rangle$ up to this order in their scheme, however, some pieces that are relevant at NNLO were not discussed in this reference. Furthermore, it also did not address the role of the operator matching coefficients in relating the SdSET one-point functions $\langle[\varphi_+^{2n}](t,\vec{x})\rangle$ to the full-theory ones when going beyond the leading-order approximation in $\sqrt{\kappa}$.

We now have all the necessary tools in place to carry out the NNLO-computation in our scheme, including the matching procedure onto the $\langle[\phi^{2n}](t,\vec{x})\rangle$, and we already computed some of the relevant pieces. The first is the anomalous dimension $\gamma_{20}^{\mu,(\kappa)}$, which was not discussed in [107]. Further, we also computed the operator matching coefficients $C_{22}^{(\kappa)}$ and $C_{20}^{(\kappa)}$, which will both become relevant for the NNLO matching equation as well. We must leave the computation of the remaining pieces for future work.

[9]These two references find a term $\sim \langle[\varphi_+^{2n-2}](t,\vec{x})\rangle$ as the NLO correction to the matching equation, which, at first, seems incompatible with our result. However, looking at the leading-order result (4.9.150) for the one-point functions one sees that $\kappa\langle[\varphi_+^n](t,\vec{x})\rangle \sim \langle[\varphi_+^{n-4}](t,\vec{x})\rangle$, so the two terms can be consistently translated into each other.

Interpretation of the self-consistent solution procedure

The self-consistent solution approach to the equation of motion (4.9.141) is analogous to the one that is typically used to solve RGEs for the running couplings in usual flat-space quantum field theory [34,35]. This procedure is known to be able to capture the contributions of infinite towers of terms, these terms being logarithms of the renormalization scale in the case of the solution of the RGEs for running couplings. In our case, solving (4.9.141) self-consistently at leading power in κ, by recasting this equation in the form of the Fokker-Planck equation, we have obtained an IR-finite and de Sitter invariant result instead of an IR-divergent and non-de Sitter-invariant result for the EFT one-point functions, see (4.9.150). We can therefore think of having achieved the "resummation" of the IR logarithms

$$\ln\left(\frac{\Lambda}{a(t)\mu}\right) \tag{4.9.161}$$

which we kept finding in perturbative SdSET computations into a form which is IR-finite, and thus amenable to taking the limit $\Lambda \to 0$, which then also removes any time-dependence from the one-point functions. However, at this point we would like to point out that, in our opinion, this procedure should not be thought of as some sort of renormalization-group improved perturbation theory, which is the more common area of application of RG-techniques in the context of EFTs. In our case the observables computed in perturbation theory are simply not well-defined, and this would not be solved by any renormalization-group improvement of the perturbative result. Instead, what we did above, in the special case of one-point functions, is to find the non-perturbative vacuum state of the theory by solving the lowest-order truncation of the equation of motion (4.9.141). This is equivalent to solving the Fokker-Planck equation of Stochastic Inflation to obtain non-perturbative results for the SdSET correlators in question which are manifestly IR-finite and de Sitter-invariant.

4.10 Conclusion

In this chapter, building on the papers [105, 107], we have constructed a consistent and well-defined formulation of the SdSET, by deriving the action of the free EFT rigorously from the full-theory action, and then showing how both the local interaction terms and the non-Gaussian initial conditions can be implemented to define the interacting SdSET. Using this formulation, we have shown how the renormalization and matching procedure in the EFT work, by defining a consistent regularization and renormalization scheme both for the SdSET action and for composite operators φ_+^n, and by carrying out several matching computations. Finally, we discussed how the issue of infrared divergences, which plague the perturbative computation of correlation functions of massless, minimally coupled scalar fields, can be addressed and resolved using the SdSET, focussing on the simplest case of renormalized one-point functions. While doing so, we have also shown how the intuition of [105, 107] about the link between the effective time evolution of renormalized composite operators $[\varphi_+^n]$ and their renormalization-group evolution is realized in our scheme. The work that we have carried out in this chapter puts the SdSET on a firm quantum-field-theoretic foundation, and paves the way towards its application to more complex observables and theories.

Appendix

4.A Derivation of the effective action for the real, non-relativistic scalar field in Minkowski space

In this appendix we go through, and expand on, the derivation of the effective action for the real, non-relativistic scalar field in Minkowski space that was presented in [120] using a non-local field redefinition that expresses the real full-theory field ϕ in terms of the complex effective fields ψ and ψ^*. This derivation inspired the derivation of the free action of the SdSET presented in the main text, and the main idea and procedure are essentially the same, up to necessary generalizations to account for the fact that we are working in a time-dependent spacetime, so it is worthwhile and instructive to go through the Minkowski case in detail.

4.A.1 Heuristic analysis and motivation

The starting point of the discussion is the Lagrangian for a free, massive scalar field in Minkowski space:

$$\mathcal{L} = \frac{1}{2}\Big[\partial_\mu\phi\partial^\mu\phi - m^2\phi^2\Big]\,, \tag{4.A.1}$$

which leads to the following equation of motion:

$$\Big[\partial_t^2 - \partial_i^2 + m^2\Big]\phi(t,\vec{x}) = 0\,. \tag{4.A.2}$$

We are interested in deriving the Lagrangian which describes systematically the effective dynamics of the theory in the nonrelativistic limit, meaning that the three-momentum of the particles associated to ϕ satisfies

$$\frac{|\vec{k}|}{m} \ll 1\,, \tag{4.A.3}$$

and correlation functions (or scattering amplitudes) computed in this theory can be expanded systematically in powers of $|\vec{k}|/m$. In this case, m therefore plays the role of the hard scale of the EFT we are after.

In the nonrelativistic limit the standard ansatz is to express the real field ϕ through a complex field ψ, where ψ and ψ^* correspond to the positive and negative frequency solutions of the equation of motion for ϕ [120]:

$$\phi = \frac{1}{\sqrt{2m}}(e^{-imt}\psi + e^{imt}\psi^*) = \frac{1}{\sqrt{2m}}\mathrm{Re}[e^{-imt}\psi]\,. \tag{4.A.4}$$

In the above equation, the leading time dependence $e^{\pm imt}$ has been factored out already, and the residual time dependence is captured by the effective fields. Equation (4.A.4) alone, however, does not fully specify the field ψ, since it is a complex field, and as such contains two real degrees of freedom. The standard procedure is to plug the field decomposition (4.A.4) into (4.A.1) and drop terms that have a coefficient $e^{\pm 2imt}$. The physical argument to justify this is that, compared to the typical time-scales that we wish to describe using the effective theory, these terms are oscillating very quickly, and their effect on observables, on average, is therefore negligible. The Lagrangian obtained in this way is then of the form

$$\mathcal{L}_{\rm nr} = \frac{i}{2}(\dot{\psi}\psi^* - \psi\dot{\psi}^*) + \frac{1}{2m}\dot{\psi}\dot{\psi}^* - \frac{1}{2m}\partial_i\psi\partial_i\psi^* \,, \tag{4.A.5}$$

where the dots on the fields denote time derivatives, which differs from the standard leading-power non-relativistic Lagrangian by the term $\dot{\psi}\dot{\psi}^*/2m$. However, since this term is suppressed by m with respect to the single time-derivative term, it is usually argued that this should more appropriately be interpreted as an interaction term, which can thus be rewritten using the leading-power equation of motion for ψ and ψ^*. Both steps, the elimination of oscillating terms and of the term $\dot{\psi}\dot{\psi}^*$, fully constrain the field ψ, since what is left at leading power in the gradient expansion is a first-order equation of motion in time for ψ,

$$i\dot{\psi} = -\frac{\partial_i^2}{2m}\psi \,, \tag{4.A.6}$$

and the complex conjugation of the above for ψ^*, which is of course just the Schrödinger equation. Through the above series of physical arguments, we have therefore obtained two decoupled first-order equations of motion for ψ and ψ^*, which therefore describe one degree of freedom each, as it should be.

Now suppose that we want to more rigorously arrive at the above result for the dynamics of ψ and ψ^*, without the need to resort to discussing away quickly oscillating terms or squared time-derivative terms. A way to do so is to additionally assume the following relation between ψ and the conjugate momentum to ϕ:

$$\dot{\phi} \equiv \pi = -i\sqrt{\frac{m}{2}}(e^{-imt}\psi - e^{imt}\psi^*) = -i\sqrt{\frac{m}{2}}\mathrm{Im}[e^{-imt}\psi] \,, \tag{4.A.7}$$

which means that we are requesting that the time evolution of the field ϕ should be determined by the leading time-dependence in the exponentials alone, which is associated to the large mass m, and not by the residual time dependence contained in ψ, ψ^*, which is instead associated to gradient corrections that scale like $|\vec{k}|/m$, and are therefore small. This is only consistent with (4.A.4) if we additionally require

$$e^{-imt}\dot{\psi} + e^{imt}\dot{\psi}^* = 0 \,. \tag{4.A.8}$$

Further, we already know what $\dot{\pi}$ needs to be, using that $\pi = \dot{\phi}$ and equation of motion of ϕ (4.A.2):

$$\dot{\pi} = \ddot{\phi} = (\partial_i^2 - m^2)\phi \,. \tag{4.A.9}$$

This, in turn, is only consistent with (4.A.7) and (4.A.4) if

$$-i\sqrt{2m}e^{-imt}\dot{\psi} = \partial_i^2\phi \quad \Rightarrow \quad \dot{\psi} = \frac{i}{2m}(\partial_i^2\psi + e^{2imt}\partial_i\partial^i\psi^*) \tag{4.A.10}$$

and again the complex conjugation of the above for ψ^*. However we still find a quickly oscillating term, which we are forced to again discuss away to get to (4.A.6). Therefore the redefinition (4.A.4) together with (4.A.7) are enough to get rid of the $\dot{\psi}^2$, $\dot{\psi}^{*2}$ and $\dot{\psi}\dot{\psi}^*$ terms in the Lagrangian, but not yet to eliminate the $e^{\pm 2imt}\partial_i\psi\partial^i\psi$-terms. This final hurdle can be overcome by means of a non-local version extension of the field redefinition (4.A.4), as was pointed out in [120]. We repeat their derivation in detail, since the same procedure, with the appropriate generalizations, can be applied to the case of the SdSET. The derivation makes use of the canonical formalism, which is very well-suited for our purposes, since in it ϕ and π are truly independent fields which we can replace by the independent non-relativistic fields ψ and ψ^* and then go back to the Lagrangian formulation. As we saw above, this is what we need to do in order to obtain a rigorous one-to-one mapping of the two degrees of freedom contained in ϕ to the two degrees of freedom contained in ψ and ψ^*.

4.A.2 Ground-up construction using a non-local field redefinition

What we want to do is find a map between the canonical pairs $\{\phi, \pi\} \to \{\psi, i\psi^*\}$ by means of a canonical transformation. We start assuming the knowledge that the local field redefinitions (4.A.4), (4.A.7) are enough to reduce the relativistic second-order equation of motion to two coupled first order equations of motion for the fields ψ, ψ^*, which describe the positive and negative frequency modes of ϕ, respectively. What is still left to do is, therefore, to reorganize the gradient terms, which are the only terms still leading to a coupling between the two effective fields. This motivates us to make the following ansatz:

$$\begin{aligned}\phi =& \frac{1}{\sqrt{2m}}\left[e^{-imt}D_1(t)\psi + e^{imt}D_2(t)\psi^*\right], &(4.A.11)\\ \pi =& -i\sqrt{\frac{m}{2}}\left[e^{-imt}P_1(t)\psi - e^{imt}P_2(t)\psi^*\right], &(4.A.12)\end{aligned}$$

where we allow for an explicit time dependence in $D_{1,2}$, $P_{1,2}$. We know that they will be related to the suppressed gradient terms and, further, we assume that they will be analytic functions of the gradient terms. They will, therefore, allow for a gradient expansion, and we require them to be unity at leading power, such that the the equations (4.A.11), (4.A.12) agree with (4.A.4), (4.A.7) up to higher corrections:

$$D_{1,2} = 1 + \mathcal{O}\left(\frac{\partial_i^2}{m^2}\right), \quad P_{1,2} = 1 + \mathcal{O}\left(\frac{\partial_i^2}{m^2}\right). \tag{4.A.13}$$

Since ϕ, π are real by assumption, this immediately implies that $D_1^* = D_2$, $P_1^* = P_2$, so we can just replace $D_1 \to D$, $P_1 \to P$ and simplify (4.A.11), (4.A.12) to

$$\begin{aligned}\phi =& \frac{1}{\sqrt{2m}}\left[e^{-imt}D(t)\psi + e^{imt}D^*(t)\psi^*\right], &(4.A.14)\\ \pi =& -i\sqrt{\frac{m}{2}}\left[e^{-imt}P(t)\psi - e^{imt}P^*(t)\psi^*\right]. &(4.A.15)\end{aligned}$$

Further, since we assume ψ and $i\psi^*$ to be a canonical pair, they have to satisfy canonical equal-time commutation relations:

$$[\psi(t,\vec{x}), i\psi^*(t,\vec{y})] = i\delta^{(3)}(\vec{x}-\vec{y}), \quad [\psi(t,\vec{x}),\psi(t,\vec{y})] = [i\psi^*(t,\vec{x}), i\psi^*(t,\vec{y})] = 0, \tag{4.A.16}$$

just like ϕ and π do, which then gives us the following constraint on the operators P and D:

$$D^*P + P^*D = 2. \tag{4.A.17}$$

Taking the time derivative of this equation we obtain the relation

$$P\dot{D}^* + \dot{P}D^* + \dot{P}^*D + P^*\dot{D} = 0, \tag{4.A.18}$$

which will be useful in the following.

The equations (4.A.14) and (4.A.15) define a canonical transformation between the canonical pairs $\{\phi, \pi\}$ and $\{\psi, i\psi^*\}$, and we now need to determine what the appropriate form of the operators D and P is. To do so, we follow the presentation of the procedure in [121]. The starting point to do so is to consider the Hamiltonian density $\mathcal{H}$ for the pair $\{\phi, \pi\}$, which is defined from the total Hamiltonian as

$$H = \int \mathrm{d}^3x\, \tilde{\mathcal{H}}, \tag{4.A.19}$$

and reads

$$\tilde{\mathcal{H}}[\phi,\pi] = \frac{1}{2}\pi^2 + \frac{1}{2}(\partial_i\phi)^2 + \frac{m^2}{2}\phi^2. \tag{4.A.20}$$

Since we will only talk about Hamiltonian densities from now on, we will refer to them as just "Hamiltonians". We now wish to derive the form of the Hamiltonian for $\{\psi, i\psi^*\}$ from (4.A.20), which we denote as $\mathcal{H}$. The two are related by the following canonical transformation [121]:

$$\mathcal{H}[\psi, i\psi^*] = \tilde{\mathcal{H}}[\psi, i\psi^*] + \frac{\partial F}{\partial t}\,, \tag{4.A.21}$$

where $\tilde{\mathcal{H}}[\psi, i\psi^*]$ denotes (4.A.20) with the expressions (4.A.14) and (4.A.15) plugged in, and $F[\psi, \phi, t]$ is the generating functional of the canonical transformation (4.A.14), (4.A.15), which we need to work out explicitly. It determining equations read [121]

$$\pi[\phi, \psi] = \frac{\partial F}{\partial \phi}\,, \quad i\psi^*[\phi, \psi] = -\frac{\partial F}{\partial \psi}\,, \tag{4.A.22}$$

where π and $i\psi^*$ need to be expressed only in terms of ϕ and ψ by inverting (4.A.14), (4.A.15) accordingly, which we indicate by their arguments in the above equation. We are being slightly sloppy with the notation in the above equation, since F is a functional, and we should be taking functional derivatives with respect to ϕ and ψ. However, for the present manipulations this distinction is immaterial, and we can write F as a product of fields and operators and treat the fields as if they were one-dimensional variables to avoid cluttering our expressions.

Making the ansatz

$$F[\psi, \phi, t] = \phi A(t)\phi + \phi B(t)\psi + \psi C(t)\psi \tag{4.A.23}$$

to solve these two differential equations, where $A(t)$, $B(t)$ and $C(t)$ should be thought of as operators acting on the fields to their right, we find:

$$F[\psi, \phi, t] = i\left[\frac{m}{2}\phi\frac{P^*}{D^*}\phi - \sqrt{2m}e^{-imt}\phi\frac{1}{D^*}\psi + \frac{1}{2}e^{-2imt}\psi\frac{D}{D^*}\psi\right]. \tag{4.A.24}$$

We now take the partial derivative of F with respect to t, where the derivative only takes into account the explicitly appearing time dependence in the exponentials and in the operators D and P, and plug the expression of ϕ in terms of ψ, ψ^* back in:

$$\frac{\partial F}{\partial t} = -m\psi^*\psi + \frac{i}{4}\left[e^{-2imt}\psi(P\dot{D} - \dot{P}D)\psi - \psi^*(P^*\dot{D} - \dot{P}^*D + \dot{P}D^* - P\dot{D}^*)\psi + e^{2imt}\psi^*(\dot{P}^*D^* - P^*\dot{D}^*)\psi^*\right]. \tag{4.A.25}$$

A first consistency check on this result is provided by the requirement that the result for the canonically transformed Hamiltonian should be real. $\tilde{\mathcal{H}}$ clearly is, and we notice that our result for $\partial F/\partial t$ is as well, so their sum will be real. Plugging (4.A.25) into (4.A.21) gives us the following expression:

$$\mathcal{H} = \frac{m}{4}\Bigg\{e^{-2imt}\psi D^2\left[-\frac{i}{m}\frac{\partial}{\partial t}\left(\frac{P}{D}\right) - \left(\frac{P}{D}\right)^2 + 1 - \frac{\partial_i^2}{m^2}\right]\psi \tag{4.A.26}$$

$$+ 2\psi^*\left[P^*P + D^*D\left(1 - \frac{\partial_i^2}{m^2}\right) - 2 - \frac{i}{2m}(P^*\dot{D} - \dot{P}^*D + \dot{P}D^* - P\dot{D}^*)\right]\psi \tag{4.A.27}$$

$$+ e^{2imt}\psi^*{D^*}^2\left[\frac{i}{m}\frac{\partial}{\partial t}\left(\frac{P^*}{D^*}\right) - \left(\frac{P^*}{D^*}\right)^2 + 1 - \frac{\partial_i^2}{m^2}\right]\psi^*\Bigg\}. \tag{4.A.28}$$

By assumption it satisfies the following canonical equations:

$$\dot{\psi} = -i\frac{\partial \mathcal{H}}{\partial \psi^*}\,, \quad i\dot{\psi}^* = -\frac{\partial \mathcal{H}}{\partial \psi}\,, \tag{4.A.29}$$

which are just

$$i\dot{\psi} = \frac{\partial \mathcal{H}}{\partial \psi^*} \tag{4.A.30}$$

and its complex conjugate.

The purpose of all these manipulations is to obtain a Hamiltonian which yields decoupled equations of motion for ψ and ψ^*, meaning

$$i\dot{\psi} = E\psi\,, \tag{4.A.31}$$

with E the equation-of-motion operator, and analogously for ψ^*. Combining this requirement with (4.A.30) fixes the desired form of $\mathcal{H}$ to be

$$\mathcal{H} = \psi^* E\psi\,. \tag{4.A.32}$$

Comparing this to (4.A.28) we see we need to choose D and P such that only mixed terms in ψ and ψ^* are left over, while the terms involving two ψ and ψ^* need to vanish. This means that, defining

$$f = \frac{P}{D}\,, \tag{4.A.33}$$

the combination f needs to satisfy the following differential equation:

$$-\frac{i}{m}\frac{\partial f}{\partial t} - f^2 + 1 - \frac{\partial_i^2}{m^2} = 0 \tag{4.A.34}$$

and its complex conjugate. Solving this equation will then tell us what the desired result for D and P is that achieves this form, and therefore the appropriate form of the canonical transformation we are seeking.

Equation (4.A.34) has the general solution

$$f(t) = -i\sqrt{1-\frac{\partial_i^2}{m^2}}\tan\left((mt+C)\sqrt{1-\frac{\partial_i^2}{m^2}}\right), \quad C = \text{const.}\,. \tag{4.A.35}$$

We know that at leading power in the gradient expansion f needs to be equal to one, since both D and P need to be unity. Expanding to leading power in the gradient terms gives:

$$f(t) = -i\tan(mt+C) + \mathcal{O}\left(\frac{\partial_i^2}{m^2}\right), \tag{4.A.36}$$

which is explicitly time dependent. To be constant for all times this expression would require a time-dependent C, which is however not allowed by (4.A.34). This means that $f = P/D$ needs to be time-independent in order to satisfy the imposed constraint. The differential equation (4.A.34) thus reduces to an algebraic equation, which has the solution

$$\frac{P}{D} = \frac{P^*}{D^*} = \sqrt{1-\frac{\partial_i^2}{m^2}}\,. \tag{4.A.37}$$

This square root should be understood as being defined via its series expansion which, indeed, as a 1 as its leading term, as it should be.

However, the fact that the ratio of P and D needs to be time-independent does not mean that D and P themselves need to be: the above result still leaves us the freedom to redefine

$$D(t) = \check{D}g\left(\frac{\partial_i^2}{m^2}, t\right), \quad P(t) = \check{P}g\left(\frac{\partial_i^2}{m^2}, t\right), \tag{4.A.38}$$

with a complex time-dependent function g and time-independent and real $\check{D}, \check{P}$ satisfying

$$\frac{\check{P}}{\check{D}} = \sqrt{1-\frac{\partial_i^2}{m^2}}\,, \tag{4.A.39}$$

provided that the function g is 1 at leading power in its gradient expansion:

$$g\left(\frac{\partial_i^2}{m^2}, t\right) = 1 + \mathcal{O}\left(\frac{\partial_i^2}{m^2}\right). \tag{4.A.40}$$

(4.A.17) then becomes:

$$g^* g \check{P} \check{D} = 1\,, \tag{4.A.41}$$

which, since it factorizes in a time-dependent and time-independent part, separately implies:

$$g^* g = 1\,, \quad \check{P}\check{D} = 1\,, \tag{4.A.42}$$

From this equation, and the above results, we infer that

$$\check{P} = \left[1 - \frac{\partial_i^2}{m^2}\right]^{\frac{1}{4}}, \quad \check{D} = \check{P}^{-1} \tag{4.A.43}$$

and that the function g must be a pure time-dependent phase:

$$g\left(\frac{\partial_i^2}{m^2}, t\right) = \exp\left[-i\gamma\left(\frac{\partial_i^2}{m^2}, t\right)\right], \tag{4.A.44}$$

$$\gamma\left(\frac{\partial_i^2}{m^2}, t\right) = 0 + \mathcal{O}\left(\frac{\partial_i^2}{m^2}\right). \tag{4.A.45}$$

The condition that γ has no $\mathcal{O}(1)$ contribution is due to the fact that we are still assuming the field redefinition to agree with (4.A.4), (4.A.7) at leading power in the gradients. If we want to allow for a small residual mass term for the effective fields by shifting $m \to m + \delta m$ in the exponents of (4.A.11), (4.A.12), which would still be incompatible with (4.A.36), we have to drop the requirement (4.A.13) and trade (4.A.45) for

$$\tilde{\gamma}\left(\frac{\partial_i^2}{m^2}, t\right) = \delta m t + \mathcal{O}\left(\frac{\partial_i^2}{m^2}\right). \tag{4.A.46}$$

We will not pursue this further here.

Plugging (4.A.38) back into the Hamiltonian gives us:

$$\mathcal{H} = m\psi^* \left[\sqrt{1 - \frac{\partial_i^2}{m^2}} - 1 - \frac{\dot{\gamma}}{m}\right]\psi\,. \tag{4.A.47}$$

Since we are considering a free scalar field propagating in flat space, energy conservation is guaranteed, which means that the Hamiltonian cannot have any explicit time dependence:

$$\frac{\partial \mathcal{H}}{\partial t} = 0\,. \tag{4.A.48}$$

This in turn means that γ can be at most linear in time, since its first derivative needs to be constant:

$$\gamma\left(\frac{\partial_i^2}{m^2}, t\right) \equiv \gamma_0\left(\frac{\partial_i^2}{m^2}\right) + mt\gamma_1\left(\frac{\partial_i^2}{m^2}\right), \tag{4.A.49}$$

which gives us the final form of our Hamiltonian:

$$\mathcal{H} = m\psi^* \left[\sqrt{1 - \frac{\partial_i^2}{m^2}} - 1 - \gamma_1\left(\frac{\partial_i \partial^i}{m^2}\right)\right]\psi\,. \tag{4.A.50}$$

We obtain the Lagrangian density from (4.A.56) via Legendre transformation:

$$\mathcal{L} = i\psi^*\dot{\psi} - \mathcal{H} = \frac{i}{2}\left[\dot{\psi}\psi^* - \psi\dot{\psi}^* + \partial_t(\psi\psi^*)\right] - m\psi^*\left[\sqrt{1 - \frac{\partial_i^2}{m^2}} - 1 - \gamma_1\left(\frac{\partial_i^2}{m^2}\right)\right]\psi \tag{4.A.51}$$

which is real up to a total time derivative term and, since the fundamental object is the action and we assume that we can drop boundary terms we obtain:

$$S = \int \mathrm{d}^4x \left\{ \frac{i}{2}\Big[\dot{\psi}\psi^* - \psi\dot{\psi}^*\Big] - m\psi^* \left[\sqrt{1 - \frac{\partial_i^2}{m^2}} - 1 - \gamma_1\bigg(\frac{\partial_i^2}{m^2}\bigg)\right]\psi \right\}. \tag{4.A.52}$$

The explicit form of the found field redefinition is then:

$$\phi(t, \vec{x}) = \frac{1}{\sqrt{2\sqrt{m^2 - \partial_i^2}}}\Big[e^{-i[\gamma_0 + m(1+\gamma_1)t]}\psi(t, \vec{x}) + e^{i[\gamma_0 + m(1+\gamma_1)t]}\psi^*(t, \vec{x})\Big], \tag{4.A.53}$$

$$\pi(t, \vec{x}) = -i\sqrt{\frac{\sqrt{m^2 - \partial_i^2}}{2}}\Big[e^{-i[\gamma_0 + m(1+\gamma_1)t]}\psi(t, \vec{x}) - e^{i[\gamma_0 + m(1+\gamma_1)t]}\psi^*(t, \vec{x})\Big]. \tag{4.A.54}$$

We thus succeeded in finding an explicit non-local field redefinition of ϕ, and its canonically conjugated momentum, which decouples the non-relativistic fields from each other in a rigorous manner. However, we are still left with the undetermined functions γ_0 and γ_1. The former function is irrelevant for the dynamics of the effective fields, since it does not appear in the action, and only contributes to the exponentials of the field redefinitions (4.A.53) and (4.A.54) as a time-independent phase, which however depends on the gradients. The latter function does explicitly appear in the action, as well as in the exponentials in (4.A.53) and (4.A.54). It determines how much of the time evolution of the original field ϕ is left in the effective modes ψ, ψ^*, and should therefore be chosen according to the physics that we want the effective modes to describe. Both a non-vanishing γ_0 and γ_1 introduce a spatial non-locality, since they appear in the exponent of the redefinition, and therefore induce infinitely many terms. The non-locality induced by the presence of γ_1 is further associated with the time evolution of ϕ, π.

Two choices are particularly of note: the first is to just choose

$$\gamma = 0, \tag{4.A.55}$$

from which we obtain the Hamiltonian

$$\mathcal{H} = m\psi^*\left[\sqrt{1 - \frac{\partial_i^2}{m^2}} - 1\right]\psi. \tag{4.A.56}$$

This is the commonly used form when considering the non-relativistic scalar field, and it is the one found in [120]. It gives us the action

$$S = \int \mathrm{d}^4x \left\{ \frac{i}{2}(\dot{\psi}\psi^* - \psi\dot{\psi}^*) - m\psi^*\left[\sqrt{1 - \frac{\partial_i^2}{m^2}} - 1\right]\psi \right\}, \tag{4.A.57}$$

and the equation of motion

$$i\dot{\psi} = m\left[\sqrt{1 - \frac{\partial_i^2}{m^2}} - 1\right]\psi = m\sum_{n=1}^{\infty}\frac{1}{n!}\left[\prod_{k=0}^{n-1}\frac{1-2k}{2}\right]\bigg(-\frac{\partial_i^2}{m^2}\bigg)^n\psi \tag{4.A.58}$$

and its complex conjugate. The reason why this choice is the standard one is precisely because it does not introduce additional modifications to the time evolution of the effective fields: the field redefinition is built to decouple the low-energy modes and not affect the dynamics any further.

The other most notable choice is

$$\gamma\bigg(\frac{\partial_i^2}{m^2}, t\bigg) = mt\left[\sqrt{1 - \frac{\partial_i^2}{m^2}} - 1\right], \tag{4.A.59}$$

which gives us a vanishing Hamiltonian,

$$\mathcal{H} = 0, \tag{4.A.60}$$

and the simple action

$$S = \frac{i}{2}\int \mathrm{d}^4x\,(\dot\psi\psi^* - \psi\dot\psi^*) \tag{4.A.61}$$

with trivial equations of motion:

$$\dot\psi = 0\,. \tag{4.A.62}$$

It is suggestive to explicitly write out this redefinition and to Fourier transform the fields in the position argument:

$$\phi(t,\vec x) = \int \frac{\mathrm{d}^3k}{(2\pi)^3}\frac{1}{\sqrt{2\omega_{\vec k}}}\Big[e^{-i(\omega_{\vec k}t-\vec k\cdot\vec x)}\psi(\vec k) + e^{i(\omega_{\vec k}t-\vec k\cdot\vec x)}\psi^*(\vec k)\Big]\,, \tag{4.A.63}$$

$$\pi(t,\vec x) = -\,i\int \frac{\mathrm{d}^3k}{(2\pi)^3}\sqrt{\frac{\omega_{\vec k}}{2}}\Big[e^{-i(\omega_{\vec k}t-\vec k\cdot\vec x)}\psi(\vec k) - e^{i(\omega_{\vec k}t-\vec k\cdot\vec x)}\psi^*(\vec k)\Big]\,, \tag{4.A.64}$$

with

$$\omega_{\vec k} \equiv \sqrt{m^2+\vec k^2}\,. \tag{4.A.65}$$

By making this choice we have therefore pieced the full relativistic time dependence back together by completely pulling it out of the effective fields. Any choice in between the two discussed ones is equally valid, although they may not be equally desirable.

4.B Field redefinition to eliminate φ_+^n-interaction terms

This appendix is dedicated to the derivation of the form of the field redefinition designed to eliminate interaction terms of the form

$$S_{\mathrm{int},\varphi_+^{2n+2}} = -\int \mathrm{d}^{d-1}x\mathrm{d}t\; a(t)^{(4-d)n+3}C_n\varphi_+^{2n+2} \tag{4.B.1}$$

in order to be able to define a power-counting scheme for the effective fields which is reflected at the level of the correlation functions. We can do so by redefining the field φ_- as

$$\varphi_- \to \varphi_- + \sum_{n=0}^{\infty} a(t)^{(4-d)n+3} r_n\varphi_+^{2n+1} \tag{4.B.2}$$

which will induce new φ_+^n-terms via the kinetic term (using that $\nu = 3/2$ in every dimension in our scheme)

$$\begin{aligned}-3\int \mathrm{d}^{d-1}x\mathrm{d}t\;\dot\varphi_+\varphi_- \to &-3\int \mathrm{d}^{d-1}x\mathrm{d}t\;\dot\varphi_+\Big[\varphi_- + \sum_{n=0}^{\infty}a(t)^{(4-d)n+3}r_n\varphi_+^{2n+1}\Big]\\ &= -3\int \mathrm{d}^{d-1}x\mathrm{d}t\;\Big[\dot\varphi_+\varphi_- + \sum_{n=0}^{\infty}a(t)^{(4-d)n+3}\frac{r_n}{2n+2}\frac{\mathrm{d}}{\mathrm{d}t}\varphi_+^{2n+2}\Big]\,,\end{aligned} \tag{4.B.3}$$

which we can use to write the offending interaction terms as total time derivatives, which we can drop, by choosing the coefficients r_n appropriately:

$$\begin{aligned}&-\int \mathrm{d}^{d-1}x\mathrm{d}t\; a(t)^{(4-d)n+3}\Big[\frac{3r_n}{2n+2}\frac{\mathrm{d}}{\mathrm{d}t}\varphi_+^{2n+2} + C_n\varphi_+^{2n+2}\Big]\\ &= -\int \mathrm{d}^{d-1}x\mathrm{d}t\;\frac{\mathrm{d}}{\mathrm{d}t}\Big[\frac{C_n}{(4-d)n+3}a(t)^{(4-d)n+3}\varphi_+^{2n+2}\Big]\end{aligned} \tag{4.B.4}$$

if we fix

$$r_n = \frac{(2n+2)C_n}{3[(4-d)n+3]}\,. \tag{4.B.5}$$

The redefinition of φ_- at a particular order in κ will, however, induce new φ_+^{2n+2} terms at higher orders in κ, which will enter the appropriate coefficients C_n, which will therefore become more and more complicated for higher n. However, these terms will also be more and more suppressed in powers of κ, so only a subset of them needs to be taken into account if one is interested in working at a certain order in κ. For our purposes in this thesis, it is enough to keep only the lowest-order term in the counting in powers of κ multiplying each power of φ_+ in the redefinition.

4.B.1 Elimination of φ_+^2-terms

We start from the interaction term

$$S_{\text{int},\varphi_+^2} = -\int \mathrm{d}^{d-1}x\mathrm{d}t\ a(t)^3 \frac{c^0_{2,0}}{2}\varphi_+^2\,, \tag{4.B.6}$$

and using the RPI-relation between effective couplings (4.3.7) we can express $c^0_{2,0}$ in terms of $c^0_{1,1}$:

$$c^0_{2,0} = H^3 c^0_{1,1}\,. \tag{4.B.7}$$

Comparing to the form of (4.B.1) we identify

$$C_0 = \frac{c^0_{1,1}}{2H^3} \tag{4.B.8}$$

and using (4.B.5)we find

$$r_0 = \frac{1}{9}\,, \tag{4.B.9}$$

which corresponds to the redefiniton

$$\varphi_- \to \varphi_- + \frac{c^0_{1,1}(a(t)H)^3}{9}\varphi_+ + \mathcal{O}(\kappa^2)\,. \tag{4.B.10}$$

This shift then induces new terms. For instance, we get a shift in the coefficient of the bilinear term $\sim \varphi_+\varphi_-$ coming from the term $\sim \varphi_-^2$,

$$a(t)^{-3}\frac{c^0_{0,2}}{2}\varphi_-^2 \to \frac{H^3 c^0_{0,2}c^0_{1,1}}{9}\varphi_+\varphi_- \sim \kappa^2\,. \tag{4.B.11}$$

However, since the induced term will always be more strongly suppressed in powers of the full-theory coupling, and in this chapter we only work with EFT-couplings matched at leading power in κ to the full theory, these terms are irrelevant in the present setting, and we disregard them. However, as soon as we will start computing sub-leading corrections to the EFT-couplings, these newly induced terms will be important in order to carry out the matching computations correctly.

4.B.2 Elimination of φ_+^4-terms

We move on to the next interaction terms we need to remove, which are

$$S_{\text{int},\varphi_+^4} = -\int \mathrm{d}^{d-1}x\mathrm{d}t\ a(t)^{7-d} \frac{c^0_{4,0}}{4!}\varphi_+^4\,. \tag{4.B.12}$$

Using (4.B.1), as well as the RPI-relation between effective couplings (4.3.7) to relate $c^0_{4,0}$ to $c^0_{3,1}$, we identify

$$C_1 = \frac{H^3 c^0_{3,1}}{4!}\,, \tag{4.B.13}$$

which, using (4.B.1) leads to

$$r_1 = \frac{H^3 c^0_{3,1}}{18(7-d)}\,, \tag{4.B.14}$$

which corresponds to the redefinition

$$\varphi_- \to \varphi_- + (a(t)H)^3 \left[\frac{c^0_{1,1}}{9}\varphi_+ + \frac{c^0_{3,1}a(t)^{4-d}}{18(7-d)}\varphi_+^3\right]. \tag{4.B.15}$$

Contrarily to the previous subsection, this redefinition induces a new φ_+^6 interaction term that is as important as $c^0_{6,0}$:

$$a(t)^{4-d}\frac{c^0_{3,1}}{6}\varphi_+^3\varphi_- \to a(t)^{11-2d}\frac{H^3(c^0_{3,1})^2}{108(7-d)}\varphi_+^6 \sim \kappa^2\,, \tag{4.B.16}$$

and we therefore need to keep track of it.

4.B.3 Elimination of φ_+^6-terms

We now need to eliminate the interaction terms

$$S_{\text{int},\varphi_+^6} = -\int \mathrm{d}^{d-1}x\mathrm{d}t\; a(t)^{11-2d}\left[\frac{c^0_{6,0}}{6!} + \frac{H^3(c^0_{3,1})^2}{108(7-d)}\right]\varphi_+^6\,, \tag{4.B.17}$$

so we identify

$$C_2 = H^3\left[\frac{c^0_{5,1}}{6!} + \frac{(c^0_{3,1})^2}{108(7-d)}\right], \tag{4.B.18}$$

where we used (4.3.7) again to express $c^0_{6,0}$ in terms of $c^0_{5,1}$. We therefore need to pick

$$r_2 = \frac{2H^3}{11-2d}\left[\frac{c^0_{5,1}}{6!} + \frac{(c^0_{3,1})^2}{108(7-d)}\right], \tag{4.B.19}$$

which corresponds to the final field redefinition

$$\varphi_- \to \varphi_- + (a(t)H)^3\left[\frac{c^0_{1,1}}{9}\varphi_+ + \frac{c^0_{3,1}a(t)^{4-d}}{18(7-d)}\varphi_+^3 + \frac{2a(t)^{2(4-d)}}{11-2d}\left[\frac{c^0_{5,1}}{6!} + \frac{(c^0_{3,1})^2}{108(7-d)}\right]\varphi_+^5\right], \tag{4.B.20}$$

which is presented in the main text.

4.C Loop integrals for the one-loop power spectrum

In this appendix we collect the explicit expressions for the evaluation of the loop integrals resulting from the insertion of the non-Gaussian initial conditions $\Xi^\sigma_{3,1}$ into the SdSET power spectrum discussed in section 4.5.

To evaluate the integral

$$\int \frac{\mathrm{d}^{d-1}l}{(2\pi)^{d-1}}\frac{1}{l_\Lambda^3}\ln\left(\frac{2e^{\gamma_E}(k_\Lambda + l_\Lambda)}{a_* H}\right) \tag{4.C.1}$$

we first write

$$\ln\left(\frac{2e^{\gamma_E}(k_\Lambda + l_\Lambda)}{a_* H}\right) = \frac{\mathrm{d}}{\mathrm{d}u}\bigg|_{u=0}\left(\frac{2e^{\gamma_E}(k_\Lambda + l_\Lambda)}{a_* H}\right)^u, \tag{4.C.2}$$

then pull the derivative out of the integral, and then use the Mellin-Barnes representation

$$\frac{1}{(k_\Lambda + l_\Lambda)^{-u}} = \frac{1}{\Gamma(-u)}\frac{1}{2\pi i}\int_{-i\infty}^{i\infty}\mathrm{d}z\;\Gamma(-u+z)\Gamma(-z)\frac{l_\Lambda^z}{k_\Lambda^{-u+z}} \tag{4.C.3}$$

to simplify the $\vec{l}$-integration, which yields:

$$\int \frac{\mathrm{d}^{d-1}l}{(2\pi)^{d-1}}\frac{1}{[l^2+\Lambda^2]^{\frac{3-z}{2}}} = \frac{\Lambda^{z-2\varepsilon}\Gamma(-\frac{z}{2}+\varepsilon)}{(4\pi)^{\frac{3}{2}-\varepsilon}\Gamma(\frac{3-z}{2})}\,. \tag{4.C.4}$$

We now substitute the factor l_Λ^z with the above result in (4.C.3), and close the contour in the right complex half-plane to evaluate the remaining z-integral. We then use the residue theorem to evaluate the resulting integral, and we only need to pick up the residues at poles that will survive the $\Lambda \to 0$ limit. Finally, we take the derivative of the result with respect to u, then set $u = 0$ and expand the resulting expression in ε. At this point, we can also let $k_\Lambda \to k$, since the result features no inverse powers of Λ. Doing so, we find the result

$$\begin{aligned}
&\left(\frac{e^{\gamma_E}\Lambda^2}{4\pi}\right)^{\varepsilon} \int \frac{\mathrm{d}^{d-1}l}{(2\pi)^{d-1}} \frac{1}{l_\Lambda^3} \ln\left(\frac{2e^{\gamma_E}(k_\Lambda + l_\Lambda)}{a_* H}\right) \\
=&\frac{1}{4\pi^2}\left\{\frac{1}{2\varepsilon^2} + \frac{1}{\varepsilon}\left[1 + \ln\left(\frac{e^{\gamma_E}\Lambda}{a_* H}\right)\right] + \ln^2\left(\frac{2k}{\Lambda}\right) - 2\ln\left(\frac{2k}{\Lambda}\right) + 2 + \frac{5\pi^2}{24}\right\}. \qquad (4.C.5)
\end{aligned}$$

For the non-trivial rational part of the integrand we can use the following Mellin-Barnes representations:

$$\frac{1}{(k_\Lambda + l_\Lambda)^2} = \frac{1}{\Gamma(2)} \frac{1}{2\pi i} \int_{-i\infty}^{i\infty} \mathrm{d}z\, \Gamma(2+z)\Gamma(-z) \frac{l_\Lambda^z}{k_\Lambda^{2+z}}\,, \qquad (4.C.6)$$

$$\frac{1}{k_\Lambda^3 + l_\Lambda^3} = \frac{1}{\Gamma(1)} \frac{1}{2\pi i} \int_{-i\infty}^{i\infty} \mathrm{d}z\, \Gamma(1+z)\Gamma(-z) \frac{l_\Lambda^{3z}}{k_\Lambda^{3+3z}}\,. \qquad (4.C.7)$$

After evaluating the $\vec{l}$-integral we then only need to pick up the poles of the remaining Mellin-Barnes integrals which give non-vanishing results as $\Lambda \to 0$, which turn out to be just isolated poles, and we never have to sum up any series of residues. The relevant integrals then read

$$\left(\frac{e^{\gamma_E}\Lambda^2}{4\pi}\right)^{\varepsilon} \int \frac{\mathrm{d}^{d-1}l}{(2\pi)^{d-1}} \frac{1}{l_\Lambda^3 (l_\Lambda + k_\Lambda)^2} = \frac{1}{2\pi^2 k^2}\left[\ln\left(\frac{2k}{\Lambda}\right) - 2\right], \qquad (4.C.8)$$

$$\left(\frac{e^{\gamma_E}\Lambda^2}{4\pi}\right)^{\varepsilon} \int \frac{\mathrm{d}^{d-1}l}{(2\pi)^{d-1}} \frac{1}{l_\Lambda^3 (l_\Lambda^3 + k_\Lambda^3)} = \frac{1}{2\pi^2 k^3}\left[\ln\left(\frac{2k}{\Lambda}\right) - 1\right], \qquad (4.C.9)$$

$$\left(\frac{e^{\gamma_E}\Lambda^2}{4\pi}\right)^{\varepsilon} \int \frac{\mathrm{d}^{d-1}l}{(2\pi)^{d-1}} \frac{1}{l_\Lambda^2 (l_\Lambda^3 + k_\Lambda^3)} = \frac{1}{3\sqrt{3}\pi k^2}\,, \qquad (4.C.10)$$

$$\left(\frac{e^{\gamma_E}\Lambda^2}{4\pi}\right)^{\varepsilon} \int \frac{\mathrm{d}^{d-1}l}{(2\pi)^{d-1}} \frac{1}{l_\Lambda (l_\Lambda^3 + k_\Lambda^3)} = \frac{1}{3\sqrt{3}\pi k}\,. \qquad (4.C.11)$$

To carry out the analytic continuation of the relevant Mellin-Barnes integrands in the limit $\varepsilon \to 0$ we used the `Mathematica` package `MB` [113], and the relevant residues were identified by hand and computed using the built-in `Mathematica` function.

4.D Loop integrals for the one-loop bispectrum of the composite operator φ_+^2 with $\vec{q} = 0$

In this appendix we collect the explicit expressions for the evaluation of non-trivial the loop integrals resulting from the insertion of the non-Gaussian initial conditions $\Xi_{3,1}^{\sigma}$ into the SdSET one-loop bispectrum of the composite operator φ_+^2 discussed in section 4.7.

To compute the integrals involving the logarithm of $l_\Lambda + k_\Lambda$, we can essentially follow the same procedure we applied in appendix 4.C: for the integral involving the logarithm we first write

$$\ln\left(\frac{2e^{\gamma_E}(l_\Lambda + k_\Lambda)}{a_* H}\right) = \frac{\mathrm{d}}{\mathrm{d}u}\bigg|_{u=0} \left(\frac{2e^{\gamma_E}(l_\Lambda + k_\Lambda)}{a_* H}\right)^u, \qquad (4.D.1)$$

and pull the u-derivative out of the integrals. We can then use the Mellin-Barnes representation [112]

$$\frac{1}{(l_\Lambda + k_\Lambda)^{-u}} = \frac{1}{\Gamma(-u)} \frac{1}{2\pi i} \int_{-i\infty}^{i\infty} \mathrm{d}z\, \Gamma(-u+z)\Gamma(-z) \frac{l_\Lambda^z}{k_\Lambda^{-u+z}} \qquad (4.D.2)$$

to simplify the $\vec{l}$-integration. After performing this integration, the z-integration can be carried out using the residue theorem, and we only need to keep the residues that give non-vanishing terms in the limit $\Lambda \to 0$. Finally, we take the u-derivative of the resulting expression, and then set $u = 0$. Similarly, we can write

$$\frac{1}{l_\Lambda + k_\Lambda} = \frac{1}{\Gamma(1)} \frac{1}{2\pi i} \int_{-i\infty}^{i\infty} \mathrm{d}z\ \Gamma(1+z)\Gamma(-z) \frac{l_\Lambda^z}{k_\Lambda^{1+z}} \tag{4.D.3}$$

to simplify the $\vec{l}$-integration for the integral with $(l_\Lambda + k_\Lambda)$ in the denominator.

Doing so, we find the following results:

$$\begin{aligned}
\left(\frac{e^{\gamma_E}\Lambda^2}{4\pi}\right)^\varepsilon \int \frac{\mathrm{d}^{d-1}l}{(2\pi)^{d-1}} \frac{1}{l_\Lambda^6} \ln\left(\frac{2e^{\gamma_E}(l_\Lambda + k_\Lambda)}{a_* H}\right) =& \frac{1}{6\pi^2}\left\{\frac{1}{k^3}\left[\ln\left(\frac{2k}{\Lambda}\right) - \frac{2}{3}\right] - \frac{3\pi}{8k^2\Lambda} + \frac{1}{k\Lambda^2}\right. \\
&\left. + \frac{3\pi}{16\Lambda^3}\ln\left(\frac{e^{\gamma_E}\Lambda}{a_* H}\right)\right\}, \qquad (4.D.4) \\
\left(\frac{e^{\gamma_E}\Lambda^2}{4\pi}\right)^\varepsilon \int \frac{\mathrm{d}^{d-1}l}{(2\pi)^{d-1}} \frac{1}{l_\Lambda^3} \ln\left(\frac{2e^{\gamma_E}(l_\Lambda + k_\Lambda)}{a_* H}\right) =& \frac{1}{8\pi^2}\left\{\frac{1}{\varepsilon^2} + \frac{2}{\varepsilon}\left[1 + \ln\left(\frac{e^{\gamma_E}\Lambda}{a_* H}\right)\right] + 2\ln^2\left(\frac{2k}{\Lambda}\right)\right. \\
&\left. - 4\ln\left(\frac{2k}{\Lambda}\right) + 4 + \frac{5\pi^2}{12}\right\}, \qquad (4.D.5) \\
\left(\frac{e^{\gamma_E}\Lambda^2}{4\pi}\right)^\varepsilon \int \frac{\mathrm{d}^{d-1}l}{(2\pi)^{d-1}} \frac{1}{l_\Lambda^4(l_\Lambda + k_\Lambda)} =& \frac{1}{2\pi^2}\left\{\frac{1}{k^2}\left[1 - \ln\left(\frac{2k}{\Lambda}\right)\right] + \frac{\pi}{4k\Lambda}\right\}. \qquad (4.D.6)
\end{aligned}$$

To carry out the analytic continuation of the relevant Mellin-Barnes integrands in the limit $\varepsilon \to 0$ we used the `Mathematica` package `MB` [113], and the relevant residues were identified by hand and computed using the built-in `Mathematica` function.

4.E Loop integrals for the one-point function of the operator φ_+^2

In this appendix we collect the explicit expressions for the evaluation of the loop integrals resulting from the insertion of the non-Gaussian initial conditions $\Xi_{3,1}^\sigma$ into the SdSET one-point function $\langle \varphi_+^2(t, \vec{x}) \rangle$ discussed in section 4.8.

The evaluation of these integrals follows the same strategy as for the ones appearing in the one-loop power spectrum, which is explained in appendix 4.C. To evaluate the integrals containing the logs we write

$$\ln\left(\frac{2e^{\gamma_E}(l_{1\Lambda} + l_{2\Lambda})}{a_* H}\right) = \frac{\mathrm{d}}{\mathrm{d}u}\bigg|_{\sigma=0} \left(\frac{2e^{\gamma_E}(l_{1\Lambda} + l_{2\Lambda})}{a_* H}\right)^u \tag{4.E.1}$$

and then we use the Mellin-Barnes representation [112]

$$\frac{1}{(l_{1\Lambda} + l_{2\Lambda})^{-u}} = \frac{1}{\Gamma(-u)} \frac{1}{2\pi i} \int_{-i\infty}^{i\infty} \mathrm{d}z\ \Gamma(-u+z)\Gamma(-z) \frac{l_{2\Lambda}^z}{l_{1\Lambda}^{-u+z}} \tag{4.E.2}$$

to simplify the $\vec{l}_{1,2}$-integrations.

To evaluate the integrals containing the rational functions of $l_{1,2}$ we can use the following algebraic manipulation to simplify the denominator structure:

$$-\frac{1}{l_{1\Lambda}^3 + l_{2\Lambda}^3}\left[\frac{l_{1\Lambda}^2 l_{2\Lambda}^2}{2(l_{1\Lambda} + l_{2\Lambda})} + \frac{2}{9}\left[7l_{1\Lambda}^3 + 3l_{1\Lambda}^2 l_{2\Lambda} + 3l_{1\Lambda} l_{2\Lambda}^2 + 7l_{2\Lambda}^3\right]\right] = -\frac{14}{9} - \frac{l_{1\Lambda}^2}{6(l_{1\Lambda} + l_{2\Lambda})^2} + \frac{l_{1\Lambda}(l_{1\Lambda}^2 - 6l_{1\Lambda} l_{2\Lambda} - 4l_{2\Lambda}^2)}{6(l_{1\Lambda}^3 + l_{2\Lambda}^3)}. \tag{4.E.3}$$

We can then use the following Mellin-Barnes representations to simplify the computations:

$$\frac{1}{(l_{1\Lambda} + l_{2\Lambda})^2} = \frac{1}{\Gamma(2)} \frac{1}{2\pi i} \int_{-i\infty}^{i\infty} \mathrm{d}z\ \Gamma(2+z)\Gamma(-z) \frac{l_{2\Lambda}^z}{l_{1\Lambda}^{2+z}}, \tag{4.E.4}$$

$$\frac{1}{l_{1\Lambda}^3 + l_{2\Lambda}^3} = \frac{1}{\Gamma(1)} \frac{1}{2\pi i} \int_{-i\infty}^{i\infty} \mathrm{d}z\ \Gamma(1+z)\Gamma(-z) \frac{l_{2\Lambda}^{3z}}{l_{1\Lambda}^{3+3z}}\,. \tag{4.E.5}$$

Following the above procedure, we find the following results for the non-trivial integrals:

$$\left(\frac{e^{\gamma_E}\Lambda^2}{4\pi}\right)^{2\varepsilon} \int \frac{\mathrm{d}^{d-1}l_1 \mathrm{d}^{d-1}l_2}{(2\pi)^{2d-2}} \frac{1}{l_{1\Lambda}^3 l_{2\Lambda}^3} \ln\left(\frac{2e^{\gamma_E}(l_{1\Lambda}+l_{2\Lambda})}{a_* H}\right) = \frac{1}{192\pi^4} \Bigg\{ \frac{9}{\varepsilon^3} + \frac{12}{\varepsilon^2}\left[1 + \ln\left(\frac{e^{\gamma_E}\Lambda}{a_* H}\right)\right] + \frac{3}{2\varepsilon^2}\left[8+\pi^2\right] + 2\pi^2 \ln\left(\frac{e^{\gamma_E}\Lambda}{a_* H}\right) + 24 - 4\pi^2 - 18\zeta(3) \Bigg\}, \tag{4.E.6}$$

$$\left(\frac{e^{\gamma_E}\Lambda^2}{4\pi}\right)^{2\varepsilon} \int \frac{\mathrm{d}^{d-1}l_1 \mathrm{d}^{d-1}l_2}{(2\pi)^{2d-2}} \frac{1}{l_{1\Lambda}^3 l_{2\Lambda}(l_{1\Lambda}+l_{2\Lambda})^2} = \frac{1}{32\pi^4}\left[\frac{1}{\varepsilon^2} - \frac{2}{\varepsilon} - 4 + \frac{7\pi^2}{6}\right], \tag{4.E.7}$$

$$\left(\frac{e^{\gamma_E}\Lambda^2}{4\pi}\right)^{2\varepsilon} \int \frac{\mathrm{d}^{d-1}l_1 \mathrm{d}^{d-1}l_2}{(2\pi)^{2d-2}} \frac{1}{l_{2\Lambda}^3 (l_{1\Lambda}^3+l_{2\Lambda}^3)} = \frac{1}{32\pi^4}\left[\frac{1}{\varepsilon^2} + \frac{2}{9\sqrt{3}}\left[8\ln(2) - 3\ln(3)\right] + \frac{5\pi^2}{54}\right], \tag{4.E.8}$$

$$\left(\frac{e^{\gamma_E}\Lambda^2}{4\pi}\right)^{2\varepsilon} \int \frac{\mathrm{d}^{d-1}l_1 \mathrm{d}^{d-1}l_2}{(2\pi)^{2d-2}} \frac{1}{l_{1\Lambda} l_{2\Lambda}^2 (l_{1\Lambda}^3+l_{2\Lambda}^3)} = \frac{1}{192\pi^4}\left[\frac{8\pi}{\sqrt{3}\varepsilon} + \frac{16\pi}{\sqrt{3}} - \frac{31\pi^2}{9} - 4\sqrt{3}\pi\ln(3) - \frac{4}{3}\psi^{(1)}\left(\frac{2}{3}\right) + \frac{2}{3}\psi^{(1)}\left(\frac{5}{6}\right)\right], \tag{4.E.9}$$

$$\left(\frac{e^{\gamma_E}\Lambda^2}{4\pi}\right)^{2\varepsilon} \int \frac{\mathrm{d}^{d-1}l_1 \mathrm{d}^{d-1}l_2}{(2\pi)^{2d-2}} \frac{1}{l_{1\Lambda}^2 l_{2\Lambda} (l_{1\Lambda}^3+l_{2\Lambda}^3)} = \frac{1}{192\pi^4}\left[\frac{8\pi}{\sqrt{3}\varepsilon} - \frac{23\pi^2}{9} + \frac{4\pi(8\ln(2) - 3\ln(3))}{3\sqrt{3}} - \frac{2}{3}\psi^{(1)}\left(\frac{1}{6}\right) + \frac{4}{3}\psi^{(1)}\left(\frac{1}{3}\right)\right], \tag{4.E.10}$$

where in the above results $\psi^{(1)}(z)$ denotes the polygamma function of order 1. To carry out the analytic continuation of the relevant Mellin-Barnes integrands in the limit $\varepsilon \to 0$ we used the `Mathematica` package `MB` [113], and the relevant residues were identified by hand and computed using the built-in `Mathematica` function.

4.F Generic equation of motion for an operator $Q(t)$ in SdSET at leading power in λ

In this appendix we derive an equation of motion for the expectation value $\langle Q(t)\rangle$ of an arbitrary operator $Q(t)$, which holds in the SdSET at leading power in λ. To this end we will use Weinberg's multiple-commutator formula for equal-time in-in correlators (1.4.6), which holds already at the operator level [37]:

$$Q(t) = \sum_{n=0}^{\infty} i^n \int_{-\infty}^{t} \mathrm{d}t_n \int_{-\infty}^{t_n} \mathrm{d}t_{n-1} \ldots \int_{-\infty}^{t_2} \mathrm{d}t_1 \left[H_I(t_1), \left[H_I(t_2), \left[\ldots\left[H_I(t_n), Q^I(t)\right]\ldots\right]\right]\right]. \tag{4.F.1}$$

Using the Leibniz rule for integrals,

$$\frac{\mathrm{d}}{\mathrm{d}t}\int_{-\infty}^{t} \mathrm{d}t'\ f(t,t') = f(t,t) + \int_{-\infty}^{t} \mathrm{d}t'\ \frac{\partial}{\partial t} f(t,t')\,, \tag{4.F.2}$$

It follows immediately from (4.F.1) that

$$\frac{\mathrm{d}}{\mathrm{d}t} Q(t) = \sum_{n=0}^{\infty} i^n \int_{-\infty}^{t} \mathrm{d}t_n \int_{-\infty}^{t_n} \mathrm{d}t_{n-1} \ldots \int_{-\infty}^{t_2} \mathrm{d}t_1 \left[H_I(t_1), \left[H_I(t_2), \left[\ldots\left[H_I(t_n), \frac{\mathrm{d}}{\mathrm{d}t} Q^I(t)\right]\ldots\right]\right]\right]$$

$$
\begin{aligned}
&+\sum_{n=1}^{\infty} i^n \int_{-\infty}^{t} \mathrm{d}t_{n-1} \int_{-\infty}^{t_{n-1}} \mathrm{d}t_{n-2} ... \int_{-\infty}^{t_2} \mathrm{d}t_1 \left[H_I(t_1), \left[H_I(t_2), \left[... \left[H_I(t_{n-1}), \left[H_I(t), Q^I(t)\right] ...\right]\right]\right]\right. \\
=&\sum_{n=0}^{\infty} i^n \int_{-\infty}^{t} \mathrm{d}t_n \int_{-\infty}^{t_n} \mathrm{d}t_{n-1} ... \int_{-\infty}^{t_2} \mathrm{d}t_1 \left[H_I(t_1), \left[H_I(t_2), \left[... \left[H_I(t_n), \frac{\mathrm{d}}{\mathrm{d}t} Q^I(t)\right] ...\right]\right]\right. \\
&+ i\sum_{n=0}^{\infty} i^n \int_{-\infty}^{t} \mathrm{d}t_n \int_{-\infty}^{t_n} \mathrm{d}t_{n-1} ... \int_{-\infty}^{t_2} \mathrm{d}t_1 \left[H_I(t_1), \left[H_I(t_2), \left[... \left[H_I(t_n), \left[H_{\mathrm{int}}(t), Q(t)\right]^I ...\right]\right]\right]\right. \\
=&i\sum_{n=0}^{\infty} i^n \int_{-\infty}^{t} \mathrm{d}t_n \int_{-\infty}^{t_n} \mathrm{d}t_{n-1} ... \int_{-\infty}^{t_2} \mathrm{d}t_1 \left[H_I(t_1), \left[H_I(t_2), \left[... \left[H_I(t_n), \left[H_0(t), Q^I(t)\right]\right] ...\right]\right]\right. \\
&+ i\left[H_{\mathrm{int}}(t), Q(t)\right] .
\end{aligned}
\tag{4.F.3}
$$

For the next-to-last and last equalities we used that an interaction picture field $A^I(t)$ satisfies, by definition [37]

$$
\frac{\mathrm{d}}{\mathrm{d}t} A^I(t) = i\left[H_0(t), A^I(t)\right] , \tag{4.F.4}
$$

which is solved by

$$
A^I(t) = U_0^{-1}(t,-\infty) A(-\infty) U_0(t,-\infty) , \tag{4.F.5}
$$

with the time-evolution operator U_0 defined by the equation

$$
\frac{\mathrm{d}}{\mathrm{d}t} U_0(t,-\infty) = -iH_0(t) U_0(t,-\infty) \tag{4.F.6}
$$

and (4.F.5) then implies that the commutator of two interaction picture fields A^I, B^I satisfies

$$
[A^I(t), B^I(t)] = [A(t), B(t)]^I . \tag{4.F.7}
$$

If the free Hamiltonian were constant in time, such that $H_0(t) = H_0(t_0)$, which would imply that $H_0(t) = H_0^I(t)$, the above would simply be the expectation value of the Heisenberg equation of motion for $Q(t)$. Since this is not the case here, we leave the above equation as it is.

So far, we have not made any assumptions about the form of the Hamiltonian $H(t)$. Now we specialize to the case of the SdSET, where we know that at leading power in λ for $\nu = 3/2$, which is fixed in any dimension in our regularization scheme, the free Hamiltonian reads

$$
H_0(t) = \frac{9}{2} \int \mathrm{d}^{d-1}x \, \varphi_+(t,\vec{x}) \left[1 - \sqrt{1 + \frac{4}{9} \frac{\partial_i^2}{(a(t)H)^2}}\right] \varphi_-(t,\vec{x}) = 0 + \mathcal{O}(\lambda^2) . \tag{4.F.8}
$$

Therefore, in the SdSET at leading power in λ the first term in (4.F.3) is simply vanishing, and only the second one is left over. Thus, we find

$$
\frac{\mathrm{d}}{\mathrm{d}t} Q(t) = i \int \mathrm{d}^{d-1}x \, \sum_{l=0}^{\infty} (a(t)\tilde{\mu})^{l(4-d)} \frac{\hat{c}^0_{2l+1,1}}{(2l+1)!} \left[\varphi_+^{2l+1}(t,\vec{x}) \varphi_-(t,\vec{x}), Q(t)\right] , \tag{4.F.9}
$$

where we plugged in the known form of the leading-power interaction Hamiltonian, expressed in terms of bare, dimensionless quantities. Since at leading power in λ we have $Z_\varphi = 1$, the only divergent quantities which appear are the dimensionless, bare couplings $\hat{c}^0_{2l+1,1}$.

Notice that in the above formula we let $\delta \to 0$, since the analytic regulator does not appear in the bilinear term of the interaction Hamiltonian. We did so because the poles in δ, which stem from the time integration associated to the bilinear interaction term $\sim \varphi_+\varphi_-$, will always be subtracted by means of the initial-condition counterterm $\sim \xi_{1,1}$. Because both the mass term and the initial-condition counterterm have the same field-operator content, and, at leading power in λ, the SdSET propagators are all time-independent, the cancellation of δ-poles between the two terms should always be exact. Specifically, no subdivergences featuring explicit δ-poles, which would need to be subtracted by means of a different counterterm, should be left over after the contributions from these two terms as subgraphs of a more complicated diagram have been added up. This line of reasoning should hold both for the renormalization of the effective couplings and for the renormalization of composite operators, so in the above expression we can safely let $\delta \to 0$ without running into ill-defined quantities in this limit.

Chapter 5

Conclusion and Outlook

In this thesis we have studied the infrared structure of the theory of the massless, minimally coupled, self-interacting scalar field in de Sitter space from several different points of view. In chapter 2 we have introduced the formalism of Stochastic Inflation and the Euclidean formulation of the theory of interest, and we used both formalisms to study the two-point function of the massless field. We were able to establish a connection between the analytic continuation of the Euclidean result, computed at fifth order in a semi-perturbative expansion scheme, and the analogous object computed in the stochastic formalism, in the leading-infrared approximation. This correspondence constitutes a fixed-order and single-field analogue of the correspondence between the Euclidean and stochastic theories observed in the context of the $O(N)$-model studied in [78–80] and [81, 82], respectively. We were not able to find a proof of the equality of the two results which holds to all orders in the semi-perturbative expansion, so we limited ourselves to formulating two conjectures about the all-order structure of the analytically continued Euclidean result. These conjectures, combined with the study of the high-order behaviour of the stochastic result, and its Borel-summability, allowed us to make a statement about the physical meaning of the analytically continued Euclidean result. In chapter 3 we then returned to the Lorentzian setting, and we studied correlation functions of the massless field in the late-time limit. We introduced the method of regions as a useful computational tool to simplify the evaluation of these objects, and illustrated its application using several examples. The region decomposition of the correlation functions naturally led to the discussion of the effective description of the late-time dynamics of the massless theory, which is provided by the Soft de Sitter Effective Theory, to which chapter 4 is dedicated. Therein, we constructed a consistent and well-defined formulation of this effective field theory, and we showed how the renormalization and matching procedures can be carried out systematically. Finally, we discussed how the theory can be used to address the effectively strongly-coupled infrared dynamics of the massless field in the case of the simplest class of correlation functions, the one-point functions.

The SdSET can be thought of as a realization of Starobinsky's original idea [60] which makes use of the modern EFT methodology, and, to us, it seems to be the framework of choice to successfully study and control the dynamics of light and massless fields in de Sitter space. Since it is formulated as a fully-fledged quantum field theory, it is extremely versatile, and it can be applied to any field-theory model formulated in a de Sitter background, after implementing the appropriate generalizations. At the same time, many of its aspects remain to be explored, and we feel that there are several directions in which the work we have carried out in this thesis can be extended. Completing the determination of all the relevant quantities that are needed to push the formalism that we have constructed to compute infrared-finite SdSET one-point functions, and to match them to the analogous full-theory objects, to next-to-next-to-leading-order accuracy in $\sqrt{\kappa}$ would constitute a further important consistency check of it. It would also be the first check of the results obtained in [107], which are the state-of-the-art at the time of writing. After the matching procedure of one-point functions has been established as being under control, it would be interesting to turn to the study of multi-point functions of massless scalar fields from this point of view, which has not yet been carried out in the literature using the SdSET. The two-point function would be the first natural candidate for this purpose. To obtain an infrared-finite and de Sitter-invariant result for this object, the same procedure that we applied to the one-point functions should be repeated in this case. Since the two-point function contains important and interesting physical information about the vacuum state of the theory one is considering, which in our case is non-perturbative, it would be worthwhile to understand this object better using the tools we developed here. It would also be a further non-trivial check of the SdSET to reproduce the next-to-leading order expression for the massless two-point function derived in [71]. The procedure used in this reference to obtain this result could also be used as a benchmark to judge the improvement in computational efficiency offered by the SdSET by implementing modern EFT tools. The lessons learned from this process would also pave the way for the computation of higher-point functions in the same manner. Finally, when the application of this framework to the massless scalar field has been understood, it can also be extended to include spinning fields, such as photons and gravitons, see [119] for some work in this direction. This would enable one to start considering more realistic inflationary models, thus building towards a generic framework to understand and control the infrared structure of massless fields during inflation, and to be able to derive accurate and reliable predictions from inflationary models.

Acknowledgements

First and foremost, I would like to thank Prof. Martin Beneke for giving me the opportunity to carry out my doctoral studies under his supervision, and for taking a chance in assigning this project to me. His guidance and support throughout the years have been invaluable, and I have learned more lessons from him than I can count.

I am indebted to Prof. Timothy Cohen for giving me the opportunity to visit CERN twice during my PhD, for taking many hours of his time to discuss the SdSET while I was there, and for generously offering his support and guidance during my first-ever postdoc application round. I would also like to thank Prof. Björn Garbrecht for mentoring me during my doctoral studies.

I would like to thank my former second master advisor, who turned into my main collaborator so far, Patrick Hager, for always being available to discuss physics, ideas, confusions and frustrations, and for offering helpful advice during the postdoc application period. I am also grateful to him for carefully proofreading a substantial portion of this thesis.

Thank you also to the members of T31: Lollo and Lea, who also helped me by proofreading parts of this thesis, Julian, Mathias, Domenico, Stefan, Michel, Tobias, Alexey, Michael, María, Nick, and Ludwig. A special thank you to Elke Hutsteiner, for expertly taking care of the administrative issues over the years, and, of course, for organizing coffee and cookies on Thursdays, despite extenuating circumstances in the department kitchen.

I also want to thank my bouldering group: Lollo, the Jedi master who started it all, Gael, Javier, Mar, Kai, and Giovanni. A special thank you to Mar for her support during a dark time.

A big thank you goes out to my bandmates in The Band With No Name, Mona&Co., Gaping Lotus Experience and Negative Feedback: Jonas, Korbinian, Giacomo, Damiano, Gael, Francesco, Matthias, Azamat, Hugo, Sebastião, Peter, and Robin. Playing music with all you guys has been one of the best parts of my stay in Munich.

Thank you also to Andreas and Matthias, for the many trips around Europe, several inside jokes, and, most of all, for being my friends since I moved to Germany.

Last, but definitely not least, I want to thank my parents for their continued and unwavering support, patience, and love throughout the years and during this process. I could not have done any of this without them.

Bibliography

[1] Planck collaboration, *Planck 2018 results. VI. Cosmological parameters*, *Astron. Astrophys.* **641** (2020) A6 [1807.06209].

[2] S. Dodelson, *Modern Cosmology*. Academic Press, Amsterdam, 2003.

[3] V. Mukhanov, *Physical Foundations of Cosmology*. Cambridge University Press, Oxford, 2005, 10.1017/CBO9780511790553.

[4] S. Weinberg, *Cosmology*. 2008.

[5] D. Baumann, *Inflation*, in *Theoretical Advanced Study Institute in Elementary Particle Physics: Physics of the Large and the Small*, pp. 523–686, 2011, DOI [0907.5424].

[6] A. A. Starobinsky, *A New Type of Isotropic Cosmological Models Without Singularity*, *Phys. Lett. B* **91** (1980) 99.

[7] A. H. Guth, *The Inflationary Universe: A Possible Solution to the Horizon and Flatness Problems*, *Phys. Rev. D* **23** (1981) 347.

[8] A. D. Linde, *A New Inflationary Universe Scenario: A Possible Solution of the Horizon, Flatness, Homogeneity, Isotropy and Primordial Monopole Problems*, *Phys. Lett. B* **108** (1982) 389.

[9] V. F. Mukhanov and G. V. Chibisov, *Quantum Fluctuations and a Nonsingular Universe*, *JETP Lett.* **33** (1981) 532.

[10] D. H. Lyth and A. Riotto, *Particle physics models of inflation and the cosmological density perturbation*, *Phys. Rept.* **314** (1999) 1 [hep-ph/9807278].

[11] D. Wands, *Multiple field inflation*, *Lect. Notes Phys.* **738** (2008) 275 [astro-ph/0702187].

[12] J. A. Vázquez, L. E. Padilla and T. Matos, *Inflationary cosmology: from theory to observations*, *Rev. Mex. Fis. E* **17** (2020) 73 [1810.09934].

[13] A. Albrecht and P. J. Steinhardt, *Cosmology for Grand Unified Theories with Radiatively Induced Symmetry Breaking*, *Phys. Rev. Lett.* **48** (1982) 1220.

[14] A. D. Linde, *Chaotic Inflation*, *Phys. Lett. B* **129** (1983) 177.

[15] C. Cheung, P. Creminelli, A. L. Fitzpatrick, J. Kaplan and L. Senatore, *The Effective Field Theory of Inflation*, *JHEP* **03** (2008) 014 [0709.0293].

[16] S. Weinberg, *Effective Field Theory for Inflation*, *Phys. Rev. D* **77** (2008) 123541 [0804.4291].

[17] S. M. Carroll, *Spacetime and Geometry: An Introduction to General Relativity*. Cambridge University Press, 7, 2019, 10.1017/9781108770385.

[18] M. Spradlin, A. Strominger and A. Volovich, *Les Houches lectures on de Sitter space*, in *Les Houches Summer School: Session 76: Euro Summer School on Unity of Fundamental Physics: Gravity, Gauge Theory and Strings*, 10, 2001, hep-th/0110007.

[19] S. W. Hawking and G. F. R. Ellis, *The Large Scale Structure of Space-Time*, Cambridge Monographs on Mathematical Physics. Cambridge University Press, 2, 2023, 10.1017/9781009253161.

[20] P. Di Francesco, P. Mathieu and D. Senechal, *Conformal Field Theory*, Graduate Texts in Contemporary Physics. Springer-Verlag, New York, 1997, 10.1007/978-1-4612-2256-9.

[21] S. Rychkov, *EPFL Lectures on Conformal Field Theory in D>= 3 Dimensions*, SpringerBriefs in Physics. 1, 2016, 10.1007/978-3-319-43626-5, [1601.05000].

[22] J. M. Maldacena and G. L. Pimentel, *On graviton non-Gaussianities during inflation*, *JHEP* **09** (2011) 045 [1104.2846].

[23] P. Creminelli, *Conformal invariance of scalar perturbations in inflation*, *Phys. Rev. D* **85** (2012) 041302 [1108.0874].

[24] N. Arkani-Hamed and J. Maldacena, *Cosmological Collider Physics*, 1503.08043.

[25] N. Arkani-Hamed, D. Baumann, H. Lee and G. L. Pimentel, *The Cosmological Bootstrap: Inflationary Correlators from Symmetries and Singularities*, *JHEP* **04** (2020) 105 [1811.00024].

[26] D. Baumann, C. Duaso Pueyo, A. Joyce, H. Lee and G. L. Pimentel, *The cosmological bootstrap: weight-shifting operators and scalar seeds*, *JHEP* **12** (2020) 204 [1910.14051].

[27] D. Baumann, C. Duaso Pueyo, A. Joyce, H. Lee and G. L. Pimentel, *The Cosmological Bootstrap: Spinning Correlators from Symmetries and Factorization*, *SciPost Phys.* **11** (2021) 071 [2005.04234].

[28] D. Baumann, W.-M. Chen, C. Duaso Pueyo, A. Joyce, H. Lee and G. L. Pimentel, *Linking the singularities of cosmological correlators*, *JHEP* **09** (2022) 010 [2106.05294].

[29] D. Baumann, D. Green, A. Joyce, E. Pajer, G. L. Pimentel, C. Sleight et al., *Snowmass White Paper: The Cosmological Bootstrap*, *SciPost Phys. Comm. Rep.* **2024** (2024) 1 [2203.08121].

[30] L. E. Parker and D. Toms, *Quantum Field Theory in Curved Spacetime: Quantized Field and Gravity*, Cambridge Monographs on Mathematical Physics. Cambridge University Press, 8, 2009, 10.1017/CBO9780511813924.

[31] N. D. Birrell and P. C. W. Davies, *Quantum Fields in Curved Space*, Cambridge Monographs on Mathematical Physics. Cambridge University Press, Cambridge, UK, 1982, 10.1017/CBO9780511622632.

[32] V. Mukhanov and S. Winitzki, *Introduction to quantum effects in gravity*. Cambridge University Press, 6, 2007.

[33] T. S. Bunch and P. C. W. Davies, *Quantum Field Theory in de Sitter Space: Renormalization by Point Splitting*, *Proc. Roy. Soc. Lond. A* **360** (1978) 117.

[34] M. E. Peskin and D. V. Schroeder, *An Introduction to quantum field theory*. Addison-Wesley, Reading, USA, 1995.

[35] M. D. Schwartz, *Quantum Field Theory and the Standard Model*. Cambridge University Press, 3, 2014.

[36] J. M. Maldacena, *Non-Gaussian features of primordial fluctuations in single field inflationary models*, *JHEP* **05** (2003) 013 [astro-ph/0210603].

[37] S. Weinberg, *Quantum contributions to cosmological correlations*, *Phys. Rev. D* **72** (2005) 043514 [hep-th/0506236].

[38] J. S. Schwinger, *Brownian motion of a quantum oscillator*, *J. Math. Phys.* **2** (1961) 407.

[39] L. V. Keldysh, *Diagram technique for nonequilibrium processes*, *Zh. Eksp. Teor. Fiz.* **47** (1964) 1515.

[40] J. Berges, *Introduction to nonequilibrium quantum field theory*, *AIP Conf. Proc.* **739** (2004) 3 [hep-ph/0409233].

[41] E. Calzetta and B. L. Hu, *Closed Time Path Functional Formalism in Curved Space-Time: Application to Cosmological Back Reaction Problems*, *Phys. Rev. D* **35** (1987) 495.

[42] X. Chen, Y. Wang and Z.-Z. Xianyu, *Schwinger-Keldysh Diagrammatics for Primordial Perturbations*, *JCAP* **12** (2017) 006 [1703.10166].

[43] A. Kaya, *On $i\epsilon$ Prescription in Cosmology*, *JCAP* **04** (2019) 002 [1810.12324].

[44] M. Baumgart and R. Sundrum, *Manifestly Causal In-In Perturbation Theory about the Interacting Vacuum*, *JHEP* **03** (2021) 080 [2010.10785].

[45] Y. Donath and E. Pajer, *The in-out formalism for in-in correlators*, *JHEP* **07** (2024) 064 [2402.05999].

[46] H. Goodhew, S. Jazayeri and E. Pajer, *The Cosmological Optical Theorem*, *JCAP* **04** (2021) 021 [2009.02898].

[47] S. Céspedes, A.-C. Davis and D.-G. Wang, *On the IR divergences in de Sitter space: loops, resummation and the semi-classical wavefunction*, *JHEP* **04** (2024) 004 [2311.17990].

[48] P. Benincasa, M. Giroux, H. S. Hannesdottir, S. Mizera, C. Pasiecznik and F. Vazão, *Records from the S-Matrix Marathon: Observables in Expanding Universes*, 9, 2024, 2409.14947.

[49] M. Garny and M. M. Muller, *Kadanoff-Baym Equations with Non-Gaussian Initial Conditions: The Equilibrium Limit*, *Phys. Rev. D* **80** (2009) 085011 [0904.3600].

[50] I. S. Gradshteyn and I. M. Ryzhik, *Table of Integrals, Series, and Products*. 1943.

[51] A. P. Prudnikov, Y. A. Brychkov and O. I. Marichev, *Integrals and Series, Volume 3: More Special Functions*. Gordon and Breach Science Publishers, New York, NY, 1990.

[52] N. A. Chernikov and E. A. Tagirov, *Quantum theory of scalar fields in de Sitter space-time*, *Ann. Inst. H. Poincare A Phys. Theor.* **9** (1968) 109.

[53] B. Allen and T. Jacobson, *Vector Two Point Functions in Maximally Symmetric Spaces*, *Commun. Math. Phys.* **103** (1986) 669.

[54] D. Marolf and I. A. Morrison, *The IR stability of de Sitter: Loop corrections to scalar propagators*, *Phys. Rev. D* **82** (2010) 105032 [1006.0035].

[55] L. H. Ford and L. Parker, *Quantized Gravitational Wave Perturbations in Robertson-Walker Universes*, *Phys. Rev. D* **16** (1977) 1601.

[56] B. Allen, *Vacuum States in de Sitter Space*, *Phys. Rev. D* **32** (1985) 3136.

[57] B.-L. Hu, *Infrared Behavior of Quantum Fields in Inflationary Cosmology – Issues and Approaches: an overview*, 1812.11851.

[58] A. A. Starobinsky, *Dynamics of Phase Transition in the New Inflationary Universe Scenario and Generation of Perturbations*, Phys. Lett. B **117** (1982) 175.

[59] A. A. Starobinsky, *STOCHASTIC DE SITTER (INFLATIONARY) STAGE IN THE EARLY UNIVERSE*, Lect. Notes Phys. **246** (1986) 107.

[60] A. A. Starobinsky and J. Yokoyama, *Equilibrium state of a selfinteracting scalar field in the De Sitter background*, Phys. Rev. D **50** (1994) 6357 [astro-ph/9407016].

[61] M. Reza Rahimi Tabar, *Analysis and Data-Based Reconstruction of Complex Nonlinear Dynamical Systems*. Springer-Verlag, Heidelberg, 2019.

[62] B. Garbrecht and G. Rigopoulos, *Self Regulation of Infrared Correlations for Massless Scalar Fields during Inflation*, Phys. Rev. D **84** (2011) 063516 [1105.0418].

[63] B. Garbrecht, G. Rigopoulos and Y. Zhu, *Infrared correlations in de Sitter space: Field theoretic versus stochastic approach*, Phys. Rev. D **89** (2014) 063506 [1310.0367].

[64] B. Garbrecht, F. Gautier, G. Rigopoulos and Y. Zhu, *Feynman Diagrams for Stochastic Inflation and Quantum Field Theory in de Sitter Space*, Phys. Rev. D **91** (2015) 063520 [1412.4893].

[65] H. Collins, R. Holman and T. Vardanyan, *The quantum Fokker-Planck equation of stochastic inflation*, JHEP **11** (2017) 065 [1706.07805].

[66] M. Mirbabayi, *Infrared dynamics of a light scalar field in de Sitter*, JCAP **12** (2020) 006 [1911.00564].

[67] T. Prokopec, N. C. Tsamis and R. P. Woodard, *Stochastic Inflationary Scalar Electrodynamics*, Annals Phys. **323** (2008) 1324 [0707.0847].

[68] M. Baumgart and R. Sundrum, *De Sitter Diagrammar and the Resummation of Time*, JHEP **07** (2020) 119 [1912.09502].

[69] J. O. Andersen, M. Eriksson and A. Tranberg, *Stochastic inflation from quantum field theory and the parametric dependence of the effective noise amplitude*, JHEP **02** (2022) 121 [2111.14503].

[70] I. Moss and G. Rigopoulos, *Effective long wavelength scalar dynamics in de Sitter*, JCAP **05** (2017) 009 [1611.07589].

[71] V. Gorbenko and L. Senatore, *$\lambda\phi^4$ in dS*, 1911.00022.

[72] M. Mirbabayi, *Markovian dynamics in de Sitter*, JCAP **09** (2021) 038 [2010.06604].

[73] S. L. Adler, *Massless, Euclidean Quantum Electrodynamics on the Five-Dimensional Unit Hypersphere*, Phys. Rev. D **6** (1972) 3445.

[74] I. T. Drummond, *Dimensional Regularization of Massless Theories in Spherical Space-Time*, Nucl. Phys. B **94** (1975) 115.

[75] A. Rajaraman, *On the proper treatment of massless fields in Euclidean de Sitter space*, Phys. Rev. D **82** (2010) 123522 [1008.1271].

[76] M. Beneke and P. Moch, *On "dynamical mass" generation in Euclidean de Sitter space*, Phys. Rev. D **87** (2013) 064018 [1212.3058].

[77] A. Higuchi, D. Marolf and I. A. Morrison, *On the Equivalence between Euclidean and In-In Formalisms in de Sitter QFT*, Phys. Rev. D **83** (2011) 084029 [1012.3415].

[78] D. López Nacir, F. D. Mazzitelli and L. G. Trombetta, *$O(N)$ model in Euclidean de Sitter space: beyond the leading infrared approximation*, *JHEP* **09** (2016) 117 [1606.03481].

[79] D. López Nacir, F. D. Mazzitelli and L. G. Trombetta, *Long distance behavior of $O(N)$-model correlators in de Sitter space and the resummation of secular terms*, *JHEP* **10** (2018) 016 [1807.05964].

[80] D. López Nacir, F. D. Mazzitelli and L. G. Trombetta, *To the sphere and back again: de Sitter infrared correlators at NTLO in 1/N*, *JHEP* **08** (2019) 052 [1905.03665].

[81] F. Gautier and J. Serreau, *Infrared dynamics in de Sitter space from Schwinger-Dyson equations*, *Phys. Lett. B* **727** (2013) 541 [1305.5705].

[82] F. Gautier and J. Serreau, *Scalar field correlator in de Sitter space at next-to-leading order in a 1/N expansion*, *Phys. Rev. D* **92** (2015) 105035 [1509.05546].

[83] G. Moreau and J. Serreau, *The $1/N$ expansion for stochastic fields in de Sitter spacetime*, *Phys. Rev. D* **102** (2020) 125015 [2004.09157].

[84] G. Moreau and J. Serreau, *Stability of de Sitter spacetime against infrared quantum scalar field fluctuations*, *Phys. Rev. Lett.* **122** (2019) 011302 [1808.00338].

[85] G. Moreau and J. Serreau, *Backreaction of superhorizon scalar field fluctuations on a de Sitter geometry: A renormalization group perspective*, *Phys. Rev. D* **99** (2019) 025011 [1809.03969].

[86] G. Moreau and J. Serreau, *Unequal Time Correlators of Stochastic Scalar Fields in de Sitter Space*, *Phys. Rev. D* **101** (2020) 045015 [1912.05358].

[87] T. Markkanen, A. Rajantie, S. Stopyra and T. Tenkanen, *Scalar correlation functions in de Sitter space from the stochastic spectral expansion*, *JCAP* **08** (2019) 001 [1904.11917].

[88] F. Tanaka, *Coherent Representation of Dynamical Renormalization Group in Bose Systems*, *Prog. Theor. Phys.* **54** (1975) 1679.

[89] D. Boyanovsky, H. J. de Vega, R. Holman and M. Simionato, *Dynamical renormalization group resummation of finite temperature infrared divergences*, *Phys. Rev. D* **60** (1999) 065003 [hep-ph/9809346].

[90] D. Boyanovsky and H. J. de Vega, *Dynamical renormalization group approach to relaxation in quantum field theory*, *Annals Phys.* **307** (2003) 335 [hep-ph/0302055].

[91] C. P. Burgess, L. Leblond, R. Holman and S. Shandera, *Super-Hubble de Sitter Fluctuations and the Dynamical RG*, *JCAP* **03** (2010) 033 [0912.1608].

[92] J. Zinn-Justin, *Quantum field theory and critical phenomena*, *Int. Ser. Monogr. Phys.* **113** (2002) 1.

[93] M. Mariño, *Instantons and Large N: An Introduction to Non-Perturbative Methods in Quantum Field Theory*. Cambridge University Press, 9, 2015, 10.1017/CBO9781107705968.

[94] M. Honda, R. Jinno, L. Pinol and K. Tokeshi, *Borel resummation of secular divergences in stochastic inflation*, *JHEP* **08** (2023) 060 [2304.02592].

[95] J. E. Avery and J. S. Avery, *Hyperspherical Harmonics and Their Physical Applications*. World Scientific Publishing Co., 5 Toh Tuck Link, Singapore 596224, 2018.

[96] S. Hollands, *Massless interacting quantum fields in deSitter spacetime*, *Annales Henri Poincare* **13** (2012) 1039 [1105.1996].

[97] M. Beneke and V. A. Smirnov, *Asymptotic expansion of Feynman integrals near threshold*, Nucl. Phys. B **522** (1998) 321 [hep-ph/9711391].

[98] V. A. Smirnov, *Applied asymptotic expansions in momenta and masses*, *Springer Tracts Mod. Phys.* **177** (2002) 1.

[99] B. Jantzen, *Foundation and generalization of the expansion by regions*, JHEP **12** (2011) 076 [1111.2589].

[100] M. Beneke, P. Hager and A. F. Sanfilippo, *Cosmological correlators in massless ϕ^4-theory and the method of regions*, JHEP **04** (2024) 006 [2312.06766].

[101] S. Melville and E. Pajer, *Cosmological Cutting Rules*, JHEP **05** (2021) 249 [2103.09832].

[102] S. Weinberg, *Quantum contributions to cosmological correlations. II. Can these corrections become large?*, Phys. Rev. D **74** (2006) 023508 [hep-th/0605244].

[103] L. Senatore and M. Zaldarriaga, *On Loops in Inflation*, JHEP **12** (2010) 008 [0912.2734].

[104] D. Seery, *Infrared effects in inflationary correlation functions*, Class. Quant. Grav. **27** (2010) 124005 [1005.1649].

[105] T. Cohen and D. Green, *Soft de Sitter Effective Theory*, JHEP **12** (2020) 041 [2007.03693].

[106] G. Ballesteros, J. Gambín Egea and F. Riccardi, *Finite parts of inflationary loops*, JHEP **06** (2025) 098 [2411.19674].

[107] T. Cohen, D. Green, A. Premkumar and A. Ridgway, *Stochastic Inflation at NNLO*, JHEP **09** (2021) 159 [2106.09728].

[108] M. Beneke and T. Feldmann, *Factorization of heavy to light form-factors in soft collinear effective theory*, Nucl. Phys. B **685** (2004) 249 [hep-ph/0311335].

[109] C. W. Bauer, D. Pirjol and I. W. Stewart, *Factorization and endpoint singularities in heavy to light decays*, Phys. Rev. D **67** (2003) 071502 [hep-ph/0211069].

[110] J.-Y. Chiu, A. Jain, D. Neill and I. Z. Rothstein, *A Formalism for the Systematic Treatment of Rapidity Logarithms in Quantum Field Theory*, JHEP **05** (2012) 084 [1202.0814].

[111] J. C. Collins, *Renormalization: An Introduction to Renormalization, The Renormalization Group, and the Operator Product Expansion*, vol. 26 of *Cambridge Monographs on Mathematical Physics*. Cambridge University Press, Cambridge, 1986, 10.1017/CBO9780511622656.

[112] V. A. Smirnov, *Analytic tools for Feynman integrals*, vol. 250. 2012, 10.1007/978-3-642-34886-0.

[113] M. Czakon, *Automatized analytic continuation of Mellin-Barnes integrals*, Comput. Phys. Commun. **175** (2006) 559 [hep-ph/0511200].

[114] A. Y. Kamenshchik and T. Vardanyan, *Renormalization group inspired autonomous equations for secular effects in de Sitter space*, Phys. Rev. D **102** (2020) 065010 [2005.02504].

[115] D. Green and A. Premkumar, *Dynamical RG and Critical Phenomena in de Sitter Space*, JHEP **04** (2020) 064 [2001.05974].

[116] T. Huber and D. Maitre, *HypExp 2, Expanding Hypergeometric Functions about Half-Integer Parameters*, Comput. Phys. Commun. **178** (2008) 755 [0708.2443].

[117] T. Cohen, D. Green and A. Premkumar, *A tail of eternal inflation*, SciPost Phys. **14** (2023) 109 [2111.09332].

[118] T. Cohen, D. Green and Y. Huang, *Operator origin of anomalous dimensions in de Sitter space*, *Phys. Rev. D* **111** (2025) 103513 [2407.08581].

[119] D. Green and K. Gupta, *Soft Metric Fluctuations During Inflation*, 2410.11973.

[120] M. H. Namjoo, A. H. Guth and D. I. Kaiser, *Relativistic Corrections to Nonrelativistic Effective Field Theories*, *Phys. Rev. D* **98** (2018) 016011 [1712.00445].

[121] H. Goldstein, C. Poole and J. Safko, *Classical Mechanics, Third Edition*. Addison Wesley, San Francisco, 2001.

[122] A. V. Manohar, *Introduction to Effective Field Theories*, 1804.05863.

[123] M. Garny and U. Reinosa, *Renormalization out of equilibrium in a superrenormalizable theory*, *Phys. Rev. D* **94** (2016) 045012 [1504.06643].

[124] M. Neubert, *Renormalization Theory and Effective Field Theories*, 1901.06573.